UNIVERSITY OF CALIFORNIA
RIVERSIDE

Transcriptomics in Ecotoxicology: Characterizing the Effects of Contaminants and Environmental Parameters on Aquatic Populations

A Dissertation submitted in partial satisfaction
of the requirements for the degree of

Doctor of Philosophy

in

Environmental Sciences

by

Nicolette Andrzejczyk

June 2020

Dissertation Committee:
Dr. Daniel Schlenk, Chairperson
Dr. David Volz
Dr. Jay Gan

The Dissertation of Nicolette Andrzejczyk is approved:

_____

_____

_____

Committee Chairperson

University of California, Riverside

Acknowledgements

This dissertation was possible due to the help of many people. First and foremost, I would like to thank my PhD advisor Dr. Daniel Schlenk for his continuous encouragement, optimism, and confidence in me. Over the years, he has helped me develop my skills as a critical thinker and scientist, opened doors to a number of research opportunities, and dedicated his time and effort into improving my research. Thank you for all of your advice and mentorship and always being there to chat about my research or anything else I needed help with! Additionally, I would like to acknowledge my committee members, Dr. David Volz and Dr. Jay Gan, who have provided me with mentorship and guidance throughout my time at UCR. Having mentors like you that I could go to for research or networking related advice has shaped me into a better scientist. Thank you to my amazing family and friends for always being so supportive of my goals.

I would also like to thank the many past and present Schlenk lab members for their mentorship, advice, and friendship, including Dr. Justin Greer, Dr. Marissa Giroux, Dr. Jason Magnuson, Dr. Elvis Xu, Dr. Luisa Bertotto, Dr. Scott Coffin, Dr. Graciel Diamante, Tori McGruer, Phil Tanabe, and GT Harraka. Additionally, thank you to my various undergraduate mentors and advisors who first got me interested in research and always pushed me to do my best, including Dr. Susan Cushman, Dr. John Halfman, Dr. Walter Bowyer, Dr. Kristy Kenyon, and Dr. Roxanne Razavi – my time spent with you at HWS is what led me to pursue a PhD. I would also like to thank Dr. Vince Palace and Lee Hrenchuk at the IISD Experimental Lakes Area who provided field support,

mentorship, and advice for Chapters 2 and 3 as well as Sonya Michaleski and Lauren Hayhurst for help in field sampling. Additionally, thank you to Kenny Sakamoto, Jeff Armstrong, Danny Tang, and the rest of the ocean monitoring crew at the Orange County Sanitation District for the many early mornings of trawling on the *Nerissa*. Thank you Lisa Peters, Dr. Gregg Tomy, and the Centre for Oil and Gas Research and Development (COGRAD) for chemistry data used in Chapter 3.

Graduate student support was provided through the University of California, Riverside. Research in Chapters 2 and 3 was made possible by a grant from The Gulf of Mexico Research Initiative, Grant No: SA-1520; Name: Relationship of Effects of Cardiac Outcomes in fish for Validation of Ecological Risk (RECOVER2). Research in Chapter 3 was possible thanks to a large multidisciplinary program that includes participation and funding from governments (Environment and Climate Change Canada, Fisheries and Oceans Canada, Natural Resources Canada, Ontario Municipal Employees Coordinating Committee, Ontario Ministry of Natural Resources and Forestry), regulators (National Energy Board), academic partners (universities of Manitoba, Ottawa, Queen's, Institut national de la recherche scientifique, Calgary, Saskatchewan, McGill) and industry (Canadian Association of Petroleum Producers, Canadian Energy Pipelines Association). Additionally, the BOREAL study referenced in Chapter 3 was funded by an NSERC Strategic Partnership Grant to Dr. Jules Blais (University of Ottawa), Dr. Mark Hanson (University of Manitoba), and Dr. Diane Orihel (Queen's University), in partnership with Dr. Bruce Hollebone (Environment and Climate Change Canada) and Dr. Vince Palace (IISD-Experimental Lakes Area). Additional funding was provided by

the UCR Dissertation Year Program Award, IISD Experimental Lakes Area Highly-Qualified Personnel Grant, and the Southern California SETAC Graduate Student Research Award. Funding for attendance of numerous conferences was provided by the UCR Graduate Student Association travel grants, Environmental Sciences Mini-Graduate Student Association travel grants, the Albert Marsh Environmental Sciences Scholarship, Pollutant Responses in Marine Organisms Student Travel Award, and the Society of Toxicology Student Travel Award.

Copyright Acknowledgements

Dedication

Dla mojej mamy i reszty mojej rodziny - dziękuję za wsparcie. Kocham was!

ABSTRACT OF THE DISSERTATION

Transcriptomics in Ecotoxicology: Characterizing the Effects of Contaminants and Environmental Parameters on Aquatic Populations

by

Nicolette Andrzejczyk

Doctor of Philosophy, Graduate Program in Environmental Sciences
University of California, Riverside, June 2020
Dr. Daniel Schlenk, Chairperson

Characterizing the potential impacts of chemical stressors from the molecular level to the population level is critical in understanding the risks of contaminants to wildlife. Use of transcriptomics is a powerful tool that may be used to identify the mechanisms of action of a chemical and, thus, to predict ecological risk through an adverse outcome pathway approach. In the present study, fish population declines thought to be a result of estrogenic contaminants from wastewater treatment effluent were explored using molecular- to population-level endpoints. Population declines were instead found to be correlated with increased water temperatures indicating that environmental stressors may alter ecosystem health in addition to contaminants. It is likely that repeated biannual sampling also contributed to population declines to some degree, warranting the development of non-lethal, catch and release sampling methods.

To assess effects of environmental factors and limit lethal sampling of populations for molecular endpoints, the toxicogenomic analysis of epidermal mucus was evaluated as a non-lethal assessment tool. Using the Canadian Experimental Lakes Area, mucus from four fish populations residing in different lakes underwent RNA sequencing. Results indicated that RNA sequencing of mucus was able to discern unique patterns of gene expression among fish populations that correlated with environmental variables, such as productivity, dissolved oxygen, and alkalinity. Thus, toxicogenomic analysis of mucus was identified as a useful tool to assess molecular effects of environmental factors on fish populations. To further develop the use of mucus for ecotoxicological studies, mucus was collected and sequenced from fish before and after additions of diluted bitumen (dilbit) into one of these lakes. Transcripts associated with oil exposure were altered in mucus of dilbit-exposed individuals, suggesting that transcriptomic analysis of mucus may be used as a non-lethal method for exposure assessment to environmental contaminants. Overall, this work explored the use of transcriptomic tools to assess exposure to environmental and chemical stressors in wild populations and identified transcriptomics of mucus as an effective non-lethal toxicogenomics-based assessment tool.

Table of Contents

List of Tables

List of Figures

Chapter 3

Transcriptomics in Ecotoxicology

The primary goal of ecotoxicology is to characterize the effects of chemical stressors on biological organisms, ultimately at the population, community, and ecosystems levels. The development of tools allowing for non-target, high-throughput screening of biomolecules has greatly enhanced the ability of toxicologists to understand molecular changes induced by chemical stressor exposure. Of these tools, use of transcriptomics in ecotoxicology has been critical in furthering our understanding of how the expression of genes is altered following exposure to environmental contaminants. Through RNA sequencing, it is possible to identify and characterize all RNA molecules in an organism, importantly messenger RNA (mRNA) transcripts which are responsible for translating DNA into proteins. Thus, the transcriptome reflects all mRNA transcripts that are actively expressed in the organism at a given time. Through profiling of all mRNA transcripts, transcriptomics has been proposed as a tool to understand the biological effects of chemical stressors by assessing changes in gene expression patterns at the transcriptome-wide level.[1–3]

Understanding the effects of a chemical at the molecular level is critical. When a chemical interacts with a biological target at the molecular- or cellular-level, a biomolecular response follows during which thousands of molecules are produced.[4] The various biomolecules produced following the chemical-target interaction results in changes throughout multiple levels of biological organization over time through subsequent biological reactions (Figure 1.1).[3–6] Transcriptomic analysis can be used to identify initial biomolecular interactions throughout the transcriptome, making it a

powerful tool for inferring the mode of action for chemicals.[2,3,7] Furthermore, understanding the effects of a chemical on the molecular-level has been deemed crucial in ecotoxicology, as molecular-level effects can be used to understand upstream adverse effects (Figure 1.1).[4,8,9]

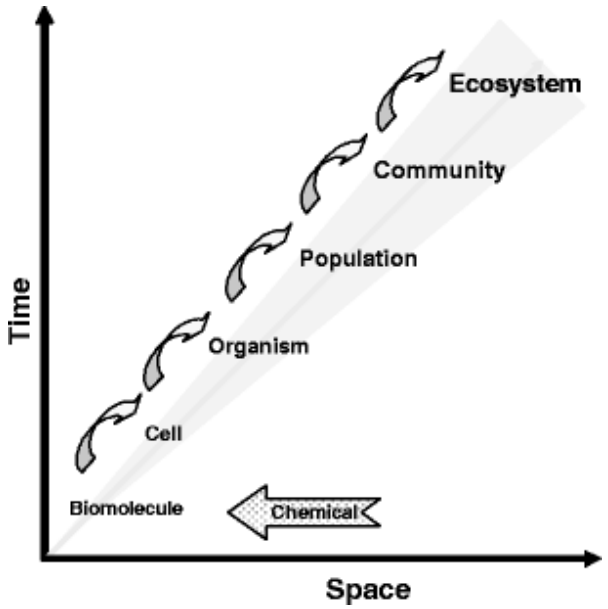

Figure 1.1. Interaction of a chemical at the biochemical or cellular level will initiate a small-scale biomolecular response that may eventually result in higher-level biological effects (from Schirmer et al., 2010).

As ecotoxicology is ultimately most concerned with effects at the population-level and above, molecular interactions identified through transcriptomics must be bridged to higher levels of biological organization in order to be meaningful.[6,10] To bridge transcriptomic data to population-level responses, Ankley et al. (2010) proposed the concept of the adverse outcome pathway: a conceptual model that uses existing knowledge to depict the linkage between a direct molecular initiating event and the subsequent adverse outcomes throughout the levels of biological organization (Figure 1.2). By identifying chemical-specific gene expression profiles, upstream biological

responses can be predicted based on the function of the differentially expressed genes and comparison of expression profiles to those of reference toxicants with established modes of action.[6,11] Development of adverse outcome pathways may therefore be an important for predictive ecological risk assessment of chemicals.

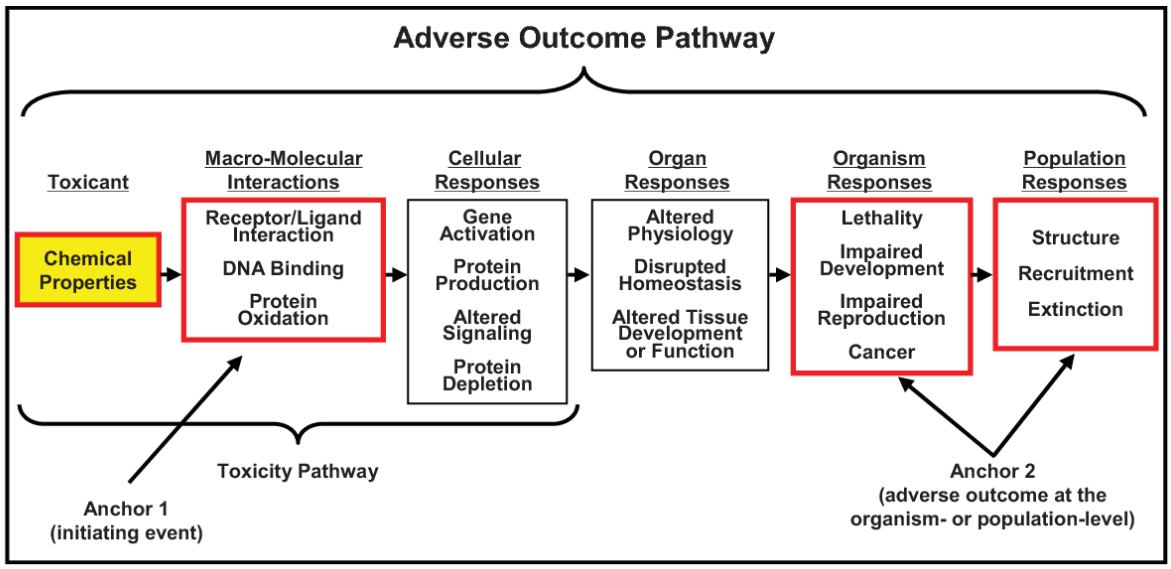

Figure 1.2. Schematic of the adverse outcome pathway framework (from Ankley et al., 2010).

Use of transcriptomic data in conjunction with an adverse outcome pathway approach has several potential applications in ecotoxicology and environmental toxicology. Firstly, understanding a chemical's mode of action may be used for development of predictive, mechanism-based ecological risk assessment of contaminants.[8] Along with this, transcriptomics may be a useful tool to characterize, classify, and predict toxicity of chemicals *in vitro*, which could reduce animal testing and expedite chemical screening.[12] Transcriptomic studies also allow for discovery of molecular biomarkers that could be used for efficient monitoring of chemical exposure in

wildlife.[8,9] Similarly, transcriptomic studies on wild populations may be used to identify causative agents contributing to observed perturbations.[8,9] Overall, toxicogenomic tools such as transcriptomics have immense utility within ecotoxicology and, consequently, within risk assessment and regulatory fields.

Contaminants of emerging concern in aquatic environments

Emerging contaminants

The use of synthetic chemicals in the modern world has become essential across a number of industries. In fact, chemical discovery has been growing at rapid pace, with the Chemicals Abstract Service (CAS REGISTRY) registering its 150 millionth unique chemical substance in May 2019.[13] In May 2011, CAS REGISTRY had only registered its 60 millionth chemical substance, showing an exponential increase in chemical discovery into present day. Through human activities, there is potential for synthetic chemicals to enter marine and freshwater ecosystems where they may exert adverse effects on aquatic species.[14]

Due to the rapid discovery of chemicals, many emerging or newly identified contaminants have been detected within aquatic environments, such as pharmaceuticals and personal care products (PPCPs), industrial additives, surfactants, and others.[15] Unlike other contaminant classes, there are no or very few regulations controlling the presence of a majority of emerging contaminants within the environment or drinking water. The lack of regulation is largely attributed to the lack of knowledge on the behavior in the environment, toxicity, and biological effects of these emerging contaminants. Emerging

contaminants may also be unique from other contaminant classes as they do not need to be persistent in order to induce adverse effects due to the fact that they are continuously discharged into the environment at rates that exceed their removal rates.[16]

One of the main sources of emerging contaminants is wastewater treatment plant effluent and, thus, most previous research on emerging contaminants has been in regards to its presence in effluent.[15,17–19] Wastewater effluent is a major contributor of emerging contaminants and their metabolites as most existing conventional water treatment plants have not been designed to remove these newly identified contaminants.[15,19] Wastewater treatment plants receive sewage from both households and industrial sources, which may contain PPCPs, industrial additives, and other emerging contaminants (Figure 1.3).[15,19] It should be noted that animal farming, agriculture, and landfills may further contribute emerging contaminants by runoff into surface water or infiltration into groundwater which introduces contaminants into drinking water systems and ultimately wastewater treatment plants (Figure 1.3). Finally, as wastewater treatment plants may not be able to efficiently remove emerging contaminants, effluent introduces these contaminants into marine and freshwater environments.

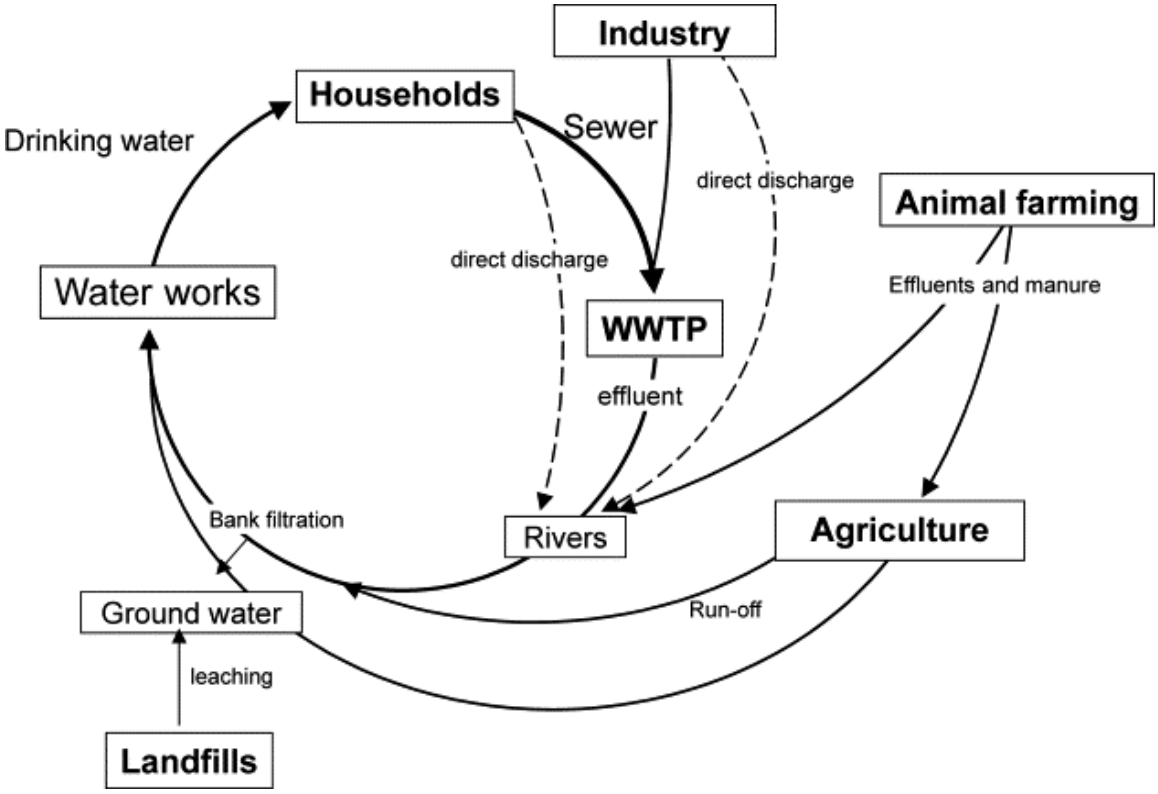

Figure 1.3. Schematic illustrating the central role wastewater treatment plants hold in releasing emerging contaminants into aquatic environments (from Petrović et al., 2003).

Emerging contaminants may induce adverse effects once in aquatic environments as many of these compounds have been shown to be endocrine disrupting chemicals (EDCs).[19] The U.S. Environmental Protection Agency (EPA) has defined EDCs as "an exogenous agent that interferes with synthesis, secretion, transport, metabolism, binding action, or elimination of natural blood-borne hormones that are present in the body and are responsible for homeostasis, reproduction, and developmental process." Initially, EDCs were thought to mainly exert actions through nuclear hormone receptors such as estrogen receptors, androgen receptors, progesterone receptors, and thyroid receptors; however, further research has shown that EDCs can act through numerous other

mechanisms, such as nonnuclear steroid hormone receptors, orphan receptors, nonsteroid receptors, enzymatic pathways involved in steroid hormone biosynthesis and metabolism, and others.[20] This wide spectrum of potential mechanisms of action reflect on the diversity in structure of EDCs. Furthermore, as EDCs are structurally diverse and often do not appear to share structural similarity, it is difficult to predict if a compound may be endocrine disrupting.[20] Nevertheless, there are certain emerging EDCs whose mechanisms of action have been relatively well-characterized. For example, bisphenol A (BPA), nonylphenol, and 17α-ethinylestradiol (EE2) contain a phenolic moiety that mimic natural estrogen and allow these compounds to interact with the estrogen receptor.[16,21–23] Estrogenic compounds detected in wastewater will be discussed in more detail as the adverse outcome pathway has been most developed for these compounds and the ability for estrogenic compounds to induce population level effects has been demonstrated.[24]

Estrogenic compounds

Estrogenic compounds can enter the aquatic environment through a number of ways, one of the most prominent being through wastewater treatment plant effluent.[25] In fact, out of all known estrogen mimicking compounds, almost all have been found in wastewater effluent.[26,27] Common estrogenic compounds found in wastewater effluent and in the environment include natural steroidal estrogens, phthalates, nonylphenol, alkylphenol-ethoxylates, bisphenol A, among hundreds of others.[25,27,28] One compound that has gained significant attention is the synthetic estrogen EE2 which is found in

hormonal contraceptives and is one of the most potent estrogens found in water systems.[29] As it is resistant to degradation in the body, EE2 is often present in wastewater treatment effluent where it is then released into aquatic environments.[30] EE2 has been identified at levels as high as 273 ng/L in U.S. rivers, as well as at lower levels ranging from 0.5 to 5 ng/L.[30–32] Estrogenic compounds in the aquatic environment are taken up by organisms through direct uptake from water through the gills, intake of suspended particles, or consumption of contaminated food, which may result in biomagnification.[33,34] Once taken up by organisms, estrogenic compounds may induce deleterious endocrine disrupting effects in aquatic organisms even at trace levels of ng/L.[24,35]

Exogenous estrogenic compounds are able to bind to the estrogen receptor, eliciting the production of estrogen and associated upstream responses.[22,23] Most notably, the increased estrogen production associated with exposure to estrogenic compounds has shown to consequently induce production of vitellogenin in fish.[24] As the egg-yolk protein vitellogenin is female-specific, the presence of the protein in male fish has become a well-recognized biomarker of exposure to xenobiotics.[28,36,37] While vitellogenin may be useful for exposure assessment, induction of vitellogenin alone is alone is not indicative of reproductive dysfunction and other biological endpoints should be considered. Changes in hormone levels due to estrogenic compounds may also affect sexual differentiation, as sex in fish is determined by the hormonal environment.[38] Increased production of estrogen during gonadogenesis and gametogenesis can change the path of development, causing differentiation of reproductive ducts and primordial

germ cells to result in characteristics opposite of the individual's genotypic sex or development of testis-ova.[39–41] Estrogenic compounds can also affect adult fish by inducing redifferentiation of germ cells, leading to formation of intersex characteristics even outside of development.[39] In addition, partial or complete inhibition of gonad growth has also been observed in male fish exposed to estrogenic compounds.[39,42,43] At the individual level, estrogenic compounds such as EE2 have been shown to alter courtship behaviors in male fish, consequently impacting mating success.[44,45] Thus, alterations induced by estrogenic compounds at the molecular, organ, and individuals levels may ultimately affect the reproductive fitness of fish.[46] Decreased reproductive success may in turn have population-level implications, as was seen with the near extirpation of a fathead minnow (*Pimephales promelas*) population following exposure to 5 ng/L of EE2 in a whole-lake experiment.[24] Moreover, the collapse of the fathead minnow population had consequent effects throughout the food web, such as declines in the lake trout (*Salvelinus namaycush*) population due to reduce prey availability.[47] The aforementioned study is an important example of how molecular-level changes induced by environmental contaminants may ultimately lead to ecosystem-level effects.

Persistent organic pollutants in aquatic environments

Persistent organic pollutants

Persistent organic pollutants (POPs) are ubiquitous environmental contaminants that are not readily degraded in the environment due to their long half-lives in environmental media.[48] The most notable examples are legacy POPs such as

polychlorinated biphenyls (PCBs), dichlorodiphenyltrichloroethanes (DDTs), chlordanes, and hexachlorobenzene (HCB) which have been banned due to their toxicity. In May 2001, the United States and 90 other countries signed a United Nations treaty under which countries agreed to reduce or eliminate the production and use of 12 key POPs, including polychlorodibenzodioxins/furans (PCDD/Fs), PCBs, and some organochlorine pesticides.[49] Since then, the production and use of other POPs have been regulated, such as mixtures of polybrominated diphenyl ethers (PBDEs), perfluorooctane sulfonic acid (PFOS), perfluoroalkyl substances (PFASs) and hexabromocyclododecanes (HBCDs). Although many POPs are not currently being released into the environment and those that are currently used are heavily regulated, they are still detected in sediments and biota at toxic concentrations due to their persistence.[50] Moreover, as POPs are typically hydrophobic and lipophilic, they partition into organic matter of sediments in aquatic environments. Thus, sediments serve as environmental reservoirs from which POPs can be mobilized and re-introduced into the aquatic environments even without present day inputs.

A major historic source of POPs in the environment was through agricultural applications. The most well-known agrochemical POP is DDT, which is an organochlorine pesticide that was extensively used on agricultural crops in the United States from 1945 until 1972 when it was banned in the United States.[49] Aside from its agricultural use, DDT was also used to protect against diseases such as malaria and typhus and continues to be used in some parts of the world today. Overall, it is estimated that 4 billion pounds of DDT has been produced and applied worldwide since 1940.[49]

Other organochlorine pesticides include aldrin, dieldrin, chlordane, and heptachlor; while these are banned in most countries, some continue to be used in certain developing countries.[51] Following pesticide application, organochlorine pesticides can enter aquatic environments through runoff, leaching of polluted wastes into groundwater, industrial discharges from manufacturers, or wastewater treatment plant effluent.[51]

Many POPs have also been useful in a variety of industrial applications, most notably the halogenated aromatic hydrocarbons PCBs, PCDDs, and PCDFs. Mixtures of PCB congeners have been used in multiple products historically, including hydraulic and heat transfer liquids, vacuum pumps, transformers, paints, adhesives, waxes, inks, carbonless copy paper, and others.[52,53] Unlike PCBs, PCDDs and PCDFs are formed unintentionally as byproducts during industrial and combustion processes, such as combustion of municipal waste, medical waste incinerators, metal smelting, and chemical manufacturing.[54,55] Exposure to these halogenated aromatic hydrocarbons has shown the induce adverse effects in fish through sustained aryl hydrocarbon receptor (AhR) activation, including carcinogenesis, endocrine disruption, altered lipid metabolism, porphyria, hepatotoxicity, cardiotoxicity, dermal toxicity, immunotoxicity, developmental toxicity, and reproductive toxicity.[56–63] Exposure to halogenated aromatic hydrocarbons in the environment may ultimately have population-level impacts, as halogenated aromatic hydrocarbons were suggested to be the key causative factor in recruitment failures observed in lake trout populations within the Great Lakes for nearly four decades.[59]

Polycyclic aromatic hydrocarbons (PAHs) are another notable group of POPs which exert similar mechanisms of toxicity as halogenated aromatic hydrocarbons. It has been suggested that combustion and subsequent emission of PAHs into the atmosphere accounts for over 90% of PAHs in the environment.[64] The major sources of PAH emissions include residential heating (coal and wood burning, oil and gas burning), mobile sources (gasoline and diesel engines), industrial processes (coke manufacturing, asphalt production, etc.), incinerations, among others.[64] PAHs from atmospheric emissions may then enter aquatic environments through atmospheric deposition in precipitation and dry deposition.[65] Wastewater effluent has shown to be a common contributor of PAHs in aquatic environments, with concentration ranges typically being less than 5 μg/L for treatment plants that serve primarily domestic wastes.[65] However, concentrations can be higher in treatment plants receiving high proportions of industrial wastes, such as the Los Angeles County Sanitation District which has had 216.5 μg/L ΣPAHs reported in effluent as a result of receiving waste from petroleum refineries.[66] Other sources include industrial outfalls, urban runoff, leaks and spills of crude oil, and sewage sludges. Following exposure, PAHs have been shown to induce toxicity through both AhR-dependent and AhR-independent pathways;[67] the toxicity of PAHs to fish will be discussed in greater detail further in the chapter.

One central way that POPs can be introduced into aquatic environments is through wastewater treatment plant effluent. POPs may enter wastewater treatment plants from urban or agricultural drainage into sewage systems as well as from industrial and domestic wastes.[68,69] In the primary stage of treatment, POPs are likely to be removed

primarily by sorption onto suspended solids and sedimentation, followed by volatilization at the air-water interface.[70] For example, sorption to sludge has shown to remove up to 70% of PCBs and 32% of heptachlor in wastewater.[71,72] In the second stage of treatment, POPs may be removed through sorption to activated sludge, biotransformation or biodegradation, and air stripping.[70] However, conventional wastewater treatment processes are not completely efficient in removing POPs, resulting in release of contaminants into aquatic environments via effluent. Moreover, research has shown that the efficiency of POP removal during wastewater treatment processes is both plant-specific and compound-dependent.[73–75]

Overall, input of POPs into aquatic environments may pose risk to ecosystem health due to their recalcitrant nature. Due to their lipophilicity, POPs are often deposited into sediments and bioaccumulated into the lipid fraction of organisms, leading to long-term exposure and effects in aquatic organisms. Thus, presence of POPs is an important factor to consider when investigating perturbations within wild populations.

Behavior and toxicity of diluted bitumen

Chemical composition

Oil sands are a form of hydrocarbon deposits composed of sand, clay, water, minerals, and bitumen. Bitumen, a naturally weathered heavy crude oil, can be extracted from oil sands where it is then processed into synthetic crude oil. As bitumen is highly dense and viscous in its natural state, it is often made into a mixture called diluted bitumen, or dilbit, to make transport through pipelines more effective. Dilbit typically

consists of approximately 70% bitumen and 30% of a diluent, usually natural gas condensate.[76] The specific diluents used and the ratio of bitumen-to-diluent varies, therefore resulting in variability in the composition of dilbit among source regions.[77,78] Dilbit has the same general composition as other crude oils which is often characterized by presence of saturated hydrocarbons, aromatic hydrocarbons, resins, and asphaltenes (SARA) within the oil industry. However, the abundances of these classes of chemicals vary greatly among oil types (Figure 1.4).[79] Compared to other crude oils, diluted bitumen has higher proportions of asphaltenes and resins, the importance of which will be discussed in the following section.

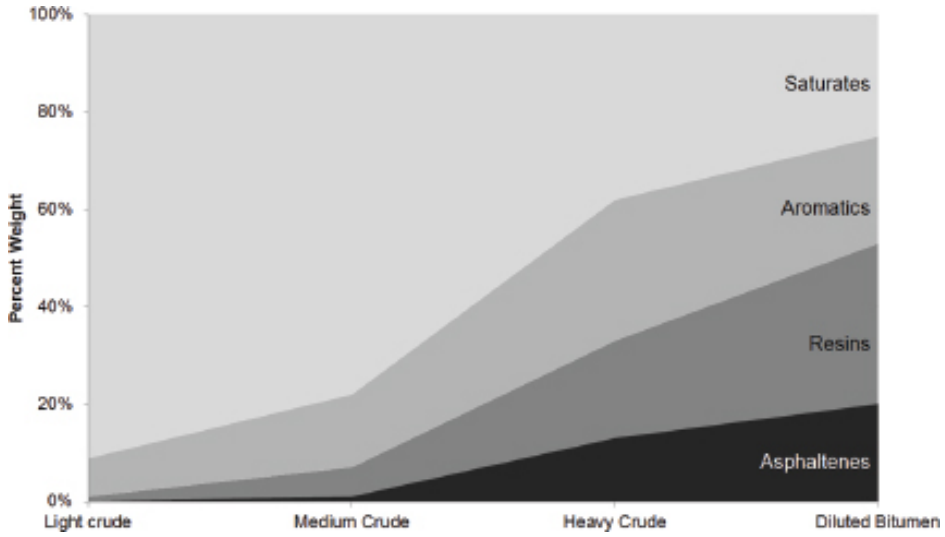

Figure 1.4. Relative composition of light crude oil, medium crude oil, heavy crude oil, and diluted bitumen in terms of the major oil constituent classes: saturates, aromatics, resins, and asphaltenes (from NASEM, 2016).

Environmental Fate and Transport of Dilbit

The Canadian oil sands in Alberta, Canada are one of the largest known reserves of bitumen, containing an estimated 50 billion cubic meters or 315 billion barrels of

bitumen.[80] A majority of crude oil exported from the Canadian oil sands is through pipelines, raising concern for potential leaks and spills into lakes and rivers located along current pipeline routes.[81] As bitumen production is projected to continue to grow,[80] the associated increase in pipeline development and dilbit transport further attributes to the risk of accidental leaks and spills. Dilbit spills into aquatic environments have historically been infrequent; however, spills that have occurred have posed novel environmental issues due to the unique chemical properties of dilbit that influence its environmental fate and behavior. Following a pipeline burst, a 2010 oil spill in Michigan released 1.15 million gallons of dilbit into the Kalamazoo River and was the largest inland oil spill in the United States.[79,82] The Kalamazoo River oil spill resulted in being the most expensive inland oil spill in United States history with the cleanup costing approximately $1.2 billion.[83] This difficult and costly cleanup was largely due to the unique weathering of dilbit, which caused the material to sink to the riverbed and coat the cobblestone bottom.

During a spill, evaporation is one of the most important weathering processes affecting crude oils and greatly alters the chemical and physical characteristics of dilbit.[79,84] The diluents added to create dilbit are typically volatile and are thus readily evaporated from the mixture, resulting in a residue that resembles the original bitumen;[79] this is an important factor that distinguishes dilbit from other crude oils. The evaporative loss of the diluent as well as other light compounds (such as saturated hydrocarbons and aromatics) affects the density, adhesion, and viscosity of dilbit (Table 1.1).[79,85] Density of dilbit increases following weathering as lighter compounds are evaporated. For example, Cold Lake Blend dilbit has a density of 0.92 g/cm^3 prior to release into the environment

and increases to 1.002 g/cm^3 after weathering.[79,85] Weathered dilbit may exceed the density of freshwater (1.00 g/cm^3) resulting in the material to sink to the bottom of freshwater bodies.[86] Unlike weathered dilbit, other forms of weathered crude oil will have densities below that of freshwater and often will float on the surface (Table 1.1).

As with density, viscosity and adhesion of dilbit also increases after weathering (Table 1.1). The viscosity of oil is dependent on the relative abundance of resins and asphaltenes as they are large, polar molecules.[79] Crude oils with greater amounts of light components and lesser amounts of resins and asphaltenes are less viscous. Following evaporative loss of lighter compounds, viscosity of weathered dilbit increases compared to the unweathered product as the relative proportion of resins and asphaltenes increases within the mixture. The increased proportion of resins and asphaltenes in weathered dilbit also results in increased adhesion.[79] Not only is weathered dilbit much more adhesive than its unweathered form, it is also highly more adhesive than other forms of crude oil, both weathered and unweathered (Table 1.1).[85] Furthermore, as dilbit is composed of higher proportions of resins and asphaltenes, dilbit spills will introduce a higher mass of adhesive material than other crude oils.[79] Due to the viscous and adhesive properties of weathered dilbit, cleanup of spills may be difficult as the dilbit residues attach to sediments, rocks, vegetation, and any other structures. This unique behavior of weathered dilbit is what resulted in the long and costly cleanup of the Kalamazoo River oil spill.

Table 1.1. Properties of unweathered and weathered several crude oils (modified from NASEM, 2016).

Type of Crude Oil	Density (g/cm^3)	Viscosity (mPa·s)	Adhesion (g/m^2)
Light Crude	0.77	1	0
Weathered Light Crude	0.84	5	9
Medium Crude	0.85	8	12
Weathered Medium Crude	0.90	112	33
Heavy Crude	0.94	820	75
Weathered Heavy Crude	0.98	475,000	600
Diluted Bitumen	0.92	270	98
Weathered Diluted Bitumen	1.002	50,000	1,580

Breakdown of dilbit in the environment is likely mainly mediated through photooxidation and biodegradation. When exposed to sunlight, constituents within dilbit are oxidized through cleavage and formation of covalent bonds, resulting in oxygenated compounds.[79] Because aromatic hydrocarbons are typically most rapidly transformed, the relative abundance of resins and asphaltenes in residual dilbit is predicted to increase which may contribute to the increases in density, viscosity, and adhesion of weathered dilbit.[87,88] The role of photooxidation on the weathering of dilbit has receive minimal study and, therefore, the specific effects of photooxidation on dilbit are largely unknown. There has also been little study on the biodegradation of dilbit; however, it is known that hydrocarbons within dilbit can be degraded by bacteria.[89] The capacity to biodegrade dilbit was examined by the U.S. EPA following the Kalamazoo River spill.[90] Dilbit collected 19-20 months following the spill was incubated with sediments for 28 days, resulting in about 25% of hydrocarbons being degraded. However, most biodegradation occurred in the first half of the experiment followed by a decrease in biodegradation

rates, indicating that the majority of the dilbit would not be biodegraded for at least several months. More research is needed to fully understand biodegradation of dilbit in both aerobic and anaerobic environments.

To better understand the fate and behavior of dilbit in aquatic systems, several mesocosm studies have been carried out in both laboratory and outdoor settings. For example, an indoor tank study designed to simulate conditions similar to discharge into surface waters identified accelerated degradation and increased viscosity of Cold Lake Blend dilbit following UV light exposure.[91] To examine the behavior of dilbit spilled at sea, another study conducted 13 day weathering studies of Access Western Blend and Cold Lake Blend dilbit in outdoor flume tanks containing seawater.[86] As a result of weathering and evaporative losses, both dilbit blends increased in density, leading to sinking of Access Western Blend dilbit after seven days. Moreover, the density of Cold Lake Blend dilbit increased at a slower rate than that of Access Western Blend due to a higher proportion of alkylated PAHs which are more resistant to degradation; these results further suggest that geographical source of dilbit may cause variability in behavior in the environment. To study behavior of dilbit in low-energy freshwater systems, Stoyanovich et al. (2019) conducted eleven day experimental spills of Cold Lake Winter Blend in outdoor mesocosms containing lake water and sediments.[92] Density and viscosity of dilbit increased within the first 24 hours as a result of evaporation loss of volatile hydrocarbons, ultimately leading to submergence of dilbit after 8 days. Along with this, there was a rapid accumulation of PAHs into the water column following addition of dilbit, most notably small 2- and 3-ring phenanthrenes, dibenzothiophenes,

and fluorenes; these tricyclic PAHs have been shown to be cardiotoxic in fish,[93,94] suggesting dilbit spills may have adverse effects on fish health. While previous mesocosm studies have been critical in furthering understanding of dilbit's fate and behavior in aquatic systems, they do not account for interaction of oil with biotic components within the aquatic environment.

Aquatic Toxicity of Dilbit

The toxicity of conventional crude oil has been well characterized in fish. In early life stage fish, the toxicity of oil has been attributed to the water soluble fraction of oil, rather than physical contact with oil droplets.[95,96] Following the 1989 *Exxon Valdez* oil spill in Prince William Sound, Alaska, experimental studies reported high toxicity of petrogenic PAHs to fish embryos, with certain 3- and 4-ring PAHs being identified as the predominant drivers of oil toxicity.[97–99] For example, toxicity in pink salmon (*Oncorhynchus gorbuscha*) embryos was correlated with PAH uptake but was not correlated with other oil constituents such as alkanes and monoaromatic hydrocarbons.[97] While initial studies on monoaromatic hydrocarbons and unweathered oil showed toxic responses at mg/L concentrations, extensive research of weathered oil following the *Exxon Valdez* identified toxic responses in embryos at μg/L PAH concentrations. Further research suggested that weathering increases the toxicity of oil due to the evaporative loss of lower molecular weight compounds, leading to proportional increases in larger PAHs which have been shown to be more toxic and more bioaccumulative due to greater hydrophobicity.[100,101] Following the 2010 *Deepwater Horizon* oil spill, studies in mahi-

mahi (*Coryphaena hippurus*) and red drum (*Sciaenops ocellatus*) at various life stages also reported increases in toxicity of naturally weathered slick oil following ultraviolet (UV) exposure.[102–106] Thus, experimental studies following past major oil spills highlight the critical role environmental weathering processes play in oil toxicity.

Due to various structures of PAHs, there are multiple mechanisms of action for crude oil toxicity in fish. As tetracyclic PAHs are strong AhR agonists, compounds such as pyrene, chrysene, and benz[*a*]anthracene initiate toxicity by AhR-dependent transcriptional activation (Figure 1.5).[107] While the exact downstream effectors of AhR-mediated toxicity remain unclear, dioxin exposure induced cardiac malformations in developing zebrafish that were linked to AhR-mediated downregulation of transcription factors critical for normal heart development, forkhead box M1 and hairy/enhancer-of-split related YRPM motif 2.[108] Moreover, reduced cardiomyocyte proliferation in zebrafish was correlated to AhR-mediated downregulation of cell cycle and cell proliferation genes. Studies in zebrafish showed that benz[*a*]anthracene and benzo[*a*]pyrene induced AhR-mediated downregulation of genes involved in calcium homeostasis of the heart, such as genes encoding the ryanodine receptor and sarcoplasmic reticulum calcium (SERCA) pumps.[109,110] Unlike tetracyclic PAHs, tricyclic PAHs have been shown to induce toxicity through AhR-independent mechanisms (Figure 1.5).[111] In the AhR-independent mechanism, PAHs prolong action potentials in cardiomyocytes by blocking the delayed rectifier potassium current and inhibiting calcium cycling, resulting in impaired excitation-contraction coupling of the heart (Figure 1.5).[112]

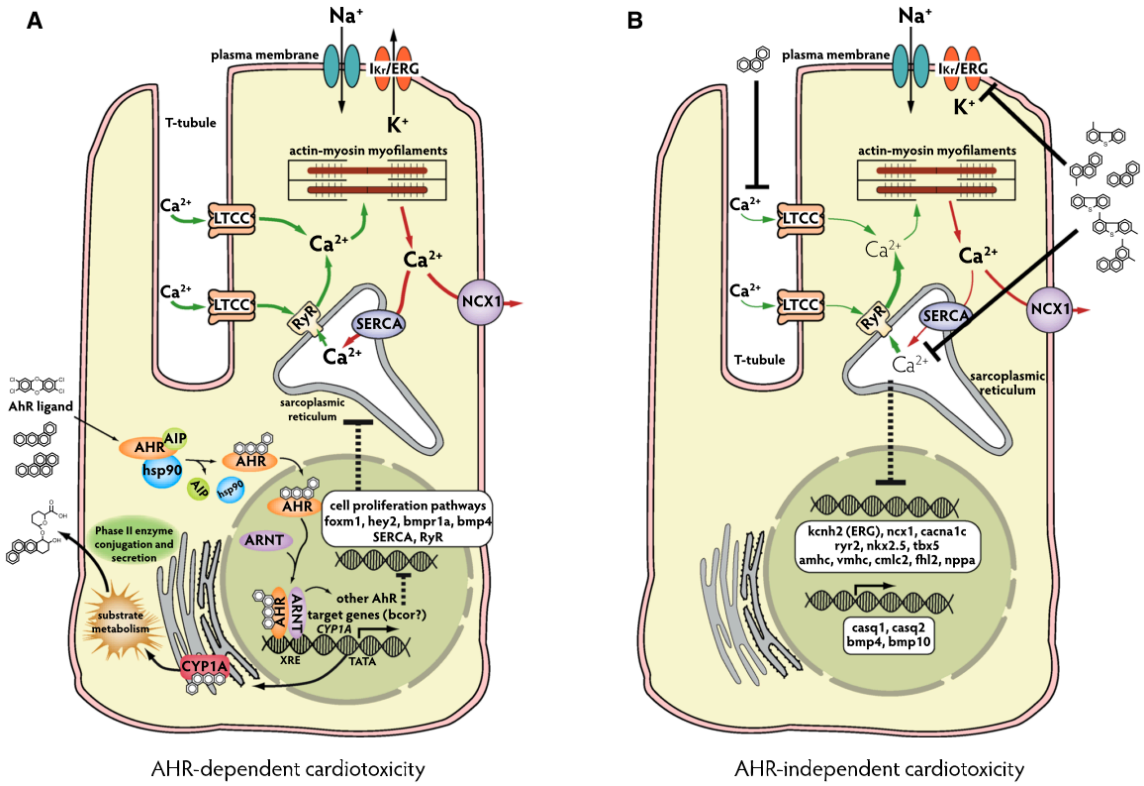

Figure 1.5. Diagrams depicting the modes of action for both aryl hydrocarbon receptor (AhR)-dependent and AhR-independent cardiotoxicity follow exposure to petrogenic polycyclic aromatic hydrocarbons (from Incardona, 2017).

The molecular effects of petrogenic PAHs are known to induce downstream cardiotoxicity in fish through both AhR-dependent and AhR-independent mechanisms.[67] Oil exposure during developmental stages has been shown to induce yolk-sac and pericardial edemas, defects in spinal curvature, craniofacial deformities, arrhythmias, reductions in contractility, decreased heart rates, and failed looping of the heart in several fish species.[113–119] Transcriptomic studies in larval mahi-mahi and red drum exposed to *Deepwater Horizon* oil later identified the eye as a potential target of oil toxicity, as suggested by gene expression changes associated with eye development and ocular

disease.[113,115] Supporting the observed gene expression changes, reductions in eye area of larval red drum were reported 48 h postfertilization at 4.74 µg/L ΣPAH.[113] Subsequent studies suggested that oil exposure may impair visual function in early-life stage fish, as exposure to weathered crude oil reduced optomotor response in embryonic red drum and sheepshead minnow (*Cyprinodon variegatus*) at 2.72 µg/L ΣPAH.[120] Overall, transcriptomic studies in larval mahi-mahi have demonstrated that the differential expression of mRNA and microRNA transcripts is linked to consequent morphological, physiological, and behavioral changes observed following exposure to *Deepwater Horizon* oil.[114,115] Thus, RNA sequencing studies following the *Deepwater Horizon* oil spill highlight the power that transcriptomics may have in identifying and predicting potential adverse outcomes at higher levels of biological organization.

In older life stage fish, impaired Ca^{2+} and K^{+} fluxes in cardiomyocyes following oil exposure can result in whole-heart effects such as cardiac arrhythmia, reduced cardiac contractility, reductions in stroke volume, and decreased cardiac output.[121–123] Ultimately, exposure to crude oil at either developmental or adult life stages may impact swim performance. For example, larval exposure to *Deepwater Horizon* crude oil resulted in decreased critical swimming velocities in juvenile mahi-mahi at 1.2 µg/L ΣPAH.[124] Moreover, acute exposure of adult mahi-mahi to *Deepwater Horizon* crude oil at 8.4 µg/L ΣPAH resulted in significant decreases in critical and optimal swimming speeds, maximum metabolic rate, and aerobic scope.[125] Thus, molecular effects of crude oil exposure at both developmental and adult life stages may have impacts on individual fitness and consequently on population success.

As the chemical composition of dilbit is similar to that of conventional crude oils, it is suspected that dilbit may induce cardiotoxic responses that have been well-characterized for crude oil exposure. Although experimental studies of dilbit toxicity have been minimal in fish, there is evidence for PAH-induced developmental and cardiac impairment following exposure to the water soluble fraction of dilbit. At the molecular level, exposure of several fish species to dilbit during development has shown to induce CYP1A activity and upregulation of *ahr*, potentially indicating AhR-mediated toxicity.[126–134] Oxidative stress has also been observed, as suggested by the upregulation of *hsp70*, *gsr*, *sod*, and *g6pdh* in Japanese medaka embryos exposed to water accommodated fractions (WAFs) and chemically-enhanced WAFs (CEWAF) of unweathered Access Western Blend dilbit for 17 days.[127] Moreover, developmental defects similar to those induced by conventional crude oil have been observed in fish following dilbit exposure, including increased prevalence of yolk sac and pericardial edema, craniofacial malformations, blue sac disease, and abnormal or uninflated swim bladders.[126,127,135,136]

Exposure of sockeye salmon parr (*Oncorhynchus nerka*) to water soluble fractions of dilbit (3.5 – 66.7 μg/L ΣPAH) resulted in concentration-dependent cardiac remodeling that correlated to reductions in swimming performance.[131] More specifically, individuals exposed at 66.7 μg/L ΣPAH showed relatively fewer myocytes and more collagen within the compact myocardium. Dilbit may also impede exercise recovery, as dilbit-exposed sockeye salmon experienced increased cellular damage following exercise as suggested by an increase in tissue leakage proteins, such as creatine kinase, in serum compared to

controls.[132] There is evidence that dilbit may also alter energetics within exposed fish. For example, early life stage exposures of Atlantic salmon (67.9 µg/L ΣPAH) and sockeye salmon (4 µg/L ΣPAH) to dilbit resulted in elevated triglyceride levels in the heart and whole-body, indicative of decreased lipid utilization for energy.[130,134] Dilbit may induce behavioral alterations, as was observed in a study where exposure to dilbit WAF (46.1 µg/L ΣPAH) altered shelter-seeking behavior in zebrafish embryos.[126] Overall, altered or impaired swim performance, energetics, and behavior may be detrimental to migratory success, predator avoidance, or impair the ability to capture prey, all of which may have adverse effects at the population-level.

Aside from direct toxicity, fish may be adversely affected by dilbit spills through impairments to the food web. Experiments in mescocosms containing water and sediment from an oligotrophic lake monitored the effects of dilbit additions to planktonic communities over 11 days.[137] Results of the study indicated that most phytoplankton and zooplankton species were sensitive to dilbit, as indicated by total abundance declines of over 70% following exposure. While nano- and microphytoplankton began to recover as dilbit sank, picoplankton and zooplankton abundances remained low throughout the exposure. As zooplankton are important food sources for organisms within multiple trophic levels, zooplankton abundance declines follow dilbit exposure may result in food web impairments.

Environmental stressors

Consideration of environmental variables is important in adequately assessing risk of environmental contaminants to organisms. Various environmental variables may potentiate the toxicity of a contaminant, and presence of both environmental stressors and contaminants may have additive or synergistic effects on exposed organisms. For example, exposure of PAHs to sunlight has shown to result in photoinduced toxicity, or increased toxicity in presence of certain wavelengths of light.[138,139] Photoinduced toxicity occurs when conjugated bonds of PAHs absorb UV radiation, exciting the compound into a triplet state.[139] The absorbed energy from the excited PAHs can transfer to dissolved oxygen, solvents, or biological molecules forming singlet-oxygen intermediaries and other oxygen free radicals.[140] The produced intermediaries and reactive species are highly oxidizing and can damage cellular constituents such as cell membranes, nucleic acids, or proteins.[139,140]

PAH photoinduced toxicity has shown increase mortality, reduce fecundity, and increase photoavoidance behavior in aquatic organisms.[141–144] Thus, organisms that remain near surface waters where they are likely to encounter UV light may be at increased risk following an oil spill. Following the *Deepwater Horizon* oil spill, significant amounts of research were conducted on PAH photoinduced toxicity to fish species such as mahi-mahi. Mahi-mahi are at risk to photoinduced toxicity as newly fertilized embryos remain buoyant in surface water and continue to remain in the upper water column following hatch.[145,146] In one study, coexposure to *Deepwater Horizon* oil and natural sunlight resulted in a significant reduction in hatching rates as well as a 5-fold

increase in toxicity in mahi-mahi embryos.[103] Moreover, coexposure with UV was shown to exacerbate sublethal cardiotoxic effects, as bradycardia was observed in mahi-mahi larvae coexposed to UV and oil at 4 and 17 μg/L ΣPAH, but was not observed in the no-UV counterpart exposures.[104] Overall, results from UV coexposure experiments indicate the importance of considering environmental parameters when assessing toxicity or risk of environmental contaminants.

Exposure to both environmental stressors and environmental contaminants may also produce additive or synergistic effects in aquatic organisms.[147] One significant environmental stressors that affects fish populations in both marine and freshwater environments is hypoxia, largely as a result of human acitivities.[148,149] Tolerance to hypoxia varies among species, life stage, and other variables, but is typically defined by the critical oxygen tension (P_{crit}), or the dissolved oxygen concentration at which a fish can no longer obtain adequate amounts of oxygen to maintain their metabolic rate.[150,151] Once dissolved oxygen levels fall below P_{crit}, fish transition to anaerobic metabolism; however, fish can only rely on anaerobic metabolism for a limited duration, ultimately resulting in mortality if the fish cannot find more oxygenated waters.[150,151] The effects of hypoxia can be exacerbated by environmental contaminants, such as oil. For example, common sole (*Solea solea*) exposed to oil for 5 days exhibited a 65% increase in P_{crit} due to reductions in active metabolic rate, suggesting that oil exposure may impair the ability of fish to tolerate hypoxic conditions.[152] Moreover, coexposure to hypoxic conditions and oil may have synergistic effects, as coexposure to hypoxia has shown to enhance toxicity of PAHs and oil in early life stage and juvenile fish.[153–156] For example, exposure to

hypoxic conditions significantly enhanced mortality in response to CEWAF prepared from Southern Louisiana Sweet Crude Oil in sheepshead minnow (*Cyprinodon variegatus*) larvae.[157] Thus, potential synergistic effects of hypoxia demonstrate the importance of considering environmental stressors in oil spill risk assessments.

Aside from their interaction with contaminants, environmental stressors alone may also contribute to perturbations observed in wild fish populations. One of the most notable and extensively researched environmental variable in relation to fish population health is water temperature. In marine fish populations, oceanographic and climatic variability have been correlated with recruitment success in various fish stocks around the world.[158–161] For example, in the North Atlantic, research has shown that the North Atlantic Oscillation Index has consistently been the most important parameter explaining abundance, growth, and assemblage composition of juvenile marine fish.[158] Moreover, increasing mean sea temperatures have been correlated to declines in recruitment, posing risk of collapse in these populations especially if warm conditions continue.[160]

As fish are ectothermic, they are especially vulnerable to temperature fluctuations as their metabolism is directly dependent on the environment.[162] Thus, increases in temperature result in increased rates of biochemical and cellular processes that are required for homeostasis as well as the energetic costs of activity, growth, and reproduction.[163,164] In order to balance increased metabolic demands, individuals may alter their behavior such as increasing food intake or reducing activity and movement patterns.[165,166] Moreover, at warmer temperatures, the maximum capacity for oxygen cannot keep up with the rate of increasing metabolic demands, which may impair vital

functions such as growth, swimming, feeding, and reproduction.[167–169] Impairments in these vital functions may ultimately result in population-level impacts.

Fish populations may cope with increased temperatures through genetic evolution or phenotypic plasticity.[167,170] Individuals may either undergo developmental acclimation which are permanent responses to the environment during early development, or reversible acclimation which are controlled in response to daily or seasonal fluctuations.[170] However, there modifications likely have energetic costs which may reduce the energy available for other vital functions, such as growth or reproduction.[171] Furthermore, research has shown that epigenetic inheritance may be involved in acclimation to warmer temperatures. In a study in common reef fish (*Acanthochromis polyacanthus*), genes involved in thermal acclimation (e.g. enhanced fatty acid oxidation and protein and carbohydrate metabolism) were upregulated in fish that were transgenerationally-exposed to warmer temperatures to help better cope with environmental conditions.[172] Aside from acclimation, fish populations may cope with increasing water temperatures by shifting their geographic distribution which has already been observed in several marine fisheries in the world.[173,174]

Another notable environmental stressor in both freshwater and marine ecosystems is acidification. In freshwater environments, deposition of acidic ions through precipitation into geologically-sensitive areas may result in acidification, or loss of acid-neutralizing capacity and decreases in pH.[175,176] Acidification of lakes has shown to be detrimental to ecosystems. In order to simulate the effects of acid precipitation on freshwater lakes, sulfuric acid was added to Lake 223 at the Experimental Lakes Area

over a three year period from 1976 to 1978.[177] Declines in pH resulted in the disappearance of *Mysis relicta* and fathead minnow as well as increases in embryonic mortality and deformities in resident lake trout in L223.[178–180] Furthermore, the collapse of lower trophic level species in the lake resulted in emaciation and decreased survival in lake trout. [181] Thus, acidification may ultimately result in population and ecosystem-level impairments.

Ocean acidification as a result of increased partial pressure of carbon dioxide (pCO_2) has also impacted marine fish populations. The increase in pCO_2 requires fish to increase energy expenditure on physiological adaptations, especially acid-base regulation and cardiorespiratory control.[182,183] For example, fish excrete excess H^+ ions in acidic conditions in order to restore normal bodily fluid pH levels, which requires additional energy expenditure.[184] Along with this, ventilatory frequency is increased at high pCO_2 levels, with research indicating that fish show little respiratory acclimation during long-term exposure to increased pCO_2.[185,186] Increased energy expenditure on physiological adaptations may thus divert energy from vital functions such as reproduction, growth, and predation. Neurosensory and behavioral alterations as a result of ocean acidification have also been extensively researched in fish.[187] Studies have identified impairment in olfaction, hearing, and vision in several fish species exposed to increased pCO_2.[188–191] In fact, these sensory disruptions have been linked to increased mortality in the field.[192,193] Moreover, impairment in sensory function may also affect predator-prey dynamics, habitat preference, recruitment, social interactions, and others, which all have the potential to impact both population and ecosystem dynamics.[187,194–198] Thus, both

warming water temperatures and acidification are important examples of how changes in environmental parameters may impact populations and ecosystems.

Non-lethal sampling methods to assess stressor effects

To prevent further disruption of wild populations, noninvasive sampling methods have become increasingly important for studying toxicological effects of environmental pollutants on aquatic organisms. While the liver has been a primary target for aquatic toxicology studies, lethal sampling is required for collection of this tissue and, thus, there is a need to identify a non-lethal alternative with similar sensitivity. For example, the use of caudal fin tissue has recently been studied for its potential to be used as a non-lethal, toxicogenomics-based assessment tool in fish. In a study exposing rainbow trout (*Oncorhynchus mykiss*) to either EE2 or cadmium for 96 hours, qPCR analysis identified estrogenic and metal-related transcript changes in caudal fin tissue that matched responses observed in the hepatic transcriptome.[199] In another study, qPCR analysis of caudal fin tissue from juvenile coho salmon (*Onchorhynchus kisutch*) exposed to low sulfur marine diesel identified gene expression changes associated with oil exposure, such as upregulation of *cyp1a*.[200] Transcriptomics of blood has also been shown to be an effective non-lethal method to assess effects of contaminant exposure on fish. Using an oligonucleotide microarray, transcriptomic changes within the whole blood and liver of fathead minnow were quantified following exposure to several types of PFAS.[201] Gene expression results from both blood and liver indicated transcriptional changes involved in cholesterol metabolism and mitochondrial function, including dysregulation of estrogen

receptor α and peroxisome proliferator activator β and γ. Aside from toxicogenomics-based assessments, nonlethal sampling of blood, tissue punches, and scales have been identified as useful tools for assessing contaminant loading in fish.[202–206]

Analysis of epidermal mucus is another promising route for development of noninvasive sampling methods in fish. Mucus is secreted from goblet cells on the skin and forms a protective layer over the epithelial cells. The roles of mucus have been extensively reviewed,[207] with critical functions including involvement in protection against pollutants and pathogens, ionic and osmotic regulation, respiration, and locomotion. Previous studies have explored the components of fish mucus, identifying the presence of proteins, RNA, DNA, lipids, and carbohydrates that could potentially be used as biomarkers.[208] In a genomic study of large yellow croaker (*Larimichthys crocea*), over 3,200 different proteins were found in epidermal mucus which accounted for over 12% of all protein-coding genes in the genome.[209] The immense number of proteins presents potential for screening of mucus for proteins or transcripts acting as biomarkers of exposure and effect. As epidermal mucus plays an important role in protecting fish from the external environment, many of the proteins identified in mucus are immune-related, including heat shock proteins, histone proteins, lectins, lysosome proteins, ribosomal proteins, complement proteins, among many others.[210,211] Studies have also identified presence of non-immune proteins that may be useful for ecotoxicology studies.

Several studies have investigated the use of fish epidermal mucus as a tool for exposure assessment following various stressors. One of the earliest studied ecotoxicological biomarkers in epidermal mucus was the vitellogenin protein.[212] In

various studies using Atlantic salmon, South American cichlid fish (*Cichlasoma dimerus*), and striped bass (*Morone saxatilis*), the presence of vitellogenin protein was detected in epidermal mucus following exposure to various estrogenic contaminants.[213–215] In another study, exposure of gilthead seabream (*Sparus aurata*) to heavy metals resulted in increased activity of enzymes related to immune responses.[216] Antioxidant responses have also been observed in mucus, such as increased activities of superoxide dismutase, catalase, and glutathione peroxidase in the mucus of oil-exposed dusky splitfin (*Goodea gracilis*).[217] Moreover, F_2-isprostanes have been identified in epidermal mucus which may be used to monitor oxidative stress.[218] Analysis of mucus has also been utilized in aquaculture-based experiments, where alterations in the composition and abundance of proteins were observed in fish epidermal mucus following food deprivation, overcrowding, and bacterial infection.[210,219–222]

There has been significantly less study on the identification of RNA in fish epidermal mucus and its potential to be used as a biomarker. In a study on channel catfish (*Ictalurus punctatus*), expression of immune-related genes in epidermal mucus was quantified through RT-qPCR following exposure to the bacterium *Flavobacterium columnare.*[223] All genes examined in the study were differentially expressed at at least one time point after exposure to the bacterium, indicating that gene expression can be quantified in epidermal mucus and that changes in environmental exposure alters the transcriptional profile in mucus. More recently, whole-transcriptome sequencing of mahi-mahi mucus was conducted following exposure to *Deepwater Horizon* slick oil at concentrations of 16.55 and 23.03 μg/L ΣPAH.[224] Results of sequencing showed

dysregulation of transcripts associated with cardiotoxicity and immunosuppression, which are common phenotypes observed in fish following oil exposure. Along with this, the well-established biomarkers of oil exposure, *cyp1a1* and *cyp1b1*, were the top differentially expressed transcripts in mucus of oil-exposed mahi-mahi. As responses in mucus paralleled common responses observed following oil exposure in previous studies, mucus is a promising source for noninvasive monitoring techniques. However, the efficacy of mucus for oil exposure assessment has yet to be tested in wild populations in the environment.

Hypotheses

Summary of Research Aims

The overarching goals of the present research were to use transcriptomic tools to assess the effects of stressors on wild aquatic populations and to develop nonlethal methods to assess gene expression changes in wild organisms (Figure 1.6). First, molecular- to population-level analyses were used to assess the potential contribution of estrogenic compounds to observed fish population declines by the Orange County Sanitation District (OCSD) wastewater outfall. Since population metrics correlated with water temperature fluctuations, it is likely that environmental conditions may alter ecosystem health. In addition, repeated lethal sampling of populations may also be a factor contributing to observed fish population declines at OCSD. Thus, using another well-controlled field setting of the Experimental Lakes Area, whole-transcriptome sequencing of epidermal mucus was explored as a potential non-lethal method to assess health of fish populations. In order to establish the ability of mucus to differentiate spatial and environmental differences in fish populations, RNA sequencing of mucus was first used to assess transcriptomic patterns in lake trout populations residing within different lakes with unique environmental conditions. Next, mucus was sequenced from lake trout that were exposed to dilbit in a whole-lake system to determine whether sequencing of mucus can be used for nonlethal exposure assessment to environmental contaminants. The hypotheses and specific aims of each chapter are described in more detail in the following pages.

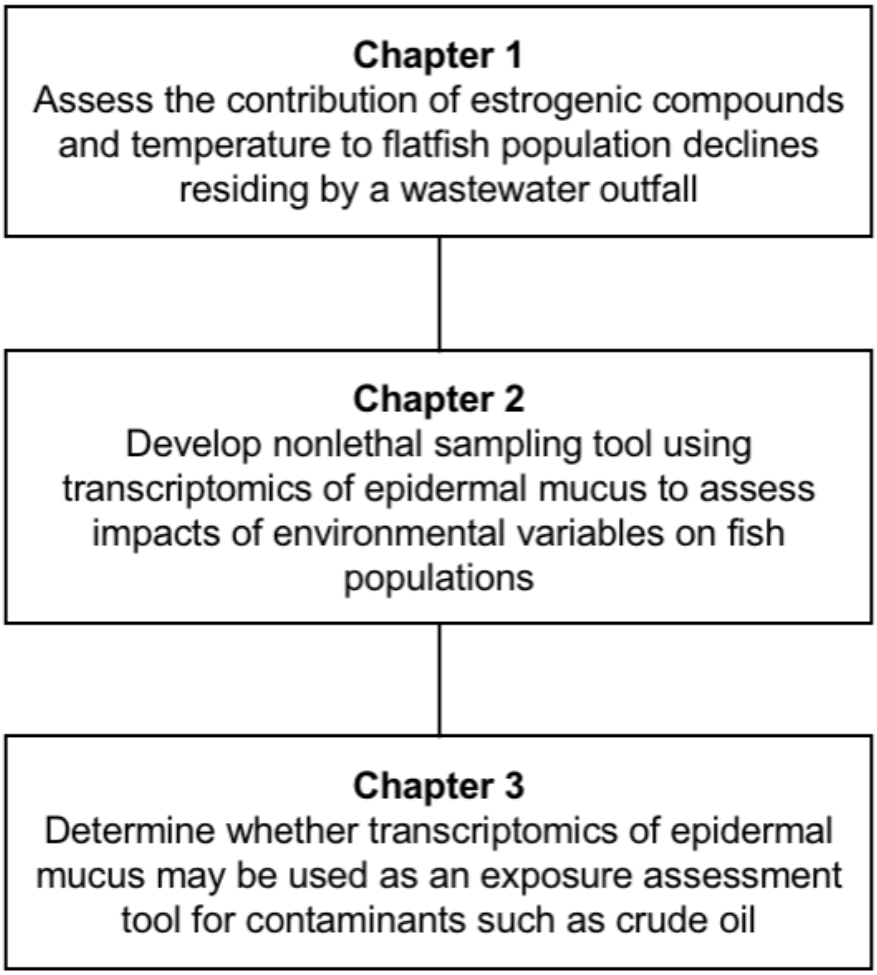

Figure 1.6. Schematic of dissertation workflow

Chapter 1: Examining the role of estrogenic activity and ocean temperature on declines of a coastal demersal flatfish population near the municipal wastewater outfall of Orange County, California, USA

In recent years, the demersal flatfish Pacific sanddab have been declining throughout the Orange County Sanitation District (OCSD) monitoring region. However, the environmental stressors that induced these population declines remain unknown. Previous studies at the OCSD outfall have identified estrogenic activity in flatfish residing at the outfall.[225–228] Along with this, inverse relationships between flatfish abundances and ocean temperature have been identified within the Southern California Bight.[229] Based on these previous studies, we hypothesize that Pacific sanddab declines may be linked to estrogenic activity stemming from the OCSD outfall or due to recent increases in ocean temperature. While RNA sequencing was planned to be used for this project, preliminary results did not indicate any perturbations in individuals and, therefore, did not signify the need for transcriptomic analysis. Therefore, the following aims were selected to address the previous hypotheses:

Aim 1: Quantify presence of estrogenic activity in Pacific sanddab collected at outfall and reference sites in the OCSD monitoring area.

Aim 2: Use statistical models to assess the relationship between historical Pacific sanddab abundances and ocean temperature as well as broader-scale climate patterns.

Aim 3: Develop an adverse outcome pathway to potentially explain population declines by quantifying endpoints at the molecular-, cellular-, organ-, individual-, population-, and community-level.

Having observed population declines, this study aims to identify stressors causing population-level perturbations in Pacific sanddab and potentially other species in the area. More specifically, the results of this research will assess the potential risks of estrogenic activity and rising ocean temperatures to marine wildlife and will help identify environmental stressors to target for future prevention and mitigation measures. Although there are many interacting environmental factors that may be affecting population abundances, this research will help narrow the focus of future research on the decline of Pacific sanddab in the OCSD monitoring region.

Chapter 2: Transcriptomics of epidermal mucus as a nonlethal method to evaluate effects of environmental variables among fish populations

Environmental variables may have direct impacts on ecosystem health, as temperature and broader-scale climate factors were shown to correlate with fish population abundances within the OCSD monitoring region. While studying the impacts of various environmental stressors on populations, the use of lethal sampling may further contribute to population perturbations. As a result, development of effective nonlethal sampling tools is warranted. Use of epidermal mucus may be a viable tool in fish, with previous studies showing dynamic regulation of proteins and transcripts following stress.[210,223,224] In order to determine the efficacy of mucus transcriptomics to identify molecular differences among populations, epidermal mucus was sequenced from four lake trout populations residing in different lakes at the Experimental Lakes Area. It is hypothesized that RNA sequencing of lake trout epidermal mucus will identify unique molecular differences that correlate with environmental variables among various populations. The previous hypothesis will be tested through the following specific aims:

Aim 1: Use RNA sequencing to identify gene expression changes in epidermal mucus among four lake trout populations.

Aim 2: Through statistical analysis of environmental variable data, identify potential factors driving transcriptomic similarities and differences among lake trout populations.

Through RNA sequencing of mucus samples collected from four lake trout populations, results of the present study will determine whether analysis of mucus is a viable nonlethal

tool for comparative population transcriptomics. If so, sequencing of mucus would be a useful tool for studying threatened or endangered fish populations without inducing further perturbations. Further research will be conducted to assess the use of mucus to identify molecular changes following exposure to environmental contaminants.

Chapter 3: RNA sequencing of lake trout epidermal mucus to assess molecular effects following exposure to diluted bitumen in a boreal lake

Diluted bitumen (dilbit) is exported from the Oil Sands region via extensive transcontinental pipeline networks, raising concern for potential leaks and spills into the environment along transportation routes. While dilbit production and export is projected to continue to increase into the future, research on the toxicity of dilbit has been minimal. Although previous laboratory studies have been critical in advancing our understanding of dilbit toxicity, they do not account for environmental parameters that may alter the chemical and physical composition of dilbit. In order to understand the biological effects of dilbit in the environment, dilbit spills were simulated within a boreal lake at the Experimental Lakes Area. Through the following specific aims, the present study will address the hypothesis that RNA sequencing of epidermal mucus may be used to assess toxicity and exposure of resident lake trout to dilbit:

> **Aim 1:** Use RNA sequencing of epidermal mucus to understand the molecular effects of dilbit exposure to lake trout in a whole-lake environment.
>
> **Aim 2:** Through transcriptomic analysis of epidermal mucus, determine whether biomarkers exist in mucus that may be used for nonlethal oil exposure assessment following an oil spill.

Results of the study will assess the molecular changes incurred in lake trout by dilbit exposure in the environment. As the exposures will account for chemical and physical changes in dilbit as well as ecological components, the results of the study will further our understanding of dilbit spill impacts in a real-world scenario. Furthermore,

transcriptomics of mucus will determine whether epidermal mucus is a viable tool for nonlethal exposure assessment following an oil spill.

References

(1) Waters, M. D.; Fostel, J. M. Toxicogenomics and Systems Toxicology: Aims and Prospects. *Nat. Rev. Genet.* **2004**, *5* (12), 936–948. https://doi.org/10.1038/nrg1493.

(2) Merrick, B. A.; Bruno, M. E. Genomic and Proteomic Profiling for Biomarkers and Signature Profiles of Toxicity. *Curr. Opin. Mol. Ther.* **2004**, *6* (6), 600–607.

(3) Ankley, G. T.; Daston, G. P.; Degitz, S. J.; Denslow, N. D.; Hoke, R. A.; Kennedy, S. W.; Miracle, A. L.; Perkins, E. J.; Snape, J.; Tillitt, D. E.; et al. Toxicogenomics in Regulatory Ecotoxicology. *Environ. Sci. Technol.* **2006**, *40* (13), 4055–4065. https://doi.org/10.1021/es0630184.

(4) Schirmer, K.; Fischer, B. B.; Madureira, D. J.; Pillai, S. Transcriptomics in Ecotoxicology. *Anal. Bioanal. Chem.* **2010**, *397* (3), 917–923. https://doi.org/10.1007/s00216-010-3662-3.

(5) National Research Council. *Toxicity Testing in the 21st Century*; The National Academies Pree: Washington, DC, 2007. https://doi.org/10.17226/11970.

(6) Ankley, G. T.; Bennett, R. S.; Erickson, R. J.; Hoff, D. J.; Hornung, M. W.; Johnson, R. D.; Mount, D. R.; Nichols, J. W.; Russom, C. L.; Schmieder, P. K.; et al. Adverse Outcome Pathways: A Conceptual Framework to Support Ecotoxicology Research and Risk Assessment. *Environ. Toxicol. Chem.* **2010**, *29* (3), 730–741. https://doi.org/10.1002/etc.34.

(7) Joseph, P. Transcriptomics in Toxicology. *Food Chem Toxicol* **2017**, *109* (1), 650–662. https://doi.org/10.1016/j.physbeh.2017.03.040.

(8) Eggen, R. I.; Behra, R.; Burkhardt-Holm, P.; Escher, B. I.; Schweigert, N. Challenges in Ecotoxicology. *Environ. Sci. Technol.* **2004**, *38* (3).

(9) Calzolai, L.; Ansorge, W.; Calabrese, E.; Denslow, N.; Part, P.; Lettieri, T. Transcriptomics and Proteomics. Applications to Ecotoxicology. *Comp. Biochem. Physiol. Part D* **2007**, *2*. https://doi.org/10.1016/j.cbd.2007.04.007.

(10) Kramer, V. J.; Etterson, M. A.; Hecker, M.; Murphy, C. A.; Roesijadi, G.; Spade, D. J.; Spromberg, J. A.; Wang, M.; Ankley, G. T. Adverse Outcome Pathways and Ecological Risk Assessment: Bridging to Population-Level Effects. *Environ. Toxicol. Chem.* **2011**, *30* (1), 64–76. https://doi.org/10.1002/etc.375.

(11) Hamadeh, H. K.; Bushel, P. R.; Jayadev, S.; Martin, K.; DiSorbo, O.; Sieber, S.; Bennett, L.; Tennant, R.; Stoll, R.; Barrett, J. C.; et al. Gene Expression Analysis

Reveals Chemical-Specific Profiles. *Toxicol. Sci.* **2002**, *67* (2), 219–231. https://doi.org/10.1093/toxsci/67.2.219.

(12) Tonk, E. C. M.; Piersma, A. H. Chapter 4.2 - Transcriptomic Approaches in In Vitro Developmental Toxicity Testing; Kleinjans, J. B. T.-T.-B. C. M., Ed.; Academic Press: San Diego, 2014; pp 143–157. https://doi.org/https://doi.org/10.1016/B978-0-12-397862-2.00008-5.

(13) Wang, L. CAS Reaches 150 Millionth Substance. *Chemical and Engineering News*. 2019.

(14) Hutchinson, T. H.; Lyons, B. P.; Thain, J. E.; Law, R. J. Evaluating Legacy Contaminants and Emerging Chemicals in Marine Environments Using Adverse Outcome Pathways and Biological Effects-Directed Analysis. *Mar. Pollut. Bull.* **2013**, *74* (2), 517–525. https://doi.org/https://doi.org/10.1016/j.marpolbul.2013.06.012.

(15) Petrović, M.; Gonzalez, S.; Barceló, D. Analysis and Removal of Emerging Contaminants in Wastewater and Drinking Water. *TrAC Trends Anal. Chem.* **2003**, *22* (10), 685–696. https://doi.org/https://doi.org/10.1016/S0165-9936(03)01105-1.

(16) Careghini, A.; Mastorgio, A. F.; Saponaro, S.; Sezenna, E. Bisphenol A, Nonylphenols, Benzophenones, and Benzotriazoles in Soils, Groundwater, Surface Water, Sediments, and Food: A Review. *Environ. Sci. Pollut. Res. Int.* **2015**, *22* (8), 5711–5741. https://doi.org/10.1007/s11356-014-3974-5.

(17) Benotti, M. J.; Trenholm, R. A.; Vanderford, B. J.; Holady, J. C.; Stanford, B. D.; Snyder, S. A. Pharmaceuticals and Endocrine Disrupting Compounds in U.S. Drinking Water. *Environ. Sci. Technol.* **2009**, *43* (3), 597–603. https://doi.org/10.1021/es801845a.

(18) Pal, A.; Gin, K. Y. H.; Lin, A. Y. C.; Reinhard, M. Impacts of Emerging Organic Contaminants on Freshwater Resources: Review of Recent Occurrences, Sources, Fate and Effects. *Sci. Total Environ.* **2010**, *408* (24), 6062–6069. https://doi.org/10.1016/j.scitotenv.2010.09.026.

(19) Bolong, N.; Ismail, A. F.; Salim, M. R.; Matsuura, T. A Review of the Effects of Emerging Contaminants in Wastewater and Options for Their Removal. *Desalination* **2009**, *239* (1–3), 229–246. https://doi.org/10.1016/j.desal.2008.03.020.

(20) Diamanti-Kandarakis, E.; Bourguignon, J.-P.; Giudice, L. C.; Hauser, R.; Prins, G. S.; Soto, A. M.; Zoeller, R. T.; Gore, A. C. Endocrine-Disrupting Chemicals: An Endocrine Society Scientific Statement. *Endocr. Rev.* **2009**, *30* (4), 293–342.

https://doi.org/10.1210/er.2009-0002.

(21) Gao, H.; Yang, B.-J.; Li, N.; Feng, L.-M.; Shi, X.-Y.; Zhao, W.-H.; Liu, S.-J. Bisphenol A and Hormone-Associated Cancers: Current Progress and Perspectives. *Medicine (Baltimore)*. **2015**, *94* (1), e211–e211. https://doi.org/10.1097/MD.0000000000000211.

(22) Blair, R. M.; Fang, H.; Branham, W. S.; Hass, B. S.; Dial, S. L.; Moland, C. L.; Tong, W.; Shi, L.; Perkins, R.; Sheehan, D. M. The Estrogen Receptor Relative Binding Affinities of 188 Natural and Xenochemicals: Structural Diversity of Ligands. *Toxicol. Sci.* **2000**, *54* (1), 138–153. https://doi.org/10.1093/toxsci/54.1.138.

(23) Tollefsen, K. E.; Mathisen, R.; Stenersen, J. Estrogen Mimics Bind with Similar Affinity and Specificity to the Hepatic Estrogen Receptor in Atlantic Salmon (Salmo Salar) and Rainbow Trout (Oncorhynchus Mykiss). *Gen. Comp. Endocrinol.* **2002**, *126* (1), 14–22. https://doi.org/10.1006/gcen.2001.7743.

(24) Kidd, K. A.; Blanchfield, P. J.; Mills, K. H.; Palace, V. P.; Evans, R. E.; Lazorchak, J. M.; Flick, R. W. Collapse of a Fish Population after Exposure to a Synthetic Estrogen. *Proc. Natl. Acad. Sci. U. S. A.* **2007**, *104* (21), 8897–8901. https://doi.org/10.1073/pnas.0609568104.

(25) Adeel, M.; Song, X.; Wang, Y.; Francis, D.; Yang, Y. Environmental Impact of Estrogens on Human, Animal and Plant Life: A Critical Review. *Environ. Int.* **2017**, *99*, 107–119. https://doi.org/10.1016/j.envint.2016.12.010.

(26) Jobling, S.; Reynolds, T.; White, R.; Parker, M. G.; Sumpter, J. P. A Variety of Environmentally Persistent Chemicals, Including Some Phthalate Plasticizers, Are Weakly Estrogenic. *Environ. Health Perspect.* **1995**, *103* (6), 582–587. https://doi.org/10.1289/ehp.95103582.

(27) Jobling, S.; Nolan, M.; Tyler, C. R.; Brighty, G.; Sumpter, J. P. Widespread Sexual Disruption in Wild Fish. *Environ. Sci. Technol.* **1998**, *32* (17), 2498–2506. https://doi.org/10.1021/es9710870.

(28) Purdom, C. E.; Hardiman, P. A.; Bye, V. J.; Eno, N. C.; Tyler, C. R.; Sumpter, J. P. Estrogenic Effects of Effluents from Sewage Treatment Works. *Chem. Ecol.* **1994**, *8* (4), 275–285. https://doi.org/10.1080/02757549408038554.

(29) Thorpe, K. L.; Cummings, R. I.; Hutchinson, T. H.; Scholze, M.; Brighty, G.; Sumpter, J. P.; Tyler, C. R. Relative Potencies and Combination Effects of Steroidal Estrogens in Fish. *Environ. Sci. Technol.* **2003**, *37* (6), 1142–1149. https://doi.org/10.1021/es0201348.

(30) Kolpin, D. W.; Furlong, E. T.; Meyer, M. T.; Thurman, E. M.; Zaugg, S. D.; Barber, L. B.; Buxton, H. T. Pharmaceuticals, Hormones, and Other Organic Wastewater Contaminants in U.S. Streams, 1999-2000: A National Reconnaissance. *Environ. Sci. Technol.* **2002**, *36* (6), 1202–1211. https://doi.org/10.1021/es011055j.

(31) Allen, Y.; Matthiessen, P.; Scott, A. P.; Haworth, S.; Feist, S.; Thain, J. E. The Extent of Oestrogenic Contamination in the UK Estuarine and Marine Environments - Further Surveys of Flounder. *Sci. Total Environ.* **1999**, *233* (1–3), 5–20. https://doi.org/10.1016/S0048-9697(99)00175-8.

(32) Ternes, T. A.; Stumpf, M.; Mueller, J.; Haberer, K.; Wilken, R. D.; Servos, M. Behavior and Occurrence of Estrogens in Municipal Sewage Treatment Plants - I. Investigations in Germany, Canada and Brazil. *Sci. Total Environ.* **1999**, *225* (1–2), 81–90. https://doi.org/10.1016/S0048-9697(98)00334-9.

(33) Ruhí, A.; Acuña, V.; Barceló, D.; Huerta, B.; Mor, J. R.; Rodríguez-Mozaz, S.; Sabater, S. Bioaccumulation and Trophic Magnification of Pharmaceuticals and Endocrine Disruptors in a Mediterranean River Food Web. *Sci. Total Environ.* **2016**, *540*, 250–259. https://doi.org/10.1016/j.scitotenv.2015.06.009.

(34) Oost, R. van der; Beyer, J.; Vermeulen, N. P. E. Fish Bioaccumulation and Biomarkers in Environmental Risk Assessment: A Review. *Environ. Toxicol. Pharmacol.* **2003**, *13* (February), 57–149.

(35) Heberer, T. Occurrence, Fate, and Removal of Pharmaceutical Residues in the Aquatic Environment: A Review of Recent Research Data. *Toxicol. Lett.* **2002**, *131*, 5–17. https://doi.org/10.1111/j.1439-0388.1936.tb00094.x.

(36) Kime, D. E.; Nash, J. P.; Scott, A. P. Vitellogenesis as a Biomarker of Reproductive Disruption by Xenobiotics. *Aquaculture* **1999**, *177* (1), 345–352. https://doi.org/https://doi.org/10.1016/S0044-8486(99)00097-6.

(37) Arukwe, A.; Celius, T.; Walther, B. T.; Goksøyr, A. Plasma Levels of Vitellogenin and Eggshell Zona Radiata Proteins in 4-Nonylphenol and O,p′-DDT Treated Juvenile Atlantic Salmon (Salmo Salar). *Mar. Environ. Res.* **1998**, *46* (1), 133–136. https://doi.org/https://doi.org/10.1016/S0141-1136(98)00002-6.

(38) Devlin, R. H.; Nagahama, Y. Sex Determination and Sex Differentiation in Fish: An Overview of Genetic, Physiological, and Environmental Influences. *Aquaculture* **2002**, *208* (3), 191–364. https://doi.org/https://doi.org/10.1016/S0044-8486(02)00057-1.

(39) Jobling, S.; Sheahan, D.; Osborne, J. A.; Matthiessen, P.; Sumpter, J. P. Inhibition of Testicular Growth in Rainbow Trout (Oncorhynchus Mykiss) Exposed to Estrogenic Alkylphenolic Chemicals. *Environ. Toxicol. Chem.* **1996**, *15* (2), 194–202. https://doi.org/10.1897/1551-5028(1996)015<0194:IOTGIR>2.3.CO;2.

(40) Wester, P. W.; Canton, J. H. Histopathological Study of Oryzias Latipes (Medaka) after Long-Term β-Hexachlorocyclohexane Exposure. *Aquat. Toxicol.* **1986**, *9* (1), 21–45. https://doi.org/https://doi.org/10.1016/0166-445X(86)90004-4.

(41) Gray, M. A.; Metcalfe, C. D. Induction of Testis-Ova in Japanese Medaka (Oryzias Latipes) Exposed to P-Nonylphenol. *Environ. Toxicol. Chem.* **1997**, *16* (5), 1082–1086. https://doi.org/10.1002/etc.5620160531.

(42) Panter, G. H.; Thompson, R. S.; Sumpter, J. P. Adverse Reproductive Effects in Male Fathead Minnows (Pimephales Promelas) Exposed to Environmentally Relevant Concentrations of the Natural Oestrogens, Oestradiol and Oestrone. *Aquat. Toxicol.* **1998**, *42* (4), 243–253. https://doi.org/10.1016/S0166-445X(98)00038-1.

(43) Tetreault, G. R.; Bennett, C. J.; Shires, K.; Knight, B.; Servos, M. R.; McMaster, M. E. Intersex and Reproductive Impairment of Wild Fish Exposed to Multiple Municipal Wastewater Discharges. *Aquat. Toxicol.* **2011**, *104* (3–4), 278–290. https://doi.org/10.1016/j.aquatox.2011.05.008.

(44) Colman, J. R.; Baldwin, D.; Johnson, L. L.; Scholz, N. L. Effects of the Synthetic Estrogen, 17α-Ethinylestradiol, on Aggression and Courtship Behavior in Male Zebrafish (Danio Rerio). *Aquat. Toxicol.* **2009**, *91* (4), 346–354. https://doi.org/10.1016/j.aquatox.2008.12.001.

(45) Saaristo, M.; Craft, J. A.; Lehtonen, K. K.; Lindström, K. An Endocrine Disrupting Chemical Changes Courtship and Parental Care in the Sand Goby. *Aquat. Toxicol.* **2010**, *97* (4), 285–292. https://doi.org/10.1016/j.aquatox.2009.12.015.

(46) Brian, J. V; Harris, C. A.; Scholze, M.; Kortenkamp, A.; Booy, P.; Lamoree, M.; Pojana, G.; Jonkers, N.; Marcomini, A.; Sumpter, J. P. Evidence of Estrogenic Mixture Effects on the Reproductive Performance of Fish. *Environ. Sci. Technol.* **2007**, *41* (1), 337–344. https://doi.org/10.1021/es0617439.

(47) Palace, V. P.; Evans, R. E.; Wautier, K. G.; Mills, K. H.; Blanchfield, P. J.; Park, B. J.; Baron, C. L.; Kidd, K. A. Interspecies Differences in Biochemical, Histopathological, and Population Responses in Four Wild Fish Species Exposed to Ethynylestradiol Added to a Whole Lake. *Can. J. Fish. Aquat. Sci.* **2009**, *66* (11), 1920–1935. https://doi.org/10.1139/F09-125.

(48) Jones, K. C.; de Voogt, P. Persistent Organic Pollutants (POPs): State of the Science. *Environ. Pollut.* **1999**, *100* (1), 209–221. https://doi.org/https://doi.org/10.1016/S0269-7491(99)00098-6.

(49) U.S. Environmental Protection Agency. Persistent Organic Pollutants: A Global Issue, A Global Response https://www.epa.gov/international-cooperation/persistent-organic-pollutants-global-issue-global-response.

(50) Johnson, L. L.; Anulacion, B. F.; Arkoosh, M. R.; Burrows, D. G.; da Silva, D. A. M.; Dietrich, J. P.; Myers, M. S.; Spromberg, J.; Ylitalo, G. M. 2 - Effects of Legacy Persistent Organic Pollutants (POPs) in Fish—Current and Future Challenges. In *Organic Chemical Toxicology of Fishes*; Tierney, K. B., Farrell, A. P., Brauner, C. J. B. T.-F. P., Eds.; Academic Press, 2013; Vol. 33, pp 53–140. https://doi.org/https://doi.org/10.1016/B978-0-12-398254-4.00002-9.

(51) Jayaraj, R.; Megha, P.; Sreedev, P. Organochlorine Pesticides, Their Toxic Effects on Living Organisms and Their Fate in the Environment. *Interdiscip. Toxicol.* **2016**, *9* (3–4), 90–100. https://doi.org/10.1515/intox-2016-0012.

(52) de Voogt, P.; Brinkman, U. A. T. Production, Preoperties, and Usage of Polychlorinated Biphenyls. In *Halogenated biphenyls, terphenyls, napthalenes, dibenzodioxins and related products*; Kimbrough, R. D., Jensen, A. A., Eds.; Elsevier: Amsterdam, 1989; pp 3–45.

(53) Breivik, K.; Alcock, R.; Li, Y.-F.; Bailey, R. E.; Fiedler, H.; Pacyna, J. M. Primary Sources of Selected POPs: Regional and Global Scale Emission Inventories. *Environ. Pollut.* **2004**, *128* (1), 3–16. https://doi.org/https://doi.org/10.1016/j.envpol.2003.08.031.

(54) U.S. Environmental Protection Agency. *An Inventory of Sources and Environmental Releases of Dioxinlike Compounds in the United States for the Years 1987, 1995, and 2000*; Washington, DC, 2006.

(55) Fiedler, H. Sources of PCDD/PCDF and Impact on the Environment. *Chemosphere* **1996**, *32* (1), 55–64. https://doi.org/https://doi.org/10.1016/0045-6535(95)00228-6.

(56) Colborn, T.; vom Saal, F. S.; Soto, A. M. Developmental Effects of Endocrine-Disrupting Chemicals in Wildlife and Humans. *Environ. Health Perspect.* **1993**, *101* (5), 378–384. https://doi.org/10.1289/ehp.93101378.

(57) Safe, S. Polychlorinated Biphenyls (PCBs), Dibenzo-P-Dioxins (PCDDs), Dibenzofurans (PCDFs), and Related Compounds: Environmental and Mechanistic Considerations Which Support the Development of Toxic

Equivalency Factors (TEFs). *Crit. Rev. Toxicol.* **1990**, *21* (1), 51–88. https://doi.org/10.3109/10408449009089873.

(58) Safe, S. H. Polychlorinated Biphenyls (PCBs): Environmental Impact, Biochemical and Toxic Responses, and Implications for Risk Assessment. *Crit. Rev. Toxicol.* **1994**, *24* (2), 87–149. https://doi.org/10.3109/10408449409049308.

(59) Tillitt, D. E.; Cook, P. M.; Giesy, J. P.; Heideman, W.; Peterson, R. E. Reproductive Impairment of Great Lakes Lake Trout by Dioxin-Like Chemicals. In *The Toxicology of Fishes*; Di Giulio, R. T., Hinton, D. E., Eds.; Taylor & Francis Group, LLC: Boca Raton, FL, 2008; pp 819–875.

(60) Walker, M. K.; Spitsbergen, J. M.; Olson, J. R.; Peterson, R. E. 2,3,7,8-Tetrachlorodibenzo-P-Dioxin (TCDD) Toxicity during Early Life Stage Development of Lake Trout (Salvelinus Namaycush). *Can. J. Fish. Aquat. Sci.* **1991**, *48* (5), 875–883. https://doi.org/10.1139/f91-104.

(61) Tanguay, R. L.; Andreasen, E.; Walker, M. K.; Peterson, R. E. Dioxin Toxicity and Aryl Hydrocarbon Receptor Signaling in Fish. In *Dioxins and Health*; Schecter, A., Gasiewicz, T. A., Eds.; John Wiley & Sons: New Jersey, 2003; pp 603–628.

(62) King-Heiden, T. C.; Mehta, V.; Xiong, K. M.; Lanham, K. A.; Antkiewicz, D. S.; Ganser, A.; Heideman, W.; Peterson, R. E. Reproductive and Developmental Toxicity of Dioxin in Fish. *Mol. Cell. Endocrinol.* **2012**, *354* (1–2), 121–138. https://doi.org/10.1016/j.mce.2011.09.027.

(63) Volz, D. C.; Hinton, D. E.; Law, J. M.; Kullman, S. W. Dynamic Gene Expression Changes Precede Dioxin-Induced Liver Pathogenesis in Medaka Fish. *Toxicol. Sci.* **2006**, *89* (2), 524–534. https://doi.org/10.1093/toxsci/kfj033.

(64) Howsam, M.; Jones, K. C. Sources of PAHs in the Environment BT - PAHs and Related Compounds: Chemistry; Neilson, A. H., Ed.; Springer Berlin Heidelberg: Berlin, Heidelberg, 1998; pp 137–174. https://doi.org/10.1007/978-3-540-49697-7_4.

(65) Latimer, J. S.; Zheng, J. The Sources, Transport, and Fate of PAHs in the Marine Environment. In *PAHs: An Ecotoxicological Perspective*; Douben, P. E. T., Ed.; John Wiley & Sons, 2003; pp 9–33.

(66) Eganhouse, R. P.; Gossett, R. W. Historical Deposition and Biogeochemical Fate of Polycyclic Aromatic Hydrocarbons in Sediments near a Major Submarine Wastewater Outfall in Southern California. In *Organic substances and sediment in water*; Baker, R. A., Ed.; Lewis Publishers: Boca Raton, FL, 1991; pp 191–220.

(67) Incardona, J. P. Molecular Mechanisms of Crude Oil Developmental Toxicity in Fish. *Arch. Environ. Contam. Toxicol.* **2017**, *73* (1), 19–32. https://doi.org/10.1007/s00244-017-0381-1.

(68) Blanchard, M.; Teil, M.-J.; Ollivon, D.; Garban, B.; Chestérikoff, C.; Chevreuil, M. Origin and Distribution of Polyaromatic Hydrocarbons and Polychlorobiphenyls in Urban Effluents to Wastewater Treatment Plants of the Paris Area (FRANCE). *Water Res.* **2001**, *35* (15), 3679–3687. https://doi.org/https://doi.org/10.1016/S0043-1354(01)00078-1.

(69) Blanchard, M.; Teil, M. J.; Ollivon, D.; Legenti, L.; Chevreuil, M. Polycyclic Aromatic Hydrocarbons and Polychlorobiphenyls in Wastewaters and Sewage Sludges from the Paris Area (France). *Environ. Res.* **2004**, *95* (2), 184–197. https://doi.org/https://doi.org/10.1016/j.envres.2003.07.003.

(70) Byrns, G. The Fate of Xenobiotic Organic Compounds in Wastewater Treatment Plants. *Water Res.* **2001**, *35* (10), 2523–2533. https://doi.org/https://doi.org/10.1016/S0043-1354(00)00529-7.

(71) Morris, S.; Lester, J. N. Behaviour and Fate of Polychlorinated Biphenyls in a Pilot Wastewater Treatment Plant. *Water Res.* **1994**, *28* (7), 1553–1561. https://doi.org/https://doi.org/10.1016/0043-1354(94)90222-4.

(72) Hannah, S. A.; Austern, B. M.; Eralp, A. E.; Wise, R. H. Comparative Removal of Toxic Pollutants by Six Wastewater Treatment Processes. *J. (Water Pollut. Control Fed.* **1986**, *58* (1), 27–34.

(73) Saleh, F. Y.; Lee, G. F.; Wolf, H. W. Selected Organic Pesticides, Occurrence, Transformation, and Removal from Domestic Wastewater. *J. (Water Pollut. Control Fed.* **1980**, *52* (1), 19–28.

(74) Petrasek, A. C.; Kugelman, I. J.; Austern, B. M.; Pressley, T. A.; Winslow, L. A.; Wise, R. H. Fate of Toxic Organic Compounds in Wastewater Treatment Plants. *J. (Water Pollut. Control Fed.* **1983**, *55* (10), 1286–1296.

(75) Pham, T.-T.; Proulx, S. PCBs and PAHs in the Montreal Urban Community (Quebec, Canada) Wastewater Treatment Plant and in the Effluent Plume in the St Lawrence River. *Water Res.* **1997**, *31* (8), 1887–1896. https://doi.org/https://doi.org/10.1016/S0043-1354(97)00025-0.

(76) Crosby, S.; Fay, R.; Groark, C.; Kani, A.; Smith, J.; Sullivan, T. Transporting Alberta's Oil Sands Products: Defining the Issues and Assessing the Risks. *NOAA Tech. Memo. NOS OR&R 44* **2013**, No. September, 153.

(77) Adams, J.; Larter, S.; Bennett, B.; Huang, H.; Westrich, J.; Larter, S.; Bennett, B.; Huang, H.; Westrich, J.; E, S. I.; et al. *The Dynamic Interplay of Oil Mixing, Charge Timing, and Biodegradation in Forming the Alberta Oil Sands: Insights from Geologic Modeling and Biogeochemistry*; 2013. https://doi.org/10.1306/13371578St643552.

(78) King, T.; Mason, J.; Thamer, P.; Wohlgeschaffen, G.; Lee, K.; Clyburne, J. A. C. Composition of Bitumen Blends Relevant to Ecological Impacts and Spill Response. *40th AMOP Tech. Semin. Environ. Contam. Response* **2017**, No. November 2018.

(79) National Academies of Sciences Medicine and Engineering. *Spills of Diluted Bitumen from Pipelines: A Comparative Study of Environmental Fate, Effects, and Response*; The National Academies Press: Washington, DC, 2016. https://doi.org/10.17226/21834.

(80) Canada National Energy Board. *Canada's Oil Sands Opportunities and Challenges To 2015: An Update*; 2006.

(81) Dupuis, A.; Ucan-Marin, F. A Literature Review on the Aquatic Toxicology of Petroleum Oil: An Overview of Oil Properties and Effects to Aquatic Biota. *DFO Can. Sci. Advis. Secr. Res. Doc.* **2015**, *2015/007* (April), 51.

(82) United States Environmental Protection Agency. *Oil Cleanup Continues on Kalamazoo River*; 2013.

(83) Enbridge Energy Partners L.P. *Form 10-Q 2014*; 2014.

(84) National Research Council. *Oil in the Sea III: Inputs, Fates, and Effects*; The National Academies Press: Washington, DC, 2003.

(85) Hollebone, B. The Oil Properties Data Appendix. In *Handbook of Oil Spill Science and Technology*; Fingas, M., Ed.; John Wiley & Sons: NY, 2015; pp 577–681.

(86) King, T. L.; Robinson, B.; Boufadel, M.; Lee, K. Flume Tank Studies to Elucidate the Fate and Behavior of Diluted Bitumen Spilled at Sea. *Mar. Pollut. Bull.* **2014**, *83* (1). https://doi.org/10.1016/j.marpolbul.2014.04.042.

(87) Aeppli, C.; Carmichael, C. A.; Nelson, R. K.; Lemkau, K. L.; Graham, W. M.; Redmond, M. C.; Valentine, D. L.; Reddy, C. M. Oil Weathering after the Deepwater Horizon Disaster Led to the Formation of Oxygenated Residues. *Environ. Sci. Technol.* **2012**, *46* (16), 8799–8807. https://doi.org/10.1021/es3015138.

(88) Prince, R. C.; Garrett, R. M.; Bare, R. E.; Grossman, M. J.; Townsend, T.; Suflita, J. M.; Lee, K.; Owens, E. H.; Sergy, G. A.; Braddock, J. F.; et al. The Roles of Photooxidation and Biodegradation in Long-Term Weathering of Crude and Heavy Fuel Oils. *Spill Sci. Technol. Bull.* **2003**, *8* (2), 145–156. https://doi.org/https://doi.org/10.1016/S1353-2561(03)00017-3.

(89) Prince, R. C. Petroleum Spill Bioremediation in Marine Environments. *Crit. Rev. Microbiol.* **1993**, *19* (4), 217–240. https://doi.org/10.3109/10408419309113530.

(90) United States Environmental Protection Agency. *Environmental Response Team's Final Bench Scale/ Screening Level Oil Biodegradation Study: Report Number 1597*; 2013.

(91) SL Ross Environmental Research. *Meso-Scale Weathering of Cold Lake Blend Bitumen*; 2012.

(92) Stoyanovich, S. S.; Yang, Z.; Hanson, M.; Hollebone, B. P.; Orihel, D. M.; Palace, V.; Rodriguez-Gil, J. L.; Faragher, R.; Mirnaghi, F. S.; Shah, K.; et al. Simulating a Spill of Diluted Bitumen: Environmental Weathering and Submergence in a Model Freshwater System. *Environ. Toxicol. Chem.* **2019**, *38* (12), 2621–2628. https://doi.org/10.1002/etc.4600.

(93) Incardona, J. P.; Collier, T. K.; Scholz, N. L. Defects in Cardiac Function Precede Morphological Abnormalities in Fish Embryos Exposed to Polycyclic Aromatic Hydrocarbons. *Toxicol. Appl. Pharmacol.* **2004**, *196* (2), 191–205. https://doi.org/https://doi.org/10.1016/j.taap.2003.11.026.

(94) Incardona, J. P.; Carls, M. G.; Teraoka, H.; Sloan, C. A.; Tracy, K.; Scholz, N. L. Aryl Hydrocarbon Receptor-Independent Toxicity of Weathered Crude Oil during Fish Development Published by : The National Institute of Environmental Health Sciences Linked References Are Available on JSTOR for This Article : Aryl Hydroc. *Environ. Health Perspect.* **2005**, *113* (12), 1755–1762.

(95) Carls, M. G.; Holland, L.; Larsen, M.; Collier, T. K.; Scholz, N. L.; Incardona, J. P. Fish Embryos Are Damaged by Dissolved PAHs, Not Oil Particles. *Aquat. Toxicol.* **2008**, *88* (2), 121–127. https://doi.org/10.1016/j.aquatox.2008.03.014.

(96) Carls, M. G.; Meador, J. P. A Perspective on the Toxicity of Petrogenic Pahs to Developing Fish Embryos Related to Environmental Chemistry. *Hum. Ecol. Risk Assess.* **2009**, *15* (6), 1084–1098. https://doi.org/10.1080/10807030903304708.

(97) Marty, G. D.; Hinton, D. E.; Short, J. W.; Heintz, R. A.; Rice, S. D.; Dambach, D. M.; Willits, N. H.; Stegeman, J. J. Ascites, Premature Emergence, Increased

Gonadal Cell Apoptosis, and Cytochrome P4501A Induction in Pink Salmon Larvae Continuously Exposed to Oil-Contaminated Gravel during Development. *Can. J. Zool.* **1997**, *75* (6), 989–1007.

(98) Carls, M. G.; Rice, S. D.; Hose, J. E. Sensitivity of Fish Embryos to Weathered Crude Oil: Part I. Low-Level Exposure during Incubation Causes Malformations, Genetic Damage, and Mortality in Larval Pacific Herring (Clupea Pallasi). *Environ. Toxicol. Chem.* **1999**, *18* (3), 481–493. https://doi.org/10.1002/etc.5620180317.

(99) Peterson, C. H.; Rice, S. D.; Short, J. W.; Esler, D.; Bodkin, J. L.; Ballachey, B. E.; Irons, D. B. Long-Term Ecosystem Response to the Exxon Valdez Oil Spill. *Science (80-.).* **2003**, *302* (5653), 2082–2086. https://doi.org/10.1126/science.1084282.

(100) Neff, J. M. *Bioaccumulation in Marine Organisms. Effect of Contaminants from Oil Well Produced Water*; Els: Boston, 2002. https://doi.org/10.1016/s0146-6380(02)00213-9.

(101) Carls, M. G.; Holland, L. G.; Short, J. W.; Heintz, R. A.; Rice, S. D. Monitoring Polynuclear Aromatic Hydrocarbons in Aqueous Environments with Passive Low-Density Polyethylene Membrane Devices. *Environ. Toxicol. Chem.* **2004**, *23* (6), 1416–1424. https://doi.org/10.1897/03-395.

(102) Alloy, M.; Garner, T. R.; Bridges, K.; Mansfield, C.; Carney, M.; Forth, H.; Krasnec, M.; Lay, C.; Takeshita, R.; Morris, J.; et al. Co-Exposure to Sunlight Enhances the Toxicity of Naturally Weathered Deepwater Horizon Oil to Early Lifestage Red Drum (Sciaenops Ocellatus) and Speckled Seatrout (Cynoscion Nebulosus). *Environ. Toxicol. Chem.* **2017**, *36* (3), 780–785. https://doi.org/10.1002/etc.3640.

(103) Alloy, M.; Baxter, D.; Stieglitz, J.; Mager, E.; Hoenig, R.; Benetti, D.; Grosell, M.; Oris, J.; Roberts, A. Ultraviolet Radiation Enhances the Toxicity of Deepwater Horizon Oil to Mahi-Mahi (Coryphaena Hippurus) Embryos. *Environ. Sci. Technol.* **2016**, *50* (4), 2011–2017. https://doi.org/10.1021/acs.est.5b05356.

(104) Sweet, L. E.; Magnuson, J.; Garner, T. R.; Alloy, M. M.; Stieglitz, J. D.; Benetti, D.; Grosell, M.; Roberts, A. P. Exposure to Ultraviolet Radiation Late in Development Increases the Toxicity of Oil to Mahi-Mahi (Coryphaena Hippurus) Embryos. *Environ. Toxicol. Chem.* **2017**, *36* (6), 1592–1598. https://doi.org/10.1002/etc.3687.

(105) Bridges, K. N.; Krasnec, M. O.; Magnuson, J. T.; Morris, J. M.; Gielazyn, M. L.; Chavez, J. R.; Roberts, A. P. Influence of Variable Ultraviolet Radiation and Oil

Exposure Duration on Survival of Red Drum (Sciaenops Ocellatus) Larvae. *Environ. Toxicol. Chem.* **2018**, *37* (9), 2372–2379. https://doi.org/10.1002/etc.4183.

(106) Esbaugh, A. J.; Mager, E. M.; Stieglitz, J. D.; Hoenig, R.; Brown, T. L.; French, B. L.; Linbo, T. L.; Lay, C.; Forth, H.; Scholz, N. L.; et al. The Effects of Weathering and Chemical Dispersion on Deepwater Horizon Crude Oil Toxicity to Mahi-Mahi (Coryphaena Hippurus) Early Life Stages. *Sci. Total Environ.* **2016**, *543*, 644–651. https://doi.org/https://doi.org/10.1016/j.scitotenv.2015.11.068.

(107) Incardona, J. P.; Day, H. L.; Collier, T. K.; Scholz, N. L. Developmental Toxicity of 4-Ring Polycyclic Aromatic Hydrocarbons in Zebrafish Is Differentially Dependent on AH Receptor Isoforms and Hepatic Cytochrome P4501A Metabolism. *Toxicol. Appl. Pharmacol.* **2006**, *217* (3), 308–321. https://doi.org/https://doi.org/10.1016/j.taap.2006.09.018.

(108) Carney, S. A.; Chen, J.; Burns, C. G.; Xiong, K. M.; Peterson, R. E.; Heideman, W. Aryl Hydrocarbon Receptor Activation Produces Heart-Specific Transcriptional and Toxic Responses in Developing Zebrafish. *Mol. Pharmacol.* **2006**, *70* (2), 549 LP-561. https://doi.org/10.1124/mol.106.025304.

(109) Fang, X.; Corrales, J.; Thornton, C.; Clerk, T.; Scheffler, B. E.; Willett, K. L. Transcriptomic Changes in Zebrafish Embryos and Larvae Following Benzo[a]pyrene Exposure. *Toxicol. Sci.* **2015**, *146* (2), 395–411. https://doi.org/10.1093/toxsci/kfv105.

(110) Jayasundara, N.; Van Tiem Garner, L.; Meyer, J. N.; Erwin, K. N.; Di Giulio, R. T. AHR2-Mediated Transcriptomic Responses Underlying the Synergistic Cardiac Developmental Toxicity of PAHs. *Toxicol. Sci.* **2015**, *143* (2), 469–481. https://doi.org/10.1093/toxsci/kfu245.

(111) Incardona, J. P.; Scholz, N. L. The Influence of Heart Developmental Anatomy on Cardiotoxicity-Based Adverse Outcome Pathways in Fish. *Aquat. Toxicol.* **2016**, *177*, 515–525. https://doi.org/10.1016/j.aquatox.2016.06.016.

(112) Brette, F.; Machado, B.; Cros, C.; Incardona, J.; Scholz, N. L.; Block, B. A. Crude Oil Impairs Cardiac Excitation-Contraction Coupling in Fish. *Science (80-.).* **2014**, *343*, 772–776. https://doi.org/10.1126/science.1248286.

(113) Xu, E. G.; Khursigara, A. J.; Magnuson, J.; Starr, E.; Hardiman, G.; Esbaugh, A. J.; Roberts, A. P.; Schlenk, D. Larval Red Drum (Sciaenops Ocellatus) Sublethal Exposure to Weathered Deepwater Horizon Crude Oil: Developmental and Transcriptomic Consequences. **2017**. https://doi.org/10.1021/acs.est.7b02037.

(114) Xu, E. G.; Magnuson, J. T.; Diamante, G.; Mager, E.; Pasparakis, C.; Grosell, M.; Roberts, A. P.; Schlenk, D. Changes in microRNA-mRNA Signatures Agree with Morphological, Physiological, and Behavioral Changes in Larval Mahi-Mahi Treated with Deepwater Horizon Oil. *Environ. Sci. Technol.* **2018**, *52* (22), 13501–13510. https://doi.org/10.1021/acs.est.8b04169.

(115) Xu, E. G.; Mager, E. M.; Grosell, M.; Pasparakis, C.; Schlenker, L. S.; Stieglitz, J. D.; Benetti, D.; Starr, E.; Courtney, S. M.; Diamante, G.; et al. Time-and Oil-Dependent Transcriptomic and Physiological Responses to Deepwater Horizon Oil in Mahi-Mahi (Coryphaena Hippurus) Embryos and Larvae. **2016**. https://doi.org/10.1021/acs.est.6b02205.

(116) Incardona, J. P.; Carls, M. G.; Holland, L.; Linbo, T. L.; Baldwin, D. H.; Myers, M. S.; Peck, K. A.; Tagal, M.; Rice, S. D.; Scholz, N. L. Very Low Embryonic Crude Oil Exposures Cause Lasting Cardiac Defects in Salmon and Herring. *Nat. Publ. Gr.* **2015**. https://doi.org/10.1038/srep13499.

(117) Incardona, J. P.; Collier, T. K.; Scholz, N. L. Defects in Cardiac Function Precede Morphological Abnormalities in Fish Embryos Exposed to Polycyclic Aromatic Hydrocarbons. *Toxicol. Appl. Pharmacol.* **2004**, *196*, 191–205. https://doi.org/10.1016/j.taap.2003.11.026.

(118) Incardona, J. P.; Carls, M. G.; Day, H. L.; Sloan, C. A.; Bolton, J. L.; Collier, T. K.; Scholz, N. L. Cardiac Arrhythmia Is the Primary Response of Embryonic Pacific Herring (Clupea Pallasi) Exposed to Crude Oil during Weathering. *Environ. Sci. Technol.* **2009**, *43* (1), 201–207. https://doi.org/10.1021/es802270t.

(119) Sørhus, E.; Incardona, J. P.; Karlsen, Ø.; Linbo, T.; Sørensen, L.; Nordtug, T.; van der Meeren, T.; Thorsen, A.; Thorbjørnsen, M.; Jentoft, S.; et al. Crude Oil Exposures Reveal Roles for Intracellular Calcium Cycling in Haddock Craniofacial and Cardiac Development. *Sci. Rep.* **2016**, *6* (1), 31058. https://doi.org/10.1038/srep31058.

(120) Magnuson, J. T.; Khursigara, A. J.; Allmon, E. B.; Esbaugh, A. J.; Roberts, A. P. Effects of Deepwater Horizon Crude Oil on Ocular Development in Two Estuarine Fish Species, Red Drum (Sciaenops Ocellatus) and Sheepshead Minnow (Cyprinodon Variegatus). *Ecotoxicol. Environ. Saf.* **2018**, *166*, 186–191. https://doi.org/https://doi.org/10.1016/j.ecoenv.2018.09.087.

(121) Brette, F.; Shiels, H. A.; Galli, G. L. J.; Cros, C.; Incardona, J. P.; Scholz, N. L.; Block, B. A. A Novel Cardiotoxic Mechanism for a Pervasive Global Pollutant. *Sci. Rep.* **2017**, *7*, 1–9. https://doi.org/10.1038/srep41476.

(122) Nelson, D.; Heuer, R. M.; Cox, G. K.; Stieglitz, J. D.; Hoenig, R.; Mager, E. M.;

Benetti, D. D.; Grosell, M.; Crossley, D. A. Effects of Crude Oil on in Situ Cardiac Function in Young Adult Mahi–mahi (Coryphaena Hippurus). *Aquat. Toxicol.* **2016**, *180*, 274–281. https://doi.org/https://doi.org/10.1016/j.aquatox.2016.10.012.

(123) Nelson, D.; Stieglitz, J. D.; Cox, G. K.; Heuer, R. M.; Benetti, D. D.; Grosell, M.; Crossley, D. A. Cardio-Respiratory Function during Exercise in the Cobia, Rachycentron Canadum: The Impact of Crude Oil Exposure. *Comp. Biochem. Physiol. Part C Toxicol. Pharmacol.* **2017**, *201*, 58–65. https://doi.org/https://doi.org/10.1016/j.cbpc.2017.08.006.

(124) Mager, E. M.; Esbaugh, A. J.; Stieglitz, J. D.; Hoenig, R.; Bodinier, C.; Incardona, J. P.; Scholz, N. L.; Benetti, D. D.; Grosell, M. Acute Embryonic or Juvenile Exposure to Deepwater Horizon Crude Oil Impairs the Swimming Performance of Mahi-Mahi (Coryphaena Hippurus). **2014**. https://doi.org/10.1021/es501628k.

(125) Stieglitz, J. D.; Mager, E. M.; Hoenig, R. H.; Benetti, D. D.; Grosell, M. Impacts of Deepwater Horizon Crude Oil Exposure on Adult Mahi-Mahi (Coryphaena Hippurus) Swim Performance. *Environ. Toxicol. Chem.* **2016**, *35* (10), 2613–2622. https://doi.org/10.1002/etc.3436.

(126) Philibert, D. A.; Philibert, C. P.; Lewis, C.; Tierney, K. B. Comparison of Diluted Bitumen (Dilbit) and Conventional Crude Oil Toxicity to Developing Zebrafish. *Environ. Sci. Technol.* **2016**, *50*, 6091–6098. https://doi.org/10.1021/acs.est.6b00949.

(127) Madison, B. N.; Hodson, P. V; Langlois, V. S. Diluted Bitumen Causes Deformities and Molecular Responses Indicative of Oxidative Stress in Japanese Medaka Embryos. *Aquat. Toxicol.* **2015**, *165*, 222–230. https://doi.org/10.1016/j.aquatox.2015.06.006.

(128) Madison, B. N.; Hodson, P. V.; Langlois, V. S. Cold Lake Blend Diluted Bitumen Toxicity to the Early Development of Japanese Medaka. *Environ. Pollut.* **2017**, *225*, 579–586. https://doi.org/10.1016/j.envpol.2017.03.025.

(129) Alsaadi, F. M.; Madison, B. N.; Brown, R. S.; Hodson, P. V.; Langlois, V. S. Morphological and Molecular Effects of Two Diluted Bitumens on Developing Fathead Minnow (Pimephales Promelas). *Aquat. Toxicol.* **2018**, *204* (June), 107–116. https://doi.org/10.1016/j.aquatox.2018.09.003.

(130) Alderman, S. L.; Lin, F.; Gillis, T. E.; Farrell, A. P.; Kennedy, C. J. Developmental and Latent Effects of Diluted Bitumen Exposure on Early Life Stages of Sockeye Salmon (Oncorhynchus Nerka). *Aquat. Toxicol.* **2018**, *202*, 6–15. https://doi.org/10.1016/j.aquatox.2018.06.014.

(131) Alderman, S. L.; Lin, F.; Farrell, A. P.; Kennedy, C. J.; Gillis, T. E. Effects of Diluted Bitumen Exposure on Juvenile Sockeye Salmon: From Cells to Performance. *Environ. Toxicol. Chem.* **2017**, *36* (2), 354–360. https://doi.org/10.1002/etc.3533.

(132) Alderman, S. L.; Dindia, L. A.; Kennedy, C. J.; Farrell, A. P.; Gillis, T. E. Proteomic Analysis of Sockeye Salmon Serum as a Tool for Biomarker Discovery and New Insight into the Sublethal Toxicity of Diluted Bitumen. *Comp. Biochem. Physiol. - Part D* **2017**, *22*, 157–166. https://doi.org/10.1016/j.cbd.2017.04.003.

(133) McDonnell, D.; Madison, B. N.; Baillon, L.; Wallace, S. J.; Brown, S. R.; Hodson, P. V.; Langlois, V. S. Comparative Toxicity of Two Diluted Bitumens to Developing Yellow Perch (Perca Flavescens). *Sci. Total Environ.* **2019**, *655*, 977–985. https://doi.org/10.1016/j.scitotenv.2018.11.199.

(134) Avey, S. R.; Kennedy, C. J.; Farrell, A. P.; Gillis, T. E.; Alderman, S. L. Effects of Diluted Bitumen Exposure on Atlantic Salmon Smolts: Molecular and Metabolic Responses in Relation to Swimming Performance. *Aquat. Toxicol.* **2020**, *221* (September 2019), 105423. https://doi.org/10.1016/j.aquatox.2020.105423.

(135) Lee, K.; Boufadel, M.; Chen, B.; Foght, J.; Hodson, P.; Swanson, S.; Venosa, A. High-Priority Research Needs for Oil Spills in Canada: Summary of a Royal Society Expert Panel Report on the Behaviour and Environmental Impacts of Crude Oil Released into Aqueous Environments. *39th AMOP Tech. Semin. Environ. Contam. Response* **2016**, No. July.

(136) Alsaadi, F.; Hodson, P. V.; Langlois, V. S. An Embryonic Field of Study: The Aquatic Fate and Toxicity of Diluted Bitumen. *Bulletin of Environmental Contamination and Toxicology*. 2018. https://doi.org/10.1007/s00128-017-2239-7.

(137) Cederwall, J.; Black, T. A.; Blais, J. M.; Hanson, M. L.; Hollebone, B. P.; Palace, V. P.; Rodríguez-Gil, J. L.; Greer, C. W.; Maynard, C.; Ortmann, A. C.; et al. Life under an Oil Slick: Response of a Freshwater Food Web to Simulated Spills of Diluted Bitumen in Field Mesocosms. *Can. J. Fish. Aquat. Sci.* **2020**, *10* (February), 1–10. https://doi.org/10.1139/cjfas-2019-0224.

(138) Oris, J. T.; Giesy, J. P. The Photo-Induced Toxicity of Polycyclic Aromatic Hydrocarbons to Larvae of the Fathead Minnow (Pimephales Promelas). *Chemosphere* **1987**, *16* (7), 1395–1404. https://doi.org/https://doi.org/10.1016/0045-6535(87)90079-8.

(139) Newsted, J. L.; Giesy, J. P. Predictive Models for Photoinduced Acute Toxicity of Polycyclic Aromatic Hydrocarbons to Daphnia Magna, Strauss (Cladocera, Crustacea). *Environ. Toxicol. Chem.* **1987**, *6* (6), 445–461.

https://doi.org/10.1002/etc.5620060605.

(140) Fu, P. P.; Xia, Q.; Sun, X.; Yu, H. Phototoxicity and Environmental Transformation of Polycyclic Aromatic Hydrocarbons (PAHs)—Light-Induced Reactive Oxygen Species, Lipid Peroxidation, and DNA Damage. *J. Environ. Sci. Heal. Part C* **2012**, *30* (1), 1–41. https://doi.org/10.1080/10590501.2012.653887.

(141) Ankley, G. T.; Burkhard, L. P.; Cook, P. M.; Diamond, S. A.; Erickson, R. J.; Mount, D. R. Photoactivated Toxicity of PAHs to Aquatic Organisms. *PAHs An Ecotoxicological Perspect.* **2003**, *4*, 275.

(142) Diamond, S. A.; Mount, D. R.; Mattson, V. R.; Heinis, L. J.; Highland, T. L.; Adams, A. D.; Simcik, M. F. Photoactivated Polycyclic Aromatic Hydrocarbon Toxicity in Medaka (Oryzias Latipes) Embryos: Relevance to Environmental Risk in Contaminated Sites. *Environ. Toxicol. Chem. An Int. J.* **2006**, *25* (11), 3015–3023.

(143) Holst, L. L.; Giesy, J. P. Chronic Effects of the Photoenhanced Toxicity of Anthracene on Daphnia Magna Reproduction. *Environ. Toxicol. Chem. An Int. J.* **1989**, *8* (10), 933–942.

(144) Bowling, J. W.; Leversee, G. J.; Landrum, P. F.; Giesy, J. P. Acute Mortality of Anthracene-Contaminated Fish Exposed to Sunlight. *Aquat. Toxicol.* **1983**, *2* (1), 79–90.

(145) Beardsley Jr, G. L. Age, Growth, and Reproduction of the Dolphin, Coryphaena Hippurus, in the Straits of Florida. *Copeia* **1967**, 441–451.

(146) Ditty, J. G.; Shaw, R. F.; Grimes, C. B.; Cope, J. S. Larval Development, Distribution, and Abundance of Common Dolphin, Coryphaena Hippurus, and Pompano Dolphin, C. Equiselis(family: Coryphaenidae), in the Northern Gulf of Mexico. *Fish. Bull.* **1994**, *92* (2), 275–291.

(147) Khursigara, A. J.; Ackerly, K. L.; Esbaugh, A. J. Oil Toxicity and Implications for Environmental Tolerance in Fish. *Comp. Biochem. Physiol. Part - C Toxicol. Pharmacol.* **2019**, *220* (December 2018), 52–61. https://doi.org/10.1016/j.cbpc.2019.03.003.

(148) Schmidtko, S.; Stramma, L.; Visbeck, M. Decline in Global Oceanic Oxygen Content during the Past Five Decades. *Nature* **2017**, *542* (7641), 335–339. https://doi.org/10.1038/nature21399.

(149) Jenny, J.-P.; Francus, P.; Normandeau, A.; Lapointe, F.; Perga, M.-E.; Ojala, A.; Schimmelmann, A.; Zolitschka, B. Global Spread of Hypoxia in Freshwater

Ecosystems during the Last Three Centuries Is Caused by Rising Local Human Pressure. *Glob. Chang. Biol.* **2016**, *22* (4), 1481–1489. https://doi.org/10.1111/gcb.13193.

(150) Speers-Roesch, B.; Mandic, M.; Groom, D. J. E.; Richards, J. G. Critical Oxygen Tensions as Predictors of Hypoxia Tolerance and Tissue Metabolic Responses during Hypoxia Exposure in Fishes. *J. Exp. Mar. Bio. Ecol.* **2013**, *449*, 239–249. https://doi.org/https://doi.org/10.1016/j.jembe.2013.10.006.

(151) Farrell, A. P.; Richards, J. G. Chapter 11 Defining Hypoxia: An Integrative Synthesis of the Responses of Fish to Hypoxia. In *Hypoxia*; Richards, J. G., Farrell, A. P., Brauner, C. J. B. T.-F. P., Eds.; Academic Press, 2009; Vol. 27, pp 487–503. https://doi.org/https://doi.org/10.1016/S1546-5098(08)00011-3.

(152) Davoodi, F.; Claireaux, G. Effects of Exposure to Petroleum Hydrocarbons upon the Metabolism of the Common Sole Solea Solea. *Mar. Pollut. Bull.* **2007**, *54* (7), 928–934. https://doi.org/https://doi.org/10.1016/j.marpolbul.2007.03.004.

(153) Matson, C. W.; Timme-Laragy, A. R.; Di Giulio, R. T. Fluoranthene, but Not Benzo[a]pyrene, Interacts with Hypoxia Resulting in Pericardial Effusion and Lordosis in Developing Zebrafish. *Chemosphere* **2008**, *74* (1), 149–154. https://doi.org/https://doi.org/10.1016/j.chemosphere.2008.08.016.

(154) Yu, R. M. K.; Ng, P. K. S.; Tan, T.; Chu, D. L. H.; Wu, R. S. S.; Kong, R. Y. C. Enhancement of Hypoxia-Induced Gene Expression in Fish Liver by the Aryl Hydrocarbon Receptor (AhR) Ligand, Benzo[a]pyrene (BaP). *Aquat. Toxicol.* **2008**, *90* (3), 235–242. https://doi.org/https://doi.org/10.1016/j.aquatox.2008.09.004.

(155) Jasperse, L.; Levin, M.; Rogers, K.; Perkins, C.; Bosker, T.; Griffitt, R. J.; Sepúlveda, M.; De Guise, S. Hypoxia and Reduced Salinity Exacerbate the Effects of Oil Exposure on Sheepshead Minnow (Cyprinodon Variegatus) Reproduction. *Aquat. Toxicol.* **2019**, *212*, 175–185. https://doi.org/https://doi.org/10.1016/j.aquatox.2019.05.002.

(156) Hedgpeth, B. M.; Griffitt, R. J. Simultaneous Exposure to Chronic Hypoxia and Dissolved Polycyclic Aromatic Hydrocarbons Results in Reduced Egg Production and Larval Survival in the Sheepshead Minnow (Cyprinodon Variegatus). *Environ. Toxicol. Chem.* **2016**, *35* (3), 645–651. https://doi.org/10.1002/etc.3207.

(157) Dasgupta, S.; Huang, I. J.; McElroy, A. E. Hypoxia Enhances the Toxicity of Corexit EC9500A and Chemically Dispersed Southern Louisiana Sweet Crude Oil (MC-242) to Sheepshead Minnow (Cyprinodon Variegatus) Larvae. *PLoS One* **2015**, *10* (6), e0128939–e0128939. https://doi.org/10.1371/journal.pone.0128939.

(158) Attrill, M. J.; Power, M. Climatic Influence on a Marine Fish Assemblage. *Nature* **2002**, *417* (6886), 275–278. https://doi.org/10.1038/417275a.

(159) Dippner, J. W. Recruitment Success of Different Fish Stocks in the North Sea in Relation to Climate Variability. *Dtsch. Hydrogr. Zeitschrift* **1997**, *49* (2), 277–293. https://doi.org/10.1007/BF02764039.

(160) O'Brien, C. M.; Fox, C. J.; Planque, B.; Casey, J. Climate Variability and North Sea Cod. *Nature* **2000**, *404* (6774), 142. https://doi.org/10.1038/35004654.

(161) Alheit, J.; Hagen, E. Long-Term Climate Forcing of European Herring and Sardine Populations. *Fish. Oceanogr.* **1997**, *6* (2), 130–139. https://doi.org/10.1046/j.1365-2419.1997.00035.x.

(162) Thackeray, S. J.; Sparks, T. H.; Frederiksen, M.; Burthe, S.; Bacon, P. J.; Bell, J. R.; Botham, M. S.; Brereton, T. M.; Bright, P. W.; Carvalho, L.; et al. Trophic Level Asynchrony in Rates of Phenological Change for Marine, Freshwater and Terrestrial Environments. *Glob. Chang. Biol.* **2010**, *16* (12), 3304–3313. https://doi.org/10.1111/j.1365-2486.2010.02165.x.

(163) Evans, D. H.; Claiborne, J. B. *The Physiology of Fishes*, 3rd ed.; CRC Press: New York, 2006.

(164) Wood, C. M.; McDonald, D. G. *Global Warming: Implications for Freshwater and Marine Fish*; Cambridge University Press: Cambridge, UK, 1997.

(165) Johansen, J. L.; Messmer, V.; Coker, D. J.; Hoey, A. S.; Pratchett, M. S. Increasing Ocean Temperatures Reduce Activity Patterns of a Large Commercially Important Coral Reef Fish. *Glob. Chang. Biol.* **2014**, *20* (4), 1067–1074. https://doi.org/10.1111/gcb.12452.

(166) Johansen, J. L.; Pratchett, M. S.; Messmer, V.; Coker, D. J.; Tobin, A. J.; Hoey, A. S. Large Predatory Coral Trout Species Unlikely to Meet Increasing Energetic Demands in a Warming Ocean. *Sci. Rep.* **2015**, *5* (1), 13830. https://doi.org/10.1038/srep13830.

(167) Veilleux, H. D.; Ryu, T.; Donelson, J. M.; Van Herwerden, L.; Seridi, L.; Ghosheh, Y.; Berumen, M. L.; Leggat, W.; Ravasi, T.; Munday, P. L. Molecular Processes of Transgenerational Acclimation to a Warming Ocean. *Nat. Clim. Chang.* **2015**, *5* (12), 1074–1078. https://doi.org/10.1038/nclimate2724.

(168) Pörtner, H. O.; Farrell, A. P. Physiology and Climate Change. *Science (80-.).* **2008**, *322* (5902), 690 LP-692. https://doi.org/10.1126/science.1163156.

(169) Del Toro-Silva, F. M.; Miller, J. M.; Taylor, J. C.; Ellis, T. A. Influence of Oxygen and Temperature on Growth and Metabolic Performance of Paralichthys Lethostigma (Pleuronectiformes: Paralichthyidae). *J. Exp. Mar. Bio. Ecol.* **2008**, *358* (2), 113–123. https://doi.org/https://doi.org/10.1016/j.jembe.2008.01.019.

(170) Donelson, J. M.; Munday, P. L.; Mccormick, M. I.; Nilsson, G. E. Acclimation to Predicted Ocean Warming through Developmental Plasticity in a Tropical Reef Fish. *Glob. Chang. Biol.* **2011**, *17* (4), 1712–1719. https://doi.org/10.1111/j.1365-2486.2010.02339.x.

(171) Angilletta, M. J.; Wilson, R. S.; Navas, C. A.; James, R. S. Tradeoffs and the Evolution of Thermal Reaction Norms. *Trends Ecol. Evol.* **2003**, *18* (5), 234–240. https://doi.org/https://doi.org/10.1016/S0169-5347(03)00087-9.

(172) Veilleux, H. D.; Ryu, T.; Donelson, J. M.; van Herwerden, L.; Seridi, L.; Ghosheh, Y.; Berumen, M. L.; Leggat, W.; Ravasi, T.; Munday, P. L. Molecular Processes of Transgenerational Acclimation to a Warming Ocean. *Nat. Clim. Chang.* **2015**, *5* (12), 1074–1078. https://doi.org/10.1038/nclimate2724.

(173) Gamito, R.; Costa, M. J.; Cabral, H. N. Fisheries in a Warming Ocean: Trends in Fish Catches in the Large Marine Ecosystems of the World. *Reg. Environ. Chang.* **2015**, *15* (1), 57–65. https://doi.org/10.1007/s10113-014-0615-y.

(174) Perry, A. L.; Low, P. J.; Ellis, J. R.; Reynolds, J. D. Climate Change and Distribution Shifts in Marine Fishes. *Science (80-.).* **2005**, *308* (5730), 1912 LP-1915. https://doi.org/10.1126/science.1111322.

(175) Henriksen, A. Acidification of Freshwaters — a Large Scale Tritration. In *Proceedings of the International Conference on the Ecological Impacts of Acid Precipitation*; Drablos, D., Tollan, A., Eds.; SNSF Project: Oslo, Norway, 1980; pp 68–74.

(176) Wright, R.; Conroy, N.; Dickson, W.; Harriman, R.; Henriksen, A.; Schofield, C. Acidified Lake Districts of the World: A Comparison of Water Chemistry of Lakes in Southern Norway, Southern Sweden, Southwestern Scotland, the Adirondack Mountains of New York, and Southeastern Ontario. In *Proceedings of the International Conference on the Ecological Impacts of Acid Precipitation*; Drabios, D., Tollan, A., Eds.; SNSF Project: Oslo, Norway, 1980; pp 377–379.

(177) Schindler, D. W.; Wagemann, R.; Cook, R. B.; Ruszczynski, T.; Prokopowich, J. Experimental Acidification of Lake 223, Experimental Lakes Area: Background Data and the First Three Years of Acidification. *Can. J. Fish. Aquat. Sci.* **1980**, *37* (3), 342–354. https://doi.org/10.1139/f80-048.

(178) Nero, R. W.; Schindler, D. W. Decline of Mysis Relicla During the Acidification of Lake 223. *Can. J. Fish. Aquat. Sci.* **1983**, *40*, 1095–1911.

(179) Kennedy, L. A. Teratogenesis in Lake Trout (Salvelinus Namaycush) in an Experimentally Acidified Lake. *Can. J. Fish. Aquat. Sci.* **1980**, *37* (12), 2355–2358. https://doi.org/10.1139/f80-282.

(180) Schindler, D. W.; Turner, M. A. Biological, Chemical and Physical Responses of Lakes to Experimental Acidification. In *Long-Range Transport of Airborne Pollutants*; Martin, H. C., Ed.; Springer Netherlands: Dordrecht, 1982; pp 259–271. https://doi.org/10.1007/978-94-009-7966-6_19.

(181) Mills, K. H.; Chalanchuk, S. M.; Mohr, L. C.; Davies, I. J. Responses of Fish Populations in Lake 223 to 8 Years of Experimental Acidification. *Can. J. Fish. Aquat. Sci.* **1987**, *44* (SUPPL. 1), 114–125. https://doi.org/10.1139/f87-287.

(182) Marshall, W. S.; Grosell, M. Ion Transport, Osmoregulation, and Acid-Base Balance. In *The Physiology of Fishes*; Evans, D., Claiborne, J. B., Eds.; CRC Press: Boca Raton, FL, 2006; pp 177–230.

(183) Ishimatsu, A.; Hayashi, M.; Kikkawa, T. Fishes in High-CO2, Acidified Oceans . *Mar. Ecol. Prog. Ser.* **2008**, *373*, 295–302.

(184) Heisler, N. Acid-Base Regulation in Fishes. In *Acid-base regulation in animals*; Heisler, N., Ed.; Elsevier: Amsterdam, 1986; pp 309–356.

(185) Hosfeld, C. D.; Engevik, A.; Mollan, T.; Lunde, T. M.; Waagbø, R.; Olsen, A. B.; Breck, O.; Stefansson, S.; Fivelstad, S. Long-Term Separate and Combined Effects of Environmental Hypercapnia and Hyperoxia in Atlantic Salmon (Salmo Salar L.) Smolts. *Aquaculture* **2008**, *280* (1–4), 146–153. https://doi.org/10.1016/j.aquaculture.2008.05.009.

(186) Fivelstad, S.; Olsen, A. B.; Kløften, H.; Ski, H.; Stefansson, S. Effects of Carbon Dioxide on Atlantic Salmon (Salmo Salar L.) Smolts at Constant pH in Bicarbonate Rich Freshwater. *Aquaculture* **1999**, *178* (1–2), 171–187. https://doi.org/10.1016/S0044-8486(99)00125-8.

(187) Heuer, R. M.; Grosell, M. Physiological Impacts of Elevated Carbon Dioxide and Ocean Acidification on Fish. *Am. J. Physiol. Integr. Comp. Physiol.* **2014**, *307* (9), R1061–R1084. https://doi.org/10.1152/ajpregu.00064.2014.

(188) Munday, P. L.; Dixson, D. L.; Donelson, J. M.; Jones, G. P.; Pratchett, M. S.; Devitsina, G. V; Døving, K. B. Ocean Acidification Impairs Olfactory

Discrimination and Homing Ability of a Marine Fish. *Proc. Natl. Acad. Sci.* **2009**, *106* (6), 1848 LP-1852. https://doi.org/10.1073/pnas.0809996106.

(189) Munday, P. L.; Pratchett, M. S.; Dixson, D. L.; Donelson, J. M.; Endo, G. G. K.; Reynolds, A. D.; Knuckey, R. Elevated CO2 Affects the Behavior of an Ecologically and Economically Important Coral Reef Fish. *Mar. Biol.* **2013**, *160* (8), 2137–2144. https://doi.org/10.1007/s00227-012-2111-6.

(190) Simpson, S. D.; Munday, P. L.; Wittenrich, M. L.; Manassa, R.; Dixson, D. L.; Gagliano, M.; Yan, H. Y. Ocean Acidification Erodes Crucial Auditory Behaviour in a Marine Fish. *Biol. Lett.* **2011**, *7* (6), 917–920. https://doi.org/10.1098/rsbl.2011.0293.

(191) Ferrari, M. C. O.; McCormick, M. I.; Munday, P. L.; Meekan, M. G.; Dixson, D. L.; Lönnstedt, O.; Chivers, D. P. Effects of Ocean Acidification on Visual Risk Assessment in Coral Reef Fishes. *Funct. Ecol.* **2012**, *26* (3), 553–558. https://doi.org/10.1111/j.1365-2435.2011.01951.x.

(192) Munday, P. L.; Dixson, D. L.; McCormick, M. I.; Meekan, M.; Ferrari, M. C. O.; Chivers, D. P. Replenishment of Fish Populations Is Threatened by Ocean Acidification. *Proc. Natl. Acad. Sci.* **2010**, *107* (29), 12930 LP-12934. https://doi.org/10.1073/pnas.1004519107.

(193) Chivers, D. P.; McCormick, M. I.; Nilsson, G. E.; Munday, P. L.; Watson, S.-A.; Meekan, M. G.; Mitchell, M. D.; Corkill, K. C.; Ferrari, M. C. O. Impaired Learning of Predators and Lower Prey Survival under Elevated CO2: A Consequence of Neurotransmitter Interference. *Glob. Chang. Biol.* **2014**, *20* (2), 515–522. https://doi.org/10.1111/gcb.12291.

(194) Briffa, M.; de la Haye, K.; Munday, P. L. High CO2 and Marine Animal Behaviour: Potential Mechanisms and Ecological Consequences. *Mar. Pollut. Bull.* **2012**, *64* (8), 1519–1528. https://doi.org/https://doi.org/10.1016/j.marpolbul.2012.05.032.

(195) Munday, P. L.; McCormick, M. I.; Nilsson, G. E. Impact of Global Warming and Rising CO2 Levels on Coral Reef Fishes: What Hope for the Future? *J. Exp. Biol.* **2012**, *215* (22), 3865 LP-3873. https://doi.org/10.1242/jeb.074765.

(196) Allan, B. J. M.; Domenici, P.; McCormick, M. I.; Watson, S.-A.; Munday, P. L. Elevated CO2 Affects Predator-Prey Interactions through Altered Performance. *PLoS One* **2013**, *8* (3), e58520–e58520. https://doi.org/10.1371/journal.pone.0058520.

(197) Devine, B. M.; Munday, P. L.; Jones, G. P. Rising CO2 Concentrations Affect

Settlement Behaviour of Larval Damselfishes. *Coral Reefs* **2012**, *31* (1), 229–238. https://doi.org/10.1007/s00338-011-0837-0.

(198) Ferrari, M. C. O.; Dixson, D. L.; Munday, P. L.; Mccormick, M. I.; Meekan, M. G.; Sih, A.; Chivers, D. P. Intrageneric Variation in Antipredator Responses of Coral Reef Fishes Affected by Ocean Acidification: Implications for Climate Change Projections on Marine Communities. *Glob. Chang. Biol.* **2011**, *17* (9), 2980–2986. https://doi.org/10.1111/j.1365-2486.2011.02439.x.

(199) Veldhoen, N.; Stevenson, M. R.; Skirrow, R. C.; Rieberger, K. J.; van Aggelen, G.; Meays, C. L.; Helbing, C. C. Minimally Invasive Transcriptome Profiling in Salmon: Detection of Biological Response in Rainbow Trout Caudal Fin Following Exposure to Environmental Chemical Contaminants. *Aquat. Toxicol.* **2013**, *142–143*, 239–247. https://doi.org/10.1016/j.aquatox.2013.08.016.

(200) Imbery, J. J.; Buday, C.; Miliano, R. C.; Shang, D.; Round, J. M.; Kwok, H.; Van Aggelen, G.; Helbing, C. C. Evaluation of Gene Bioindicators in the Liver and Caudal Fin of Juvenile Pacific Coho Salmon in Response to Low Sulfur Marine Diesel Seawater-Accommodated Fraction Exposure. *Environ. Sci. Technol.* **2019**, *53* (3), 1627–1638. https://doi.org/10.1021/acs.est.8b05429.

(201) Rodríguez-Jorquera, I. A.; Colli-Dula, R. C.; Kroll, K.; Jayasinghe, B. S.; Parachu Marco, M. V.; Silva-Sanchez, C.; Toor, G. S.; Denslow, N. D. Blood Transcriptomics Analysis of Fish Exposed to Perfluoro Alkyls Substances: Assessment of a Non-Lethal Sampling Technique for Advancing Aquatic Toxicology Research. *Environ. Sci. Technol.* **2019**, *53* (3), 1441–1452. https://doi.org/10.1021/acs.est.8b03603.

(202) Razavi, N. R.; Halfman, J. D.; Cushman, S. F.; Massey, T.; Beutner, R.; Foust, J.; Gilman, B.; Cleckner, L. B. Mercury Concentrations in Fish and Invertebrates of the Finger Lakes in Central New York, USA. *Ecotoxicology* **2019**. https://doi.org/10.1007/s10646-019-02132-z.

(203) Lake, J. L.; Ryba, S. A.; Serbst, J. R.; Libby, A. D. Mercury in Fish Scales as an Assessment Method for Predicting Muscle Tissue Mercury Concentrations in Largemouth Bass. *Arch. Environ. Contam. Toxicol.* **2006**, *50* (4), 539–544. https://doi.org/10.1007/s00244-005-5052-y.

(204) Baker, R. F.; Blanchfield, P. J.; Paterson, M. J.; Flett, R. J.; Wesson, L. Evaluation of Nonlethal Methods for the Analysis of Mercury in Fish Tissue. *Trans. Am. Fish. Soc.* **2004**, *133* (3), 568–576. https://doi.org/10.1577/t03-012.1.

(205) Brumbaugh, W. G.; Schmitt, C. J.; May, T. W. Concentrations of Cadmium, Lead, and Zinc in Fish from Mining-Influenced Waters of Northeastern Oklahoma:

Sampling of Blood, Carcass, and Liver for Aquatic Biomonitoring. *Arch. Environ. Contam. Toxicol.* **2005**, *49* (1), 76–88. https://doi.org/10.1007/s00244-004-0172-3.

(206) Henderson, T. F.; Stevens, S. Y.; Lee, C. J. Assessing the Suitability of a Non-Lethal Biopsy Punch for Sampling Fish Muscle Tissue. *Fish Physiol Biochem* **2016**, *42*, 1521–1526. https://doi.org/10.1007/s10695-016-0237-z.

(207) Shephard, K. L. Functions for Fish Mucus. *Rev. Fish Biol. Fish.* **1994**, *4* (4), 401–429. https://doi.org/10.1007/BF00042888.

(208) Brinchmann, M. F. Immune Relevant Molecules Identified in the Skin Mucus of Fish Using -Omics Technologies. *Mol. BioSyst.* **2016**, *12* (7), 2056–2063. https://doi.org/10.1039/C5MB00890E.

(209) Ao, J.; Mu, Y.; Xiang, L.-X.; Fan, D.; Feng, M.; Zhang, S. Genome Sequencing of the Perciform Fish Larimichthys Crocea Provides Insights into Molecular and Genetic Mechanisms of Stress Adaptation. *PLoS Genet* **2015**, *11* (4), 1005118. https://doi.org/10.1371/journal.pgen.1005118.

(210) Provan, F.; Jensen, L. B.; Uleberg, K. E.; Larssen, E.; Rajalahti, T.; Mullins, J.; Obach, A. Proteomic Analysis of Epidermal Mucus from Sea Lice-Infected Atlantic Salmon, Salmo Salar L. *J. Fish Dis.* **2013**, *36* (3), 311–321. https://doi.org/10.1111/jfd.12064.

(211) Cordero, H.; Brinchmann, M. F.; Cuesta, A.; Meseguer, J.; Esteban, M. A. Skin Mucus Proteome Map of European Sea Bass (Dicentrarchus Labrax). *Proteomics* **2015**, *15* (23–24), 4007–4020. https://doi.org/10.1002/pmic.201500120.

(212) Van Veld, P. A.; Rutan, B. J.; Sullivan, C. A.; Johnston, L. D.; Rice, C. D.; Fisher, D. F.; Yonkos, L. T. A Universal Assay for Vitellogenin in Fish Mucus and Plasma. *Environ. Toxicol. Chem.* **2005**, *24* (12), 3048–3052. https://doi.org/10.1897/05-363R.1.

(213) Kishida, M.; Anderson, T. R.; Specker, J. L. Induction by Beta-Estradiol of Vitellogenin in Striped Bass (Morone Saxatilis): Characterization and Quantification in Plasma and Mucus. *Gen. Comp. Endocrinol.* **1992**, *88*, 29–39.

(214) Meucci, V.; Arukwe, A. Detection of Vitellogenin and Zona Radiata Protein Expressions in Surface Mucus of Immature Juvenile Atlantic Salmon (Salmo Salar) Exposed to Waterborne Nonylphenol. *Aquat. Toxicol.* **2005**, *73*, 1–10. https://doi.org/10.1016/j.aquatox.2005.03.021.

(215) Moncaut, N.; Nostro, F. Lo; Maggese, M. C. Vitellogenin Detection in Surface Mucus of the South American Cichlid Fish Cichlasoma Dimerus (Heckel, 1840) Induced by Estradiol-17β. Effects on Liver and Gonads. *Aquat. Toxicol.* **2003**, *63*

(2), 127–137. https://doi.org/https://doi.org/10.1016/S0166-445X(02)00175-3.

(216) Guardiola, F. A.; Dioguardi, M.; Parisi, M. G.; Trapani, M. R.; Meseguer, J.; Cuesta, A.; Cammarata, M.; Esteban, M. A. Evaluation of Waterborne Exposure to Heavy Metals in Innate Immune Defences Present on Skin Mucus of Gilthead Seabream (Sparus Aurata). *Fish Shellfish Immunol.* **2015**. https://doi.org/10.1016/j.fsi.2015.02.010.

(217) Dzul-Caamal, R.; Salazar-Coria, L.; Olivares-Rubio, H. F.; Rocha-Gómez, M. A.; Girón-Pérez, M. I.; Vega-López, A. Oxidative Stress Response in the Skin Mucus Layer of Goodea Gracilis (Hubbs and Turner, 1939) Exposed to Crude Oil: A Non-Invasive Approach. *Comp. Biochem. Physiol. -Part A Mol. Integr. Physiol.* **2016**. https://doi.org/10.1016/j.cbpa.2016.05.008.

(218) Bulloch, P.; Schur, S.; Muthumuni, D.; Xia, Z.; Johnson, W.; Chu, M.; Palace, V.; Su, G.; Letcher, R.; Tomy, G. T. F2-Isoprostanes in Fish Mucus: A New, Non-Invasive Method for Analyzing a Biomarker of Oxidative Stress. *Chemosphere* **2020**, *239*.

(219) Cordero, H.; Morcillo, P.; Cuesta, A.; Brinchmann, M. F.; Esteban, M. A. Differential Proteome Profile of Skin Mucus of Gilthead Seabream (Sparus Aurata) after Probiotic Intake And/or Overcrowding Stress. *J. Proteomics* **2016**, *132*, 41–50. https://doi.org/10.1016/j.jprot.2015.11.017.

(220) Easy, R. H.; Ross, N. W. Changes in Atlantic Salmon (Salmo Salar) Epidermal Mucus Protein Composition Profiles Following Infection with Sea Lice (Lepeophtheirus Salmonis). *Comp. Biochem. Physiol. - Part D Genomics Proteomics* **2009**. https://doi.org/10.1016/j.cbd.2009.02.001.

(221) Guardiola, F. A.; Cuesta, A.; Arizcun, M.; Meseguer, J.; Esteban, M. A. Comparative Skin Mucus and Serum Humoral Defence Mechanisms in the Teleost Gilthead Seabream (Sparus Aurata). *Fish Shellfish Immunol.* **2014**, *36* (2), 545–551. https://doi.org/10.1016/j.fsi.2014.01.001.

(222) Rajan, B.; Lokesh, J.; Kiron, V.; Brinchmann, M. F. Differentially Expressed Proteins in the Skin Mucus of Atlantic Cod (Gadus Morhua) upon Natural Infection with Vibrio Anguillarum. *BMC Vet. Res.* **2013**, *9*. https://doi.org/10.1186/1746-6148-9-103.

(223) Ren, Y.; Zhao, H.; Su, B.; Peatman, E.; Li, C. Expression Profiling Analysis of Immune-Related Genes in Channel Catfish (Ictalurus Punctatus) Skin Mucus Following Flavobacterium Columnare Challenge. *Fish Shellfish Immunol.* **2015**, *46* (2), 537–542. https://doi.org/10.1016/j.fsi.2015.07.021.

(224) Greer, J. B.; Andrzejczyk, N. E.; Mager, E. M.; Stieglitz, J. D.; Benetti, D.; Grosell, M.; Schlenk, D. Whole-Transcriptome Sequencing of Epidermal Mucus as a Novel Method for Oil Exposure Assessment in Juvenile Mahi-Mahi (Coryphaena Hippurus). *Environ. Sci. Technol. Lett.* **2019**, *6*, 538–544. https://doi.org/10.1021/acs.estlett.9b00479.

(225) Roy, L. a; Armstrong, J. L.; Sakamoto, K.; Steinert, S.; Perkins, E.; Lomax, D. P.; Johnson, L. L.; Schlenk, D. The Relationships of Biochemical Endpoints to Histopathology and Population Metrics in Feral Flatfish Species Collected near the Municipal Wastewater Outfall of Orange County, California, USA. *Environ. Toxicol. Chem.* **2003**, *22* (6), 1309–1317. https://doi.org/10.1897/1551-5028(2003)022<1309:TROBET>2.0.CO;2.

(226) Ann Rempel, M.; Reyes, J.; Steinert, S.; Hwang, W.; Armstrong, J.; Sakamoto, K.; Kelley, K.; Schlenk, D. Evaluation of Relationships between Reproductive Metrics, Gender and Vitellogenin Expression in Demersal Flatfish Collected near the Municipal Wastewater Outfall of Orange County, California, USA. *Aquat. Toxicol.* **2006**, *77* (3), 241–249. https://doi.org/10.1016/j.aquatox.2005.12.007.

(227) Bay, S. M.; Vidal-Dorsch, D. E.; Schlenk, D.; Kelley, K. M.; Maruya, K. A.; Gully, J. R. Integrated Coastal Effects Study: Synthesis of Findings. *Environ. Toxicol. Chem.* **2012**, *31* (12), 2711–2722. https://doi.org/10.1002/etc.2007.

(228) Forsgren, K. L.; Bay, S. M.; Vidal-Dorsch, D. E.; Deng, X.; Lu, G.; Armstrong, J.; Gully, J. R.; Schlenk, D. Annual and Seasonal Evaluation of Reproductive Status in Hornyhead Turbot at Municipal Wastewater Outfalls in the Southern California Bight. *Environ. Toxicol. Chem.* **2012**, *31* (12), 2701–2710. https://doi.org/10.1002/etc.2006.

(229) Allen, M. J.; Smith, R. W.; Jarvis, E. T.; Raco-Rands, V.; Bernstein, B. B.; Herbinson, K. T. *Temporal Trends in Southern California Coastal Fish Populations Relative to 30-Year Trends in Oceanic Conditions*; 2004.

Chapter 1: Examining the role of estrogenic activity and ocean temperature on declines of a coastal demersal flatfish population near the municipal wastewater outfall of Orange County, California, USA

Abstract

Wastewater treatment plant effluent introduces a mixture of pollutants into marine environments; however, the impacts of chronic sublethal exposures on populations is often unclear. Presence of estrogenic agents in sediments and uptake of these compounds by demersal flatfishes has been reported at the Orange County Sanitation District (OCSD) wastewater outfall. Furthermore, estrogenic activity has been identified in male flatfish in the area, potentially contributing to observed population declines in the OCSD region. Rising ocean temperatures may further contribute to flatfish declines as relationships between temperature and abundance have been reported in the Southern California Bight. To investigate declines, sex ratios, condition factor, organ health indices, hormones, and vitellogenin were quantified in flatfish collected at OCSD outfall and reference sites. Additionally, historical temperature data was examined for trends with population abundances. Rather than being linked to estrogenic activity, results indicated that population declines were more correlated to increases in ocean temperature.

Introduction

Exposure to compounds with estrogenic modes of action has been linked to endocrine disrupting effects among wild fish populations in freshwater and marine environments.[1–5] The presence of estrogenic agents in aquatic environments is a result of anthropogenic activities, with wastewater treatment plant effluent being one of the major contributors.[2,6,7] As a result of large-scale urbanization, wastewater treatment plant effluent may pose risks to aquatic ecosystems receiving effluent from highly developed areas, such as Southern California. The Southern California Bight alone receives a total of over 1 billion gallons of treated wastewater per day, often containing several contaminants of emerging concern not removed by the treatment process.[8–10]

At the Orange County Sanitation District (OCSD) wastewater treatment plant outfall, a variety of estrogenic agents have been identified in sediments, including 17β-estradiol (E_2), nonylphenol, alkylphenol ethoxylates, triclosan, and various pharmaceutical and personal care products, among others.[11,12] Furthermore, bioaccumulation of compounds deposited in sediments at the OCSD has been observed in the demersal flatfish hornyhead turbot (*Pleuronichthys verticalis*).[12–14] Compounds identified in sediments and organisms at the OCSD outfall may pose risks to marine health as E_2, nonylphenol, and alkylphenol ethoxylates have been shown to alter steroidogenesis in several fish species.[15–18]

Previous studies have investigated the occurrence of endocrine disrupting effects in hornyhead turbot residing at the OCSD outfall. These studies reported elevated E_2 and vitellogenin levels in hornyhead turbot males as well as skewed population sex ratios.[8,19–

[21] Although estrogenic activity has been identified, population abundances of hornyhead turbot have remained unchanged indicating little or no population-level effects.[21] While hornyhead turbot populations appear to be stable, there may be other more sensitive species that respond differently to contaminants deposited in sediments at the OCSD outfall.

In addition to anthropogenic chemical inputs, trends in environmental variables may further impact population abundances. Of these environmental variables, temperature and shifts in climate cycles are likely to mediate demersal flatfish populations as we are currently in the 3rd consecutive decade of record high ocean.[22,23] In the Southern California Bight specifically, demersal flatfish abundances have shown to correlate with shoreline and offshore ocean temperatures, the Pacific Decadal Oscillation (PDO) index, and the El Niño Southern Oscillation (ENSO) cycle;[24] these results indicate that temperature plays an important role in population fluctuations.

Unlike previously studied demersal flatfish species, Pacific sanddab (*Citharichthys sordidus*) have experienced population declines throughout the OCSD monitoring region.[14,25–34] Pacific sanddab and other demersal flatfishes are ideal study species as they are exposed to compounds deposited in sediments through direct dermal absorption and through their diet of infaunal and epibenthic organisms.[35,36] Having identified population-level disturbances in Pacific sanddab, this study aims to identify potential mechanisms responsible for population declines. We hypothesized that declines may be linked to estrogenic activity given the previous detection of estrogenic agents in OCSD sediments and identification of estrogenic activity in other flatfish species.

Additionally, it was hypothesized that population declines may be correlated to shifts in ocean temperature as significant relationships between abundance and temperature as well as broader climate cycles have previously been identified among demersal flatfish populations in the Southern California Bight.

Materials and methods

Sampling Area

All samples were collected within the OCSD ocean monitoring area located on the southern portion of the San Pedro Shelf within the Southern California Bight (Figure 2.1). The OCSD outfall, T1, is located 7 km offshore at a depth of 55 m (33° 34.641' N, 118° 00.567' W), while the reference site, T11, is located 7.7 km north of the outfall at a depth of 60 m (33° 36.055' N, 118° 05.199' W). The reference site has over 25 years of monitoring data by the OCSD Ocean Monitoring division and was confirmed by USEPA Region IX. Trawling paths were determined using differential Global Positioning System (GPS) navigation to accurately locate the sampling sites and to control the speed of the trawl (2.0-2.5 knots over the bottom). Currents in the lower water column layer, where effluent is discharged, are directed upcoast.[27] Full secondary treatment for all OCSD effluent has been implemented since 2011.

Fish Collection

Sexually mature Pacific sanddab were collected in February 2017 and March 2017 from the OCSD outfall and reference sites using a 7.6m wide semi-balloon otter

trawl. Individuals were counted, weighed, and measured upon collection. For February 2017 sampling, n = 11 individuals were collected at the outfall with average lengths of 17.59 ± 2.02 cm and average weights of 87.55 ± 39.56 g; n = 12 individuals were collected at the reference with average lengths of 19.23 ± 2.10 cm and average weights of 119.83 ± 48.89 g. For March 2017 sampling, n = 17 individuals were collected at the outfall with average lengths of 16.38 ± 1.59 cm and average weights of 66.25 ± 10.85 g; no individuals were collected at the reference site. Sex of each individual was determined by gross morphology of the gonads. Additionally, sex ratios were tallied at the outfall site of each individual collected during March 2017 sampling (n males = 39, n females = 41). Fish were kept in a flow-through holding tank receiving fresh seawater prior to processing. About >1 mL of blood was collected from the dorsal aorta using a 22-gauge syringe and was immediately centrifuged for 10 minutes at 10,000 rpm. The plasma supernatant was transferred to a new tube and kept on dry ice until long-term storage at -80°C for further analysis. Individuals were sacrificed by severing of the spinal cord, followed by harvesting of liver and gonad tissues. Tissues were kept on dry ice until transferred to storage at -80°C where they were stored until analysis.

Current Data

For individuals collected during February 2017 sampling, hepatic mRNA transcript levels for vitellogenin were quantified through real-time quantitative PCR (RT-qPCR) and normalized to 18S rRNA using primers in Table 2.1. Total RNA extractions from liver tissue were performed using Qiagen RNeasy® Mini Kit (Valencia, CA)

according to the manufacturer's protocol. RNA concentration and integrity was measured on a NanoDrop® ND-1000 UV-Vis Spectrophotometer (Wilmington, DE) prior to cDNA synthesis. First strand cDNA was synthesized using Promega™ Reverse Transcription System (Madison, WI) with random primers according to manufacturer's protocol. cDNA products were then utilized for the RT-qPCR reaction using Bio-Rad SsoAdvanced™ Universal SYBR® Green Supermix (Hercules, CA) on a Bio-Rad CFX96 real-time PCR Detection System (Hercules, CA). The thermal cycling profile consisted of an initial denaturation at 95 °C for 3 minutes, followed by 40 cycles of denaturation at 95 °C for 10 seconds, annealing at 55°C for 30 seconds, and extension at 95 °C for 10 seconds. qPCR products were verified using gel electrophoresis. Each sample was run in duplicate and mean values were calculated. Relative gene expression of vitellogenin between fish from outfall and reference sites was derived using the $2^{-\Delta\Delta CT}$ method among males and females individually.

Plasma testosterone and E_2 were quantified in Pacific sanddab plasma samples collected in February and March 2017 using ELISA assay kits from Cayman Chemical (Ann Arbor, MI). Standard curves were produced following the manufacturer's protocol to obtain plasma testosterone and E_2 levels. GSI and LSI values were calculated using the equation GSI/LSI $= \frac{organ\ weight}{body\ weight}\ x\ 100$ for all Pacific sanddab collected during February 2017 sampling. Additionally, population sex ratios from February and March 2017 sampling were tabulated using gross morphology of gonads.

Historical Population Data

Historical OCSD trawl data, containing length and weight information on individuals captured during trawls, was used to calculate Fulton's condition factor (K) for Pacific sanddab using the equation $K = \frac{\text{body weight}}{\text{length}^3} \times 100$. Average yearly condition factor was calculated for all individuals collected at outfall and reference sites from 2006 to 2014. Historical trawl data was used to obtain Pacific sanddab abundances at outfall and reference sites from August 2005 to January 2017. These abundance values represent the total number of Pacific sanddab individuals collected during each biannual OCSD trawl at a given site. Fish community Shannon Weiner diversity indices (H) were gathered from OCSD Ocean Monitoring Annual reports (www.ocsd.com) from 2009 to 2015 for both outfall and reference sites from summer trawls.

Oceanographic Variable Data

Long-term ocean temperature data at the outfall and reference sites were acquired from OCSD from August 2005 to January 2017. Temperatures for the 50 to 60 m water column range were averaged for each year at outfall and reference sites to reflect temperatures Pacific sanddab are exposed to. Additional temperature data from OCSD Ocean Monitoring Annual Reports were used to substitute missing values in the long-term temperature data. Ocean temperature data were also obtained from California Cooperative Oceanic Fisheries Investigations (CalCOFI) cruise data reports at Station 90.0 30.0 (33° 25.1' N, 117° 54.4' W) at depths of 50m and 60 m (www.calcofi.org). Pacific Decadal Oscillation index values, which represent the long-term patterns in

Pacific climate variability, were obtained from the Joint Institute for the Study of the Atmosphere and Ocean (http://research.jisao.washington.edu/pdo/). Finally, Multivariate ENSO Index (MEI) values were obtained from the National Oceanic and Atmospheric Administration (https://www.esrl.noaa.gov/psd/enso/mei/). All oceanographic variable data were acquired from August 2005 to January 2017 for points in time corresponding to biannual OCSD trawls during which Pacific sanddab were collected.

Statistical Analyses

Statistical analyses were done using RStudio Version 1.1.447. The level of significance for all statistical analyses was determined at $p < 0.05$. Data were assessed for normality of distribution and homogeneity of variance using Shaprio-Wilk and F-tests. For normal data with equal variance, difference in means among two groups were assessed using a Student's t-test. For non-normal data, a Mann-Whitney U test was used to assess the difference in means between two groups. A chi-square goodness of fit test was used to determine whether observed frequencies significantly varied from the expected frequencies. To test for monotonic trends in a series of observations over time, a simple linear regression was used for normal data and a Mann-Kendall trend test was used for non-normal data.

To assess the relationship between Pacific sanddab abundances at OCSD sites and various oceanographic variables, statistical methods outlined in Allen et al. (2004) were followed. Oceanographic variables, the independent variables, included in the analysis were ocean temperature at the OCSD outfall and reference sites, CalCOFI ocean

temperatures at 50m and 60m depth, PDO index, and MEI. Prior to analysis, abundance and oceanographic variable values were converted to z-scores to standardize the data. Linear regression analyses were run to model the relationships between Pacific sanddab abundances at both outfall and reference sites and the various oceanographic variables. Regression models were created for time lags of 0, 1, 2, and 3 years for each independent variable as there may be a delay in response of fish populations to changes in oceanographic parameters.

Results

Current Data

Hepatic vitellogenin expression in male fish collected in February 2017 did not significantly differ between reference and outfall sites (Mann-Whitney U test; p = 0.5556) (Figure 2.S1). Similarly, testosterone levels between outfall and reference sites were not significantly different in males collected in February or June of 2017 (Mann-Whitney U test; p = 0.9096) (Figure 2.S2). E_2 in males could not be quantified as levels were below the detection limit of 0.65 pg/mL.

Average GSI values of male and female Pacific sanddab were unchanged (Student's t-test; p = 0.7212, p = 0.3960, respectively) but GSI trended higher at the outfall site (Figure 2.2). Average HSI of male Pacific sanddab trended higher at the outfall site relative to the reference site but this difference was not statistically significant (Student's t-test; p = 0.6000). As for females, there was a non-significant trend of higher HSI values at the outfall site relative to the reference site (Student's t-test; p = 0.2029).

Pacific sanddab population sex ratios were derived for outfall (n = 80) and reference sites (n = 12) using population survey data collected during March 2017 trawl sampling (Figure 2.S3). Pacific sanddab sex distributions did not significantly deviate from the hypothesized 50% distribution of males and females at either outfall (Chi-square goodness of fit; $\chi^2 = 0.05$, $p = 0.8231$) or reference sites (Chi-square goodness of fit; $\chi^2 = 0.3333$, $p = 0.5637$).

Historical Population Data

Condition factor in individuals remained relatively constant from 2006 to 2014 at both outfall and reference sites (Figure 2.S4). There was no significant upward or downward monotonic trend in condition factor at either outfall (Mann-Kendall; $p = 0.6022$) or reference sites (Mann-Kendall; $p = 0.7544$) throughout the time period. Pacific sanddab population abundance showed significant downward trends at both outfall (Linear regression; $p = 0.0009$) and reference sites (Linear regression; $p = 0.0218$) from 2005 to 2017 (Figure 2.3). For species diversity, there was no significant upward or downward trend in the H index at the outfall (Linear regression; $p = 0.4091$) and reference sites (Linear regression; $p = 0.8403$), suggesting constant species diversity throughout the timeframe (Figure 2.S5).

Oceanographic Variable Data

Pacific sanddab abundances and oceanographic variables in question were presented in LOESS-smoothed plots to visualize temporal patterns (Figure 2.4). To assess

the influence of the oceanographic variables on Pacific sanddab abundances, regression models were computed among abundance and each independent variable for time lags of 0, 1, 2, and 3 years (Table 2.2). Pacific sanddab abundances at the OCSD outfall site had a significant relationship with PDO (Linear regression; $p = 0.014$; 2-year lag) and MEI (Linear regression; $p = 0.021$; 2-year lag). Abundance at the reference site showed a significant relationship with ocean temperature at the OCSD reference site (Linear regression; $p = 0.01$; no lag) for the CalCOFI 50m depth ocean temperature measurements (Linear regression; $p = 0.018$; no lag), CalCOFI 60m depth ocean temperature measurements (Linear regression; $p = 0.023$; no lag), and PDO (Linear regression; $p = 0.01$; 3-year lag).

Discussion

Previously, male hornyhead turbot have demonstrated induction of vitellogenin production at the OCSD outfall site.[20,21,37] However, in the present study, vitellogenin expression in male Pacific sanddab did not differ among individuals collected at outfall and reference sites. Lack of vitellogenin induction in male Pacific sanddab could be due to limited exposure to xenoestrogens or absence of measureable plasma E_2, the principal hormone believed to control vitellogenin production.[38] Species differences in sensitivity to environmental estrogens[39,40] or variation in sensitivity and responsiveness of the estrogen receptor[41–44] may also contribute to observed species differences in vitellogenin production. Furthermore, variation in life histories or in detoxification strategies may account for these differences in how species react to exposure to estrogenic agents in the

environment. In female Pacific sanddab, a trend of higher vitellogenin levels at the outfall site relative to the reference site was observed. Rather than being linked to alterations due to environmental estrogens, females may have higher vitellogenin production due to greater reproductive success as a result of more resources and energy reserves at the outfall site.[45]

Unlike previous studies where E_2 was observed in male hornyhead turbot at the OCSD outfall,[20] E_2 was below the detection limit in male Pacific sanddab. The lack of effect in Pacific sanddab may be related to species differences in E_2 production caused by a number of factors, such as processing and turnover of contaminants, differential chemical uptake, species-specific receptor interactions, and variability in bioconcentration.[46] Other factors such as differences in species behavior, such as movement and trophic status, could also influence chemical exposure,[47,48] and, therefore, E_2 production as well. As testosterone levels in males were likewise unaltered between outfall and reference sites, hormone impairment does not appear to be present in Pacific sanddab at the OCSD outfall.

GSI and HSI were similarly not statistically different in male and female Pacific sanddab between outfall and reference sites. In females, GSI tended to be higher at the outfall site which is likely correlated to elevated vitellogenin production in females at the outfall site.[49] HSI trended higher in both males and females at the outfall site relative to the reference site. As the main reserve of fat in demersal flatfish is stored in the liver, HSI is considered a measure of energy reserves in fish.[50–52] Higher HSI values at the outfall

indicate higher energy storage in these individuals, likely as a result of greater availability of prey and resources as reflected by higher H index values at the outfall.

Pacific sanddab populations at the OCSD outfall and reference sites did not exhibit altered sex ratios. Previous studies have observed that exposure to wastewater treatment plant effluent can alter estrogenic pathways involved in sexual development and, therefore, may alter sex ratios in fish populations.[16,53,54] However, the observed evenly-distributed sex ratios among OCSD Pacific sanddab populations suggests there may not be alterations in estrogenic pathways that would result in skewed sex ratios. Altogether, data collected from 2017 sampling show no evidence that estrogenic activity is contributing to declines.

As for historical population data, condition factor of Pacific sanddab at outfall and reference sites from 2006 to 2014 have remained constant and have not shown a distinct upward or downward trend. This suggests that energy and nutritional status of Pacific sanddab at the OCSD sites have remained relatively unaltered throughout this time frame.[55] Biological communities at the OCSD outfall area do not appear to be impaired as reflected by measures of diversity. H indices remained relatively constant at both the OCSD outfall and reference sites from 2009 to 2015, suggesting no major perturbations at the outfall during the timeframe. In fact, H index was consistently higher at the outfall than the reference site, suggesting the outfall may provide higher quality habitat for its constituents. While the OCSD outfall provides artificial reef structure and supports communities typically found within hard substrate habitats, the OCSD reference site is composed of soft sandy bottoms.[56,57] Hard substrate habitats typically have higher species

diversity than soft substrate habitats by providing greater availability and variety of habitat,[29,58,59] potentially explaining the higher H index values observed at the outfall site.

Since there were no significant changes in estrogenic parameters for Pacific sanddab throughout the OCSD monitoring area, other environmental endpoints were explored as a potential cause for population reductions. Significant inverse relationships were observed between Pacific sanddab abundance and ocean temperature, PDO, and MEI. During periods of warmer ocean temperatures or warmer climate regimes, there was a corresponding decrease in population abundances, especially in the most recent years (Figure 2.4). In the worst-case scenario, warmer temperatures could be outside the optimal physiological range of Pacific sanddab, causing increased mortality and reduced fitness and, thus, population declines.[60] Alternatively, warmer ocean temperatures may cause individuals to move to colder waters where they are not accounted for during OCSD surveys. Migration of Pacific sanddab to deeper, colder waters is probable as Citharichthids are known to relocate in response to temperature fluctuations.[61] In a related species, the speckled sanddab (*Citharichthys stigmaeus*), temperature has been shown to have an effect on the distribution of individuals within localized regions.[61] While a causal link cannot be concluded at this time, the association observed in the current study warrants additional evaluation of the effects of temperature on behavior or recruitment of Pacific sanddab in this region.

While temperature indicated a significant association with populations of this species, other environmental factors should not be ignored. Wild fish populations are susceptible to the effects of several interacting biotic and abiotic factors, making it is

difficult to elucidate the mechanisms for population declines. Of these factors, disease and parasites likely are not contributing to population declines in the OCSD monitoring region; during the 2016-2017 sampling season, less than 1% of fishes exhibited external parasites or other external abnormalities, such as tumors, fin erosion, and skin lesions.[34] Furthermore, demersal flatfish muscle and liver tissue concentrations of mercury, ΣDDT, ΣPCB, and chlorinated pesticides were similar at outfall and non-outfall sites, were within the historical ranges at the OCSD monitoring region, and were below federal and state human consumption guidelines.[34] These tissue contaminant results indicate that other toxicants likely do not play a major role in population declines. More data is needed on the prevalence of other stressors (habitat loss, fishing pressure, predation, etc.) in order to understand the role of interacting biotic and abiotic factors on Pacific sanddab population declines.

In summary, our results do not provide evidence that estrogenic activity is contributing to observed declines in Pacific sanddab within the OCSD ocean monitoring area. Individuals did not show any impairment in terms of population sex ratios, condition factor, organ health indices, hormones, or vitellogenin production which are typically observed when estrogenic contaminants are present and exposure occurs to fish. Based on our preliminary assessments of environmental parameters, a more careful examination of temperature impacts on fish populations may provide more fruitful results to better understand fishery population dynamics in the Southern California Bight as well as other coastal regions.

References

(1) Lye, C. M.; Frid, C. L. J.; Gill, M. E.; Mccormickt, D. Abnormalities in the Reproductive Exposed to Effluent from a Sewage Treatment Works. *Mar. Pollut. Bull.* **1997**, *34* (1), 34–41.

(2) Jobling, S.; Nolan, M.; Tyler, C. R.; Brighty, G.; Sumpter, J. P. Widespread Sexual Disruption in Wild Fish. *Environ. Sci. Technol.* **1998**, *32* (17), 2498–2506. https://doi.org/10.1021/es9710870.

(3) Allen, Y.; Matthiessen, P.; Scott, A. P.; Haworth, S.; Feist, S.; Thain, J. E. The Extent of Oestrogenic Contamination in the UK Estuarine and Marine Environments - Further Surveys of Flounder. *Sci. Total Environ.* **1999**, *233* (1–3), 5–20. https://doi.org/10.1016/S0048-9697(99)00175-8.

(4) Kidd, K. A.; Blanchfield, P. J.; Mills, K. H.; Palace, V. P.; Evans, R. E.; Lazorchak, J. M.; Flick, R. W. Collapse of a Fish Population after Exposure to a Synthetic Estrogen. *Proc. Natl. Acad. Sci. U. S. A.* **2007**, *104* (21), 8897–8901. https://doi.org/10.1073/pnas.0609568104.

(5) Palace, V. P.; Evans, R. E.; Wautier, K.; Baron, C.; Vandenbyllardt, L.; Vandersteen, W.; Kidd, K. Induction of Vitellogenin and Histological Effects in Wild Fathead Minnows from a Lake Experimentally Treated with the Synthetic Estrogen, Ethynylestradiol. *Water Qual. Res. J.* **2002**, *37* (3), 637–650. https://doi.org/10.2166/wqrj.2002.042.

(6) Jobling, S.; Reynolds, T.; White, R.; Parker, M. G.; Sumpter, J. P. A Variety of Environmentally Persistent Chemicals, Including Some Phthalate Plasticizers, Are Weakly Estrogenic. *Environ. Health Perspect.* **1995**, *103* (6), 582–587. https://doi.org/10.1289/ehp.95103582.

(7) Thomas, K. V; Hurst, M. R.; Matthiessen, P.; Waldock, M. J. Characterization of Estrogenic Compounds in Water Samples Collected from United Kingdom Estuaries. *Environ. Toxicol. Chem.* **2001**, *20* (10), 2165–2170. https://doi.org/10.1897/1551-5028(2001)020<2165:coeciw>2.0.co;2.

(8) Bay, S. M.; Vidal-Dorsch, D. E.; Schlenk, D.; Kelley, K. M.; Maruya, K. A.; Gully, J. R. Integrated Coastal Effects Study: Synthesis of Findings. *Environ. Toxicol. Chem.* **2012**, *31* (12), 2711–2722. https://doi.org/10.1002/etc.2007.

(9) Vidal-Dorsch, D. E.; Bay, S. M.; Maruya, K.; Snyder, S. A.; Trenholm, R. A.; Vanderford, B. J. Contaminants of Emerging Concern in Municipal Wastewater Effluents and Marine Receiving Water. *Environ. Toxicol. Chem.* **2012**, *31* (12), 2674–2682. https://doi.org/10.1002/etc.2004.

(10) Lyon, G. S.; Sutula, M. A. Effluent Discharges to the Southern California Bight from Large Municipal Wastewater Treatment Facilities from 2005 to 2009. **2006**.

(11) Schlenk, D.; Sapozhnikova, Y.; Irwin, M. A.; Xie, L.; Hwang, W.; Reddy, S.; Brownawell, B. J.; Armstrong, J.; Kelly, M.; Montagne, D. E.; et al. In Vivo Bioassay-Guided Fractionation of Marine Sediment Extracts From the Southern California Bight, Usa, for Estrogenic Activity. *Environ. Toxicol. Chem.* **2005**, *24* (11), 2820. https://doi.org/10.1897/05-116R.1.

(12) Maruya, K. A.; Vidal-Dorsch, D. E.; Bay, S. M.; Kwon, J. W.; Xia, K.; Armbrust, K. L. Organic Contaminants of Emerging Concern in Sediments and Flatfish Collected near Outfalls Discharging Treated Wastewater Effluent to the Southern California Bight. *Environ. Toxicol. Chem.* **2012**, *31* (12), 2683–2688. https://doi.org/10.1002/etc.2003.

(13) Bay, S. M.; Vidal-Dorsch, D. E.; Schlenk, D.; Kelley, K. M.; Baker, M. E.; Maruya, K. A.; Gully, J. R. *Sources and Effects of Endocrine Disruptors and Other Contaminants of Emerging Concern in the Southern California Bight Coastal Ecosystem*; 2011.

(14) Orange County Sanitation District. *Ocean Monitoring Annual Report 2011-2012*; 2012.

(15) Jobling, S.; Sheahan, D.; Osborne, J. A.; Matthiessen, P.; Sumpter, J. P. Inhibition of Testicular Growth in Rainbow Trout (Oncorhynchus Mykiss) Exposed to Estrogenic Alkylphenolic Chemicals. *Environ. Toxicol. Chem.* **1996**, *15* (2), 194–202. https://doi.org/10.1897/1551-5028(1996)015<0194:IOTGIR>2.3.CO;2.

(16) Nimrod, A. C.; Benson, W. H. Reproduction and Development of Japanese Medaka Following an Early Life Stage Exposure to Xenoestrogens. *Aquat. Toxicol.* **1998**, *44*, 141–156.

(17) Desbrow, C.; Routledge, E. J.; Brighty, G. C.; Sumpter, J. P.; Waldock, M. Identification of Estrogenic Chemicals in STW Effluent. 1. Chemical Fractionation and in Vitro Biological Screening. *Environ. Sci. Technol.* **1998**, *32* (11), 1549–1558.

(18) Nakamura, M.; Nagoya, H.; Hirai, T. Nonylphenol Induces Complete Feminization of the Gonad in Genetically Controlled All-Male Amago Salmon. *Fish. Sci.* **2002**, *68* (6), 1387–1389. https://doi.org/10.1046/j.1444-2906.2002.00579.x.

(19) Roy, L. a; Armstrong, J. L.; Sakamoto, K.; Steinert, S.; Perkins, E.; Lomax, D. P.;

Johnson, L. L.; Schlenk, D. The Relationships of Biochemical Endpoints to Histopathology and Population Metrics in Feral Flatfish Species Collected near the Municipal Wastewater Outfall of Orange County, California, USA. *Environ. Toxicol. Chem.* **2003**, *22* (6), 1309–1317. https://doi.org/10.1897/1551-5028(2003)022<1309:TROBET>2.0.CO;2.

(20) Ann Rempel, M.; Reyes, J.; Steinert, S.; Hwang, W.; Armstrong, J.; Sakamoto, K.; Kelley, K.; Schlenk, D. Evaluation of Relationships between Reproductive Metrics, Gender and Vitellogenin Expression in Demersal Flatfish Collected near the Municipal Wastewater Outfall of Orange County, California, USA. *Aquat. Toxicol.* **2006**, *77* (3), 241–249. https://doi.org/10.1016/j.aquatox.2005.12.007.

(21) Forsgren, K. L.; Bay, S. M.; Vidal-Dorsch, D. E.; Deng, X.; Lu, G.; Armstrong, J.; Gully, J. R.; Schlenk, D. Annual and Seasonal Evaluation of Reproductive Status in Hornyhead Turbot at Municipal Wastewater Outfalls in the Southern California Bight. *Environ. Toxicol. Chem.* **2012**, *31* (12), 2701–2710. https://doi.org/10.1002/etc.2006.

(22) Levitus, S.; Antonov, J. I.; Boyer, T. P.; Stephens, C. Warming of the World Ocean. *Science (80-.).* **2000**, *287*, 2225–2229.

(23) Hansen, J.; Ruedy, R.; Sato, M.; Lo, K. Global Surface Temperature Change. *Rev. Geophys* **2010**, *48*. https://doi.org/10.1029/2010RG000345.

(24) Allen, M. J.; Smith, R. W.; Jarvis, E. T.; Raco-Rands, V.; Bernstein, B. B.; Herbinson, K. T. *Temporal Trends in Southern California Coastal Fish Populations Relative to 30-Year Trends in Oceanic Conditions*; 2004.

(25) Orange County Sanitation District. *Ocean Monitoring Annual Report 2006-2007*; 2007.

(26) Orange County Sanitation District. *Ocean Monitoring Annual Report 2007-2008*; 2008.

(27) Orange County Sanitation District. Ocean Monitoring Annual Report 2008-2009, 2009.

(28) Orange County Sanitation District. *Ocean Monitoring Annual Report 2009-2010*; 2010.

(29) Orange County Sanitation District. *Ocean Monitoring Annual Report 2010-2011*; 2011.

(30) Orange County Sanitation District. *Ocean Monitoring Annual Report 2012-2013*;

2013.

(31) Orange County Sanitation District. *Ocean Monitoring Annual Report Year 2013-2014*; 2014.

(32) Orange County Sanitation District. *Ocean Monitoring Annual Report 2014-2015*; 2015.

(33) Orange County Sanitation District. *Ocean Monitoring Annual Report 2015-2016*; 2016.

(34) Orange County Sanitation District. *Ocean Monitoring Annual Report 2016-2017*; 2017.

(35) Allen, M. J. Functional Structure of Soft-Bottom Fish Communities of the Southern California Shelf, University of California, San Diego, 1982.

(36) Love, M. S.; Goldberg, S. R. A Histological Examination of the Ovaries of Pacific Sanddab, Citharichthys Sordidus, Captured at Two Oil Platforms and Two Natural Sites in the Southern California Bight. *Bull. South. Calif. Acad. Sci.* **2009**, *108* (2), 45–51.

(37) Deng, X.; Rempel, M. A.; Armstrong, J.; Schlenk, D. Seasonal Evaluation of Reproductive Status and Exposure to Environmental Estrogens in Hornyhead Turbot at the Municipal Wastewater Outfall of Orange County, CA. *Environ. Toxicol.* **2007**, *22* (5), 464–471. https://doi.org/10.1002/tox.20287.

(38) von der Decken, A.; Waters, S. Modulation of Hepatic Chromatin Structure in Response to 17-Beta Estradiol Induced Activation of the Vitellogenin Gene Regions in Atlantic Salmon, Salmo Salar. *Acta Biochim. Pol.* **1993**, *40* (1), 23–28.

(39) Matthiessen, P. Endocrine Disruption in Marine Fish. *Pure Appl. Chem* **2003**, *75*, 11–12.

(40) Van Den Belt, K.; Verheyen, R.; Witters, H. Comparison of Vitellogenin Responses in Zebrafish and Rainbow Trout Following Exposure to Environmental Estrogens. *Ecotoxicol. Environ. Saf.* **2003**, *56*, 271–281. https://doi.org/10.1016/S0147-6513(03)00004-6.

(41) Matthews, J.; Zacharewski, T. Differential Binding Affinities of PCBs, HO-PCBs, and Aroclors with Recombinant Human, Rainbow Trout (Onchorhynkiss Mykiss), and Green Anole (Anolis Carolinensis) Estrogen Receptors, Using a Semi-High Throughput Competitive Binding Assay. *Toxicol. Sci.* **2000**, *53* (326–339).

(42) Harris, H. A.; Bapat, A. R.; Gonder, D. S.; Frail, D. E. The Ligand Binding Profiles of Estrogen Receptors and Are Species Dependent. *Steroids* **2002**, *67*, 379–884.

(43) Lange, A.; Katsu, Y.; Miyagawa, S.; Ogino, Y.; Urushitani, H.; Kobayashi, T.; Hirai, T.; Shears, J. A.; Nagae, M.; Yamamoto, J.; et al. Comparative Responsiveness to Natural and Synthetic Estrogens of Fish Species Commonly Used in the Laboratory and Field Monitoring. *Aquat. Toxicol.* **2012**, *109*, 250–258. https://doi.org/10.1016/j.aquatox.2011.09.004.

(44) Le Dréan, Y.; Kern, L.; Pakdel, F.; Valotaire, Y. Rainbow Trout Estrogen Receptor Presents an Equal Specificity but a Differential Sensitivity for Estrogens than Human Estrogen Receptor. *Mol. Cell. Endocrinol.* **1995**, *109* (1), 27–35. https://doi.org/10.1016/0303-7207(95)03482-m.

(45) Kjesbu, S.; Kryvi, H.; Witthames, P. W.; Greer Walker, M. Fecundity, Atresia, and Egg Size of Captive Atlantic Cod N Relation to Proximate Body Composition. *Can. J. Fish. Aquat. Sci.* **1991**, *48*, 2333–2343.

(46) Tyler, C. R.; Spary, C.; Gibson, R.; Santos, E. M.; Shears, J.; Hill, E. M. Accounting for Differences in Estrogenic Responses in Rainbow Trout (Oncorhynchus Mykiss: Salmonidae) and Roach (Rutilus Rutilus: Cyprinidae) Exposed to Effluents from Wastewater Treatment Works. *Environ. Sci. Technol.* **2005**, *39*, 2599–2607. https://doi.org/10.1021/es0488939.

(47) Young, D. R.; Mearns, A. J. *Pollutant Flow through Food Webs*; El Segundo, CA, 1978.

(48) Mann, R. A.; Ajani, P. Bioaccumulation of Organochlorines and Trace Metals in fish—Sydney Deepwater Outfalls Environmental Monitoring Program. In *Proceedings of a Bioaccumulation Workshop: Assessment of the Distribution, Impacts and Bioaccumulation of Contaminants in Aquatic Environments*; Water Board and Australian Marine Sciences Association Inc, 1992; pp 65–79.

(49) Tyler, C. R.; Sumpter, J. P.; Sumpter, T. Oocyte Growth and Development in Teleosts. *Rev. Fish Biol. Fish.* **1996**, *6*, 287–318.

(50) Jensen, A. J. The "Gut Index", a New Parameter to Measure the Gross Nutritional State of Arctic Char, Salvelinus Alpinus (L.) and Brown Trout, Salmo Trutta L. *J. Fish Biol.* **1980**, *17* (6), 741–747. https://doi.org/10.1111/j.1095-8649.1980.tb02805.x.

(51) Adams, S. M. Ecological Role of Lipids in the Health and Success of Fish Populations BT - Lipids in Freshwater Ecosystems; Arts, M. T., Wainman, B. C.,

Eds.; Springer New York: New York, NY, 1999; pp 132–160. https://doi.org/10.1007/978-1-4612-0547-0_8.

(52) Shulman, G. E.; Love, R. . M. *The Biochemical Ecology of Marine Fishes*; Southward, A. J., Tyler, P. A., Young, C. M., Eds.; Academic Press, 1999.

(53) Jobling, S.; Williams, R.; Johnson, A.; Taylor, A.; Gross-Sorokin, M.; Nolan, M.; Tyler, C. R.; van Aerle, R.; Santos, E.; Brighty, G. Predicted Exposures to Steroid Estrogens in U.K. Rivers Correlate with Widespread Sexual Disruption in Wild Fish Populations. *Environ. Health Perspect.* **2006**, *114* (Supplement 1), 32–39. https://doi.org/10.1289/ehp.8050.

(54) Vajada, A. M.; Barber, L. B.; Gray, J. L.; Lopez, E. M.; Woodling, J. D.; Norris, D. O. Reproductive Disruption in Fish Downstream from an Estrogenic Wastewater Effluent. *Environ. Sci. Technol.* **2008**, *42*, 3407–3414. https://doi.org/10.1021/es0720661.

(55) Lambert, Y.; Dutil, J.-D.; Dutil, L. Energetic Consequences of Reproduction in Atlantic Cod (Gadus Morhua) in Relation to Spawning Level of Somatic Energy Reserves. *Can. J. Fish. Aquat. Sci.* **2000**, *57*, 815–825.

(56) Lewis, R. D.; McKee, K. *A Guide to Artificial Reefs in Southern California*; 1989.

(57) Orange County Sanitation District. *Ocean Monitoring Annual Report 1999-2000*; 2000.

(58) Thorson, G. Havbundens Dyreliv. Infaunaen, Den Jævne Havbunds Dyresamfund. In *Danmarks natur: Havet*; Nørrevang, A., Meyer, T. J., Eds.; Politikens Forlag: Copenhagen, 1968; pp 82–143.

(59) Niesen, T. M. Intertidal Habitats and Marine Biogeography of the Oregonian Province. In *The Light and Smith Manual-Intertidal Invertebrates from Central California to Oregon (Fourth Edition)*; Carlton, J. T., Ed.; The University of California Press: Richmond, CA, 2007; pp 3–17.

(60) Perry, A. L.; Low, P. J.; Ellis, J. A.; Reynolds, J. D. Climate Change and Distribution Shifts in Marine Fishes. *Science (80-.).* **2005**, *308* (5730), 1912–1915.

(61) Ehrlich, K.; Stephens, J. S.; Muszynski, G.; Hood, J. Thermal Behavior of the Speckled Sanddab, Citharichthys Stigmaeus: Laboratory and Field Investigations. *U.S. Natl. Mar. Fish. Serv. Fish. Bull. 76* **1979**, 867–872.

Figures and Tables

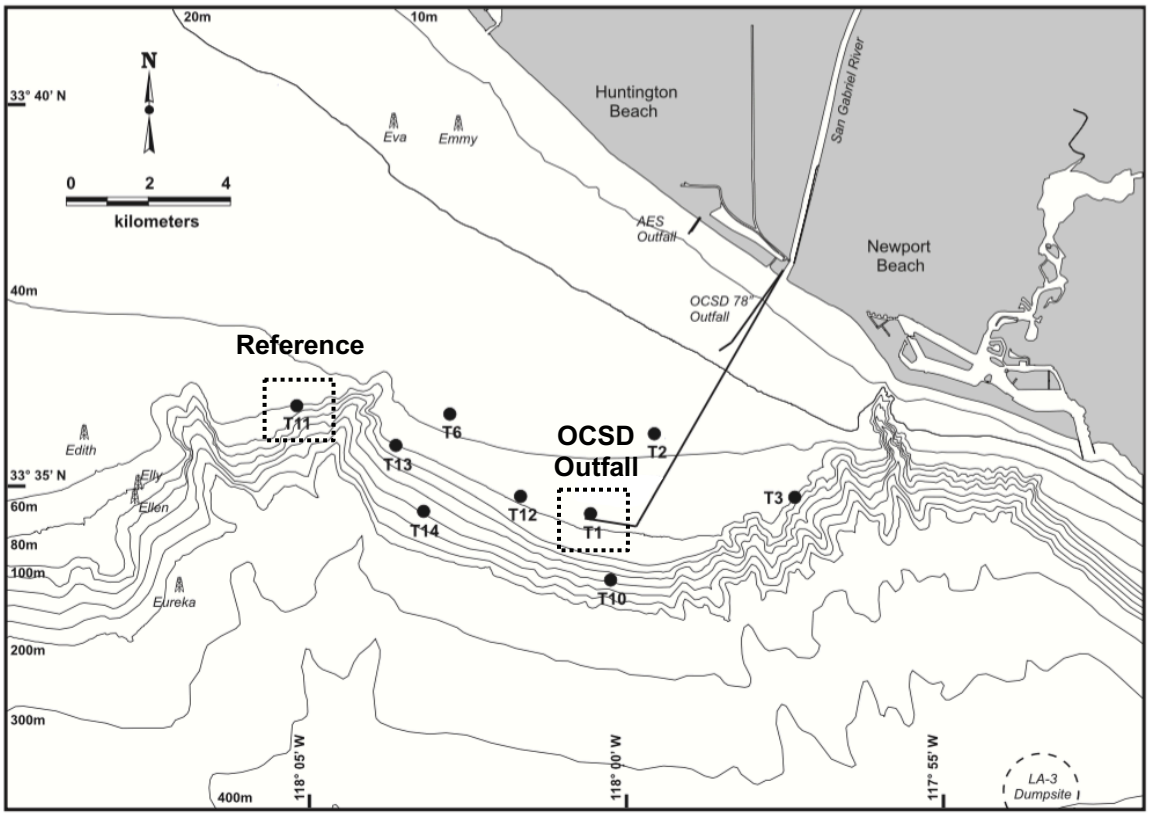

Figure 2.1. The study area for the Orange County Sanitation District (OCSD) ocean monitoring program showing the outfall (T1) and reference (T11) sites (modified from OCSD, 2011).

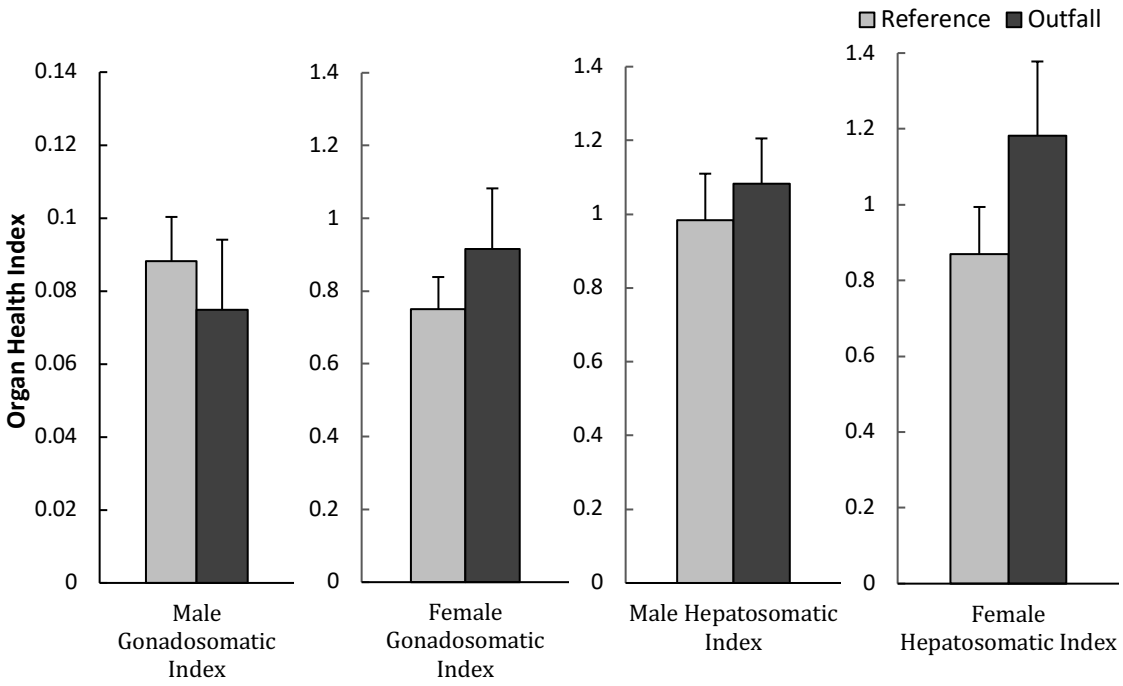

Figure 2.2. Gonadosomatic and hepatosomatic index values for male and female Pacific sanddab (*Citharichthys sordidus*) collected during February 2017 sampling at the Orange County Sanitation District outfall and reference sites.

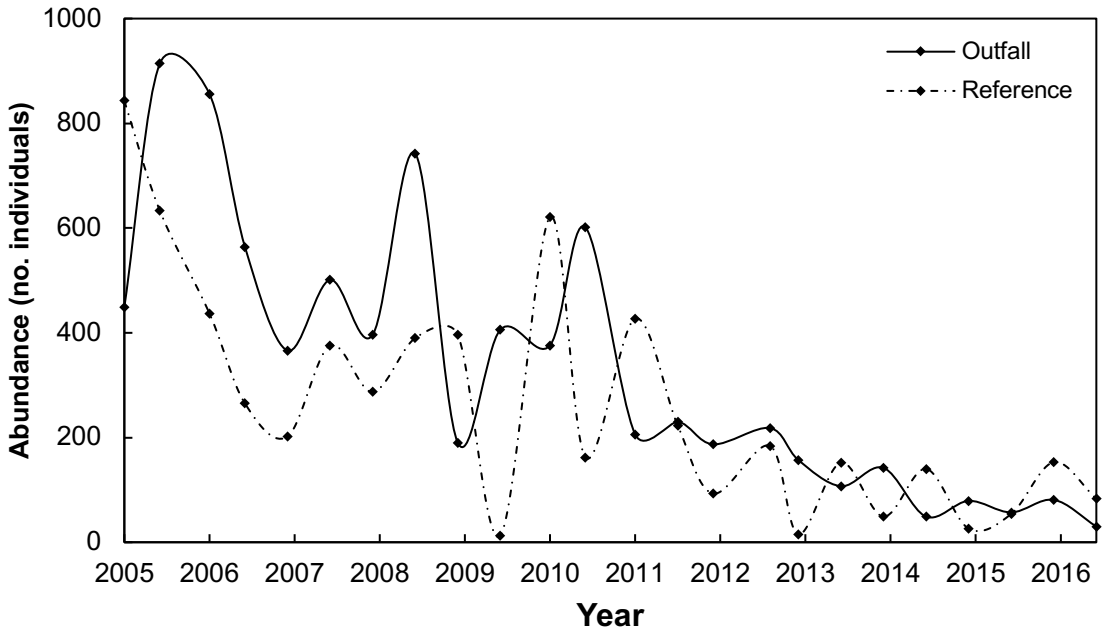

Figure 2.3. Population abundances of Pacific sanddab (*Citharichthys sordidus*) collected at the Orange County Sanitation District outfall and reference sites during biannual trawls from August 2005 to January 2017.

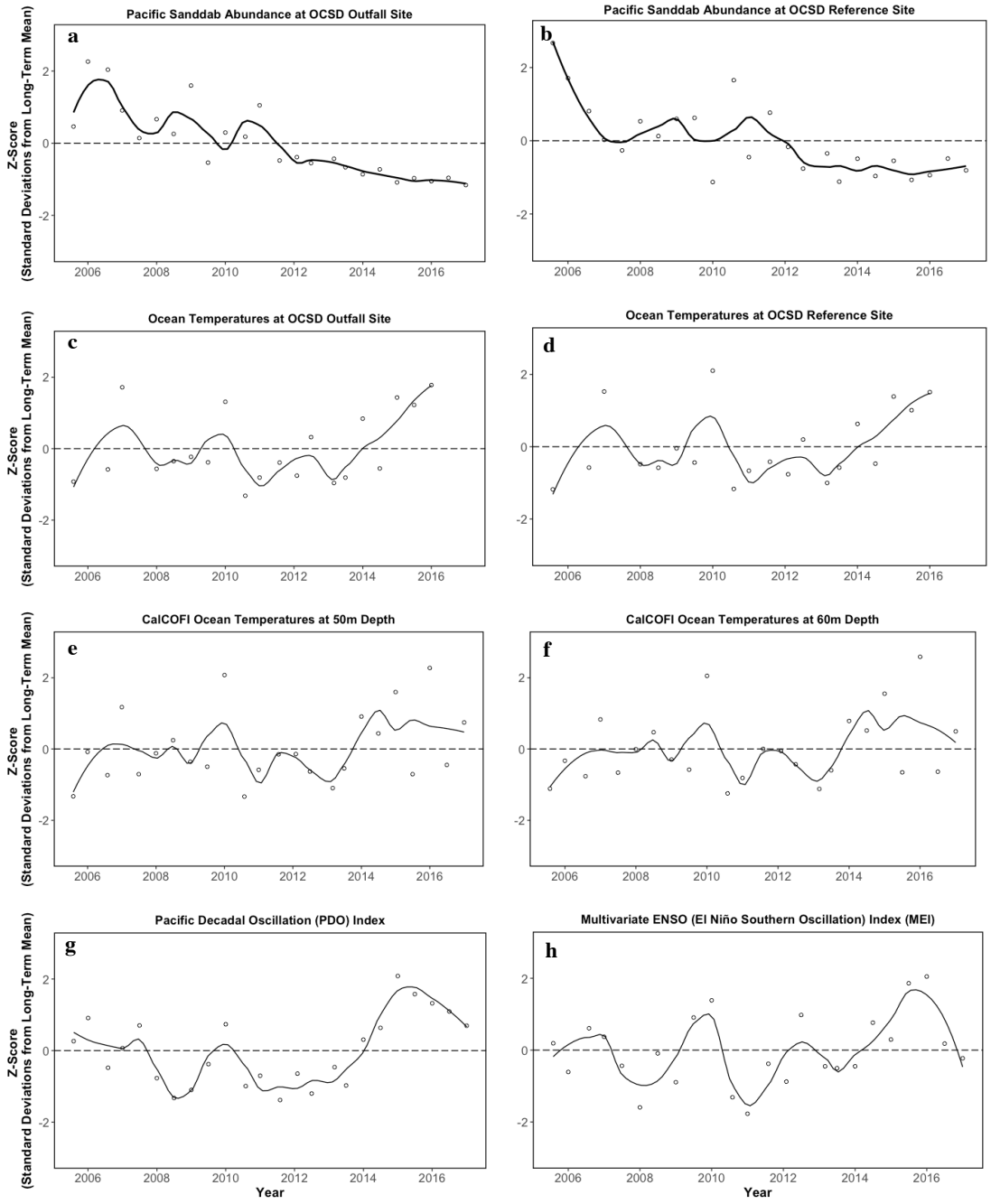

Figure 2.4. LOESS-smoothed temporal trends of a) Pacific sanddab (*Citharichthys sordidus*) abundance at the Orange County Sanitation District (OCSD) outfall site, b) Pacific sanddab abundance at the OCSD reference site, c) ocean temperatures averaged for the 50 to 60m water column at the OCSD outfall site, d) ocean temperatures averaged for the 50 to 60m water column at the OCSD reference site, e) ocean temperatures at 50

m depth from California Cooperative Oceanic Fisheries Investigations (CalCOFI) cruises, f) ocean temperatures at 60 m depth from CalCOFI cruises, g) the Pacific Decadal Oscillation index, and h) the Multivariate El Niño Southern Oscillation Index.

Table 2.1. Primer sequences used for realtime-qPCR quantification of gene expression in Pacific Sanddab (*Citharichthys sordidus*).

Gene	**Forward Primer (5' → 3')**	**Reverse Primer (3' → 5')**	**Source**
18S rRNA	GGTCTGTGATGCCCTTAGATGTC	AGTGGGGTTCAGCGGGTTAC	Zheng and Sun, 2011
Vitellogenin	ATGAAGGGACAGACCTGTGG	AACCCAGGAATGAGCATAGC	Baker et al. 2014

Table 2.2. *p*-values yielded from linear regression analyses between Pacific sanddab (*Citharichthys sordidus*) abundances at Orange County Sanitation District (OCSD) sites and oceanographic variables at time lags of 0, 1, 2, and 3 years. Only values $p \leq 0.1$ were included in the table. Asterisks denotes significant relationship among abundance and the given independent variable at a significance level of $p \leq 0.05$.

	***p*-values**							
	Pacific Sanddab Abundance at Outfall Site				Pacific Sanddab Abundance at Reference Site			
	No Lag	1-Year	2-Year	3-Year	No Lag	1-Year	2-Year	3-Year
Ocean Temperature at OCSD Outfall	-	-	0.080	-	N/A	N/A	N/A	N/A
Ocean Temperature at OCSD Reference	N/A	N/A	N/A	N/A	0.010*	-	-	-
CalCOFI Ocean Temperature at 50 m	-	-	-	-	0.018*	-	-	-
CalCOFI Ocean Temperature at 60 m	-	-	-	-	0.023*	-	-	-
Pacific Decadal Oscillation (PDO) Index	-	-	0.014*	0.053	-	0.087	0.082	0.010*
Multivariate ENSO Index (MEI)	0.083	-	0.021*	-	0.081	-	-	-

Supplemental Information

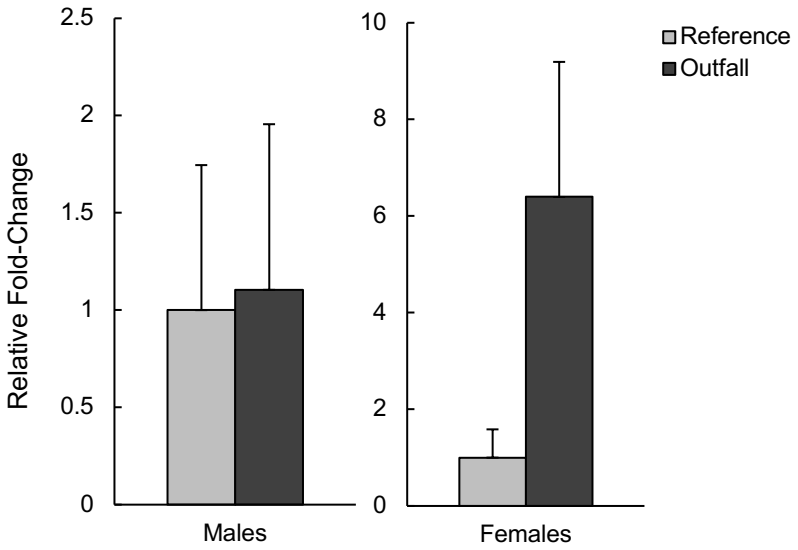

Figure 2.S1. Relative fold-change in hepatic vitellogenin expression among male and female Pacific sanddab (*Citharichthys sordidus*) at Orange County Sanitation District outfall and reference sites collected during February 2017 sampling. Vitellogenin values were normalized to 18S.

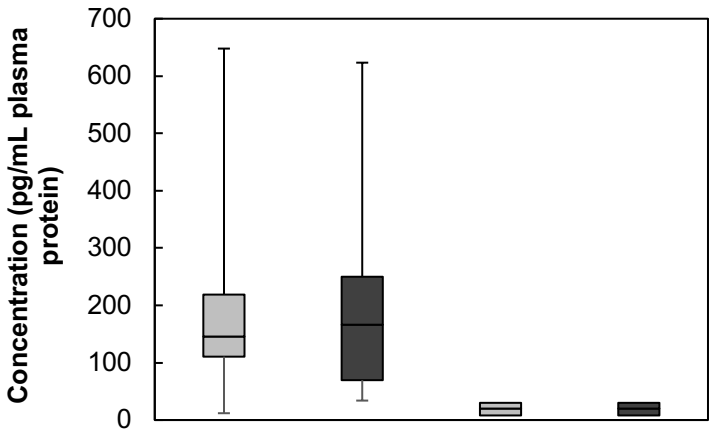

Figure 2.S2. Plasma testosterone and estradiol measurements in male Pacific sanddab (*Citharichthys sordidus*) collected during February and March 2017 sampling at the Orange County Sanitation District outfall and reference sites.

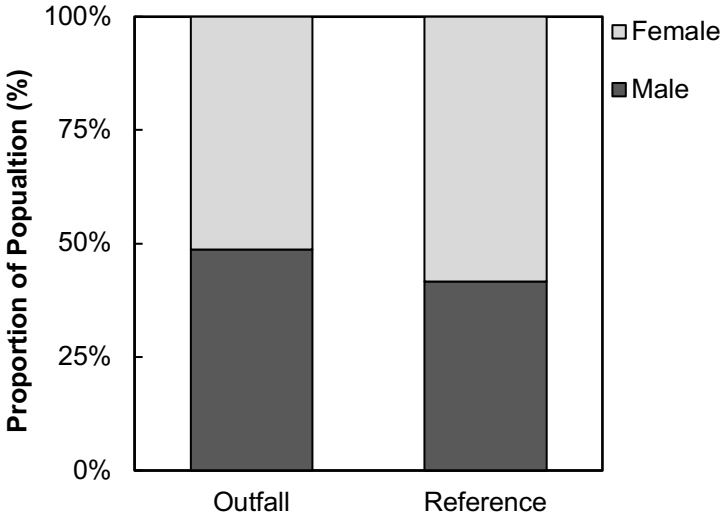

Figure 2.S3. Population sex ratios of Pacific sanddab (*Citharichthys sordidus*) collected at the Orange County Sanitation District outfall (February 2017) and reference sites (March 2017).

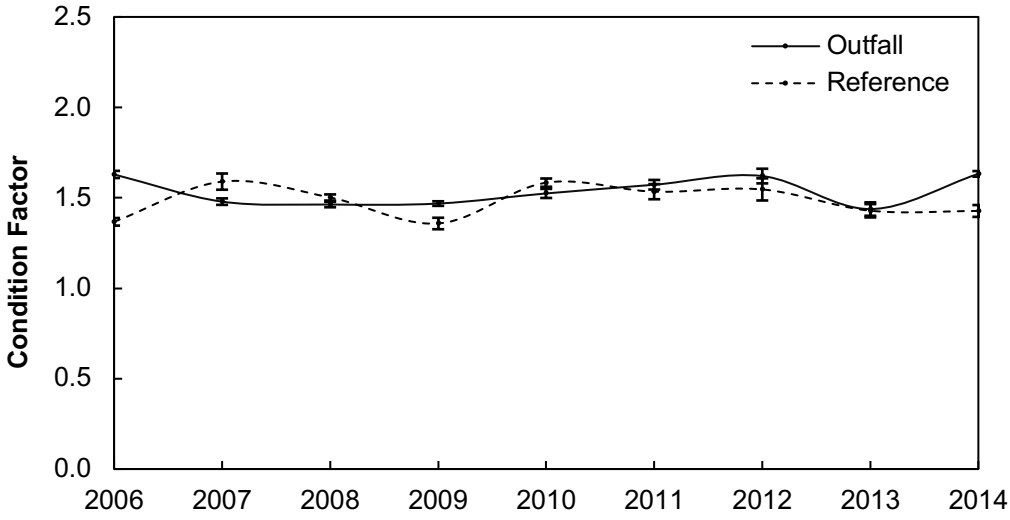

Figure 2.S4. Yearly averages of Fulton's condition factor for Pacific sanddab (*Citharichthys sordidus*) collected during Orange County Sanitation District trawls from 2006 to 2014. Asterisks denote significant difference in condition factor among sites during a given year ($p > 0.05$).

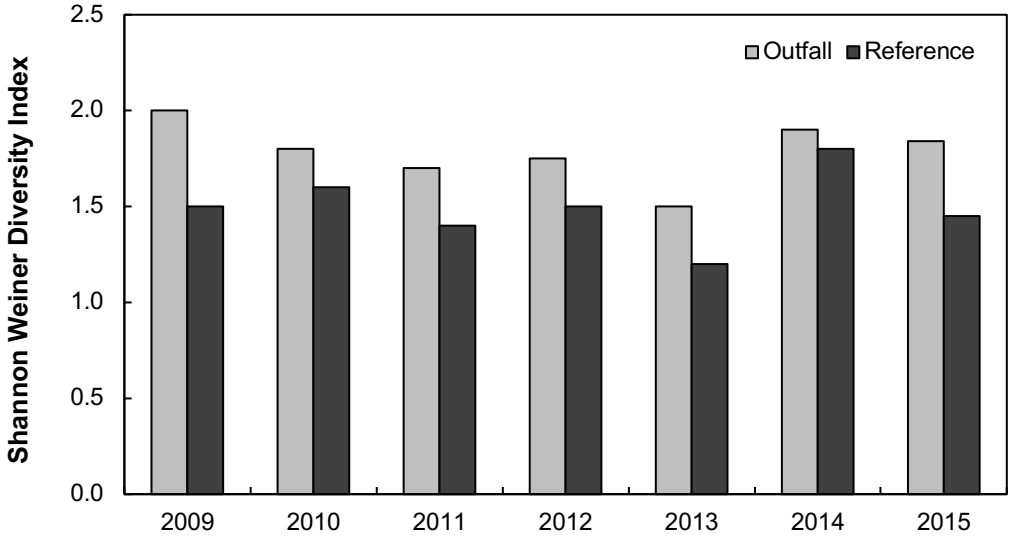

Figure 2.S5. Fish community Shannon Weiner diversity index values (H) at the Orange County Sanitation District outfall and reference sites from 2009 to 2015 during summer trawls.

Chapter 2: Transcriptomics of epidermal mucus as a nonlethal method to evaluate effects of environmental variables among fish populations

Abstract

Although transcriptomic analysis of wild organisms is a powerful tool to understand molecular differences among populations, most methods employed today require the use of lethal sampling. In fish, the use of epidermal mucus is a promising method for the development of nonlethal sampling tools. Previous studies have shown that mRNA is dynamically regulated in fish epidermal mucus following stressor exposure, suggesting that mucus is reflective of molecular changes occurring within the organism in response to its environment. The aim of the present study was to determine whether transcriptomics of mucus could be used discern molecular differences among populations of lake trout. In order to do so, mucus was collected and sequenced from four geographically-distinct lake trout (*Salvelinus namaycush*) populations at the IISD Experimental Lakes Area. Principal component analysis (PCA) and hierarchical clustering of read data showed that each lake trout population had unique transcriptomic profiles, suggesting that RNA sequencing of mucus is able to discern molecular differences among fish populations. Furthermore, differential gene expression analysis identified regulation of immune-related transcripts and viral gene expression transcripts among populations. PCA and a mixed linear model of water quality parameters indicated that environmental variables accounted for transcriptomic variation among populations. However, 32% of transcriptomic variance was unaccounted for by the mixed linear

model, suggesting that other variables may influence transcription, such as epigenetics and presence of pathogens. Overall, results indicate that RNA sequencing of epidermal mucus is an effective, nonlethal method to study transcriptional differences among fish populations and may be especially useful for studies of endangered species.

Introduction

In both laboratory and field experiments, lethal techniques have traditionally been employed in the collection of wildlife tissue for analysis of gene expression, contaminant loading, stable isotopes, and other endpoints of interest. However, there has been pressure in the scientific community to develop nonlethal sampling techniques as sacrifice of wildlife raises concerns, particularly in the study of threatened species.[1,2] To minimize impact on animal welfare, nonlethal analyses of fish health have been increasingly used in scientific studies, including blood sampling,[3,4] fin clipping,[5,6] tissue biopsies,[7–9] and collection of scales.[10,11] The use of fish epidermal mucus for nonlethal assessment of animal health has also become of more interest in the past decade.[12–19] As collection of epidermal mucus is minimally-invasive, inexpensive, rapid, and requires little training, mucus-based analyses are a promising route for furthering the development of nonlethal sampling techniques in fish.

Epidermal mucus has several biological and ecological roles that influence fish health and interaction with the external environment.[20] Mucus is secreted by epidermal goblet cells, forming a protective layer over the epithelial cells of fish skin. Among other functions, mucus is crucial for ionic and osmotic regulation, respiration, locomotion, and

protection against pollutants, pathogens, and abrasion.[21] The multiple roles of epidermal mucus can be attributed to its physical properties as well as its biologically-active composition of various RNA, DNA, lipids, carbohydrates, metabolites, and microbiota.[15,20] Moreover, the chemical composition of mucus is altered following exposure to biotic and abiotic stressors. For example, aquaculture-based studies in fish have identified alterations in the composition and abundance of proteins, especially those with immune-related functions, following food deprivation, overcrowding, and bacterial infection.[14,16,22–24] Exposure to environmental contaminants can also induce changes in mucus composition, such as alterations in protein profiles of gilthead seabream (*Sparus aurata*) mucus exposed to heavy metals,[25] increases of antioxidant response in mucus of oil-exposed dusky splitfin (*Goodea gracilis*),[18] and potential changes in mucosal F_2-isoprostanes following oxidative stress.[19] Thus, analysis of mucus may be a useful tool for monitoring fish health.

In addition to proteomic profiles, expression patterns of mRNA in fish mucus can also provide insight on organism health following various stress conditions. Following *Deepwater Horizon* slick oil exposure, the mucosal transcriptome of juvenile mahi-mahi (*Coryphaena hippurus*) showed differential expression of transcripts involved in immune response, cardiotoxicity, and calcium homeostasis which are phenotypes commonly associated with crude oil or polycyclic aromatic hydrocarbon exposure.[12] Moreover, using quantitative polymerase chain reaction (qPCR), differential expression of immune-related genes was detected in mucus of channel catfish (*Ictalurus punctatus*) following bacterial challenge.[13] Results from previous studies suggest that the mucus transcriptome

captures gene expression changes associated with biotic and abiotic stressors and, thus, is a viable method to assess fish health. However, mRNA-based analysis of epidermal mucus has yet to be tested in the field and may be a promising nonlethal method for studying wild fish populations.

Transcriptomic analysis of wild populations is a powerful tool in molecular ecology as it can be used to assess gene expression variation among populations and to explore mechanisms by which populations respond to environmental stimuli.[26–30] More specifically, transcriptome-wide assessments have been crucial in understanding mechanistic responses to different environmental conditions and how those responses vary in different wild populations. For example, Whitehead et al. (2010) compared transcriptomic responses in killifish (*Fundulus heteroclitus*) to polychlorinated biphenyl (PCB) within a pollutant-tolerant population and a nearby sensitive population. PCB exposure within the sensitive population caused significant transcriptomic changes that were linked to developmental deformities, whereas physiological and transcriptomic responses within the tolerant population where comparatively negligible. Through comparative transcriptomics, PCB tolerance was likely attributed to the blockade of the aryl hydrocarbon receptor (AhR) signaling pathway in the tolerant population, a key mediator in PCB toxicity. Although transcriptomics studies are useful in providing insight on global molecular differences among populations, they often rely on lethal sampling which may make it difficult to study threatened species.

While mucus has proven to be useful as a diagnostic metric in laboratory studies, efficacy of mucus-based gene expression analysis to evaluate environmental stressors or

population differences has yet to be assessed in wild fish populations. To determine whether mucus can be used to nonlethally assess transcriptomic differences in geographically-distinct fish populations, RNA sequencing was conducted on epidermal mucus collected from four lake trout (*Salvelinus namaycush)* populations residing in different boreal lakes at the IISD Experimental Lakes Area (IISD-ELA) research station in Northwestern Ontario, Canada. Through sequencing, differential gene expression analysis will elucidate molecular mechanisms that vary among lake trout populations due to ecological differences or epigenetic factors. Transcriptomics of epidermal mucus may be useful for assessing effects of environmental contaminants, varying ecological conditions, epigenetic modifications, and other variables among fish populations without the use of lethal sampling.

Materials and Methods

Sampling Region

The IISD Experimental Lakes Area (IISD-ELA), located in Northwestern Ontario, Canada, is a series of 58 small boreal lakes and their watersheds which have been set aside for scientific research since 1968 (https://www.iisd.org/ela/). Being located in a sparsely populated region, the lakes at IISD-ELA are mostly unaffected by anthropogenic influences. For the present study, Lakes 260, 223, 224, and 373 were selected for comparison as they have extensive, long-term databases for abiotic and biological components of the ecosystem (Figure 3.1). L223 and L224 are connected by a shallow ~300 m stream flowing from L224 into L223; however, there is no movement of

lake trout populations between the lakes (personal communication, Michael D. Rennie, Lakehead University). Furthermore, L223 and L224 are located about 3 km from L260 and about 8 km from L373, with L260 and L373 being about 6 km apart. All four of the lakes are located within the same quaternary watershed (Figure 3.1). Key hydrologic characteristics for the lakes are listed in Table 1a. In terms of area, L260 is the largest of the four lakes. However, L224 and L373 are about 33% greater in volume and are deeper than L260 and L223. Overall, L224 and L373 are comparable in terms of volume and depth, whereas L260 and L223 contain less volume and are shallower.

Collection of Samples

Epidermal mucus was collected from seven lake trout captured in each of L260, L223, L224, and L373 in late September/early October 2017. Fish were captured from a boat using hook and line and, upon capture, were placed in separate bins of fresh lake water until processing (held < 5 min). Retrieval and post-capture air exposure were minimized to reduce physiological stress.[31] Water was renewed for each fish to prevent cross-contamination between individuals. Prior to collecting mucus, lake trout were placed in a solution of 0.1g/L pH buffered (7.0) tricaine methanesulfonate (MS-222) mixed in lake water until fin movement ceased and fish were unresponsive to light pressure on the caudal fin. Total length, fork length, weight, and sex of the individuals were recorded. Sex was determined through external morphological characteristics if possible, or by expressing a small volume of gametes through gentle pressure on the abdomen. Mucus was collected by gently scraping the skin with a stainless steel spatula,

avoiding displacement of scales, to aggregate the mucus along the body axis in the anterior to posterior direction. The aggregated mucus was aspirated using a syringe, dispensed into a microcentrifuge tube, placed on crushed dry ice, and stored at -80°C until analyzed. All tools and work area were cleansed with 95% ethanol and then lake water between fish to prevent cross-contamination of mucus.

Sample collection, cDNA library generation, and Illumina sequencing

Total RNA was extracted from bulk mucus samples (n = 4 per lake) using the RNeasy Lipid Tissue Mini Kit (Qiagen, Qiagen, Germantown, MD) following the manufacturer's protocol. Total RNA concentrations were quantified using an Invitrogen™ Qubit™ 4 Fluorometer (Invitrogen, Carlsbad, CA) and a NanoDrop™ ND-1000 Spectrophotometer (Thermo Fisher Scientific, Waltham, MA). Prior to cDNA library construction, RNA integrity was assessed on an Agilent 2100 Bioanalyzer (Agilent Technologies, Palo Alto, CA).

Sequencing cDNA libraries were prepared using the NEBNext® Ultra™ II Directional RNA Library Prep Kit for Illumina® (New England Biolabs, Ipswich, MA) with the NEBNext® rRNA Depletion Kit using 500 ng of total RNA as input. NEBNext® Multiplex Oligos for Illumina® Index Primer Sets were used to enable multiplexing of cDNA libraries. Final cDNA libraries were assessed on an Agilent 2100 Bioanalyzer to verify proper fragment sizes and to quantify final library concentrations. All cDNA libraries (n = 16) were pooled and the pooled sample was assessed on an Agilent 2100 Bioanalyzer prior to sequencing. Pooled, multiplexed libraries underwent 1

x 75 bp sequencing on one lane on an Illumina NextSeq™ 500 at the Institute for Integrative Genome Biology at the University of California, Riverside.

De novo transcriptome assembly and quality assessment

Quality of raw read data was assessed with FastQC[32] v.0.11.7 prior to downstream analysis. Removal of adapter sequences and poor quality reads was performed using Trimmomatic[33] v.0.36 with the following parameters: ILLUMINACLIP: TruSeq3-SE.fa:2:30:10 LEADING: 3 TRAILING: 3 SLIDINGWINDOW: 4:15 MINLEN: 36. Read quality was again assessed with FastQC following trimming. Trimmed read files from all samples were concatenated and used to build a *de novo* transcriptome using Trinity[34] v.2.8.4 with in silico read normalization and a default *k-mer* size of 25. Alignment statistics were used to assess accuracy and completeness of the assembly. To further assess completeness of the *de novo* transcriptome, BUSCO[35] v.3.0.2 was used to quantify the percentage of complete, fragmented, and missing single copy orthologs by aligning the transcriptome to highly-conserved single copy orthologs within the 'eukaryota_odb10' BUSCO dataset. As these single copy orthologs are evolutionarily-conserved, it is expected that a well-assembled transcriptome will have a high percentage of complete single copy orthologs matching the BUSCO dataset.

Functional annotation of the de novo transcriptome

Functional annotation of the Trinity assembly was performed using Trinotate[36] v.3.1.1. The assembled putative genes were searched against several databases, including

the NCBI non-redundant protein database (http://www.ncbi.nlm.nih.gov/), the UniProtKB/Swiss-Prot database (http://www.ebi.ac.uk/uniprot/), the Kyoto Encyclopedia of Genes and Genomes (KEGG) (http://www.genome.jp/kegg/), the Gene Ontology (GO) knowledgebase (http://www.geneontology.org/), and the EMBL EggNOG database (http://eggnogdb.embl.de), using NCBI-BLASTx v.2.8.1+ reporting only the top hit (-max_target_seqs 1). Next, TransDecoder v.5.0.2 (http://transdecoder.github.io) was used to extract open read frames (ORFs) from the assembly and to predict which ORFs are likely to be coding sequences. The extracted ORFs were searched against the UniProtKB/Swiss-Prot database using NCBI-BLASTp v.2.8.1+ reporting only the top hit. Using extracted ORFs as input, HMMR[37] v.3.1b2 was used to identify functional protein domains from the Pfam domain database, TMHMM[38] v.2.0c was used to predict transmembrane regions, and SignalP[39] v.4.1c was used to predict signal peptide cleavage sites.

Hierarchical Clustering and Principle Component Analysis

Using Bowtie2[40] and RSEM[41] v.1.3.1, trimmed reads for each sample were aligned back to the annotated Trinity assembly and transcript abundances were quantified. In order to visualize transcriptome-wide similarities among samples, unsupervised hierarchical clustering was used to generate a sample-to-sample Euclidian distance heat map using the RSEM count matrix that underwent a regularized-logarithm transformation. Principal component analysis (PCA) was also performed on the transformed RSEM count matrix. Unsupervised hierarchical clustering was used to

produce a heat map of the top 500 most-variable transcripts among all samples to further visualize sample similarities. The top 500 most-variable transcripts were extracted from the transformed count matrix using the *genefilter*[42] R package and were used as input for hierarchical clustering.

Differential Gene Expression and Pathway Analysis

The non-transformed transcript count matrix was input into DESeq2[43] v.1.23.6 to determine differentially expressed transcripts among each lake-by-lake comparison at $p \leq 0.05$ after Benjamini-Hochberg false discovery rate (FDR) correction. Differentially-expressed transcripts that were annotated were input into ToppGene Suite[44] to identify altered KEGG pathways and GO terms among lakes.

qPCR Validation

cDNA was created for all samples using the Promega Reverse Transcription System (Promega, Madison, WI) with 500 ng of total RNA as input. Melt curve analysis and agarose gel electrophoresis were performed prior to qPCR to confirm primer specificity. The reactions for qPCR consisted of 10 µL SsoAdvanced Universal SYBR Green Supermix (Bio-Rad, Hercules, CA), 0.2 µM forward and reverse primers, and 2 µL of cDNA in a final volume of 20 µL. Samples were run in triplicate for each gene on a CFX Connect Real-Time PCR Detection System (Bio-Rad, Hercules, CA) with the following thermal cycler conditions: 95 °C for 10 min, 40 cycles of 95 °C for 15 s, 58 °C for 30 s, and 72 °C for 30 s. Relative expression was determined by the $2^{-\Delta\Delta Ct}$ method[31]

with β-actin as the normalizing gene. Primer sequences were designed using IDT PrimerQuest Tool® using transcript sequences. Primer information is listed in Table 3.S1.

Characterization of lake systems

Lake trout populations in L260, L223, L224, and L373 are sampled in autumn of each year for various parameters including abundance, growth, and condition. Total length and weight for lake trout sampled in 2017 were extracted from the IISD-ELA database. Fulton's condition factor (K) was calculated for each individual using the formula $K = 100 \times \text{weight}/\text{length}^3$. Statistical differences in average total length, weight, and condition factor among each lake-by-lake comparison were assessed using a one-way analysis of variance (ANOVA) followed by a Tukey's Honest Significant Difference (HSD) test using a significance threshold of adj-$p \leq 0.05$.

As zooplankton are an important food source for lake trout, zooplankton abundances by species for L260, L223, L224, and L373 in late September/early October 2017 were extracted from the IISD-ELA database. For each lake, total abundance of zooplankton, species richness (no. of species), Shannon Weiner diversity indices (H'), and Shannon equitability indices (E_H) were calculated. The Shannon Weiner diversity index measures biodiversity, accounting for both species richness and evenness, and was calculated using $H' = -\sum p_i \ln p_i$, where p_i is the proportion of total individuals found in species i. The Shannon equitability index measures evenness of the community and was

calculated using $E_H = H'/H_{max}$, where H_{max} is ln(species richness). Equitability is a value between 0 and 1, with 1 being complete evenness.

Since 1968, data for water quality, biological variables, and atmospheric conditions have been collected at the IISD-ELA. Data from September and October 2017 were extracted from the database for each target lake, which included the following environmental parameters: temperature (°C), dissolved oxygen (mg/L), conductivity (S/m), pH, alkalinity (µEq/L), chlorophyll a (µg/L), total dissolved nitrogen (µg/L), total dissolved phosphorus (µg/L), suspended carbon (µg/L), suspended phosphorus (µg/L), suspended nitrogen (µg/L), ammoniacal nitrogen (NH_3-N; µg/L), and nitrate-nitrogen (NO_3-N; µg/L). For consistency, values for each parameter were extracted for the epilimnion and metalimnion in each lake and averaged to obtain representative values for each lake. Statistical differences in average water quality parameters among each lake-by-lake comparison were assessed using a one-way ANOVA followed by a Tukey's Honest Significant Difference (HSD) test using a significance threshold of adj-$p \leq 0.05$. Using the aforementioned variables for each lake, PCA was used to reduce multidimensionality of water quality data and to graphically visualize similarity in lakes based on water quality characteristics. As the water quality parameters possess different units, all values were scaled to a unitless form of zero mean and variance of one prior to analysis in order to make the variables comparable. Results of the PCA were also used to examine the relationships between variables and the magnitude of importance of each variable on the principal components. Unsupervised hierarchical clustering of water quality parameters for each lake was used to further visualize similarities among lakes.

Water quality effects on transcriptome

A linear mixed model was used to assess percentages of transcriptional variance accounted for by selected environmental parameters. The linear mixed model was conducted using the R package *variancePartition*[45] v.1.17.6 and included lake as a random effect (categorical) as well as dissolved oxygen, conductivity, pH, alkalinity, chlorophyll a, suspended phosphorus, suspended carbon, and total dissolved nitrogen as fixed effects (continuous). Gene expression, or the transcriptome-wide count data, was the response variable of interest. Not all environmental parameters were included in the model due to collinearity of certain variables. For example, total dissolved nitrogen, NO_3-N, and NH_3-N are positively correlated which may produce misleading results and overestimated the contribution of these variables; thus, covariates were dropped. *variancePartition* fit a linear mixed model that jointly considered the contribution of all variables on the expression of each gene in the normalized transcriptome-wide gene count matrix. Using a multiple regression model, *variancePartition* assessed the effect of each individual variable on gene expression while correcting for all other variables included in the model (see *variancePartition* documentation for further statistical details).

Results

Lake trout sampling

Seven lake trout were collected by hook and line angling from each of the four target lakes in late September/early October of 2017. Weight and total length of collected lake trout were comparable among L223 (703.7 ± 30.27 g, 449.7 ± 6.0 mm), L224 (641.3

± 54.32 g, 437.6 ± 10.96 mm), L260 (644.3 ± 87.99 g; 425.9 ± 19.77 mm), and L373 (574.4 ± 40.22 g, 420.1 ± 9.55 mm). Full characterization of collected lake trout is available in Table 3.S2.

Sequencing output and de novo transcriptome assembly

Illumina sequencing generated a total number of 405,026,380 single-end raw reads across the 16 FASTQ files accounting for 80.4 GB of data (Table 3.S3). A total of 175,910,591 reads remained following trimming of adapters and poor quality reads and removal of rRNA (Table 3.S3). Average reads per sample after trimming and rRNA removal was 10,994,412 reads. Thus, rRNA was a large proportion of total raw reads, as was observed in a previous RNA sequencing study of epidermal mucus.[12] The remaining 175 million total reads were used for *de novo* transcriptome assembly. Trinity assembled 268,935 genes with an N50 contig length of 810 bp and an average contig length of 589 bp based on the longest isoform per gene (Table 3.S4). Of the 268,935 Trinity genes, 89,209 (33%) were annotated by BLASTX (Table 3.S4). Analysis of transcriptome completeness with BUSCO indicated 67% complete, 28.6% fragmented, and 4.4% missing single copy orthologs, indicating a fair reconstruction of the transcriptome. The incidence of fragmented single copy orthologs is likely due to the fact that RNA in epidermal mucus was partially degraded (RIN < 7) which may also explain the relatively low percentage of transcripts receiving a BLASTX annotation.

Transcriptomic variation among lakes

In order to visualize similarities in transcriptomes among lake trout populations, hierarchical clustering and PCA was conducted on transcriptome-wide count data. Results of sample-to-sample Euclidian distance clustering indicated an approximate clustering of L223 and L373 populations and clustering of L260 and L223 populations within separate clades (Figure 3.S1). Transcriptomic differences among the lakes were further elucidated by the PCA of transcriptome-wide count data, which clearly showed that samples clustered by lake from which they were collected (Figure 3.2A). Again, L224 and L373 lake trout clustered more closely together, whereas L260 and L223 lake trout clustered apart from all other lakes. The eigenvalues of the two first principal components represented 53% of the total variance (PC1 33%; PC2 20%). There were no patterns based on sex of the lake trout in the PCA results, suggesting transcriptomic patterns were most likely driven by lake (Figure 3.S2).

Hierarchical clustering of the top 500 most-variable transcripts revealed similar results, with individuals clustering into clearly defined clades by lake (Figure 3.2B). As with the PCA results, L224 and L373 lake trout clustered together, whereas L260 and L223 each clustered apart from the other lakes. These data suggest that individuals from L224 and L373 were most similar in terms of transcriptomic profiles, with L260 and L223 being the most different from the other lakes. Results of the hierarchical clustering and PCA overall suggest that there were clear transcriptomic differences among individuals collected from different lakes and that these differences can be detected nonlethally in epidermal fish mucus.

Differential Gene Expression and Pathway Analysis

There were significant differences in gene expression among the four lakes (Figure 3.3; Table A-1). The greatest numbers of differentially expressed transcripts were found among the comparisons between L223 and L260 (6,708 transcripts, 1,208 annotated transcripts), L224 and L260 (8,276 transcripts, 1,012 annotated transcripts), L260 and L373 (7,190 transcripts, 879 annotated transcripts), and L223 and L224 (8,123 transcripts, 1,629 annotated transcripts) (Figure 4.3). The lowest numbers of differentially expressed transcripts were among the comparisons between L223 and L373 (4,659 transcripts; 872 annotated transcripts) and L224 and L373 (4,098 transcripts, 426 annotated transcripts) (Figure 3.3). Again, the relatively low degree of annotation of transcripts was likely due to the high fragmentation of RNA transcripts in mucus, a result of RNAse present in the mucus [15]. The results of RNA sequencing were confirmed through RT-qPCR (Figure 3.S3). A full list of all annotated differentially expressed transcripts for each lake-by-lake comparison may be found in Table A-1. Only transcripts which were annotated were used for further pathway analysis.

Due to the high number of differentially expressed transcripts, pathway analyses were used to understand biological pathways and functions that differ among lake trout populations. A list of all GO biological processes and KEGG pathways for each lake-by-lake comparison can be found in Table 3.S5 and Table 3.S6. There was a high prevalence of immune-related pathways among the top ten biological process GO terms for most lake-by-lake comparisons (Table 3.2). Comparing L223 and L224, a notable observation was the presence of pathways related to viral infection within the top ranked GO

biological functions, including ‘viral process’ (rank 11), ‘viral gene expression’ (rank 8), and ‘viral transcription’ (rank 9). Furthermore, several KEGG pathways among L223 and L224 were related to pathogens, such as ‘Salmonella infection’ (rank 9), ‘Vibrio choerae infection’ (rank 5), ‘epithelial cell signaling in Helicobacter pylori infection’ (rank 10), bacterial invasion of epithelial cells’ (15), and ‘shigellosis’ (rank 13). Comparing L223 and L260, ‘viral process’ (rank 2) and ‘viral gene expression’ (rank 52) were also identified as altered GO biological functions as well as the KEGG pathways ‘Salmonella infection’ (rank 3), ‘Shigellosis’ (rank 7), ‘hepatitis C’ (rank 14), ‘viral carcinogenesis’ (rank 16), and others. As for the comparison among L233 and L373, several of the top GO biological pathways were related to cell adhesion and cell migration involved in the inflammatory response, such as ‘biological adhesion’ (rank 1), ‘cell adhesion’ (rank 2), ‘cell-cell adhesion’ (rank 4), ‘T cell activation’ (rank 12), and ‘T cell differentiation’ (rank 15) (Table 3.2; Table 3.S5). Comparison of L223 with all other lakes identified several immune- and infection-related pathways, suggesting L223 lake trout may be exposed to pathogens. Top GO biological functions among L224 and L373, the most transcriptionally-similar lakes, were mainly related to interleukin-1 beta (Table 3.2). Finally, comparisons of L260 with L224 and L373 both identified a high prevalence of pathways related to cell death and apoptosis among top GO biological pathways, such as ‘regulation of cell death’ and ‘regulation of apoptotic process’ (Table 3.2).

As immune- and pathogen-related pathways were identified within the top GO biological processes among L223 and all other lakes, immune-related transcripts differentially regulated in L223 were visualized based on normalized count data (Figure

3.4). Many immune- and stress-related transcripts were expressed to a greater degree in L223 lake trout compared to all other populations, among them members of the GTPase of immunity-associated protein family, cytokines, interferons, and heat shock proteins (Figure 3.4). Furthermore, many transcripts involved in viral transcription were found to be consistently upregulated in L223 relative to all other lakes (Figure 3.5). Aside from immune transcripts, other notable gene expression patterns included that of cytosolic phospholipase A2 gamma (*PLA2G4C*), which was the top differentially-expressed transcript and strongly upregulated (fold change > 7) in L260 lake trout in comparison with all other lakes (Table A-1). Up-regulator of cell proliferation (*URGCP*) was among the top differentially expressed transcripts in all lake-by-lake comparisons.

Abiotic and biotic variables of lakes

There were significant differences in average total length and weight among lake trout collected throughout 2017 annual sampling from L260, L223, L224, and L373 (ANOVA, $p \leq 0.05$) (Table 3.1b; Figure 3.S4). Average total length and weight of lake trout in Lake 260 were significantly greater than average total length and weight of lake trout in L223, L224, and L373 (Tukey HSD, adj-$p \leq 0.0001$ for all comparisons). Furthermore, average total length and weight of lake trout in Lake 223 were greater than average total length and weight of lake trout in L224 (Tukey HSD, adj-$p \leq 0.002$ for both comparisons). There were no significant differences in average total length and weight among L224 and L373 and among L223 and L373 (Tukey HSD, adj-$p > 0.05$ for all comparisons). Although there were differences in length and weight, average condition

factors did not significantly differ among populations (ANOVA, $p = 0.1$) (Table 3.1b; Figure 3.S4).

Total zooplankton abundance ranked from highest to lowest was as follows: L223 > L260 > L224 > L373 (Table 3.1c). L223 and L260 also had the highest zooplankton species richness (38 species), whereas species richness was lower in L224 (29 species) and L373 (26 species) (Table 3.1c). The most abundant zooplankton within all lakes were rotifers (e.g. *Keratella cochlearis*, *Kellicottia bostoniensis*, *Polyarthra remata*, *Polyarthra vulgaris*, *Kellicottia longspina*) and copepods (e.g. *cyclopoida nauplii*) (Figure 3.S5). L373 had the highest H' index of 2.50, followed by L260 with 2.08, then L223 with 1.93, and finally L224 with 1.67 (Table 3.1c). L373 and L260 also had the greatest evenness of zooplankton species with equitability index values of 0.77, followed by L223 and L224 with equitability values of 0.53 and 0.50, respectively. Thus, L373 and L260 contain the most diverse, evenly-distributed zooplankton communities.

Average water quality parameters are presented in Table 3.1d and visualized in Figure 3.S6. There were no significant differences in average suspended phosphorus, suspended nitrogen, suspended carbon, and total dissolved phosphorus among lakes (Tukey HSD, adj-$p > 0.05$ for all comparisons). However, L223 and L260 had significantly higher levels of total dissolved nitrogen than L224 and L373 (Tukey HSD, adj-$p \leq 0.0001$ for both comparisons). Chlorophyll-a levels were significantly lower in L224 compared to Lakes 223 and 260 (Tukey HSD, adj-$p > 0.03$ for both comparisons), while chlorophyll-a levels did not significantly differ among L223, L260, and L373 (Tukey HSD, adj-$p > 0.05$ for all comparisons). However, there was a visible trend of

increased chlorophyll-a in L223 and L260 (Figure 3.S6). Average dissolved oxygen levels in L260 were significantly lower compared to all other lakes (Tukey HSD, adj-$p \leq$ 0.0001 for all comparisons). Average alkalinity was significantly higher in L373 compared to all other lakes (Tukey HSD, adj-$p \leq 0.0001$ for all comparisons), whereas alkalinity was significantly lower in L224 compared to all other lakes (Tukey HSD, adj-$p \leq 0.0001$ for all comparisons). Furthermore, average pH was significantly higher in L373 as compared to L224 and L260 (Tukey HSD, adj-$p \leq 0.01$ for all comparisons) but pH did not significantly differ among L223, L224 and L260 (Tukey HSD, adj-$p > 0.05$ for all comparisons). Average temperature was comparable among the lakes; however, water temperature of L373 was significantly lower than in L223 and L224 (Tukey HSD, adj-$p \leq$ 0.03 for all comparisons) whereas temperature did not significantly differ among L223, L224, and L260 (Tukey HSD, adj-$p > 0.05$ for all comparisons). Finally, average conductivity was significantly lower in L224 compared to all other lakes (Tukey HSD, adj-$p \leq 0.02$ for all comparisons).

PCA of 11 variables for the four lakes was used to identify variation in water quality characteristics (Table 3.S7). Proportions of variance explained by PC1, PC2, and PC3 were 50.39%, 29.53%, and 20.08%, respectively. PC1 and PC2 explained the maximum amount of total variance (79.92%). Variable loadings on each PC are presented in Table 3.S2 and are graphically represented in a PCA biplot (Figure 3.6). PC1 had strong positive loadings from suspended nitrogen (0.42), suspended carbon (0.38), conductivity (0.38), and chlorophyll a (0.36) (Figure 3.2; Table 3.S7). The highest scoring lakes for PC1 were L223 (1.18) and L260 (1.68), while the PC1 score was

weakest for L373 (0.61) and was strongly negative for L224 (-3.47). Furthermore, the strong negative PC1 score of L224 and strong negative PC1 loading of total dissolved phosphorus (-0.39) suggest that L224 had high total dissolved phosphorus relative to lakes scoring positively on PC1 and that total dissolved phosphorus likely drove the variation of L224 from other lakes.

PC2 had strong positive loadings from pH (0.55), alkalinity (0.42), and dissolved oxygen (0.34) as well as negative loading from chlorophyll-a (-0.24) (Figure 3.6; Table 3.S7). L223 was the only lake with a positive PC2 score (2.49) out of the lakes of interest (Figure 3.6). Overall, PCA suggested that L260 and L223 were most similar in terms of water quality characteristics while L224 and L373 varied from all other lakes (Figure 3.6). Hierarchical clustering analysis confirmed that L223 and L260 were most closely related based on water quality characteristics whereas L224 and L373 clustered apart from L223 and L260 (Figure 3.S7).

Relationships of environmental variables to mucus transcriptomic profiles

A linear mixed model was used to quantify the percent variance in transcriptome-wide gene expression that could be explained by water quality variables. The variables included in the model explained a median of 68.1% across all genes in the transcriptome-wide count matrix, leaving a median residual of 31.9% variance unexplained (Figure 3.7). Conductivity, chlorophyll a, alkalinity, and dissolved oxygen explained the greatest proportion of variance within the transcriptome (Figure 3.3).

Discussion

Mucus transcriptome differs among lakes

Following exposure to crude oil, Greer et al. (2019) demonstrated that sequencing of mahi-mahi mucus was effectively able to distinguish transcriptomes of oil-exposed and non-exposed individuals. Our results from the present study expand the utility of mucus as a nonlethal sampling tool by demonstrating that sequencing of RNA in mucus can distinguish transcriptomic differences among geographically-distinct populations (Figure 3.2). In terms of transcriptomic similarity, individuals from L224 and L373 were most similar whereas individuals from L260 and L223 clustered apart from all other lakes (Figure 3.2). It should be noted that the lakes of interest in the present study are located in close proximity to one another and within the same ecozone and, thus, vary only slightly in terms of ecological conditions. Even so, unique transcriptome profiles by lake were captured within lake trout mucus indicating that sequencing of mucus is able to robustly capture gene expression changes among fish populations. Therefore, analysis of mucus may be a viable tool for ecological studies interested in assessing gene expression differences among fish populations. As mucus sampling is nonlethal and minimally-invasive, this method could be especially useful for assessing threatened and endangered populations without inducing further perturbations. Moreover, differential gene expression analysis and subsequent gene ontology analysis can be used to further elucidate transcriptomic relationships among populations and identify abiotic and biotic factors driving population differences.

Differentially regulated genes and pathways among lakes

Differential gene expression analysis and pathway analysis was used to understand the underlying biological meaning of transcriptional differences among lake trout populations. Among each lake-by-lake comparison, there was a high prevalence of transcripts and gene ontology biological processes related to the immune system, suggesting an active response to stress in lake trout populations (Table 3.S5; Table A-1).[46] Transcripts that were commonly differentially regulated among most lake-by-lake comparisons included members of the GTPase of immunity-associated protein family (*GIMAP2*, *GIMAP4*, *GIMAP7*, *GIMAP8*, etc.), chemokine transcripts (*CCL2*, *CCL3*, *CCL12*, *CCL20*, etc.), interferon-related transcripts (*IRF1*, *IRF3*, *IFI44*, etc.), and others (Figure 3.4). Expression of immune-related genes is not surprising as fish epidermal mucus is full of various immune relevant molecules[15] and differential regulation of immune-related genes in mucus has been identified in previous studies.[12,13] Aside from immune response transcripts, expression of viral RNA was also observed among lake trout populations.

RNA sequencing of epidermal mucus suggested the presence of retroviral infection in the sampled lake trout populations. Presence of retroviruses among lakes was evidenced by the expression of transcripts involved in transcription and replication of viral RNA, including transcripts coding for pol polyprotein, gag-pol polyprotein, replicase polyprotein, RNA-directed RNA polymerase, and RNA-dependent RNA polymerase (Table A-1).[47–49] Interestingly, the transcript *gag-pol* encodes the gag-pol polyprotein of the Walleye dermal sarcoma virus (WDSV) (UniProt ID: POL_WDSV),

an exogenous retrovirus inducing dermal lesions and sarcomas in walleye (*Sander vitreus*).[50,51] Gag, a major structural protein, and pol, the reverse transcriptase, are essential proteins encoded within retroviral genomes and within the WDSV genome specifically.[51–53] Elevated expression of viral RNA has been identified in dermal sarcomas of WDSV-infected fish.[54] While WDSV is specific to walleye, only six tumorigenic piscine retroviruses have been fully or partially sequenced and, thus, it is likely that the *gag-pol* transcript detected in the present study is endogenous to a closely related retrovirus that has not yet been sequenced.[55]

Following infection, cyclins encoded by WDSV induce cells to proliferate abnormally, resulting in lesions and tumors.[56] Interestingly, *URGCP* was consistently among the top differentially regulated transcripts among all lake-by-lake comparisons. *URGCP* stimulates cyclin to accelerate cell growth and promote tumor formation, and overexpression of *URGCP* has been implicated in virus-induced carcinomas in humans.[57,58] As lymphocytes have been shown to aggregate around WSDV dermal lesions, the differential regulation of transcripts involved in lymphocyte development, trafficking, and function (e.g. *GIMAP2*, *GIMAP4*, *GIMAP7*, *GIMAP8, CCL2*, *CCL3*, *CCL12*, *CCL20*, *IL1B*, etc.) may also indicate antiviral response to epidermal lesions.[59–61] Differential regulation of interferon-related transcripts (*IRF1*, *IRF3*, *IFI44*, etc.) further suggests antiviral response as interferon regulatory factors play a critical role in the antiviral immune response in fish and transcription of interferon regulatory factors, interferons, and interferon-stimulated genes has been shown to be upregulated following viral infection in fish.[62–66] Overall, expression of WDSV-specific *gag-pol*, transcripts

involved in cell proliferation, and immune transcripts associated with antiviral response suggest that viral carcinogenesis may be present in the studied lake trout populations. Further research will be needed to characterize the presence of viruses within the lakes.

Although transcripts for viral RNA transcription were differentially regulated among all lake-by-lake comparisons, these transcripts were only consistently upregulated within L223 lake trout, providing compelling evidence that prevalence of viral infection may be greatest within L223 (Figure 3.5). Comparison of L233 lake trout to all other lakes indicated that *URGCP* was consistently among the top ten transcripts differentially expressed in L223 and was strongly upregulated in L223 lake trout (FC > 5). Along with this, viral-related processes were among the top altered GO biological processes in L223 comparisons, including viral gene expression, viral transcription, and viral process among L223 and L224 and among L223 and L260 (Table 3.2). While immune response was evident among most lakes, immune-related transcripts were most consistently upregulated in L223 lake trout and upregulation of certain transcripts was unique to L223 (e.g. interleukin-8 (*CXCL8*), interleukin 1 beta (*IL1B*), etc.) (Figure 3.4).

Aside from immune-specific transcripts, transcripts coding for various heat shock proteins were upregulated in lake trout from L223 compared to all other lakes, including *HSP90AA1*, *hsp90a.1*, *hsp90ab1*, and *HSPA12A* (Figure 3.4; Table A-1). In fish, heat shock proteins are expressed in response to a range of biotic and abiotic stressors, such as environmental contaminants, heat and cold shock, food deprivation, and infectious pathogens.[67–70] Given the evidence for viral transcription in L223 lake trout, the upregulation of heat shock protein transcripts may be in response to pathogens. For

example, Hsp90 isoforms have been shown to be upregulated in several fish species following viral infection and bacterial challenge.[71–73] Upregulation of Hsp90 alpha and beta proteins has also been observed in epidermal mucus of sea-lice infected Atlantic salmon (*Salmo salar* L.).[14] Along with this, Hsp90 is one of the most frequently observed host chaperone for viruses, aiding in synthesis, localization, and folding of viral proteins.[74–77] As dependence of viruses on Hsp90 appears to be nearly universal,[75] the upregulation of Hsp90 isoforms in L223 may further suggest viral response. However, these results are not conclusive as Hsp90 is responsive to multiple different stressors.

Discussion of *PLA2G4C*, encoding cytosolic phospholipase A2 gamma (cPLA2γ), is warranted as it was consistently among the top upregulated gene in L260. While the function of cPLA2γ specifically has not been characterized in fish, it is known that cPLA2γ a lipolytic enzyme that catalyzes the release of arachidonic acid from membrane phospholipids in humans.[78] In fish, arachidonic acid is a precursor for a wide spectrum of eicosanoids involved in hemodynamic regulation, immune and inflammatory responses, reproduction, renal and neural functions.[79] It has been suggested that cPLA2γ specifically is involved in the inflammatory response, as *PLA2G4C* was upregulated in rodents following pathogen infection and also has been shown to contribute to formation, replication, and assembly of hepatitis C virus.[80,81] Due to the number of biological processes affected by arachidonic acid release, further work will be required to identify the downstream pathways associated with *PLA2G4C* upregulation in lake trout from L260.

Abiotic and biotic variable comparison among lakes

Lake trout from L260 had the greatest average total length and weight, followed by lake trout from L223. Although there were significant differences in average length and weight among lake trout populations, condition factor did not significantly differ suggesting a similar degree of health among populations. In terms of zooplankton populations, L260 and L223 contained the most abundant and species rich populations. As zooplankton represent a significant source of food for lake trout, the greatest abundance of zooplankton in L260 and L223 may explain the trend of larger individuals residing in those lakes. Moreover, L373 and L260 contained the most diverse, evenly-distributed zooplankton communities as suggested by Shannon diversity and equitability indices. Diversity and equitability were lower in L223 likely because the zooplankton community here was dominated by rotifer species (*Keratella cochlearis*, *Kellicottia bostoniensis*, *Polyarthra remata*, *Polyarthra vulgaris*, *Kellicottia longspina*) (Figure 3.S4). High rotifer dominance in lakes has shown to increase bacterial abundance through top-down control of flagellates[82] and, thus, the observed pathogen responses in L223 lake trout may potentially be explained by greater rotifer abundance and, consequently, bacterial abundance. However, more research is needed to establish a causative link among rotifer and bacterial abundances at IISD-ELA.

Average water quality parameters were input into PCA to elucidate similarities and differences among the four lakes based on their water quality characteristics. L260 and L223 were most similar in terms of water quality parameters, whereas L373 and L224 deviated from all other lakes (Figure 3.6). L260 and L223 had high scores on PC1,

which received highest positive loadings from suspended nitrogen, suspended carbon, conductivity, and chlorophyll a. As nitrogen and carbon are important for zooplankton productivity[83,84] and chlorophyll-a is an indicator of productivity in aquatic environments, PC1 represents lakes with high productivity. The high positive PC1 scores for L223 and L260 suggest they had higher productivity relative to the other lakes, which is further supported by the fact that L260 and L223 had the greatest zooplankton, chlorophyll-a, and total dissolved nitrogen levels (Table 3.1). PC1 scores were weakest for L373 and were strongly negative for L224, suggesting L373 and L224 were less productive than L223 and L260. Lake 224 scored strongly on PC2 which had strong positive loadings from pH, alkalinity, and dissolved oxygen (Figure 3.6). These PCA results further demonstrate that Lake 224 was lower productivity as high pH levels limit phytoplankton growth.[85] Furthermore, the positive loading of dissolved oxygen and negative loading of chlorophyll-a on PC2 is indicative of oligotrophic conditions.

Overall, results of the PCA suggest that L260 and L223 were most similar in terms of water quality characteristics likely driven by their higher productivity (Figure 3.6). Moreover, L224 and L373 varied from all other lakes, with variability likely being driven by more alkaline conditions in L373 and higher total dissolved phosphorus content in L224 (Figure 3.6). Unlike L260 and L223, water quality parameters and PCA results suggest that L373 and L224 were lower productivity lakes. Hierarchical clustering analysis confirmed that L223 and L260 were most similar based on water quality whereas L224 and L373 clustered apart from L223 and L260 (Figure 3.S6).

Relationships between environmental variables and mucus transcriptomic profiles

As the transcriptome responds to environmental changes, differences and similarities in environmental variables may explain mucus transcriptome variation among lake trout populations.[86] The high degree of transcriptomic similarity among L224 and L373 populations could potentially be explained by the fact that both lakes were fairly oligotrophic whereas L260 and L223, while still oligotrophic, tended to be more productive. However, comparison of results from the water quality PCA and transcriptome PCA suggests there are environmental factors not accounted for in the study. For example, while L260 and L373 were most similar in their water quality characteristics (Figure 3.6), lake trout from those lakes deviated from each other in terms of their transcriptomic profiles (Figure 3.2). Therefore, it is likely that there were other abiotic and biotic variables influencing gene expression changes other than those taken into account in the water quality PCA, such as pathogen loading, epigenetics, or food availability.

While PCA was used to characterize similarity in water quality profiles among lakes, a linear mixed model was used to quantify the percent variance in transcriptome-wide gene expression explained by those water quality variables. As the linear mixed model accounted for 68.1% of transcriptional variance, results suggest that variation in water quality contributes to transcriptional differences among lake trout populations (Figure 3.7). Conductivity, chlorophyll a, alkalinity, and dissolved oxygen explained the greatest proportion of variance within the transcriptome, suggesting these variables had the greatest influence on gene expression differences among lakes (Figure 3.7). Variables

identified by the linear mixed model as accounting for the most transcriptomic variation among lake trout populations were also among the variables identified in the PCA as driving inter-lake water quality differences. However, a median of 31.9% of transcriptomic variance was not explained by the water quality variables in the model. Therefore, both the water quality PCA and linear mixed model suggest that the variables considered in the present study did not fully explain transcriptional variance and, thus, other variables could be driving transcriptomic differences among populations albeit similar water quality conditions. As suggested by differential gene expression data, an additional source of transcriptional variance among populations may stem from presence of pathogens. For example, despite their fairly similar water quality profiles, the divergence in transcriptomic profiles of L223 and L260 lake trout may be partially explained by the strong immune response in L223. Overall, it is challenging to robustly quantify the effects of environmental variables on gene expression patterns as transcription may be affected by even small changes in environment.[26]

Aside from environmental factors, epigenetic modifications are another potential source of gene expression variation among populations, with studies showing that genes may be transgenerationally dysregulated following exposure to stressors in prior generations. Transgenerational alterations in the transcriptome are well-illustrated in a study which examined responses to increased temperature across generations in common reef fish (*Acanthochromis polyacanthus*).[87] Compared to controls, fish that were transgenerationally exposed to higher temperatures showed upregulation of metabolic, immune, and stress-responsive genes, likely an adaptive mechanism to maintain

performance and cope with higher temperatures. Epigenetic modifications are highly possible in lake trout populations at IISD-ELA as L260 and L223 have been used for whole-lake experiments in the past. In an effort to understand population-level impacts of environmental estrogens, L260 was subject to whole-lake ethynylestradiol additions for three years starting in 2001, resulting in feminization and a near extirpation of fathead minnow (*Pimephales promelas*) as well as population declines of lake trout.[88,89] To simulate the effects of acid precipitation on freshwater lakes, sulfuric acid was added to L223 over a three year period from 1976 to 1978,[90] resulting in disappearance of fathead minnow, increased lake trout embryonic mortality and deformities, and decreased survival of lake trout due to emaciation.[91–94] Interestingly, L224 and L373, which have not been subject to experimental modifications, had highly similar transcriptomic profiles, whereas the experimentally-modified L260 and L223 diverge from all other lakes (Figure 3.2); these observations suggest that epigenetic modifications in response to past stressful conditions may contribute to the observed transcriptional variations.

As the transcriptome reflects both short-term plastic responses and transgenerational plasticity,[86] it is difficult to adequately discern whether transcriptional variation among populations stems from environmental changes or transgenerational alterations. Although concrete identification of explanatory variables requires further development, RNA sequencing of mucus provides meaningful information on transcriptomic variation among fish populations and can be used to identify molecular differences driving variation in a nonlethal manner.

Application of method

The results of the present study demonstrate that RNA sequencing of epidermal mucus can generate a wealth of information on molecular differences among wild fish populations without the use of lethal sampling. Although the populations considered in the present study were located in closely-situated, ecologically-similar lakes, our method was still able to clearly separate individual transcriptomic profiles by lake. Sequencing of mucus could be useful in comparative transcriptomic studies of populations residing in ecologically different conditions, such as studying ecologically-divergent populations residing in two different habitat types or comparing a reference population to one at a polluted site. Moreover, using mucus for gene expression analysis can be applied to various freshwater and marine species as mRNA-based mucus analysis has been successful in mahi-mahi,[12] channel catfish,[13] largemouth bass (unpublished), and now lake trout. As mucus sampling is nonlethal, transcriptomic studies of mucus would be of most value to studies concerned with threatened and endangered fish species. mRNA-based analysis of mucus can be used in conjunction with other nonlethal sampling methods, such as blood sampling for biomarkers of interest, as well as individual- and population-level metrics (e.g. through eDNA sampling[95]) to gain insight on health at multiple levels of biological organization.

References

(1) Sloman, K. A.; Bouyoucos, I. A.; Brooks, E. J.; Sneddon, L. U. Ethical Considerations in Fish Research. *J. Fish Biol.* **2019**, *94* (4), 556–577. https://doi.org/10.1111/jfb.13946.

(2) Bennett, R. H.; Ellender, B. R.; Mäkinen, T.; Miya, T.; Pattrick, P.; Wasserman, R. J.; Woodford, D. J.; Weyl, O. L. F. Ethical Considerations for Field Research on Fishes. *Koedoe* **2016**, *58* (1), 1–15. https://doi.org/10.4102/koedoe.v58i1.1353.

(3) Rodríguez-Jorquera, I. A.; Colli-Dula, R. C.; Kroll, K.; Jayasinghe, B. S.; Parachu Marco, M. V.; Silva-Sanchez, C.; Toor, G. S.; Denslow, N. D. Blood Transcriptomics Analysis of Fish Exposed to Perfluoro Alkyls Substances: Assessment of a Non-Lethal Sampling Technique for Advancing Aquatic Toxicology Research. *Environ. Sci. Technol.* **2019**, *53* (3), 1441–1452. https://doi.org/10.1021/acs.est.8b03603.

(4) Brumbaugh, W. G.; Schmitt, C. J.; May, T. W. Concentrations of Cadmium, Lead, and Zinc in Fish from Mining-Influenced Waters of Northeastern Oklahoma: Sampling of Blood, Carcass, and Liver for Aquatic Biomonitoring. *Arch. Environ. Contam. Toxicol.* **2005**, *49* (1), 76–88. https://doi.org/10.1007/s00244-004-0172-3.

(5) Sanderson, B. L.; Tran, C. D.; Coe, H. J.; Pelekis, V.; Steel, E. A.; Reichert, W. L. Nonlethal Sampling of Fish Caudal Fins Yields Valuable Stable Isotope Data for Threatened and Endangered Fishes. *Trans. Am. Fish. Soc.* **2009**, *138* (5), 1166–1177. https://doi.org/10.1577/t08-086.1.

(6) Imbery, J. J.; Buday, C.; Miliano, R. C.; Shang, D.; Round, J. M.; Kwok, H.; Van Aggelen, G.; Helbing, C. C. Evaluation of Gene Bioindicators in the Liver and Caudal Fin of Juvenile Pacific Coho Salmon in Response to Low Sulfur Marine Diesel Seawater-Accommodated Fraction Exposure. *Environ. Sci. Technol.* **2019**, *53* (3), 1627–1638. https://doi.org/10.1021/acs.est.8b05429.

(7) Henderson, T. F.; Stevens, S. Y.; Lee, C. J. Assessing the Suitability of a Non-Lethal Biopsy Punch for Sampling Fish Muscle Tissue. *Fish Physiol Biochem* **2016**, *42*, 1521–1526. https://doi.org/10.1007/s10695-016-0237-z.

(8) Razavi, N. R.; Halfman, J. D.; Cushman, S. F.; Massey, T.; Beutner, R.; Foust, J.; Gilman, B.; Cleckner, L. B. Mercury Concentrations in Fish and Invertebrates of the Finger Lakes in Central New York, USA. *Ecotoxicology* **2019**. https://doi.org/10.1007/s10646-019-02132-z.

(9) Baker, R. F.; Blanchfield, P. J.; Paterson, M. J.; Flett, R. J.; Wesson, L. Evaluation of Nonlethal Methods for the Analysis of Mercury in Fish Tissue. *Trans. Am. Fish.*

Soc. **2004**, *133* (3), 568–576. https://doi.org/10.1577/t03-012.1.

(10) Lake, J. L.; Ryba, S. A.; Serbst, J. R.; Libby, A. D. Mercury in Fish Scales as an Assessment Method for Predicting Muscle Tissue Mercury Concentrations in Largemouth Bass. *Arch. Environ. Contam. Toxicol.* **2006**, *50* (4), 539–544. https://doi.org/10.1007/s00244-005-5052-y.

(11) Fincel, M. J.; Vandehey, J. A.; Chipps, S. R. Non-Lethal Sampling of Walleye for Stable Isotope Analysis: A Comparison of Three Tissues. *Fish. Manag. Ecol.* **2012**, *19* (4), 283–292. https://doi.org/10.1111/j.1365-2400.2011.00830.x.

(12) Greer, J. B.; Andrzejczyk, N. E.; Mager, E. M.; Stieglitz, J. D.; Benetti, D.; Grosell, M.; Schlenk, D. Whole-Transcriptome Sequencing of Epidermal Mucus as a Novel Method for Oil Exposure Assessment in Juvenile Mahi-Mahi (Coryphaena Hippurus). *Environ. Sci. Technol. Lett.* **2019**, *6*, 538–544. https://doi.org/10.1021/acs.estlett.9b00479.

(13) Ren, Y.; Zhao, H.; Su, B.; Peatman, E.; Li, C. Expression Profiling Analysis of Immune-Related Genes in Channel Catfish (Ictalurus Punctatus) Skin Mucus Following Flavobacterium Columnare Challenge. *Fish Shellfish Immunol.* **2015**, *46* (2), 537–542. https://doi.org/10.1016/j.fsi.2015.07.021.

(14) Provan, F.; Jensen, L. B.; Uleberg, K. E.; Larssen, E.; Rajalahti, T.; Mullins, J.; Obach, A. Proteomic Analysis of Epidermal Mucus from Sea Lice-Infected Atlantic Salmon, Salmo Salar L. *J. Fish Dis.* **2013**, *36* (3), 311–321. https://doi.org/10.1111/jfd.12064.

(15) Brinchmann, M. F. Immune Relevant Molecules Identified in the Skin Mucus of Fish Using -Omics Technologies. *Mol. BioSyst.* **2016**, *12* (7), 2056–2063. https://doi.org/10.1039/C5MB00890E.

(16) Rajan, B.; Lokesh, J.; Kiron, V.; Brinchmann, M. F. Differentially Expressed Proteins in the Skin Mucus of Atlantic Cod (Gadus Morhua) upon Natural Infection with Vibrio Anguillarum. *BMC Vet. Res.* **2013**, *9*. https://doi.org/10.1186/1746-6148-9-103.

(17) Cordero, H.; Brinchmann, M. F.; Cuesta, A.; Meseguer, J.; Esteban, M. A. Skin Mucus Proteome Map of European Sea Bass (Dicentrarchus Labrax). *Proteomics* **2015**, *15* (23–24), 4007–4020. https://doi.org/10.1002/pmic.201500120.

(18) Dzul-Caamal, R.; Salazar-Coria, L.; Olivares-Rubio, H. F.; Rocha-Gómez, M. A.; Girón-Pérez, M. I.; Vega-López, A. Oxidative Stress Response in the Skin Mucus Layer of Goodea Gracilis (Hubbs and Turner, 1939) Exposed to Crude Oil: A Non-Invasive Approach. *Comp. Biochem. Physiol. -Part A Mol. Integr. Physiol.*

2016. https://doi.org/10.1016/j.cbpa.2016.05.008.

(19) Bulloch, P.; Schur, S.; Muthumuni, D.; Xia, Z.; Johnson, W.; Chu, M.; Palace, V.; Su, G.; Letcher, R.; Tomy, G. T. F2-Isoprostanes in Fish Mucus: A New, Non-Invasive Method for Analyzing a Biomarker of Oxidative Stress. *Chemosphere* **2020**, *239*.

(20) Reverter, M.; Tapissier-Bontemps, N.; Lecchini, D.; Banaigs, B.; Sasal, P. Biological and Ecological Roles of External Fish Mucus: A Review. *Fishes* **2018**, *3* (4), 41. https://doi.org/10.3390/fishes3040041.

(21) Shephard, K. L. Functions for Fish Mucus. *Rev. Fish Biol. Fish.* **1994**, *4* (4), 401–429. https://doi.org/10.1007/BF00042888.

(22) Easy, R. H.; Ross, N. W. Changes in Atlantic Salmon (Salmo Salar) Epidermal Mucus Protein Composition Profiles Following Infection with Sea Lice (Lepeophtheirus Salmonis). *Comp. Biochem. Physiol. - Part D Genomics Proteomics* **2009**. https://doi.org/10.1016/j.cbd.2009.02.001.

(23) Guardiola, F. A.; Cuesta, A.; Arizcun, M.; Meseguer, J.; Esteban, M. A. Comparative Skin Mucus and Serum Humoral Defence Mechanisms in the Teleost Gilthead Seabream (Sparus Aurata). *Fish Shellfish Immunol.* **2014**, *36* (2), 545–551. https://doi.org/10.1016/j.fsi.2014.01.001.

(24) Cordero, H.; Morcillo, P.; Cuesta, A.; Brinchmann, M. F.; Esteban, M. A. Differential Proteome Profile of Skin Mucus of Gilthead Seabream (Sparus Aurata) after Probiotic Intake And/or Overcrowding Stress. *J. Proteomics* **2016**, *132*, 41–50. https://doi.org/10.1016/j.jprot.2015.11.017.

(25) Guardiola, F. A.; Dioguardi, M.; Parisi, M. G.; Trapani, M. R.; Meseguer, J.; Cuesta, A.; Cammarata, M.; Esteban, M. A. Evaluation of Waterborne Exposure to Heavy Metals in Innate Immune Defences Present on Skin Mucus of Gilthead Seabream (Sparus Aurata). *Fish Shellfish Immunol.* **2015**. https://doi.org/10.1016/j.fsi.2015.02.010.

(26) Alvarez, M.; Schrey, A. W.; Richards, C. L. Ten Years of Transcriptomics in Wild Populations: What Have We Learned about Their Ecology and Evolution? *Mol. Ecol.* **2015**, *24* (4), 710–725. https://doi.org/10.1111/mec.13055.

(27) Whitehead, A.; Dubansky, B.; Bodinier, C.; Garcia, T. I.; Miles, S.; Pilley, C.; Raghunathan, V.; Roach, J. L.; Walker, N.; Walter, R. B.; et al. Genomic and Physiological Footprint of the Deepwater Horizon Oil Spill on Resident Marsh Fishes. *Proc. Natl. Acad. Sci. U. S. A.* **2012**, *109* (50), 20298–20302. https://doi.org/10.1073/pnas.1109545108.

(28) Meier, K.; Hansen, M. M.; Normandeau, E.; Mensberg, K. L. D.; Frydenberg, J.; Larsen, P. F.; Bekkevold, D.; Bernatchez, L. Local Adaptation at the Transcriptome Level in Brown Trout: Evidence from Early Life History Temperature Genomic Reaction Norms. *PLoS One* **2014**, *9* (1). https://doi.org/10.1371/journal.pone.0085171.

(29) Richards, C. L.; Rosas, U.; Banta, J.; Bhambhra, N.; Purugganan, M. D. Genome-Wide Patterns of Arabidopsis Gene Expression in Nature. *PLoS Genet.* **2012**, *8* (4). https://doi.org/10.1371/journal.pgen.1002662.

(30) Oleksiak, M. F.; Churchill, G. A.; Crawford, D. L. Variation in Gene Expression within and among Natural Populations. *Nat. Genet.* **2002**, *32* (2), 261–266. https://doi.org/10.1038/ng983.

(31) Cooke, S. J.; Donaldson, M. R.; O'connor, C. M.; Raby, G. D.; Arlinghaus, R.; Danylchuk, A. J.; Hanson, K. C.; Hinch, S. G.; Clark, T. D.; Patterson, D. A.; et al. The Physiological Consequences of Catch-and-Release Angling: Perspectives on Experimental Design, Interpretation, Extrapolation and Relevance to Stakeholders. *Fish. Manag. Ecol.* **2013**, *20* (2–3), 268–287. https://doi.org/10.1111/j.1365-2400.2012.00867.x.

(32) Andrews, S. FastQC: A Quality Control Tool for High Throughput Sequence Data. **2010**.

(33) Bolger, A. M.; Lohse, M.; Usadel, B. Trimmomatic: A Flexible Trimmer for Illumina Sequence Data. *Bioinformatics* **2014**, btu170.

(34) Haas, B. J.; Papanicolaou, A.; Yassour, M.; Grabherr, M.; Blood, P. D.; Bowden, J.; Couger, M. B.; Eccles, D.; Li, B.; Lieber, M.; et al. De Novo Transcript Sequence Reconstruction from RNA-Seq Using the Trinity Platform for Reference Generation and Analysis. *Nat. Protoc.* **2013**, *8* (8), 1494–1512. https://doi.org/10.1038/nprot.2013.084.

(35) Simão, F. A.; Waterhouse, R. M.; Ioannidis, P.; Kriventseva, E. V; Zdobnov, E. M. BUSCO: Assessing Genome Assembly and Annotation Completeness with Single-Copy Orthologs. *Bioinformatics* **2015**, *31* (19), 3210–3212. https://doi.org/10.1093/bioinformatics/btv351.

(36) Bryant, D. M.; Johnson, K.; DiTommaso, T.; Tickle, T.; Couger, M. B.; Payzin-Dogru, D.; Lee, T. J.; Leigh, N. D.; Kuo, T. H.; Davis, F. G.; et al. A Tissue-Mapped Axolotl De Novo Transcriptome Enables Identification of Limb Regeneration Factors. *Cell Rep.* **2017**, *18* (3), 762–776. https://doi.org/10.1016/j.celrep.2016.12.063.

(37) Finn, R. D.; Clements, J.; Eddy, S. R. HMMER Web Server: Interactive Sequence Similarity Searching. *Nucleic Acids Res.* **2011**, *39*, W29–W37.

(38) Krogh, A.; Karsson, B.; von Heijne, G.; Sonnhammer, E. L. Predicting Transmembrane Protein Topology with a Hidden Markov Model: Application to Complete Genomes. *J. Mol. Biol.* **2001**, *305* (3), 567–580.

(39) Petersen, T.; Brunak, S.; von Heijne, G.; Nielsen, H. SignalP 4.0: Discriminating Signal Peptides from Transmembrane Regions. *Nat. Methods* **2011**, *8* (10), 785–786.

(40) Langmead, B.; Salzberg, S. Fast Gapped-Read Alignment with Bowtie 2. *Nat Methods* **2012**, *9* (4), 357–359.

(41) Li, B.; Dewey, C. RSEM: Accurate Transcript Quantification from RNA-Seq Data with or without a Reference Genome. *BMC Bioinformatics* **2011**, *12* (323). https://doi.org/10.1186/1471-2105-12-323.

(42) Gentleman, R.; Carey, V.; Huber, W.; Hahne, F. Genefilter: Methods for Filtering Genes from High-Throughput Experiments. *R Packag. version 1.68.0* **2019**.

(43) Love, M. I.; Huber, W.; Anders, S. Moderated Estimation of Fold Change and Dispersion for RNA-Seq Data with DESeq2. *Genome Biol.* **2014**, *15* (550). https://doi.org/https://doi.org/10.1186/s13059-014-0550-8.

(44) Kaimal, V.; Bardes, E.; Tabar, S.; Jegga, A.; Aronow, B. ToppGene Suite for Gene List Enrichment Analysis and Candidate Gene Prioritization. *Nucleic Acids Res.* **2009**, *37*, W305–W311. https://doi.org/https://doi.org/10.1093/nar/gkp427.

(45) Hoffman, G. E.; Schadt, E. E. variancePartition: Interpreting Drivers of Variation in Complex Gene Expression Studies. *BMC Bioinformatics* **2016**, *17*. https://doi.org/10.1186/s12859-016-1323-z.

(46) Tort, L. Stress and Immune Modulation in Fish. *Dev. Comp. Immunol.* **2011**, *35* (12), 1366–1375. https://doi.org/10.1016/j.dci.2011.07.002.

(47) Ahlquist, P. RNA-Dependent RNA Polymerases, Viruses, and RNA Silencing. *Science (80-.).* **2002**, *296* (5571), 1270–1273.

(48) Lepa, A.; Siwicki, A. K. Retroviruses of Wild and Cultured Fish. *Polish Journal of Veterinary Sciences*. 2011, pp 703–709. https://doi.org/10.2478/V10181-011-0106-8.

(49) Fodor, E. The RNA Polymerase of Influenza A Virus: Mechanisms of Viral Transcription and Replication. *Acta Virol.* **2013**, *57*, 113–122. https://doi.org/10.4149/av.

(50) Xu, K.; Zhang, T. T.; Wang, L.; Zhang, C. F.; Zhang, L.; Ma, L. X.; Xin, Y.; Ren, C. H.; Zhang, Z. Q.; Yan, Q.; et al. Walleye Dermal Sarcoma Virus: Expression of a Full-Length Clone or the Rv-Cyclin (Orf a) Gene Is Cytopathic to the Host and Human Tumor Cells. *Mol. Biol. Rep.* **2013**, *40* (2), 1451–1461. https://doi.org/10.1007/s11033-012-2188-5.

(51) Holzschu, D. L.; Martineau, D.; Fodor, S. K.; Vogt, V. M.; Bowser, P. R.; Casey, J. W. Nucleotide Sequence and Protein Analysis of a Complex Piscine Retrovirus, Walleye Dermal Sarcoma Virus. *J. Virol.* **1995**, *69* (9), 5320–5331. https://doi.org/10.1128/jvi.69.9.5320-5331.1995.

(52) Katz, R. The Retroviral Enzymes. *Annu. Rev. Biochem.* **1994**, *63* (1), 133–173. https://doi.org/10.1146/annurev.biochem.63.1.133.

(53) Rovnak, J.; Quackenbush, S. L. Walleye Dermal Sarcoma Virus: Molecular Biology and Oncogenesis. *Viruses* **2010**, *2* (9), 1984–1999. https://doi.org/10.3390/v2091984.

(54) Poulet, F. M.; Vogt, V. M.; Bowser, P. R.; Casey, J. W. In Situ Hybridization and Immunohistochemical Study of Walleye Dermal Sarcoma Virus (WDSV) Nucleic Acids and Proteins in Spontaneous Sarcomas of Adult Walleyes (Stizostedion Vitreum). *Vet. Pathol.* **1995**, *32* (2), 162–172. https://doi.org/10.1177/030098589503200210.

(55) Quackenbush, S. L.; Rovnak, J.; Casey, R. N.; Paul, T. A.; Bowser, P. R.; Sutton, C.; Casey, J. W. Genetic Relationship of Tumor-Associated Piscine Retroviruses. *Mar. Biotechnol.* **2001**, *3* (0), S088–S099. https://doi.org/10.1007/s10126-01-0030-5.

(56) LaPierre, L. A.; Casey, J. W.; Holzschu, D. L. Walleye Retroviruses Associated with Skin Tumors and Hyperplasias Encode Cyclin D Homologs. *J. Virol.* **1998**, *72* (11), 8765–8771. https://doi.org/10.1128/jvi.72.11.8765-8771.1998.

(57) Dodurga, Y.; Gundogdu, G.; Tekin, V.; Koc, T.; Satiroglu-Tufan, N. L.; Bagci, G.; Kucukatay, V. Valproic Acid Inhibits the Proliferation of SHSY5Y Neuroblastoma Cancer Cells by Downregulating URG4/URGCP and CCND1 Gene Expression. *Mol. Biol. Rep.* **2014**, *41* (7), 4595–4599. https://doi.org/10.1007/s11033-014-3330-3.

(58) Lale Satiroglu Tufan, N.; Lian, Z.; Liu, J.; Pan, J.; Arbuthnot, P.; Kew, M.;

Clayton, M. M.; Zhu, M.; Feitelson, M. A. Hepatitis Bx Antigen Stimulates Expression of a Novel Cellular Gene, URG4, That Promotes Hepatocellular Growth and Survival. *Neoplasia* **2002**, *4* (4), 355–368. https://doi.org/10.1038/sj.neo.7900241.

(59) Ciucci, T.; Bosselut, R. Gimap and T Cells: A Matter of Life or Death. *Eur. J. Immunol.* **2014**, *44* (2), 348–351.

(60) Filén, S.; Lahesmaa, R. GIMAP Proteins in T-Lymphocytes. *J. Signal Transduct.* **2010**, *2010*, 268589. https://doi.org/10.1155/2010/268589.

(61) Reyes-Cerpa, S.; Maisey, K.; Reyes-Lopez, F.; Toro-Ascuy, D.; Sandino, A. .; Imarai, M. Fish Cytokines and Immune Response. In *New Advances and Contributions to Fish Biology*; Türker, H., Ed.; InTechOpen, 2012. https://doi.org/http://dx.doi.org/10.5772/53504.

(62) Huang, Y.; Huang, X.; Cai, J.; OuYang, Z.; Wei, S.; Wei, J.; Qin, Q. Identification of Orange-Spotted Grouper (Epinephelus Coioides) Interferon Regulatory Factor 3 Involved in Antiviral Immune Response against Fish RNA Virus. *Fish Shellfish Immunol.* **2015**, *42* (2), 345–352. https://doi.org/10.1016/j.fsi.2014.11.025.

(63) Collet, B.; Secombes, C. J. Type I-Interferon Signalling in Fish. *Fish Shellfish Immunol.* **2002**, *12* (5), 389–397. https://doi.org/10.1006/fsim.2001.0405.

(64) Zou, J.; Secombes, C. J. Teleost Fish Interferons and Their Role in Immunity. *Dev. Comp. Immunol.* **2011**, *35* (12), 1376–1387. https://doi.org/10.1016/j.dci.2011.07.001.

(65) Robertsen, B. The Role of Type I Interferons in Innate and Adaptive Immunity against Viruses in Atlantic Salmon. *Dev. Comp. Immunol.* **2018**. https://doi.org/10.1016/j.dci.2017.02.005.

(66) Yao, C. L.; Huang, X. N.; Fan, Z.; Kong, P.; Wang, Z. Y. Cloning and Expression Analysis of Interferon Regulatory Factor (IRF) 3 and 7 in Large Yellow Croaker, Larimichthys Crocea. *Fish Shellfish Immunol.* **2012**. https://doi.org/10.1016/j.fsi.2012.02.015.

(67) Iwama, G. K.; Thomas, P. T.; Forsyth, R. B.; Vijayan, M. M. Heat Shock Protein Expression in Fish. *Rev. F* **1998**, *8*, 35–56.

(68) Basu, N.; Todgham, A. E.; Ackerman, P. A.; Bibeau, M. R.; Nakano, K.; Schulte, P. M.; Iwama, G. K. Heat Shock Protein Genes and Their Functional Significance in Fish. *Gene* **2002**, *295* (2), 173–183. https://doi.org/10.1016/S0378-1119(02)00687-X.

(69) Roberts, R. J.; Agius, C.; Saliba, C.; Bossier, P.; Sung, Y. Y. Heat Shock Proteins (Chaperones) in Fish and Shellfish and Their Potential Role in Relation to Fish Health: A Review. *J. Fish Dis.* **2010**, *33* (10), 789–801. https://doi.org/10.1111/j.1365-2761.2010.01183.x.

(70) Cara, J. B.; Aluru, N.; Moyano, F. J.; Vijayan, M. M. Food-Deprivation Induces HSP70 and HSP90 Protein Expression in Larval Gilthead Sea Bream and Rainbow Trout. *Comp. Biochem. Physiol. - Part B Biochem. Mol. Biol.* **2005**, *142* (4), 426–431.

(71) Wei, T.; Gao, Y.; Wang, R.; Xu, T. A Heat Shock Protein 90 β Isoform Involved in Immune Response to Bacteria Challenge and Heat Shock from Miichthys Miiuy. *Fish Shellfish Immunol.* **2013**, *35* (2), 429–437.

(72) Xie, Y.; Song, L.; Weng, Z.; Liu, S.; Liu, Z. Hsp90, Hsp60 and sHsp Families of Heat Shock Protein Genes in Channel Catfish and Their Expression after Bacterial Infections. *Fish Shellfish Immunol.* **2015**, *44* (2), 642–651.

(73) Chen, Y. M.; Kuo, C. E.; Wang, T. Y.; Shie, P. S.; Wang, W. C.; Huang, S. L.; Tsai, T. J.; Chen, P. P.; Chen, J. C.; Chen, T. Y. Cloning of an Orange-Spotted Grouper Epinephelus Coioides Heat Shock Protein 90AB (HSP90AB) and Characterization of Its Expression in Response to Nodavirus. *Fish Shellfish Immunol.* **2010**, *28* (5–6), 895–904. https://doi.org/10.1016/j.fsi.2010.02.004.

(74) Nagy, P. D.; Wang, R. Y.; Pogany, J.; Hafren, A.; Makinen, K. Emerging Picture of Host Chaperone and Cyclophilin Roles in RNA Virus Replication. *Virology*. 2011. https://doi.org/10.1016/j.virol.2010.12.061.

(75) Geller, R.; Taguwa, S.; Frydman, J. Broad Action of Hsp90 as Host Chaperone Required for Viral Replication. *Biochim. Biophys. Acta* **2012**, *1823* (3), 698–706. https://doi.org/10.1097/MCA.0000000000000178.Endothelial.

(76) Hu, J.; Seeger, C. Hsp90 Is Required for the Activity of a Hepatitis B Virus Reverse Transcriptase. *Proc. Natl. Acad. Sci. U. S. A.* **1996**, *93* (3), 1060–1064. https://doi.org/10.1073/pnas.93.3.1060.

(77) Kampmueller, K. M.; Miller, D. J. The Cellular Chaperone Heat Shock Protein 90 Facilitates Flock House Virus RNA Replication in Drosophila Cells. *J. Virol.* **2005**, *79* (11), 6827–6837. https://doi.org/10.1128/jvi.79.11.6827-6837.2005.

(78) Murakami, M.; Masuda, S.; Kudo, I. Arachidonate Release and Prostaglandin Production by Group IVC Phospholipase A2 (Cytosolic Phospholipase A2γ). *Biochem. J.* **2003**, *372* (3), 695–702. https://doi.org/10.1042/BJ20030061.

(79) Tocher, D. R. Metabolism and Functions of Lipids and Fatty Acids in Teleost Fish. *Rev. Fish. Sci.* **2003**, *11* (2), 107–184. https://doi.org/10.1080/713610925.

(80) Xu, S.; Pei, R.; Guo, M.; Han, Q.; Lai, J.; Wang, Y.; Wu, C.; Zhou, Y.; Lu, M.; Chen, X. Cytosolic Phospholipase A2 Gamma Is Involved in Hepatitis C Virus Replication and Assembly. *J. Virol.* **2012**, *86* (23), 13025–13037. https://doi.org/10.1128/jvi.01785-12.

(81) Brown, J. K.; Knight, P. A.; Thornton, E. M.; Pate, J. A.; Coonrod, S.; Miller, H. R. P.; Pemberton, A. D. Trichinella Spiralis Induces de Novo Expression of Group IVC Phospholipase A2 in the Intestinal Epithelium. *Int. J. Parasitol.* **2008**, *38* (2), 143–147. https://doi.org/10.1016/j.ijpara.2007.10.002.

(82) Fermani, P.; Diovisalvi, N.; Torremorell, A.; Lagomarsino, L.; Zagarese, H. E.; Unrein, F. The Microbial Food Web Structure of a Hypertrophic Warm-Temperate Shallow Lake, as Affected by Contrasting Zooplankton Assemblages. *Hydrobiologia* **2013**, *714* (1), 115–130. https://doi.org/10.1007/s10750-013-1528-3.

(83) Loick-Wilde, N.; Weber, S. C.; Conroy, B. J.; Capone, D. G.; Coles, V. J.; Medeiros, P. M.; Steinberg, D. K.; Montoya, J. P. Nitrogen Sources and Net Growth Efficiency of Zooplankton in Three Amazon River Plume Food Webs. *Limnol. Oceanogr.* **2016**, *61* (2), 460–481. https://doi.org/10.1002/lno.10227.

(84) Brett, M. T.; Arhonditsis, G. B.; Chandra, S.; Kainz, M. J. Mass Flux Calculations Show Strong Allochthonous Support of Freshwater Zooplankton Production Is Unlikely. *PLoS One* **2012**, *7* (6), 1–9. https://doi.org/10.1371/journal.pone.0039508.

(85) Chen, C. Y.; Durbin, E. G. Effects of pH on the Growth and Carbon Uptake of Marine Phytoplankton. *Mar. Ecol. Prog. Ser.* **1994**, *109* (1), 83–94. https://doi.org/10.3354/meps109083.

(86) Oomen, R. A.; Hutchings, J. A. Transcriptomic Responses to Environmental Change in Fishes: Insights from RNA Sequencing. *Facets* **2017**, *2* (2), 610–641. https://doi.org/10.1139/facets-2017-0015.

(87) Veilleux, H. D.; Ryu, T.; Donelson, J. M.; Van Herwerden, L.; Seridi, L.; Ghosheh, Y.; Berumen, M. L.; Leggat, W.; Ravasi, T.; Munday, P. L. Molecular Processes of Transgenerational Acclimation to a Warming Ocean. *Nat. Clim. Chang.* **2015**, *5* (12), 1074–1078. https://doi.org/10.1038/nclimate2724.

(88) Kidd, K. A.; Blanchfield, P. J.; Mills, K. H.; Palace, V. P.; Evans, R. E.;

Lazorchak, J. M.; Flick, R. W. Collapse of a Fish Population after Exposure to a Synthetic Estrogen. *Proc. Natl. Acad. Sci. U. S. A.* **2007**, *104* (21), 8897–8901. https://doi.org/10.1073/pnas.0609568104.

(89) Palace, V. P.; Evans, R. E.; Wautier, K. G.; Mills, K. H.; Blanchfield, P. J.; Park, B. J.; Baron, C. L.; Kidd, K. A. Interspecies Differences in Biochemical, Histopathological, and Population Responses in Four Wild Fish Species Exposed to Ethynylestradiol Added to a Whole Lake. *Can. J. Fish. Aquat. Sci.* **2009**, *66* (11), 1920–1935. https://doi.org/10.1139/F09-125.

(90) Schindler, D. W.; Wagemann, R.; Cook, R. B.; Ruszczynski, T.; Prokopowich, J. Experimental Acidification of Lake 223, Experimental Lakes Area: Background Data and the First Three Years of Acidification. *Can. J. Fish. Aquat. Sci.* **1980**, *37* (3), 342–354. https://doi.org/10.1139/f80-048.

(91) Nero, R. W.; Schindler, D. W. Decline of Mysis Relicla During the Acidification of Lake 223. *Can. J. Fish. Aquat. Sci.* **1983**, *40*, 1095–1911.

(92) Kennedy, L. A. Teratogenesis in Lake Trout (Salvelinus Namaycush) in an Experimentally Acidified Lake. *Can. J. Fish. Aquat. Sci.* **1980**, *37* (12), 2355–2358. https://doi.org/10.1139/f80-282.

(93) Schindler, D. W.; Turner, M. A. Biological, Chemical and Physical Responses of Lakes to Experimental Acidification. In *Long-Range Transport of Airborne Pollutants*; Martin, H. C., Ed.; Springer Netherlands: Dordrecht, 1982; pp 259–271. https://doi.org/10.1007/978-94-009-7966-6_19.

(94) Mills, K. H.; Chalanchuk, S. M.; Mohr, L. C.; Davies, I. J. Responses of Fish Populations in Lake 223 to 8 Years of Experimental Acidification. *Can. J. Fish. Aquat. Sci.* **1987**, *44* (SUPPL. 1), 114–125. https://doi.org/10.1139/f87-287.

(95) Adams, C. I. M.; Knapp, M.; Gemmell, N. J.; Jeunen, G.-J.; Bunce, M.; Lamare, M. D.; Taylor, H. R. Beyond Biodiversity: Can Environmental DNA (eDNA) Cut It as a Population Genetics Tool? *Genes (Basel)*. **2019**, *10* (3), 192. https://doi.org/10.3390/genes10030192.

Figures and Tables

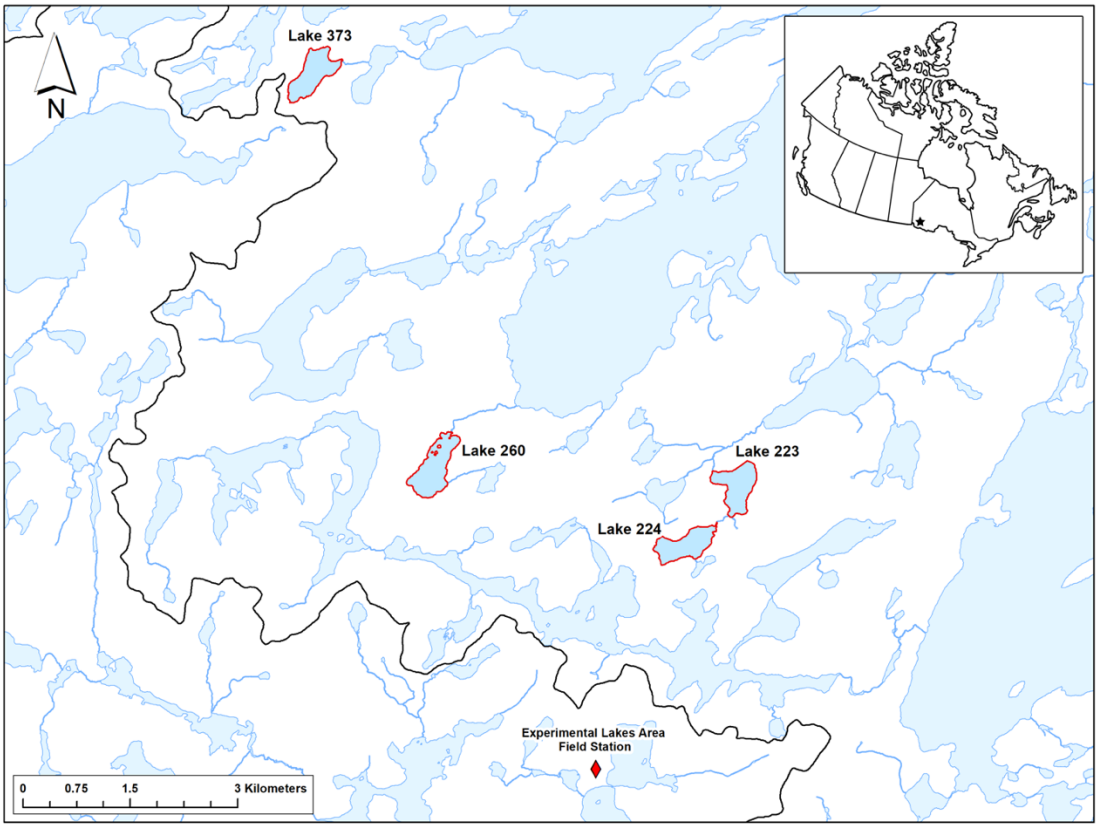

Figure 3.1. Map of the IISD Experimental Lakes Area, located in northwestern Ontario, Canada, indicating the locations of the four lakes used in the present study. Black line denotes quaternary watershed boundaries. Data source: Ontario Integrated Hydrology Data (Ontario Ministry of Natural Resources and Forestry - Provincial Mapping Unit).

Table 3.1. For each lake, (a) hydrological characteristics, (b) average metrics for lake trout collected in 2017 (± standard error of mean), (c) zooplankton population metrics, including total abundance, richness, Shannon Weiner diversity index (H'), and Shannon's equitability (E_H), and (d) average water quality parameters (± standard error of mean) (TDN = total dissolved nitrogen, TDP = total dissolved phosphorus). The n for Lake 373 is relatively lower as it was not sampled for population data in 2017.

		Lake 260	Lake 223	Lake 224	Lake 373
(a)					
	Area (m^2)	332,328	268,951	261,450	273,653
	Volume (m^3)	1,975,971	1,891,984	3,066,672	3,107,474
	Maximum Depth (m)	15.7	14.4	27.3	21.2
	Average Depth (m)	5.9	7.0	11.7	11.4
(b)					
	Total Length (mm)	472.1 ± 2.7	436.8 ± 1.5	426.0 ± 2.2	420.1 ± 9.5
	Weight (g)	845.4 ± 13.2	662.2 ± 7.1	612.4 ± 10.2	574.4 ± 40.2
	Condition Factor	0.7911 ± 0.0038	0.7894 ± 0.0041	0.7797 ± 0.0042	0.7603 ± 0.0176
	n	193	248	189	7
(c)					
	Abundance (count/L)	174.43	224.80	145.31	75.89
	Richness (# species)	38	38	29	26
	H' Index	2.08	1.93	1.67	2.50
	E_H	0.77	0.53	0.50	0.77
(d)					
	Alkalinity (µEq/L)	133.1 ± 2.16	126.6 ± 0.08	106.7 ± 1.57	174.6 ± 1.25
	Conductivity (S/m)	17.86 ± 0.86	21.32 ± 2.60	12.22 ± 0.12	18.97 ± 1.37
	pH	6.82 ± 0.08	7.02 ± 0.06	6.971 ± 0.06	7.22 ± 0.03
	Dissolved Oxygen (mg/L)	8.04 ± 0.32	11.31 ± 0.33	10.73 ± 0.25	10.78 ± 0.26
	Temperature (°C)	11.15 ± 0.53	12.85 ± 0.59	11.92 ± 0.43	10.21 ± 0.45
	Chlorophyll-a (µg/L)	3.82 ± 1.01	4.08 ± 1.36	1.52 ± 0.15	2.22 ± 0.22
	Suspended Carbon (µg/L)	421.1 ± 19.38	453.8 ± 43.01	364.1 ± 21.94	442.3 ± 22.04
	Suspended Nitrogen (µg/L)	44.65 ± 3.32	44.15 ± 4.96	33.46 ± 3.56	40.8 ± 4.76
	Suspended Phosphorus (µg/L)	3.5 ± 0.29	2.75 ± 0.25	2.6 ± 0.16	3.13 ± 0.23
	TDP (µg/L)	2.38 ± 0.21	2.25 ± 0.09	3.22 ± 0.40	2.11 ± 0.10
	TDN (µg/L)	246.3 ± 5.31	230 ± 1.96	198.7 ± 2.82	199.5 ± 3.61
	NO_3-N (µg/L)	1.75 ± 0.85	1.75 ± 0.48	1.4 ± 0.31	0.5 ± 0.33
	NH_3-N (µg/L)	0.5 ± 0.29	6.75 ± 0.75	4.7 ± 0.52	1.13 ± 0.74

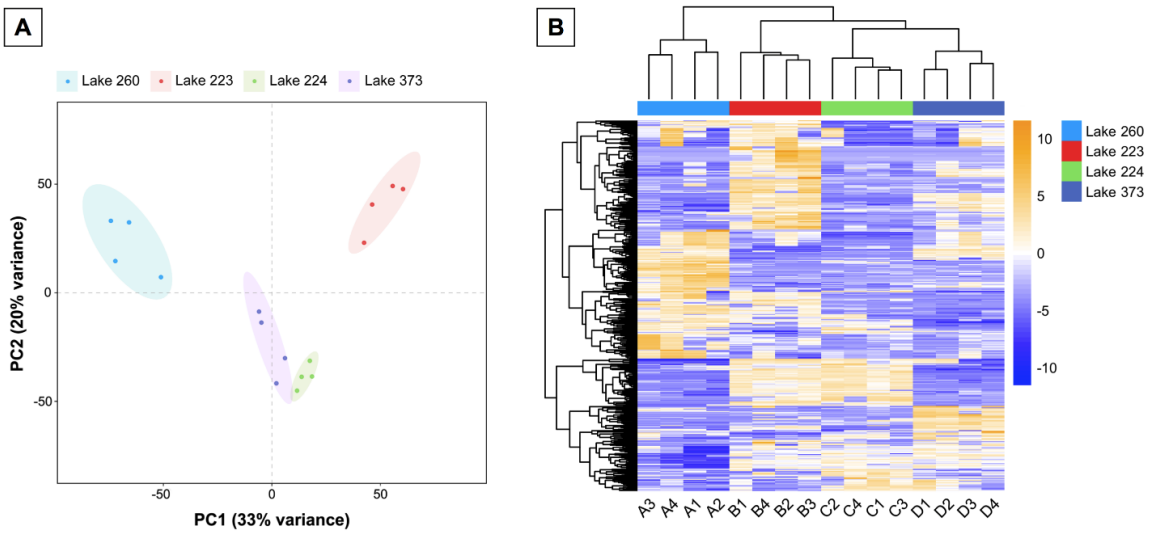

Figure 3.2. A) Principal component analysis of transcriptome-wide count data with individual lake trout colored by lake and B) unsupervised hierarchical clustering of the top 500 most variable transcripts in epidermal mucus of lake trout collected from Lakes 260, 223, 224, and 373 at the IISD Experimental Lakes Area.

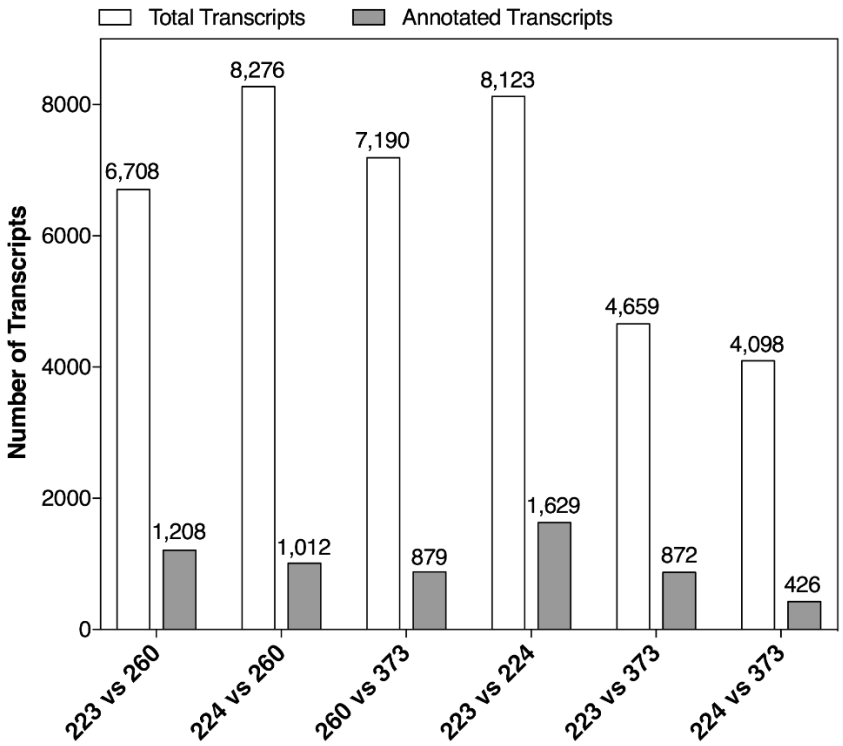

Figure 3.3. The number of differentially regulated transcripts identified by RNA sequencing in epidermal mucus collected from lake trout populations residing in different lakes. The total number of differentially regulated transcripts is presented for each lake-by-lake comparison as well as the subset of transcripts which were functionally annotated by BLASTX.

Table 3.2. The top ten gene ontology biological processes among each lake-by-lake comparison, including the FDR adjusted-*p* values and number of transcripts associated with the pathway.

Gene Ontology ID	Pathway Name	FDR adj-*p*	# Transcripts
	L223 vs L224		
GO:0006613	cotranslational protein targeting to membrane	1.58E-45	61
GO:0006614	SRP-dependent cotranslational protein targeting to membrane	2.21E-44	59
GO:0045047	protein targeting to ER	3.52E-40	59
GO:0000184	nuclear-transcribed mRNA catabolic process, nonsense-mediated decay	3.52E-40	59
GO:0072599	establishment of protein localization to endoplasmic reticulum	3.20E-39	59
GO:0070972	protein localization to endoplasmic reticulum	4.68E-37	62
GO:0006413	translational initiation	1.34E-36	70
GO:0019080	viral gene expression	1.35E-33	69
GO:0019083	viral transcription	7.79E-33	66
GO:0006612	protein targeting to membrane	1.41E-32	68
	L223 vs L373		
GO:0022610	biological adhesion	2.56E-11	94
GO:0007155	cell adhesion	2.67E-11	93
GO:0007010	cytoskeleton organization	1.31E-08	92
GO:0098609	cell-cell adhesion	2.87E-07	59
GO:0000902	cell morphogenesis	1.18E-06	68
GO:0043085	positive regulation of catalytic activity	1.18E-06	84
GO:0032989	cellular component morphogenesis	3.04E-06	71
GO:0034330	cell junction organization	3.04E-06	29
GO:0010256	endomembrane system organization	3.73E-06	42
GO:0001775	cell activation	3.89E-06	80
	L223 vs L260		
GO:0044403	symbiotic process	3.83E-15	93
GO:0016032	viral process	9.66E-15	88
GO:0044419	interspecies interaction between organisms	1.31E-14	94
GO:0010941	regulation of cell death	9.35E-12	142
GO:0016050	vesicle organization	2.82E-11	131
GO:0007010	cytoskeleton organization	4.53E-11	124
GO:0072657	protein localization to membrane	5.69E-11	69
GO:0034097	response to cytokine	9.23E-11	103
GO:0042981	regulation of apoptotic process	1.48E-10	128
GO:0043067	regulation of programmed cell death	2.18E-10	129
	L224 vs L373		
GO:0032691	negative regulation of interleukin-1 beta production	5.96E-04	7
GO:0032611	interleukin-1 beta production	5.96E-04	10
GO:0032692	negative regulation of interleukin-1 production	8.33E-04	7
GO:0032651	regulation of interleukin-1 beta production	1.00E-03	9
GO:0032612	interleukin-1 production	1.00E-03	10
GO:0032652	regulation of interleukin-1 production	2.78E-03	9
GO:0019226	transmission of nerve impulse	4.29E-03	8
GO:0000904	cell morphogenesis involved in differentiation	5.43E-03	25
GO:0050713	negative regulation of interleukin-1 beta secretion	7.60E-03	4
GO:0007626	locomotory behavior	9.31E-03	12
	L260 vs L224		
GO:0034097	response to cytokine	2.84E-08	82
GO:0071345	cellular response to cytokine stimulus	7.39E-06	71
GO:0007623	circadian rhythm	2.24E-05	25
GO:0061919	process utilizing autophagic mechanism	2.24E-05	40
GO:0006914	autophagy	2.24E-05	40
GO:0010941	regulation of cell death	2.65E-05	98
GO:0007010	cytoskeleton organization	3.55E-05	86
GO:0010942	positive regulation of cell death	5.03E-05	53
GO:0031331	positive regulation of cellular catabolic process	6.44E-05	32

GO:0048511	rhythmic process	1.03E-04	29
	L260 vs 373		
GO:0042981	regulation of apoptotic process	8.77E-08	94
GO:0010941	regulation of cell death	8.77E-08	100
GO:0043067	regulation of programmed cell death	8.77E-08	94
GO:0007009	plasma membrane organization	8.77E-08	27
GO:0046903	secretion	1.12E-07	94
GO:0044403	symbiotic process	2.64E-07	58
GO:0070201	regulation of establishment of protein localization	3.74E-07	56
GO:0016032	viral process	3.78E-07	55
GO:0070268	cornification	4.22E-07	18
GO:0044419	interspecies interaction between organisms	4.22E-07	59

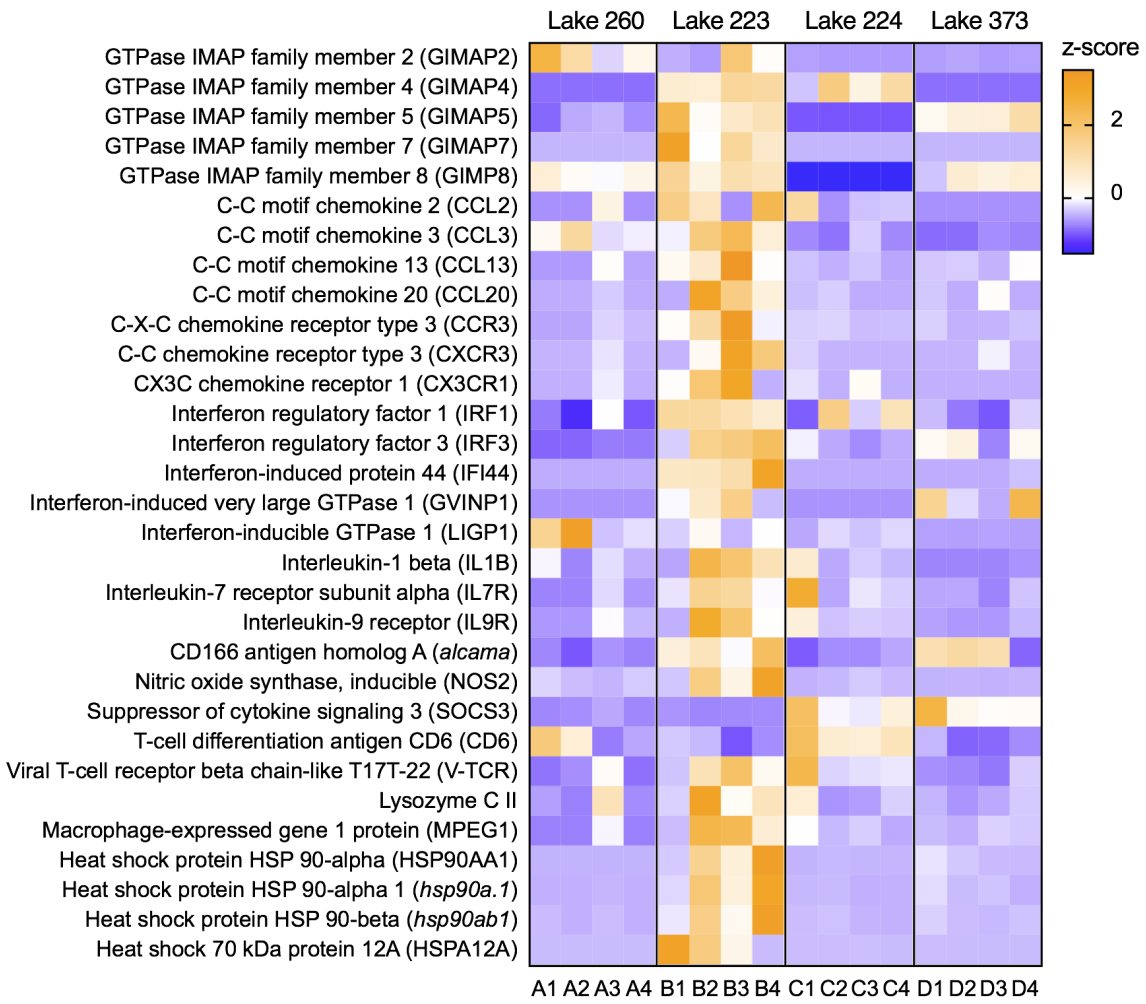

Figure 3.4. Relative expression of immune-related transcripts in epidermal mucus of lake trout collected from Lakes 260, 223, 224, and 373 at the IISD Experimental Lakes Area. Expression data are presented as the normalized count data, centered and scaled, from each individual in order to provide direct comparison of gene expression levels due to lack of a control group. Thus, orange represents higher count level of a particular transcript, whereas blue suggests lower count level. Transcripts shown were differentially-expressed in at least one lake-by-lake comparison.

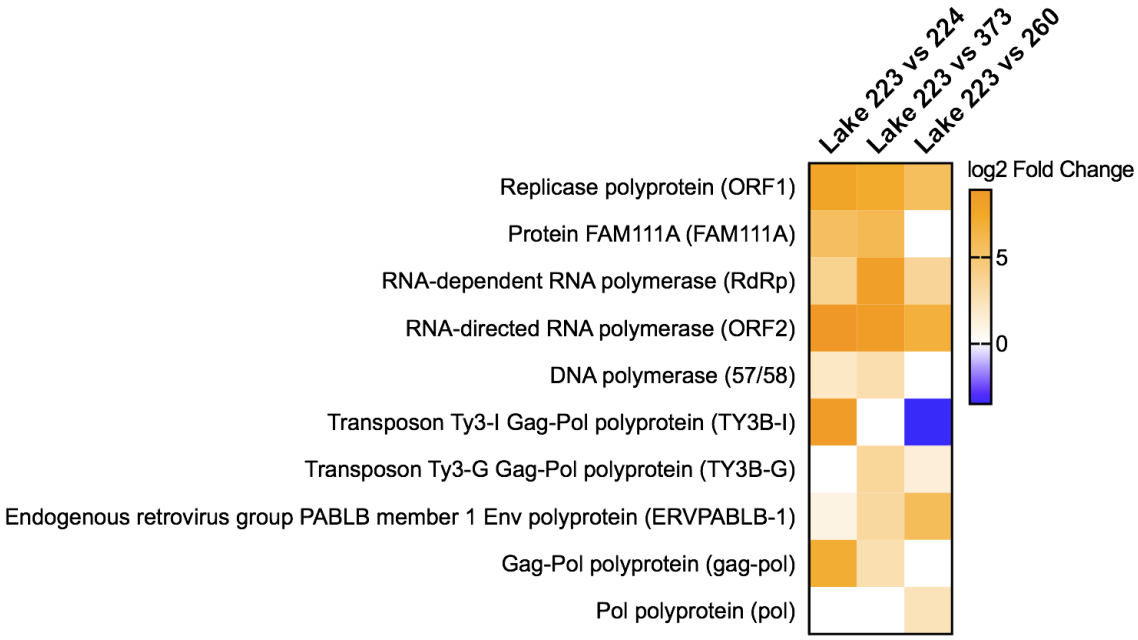

Figure 3.5. Differential expression of transcripts involved in viral gene transcription in lake trout from Lake 223 compared to Lakes 224, 373, and 260.

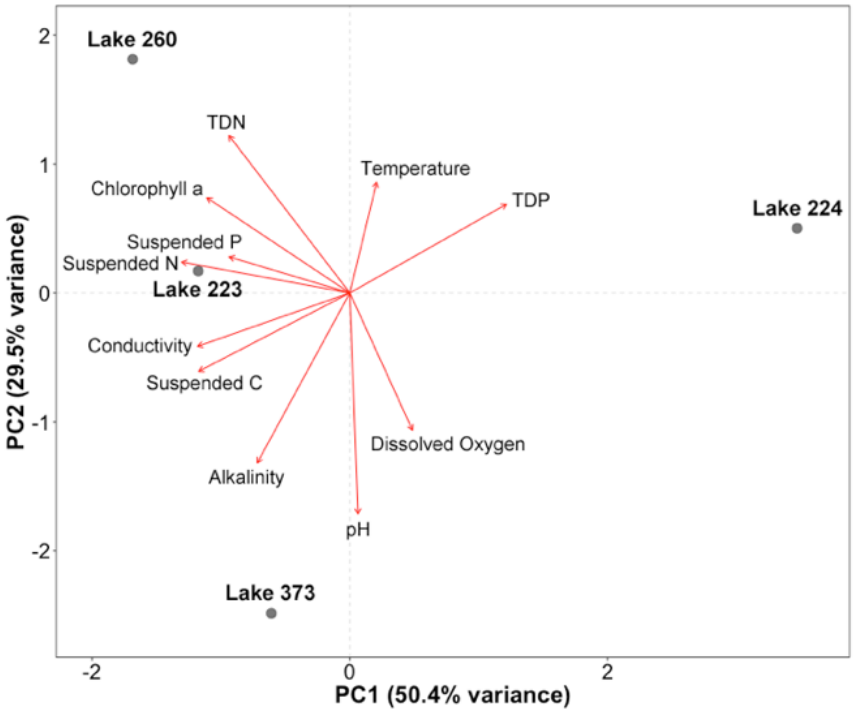

Figure 3.6. Principal component analysis of average water quality parameters for Lakes 260, 223, 224, and 373 with arrows indicating the loadings of each water quality variable.

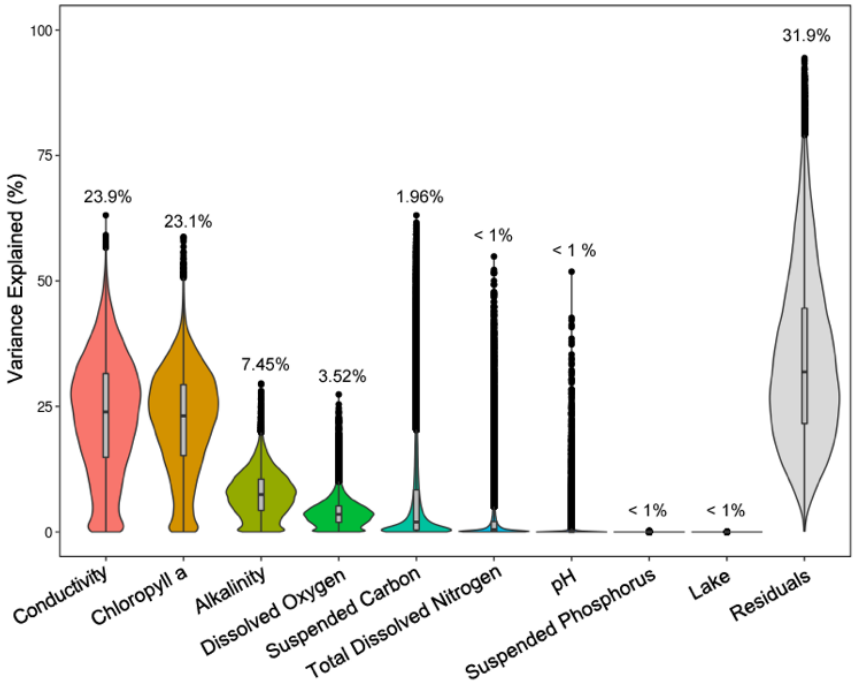

Figure 3.7. Results of the linear mixed model indicating the median variance explained by water quality parameters across all genes within the lake trout transcriptome-wide read count data. Each variable explains a certain percent of variation across all genes after correcting for all other variables.

Supplemental Materials

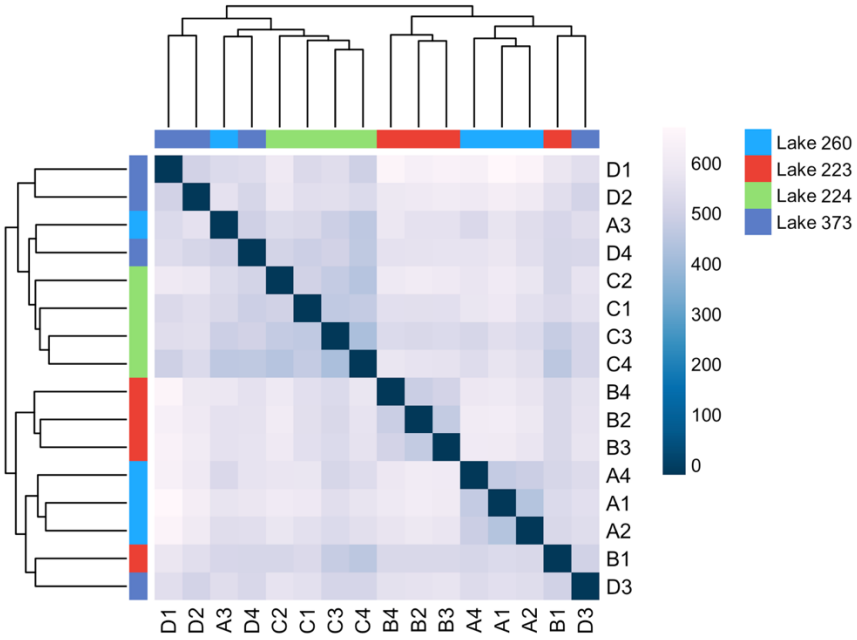

Figure 3.S1. Sample-to-sample Euclidian distance heat map based on transcriptome-wide count data from lake trout collected from four lakes at the IISD Experimental Lakes Area.

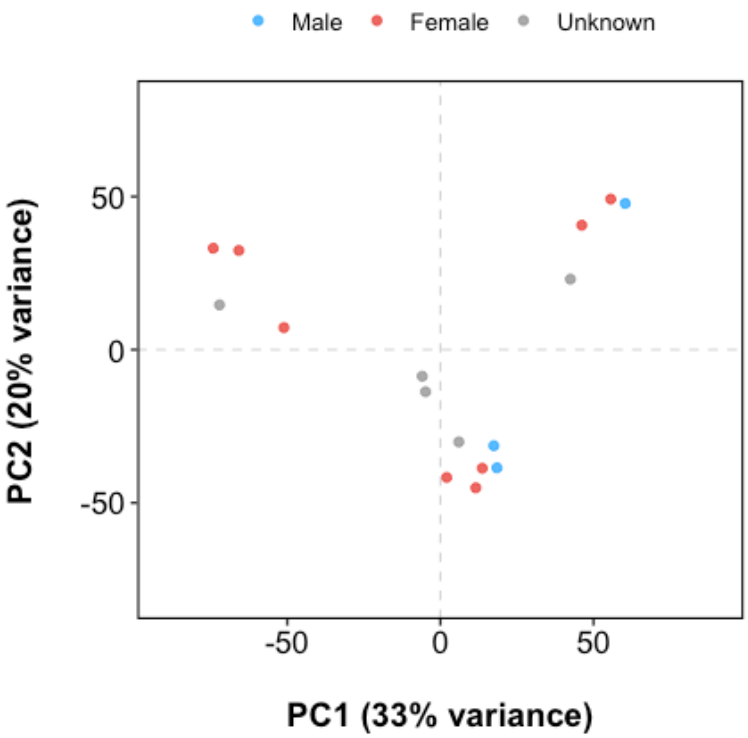

Figure 3.S2. Principal component analysis of transcriptome-wide count data with individual lake trout colored by sex. Sex of some individuals is unknown as sex determination was done through external observations which may not always be conclusive.

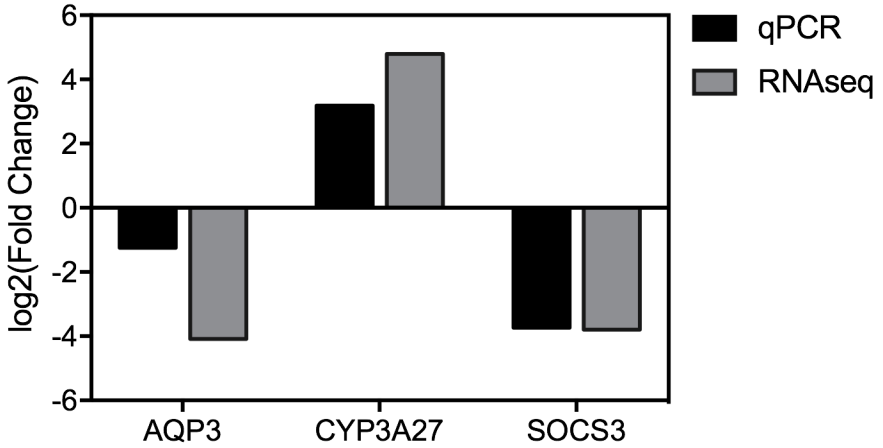

Figure 3.S3. Results of qPCR analysis used to verify the RNA sequencing results among Lake 223 and Lake 373 (AQP3 = aquaporin 3, CYP3A27 = cytochrome P450 3A27, SOCS3 = suppressor of cytokine signaling 3). Relative expression was determined by the $2^{-\Delta\Delta Ct}$ method with β-actin as the normalizing gene.

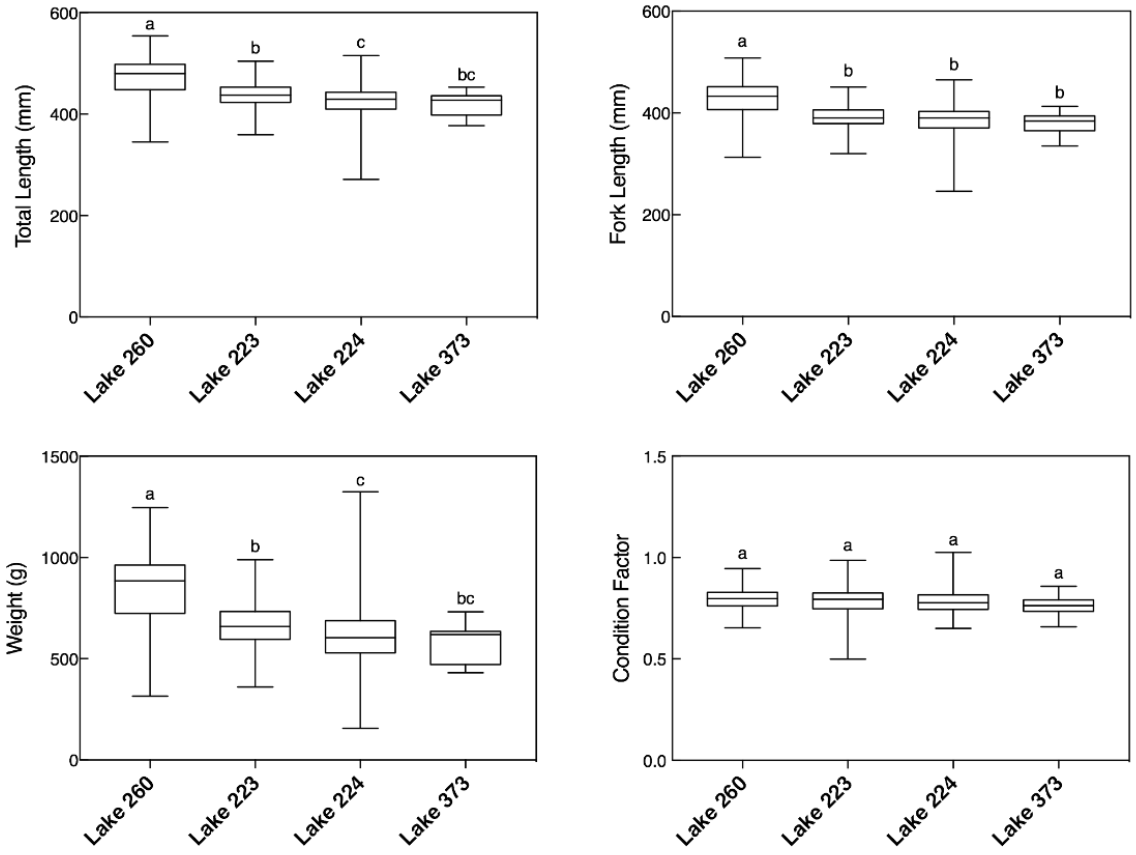

Figure 3.S4. Average length, weight, and condition factor (± SEM) of lake trout collected from L260, L223, L224, and L260 throughout 2017.

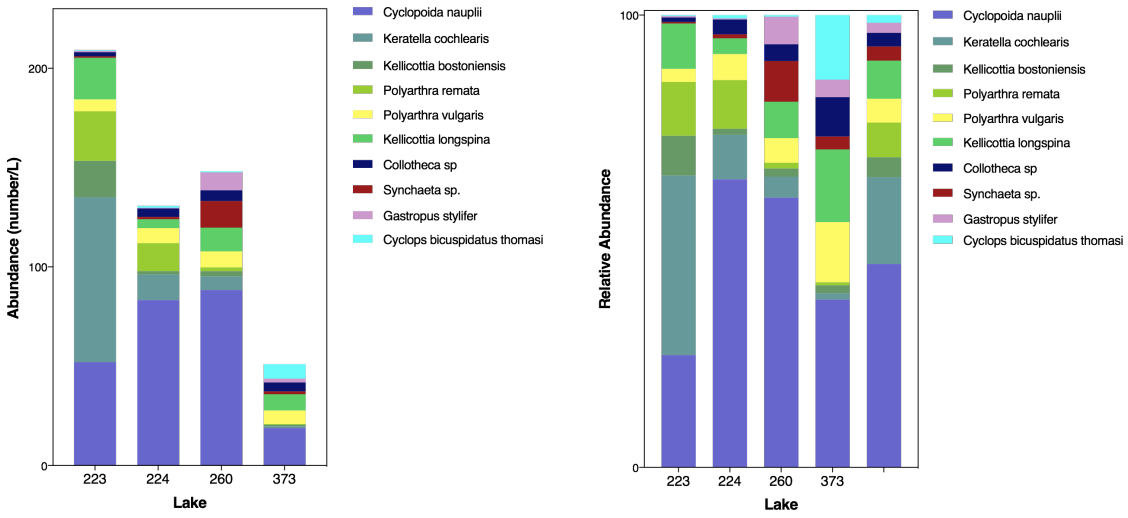

Figure 3.S5. Abundance (number/L) and relative abundance of the top ten most abundant zooplankton populations in L223, L224, L260, and L373.

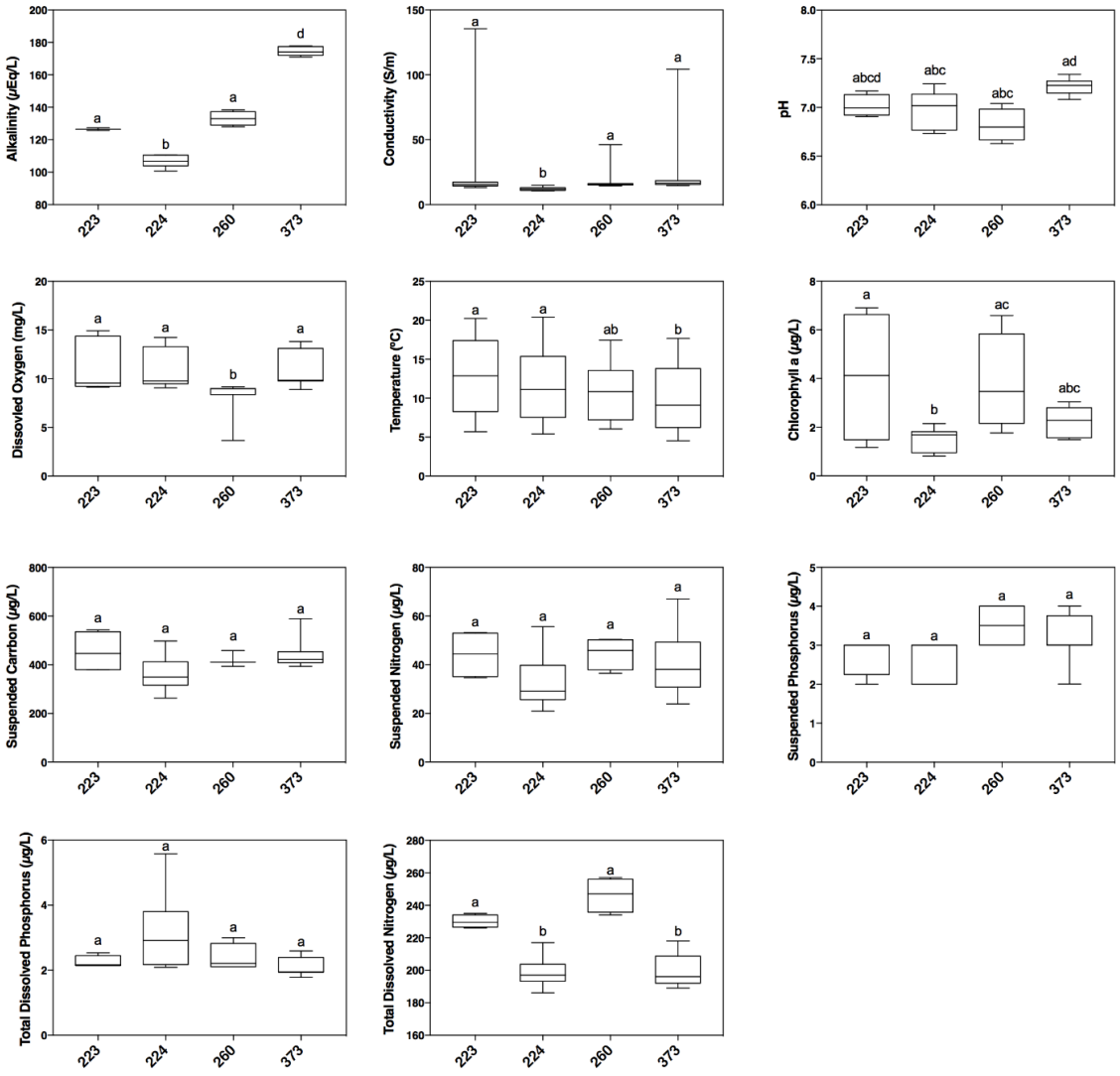

Figure 3.S6. Water quality parameters averaged from epilimnion and metalimnion data for L223, L224, L260, and L373 from sampling during September and October 2017.

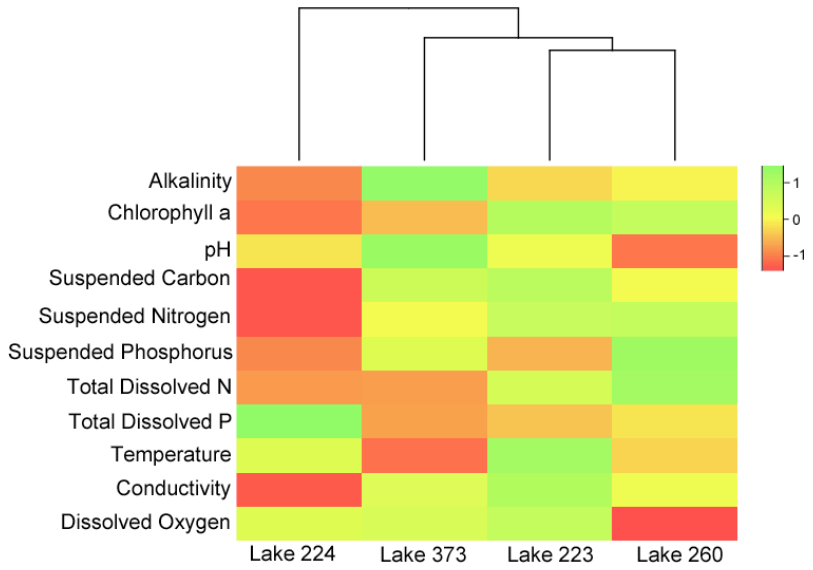

Figure 3.S7. Unsupervised hierarchical clustering of L224, L373, L223, and L260 based on average water quality parameters.

Table 3.S1. Forward and reverse primer sequences used for qPCR analysis.

Gene	Forward Sequence	Reverse Sequence
Aquaporin 3 (*aqp*3)	TGTGCTACGGGTTCATCT	GTCCTCAGTTTGGCTCTTG
Suppressor of cytokine signaling 3 (*socs3*)	TGACAACCGACATTTCTTCACC	TGCTGGAATCACACTGGACAC
Cytochrome P450 3A27 (*cyp3a27*)	GAACCGGAGGAAAGATGATG	GGACCAGGGATACCCATCTTA
Beta-actin	AGAGCTACGAGCTGCCTGAC	GCAAGACTCCATACCGAGGA

Table 3.S2. Information on lake trout collected during 2017 sampling. N/A indicated that the sex of the individual could not be inferred based on morphological observations.

Lake	ID	Date of Collection	Weight (g)	Total Length (mm)	Fork Length (mm)	Sex	Sequenced? (if yes, sample ID)
223	M17-223-01	2017-09-28	834	478	427	M	N
223	M17-223-02	2017-09-28	693	450	400	n/a	Y (B1)
223	M17-223-03	2017-09-28	648	431	385	M	Y (B2)
223	M17-223-04	2017-09-28	740	448	402	F	Y (B3)
223	M17-223-05	2017-09-28	578	462	420	F	N
223	M17-223-06	2017-09-28	737	440	398	F	N
223	M17-223-07	2017-09-28	696	439	391	M	Y (B4)
224	M17-223-01	2017-09-27	657	449	406	M	Y (C1)
224	M17-223-02	2017-09-27	688	459	415	F	Y (C2)
224	M17-223-03	2017-09-27	752	450	408	M	N
224	M17-223-04	2017-09-27	676	442	403	F	N
224	M17-223-05	2017-09-27	715	445	405	F	Y (C3)
224	M17-223-06	2017-09-27	613	445	405	F	Y (C4)
224	M17-223-07	2017-10-10	388	373	337	n/a	N
260	M17-260-01	2017-09-26	567	405	366	M	Y (A1)
260	M17-260-02	2017-09-26	362	368	334	M	N
260	M17-260-03	2017-09-26	978	500	455	F	N
260	M17-260-04	2017-09-26	378	362	324	n/a	Y (A2)
260	M17-260-05	2017-09-26	877	479	433	M	N
260	M17-260-06	2017-09-26	648	426	384	M	Y (A3)
260	M17-260-07	2017-09-26	700	441	394	M	Y (A4)
373	M17-373-01	2017-09-26	620	436	390	M	Y (D1)
373	M17-373-02	2017-10-08	619	430	384	F	N
373	M17-373-03	2017-10-08	512	427	377	n/a	N
373	M17-373-04	2017-10-08	430	377	335	n/a	N
373	M17-373-05	2017-10-10	636	420	394	n/a	Y (D2)
373	M17-373-06	2017-10-10	472	398	365	n/a	Y (D3)
373	M17-373-07	2017-10-10	732	453	413	n/a	Y (D4)

Table 3.S3. Sample RNA integrity numbers (RIN), raw read counts, and read counts following processing.

Sample	RIN	Raw Read Count	Read Count after rRNA removal and Adapter Trimming
A1	3.1	19,840,892	6,268,587
A2	3.5	19,931,020	4,981,717
A3	5.5	24,288,841	11,910,843
A4	6.4	22,146,500	8,561,001
B1	3.4	25,665,873	8,537,426
B2	4.1	27,485,398	8,468,937
B3	3.7	25,672,179	5,895,574
B4	4.1	29,436,562	6,795,667
C1	3.8	23,583,863	17,053,048
C2	3	21,060,335	9,573,289
C3	3.1	30,423,526	15,219,702
C4	3.2	31,195,629	18,990,682
D1	4.5	23,665,391	18,735,086
D2	3.3	23,097,315	8,896,490
D3	2.6	27,908,675	11,506,804
D4	4.3	29,624,381	14,515,738

Table 3.S4. Trinity *de novo* transcriptome assembly statistics and annotation information.

	Trinity Assembly
Total Trinity Genes	268,935
Total Trinity Transcripts	365,521
Percent GC	46.79
Contig N10	2,369 bp
Contig N20	1,366 bp
Contig N30	918 bp
Contig N40	659 bp
Contig N50	501 bp
Median Contig Length	312 bp
Average Contig Length	463.92 bp
Total Assembled Bases	124,764,044 bp
BLATX Hit	89,209
ThHMM	8,413
eggnog	21,060
SignalP	3,223
KEGG	20,616
Gene Ontology	24,769

Table 3.S5. The top 50 gene ontology biological pathways identified from differential gene expression analysis from all lake-to-lake comparisons.

Rank	GO ID	Pathway	*p*-value	No. Genes
		LAKE 223 VS LAKE 224		
1	GO:0006613	cotranslational protein targeting to membrane	1.58E-45	61
2	GO:0006614	SRP-dependent cotranslational protein targeting to membrane	2.21E-44	59
3	GO:0045047	protein targeting to ER	3.52E-40	59
4	GO:0000184	nuclear-transcribed mRNA catabolic process, nonsense-mediated decay	3.52E-40	59
5	GO:0072599	establishment of protein localization to endoplasmic reticulum	3.20E-39	59
6	GO:0070972	protein localization to endoplasmic reticulum	4.68E-37	62
7	GO:0006413	translational initiation	1.34E-36	70
8	GO:0019080	viral gene expression	1.35E-33	69
9	GO:0019083	viral transcription	7.79E-33	66
10	GO:0006612	protein targeting to membrane	1.41E-32	68
11	GO:0016032	viral process	2.30E-30	137
12	GO:0000956	nuclear-transcribed mRNA catabolic process	8.20E-30	65
13	GO:0044403	symbiotic process	1.21E-29	141
14	GO:0044419	interspecies interaction between organisms	7.28E-29	144
15	GO:0090150	establishment of protein localization to membrane	2.22E-28	82
16	GO:0006605	protein targeting	1.87E-24	88
17	GO:0072657	protein localization to membrane	1.11E-21	106
18	GO:0006402	mRNA catabolic process	7.43E-21	74
19	GO:0006401	RNA catabolic process	1.94E-19	76
20	GO:0072594	establishment of protein localization to organelle	1.94E-19	95
21	GO:0046700	heterocycle catabolic process	1.29E-17	92
22	GO:0034655	nucleobase-containing compound catabolic process	1.29E-17	87
23	GO:0044270	cellular nitrogen compound catabolic process	1.31E-17	92
24	GO:0043604	amide biosynthetic process	3.40E-17	118
25	GO:0019439	aromatic compound catabolic process	4.06E-17	92
26	GO:0006886	intracellular protein transport	6.57E-17	164
27	GO:0009057	macromolecule catabolic process	1.38E-16	157
28	GO:0043043	peptide biosynthetic process	1.39E-16	105
29	GO:1901361	organic cyclic compound catabolic process	2.20E-16	94
30	GO:0043603	cellular amide metabolic process	6.84E-16	138
31	GO:0006412	translation	8.11E-16	101
32	GO:0006414	translational elongation	8.11E-16	101
33	GO:0006518	peptide metabolic process	2.53E-14	112
34	GO:0044265	cellular macromolecule catabolic process	1.62E-13	130
35	GO:0033365	protein localization to organelle	6.04E-13	143
36	GO:0002181	cytoplasmic translation	7.32E-13	30
37	GO:0016071	mRNA metabolic process	9.99E-11	100
38	GO:0007010	cytoskeleton organization	1.57E-10	154
39	GO:0000902	cell morphogenesis	3.61E-09	116
40	GO:0032989	cellular component morphogenesis	4.45E-09	124
41	GO:0030029	actin filament-based process	4.79E-09	90
42	GO:0120036	plasma membrane bounded cell projection organization	1.14E-08	156
43	GO:0030030	cell projection organization	2.85E-08	157
44	GO:0010941	regulation of cell death	3.14E-08	166
45	GO:0042776	mitochondrial ATP synthesis coupled proton transport	5.16E-08	12
46	GO:0010942	positive regulation of cell death	6.17E-08	88
47	GO:0042981	regulation of apoptotic process	7.81E-08	152
48	GO:0043067	regulation of programmed cell death	8.10E-08	154
49	GO:0030036	actin cytoskeleton organization	8.33E-08	78
50	GO:0002275	myeloid cell activation involved in immune response	1.44E-07	65
		LAKE 223 VS LAKE 373		
1	GO:0022610	biological adhesion	2.56E-11	94
2	GO:0007155	cell adhesion	2.67E-11	93
3	GO:0007010	cytoskeleton organization	1.31E-08	92
4	GO:0098609	cell-cell adhesion	2.87E-07	59

5	GO:0000902	cell morphogenesis	1.18E-06	68
6	GO:0043085	positive regulation of catalytic activity	1.18E-06	84
7	GO:0032989	cellular component morphogenesis	3.04E-06	71
8	GO:0034330	cell junction organization	3.04E-06	29
9	GO:0010256	endomembrane system organization	3.73E-06	42
10	GO:0001775	cell activation	3.89E-06	80
11	GO:0045321	leukocyte activation	6.20E-06	73
12	GO:0042110	T cell activation	6.71E-06	39
13	GO:0034329	cell junction assembly	8.57E-06	25
14	GO:0007049	cell cycle	8.57E-06	93
15	GO:0030217	T cell differentiation	1.30E-05	26
16	GO:0022402	cell cycle process	1.80E-05	80
17	GO:0033043	regulation of organelle organization	2.29E-05	71
18	GO:0042127	regulation of cell population proliferation	2.97E-05	89
19	GO:0007088	regulation of mitotic nuclear division	2.97E-05	20
20	GO:0000278	mitotic cell cycle	2.97E-05	59
21	GO:1903047	mitotic cell cycle process	2.97E-05	59
22	GO:0140014	mitotic nuclear division	2.97E-05	59
23	GO:0097435	supramolecular fiber organization	3.12E-05	45
24	GO:0030098	lymphocyte differentiation	3.13E-05	31
25	GO:0030029	actin filament-based process	3.13E-05	49
26	GO:0007009	plasma membrane organization	4.82E-05	22
27	GO:0032880	regulation of protein localization	4.90E-05	62
28	GO:0071345	cellular response to cytokine stimulus	4.90E-05	62
29	GO:0140352	export from cell	5.75E-05	81
30	GO:0030155	regulation of cell adhesion	6.19E-05	46
31	GO:0032940	secretion by cell	6.83E-05	79
32	GO:0034097	response to cytokine	6.86E-05	65
33	GO:0002682	regulation of immune system process	7.15E-05	82
34	GO:0046903	secretion	7.15E-05	84
35	GO:0000904	cell morphogenesis involved in differentiation	1.04E-04	49
36	GO:0022008	neurogenesis	1.38E-04	84
37	GO:0070970	interleukin-2 secretion	1.43E-04	6
38	GO:0051783	regulation of nuclear division	1.70E-04	20
39	GO:0009967	positive regulation of signal transduction	1.78E-04	82
40	GO:0002252	immune effector process	1.81E-04	65
41	GO:0000070	mitotic sister chromatid segregation	1.81E-04	17
42	GO:0032612	interleukin-1 production	1.81E-04	15
43	GO:0046649	lymphocyte activation	1.81E-04	46
44	GO:0030036	actin cytoskeleton organization	1.86E-04	42
45	GO:0000280	nuclear division	2.01E-04	62
46	GO:0009607	response to biotic stimulus	2.14E-04	75
47	GO:0051707	response to other organism	2.14E-04	74
48	GO:0043207	response to external biotic stimulus	2.20E-04	74
49	GO:0080134	regulation of response to stress	2.52E-04	76
50	GO:0045619	regulation of lymphocyte differentiation	2.52E-04	19

LAKE 223 VS LAKE 260

1	GO:0044403	symbiotic process	3.83E-15	93
2	GO:0016032	viral process	9.66E-15	88
3	GO:0044419	interspecies interaction between organisms	1.31E-14	94
4	GO:0010941	regulation of cell death	9.35E-12	142
5	GO:0016050	vesicle organization	2.82E-11	131
6	GO:0007010	cytoskeleton organization	4.53E-11	124
7	GO:0072657	protein localization to membrane	5.69E-11	69
8	GO:0034097	response to cytokine	9.23E-11	103
9	GO:0042981	regulation of apoptotic process	1.48E-10	128
10	GO:0043067	regulation of programmed cell death	2.18E-10	129
11	GO:0090150	establishment of protein localization to membrane	4.30E-10	45
12	GO:0032940	secretion by cell	6.15E-10	121
13	GO:0071345	cellular response to cytokine stimulus	6.17E-10	95
14	GO:0140352	export from cell	6.86E-10	123
15	GO:0006613	cotranslational protein targeting to membrane	6.86E-10	24
16	GO:0045055	regulated exocytosis	6.86E-10	75
17	GO:0006906	vesicle fusion	2.57E-09	83

18	GO:0099500	vesicle fusion to plasma membrane	2.64E-09	80
19	GO:0006887	exocytosis	2.64E-09	80
20	GO:0140029	exocytic process	2.64E-09	80
21	GO:0046903	secretion	2.64E-09	126
22	GO:0090174	organelle membrane fusion	2.71E-09	83
23	GO:0048284	organelle fusion	3.31E-09	84
24	GO:0061025	membrane fusion	3.43E-09	88
25	GO:0006413	translational initiation	3.43E-09	31
26	GO:0045047	protein targeting to ER	3.43E-09	24
27	GO:0000184	nuclear-transcribed mRNA catabolic process, nonsense-mediated decay	3.43E-09	24
28	GO:0043604	amide biosynthetic process	3.73E-09	78
29	GO:0043603	cellular amide metabolic process	3.78E-09	94
30	GO:0006886	intracellular protein transport	4.05E-09	110
31	GO:0007264	small GTPase mediated signal transduction	4.85E-09	58
32	GO:0033043	regulation of organelle organization	5.84E-09	102
33	GO:0072599	establishment of protein localization to endoplasmic reticulum	5.84E-09	24
34	GO:0002274	myeloid leukocyte activation	7.04E-09	63
35	GO:0006614	SRP-dependent cotranslational protein targeting to membrane	7.21E-09	22
36	GO:0002275	myeloid cell activation involved in immune response	9.21E-09	55
37	GO:0043299	leukocyte degranulation	1.28E-08	54
38	GO:0006612	protein targeting to membrane	1.37E-08	31
39	GO:0042119	neutrophil activation	1.60E-08	51
40	GO:0002444	myeloid leukocyte mediated immunity	1.74E-08	55
41	GO:0007249	I-kappaB kinase/NF-kappaB signaling	1.79E-08	36
42	GO:0051707	response to other organism	1.85E-08	111
43	GO:0043207	response to external biotic stimulus	1.95E-08	111
44	GO:0036230	granulocyte activation	2.17E-08	51
45	GO:0009607	response to biotic stimulus	2.40E-08	112
46	GO:1901700	response to oxygen-containing compound	2.55E-08	122
47	GO:0002366	leukocyte activation involved in immune response	3.14E-08	64
48	GO:0060341	regulation of cellular localization	3.54E-08	82
49	GO:0002263	cell activation involved in immune response	3.74E-08	64
50	GO:0070972	protein localization to endoplasmic reticulum	3.74E-08	25

LAKE 224 VS LAKE 373

1	GO:0032691	negative regulation of interleukin-1 beta production	5.96E-04	7
2	GO:0032611	interleukin-1 beta production	5.96E-04	10
3	GO:0032692	negative regulation of interleukin-1 production	8.33E-04	7
4	GO:0032651	regulation of interleukin-1 beta production	1.00E-03	9
5	GO:0032612	interleukin-1 production	1.00E-03	10
6	GO:0032652	regulation of interleukin-1 production	2.78E-03	9
7	GO:0019226	transmission of nerve impulse	4.29E-03	8
8	GO:0000904	cell morphogenesis involved in differentiation	5.43E-03	25
9	GO:0050713	negative regulation of interleukin-1 beta secretion	7.60E-03	4
10	GO:0007626	locomotory behavior	9.31E-03	12
11	GO:0032989	cellular component morphogenesis	1.19E-02	31
12	GO:0000902	cell morphogenesis	1.20E-02	29
13	GO:0050711	negative regulation of interleukin-1 secretion	1.44E-02	4
14	GO:0048667	cell morphogenesis involved in neuron differentiation	2.05E-02	20
15	GO:0042776	mitochondrial ATP synthesis coupled proton transport	2.76E-02	4
16	GO:1900924	negative regulation of glycine import across plasma membrane	2.99E-02	2
17	GO:0031175	neuron projection development	3.52E-02	27
18	GO:0050706	regulation of interleukin-1 beta secretion	4.66E-02	5

LAKE 260 VS 224

1	GO:0034097	response to cytokine	2.84E-08	82
2	GO:0071345	cellular response to cytokine stimulus	7.39E-06	71
3	GO:0007623	circadian rhythm	2.24E-05	25
4	GO:0061919	process utilizing autophagic mechanism	2.24E-05	40
5	GO:0006914	autophagy	2.24E-05	40
6	GO:0010941	regulation of cell death	2.65E-05	98
7	GO:0007010	cytoskeleton organization	3.55E-05	86
8	GO:0010942	positive regulation of cell death	5.03E-05	53
9	GO:0031331	positive regulation of cellular catabolic process	6.44E-05	32

10	GO:0048511	rhythmic process	1.03E-04	29
11	GO:0033043	regulation of organelle organization	1.55E-04	73
12	GO:0044403	symbiotic process	1.55E-04	54
13	GO:0042981	regulation of apoptotic process	1.84E-04	87
14	GO:0033993	response to lipid	2.12E-04	57
15	GO:0051254	positive regulation of RNA metabolic process	2.56E-04	88
16	GO:0044419	interspecies interaction between organisms	2.56E-04	55
17	GO:0019221	cytokine-mediated signaling pathway	2.56E-04	49
18	GO:0043067	regulation of programmed cell death	2.82E-04	87
19	GO:0043903	regulation of symbiosis, encompassing mutualism through parasitism	2.93E-04	22
20	GO:0016032	viral process	3.62E-04	50
21	GO:0009896	positive regulation of catabolic process	4.16E-04	33
22	GO:0001890	placenta development	4.16E-04	19
23	GO:1901700	response to oxygen-containing compound	4.16E-04	87
24	GO:2000114	regulation of establishment of cell polarity	4.42E-04	7
25	GO:0014070	response to organic cyclic compound	4.42E-04	58
26	GO:0042127	regulation of cell population proliferation	6.48E-04	89
27	GO:0002520	immune system development	1.05E-03	59
28	GO:0043065	positive regulation of apoptotic process	1.05E-03	45
29	GO:0010876	lipid localization	1.17E-03	31
30	GO:0030029	actin filament-based process	1.17E-03	47
31	GO:0043901	negative regulation of multi-organism process	1.17E-03	21
32	GO:1903508	positive regulation of nucleic acid-templated transcription	1.17E-03	81
33	GO:0043068	positive regulation of programmed cell death	1.17E-03	45
34	GO:1902680	positive regulation of RNA biosynthetic process	1.17E-03	81
35	GO:0009725	response to hormone	1.17E-03	56
36	GO:0038127	ERBB signaling pathway	1.17E-03	16
37	GO:0010035	response to inorganic substance	1.17E-03	39
38	GO:0001818	negative regulation of cytokine production	1.27E-03	25
39	GO:0032878	regulation of establishment or maintenance of cell polarity	1.27E-03	7
40	GO:0001817	regulation of cytokine production	1.27E-03	45
41	GO:0009719	response to endogenous stimulus	1.27E-03	84
42	GO:0032480	negative regulation of type I interferon production	1.27E-03	9
43	GO:0030036	actin cytoskeleton organization	1.27E-03	42
44	GO:0001816	cytokine production	1.61E-03	48
45	GO:0043900	regulation of multi-organism process	1.61E-03	46
46	GO:0030155	regulation of cell adhesion	1.68E-03	44
47	GO:0031532	actin cytoskeleton reorganization	1.79E-03	13
48	GO:0001701	in utero embryonic development	1.79E-03	33
49	GO:0048534	hematopoietic or lymphoid organ development	1.87E-03	55
50	GO:0032922	circadian regulation of gene expression	2.00E-03	10

LAKE 260 VS LAKE 373

1	GO:0042981	regulation of apoptotic process	8.77E-08	94
2	GO:0010941	regulation of cell death	8.77E-08	100
3	GO:0043067	regulation of programmed cell death	8.77E-08	94
4	GO:0007009	plasma membrane organization	8.77E-08	27
5	GO:0046903	secretion	1.12E-07	94
6	GO:0044403	symbiotic process	2.64E-07	58
7	GO:0070201	regulation of establishment of protein localization	3.74E-07	56
8	GO:0016032	viral process	3.78E-07	55
9	GO:0070268	cornification	4.22E-07	18
10	GO:0044419	interspecies interaction between organisms	4.22E-07	59
11	GO:0032940	secretion by cell	4.22E-07	86
12	GO:0050709	negative regulation of protein secretion	4.22E-07	22
13	GO:0010942	positive regulation of cell death	4.39E-07	54
14	GO:0010256	endomembrane system organization	4.39E-07	43
15	GO:1903575	cornified envelope assembly	4.46E-07	18
16	GO:0051223	regulation of protein transport	4.46E-07	53
17	GO:0034097	response to cytokine	4.46E-07	71
18	GO:0140352	export from cell	4.60E-07	87
19	GO:0032880	regulation of protein localization	5.09E-07	67
20	GO:0002792	negative regulation of peptide secretion	6.95E-07	22
21	GO:0090087	regulation of peptide transport	6.95E-07	54
22	GO:1901700	response to oxygen-containing compound	6.95E-07	90

23	GO:0043588	skin development	7.31E-07	36
24	GO:0033993	response to lipid	7.90E-07	59
25	GO:0006952	defense response	8.20E-07	90
26	GO:0050708	regulation of protein secretion	8.81E-07	40
27	GO:0051707	response to other organism	1.00E-06	81
28	GO:0009607	response to biotic stimulus	1.00E-06	82
29	GO:0043207	response to external biotic stimulus	1.00E-06	81
30	GO:0014070	response to organic cyclic compound	1.14E-06	61
31	GO:0043065	positive regulation of apoptotic process	1.53E-06	49
32	GO:0002791	regulation of peptide secretion	1.67E-06	41
33	GO:0001816	cytokine production	1.67E-06	53
34	GO:0009913	epidermal cell differentiation	1.68E-06	32
35	GO:0030855	epithelial cell differentiation	1.91E-06	53
36	GO:0043068	positive regulation of programmed cell death	1.91E-06	49
37	GO:0051046	regulation of secretion	2.38E-06	56
38	GO:0001817	regulation of cytokine production	2.51E-06	49
39	GO:0000902	cell morphogenesis	2.60E-06	64
40	GO:0007169	transmembrane receptor protein tyrosine kinase signaling pathway	2.66E-06	48
41	GO:0030216	keratinocyte differentiation	2.76E-06	28
42	GO:0009628	response to abiotic stimulus	2.80E-06	71
43	GO:0098542	defense response to other organism	3.99E-06	66
44	GO:0007155	cell adhesion	4.97E-06	75
45	GO:0051224	negative regulation of protein transport	5.75E-06	23
46	GO:0022610	biological adhesion	5.75E-06	75
47	GO:0032989	cellular component morphogenesis	6.41E-06	67
48	GO:0050710	negative regulation of cytokine secretion	6.41E-06	14
49	GO:0071345	cellular response to cytokine stimulus	6.41E-06	63
50	GO:1903530	regulation of secretion by cell	6.67E-06	52

Table 3.S6. KEGG pathways identified from differential gene expression analysis among all lake-to-lake comparisons.

Rank	ID	Pathway	p-value	No. Genes
LAKE 223 vs LAKE 224				
1	83036	Ribosome	1.13E-28	59
2	82942	Oxidative phosphorylation	2.82E-06	28
3	83071	Tight junction	3.17E-06	32
4	83098	Parkinson's disease	8.18E-05	26
5	83101	Vibrio cholerae infection	1.60E-04	14
6	83097	Alzheimer's disease	2.12E-04	28
7	99052	Lysosome	4.65E-04	22
8	83100	Huntington's disease	6.04E-04	29
9	375172	Salmonella infection	3.54E-03	16
10	83102	Epithelial cell signaling in Helicobacter pylori infection	1.07E-02	13
11	83060	Apoptosis	1.44E-02	20
12	122191	NOD-like receptor signaling pathway	1.44E-02	23
13	83104	Shigellosis	1.92E-02	12
14	83083	Leukocyte transendothelial migration	2.14E-02	17
15	149807	Bacterial invasion of epithelial cells	2.15E-02	13
16	102279	Endocytosis	2.56E-02	30
17	1474302	Fluid shear stress and atherosclerosis	3.42E-02	19
18	1496831	Mitophagy - animal	4.62E-02	11
19	782000	Proteoglycans in cancer	4.62E-02	24
LAKE 223 VS LAKE 373				
1	83070	Adherens junction	4.14E-03	11
2	122191	NOD-like receptor signaling pathway	4.14E-03	17
3	375172	Salmonella infection	3.57E-02	10
4	126909	Oocyte meiosis	4.04E-02	12
5	119304	Progesterone-mediated oocyte maturation	4.91E-02	10
6	83101	Vibrio cholerae infection	4.91E-02	7
LAKE 223 VS LAKE 260				
1	122191	NOD-like receptor signaling pathway	1.44E-08	31
2	83071	Tight junction	6.93E-07	28
3	375172	Salmonella infection	1.84E-04	16
4	83060	Apoptosis	3.19E-04	20
5	83089	Regulation of actin cytoskeleton	3.19E-04	26
6	83058	Autophagy - animal	3.19E-04	19
7	83104	Shigellosis	3.19E-04	13
8	99052	Lysosome	5.54E-04	18
9	83048	MAPK signaling pathway	7.17E-04	28
10	83036	Ribosome	9.13E-04	20
11	83083	Leukocyte transendothelial migration	1.87E-03	16
12	114228	Fc gamma R-mediated phagocytosis	1.87E-03	14
13	1474301	IL-17 signaling pathway	2.20E-03	14
14	173973	Hepatitis C	2.41E-03	17
15	634527	NF-kappa B signaling pathway	2.41E-03	14
16	658418	Viral carcinogenesis	3.18E-03	22
17	469200	Legionellosis	3.31E-03	10
18	102279	Endocytosis	3.31E-03	26
19	83102	Epithelial cell signaling in Helicobacter pylori infection	4.39E-03	11
20	83105	Pathways in cancer	6.07E-03	34
21	1496831	Mitophagy - animal	1.13E-02	10
22	1474302	Fluid shear stress and atherosclerosis	1.27E-02	16
23	694606	Hepatitis B	1.41E-02	16
24	217173	Influenza A	1.47E-02	18
25	101143	Neurotrophin signaling pathway	1.51E-02	14
26	1319988	AGE-RAGE signaling pathway in diabetic complications	2.45E-02	12

27	83067	Focal adhesion	2.64E-02	19
28	147809	Chagas disease (American trypanosomiasis)	2.93E-02	12
29	782000	Proteoglycans in cancer	3.08E-02	19
30	83103	Pathogenic Escherichia coli infection	3.72E-02	8
31	213306	Measles	3.72E-02	14
32	167324	Amoebiasis	4.65E-02	11

LAKE 224 VS LAKE 373

1	82996	Glycosphingolipid biosynthesis - globo and isoglobo series	6.32E-03	4
2	83097	Alzheimer's disease	3.04E-02	9
3	83098	Parkinson's disease	3.04E-02	8
4	83100	Huntington's disease	4.00E-02	9

LAKE 260 VS 224

1	812256	TNF signaling pathway	1.88E-04	16
2	193147	Osteoclast differentiation	1.13E-03	16
3	83058	Autophagy - animal	2.60E-03	15
4	122191	NOD-like receptor signaling pathway	4.57E-03	17
5	375172	Salmonella infection	8.24E-03	11
6	83105	Pathways in cancer	8.87E-03	28
7	83060	Apoptosis	9.74E-03	14
8	694606	Hepatitis B	1.23E-02	14
9	83052	Phosphatidylinositol signaling system	1.23E-02	11
10	169642	Toxoplasmosis	1.23E-02	12
11	1474301	IL-17 signaling pathway	2.98E-02	10
12	634527	NF-kappa B signaling pathway	3.22E-02	10
13	83071	Tight junction	4.12E-02	14
14	952859	Oxytocin signaling pathway	4.12E-02	13
15	83093	Adipocytokine signaling pathway	4.12E-02	8
16	147809	Chagas disease (American trypanosomiasis)	4.13E-02	10
17	83048	MAPK signaling pathway	4.37E-02	18
18	373901	HTLV-I infection	4.37E-02	18

LAKE 260 VS LAKE 373

1	169642	Toxoplasmosis	1.62E-02	13

Table 3.S7A. Component matrix and total variance explained from principal component analysis of water quality data.

	PC1	PC2	PC3	PC4
Alkalinity	0.2302	0.4225	-0.2392	0.6792
Chlorophyll-a	0.3554	-0.2367	0.2312	0.0427
pH	-0.0203	0.5493	0.0892	0.2114
Suspended C	0.3759	0.1950	0.2056	-0.0838
Suspended N	0.4182	-0.0769	0.0720	0.0010
Suspended P	0.3001	-0.0897	-0.4636	-0.0885
TDN	0.3005	-0.3913	0.0304	0.3134
TDP	-0.3894	-0.2206	-0.0277	0.1763
Temperature	-0.0667	-0.2753	0.5745	0.4591
Conductivity	0.3787	0.1329	0.2588	-0.3382
DO	-0.1559	0.3414	0.4694	-0.1513

Table 3.S7B. Principal component scores from analysis of water quality parameters.

Lake	PC1	PC2	PC3	PC4
Lake 223	1.1757	-0.1705	7.91E-16	7.91E-16
Lake 224	-3.4693	-0.5019	1.17E-15	1.17E-15
Lake 260	1.6846	-1.8130	2.22E-16	2.22E-16
Lake 373	0.6090	2.4854	-4.72E-16	-4.72E-16

Chapter 3: RNA sequencing of lake trout epidermal mucus to assess molecular effects following exposure to diluted bitumen in a boreal lake

Abstract

Transport of diluted bitumen (dilbit) from Canada's Oil Sands region poses risk for leaks and spills of petroleum-derived contaminants into the environment. Exposure of fish to dilbit is known to cause cardiotoxicity, developmental deformities, and impairment in swim performance. However, previous studies have examined the toxicity of dilbit in laboratory settings which does not account for environmental and biological food-web variables that may alter exposure and/or toxicity of dilbit. Moreover, most methods of assessing organism health following oil exposure require lethal sampling. In order to better understand impacts of dilbit in an ecosystem setting without use of lethal sampling, epidermal mucus was collected and sequenced from lake trout (*Salvelinus namaycush*) exposed to low levels of dilbit in a boreal lake. While concentrations reached a maximum of 4.4 µg/L of total polyaromatic hydrocarbons (PAH) within surface waters, PAH concentrations generally remained below 1 µg/L. Results of RNA sequencing were compared to sequencing data from mucus collected prior to dilbit additions. Differential gene expression and pathway analyses indicated dysregulation of genes associated with intermediary and energy metabolism following dilbit exposure. Thus, results of the present study support that lake trout undergo consistent biological responses following a simulated dilbit spill and that mRNA-based analysis of mucus may be a viable method for non-lethal oil exposure assessment.

Introduction

The Oil Sands region of Alberta, Canada has one of the largest known reserves of bitumen, containing an estimated 50 billion cubic meters of the heavy type crude oil.[1] Due to its viscous nature, bitumen is mixed with diluents (e.g. natural gas condensate or synthetic oils) to decrease viscosity for more efficient transport, thus forming diluted bitumen (dilbit). Dilbit is primarily exported from the Oil Sands region via extensive transcontinental pipeline networks, raising concern for potential leaks and spills into lakes and rivers located along transportation routes.[2,3] Although export by rail has increased in recent years, volumes remain small compared to pipelines but present an additional potential spill vector.[3] Multiple significant dilbit spills have occurred in North America, with the largest being the 2010 Enbridge Line 6B pipeline rupture which released 1.15 million gallons of dilbit into the Kalamazoo River in Michigan.[4,5] Although major dilbit spills have occurred in the past and future spills are inevitable, there remain significant research gaps on the behavior of dilbit in the environment and its toxicity to aquatic organisms. Furthermore, Oil Sands dilbit production and export is projected to continue to expand due to significant economic incentives.[4,6] Continual increases in transport of dilbit and proposed expansions of existing pipeline networks make it critical to fully characterize the effects of dilbit on aquatic ecosystems for adequate risk assessment of future spills and proper guidance in spill response decision making.

As bitumen is heavily biodegraded over geological time, dilbit contains a high proportion of heavy molecular weight compounds such as resins, asphaltenes, and high molecular weight polycyclic aromatic hydrocarbons (PAHs) and alkylated PAHs.[5,7]

Moreover, the specific chemical fingerprint of dilbit product is highly variable depending on extraction and refining processes, geographic source, and the composition and volume of diluent added by the producer.[8,9] Following a spill, the chemical properties of dilbit are further modified by complex weathering processes such as photo-oxidation, biodegradation, evaporation, emulsification, dispersion, and sedimentation.[5,10] Due to its complex chemical composition and multiple factors affecting its chemical properties, it may be difficult to understand the fate and behavior of spilled dilbit in freshwater environments. In order to better understand dilbit's behavior in low-energy lake systems, Stoyanovich et al. 2019 conducted experimental releases of dilbit in outdoor microcosms containing natural lake water and sediments.[11] As volatile hydrocarbons evaporated, dilbit increased in density and viscosity, resulting in its submergence after 8 days. Furthermore, there was a rapid accumulation of PAHs in the water column, which tend to be drivers of oil toxicity in aquatic organisms.

The toxicity of dilbit in freshwater environments has been minimally studied and has only recently begun to receive more extensive research.[2,5] Similar to toxic endpoints associated with conventional crude oil, dilbit exposure in fish has shown to induce mortality, decreased utilization of energy stores, metabolic alterations, reduced growth, oxidative stress, behavioral changes, developmental malformations, delayed hatching, changes in heart rate, impaired swim bladder inflation, among other adverse effects.[12–18] Impairments induced by dilbit exposure may have impacts on organismal fitness and, thus, population health. For example, exposure of sockeye salmon parr (*Oncorhynchus nerka*) to water soluble fractions of dilbit (3.5 – 66.7 µg/L ΣPAH) resulted in

concentration-dependent cardiac remodeling that correlated to reductions in swimming performance.[19] Dilbit may also impede exercise recovery, as dilbit-exposed sockeye salmon experienced increased cellular damage following exercise as suggested by an increase in tissue leakage proteins, such as creatine kinase, in serum compared to controls.[20] As reduced swim performance may impair migratory success, dilbit spills may pose risk to sensitive salmonid populations in freshwater ecosystems.

Following a freshwater oil spill, there is a need for rapid exposure assessment of biota in the impacted area. Use of exposure assessment tools which are nonlethal and minimally invasive is also important in order to reduce further perturbations of sampling on animal populations. In fish, molecular analysis of epidermal mucus may be a viable solution for monitoring effects of oil exposure as it is nonlethal, rapid, inexpensive, and requires little training. Following exposure to *Deepwater Horizon* slick oil, RNA sequencing of mucus from juvenile mahi-mahi (*Coryphaena hippurus*) identified molecular changes in mucus associated with oil toxicity, such as upregulation of cytochrome P450 1A (CYP1A) and dysregulation of transcripts associated with cardiotoxicity and immunosuppression.[21] Moreover, exposure of dusky splitfin (*Goodea gracilis*) to crude oil resulted in increased antioxidant defense response in the epidermal mucus.[22] Results from these previous studies suggest that epidermal mucus may be a useful target for environmental monitoring following oil spills. However, previous studies were laboratory-based and may not reflect changes in chemical properties of oil brought about by environmental conditions such as a evaporation, photo-oxidation, emulsification, dispersion, biodegradation, and sedimentation.[5]

Although research suggests that mucus may be a promising method for nonlethal sampling, the efficacy of mucus as an oil exposure assessment tool has not yet been assessed on wild populations in the field. In the present study, epidermal mucus was collected from lake trout (*Salvelinus namaycush*) residing in a pristine Canadian boreal shield lake at the IISD Experimental Lakes Area where experimental dilbit spills were conducted within enclosures on the lake. While experimental spills were conducted within enclosures, minute levels of dilbit entered the surrounding lake environment leading to potential exposure of resident lake trout. RNA sequencing was conducted on lake trout mucus collected prior to and after dilbit additions in order to identify potential biomarkers of exposure associated with dilbit. Lake trout may serve as a model species for the study as many dilbit pipelines are concentrated in areas of Canada where they intersect rivers containing other sensitive salmonid species, such as the sockeye salmon of the Fraser River. Results of the present study will identify molecular pathways altered by dilbit in a whole-lake setting and further contribute to the development of mucus as a nonlethal tool for oil exposure assessment. Moreover, water chemistry results will help establish concentration thresholds at which molecular markers of dilbit exposure begin to be seen in salmonids in a whole-ecosystem setting.

Materials and Methods

Study area and diluted bitumen additions

The study was conducted at the IISD Experimental Lakes Area (IISD-ELA), a freshwater research center located near Kenora, Ontario, Canada (49°40'N, 93°44'W)

(https://www.iisd.org/ela/). Being located in a sparsely populated region, the lakes at IISD-ELA are mostly unaffected by anthropogenic influences. IISD-ELA's Lake 260 was selected for the present study (49°42'N, 93°46'W) which has an area of 331,328 m^2, a volume of 1,975,971 m^3, an average depth of 5.9 m, and a maximum depth of 15.7 m (Figure 5.1). Lake 260 is a boreal lake and serves as a model for freshwater water bodies in Canada's Boreal Shield ecozone.

In order to examine the fate, behavior and potential impacts of spilled dilbit in freshwater aquatic environments, dilbit spills were simulated within 10m diameter limnocorrals on Lake 260 beginning in 2018 (Figure 4.2; Figure 4.3). Limnocorrals consist of a floatation collar that supports an impermeable curtain that extends to the bottom of the lake where it is sealed to the sediments using sandbags, providing an enclosed ecosystem to model whole lake processes. A series of 9 limnocorrals were constructed and deployed in water depths of ~1.5m. After installation and pre-spill monitoring, Cold Lake Winter Blend dilbit was added to seven limnocorrals using a regression with added volumes ranging from 1:100,000 – 1:100 dilbit to water (v:v). The total volume of dilbit added to the enclosures was ~382 litres. Chemical and physical weathering, as well as potential toxicity, of the dilbit were studied for 70 days, after which residual surface dilbit was removed from the limnocorrals. The limnocorral curtains were then cut at mid water column depth prior to winter freeze up to allow continued study of the dilbit that remained on the lake bottom. As a result, there was potential for dilbit to enter the lake water column throughout the duration of the winter months and prior to final sediment cleaning, which took place in August 2019.

Additionally, in June 2019 fourteen shoreline enclosures (5x15m and enclosing volumes of 25,000-30,000 liters of lake water) were treated with 1.5 liters of weathered dilbit (Figure 4.2; Figure 4.4). While the environments were enclosed, tracer studies indicated that some leakage to the outside lake environment occurred, potentially contributing to enriched PAH concentrations in the lake. The present study will thus examine the potential effects that dilbit entering the lake environment from previous enclosure studies had on resident fish.

Water extractions and analytical chemistry

Surface water samples (1L) were collected from each enclosure at 10 time points during the study: 3 days before oil addition and on days 1,2,3,5,9,13, 18, 53, and 80 after application. Samples were filtered first using Whatman GF/C filters and then transferred to 2 L separatory funnels. Each funnel was spiked with 20 uL of 5 ppm of a recovery internal standard which consisted of d8-naphthalene, d8-acenaphthylene, d10-acenaphthene, d10-fluorene, d10-phenanthrene, d10-pyrene, d12-Benz(a)anthracene, d12-chrysene, d12-benzo(b)fluoranthene, d12-benzo(k)fluoranthene, d12-benzo(a)pyrene, d12-indeno(1,2,3-c,d)pyrene, d14-dibenzo(a,h)anthracene, and d14-benzo(g,h,i)perylene. Ten grams of NaCl was dissolved into each sample prior to the liquid:liquid extraction. The samples were extracted by adding 50 mL of dichloromethane (DCM) to each funnel and gently swirling for 1 minute. The DCM was drained into a round bottom flask and the water extraction was repeated. The combined 100 mL DCM extract was then evaporated to a final volume of 1 mL and spike with 20 uL of 5 ng/uL

d10-anthracene as an instrument performance internal standard. Samples were vortexed and transferred to 2 mL amber glass autosampler vials for storage at 4°C until analysis by GC-MS/MS.

The instrument used for the native and d-labelled PAH and alkyl PAH quantification was an Agilent 7890 GC coupled to a 7000C triple quadrupole mass spectrophotometer fitted with an electron ionization (EI) source. Helium was used as the carrier gas at a flow rate of 1.2mL/min with an Agilent J&W HP-5ms ultra inert column (30 m × 0.25 mm, 0.25 μm film thickness). Sample volumes of 1μl were injected by a PAL RSI 85 auto sampler at a temperature of 60°C. GC conditions and details of the multiple reaction monitoring precursor and product ion transitions for the 16 priority PAHs and alkylated PAHs that were analyzed in the samples can be found in Idowu et al. 2018.

Sample collection

Epidermal mucus was collected from lake trout prior to dilbit additions in September of 2017 (Figure 4.2). In September 2018, additional mucus samples were collected prior to cutting of limnocorral curtains and exposure of the lake water column to sunken dilbit. Finally, mucus was collected in September 2019 following exposure of dilbit to the lake water column. Thus, the experimental design is a temporal comparison pre- and post-exposure. Fish were captured from a boat using hook and line and were placed in separate bins of fresh lake water until processing (held < 5 min). Retrieval and post-capture air exposure were minimized to reduce physiological stress.[23] Water was

renewed for each fish to prevent cross-contamination. Lake trout were placed in a solution of 0.1g/L pH buffered (7.0) tricaine methanesulfonate (MS-222) mixed in lake water until fin movement ceased and fish were unresponsive to light pressure on the caudal fin. Total length, fork length, and weight of the individuals were recorded. Sex was determined through external morphological characteristics if possible. Mucus was collected by gently scraping the skin with a stainless steel spatula, avoiding displacement of scales, to aggregate the mucus along the body axis in the anterior to posterior direction. Mucus was aspirated using a syringe, dispensed into a microcentrifuge tube, placed on dry ice, and stored at -80°C until analyzed. Tools and work area were cleansed with ethanol and then lake water between fish to prevent cross-contamination. Condition factor (K) was calculated for each individual using the formula $K = \text{weight}/\text{length}^3 \times 100$. Statistical differences in average weight, total length, and condition factor among 2017, 2018, and 2019 lake trout were tested using a one-way ANOVA and Tukey multiple comparisons test at a significance threshold of $p \leq 0.05$. All capture and handling procedures were conducted in accordance with the Canadian Council on Animal Care approved protocols.

cDNA library generation and Illumina sequencing

Total RNA was extracted from bulk mucus samples (n = 4 per year) using the RNeasy Lipid Tissue Mini Kit (Qiagen, Qiagen, Germantown, MD). Total RNA concentrations were quantified using an Invitrogen™ Qubit™ 4 Fluorometer (Invitrogen, Carlsbad, CA) and a NanoDrop™ ND-1000 Spectrophotometer (Thermo Fisher

Scientific, Waltham, MA). RNA integrity was assessed on an Agilent 2100 Bioanalyzer (Agilent Technologies, Palo Alto, CA). Sequencing cDNA libraries were prepared using the NEBNext® Ultra™ II Directional RNA Library Prep Kit for Illumina® (New England Biolabs, Ipswich, MA) with the NEBNext® rRNA Depletion Kit using 500 ng of total RNA as input. NEBNext® Multiplex Oligos for Illumina® Index Primer Sets were used to multiplex cDNA libraries. Final cDNA libraries were assessed on an Agilent 2100 Bioanalyzer to verify proper fragment sizes and to quantify final library concentrations. The 2018 and dilbit-exposed samples (2019) cDNA libraries (n = 8) were pooled according to treatment group and the resulting samples were assessed on an Agilent 2100 Bioanalyzer. Pooled, multiplexed libraries underwent 1 x 75 bp sequencing on an Illumina NextSeq™ 500 at the Institute for Integrative Genome Biology at the University of California, Riverside. The 2017 cDNA libraries (n = 4) were processed using the same methods but were analyzed on a separate run prior to running the 2018 and 2019 libraries.

Bioinformatics analysis

Quality of raw read data was assessed with FastQC v.0.11.7[24] prior to downstream analysis. Removal of adapter sequences and poor quality reads was performed using Trimmomatic v.0.36[25] with the following parameters: ILLUMINACLIP: TruSeq3-SE.fa:2:30:10 LEADING: 3 TRAILING: 3 SLIDINGWINDOW: 4:15 MINLEN: 36. Read quality was again assessed with FastQC following trimming. Using Bowtie2,[26] read data for each sample was aligned to a *de novo* brook trout (*Salvelinus*

fontinalis) transcriptome available for download at the PhyloFish database (http://phylofish.sigenae.org/index.html).[27] The transcriptome was annotated against the UniProtKB/Swiss-Prot database (http://www.ebi.ac.uk/uniprot/) using NCBI-BLASTx v.2.8.1+ reporting only the top hit (-max_target_seqs 1).

The comparisons of interest in the study were 1) 2017 and 2018 to determine yearly gene expression changes in baseline samples and 2) 2018 and dilbit-exposed samples (2019) to determine gene expression changes following potential dilbit exposure. RSEM[28] was used to quantify abundance of transcripts in each sample. To visualize transcriptome-wide patterns among 2018 baseline and 2019 dilbit-treated samples, unsupervised hierarchical clustering was used to generate a sample-to-sample Euclidian distance heat map using the RSEM count matrix that underwent a regularized-logarithm transformation. Principal component analysis (PCA) was also performed on the transformed RSEM count matrix for baseline and dilbit-treated samples. Unsupervised hierarchical clustering was used to produce a heat map of the top 500 most-variable transcripts among 2018 and dilbit-treated samples. The top 500 most-variable transcripts were extracted from the transformed count matrix using the *genefilter* R package.[29] The non-transformed transcript count matrix was input into DESeq2 v.1.23.6[30] to determine differentially expressed transcripts among 2018 and dilbit-treated samples at $p \leq 0.05$ after Benjamini-Hochberg false discovery rate (FDR) correction. Differential expression analysis was also conducted among 2017 and 2018 baseline data to examine yearly changes in gene expression. Differentially-expressed transcripts were input into DAVID

for gene ontology (GO) and KEGG pathway analysis as well as into Ingenuity Pathway Analysis (IPA).

qPCR validation of RNA sequencing results

cDNA was created for 2018 baseline samples and dilbit-exposed samples using the Promega Reverse Transcription System (Promega, Madison, WI) with 500 ng of total RNA as input. Melt curve analysis and agarose gel electrophoresis were performed prior to qPCR to confirm primer specificity. The reactions for qPCR consisted of 10 µL SsoAdvanced Universal SYBR Green Supermix (Bio-Rad, Hercules, CA), 0.2 µM forward and reverse primers, and 2 µL of cDNA in a final volume of 20 µL. Samples were run in triplicate for each gene on a CFX Connect Real-Time PCR Detection System (Bio-Rad, Hercules, CA) with the following thermal cycler conditions: 95 °C for 10 min, 40 cycles of 95 °C for 15 s, 58 °C for 30 s, and 72 °C for 30 s. Relative expression was determined by the $2^{-\Delta\Delta Ct}$ method[31] with β-actin as the normalizing gene. Primer sequences were designed using IDT PrimerQuest Tool® with transcript sequences from the brook trout assembly. Primer information is listed in Table 4.S1.

Results and Discussion

Soluble dilbit constituents in Lake 260

In order to better evaluate the effects of dilbit on aquatic biota, dilbit experiments were carried out within limnocorrals and shoreline enclosures in a boreal lake to account for physical and chemical changes in dilbit induced by environmental factors. There were

two potential vectors for dilbit constituents entering the surrounding lake environment. Following cutting of the limnocorral curtains, sunken dilbit remained on the sediment and open to the lake environment for 323 days until cleanup on August 16, 2019. Second, following the addition of dilbit to shoreline enclosures on June 22, 2019, tracer studies indicated that some leakage from the enclosures to the outside lake environment occurred. Thus, leakage may have contributed water soluble compounds from dilbit into the lake. Prior to dilbit additions into shoreline enclosures, 0.50 μg/L ΣPAH was detected in surface waters, likely contributed from residual dilbit on lake sediments following the limnocorral experiments (Figure 4.5). Following the additions of dilbit to shoreline enclosures on June 22, there was an increase in PAH concentrations within surface waters, reaching a maximum concentration of 4.4 μg/L ΣPAH on June 26 (Figure 4.5). PAH concentrations in Lake 260 declined to 1.1 μg/L ΣPAH on June 27 and further declined to 0.86 μg/L on July 11. As residual dilbit from limnocorral studies contributed to PAH levels in the lake and remained on the sediments until August 16, 2019, it is likely that PAHs remained in the water column until removal of sunken dilbit in August; further chemistry data will provide exact exposure concentrations at the time of lake trout sampling in September 2019. Moreover, 3- and 4-ring PAHs comprised about 96% of the ΣPAHs with phenanthrenes, dibenzothiophenes, retene, and fluorenes being the most abundant compounds detected in lake water (Table 4.S2). As experiments were performed in the environment, it is likely that lighter molecular weight compounds volatilized, leaving an increased proportion of higher molecular weight 3- and 4-ring PAHs. Chemistry results are supported by previous studies simulating dilbit spills in

outdoor tanks containing lake water and sediments where rapid desorption of PAHs into the water column was observed, most notably phenanthrenes, dibenzothiophenes, and fluorenes.[11]

Routes of exposure to oil constituents in fish have been shown to occur through ventilation through gills, dermal uptake, and ingestion.[32,33] As dilbit constituents were detected within the water column, absorption of waterborne compounds through skin and gills was one probable route of exposure. Life history may have a significant impact the routes and degree of exposure to PAHs following an oil spill.[34] In this particular case, lake trout may have had potential contact with sunken dilbit during the fall and late winter when lake turnover occurs as lake trout utilize the entire water column during this time. However, as the lake stratifies in spring and summer, lake trout tend to stay in deeper, cooler waters and likely did not have contact with sunken dilbit during this time before cleanup in August 2019. Lake trout may also have ingested oil-contaminated organisms, such as zooplankton and forage fish which were more likely to have contact with sunken dilbit.[5,33] Through consumption of oil-contaminated material, PAHs may be transferred to apex predatory species through the food web. Thus, exposure to PAHs may continue even after most constituents have volatilized from the water column. Additional studies on the trophic movement of dilbit constituents in lakes are needed to better understand bioaccumulation processes in boreal lake systems.

Bioinformatics output and transcriptomic responses

Lake trout were collected by hook and line angling from Lake 260 in September of 2017 and 2018 (prior to dilbit exposure) and September of 2019 after dilbit exposure (Table 4.S3). Average weights for 2017, 2018, and 2019 lake trout were 644.3 ± 87.9 g, 814.3 ± 92.8 g, and 961.9 ± 71.5 g, respectively (Figure 4.S1). Average total lengths were 42.59 ± 1.9 cm in 2017, 46.8 ± 1.7 cm in 2018, and 48.74 ± 1.3 cm in 2019 (Figure 4.S1). Moreover, average condition factors were 0.80 ± 0.02 in 2017, 0.78 ± 0.02 in 2018, and 0.82 ± 0.02 in 2019 (Figure 4.S1). Average weight and total lengths were significantly lower in 2017 compared to 2019 ($p \leq 0.04$ for both comparisons), but there were no significant differences in weight and length among 2018 baseline and 2019 dilbit-treated individuals. There were no significant differences in condition factor among all years. Mucus samples from four individuals from each year were sequenced. The 12 FASTQ files generated from Illumina sequencing encompassed a total of 616M single-end raw reads, with an average of 51M reads per sample (Table 4.S4).

To determine year-year differences in background transcriptional signatures, comparisons were made in fish sampled prior to dilbit exposure in 2017 and 2018. A total of 1,576 transcripts were differentially expressed among 2017 and 2018 baseline years at a FDR adjusted p-value ≤ 0.05 (Table B-1). The top GO biological processes were ‘translation’, ‘ribosomal small unit assembly’, and ‘in utero embryonic development’, whereas the top GO molecular functions were ‘structural constituent of ribosome’, ‘poly(A) RNA binding’, and ‘mRNA binding’ (Table 4.S5; Table 4.S6).

Comparing animals pre- and post-dilbit exposure, the sample-to-sample Euclidian distance heat map (Figure 4.S2) and PCA of transcriptome-wide count data (Figure 4.6A) indicated clustering of individuals based on treatment. Unsupervised hierarchical clustering of the top 500 most-variable transcripts also clustered individuals by treatment (Figure 4.6B). Thus, results of clustering analyses indicate that there were clear differences in the mucus transcriptomic profiles of lake trout following additions of dilbit. PCA of transcriptome-wide count data did not show distinct clustering patterns based on sex, suggesting that transcriptomic changes among years were driven by treatment (Figure 4.S3). A total of 714 transcripts were differentially expressed at a FDR adjusted p-value ≤ 0.05 among individuals sampled in pre-and post-dilbit (Table B-2). The RNA sequencing results were confirmed through qPCR (Figure 4.S4). Among all pathway analyses, there was prevalence of biological pathways related to intermediary metabolism, more specifically relating to carbohydrates and amino acids. For example, of the 12 KEGG pathways identified, three were related to intermediary metabolism including 'arginine biosynthesis' (rank 3), 'alanine, aspartate, and glutamate metabolism' (rank 5), and 'carbon metabolism' (rank 11) (Figure 4.7; Table 4.S7). Intermediary metabolism pathways were also identified in the GO analysis, including the biological process 'urea cycle' (rank 11) as well as the molecular functions 'glucose binding' (rank 9) and 'carbamoyl-phosphate synthase activity' (rank 18) (Figure 4.7; Table 4.S8; Table 5.S9). This trend was also seen in the IPA results, where the top canonical pathways (ranked by p value) included 'superpathway of citrulline metabolism' (rank 1), 'arginine degradation 1' (rank 10), 'urea cycle' (rank 18), and 'arginine degradation VI (arginase 2

pathway)' (rank 19) (Figure 4.8). Taken together, results of the pathway analyses suggest molecular changes in metabolic and energetic processes in lake trout following dilbit exposure.

Several studies in fish have shown that exposure to PAHs and oil, can alter energy metabolism mechanics and induce energy mobilization causing increased energy demands due to stress.[35–40] Stress-induced changes in metabolism are associated with a surge of cortisol, which results in activation of gluconeogenesis and, consequently, increased plasma glucose concentrations.[35,41,42] Moreover, gluconeogenesis relies on non-carbohydrate sources such as lactate, glycerol, and amino acids for the formation of glucose. Due to the multiple pathways associated with amino acid metabolism, it is suggested that lake trout catabolized and degraded protein for energy production (Figure 4.6; Figure 4.7). Metabolism of amino acids for energy is further supported by the upregulation of alanine aminotransferase 2 (*gpt2*) which converts alanine into pyruvate for glucose production and has been shown to be enhanced in response to stress for gluconeogenesis (Figure 4.9).[42–44] Other gluconeogenic and amino acid catabolism transcripts were also upregulated, including glutamate dehydrogenase (*glud1*), glutamine-fructose-6-phosphate aminotransferase (*gfpt1*), and ornithine aminotransferase (*oat*) (Figure 4.9). Furthermore, several of these transcripts are also involved in the urea cycle, likely enhancing the urea cycle to convert excess ammonia following breakdown of amino acids (Figure 4.7; Figure 4.8; Figure 4.9). Cortisol also elicits decreased potential for glycolysis in fish through decreased activities of pyruvate kinase, hexokinase, fructose 1,6-bisphosphate, and glucose-6-phosphate 1-dehydrogenase.[41] In the present

study, glycolytic transcripts such hexokinase-1 (*hk-1*) and glucose-6-phosphate 1-dehydrogenase (*g6pd*) were downregulated in lake trout mucus following dilbit exposure (Figure 4.9). As hexokinase is a rate-limiting enzyme of glycolysis, decreased transcription of *hk-1* and other glycolytic transcripts supports the utilization of gluconeogenesis during stress-induced energy production. Although molecular changes suggested a shift in energetics, there were no differences in condition factor pre- and post-dilbit exposure, suggesting that the disruption was inadequate enough to elicit changes in body mass.

Shifts in energy metabolism have been observed in fish following dilbit exposure. Previous studies exposing Atlantic salmon (*Salmo salar*) smolts and sockeye salmon embryos to dilbit resulted in elevated cardiac and total body triglyceride levels, suggesting decreased lipid utilization for energy compared to controls.[17,18] In the present study, decreased lipid utilization was suggested by downregulation of the transcript encoding for carnitine palmitoyltransferase I (*cpt1a*) which is the rate limiting step in long-chain fatty acid oxidation (Figure 4.9).[45,46] Furthermore, expression of genes involved in protein degradation was increased in muscle of dilbit-exposed Atlantic salmon smolts, namely ubiquitin which labels protein for proteasomal degradation.[18] Although ubiquitin was not upregulated in lake trout mucus, several transcripts encoding for enzymes involved in ubiquitination of proteins were significantly upregulated, including polyubiquitin, ubiquitin conjugating enzyme E2 D2, and others (Table B-2). Thus, results from the present and previous studies together suggest that dilbit may induce shifts in energy metabolism, such as increased protein degradation and potentially

greater utilization of amino acids for energy. Although dilbit exposure has been shown to increase muscle damage in sockeye salmon,[19] it is not known whether muscle damage is correlated to transcriptional changes involved in muscle protein degradation and catabolism.

Perturbations in metabolism following dilbit exposure was also suggested by the upregulation of cytochrome c oxidase subunit 1 (*mt-co1*) and cytochrome c oxidase subunit 2 (*mt-co2*) which encode for catalytic subunits of cytochrome C oxidase (COX) (Figure 5.8).[47] COX functions as an aerobic respiratory enzyme and catalyzes the final step of the mitochondrial electron transport chain.[47,48] In fish, the enzymatic activity of COX is an indicator of metabolic capacity and a biomarker of metabolic perturbation following exposure to petroleum hydrocarbons.[49–51] Following waterborne exposures to crude oil water-accommodated fractions, COX activity in the gills and liver of Australian bass (*Macquaria novemaculeata*) either increased or decreased compared to controls depending on concentration (14 – 134 μg/L Σpetroleum hydrocarbons).[50] Similarly, COX activity was altered in the heart and red muscle of Atlantic salmon smolts following subchronic exposure to dilbit, being either increased or decreased relative to controls depending on tissue type and concentration (9.65 and 67.9 μg/L ΣPAC).[18] Thus, dysregulation of *mt-co1* and *mt-co2* in dilbit-exposed lake trout corroborates previous studies suggesting that crude oil induces alterations in COX and, thus, changes in energy metabolism. Although there are many abiotic and biotic factors that may contribute to stress response in the environment, the lack of molecular evidence for energetic changes among baseline years 2017-2018 provides a degree of support that the suggested energy

metabolism changes in 2019 were a result of dilbit additions. For example, there were no GO pathways related to intermediary metabolism or energetics among 2017 and 2018, suggesting no molecular changes in energy metabolism year-to-year at baseline conditions. Furthermore, only two genes (*g6pd* and *gpt2*) relating to energy metabolism were dysregulated among baseline conditions of the genes identified to be altered following dilbit additions (Figure 5.9).

Identification of biomarkers

The expression patterns of certain genes may be used as biomarkers of exposure and can help researchers quickly assess whether an individual has been exposed to a contaminant of interest. The induction of CYP1A has commonly been used as biomarker of exposure to petroleum hydrocarbons and other organic pollutants[52–54] and exposure to dilbit has also been shown to induce CYP1A activity in several fish species.[13–15,17,19,20,55] In the present study, there was a trend of *cyp1a3* upregulation in lake trout following dilbit additions (FDR-adj p = 0.08) (Figure 4.9; Table B-2). Although not statistically significant, upregulation of *cyp1a3* may have biological significance and may be a viable biomarker in mucus, especially at higher PAH concentrations seen following an oil spill. qPCR analysis was used to confirm the trend of *cyp1a3* upregulation that was identified in the RNA sequencing results. Results of qPCR indicated a 1.2-fold increase in *cpy1a3* transcripts in lake trout mucus after dilbit exposure, though this increase was not statistically significant (Figure 4.S4). The trend of *cyp1a3* upregulation indicates a molecular response specific to petrogenic PAHs and, thus, further suggests that the

observed energetic responses were also likely due to dilbit-induced stress rather than other environmental factors. Moreover, upregulation of *cyp1a3* in September 2019 even after removal of residual dilbit from the lake sediments in August 2019 suggests that diet may be a primary route of exposure to PAHs; as PAH levels were quickly depleted in lake water following dilbit additions, PAHs were not present during the time of sampling in September. Finally, our results support findings of a previous study in which *cyp1a1* and *cyp1b1* were the top upregulated transcript in mahi-mahi mucus following exposure to *Deepwater Horizon* slick oil (16.55 μg/L ΣPAH).[21] In the present study, there was a clear trend of *cyp1a3* upregulation even at relatively low environmental concentrations (0.84 – 4.4 μg/L ΣPAH), suggesting that CYP1A induction is a sensitive endpoint in mucus and is a viable tool for monitoring oil exposure of fish populations.

Applications and implications

Overall, results of RNA sequencing suggest stress following dilbit exposure, as indicated by upregulation of transcripts involved in cortisol-induced energy metabolism. More specifically, evidence suggests that there was an increased reliance on amino acid metabolism and decreased reliance on fatty acid oxidation for energy production in dilbit-exposed lake trout compared to controls. The changes in energy metabolism and utilization support previous studies which have also shown that crude oil and dilbit specifically may induce changes in energy metabolism. Moreover, *cyp1a3* was upregulated in lake trout mucus, suggesting a molecular response to dilbit. As RNA sequencing identified molecular changes related to energy metabolism and PAH exposure

in lake trout mucus, results of the present study indicate that transcriptomic analysis of epidermal mucus is a promising vector for nonlethal oil exposure assessment of fish populations.

There are some realities that should be considered when using molecular analysis of mucus for exposure assessment following an oil spill. Although RNA sequencing is a holistic approach to capturing molecular changes in an organism, use of targeted qPCR for genes such as *cyp1a* and *ahr* may be a more rapid and inexpensive method for monitoring exposure following an oil spill. Along with this, mucus from reference individuals will be needed for both RNA sequencing or qPCR analysis. Although use of baseline mucus samples from the population of interest would be ideal to minimize confounding variables, it may not be feasible. Instead, mucus from individuals from a well-characterized reference location may be used. Use of other nonlethal endpoints in conjunction with analysis of mucus for target genes of interest may provide a more complete insight on organism health. Examples include analysis of blood for enzymatic activity or use of muscle plugs for contaminant loading assessment. There are also logistical issues that require further research before the method may be applied for spill monitoring to determine magnitude and geographic extent of effects. For example, further research is needed to identify how rapidly the mucus transcriptome responds to external conditions as well as to determine the turnover rate of the mucus transcriptome. Furthermore, the relationship among gene expression in actively metabolizing tissues, such as liver, and the mucus should be identified in order to better understand the physiological significance of differential expression in the mucus. While additional

research is needed, use of epidermal mucus is a promising method for oil exposure assessment without the use of lethal sampling.

References

(1) Canada National Energy Board. *Canada's Oil Sands Opportunities and Challenges To 2015: An Update*; 2006.

(2) Dupuis, A.; Ucan-Marin, F. A Literature Review on the Aquatic Toxicology of Petroleum Oil: An Overview of Oil Properties and Effects to Aquatic Biota. *DFO Can. Sci. Advis. Secr. Res. Doc.* **2015**, *2015/007* (April), 51.

(3) Canada Energy Regulator. Crude Oil Annual Export Summary – 2018 https://www.cer-rec.gc.ca/nrg/sttstc/crdlndptrlmprdct/stt/crdlsmmr/crdlsmmr-eng.html.

(4) Crosby, S.; Fay, R.; Groark, C.; Kani, A.; Smith, J.; Sullivan, T. Transporting Alberta's Oil Sands Products: Defining the Issues and Assessing the Risks. *NOAA Tech. Memo. NOS OR&R 44* **2013**, No. September, 153.

(5) National Academies of Sciences Medicine and Engineering. *Spills of Diluted Bitumen from Pipelines: A Comparative Study of Environmental Fate, Effects, and Response*; The National Academies Press: Washington, DC, 2016. https://doi.org/10.17226/21834.

(6) Boufadel, M.; Chen, B.; Foght, J.; Hodson, P.; Lee, K.; Swanson, S.; Venosa, A. *The Behaviour and Environmental Impacts of Crude Oil Released into Aqueous Environments Fall*; 2015.

(7) Yang, C.; Wang, Z.; Yang, Z.; Hollebone, B.; Brown, C. E.; Landriault, M.; Fieldhouse, B. Chemical Fingerprints of Alberta Oil Sands and Related. *Environ. Forensics* **2011**, *12* (2), 173–188. https://doi.org/10.1080/15275922.2011.574312.

(8) Adams, J.; Larter, S.; Bennett, B.; Huang, H.; Westrich, J.; Larter, S.; Bennett, B.; Huang, H.; Westrich, J.; E, S. I.; et al. *The Dynamic Interplay of Oil Mixing, Charge Timing, and Biodegradation in Forming the Alberta Oil Sands: Insights from Geologic Modeling and Biogeochemistry*; 2013. https://doi.org/10.1306/13371578St643552.

(9) Lee, K.; Boufadel, M.; Chen, B.; Foght, J.; Hodson, P.; Swanson, S.; Venosa, A. High-Priority Research Needs for Oil Spills in Canada: Summary of a Royal Society Expert Panel Report on the Behaviour and Environmental Impacts of Crude Oil Released into Aqueous Environments. *39th AMOP Tech. Semin. Environ. Contam. Response* **2016**, No. July.

(10) Dew, W. A.; Hontela, A.; Rood, S. B.; Pyle, G. G. Biological Effects and Toxicity of Diluted Bitumen and Its Constituents in Freshwater Systems. *Journal of Applied*

Toxicology. 2015. https://doi.org/10.1002/jat.3196.

(11) Stoyanovich, S. S.; Yang, Z.; Hanson, M.; Hollebone, B. P.; Orihel, D. M.; Palace, V.; Rodriguez-Gil, J. L.; Faragher, R.; Mirnaghi, F. S.; Shah, K.; et al. Simulating a Spill of Diluted Bitumen: Environmental Weathering and Submergence in a Model Freshwater System. *Environ. Toxicol. Chem.* **2019**, *38* (12), 2621–2628. https://doi.org/10.1002/etc.4600.

(12) Philibert, D. A.; Philibert, C. P.; Lewis, C.; Tierney, K. B. Comparison of Diluted Bitumen (Dilbit) and Conventional Crude Oil Toxicity to Developing Zebrafish. *Environ. Sci. Technol.* **2016**, *50*, 6091–6098. https://doi.org/10.1021/acs.est.6b00949.

(13) Madison, B. N.; Hodson, P. V.; Langlois, V. S. Cold Lake Blend Diluted Bitumen Toxicity to the Early Development of Japanese Medaka. *Environ. Pollut.* **2017**, *225*, 579–586. https://doi.org/10.1016/j.envpol.2017.03.025.

(14) Madison, B. N.; Hodson, P. V; Langlois, V. S. Diluted Bitumen Causes Deformities and Molecular Responses Indicative of Oxidative Stress in Japanese Medaka Embryos. *Aquat. Toxicol.* **2015**, *165*, 222–230. https://doi.org/10.1016/j.aquatox.2015.06.006.

(15) Alsaadi, F. M.; Madison, B. N.; Brown, R. S.; Hodson, P. V.; Langlois, V. S. Morphological and Molecular Effects of Two Diluted Bitumens on Developing Fathead Minnow (Pimephales Promelas). *Aquat. Toxicol.* **2018**, *204* (June), 107–116. https://doi.org/10.1016/j.aquatox.2018.09.003.

(16) Alsaadi, F.; Hodson, P. V.; Langlois, V. S. An Embryonic Field of Study: The Aquatic Fate and Toxicity of Diluted Bitumen. *Bulletin of Environmental Contamination and Toxicology*. 2018. https://doi.org/10.1007/s00128-017-2239-7.

(17) Alderman, S. L.; Lin, F.; Gillis, T. E.; Farrell, A. P.; Kennedy, C. J. Developmental and Latent Effects of Diluted Bitumen Exposure on Early Life Stages of Sockeye Salmon (Oncorhynchus Nerka). *Aquat. Toxicol.* **2018**, *202*, 6–15. https://doi.org/10.1016/j.aquatox.2018.06.014.

(18) Avey, S. R.; Kennedy, C. J.; Farrell, A. P.; Gillis, T. E.; Alderman, S. L. Effects of Diluted Bitumen Exposure on Atlantic Salmon Smolts: Molecular and Metabolic Responses in Relation to Swimming Performance. *Aquat. Toxicol.* **2020**, *221* (September 2019), 105423. https://doi.org/10.1016/j.aquatox.2020.105423.

(19) Alderman, S. L.; Lin, F.; Farrell, A. P.; Kennedy, C. J.; Gillis, T. E. Effects of Diluted Bitumen Exposure on Juvenile Sockeye Salmon: From Cells to Performance. *Environ. Toxicol. Chem.* **2017**, *36* (2), 354–360.

https://doi.org/10.1002/etc.3533.

(20) Alderman, S. L.; Dindia, L. A.; Kennedy, C. J.; Farrell, A. P.; Gillis, T. E. Proteomic Analysis of Sockeye Salmon Serum as a Tool for Biomarker Discovery and New Insight into the Sublethal Toxicity of Diluted Bitumen. *Comp. Biochem. Physiol. - Part D* **2017**, *22*, 157–166. https://doi.org/10.1016/j.cbd.2017.04.003.

(21) Greer, J. B.; Andrzejczyk, N. E.; Mager, E. M.; Stieglitz, J. D.; Benetti, D.; Grosell, M.; Schlenk, D. Whole-Transcriptome Sequencing of Epidermal Mucus as a Novel Method for Oil Exposure Assessment in Juvenile Mahi-Mahi (Coryphaena Hippurus). *Environ. Sci. Technol. Lett.* **2019**, *6*, 538–544. https://doi.org/10.1021/acs.estlett.9b00479.

(22) Dzul-Caamal, R.; Salazar-Coria, L.; Olivares-Rubio, H. F.; Rocha-Gómez, M. A.; Girón-Pérez, M. I.; Vega-López, A. Oxidative Stress Response in the Skin Mucus Layer of Goodea Gracilis (Hubbs and Turner, 1939) Exposed to Crude Oil: A Non-Invasive Approach. *Comp. Biochem. Physiol. -Part A Mol. Integr. Physiol.* **2016**. https://doi.org/10.1016/j.cbpa.2016.05.008.

(23) Cooke, S. J.; Donaldson, M. R.; O'connor, C. M.; Raby, G. D.; Arlinghaus, R.; Danylchuk, A. J.; Hanson, K. C.; Hinch, S. G.; Clark, T. D.; Patterson, D. A.; et al. The Physiological Consequences of Catch-and-Release Angling: Perspectives on Experimental Design, Interpretation, Extrapolation and Relevance to Stakeholders. *Fish. Manag. Ecol.* **2013**, *20* (2–3), 268–287. https://doi.org/10.1111/j.1365-2400.2012.00867.x.

(24) Andrews, S. FastQC: A Quality Control Tool for High Throughput Sequence Data. **2010**.

(25) Bolger, A. M.; Lohse, M.; Usadel, B. Trimmomatic: A Flexible Trimmer for Illumina Sequence Data. *Bioinformatics* **2014**, btu170.

(26) Langmead, B.; Salzberg, S. Fast Gapped-Read Alignment with Bowtie 2. *Nat Methods* **2012**, *9* (4), 357–359.

(27) Pasquier, J.; Cabau, C.; Nguyen, T.; Jouanno, E.; Severac, D.; Braasch, I.; Journot, L.; Pontarotti, P.; Klopp, C.; Postlethwait, J. H.; et al. Gene Evolution and Gene Expression after Whole Genome Duplication in Fish: The PhyloFish Database. *BMC Genomics* **2016**, *17* (1), 1–10. https://doi.org/10.1186/s12864-016-2709-z.

(28) Li, B.; Dewey, C. RSEM: Accurate Transcript Quantification from RNA-Seq Data with or without a Reference Genome. *BMC Bioinformatics* **2011**, *12* (323). https://doi.org/10.1186/1471-2105-12-323.

(29) Gentleman, R.; Carey, V.; Huber, W.; Hahne, F. Genefilter: Methods for Filtering Genes from High-Throughput Experiments. *R Packag. version 1.68.0* **2019**.

(30) Love, M. I.; Huber, W.; Anders, S. Moderated Estimation of Fold Change and Dispersion for RNA-Seq Data with DESeq2. *Genome Biol.* **2014**, *15* (550). https://doi.org/https://doi.org/10.1186/s13059-014-0550-8.

(31) Livak, K. J.; Schmittgen, T. D. Analysis of Relative Gene Expression Data Using Real-Time Quantitative PCR and the 2−ΔΔCT Method. *Methods* **2001**, *25* (4), 402–408. https://doi.org/https://doi.org/10.1006/meth.2001.1262.

(32) Nichols, J. W.; McKim, J. M.; Lien, G. J.; Hoffman, A. D.; Bertelsen, S. L.; Elonen, C. M. A Physiologically Based Toxicokinetic Model for Dermal Absorption of Organic Chemicals by Fish. *Fundam. Appl. Toxicol.* **1996**, *31* (2), 229–242. https://doi.org/10.1006/faat.1996.0095.

(33) Almeda, R.; Wambaugh, Z.; Chai, C.; Wang, Z.; Liu, Z.; Buskey, E. J. Effects of Crude Oil Exposure on Bioaccumulation of Polycyclic Aromatic Hydrocarbons and Survival of Adult and Larval Stages of Gelatinous Zooplankton. *PLoS One* **2013**, *8* (10), 20–21. https://doi.org/10.1371/journal.pone.0074476.

(34) Snyder, S. M.; Pulster, E. L.; Wetzel, D. L.; Murawski, S. A. PAH Exposure in Gulf of Mexico Demersal Fishes, Post- Deepwater Horizon. *Environ. Sci. Technol.* **2015**, *49* (14), 8786–8795. https://doi.org/10.1021/acs.est.5b01870.

(35) Vijayan, M. M.; Aluru, N.; Leatherland, J. F. Stress Response and the Role of Cortisol. In *Fish Diseases and Disorders, vol. 2*; Leatherland, J. F., Woo, P. T. K., Eds.; CAB International: Wallingford, 2010; pp 182–201.

(36) Ings, J. S.; Vijayan, M. M.; Servos, M. R. Tissue-Specific Metabolic Changes in Response to an Acute Handling Disturbance in Juvenile Rainbow Trout Exposed to Municipal Wastewater Effluent. *Aquat. Toxicol.* **2012**, *108*, 53–59. https://doi.org/10.1016/j.aquatox.2011.09.009.

(37) Tintos, A.; Gesto, M.; Míguez, J. M.; Soengas, J. L. β-Naphthoflavone and Benzo(a)pyrene Treatment Affect Liver Intermediary Metabolism and Plasma Cortisol Levels in Rainbow Trout Oncorhynchus Mykiss. *Ecotoxicol. Environ. Saf.* **2008**, *69* (2), 180–186. https://doi.org/10.1016/j.ecoenv.2007.03.009.

(38) Frasco, M. F.; Guilhermino, L. Effects of Dimethoate and Beta-Naphthoflavone on Selected Biomarkers of Poecilia Reticulata. *Fish Physiol. Biochem.* **2002**, *26* (2), 149–156. https://doi.org/10.1023/A:1025457831923.

(39) Wendelaar Bonga, S. . The Stress Response in Fish. *Physiol. Rev.* **1977**, *77*, 591–

625.

(40) Hook, S. E.; Mondon, J.; Revill, A. T.; Greenfield, P. A.; Stephenson, S. A.; Strzlecki, J.; Corbett, P.; Armstrong, E.; Song, J.; Doan, H.; et al. Monitoring Sublethal Changes in Fish Physiology Following Exposure to a Light, Unweathered Crude Oil. *Aquat. Toxicol.* **2018**, *204* (August), 27–45. https://doi.org/10.1016/j.aquatox.2018.08.013.

(41) Laiz-Carrión, R.; Martín Del Río, M. P.; Miguez, J. M.; Mangera, J. M.; Soengas, J. L. Influence of Cortisol on Osmoregulation and Energy Metabolism in Gilthead Seabream Sparus Aurata. *J. Exp. Zool. Part A Comp. Exp. Biol.* **2003**, *298* (2), 105–118. https://doi.org/10.1002/jez.a.10256.

(42) Mommsen, T. P.; Vijayan, M. M.; Moon, T. W. Cortisol in Teleosts: Dynamics, Mechanisms of Action, and Metabolic Regulation. *Rev. Fish Biol. Fish.* **1999**, *9* (3), 211–268. https://doi.org/10.1023/A:1008924418720.

(43) Kumar, V.; Sahu, N. P.; Pal, A. K.; Kumar, S.; Sinha, A. K.; Ranjan, J.; Baruah, K. Modulation of Key Enzymes of Glycolysis, Gluconeogenesis, Amino Acid Catabolism, and TCA Cycle of the Tropical Freshwater Fish Labeo Rohita Fed Gelatinized and Non-Gelatinized Starch Diet. *Fish Physiol. Biochem.* **2010**, *36* (3), 491–499. https://doi.org/10.1007/s10695-009-9319-5.

(44) Qian, K.; Zhong, S.; Xie, K.; Yu, D.; Yang, R.; Gong, D. W. Hepatic ALT Isoenzymes Are Elevated in Gluconeogenic Conditions Including Diabetes and Suppressed by Insulin at the Protein Level. *Diabetes. Metab. Res. Rev.* **2015**, *31* (6), 562–571. https://doi.org/10.1002/dmrr.2655.

(45) Frøyland, L.; Madsen, L.; Eckhoff, K. M.; Lie, Ø.; Berge, R. K. Carnitine Palmitoyltransferase I, Carnitine Palmitoyltransferase II, and Acyl-CoA Oxidase Activities in Atlantic Salmon (Salmo Salar). *Lipids* **1998**, *33* (9), 923–930. https://doi.org/10.1007/s11745-998-0289-4.

(46) Qu, Q.; Zeng, F.; Liu, X.; Wang, Q. J.; Deng, F. Fatty Acid Oxidation and Carnitine Palmitoyltransferase I: Emerging Therapeutic Targets in Cancer. *Cell Death Dis.* **2016**, *7* (5), 1–9. https://doi.org/10.1038/cddis.2016.132.

(47) Capaldi, R. A. Structure and Function of Cytochrome c Oxidase. *Annu. Rev. Biochem.* **1990**, *59* (1), 569–596.

(48) Barrientos, A.; Barros, M. H.; Valnot, I.; Rotig, A.; Rustin, P.; Tzagoloff, A. Cytochrome Oxidase in Health and Disease. *Gene* **2002**, *286* (1), 53–63.

(49) Gagnon, M. M.; Holdway. Metabolic Enzyme Activities in Fish Gills as

Biomarkers of Exposure to Petroleum Hydrocarbons. *Ecotoxicol. Environ. Saf.* **1999**, *44*, 92–99.

(50) Cohen, A.; Gagnon, M. M.; Nugegoda, D. Alterations of Metabolic Enzymes in Australian Bass, Macquaria Novemaculeata, after Exposure to Petroleum Hydrocarbons. *Arch. Environ. Contam. Toxicol.* **2005**, *49* (2), 200–205. https://doi.org/10.1007/s00244-004-0174-1.

(51) Pelletier, D.; Dutil, J. D.; Blier, P.; Guderley, H. Relation between Growth Rate and Metabolic Organization of White Muscle, Liver and Digestive Tract in Cod, Gadus Morhua. *J. Comp. Physiol. B* **1994**, *164* (3), 179–190. https://doi.org/10.1007/BF00354078.

(52) Woodin, B. R.; Smolowitz, R. M.; Stegeman, J. J. Induction of Cytochrome P4501A in the Intertidal Fish Anoplarchus Purpurescens by Prudhoe Bay Crude Oil and Environmental Induction in Fish from Prince William Sound. *Environ. Sci. Technol.* **1997**, *31* (4), 1198–1205. https://doi.org/10.1021/es9607190.

(53) Goksøyr, A. Use of Cytochrome P450 1A (CYP1A) in Fish as a Biomarker of Aquatic Pollution BT - Toxicology in Transition; Degen, G. H., Seiler, J. P., Bentley, P., Eds.; Springer Berlin Heidelberg: Berlin, Heidelberg, 1995; pp 80–95.

(54) Whyte, J. J.; Jung, R. E.; Schmitt, C. J.; Tillitt, D. E. Ethoxyresorufin-O-Deethylase (EROD) Activity in Fish as a Biomarker of Chemical Exposure. *Crit. Rev. Toxicol.* **2000**, *30* (4), 347–570. https://doi.org/10.1080/10408440091159239.

(55) McDonnell, D.; Madison, B. N.; Baillon, L.; Wallace, S. J.; Brown, S. R.; Hodson, P. V.; Langlois, V. S. Comparative Toxicity of Two Diluted Bitumens to Developing Yellow Perch (Perca Flavescens). *Sci. Total Environ.* **2019**, *655*, 977–985. https://doi.org/10.1016/j.scitotenv.2018.11.199.

(56) Beyer, J.; Sandvik, M.; Skåre, J. U.; Egaas, E.; Hylland, K.; Waagbø, R.; Goksøyr, A. Time- and Dose-Dependent Biomarker Responses in Flounder (Platichthys Flesus L.) Exposed to Benzo[a]pyrene, 2,3,3′,4,4′, 5-Hexachlorobiphenyl (PCB-156) and Cadmium. *Biomarkers* **1997**, *2* (1), 35–44. https://doi.org/10.1080/135475097231959

Figures and Tables

Figure 4.1. Bathymetric map of Lake 260 (Credit: IISD Experimental Lakes Area).

Figure 4.2. Timeline of limnocorral and shoreline enclosure dilbit experiments and sampling of lake trout in Lake 260. Areas depicted in red indicate times during which the surrounding lake environment may have been exposed to dilbit. In September 2018, curtains of the limnocorrals were cut and sunken dilbit remained on the lake bottom until final clean up in August 2019. In June 2019, tracer studies indicated leakage of water from shoreline enclosures following additions of dilbit, potentially contributing polycyclic aromatic hydrocarbons to the lake.

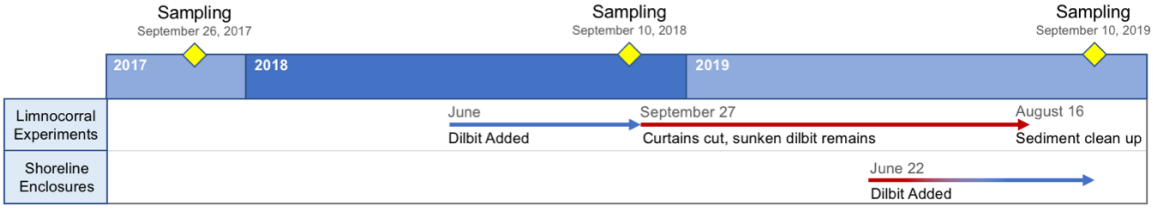

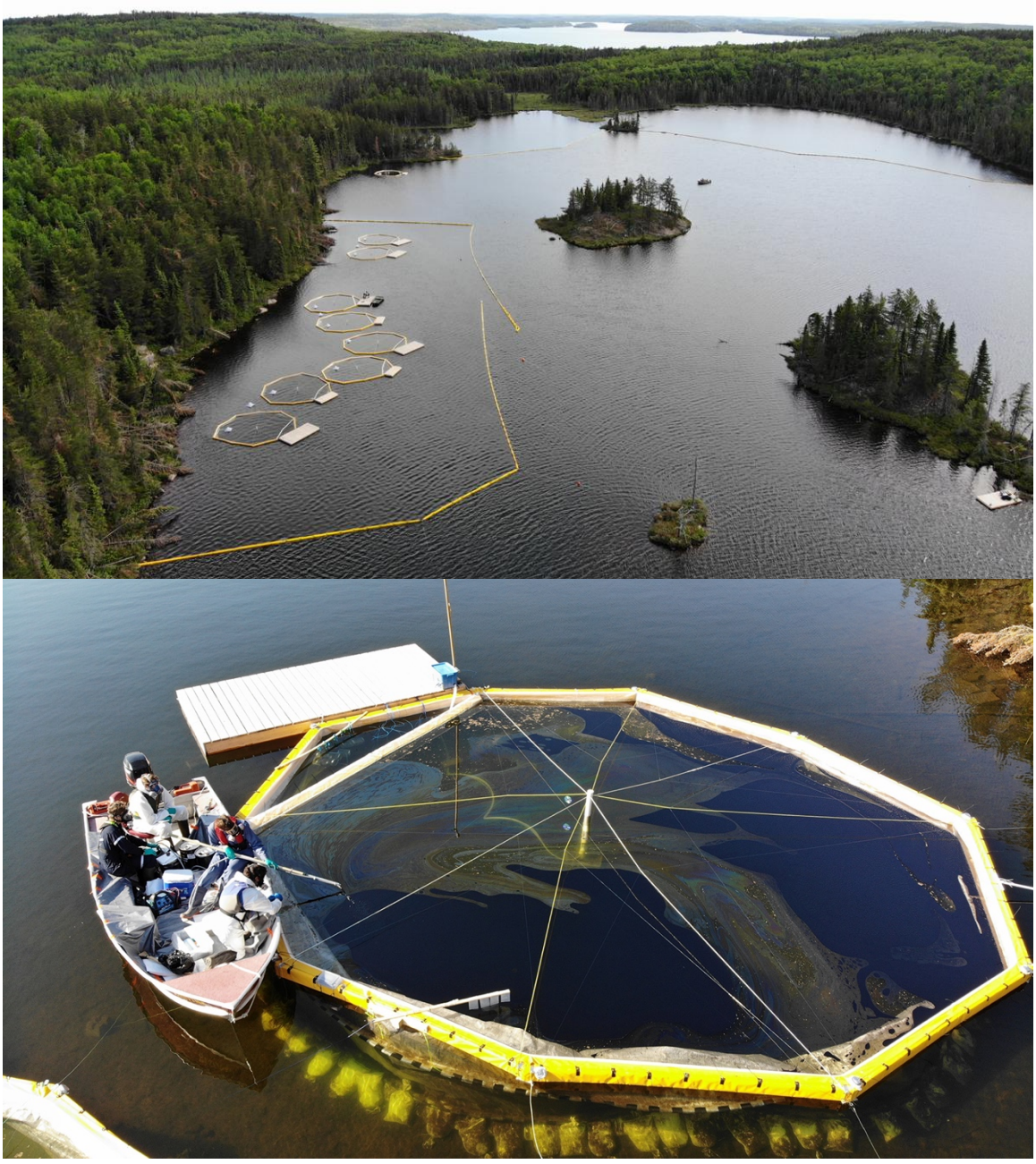

Figure 4.3. Limnocorrals experiments designed to stimulate pipeline spills of diluted bitumen on a boreal lake at the Experimental Lakes Area (Credit: Jose Luis Rodriguez Gil).

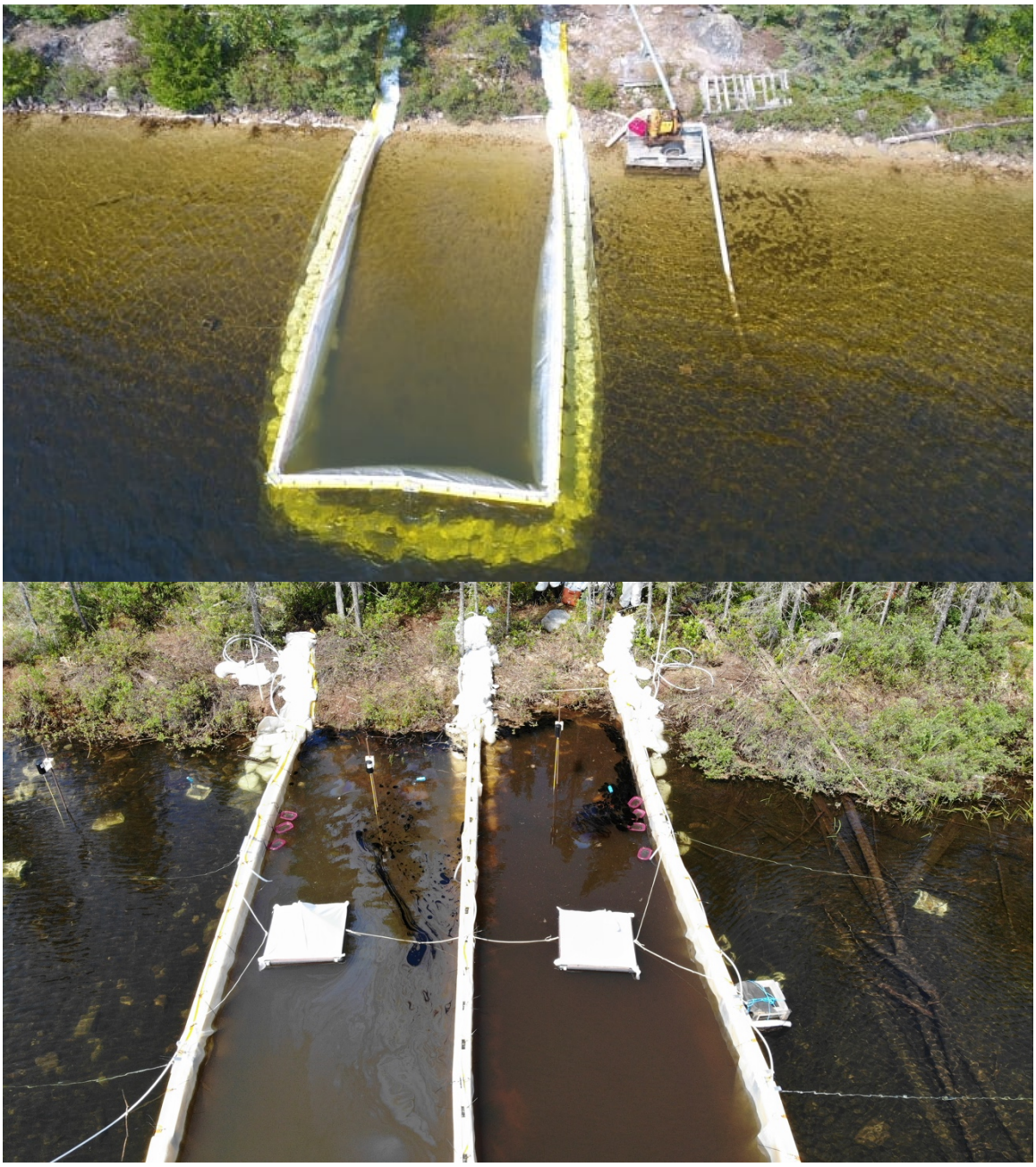

Figure 4.4. Shoreline enclosure experiments designed to stimulate pipeline spills of diluted bitumen and interaction with the shoreline within a boreal lake at the Experimental Lakes Area (Credit: Scott Higgins and IISD Experimental Lakes Area).

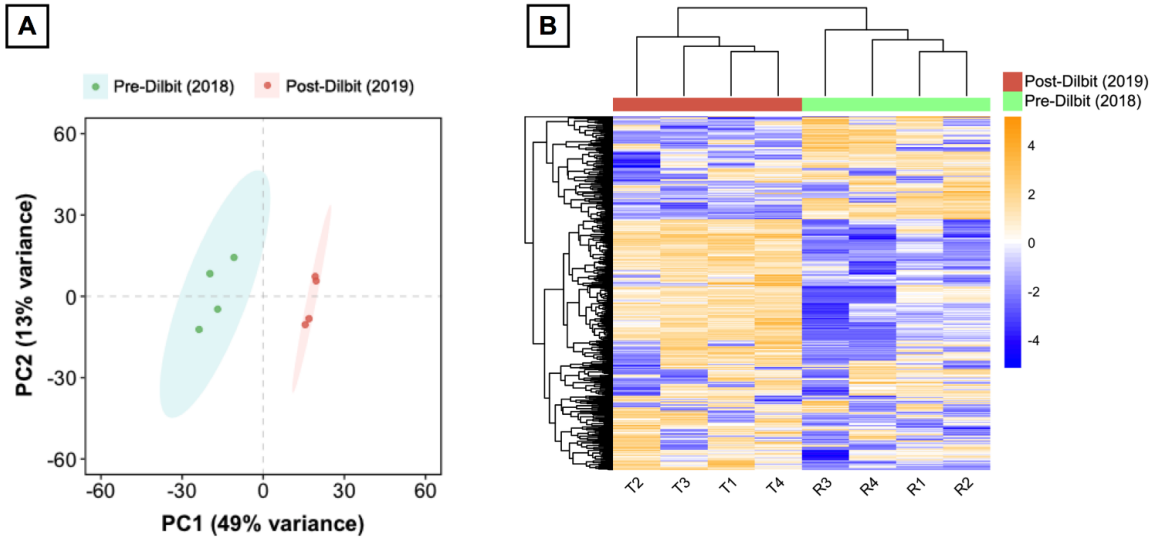

Figure 4.5. Comparison of pre- and post-dilbit exposed lake trout using (A) principal component analysis of transcriptome-wide count data and (B) unsupervised hierarchical clustering of the top 500 most variable transcripts.

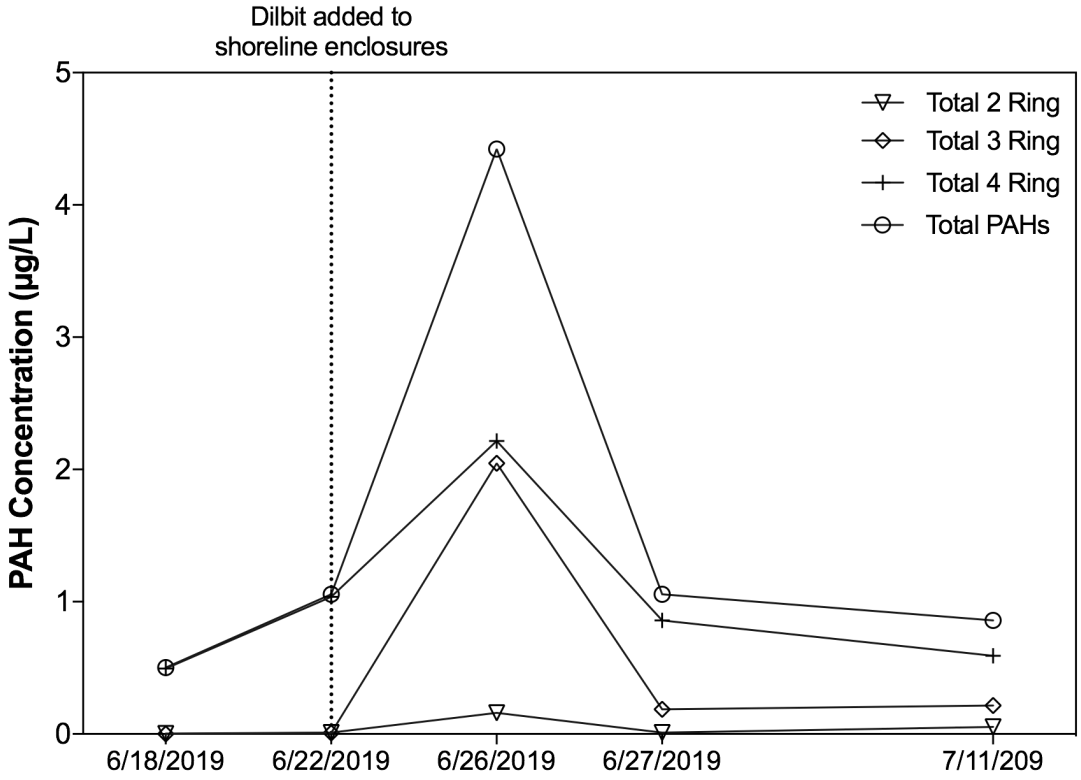

Figure 4.6. Concentrations of polycyclic aromatic hydrocarbons (PAHs) in surface waters of Lake 260 in June and July 2019. Data from June 22 and beyond is following the additions of weathered dilbit into fourteen shoreline enclosures on Lake 260. PAHs were present in Lake 260 surface waters prior to enclosure experiments as a result of the previous limnocorral experiments.

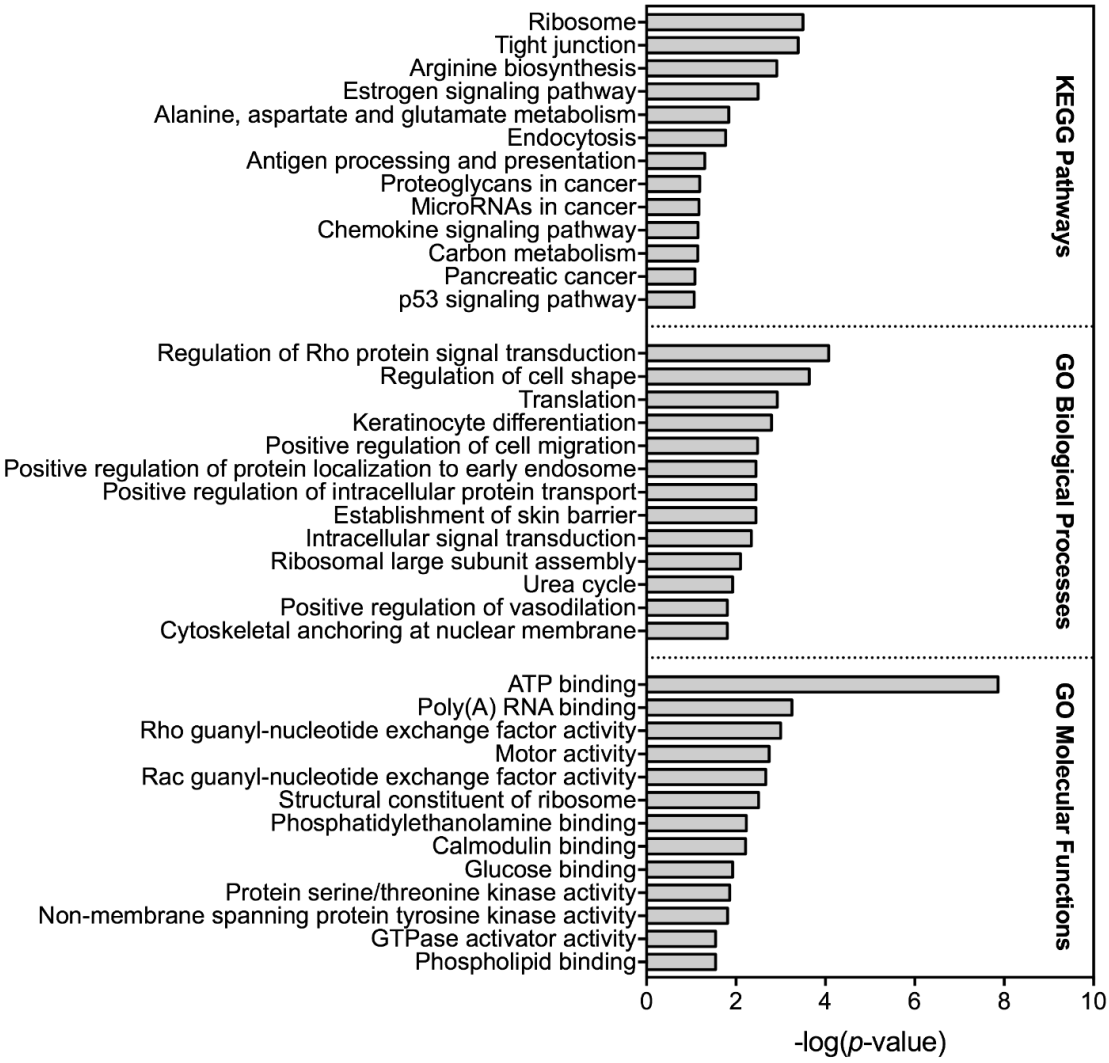

Figure 4.7. Top KEGG pathways as well as gene ontology (GO) biological processes and molecular functions altered based on differential gene expression analysis among 2018 pre-dilbit lake trout and 2019 post-dilbit lake trout.

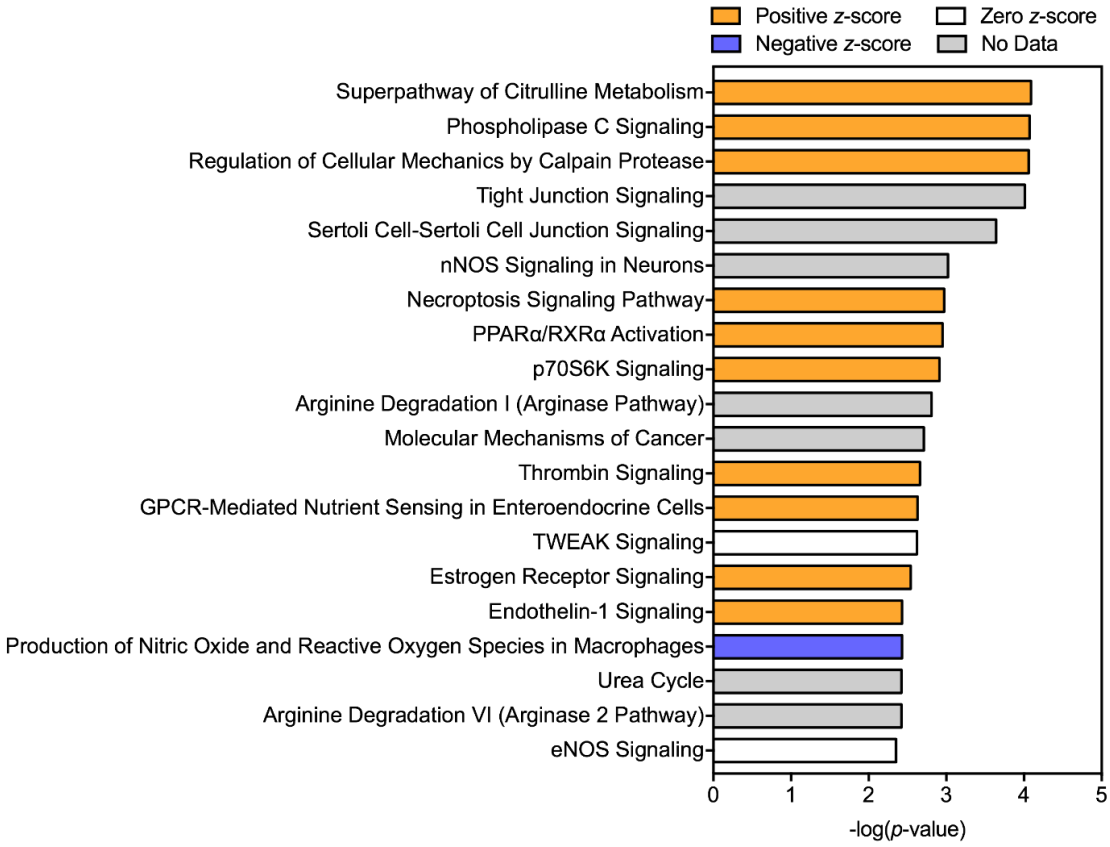

Figure 4.8. Top canonical pathways predicted by Ingenuity Pathway Analysis (IPA) to be affected following dilbit exposure. A positive *z*-score indicates predicted activation whereas a negative *z*-score indicates a predicted inhibition.

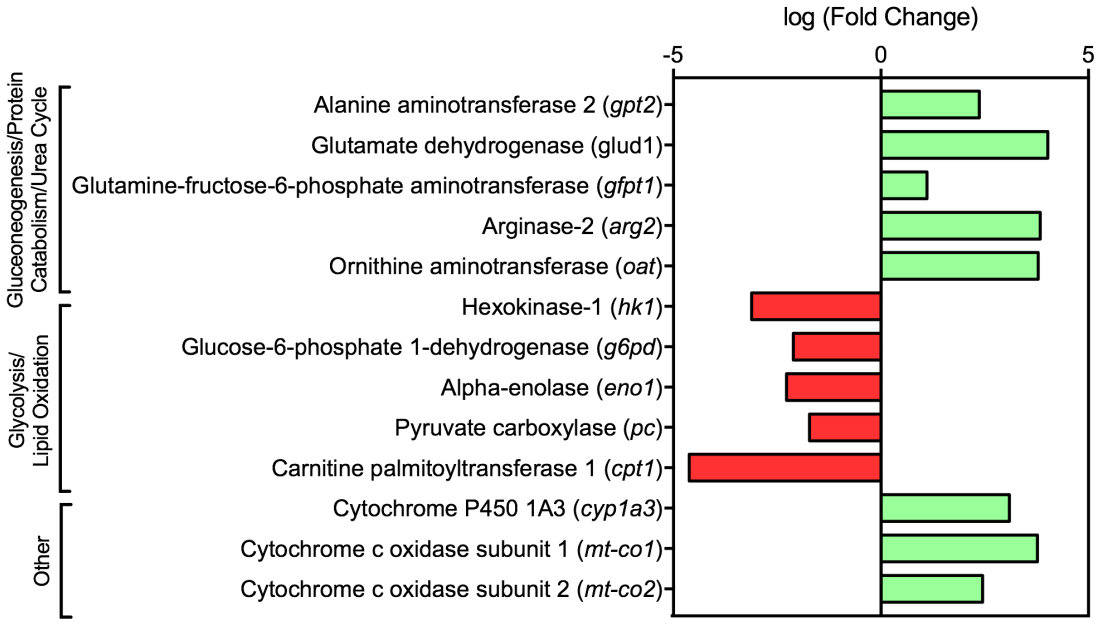

Figure 4.9. Fold change of select transcripts dysregulated in dilbit-exposed lake trout relating to energy metabolism and stress response from RNA sequencing results. All transcripts were significant at FDR adjusted p-value ≤ 0.05, except *cyp1a3* which was significant at a FDR adjusted p-value ≤ 0.1.

Supplemental Materials

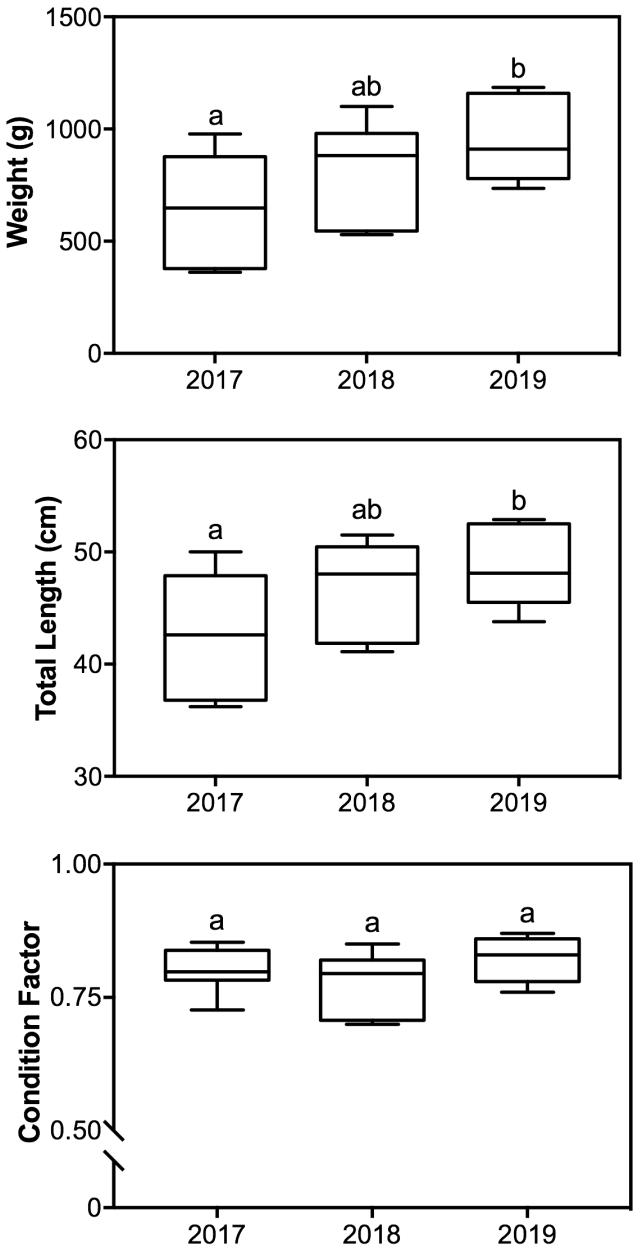

Figure 4.S1. Average weight, total length, and condition factors of lake trout sampled in 2017 (n = 7), 2018 (n = 6), and 2019 (n = 7).

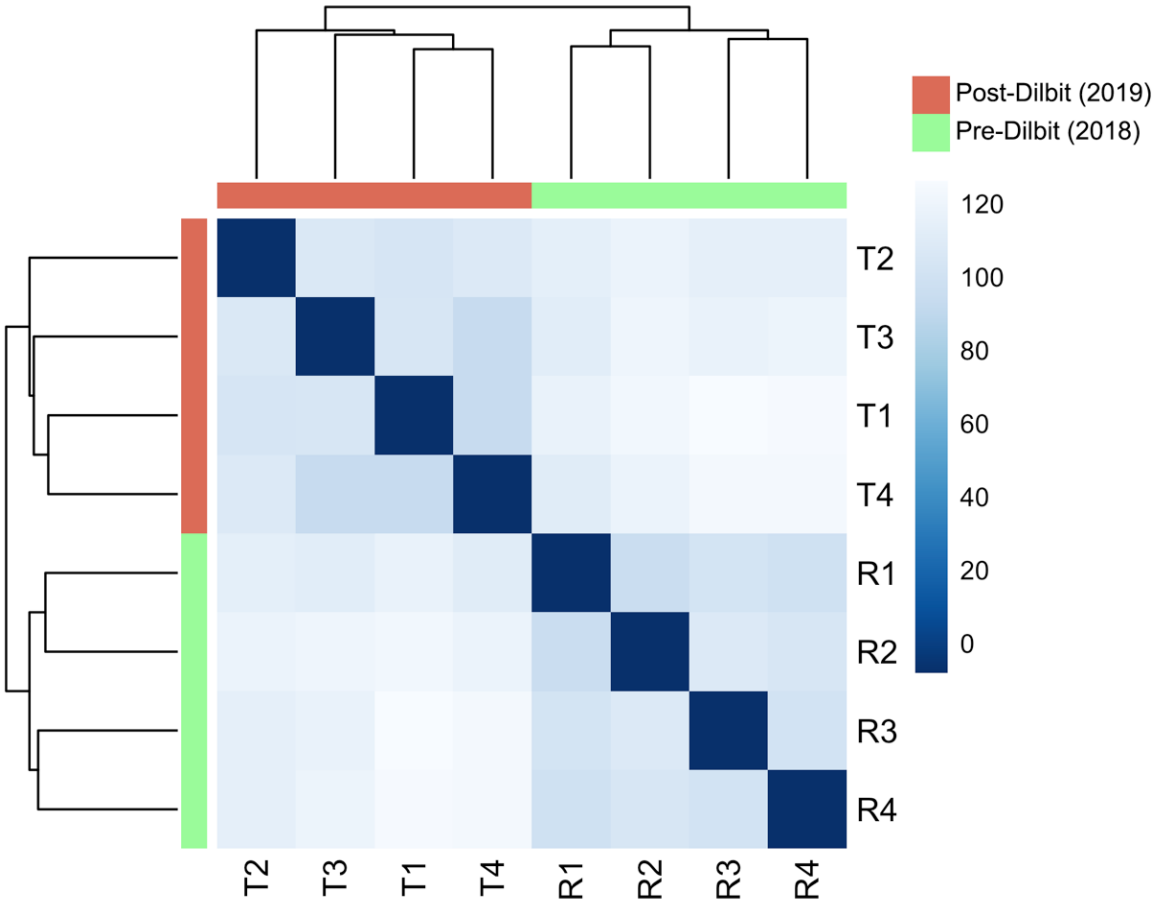

Figure 4.S2. Sample-to-sample Euclidian distance heat map of transcriptome-wide count data from 2018 and 2019 lake trout.

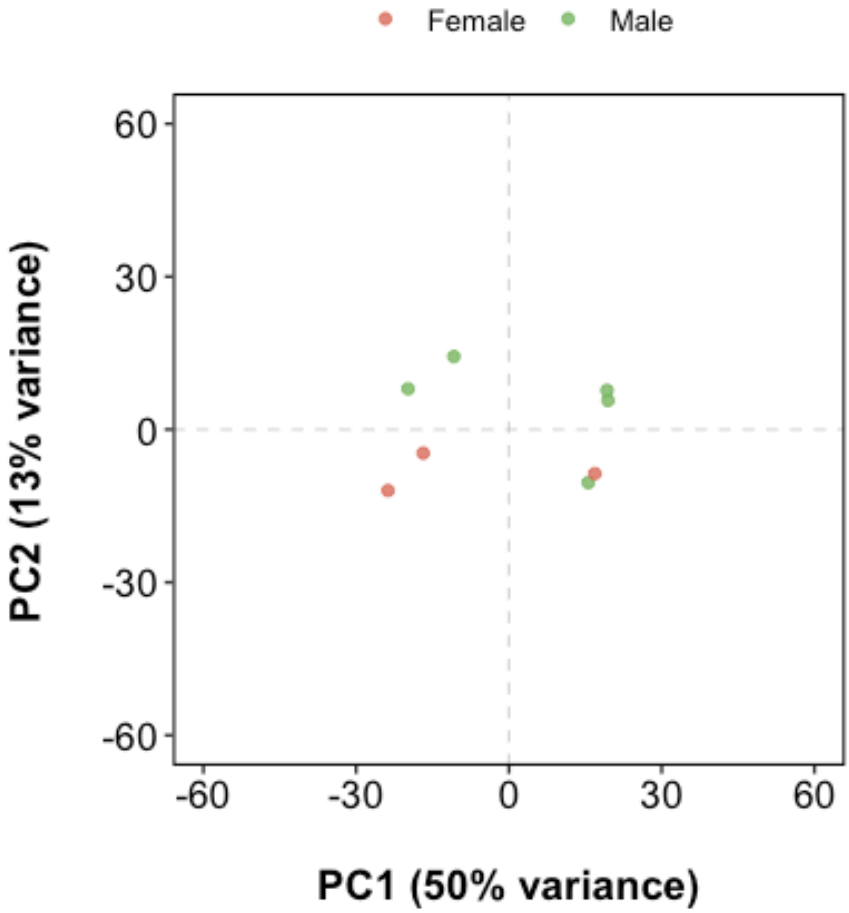

Figure 4.S3. Principal component analysis of transcriptome-wide count data by sex for 2018 and 2019 sequencing data.

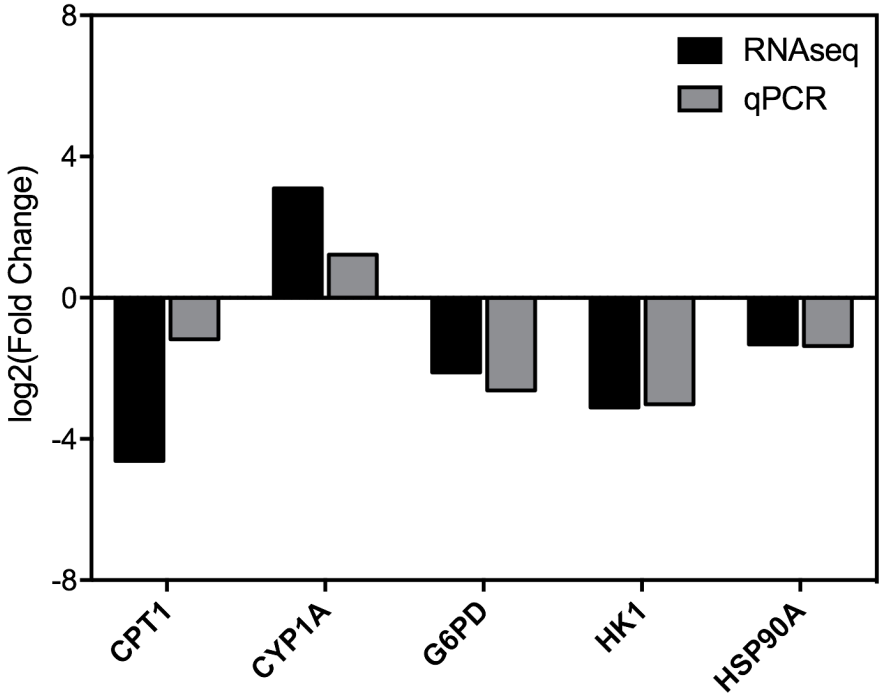

Figure 4.S4. Confirmation of RNA sequencing results through qPCR. qPCR data calculated using $2^{-\Delta\Delta Ct}$ method and normalized by β-actin. (CPT1 = Carnitine palmitoyltransferase 1, CYP1A = Cytochrome P450 1A, G6PD = Glucose-6-phosphate 1-dehydrogenase, HK1 = Hexokinase 1, HSP90A = Heat shock protein 90A).

Table 4.S1. Information for primers used for qPCR confirmation of RNA sequencing results (β-actin = beta-actin, CPT1 = Carnitine palmitoyltransferase 1, CYP1A = Cytochrome P450 1A, G6PD = Glucose-6-phosphate 1-dehydrogenase, HK1 = Hexokinase 1, HSP90A = Heat shock protein 90A).

Gene	F Sequence	R Sequence
β-actin	AGAGCTACGAGCTGCCTGAC	GCAAGACTCCATACCGAGGA
CPT1	ATGAGGAATGCCCTCAAGTG	GCTTCCTGCCAGAGAACAAC
CYP1A	CCAACTTACCTCTGCTGGAAGC	GGTGAACGGCAGGAAGGA
G6PD	TGGTGCAGAACCTCATGGTCCTCA	ATCCCGGATGATTCCAAAGTCGTC
HK1	CTGGGACGCTGAAGACCAGA	CGGTGCTGCATACCTCCTTG
HSP90A	TCCAGCAGCTGAAGGAGTTT	TGAGCTTGCAGAGGTTCTCA

Table 4.S2. Water chemistry results for polycyclic aromatic compounds in Lake 260.

ng/L of water	6/18/19	6/22/19	6/26/19	6/27/19	7/11/19
1-Methylnaphthalene	0.00	1.78	2.37	1.82	0.87
2-Methylnaphthalene	0.00	3.27	1.47	1.26	0.00
C2 Naphthalene	0.00	0.11	1.87	0.02	1.06
C3 Naphthalene (Trimethyl)	4.27	0.18	14.25	0.00	13.55
C4 Naphthalene (Tetramethyl)	0.00	5.87	139.89	8.17	38.05
Total 2 rings	**4.27**	**11.22**	**159.86**	**11.26**	**53.52**
1-Methylphenanthrene	0.00	0.30	40.31	10.79	1.17
2-Methylphenanthrene	0.00	0.08	28.79	8.93	0.57
1,7-Dimethylphenanthrene	0.00	0.54	116.33	27.50	1.73
1,8-Dimethylphenanthrene	0.00	0.56	70.77	4.95	0.00
2,6-Dimethylphenanthrene	0.00	2.34	19.41	2.13	0.28
3,6-Dimethylphenanthrene	0.10	1.44	6.30	7.02	0.53
C2 Phenanthrene	0.00	0.00	95.59	20.79	0.60
3-Methylphenanthrene	0.00	0.14	14.39	2.84	0.36
9/4-Methylphenanthrene	0.00	0.44	37.16	11.26	1.43
C3 Phenanthrene	0.00	0.00	364.34	65.20	42.15
C4 Phenanthrene	0.96	1.76	1254.03	25.29	166.79
Total 3 rings	**1.06**	**7.61**	**2047.43**	**186.68**	**215.62**
C1 Chrysene	0.00	0.00	20.14	0.79	5.02
C3 Chrysene	3.65	3.23	64.98	0.62	33.77
Retene	0.00	0.00	402.18	83.82	10.17

C1 Benzo[a]pyrene	0.00	0.96	2.89	0.00	0.00
C1 Dibenzothiophene	5.46	3.75	226.51	86.25	28.27
C1 Fluorene	3.78	158.57	200.50	212.27	287.52
C1 Pyrene	1.29	0.62	85.19	34.44	10.84
C2 Dibenzothiophene	36.12	6.49	877.19	8.62	156.75
C2 Fluorene	0.00	53.14	317.07	116.53	17.96
C3 Dibenzothiophene	445.39	810.16	17.83	314.03	40.09
Dibenzothiophene	0.64	0.00	0.16	0.54	0.00
Total 4 rings	**496.34**	**1036.93**	**2214.65**	**857.91**	**590.40**
Total PAHs	**501.67**	**1055.76**	**4421.94**	**1055.86**	**859.53**

Table 4.S3. Information on lake trout sampled in 2017, 2018, and 2019 sampling from Lake 260.

Year	Sample	Weight (g)	Total Length (cm)	Fork Length (cm)	Condition Index	Sex	Sequenced?
Sep-19	2019-260-01	1159	52.90	47.80	0.78	M	Y (T1)
Sep-19	2019-260-02	910	47.70	43.20	0.84	M	N
Sep-19	2019-260-03	1186	52.50	47.70	0.82	F	N
Sep-19	2019-260-04	1118	50.70	45.90	0.86	F	N
Sep-19	2019-260-05	779	45.50	41.30	0.83	M	Y (T2)
Sep-19	2019-260-06	735	43.80	39.50	0.87	F	Y (T3)
Sep-19	2019-260-07	846	48.10	43.50	0.76	F	Y (T4)
Sep-18	M18-260-01	941	48.00	44.80	0.85	M	Y (R1)
Sep-18	M18-260-02	885	48.10	42.30	0.80	F	N
Sep-18	M18-260-03	879	50.10	45.60	0.70	F	Y (R2)
Sep-18	M18-260-04	551	41.10	37.80	0.79	immature	N
Sep-18	M18-260-05	529	42.10	37.50	0.71	M	Y (R3)
Sep-18	M18-260-06	1101	51.50	47.00	0.81	M	Y (R4)
Sept-17	M17-260-01	567	40.5	36.6	0.85	M	Y (A1)
Sept-17	M17-260-02	362	36.8	33.4	0.72	M	N
Sept-17	M17-260-03	978	50.0	45.5	0.78	F	N
Sept-17	M17-260-04	378	36.2	32.4	0.79	?	Y (A2)
Sept-17	M17-260-05	877	47.9	43.3	0.79	M	N
Sept-17	M17-260-06	648	42.6	38.4	0.84	M	Y (A3)
Sept-17	M17-260-07	700	44.1	39.4	0.82	M	Y (A4)

Table 4.S4. Results from 1 x 75 bp single-end sequencing and bioinformatics analysis.

Sample	Read Count
T1	52,481,921
T2	65,117,353
T3	45,903,972
T4	74,522,170
R1	83,414,656
R2	60,264,337
R3	78,306,002
R4	70,278,578
A1	19,840,892
A2	19,931,020
A3	24,288,841
A4	22,146,500
TOTAL	616,496,242
AVERAGE	51,374,687

Table 4.S5. Gene ontology biological processes identified among 2017 and 2018 baseline lake trout data.

Term	Count	Genes
GO:0006412~translation	23	RPL17, RPSA, RPL36A, RPL14, RPL27A, RPL24, RPL38, RPS2, RPS6, RPS5, RPS8, RPS27, RPL32, RPL13A, RPS14, RPL3L, SLC25A1, RPL5, RPL12, RPL7A, RPS20, RPS21, RPS24
GO:0000028~ribosomal small subunit assembly	4	RPSA, RPS27, RPS10, RPS5
GO:0001701~in utero embryonic development	11	TAPT1, APOB, MYO18B, CHD7, TANC2, PTPRR, ETNK2, MYH9, GLI2, RBBP6, YBX1
GO:0098609~cell-cell adhesion	7	F11R, DBNL, VAPA, RPL24, RPL7A, RPS2, TES
GO:0045860~positive regulation of protein kinase activity	5	LAT, SNX9, CCL21, RPLP1, CD4
GO:0000027~ribosomal large subunit assembly	4	RPL3L, RPL5, RPL24, RPL12
GO:0031532~actin cytoskeleton reorganization	5	PARVG, TNIK, MINK1, MYH9, CXADR
GO:0008015~blood circulation	3	CHD7, F5, STAT1
GO:0006351~transcription, DNA-templated	24	HMGB2, IL16, EPAS1, CEBPD, SCAI, RORB, NFYB, NR3C1, TEAD3, NLRP3, STAT1, YBX1, GTF2H2, SRY, MURC, FAM120B, ASCC3, PNRC2, JUN, ACTR8, VPS36, SMARCA4, PEG3
GO:0045087~innate immune response	12	SERINC3, HMGB2, CLEC4E, ATG12, TRIM14, MSRB1, TRIM25, NLRP3, MX2, TRIM11, MATK, B2M
GO:0002181~cytoplasmic translation	4	RPL31, RPLP0, RPL9, RPLP1
GO:0030154~cell differentiation	12	MURC, SRY, PBXIP1, RXFP1, FAM120B, NME1, PRKCH, PRRC2A, PRRC2B, AGR2, MATK
GO:0043547~positive regulation of GTPase activity	9	ARHGAP21, F11R, SNX9, LAMTOR4, PSD, ITGA6, CCL21, GNAS, TBC1D2
GO:0090004~positive regulation of establishment of protein localization to plasma membrane	4	PLS1, ITGA3, AGR2, DLG1
GO:0072659~protein localization to plasma membrane	5	EPB41L3, GPR158, TNIK, GPR179, DLG1
GO:0009142~nucleoside triphosphate biosynthetic process	3	NME3, NME1, SUCLG1
GO:0000226~microtubule cytoskeleton organization	5	NEFH, DOCK7, MAP7D1, MAP7D2, GAPDH
GO:0032088~negative regulation of NF-kappaB transcription factor activity	5	NLRC3, CMKLR1, NLRP12, TNFAIP3, NLRP3
GO:0009887~organ morphogenesis	4	VEGFC, NEK8, PALB2, PHLDA2
GO:0043124~negative regulation of I-kappaB kinase/NF-kappaB signaling	4	NLRC3, NLRP12, TNFAIP3, STAT1
GO:0000461~endonucleolytic cleavage to generate mature 3'-end of SSU-rRNA from (SSU-rRNA, 5.8S rRNA, LSU-rRNA)	2	RPSA, RPS21

GO:0016567~protein ubiquitination	9	SOCS3, RNF128, FBXO2, SKP1, TNFAIP3, KLHL3, KLHL33, BARD1, TRIM11
GO:0070681~glutaminyl-tRNAGln biosynthesis via transamidation	2	GATB, GATC
GO:0007613~memory	4	GIP, TH, ITGA3, ITPR3
GO:0017148~negative regulation of translation	4	EIF4A3, RPL13A, GAPDH, SAMD4B
GO:0090023~positive regulation of neutrophil chemotaxis	3	CCL21, DAPK2, CD74
GO:0009791~post-embryonic development	5	TAPT1, APOB, ETNK2, PRDM1, SERP1
GO:1990266~neutrophil migration	2	UMOD, DAPK2
GO:0007399~nervous system development	5	FOS, APOB, NME1, SMARCA4, DLG1
GO:0031032~actomyosin structure organization	3	EPB41L3, F11R, MYH9
GO:0043484~regulation of RNA splicing	3	ESRP1, SNRNP70, AHNAK

Table 4.S6. Gene ontology molecular functions identified among 2017 and 2018 baseline lake trout data.

Term	Count	Genes
GO:0003735~structural constituent of ribosome	27	RPL17, RPL36A, RPL14, RPL27A, RPL38, RPS2, RPS27, RPL32, RPL31, RPLP0, RPL9, RPLP1, SLC25A1, RPL5, RPL12, RPS20, RPS21, RPS24, RPSA, RPL24, RPS6, RPS5, RPS8, RPL13A, RPS14, RPL3L, RPS10
GO:0044822~poly(A) RNA binding	47	CAST, HMGB2, RPL14, FKBP3, TCOF1, EIF5, PRRC2A, PRRC2B, CANX, YBX1, GOT2, RPS27, TCERG1, BUD13, RPL32, RPLP0, SRRM1, ZNF106, RPL12, RPL7A, RPS20, AHNAK, TES, HNRNPAB, RPS24, ZC3H13, SSRP1, SUCLG1, LGALS1, YTHDC1, RPL24, TRIM25, RPS6, MYH9, RBBP6, RPS8, NOP14, SYNE1, SRSF4, ASCC3, NME1, TBCA, EIF4A2, JUN, EIF4A1, ANXA11, SUPT6H
GO:0003729~mRNA binding	9	EIF4A3, RPL13A, ESRP1, CPSF6, SNRNP70, RPS2, RPS5, RBM25, SAMD4B
GO:0098641~cadherin binding involved in cell-cell adhesion	7	F11R, DBNL, VAPA, RPL24, RPL7A, RPS2, TES
GO:0008134~transcription factor binding	7	FOS, SRY, HMGB2, MDFIC, JUN, NLRP3, TRIM11
GO:0003779~actin binding	7	LRRC10, DNASE1, MARCKSL1, MSRB1, KLHL3, KLHL33, SYNPO2L
GO:0001948~glycoprotein binding	5	FOXRED2, FBXO2, ITGA3, CD4, B2M
GO:0043120~tumor necrosis factor binding	2	TNFRSF1A, A2M
GO:0050567~glutaminyl-tRNA synthase (glutamine-hydrolyzing) activity	2	GATB, GATC
GO:0005246~calcium channel regulator activity	3	GRM3, STIM1, CACNA2D4
GO:0035255~ionotropic glutamate receptor binding	2	GNAS, DLG1

Table 4.S7. KEGG pathways as well as associated genes with each pathway in dilbit-exposed lake trout.

Term	Genes
cfa03010:Ribosome	RPL14, RPS3A, RPLP0, RPL9, RPS14, RPL3, RPL5, RPS20, RPL12, RPS6, RPS2, RPL29, RPS7
cfa04530:Tight junction	CLDN8, PARD6B, TJP1, OCLN, ACTN4, CLDN4, CGN, MYH11, TJP3, MYH9
cfa00220:Arginine biosynthesis	GLUD1, ARG2, NOS2, CPS1, GPT2
cfa04915:Estrogen signaling pathway	HSP90AB1, ADCY9, GNAQ, FKBP5, ADCY5, HBEGF, PRKCD, HSPA8, ITPR2
cfa00250:Alanine, aspartate and glutamate metabolism	GFPT1, GLUD1, CAD, CPS1, GPT2
cfa04144:Endocytosis	PARD6B, CLTA, LDLR, KIF5C, PSD4, CAPZB, RAB11A, NEDD4L, GRK5, RAB11FIP1, VPS36, HSPA8, ARAP1
cfa04612:Antigen processing and presentation	HSP90AB1, PDIA3, IFI30, HSPA8, B2M
cfa05205:Proteoglycans in cancer	CCND1, EZR, ANK3, ERBB3, TIAM1, HBEGF, RDX, RPS6, SDC4, ITPR2
cfa05206:MicroRNAs in cancer	CCND1, EZR, ERBB3, ST14, CDK6, RDX, IKBKB, ATM
cfa04062:Chemokine signaling pathway	DOCK2, CCL3, ADCY9, TIAM1, ADCY5, PREX1, GRK5, IKBKB, CCL28
cfa01200:Carbon metabolism	G6PD, GLUD1, HK1, CPS1, GPT2, PC, ENO1
cfa05212:Pancreatic cancer	CCND1, JAK1, CDK6, IKBKB, RALGDS
cfa04115:p53 signaling pathway	CCND1, RRM2, CDK6, CCNG2, ATM

Table 4.S8. All GO Biological Processes with genes associated with each pathway in dilbit-exposed lake trout.

Term	Genes
GO:0035023~regulation of Rho protein signal transduction	TIAM1, PREX1, TRIO, PLEKHG4B, ARHGEF15, EPS8L2, MCF2L, FGD3, EPS8L1, DNMBP
GO:0008360~regulation of cell shape	CSNK1A1, SYNE3, BRWD3, CCL3, CORO1A, EZR, PLXNB1, RDX, CDC42EP4, MYH9, ARAP1
GO:0006412~translation	RPL14, RPS3A, SLC25A5, RRBP1, RPS14, RPL3, RPL5, EEF2, RPS20, RPL12, RPS6, RPS2, RPS7
GO:0030216~keratinocyte differentiation	EVPL, ST14, TGM1, YAP1, SCEL, ADAM9
GO:0030335~positive regulation of cell migration	SPAG9, CCL3, CORO1A, SYNE2, SEMA4G, ACTN4, SEMA6D, F2RL1, RDX, GRB7
GO:1902966~positive regulation of protein localization to early endosome	EZR, SORL1, RDX
GO:0090316~positive regulation of intracellular protein transport	ICE1, PCNT, KIF20B, PCM1
GO:0061436~establishment of skin barrier	ALOXE3, CLDN4, GRHL3, ABCA12
GO:0035556~intracellular signal transduction	ADCY5, PREX1, WNK1, MKNK2, STK17A, PRKCD, MCF2L, DNMBP, ADCY9, SNRK, TIAM1, MYZAP, JAK1, PLCD1, CIT, MELK
GO:0000027~ribosomal large subunit assembly	RPL3, RPL5, RPL12, MDN1
GO:0000050~urea cycle	ARG2, CAD, CPS1
GO:0045909~positive regulation of vasodilation	F2RL1, NOS2, CPS1
GO:0090286~cytoskeletal anchoring at nuclear membrane	SYNE3, SYNE1, SYNE2
GO:0031532~actin cytoskeleton reorganization	TNIK, EZR, SIPA1L1, CXADR, MYH9
GO:0007010~cytoskeleton organization	ABLIM1, BRWD3, CCL3, DOCK1, SVIL, KRT13
GO:0046777~protein autophosphorylation	TNIK, ULK2, STK10, MKNK2, GRK5, PIM2, DDR2, MELK
GO:0006413~translational initiation	EIF4A2, EIF4A1, LARP1
GO:0030033~microvillus assembly	TNIK, EZR, RDX
GO:0007264~small GTPase mediated signal transduction	DOCK2, RAB44, DOCK1, RAB11A, RHOBTB1, DOCK8, DOCK10, LRRK1, RALGDS, RGL1, BCAR3
GO:0001570~vasculogenesis	ZFP36L1, SGPL1, MYO1E, YAP1, JUNB
GO:0010761~fibroblast migration	ZFAND5, SGPL1, SYNE2

GO:0009791~post-embryonic development	SGPL1, GNAQ, KMT2A, PRDM1, CELA1, KDM5B
GO:0007076~mitotic chromosome condensation	NCAPG, SMC2, NCAPD2
GO:0000226~microtubule cytoskeleton organization	PCNT, CUL9, MAP2, MAP7D1, TACC1
GO:0061028~establishment of endothelial barrier	EZR, F2RL1, RDX
GO:0010628~positive regulation of gene expression	CCL3, EZR, LDLR, ERBB3, CDK6, RDX, PRDM1, KDM5B
GO:0042127~regulation of cell proliferation	FRK, ERBB3, JAK1, PLCD1, NOS2, CELA1, JUNB, BTK
GO:0043407~negative regulation of MAP kinase activity	HMGCR, SORL1, NF1, PRKCD
GO:0090002~establishment of protein localization to plasma membrane	EZR, RDX, IKBKB, TMEM150A
GO:0051295~establishment of meiotic spindle localization	SPIRE1, MYH9
GO:0071709~membrane assembly	ANK3, SPTBN1
GO:0032796~uropod organization	CORO1A, MYH9
GO:1902115~regulation of organelle assembly	EZR, RDX
GO:0051490~negative regulation of filopodium assembly	CAPZB, PRKCD
GO:0007189~adenylate cyclase-activating G-protein coupled receptor signaling pathway	ADCY9, GNAQ, GHRH, ADCY5
GO:0002244~hematopoietic progenitor cell differentiation	DOCK1, PTPRZ1, ANLN, EEF2, TOP2A
GO:0045444~fat cell differentiation	CCND1, ALOXE3, GRK5, SOX8, KLF4
GO:0070830~bicellular tight junction assembly	TJP1, OCLN, ACTN4
GO:0031175~neuron projection development	MAP2, RAB11A, GDPD5, HERC1, CAPZB
GO:0006509~membrane protein ectodomain proteolysis	SPPL2A, MYH9, ADAM9
GO:0006364~rRNA processing	RPL5, RPS6, MDN1, RPS7
GO:0043525~positive regulation of neuron apoptotic process	CCL3, NF1, ATM
GO:0010629~negative regulation of gene expression	CCL3, LDLR, NOS2, SFMBT2, PC
GO:0033077~T cell differentiation in thymus	ZFP36L1, CDK6, B2M
GO:0045746~negative regulation of Notch signaling pathway	SLC35C1, CHAC1, GDPD5
GO:0006909~phagocytosis	CSNK1A1, LEPR, ANXA11
GO:0000281~mitotic cytokinesis	ANK3, SPTBN1, ANLN
GO:0016572~histone phosphorylation	PRKCD, ATM
GO:0035166~post-embryonic hemopoiesis	MYO1E, KLF4
GO:0010032~meiotic chromosome condensation	SMC2, NCAPD2
GO:0001768~establishment of T cell polarity	DOCK2, MYH9
GO:0042159~lipoprotein catabolic process	LDLR, ATM
GO:0030036~actin cytoskeleton organization	DOCK2, CORO1A, WASF2, NF1, CAPZB

Table 4.S9. All GO Molecular Functions with genes associated with each pathway in dilbit-exposed lake trout.

Term	Genes
GO:0005524~ATP binding	HSP90AB1, ADCY5, CAD, DDR2, BTK, DDX17, NLRC3, ATP8B1, TOP2A, MDN1, TNIK, KIF5C, WNK1, CDK6, PIM2, MYH9, MCM3, PRKCD, NLRP1, MAP4K5, EIF4A2, EIF4A1, ERN1, MAP3K14, LRRK1, MELK, FRK, ERBB3, STK10, MKNK2, HK1, STK17A, CDC34, DNAH6, CHD9, UBE2D2, SNRK, HSPA8, RUNX3, MYO5B, ABCA12, CSNK1A1, MSH6, TAOK1, MYO1E, TRIO, CENPE, LARS2, CPS1, SMC2, ATM, ULK2, MYH11, KIF20B, JAK1, CHTF18, GRK5, MYO19, CIT, IKBKB, PC
GO:0044822~poly(A) RNA binding	CAST, HSP90AB1, HELZ2, U2SURP, RDX, YBX1, EZR, SPATS2, RPS3A, SAFB, RPL5, NQO1, CDC42EP4, TNRC6A, TOP2A, HSPA8, NSUN5, ENO1, PLEC, RBMS1, MKI67, ACTN4, RRBP1, SLC25A5, EEF2, SPEN, MYH9, NCL, RPS7, CORO1A, SYNE1, LRP1, EIF4A2, ANXA11, EIF4A1, SPTBN1
GO:0005089~Rho guanyl-nucleotide exchange factor activity	TIAM1, PREX1, TRIO, PLEKHG4B, ARHGEF15, MCF2L, FGD3, DNMBP
GO:0003774~motor activity	CGNL1, CGN, MYO1E, MYH11, MYO19, MYO5B
GO:0030676~Rac guanyl-nucleotide exchange factor activity	DOCK2, TIAM1, EPS8L2, EPS8L1
GO:0003735~structural constituent of ribosome	RPL14, RPS3A, SLC25A5, RPLP0, RPL9, RPS14, RPL3, RPL5, RPS20, RPL12, RPS6, RPS2, RPS7
GO:0008429~phosphatidylethanolamine binding	ANXA11, NF1, ESYT2
GO:0005516~calmodulin binding	TJP1, MKNK2, NOS2, MYH9, ASPM
GO:0005536~glucose binding	G6PD, SLC2A3, HK1
GO:0004674~protein serine/threonine kinase activity	CSNK1A1, SNRK, ULK2, ERN1, WNK1, TRIO, STK17A, PIM2, CIT, PRKCD, MELK, ATM
GO:0004715~non-membrane spanning protein tyrosine kinase activity	FRK, JAK1, PRKCD, MELK, BTK
GO:0005096~GTPase activator activity	DOCK2, DOCK1, RABGAP1, GNAQ, SIPA1L1, NF1, TBC1D5, CDC42EP4, AXIN2, ARAP1
GO:0005543~phospholipid binding	PREX1, WDFY4, PSD4, SPTBN1, NBEAL1
GO:0035091~phosphatidylinositol binding	HIP1R, MYO1E, ESYT2, GRB7, MCF2L, ITPR2
GO:0005085~guanyl-nucleotide exchange factor activity	DOCK1, DOCK8, DOCK10, RALGDS, BCAR3
GO:0005198~structural molecule activity	CLDN8, CLTA, EVPL, CLDN4, KRT42,

	CROCC, KRT13, MAP7D1
GO:0004070~aspartate carbamoyltransferase activity	CAD, CPS1
GO:0004088~carbamoyl-phosphate synthase (glutamine-hydrolyzing) activity	CAD, CPS1
GO:0004151~dihydroorotase activity	CAD, CPS1
GO:0004087~carbamoyl-phosphate synthase (ammonia) activity	CAD, CPS1
GO:0004702~receptor signaling protein serine/threonine kinase activity	MAP4K5, TNIK, TAOK1, STK10, MAP3K14
GO:0043531~ADP binding	MSH6, ERN1, MYH9
GO:0004198~calcium-dependent cysteine-type endopeptidase activity	CAPN5, CAPN8, CAPN9
GO:0004672~protein kinase activity	CCL3, CCND1, SNRK, ERBB3, ERN1, STK17A, LRRK1
GO:0016887~ATPase activity	MSH6, KIF20B, MYH9, MDN1, RNF213, DNAH6
GO:0001882~nucleoside binding	ACTN4, PNP

Conclusions

The general aims of the research presented were to assess the effects of both environmental variables and environmental contaminants on wild fish populations through use of transcriptomic tools. Research was carried out in a marine and a freshwater ecosystem that have both been monitored extensively for biotic and abiotic components. By considering long-term environmental data, the impacts of environmental variables and contaminants to fish populations were better discerned.

First, while population declines in flatfish have been observed at the OCSD outfall, the stressors driving declines had not yet been identified. It was first suggested that estrogenic activity was involved in population declines due to previous research identifying presence of EDCs in sediments at the OCSD outfall, including E_2, nonylphenol, alkylphenol ethoxylates, triclosan, and various pharmaceutical and personal care products.[1,2] Moreover, previous studies identified induction of vitellogenin and increases in E_2 in male flatfish in the area.[3,4] However, molecular- through population-level metrics measured in the present study did not identify estrogenic activity within Pacific sanddab at the OCSD outfall. More specifically, hormone levels, vitellogenin levels, organ health metrics, and population sex ratios did not provide evidence of impairment in Pacific sanddab due to estrogenic activity. While previous studies identified estrogenic activity in related species, it is possible that the lack of effect in Pacific sanddab was due to species differences such as variation in movement and trophic status, species-specific receptor interactions, differential processing and turnover of contaminants, and others. More recently, acoustic telemetry was used to characterize

movement patterns of demersal flatfish at the OCSD outfall which showed that most species, including Pacific sanddab, spent less than 10% of the study duration at the outfall site.[5] Thus, the duration of exposure to contaminants within the outfall sediments may not be adequate enough to induce biological effects.

Rather than being linked to contaminants at the OCSD outfall, statistical analysis of long-term environmental data indicated that Pacific sanddab population abundances were instead correlated to ocean temperatures as well as the Pacific Decadal Oscillation index and the Multivariate ENSO Index. It is possible that warmer ocean temperatures resulted in reduced fitness and increased mortality, leading to population declines. However, it is more likely that increases in temperature resulted in the migration of Pacific sanddab to colder, deeper waters where they are not accounted for during OCSD population sampling. Thus, further research will be needed to discern the effects of warming ocean temperatures on fish assemblages in the Southern California Bight and other coastal regions. An effective method to confirm relocation of Pacific sanddab and other fish species to deeper waters is through use of acoustic telemetry. Moreover, targeted qPCR or RNA sequencing could be used to identify any potential molecular changes associated with heat stress. Overall, results of the study indicate that environmental variables have direct implications on ecosystem health and should be considering when assessing observed perturbations.

In addition to environmental variables, it is likely that biannual sampling of fish populations at the OCSD may have contributed to population declines. Thus, the development of a nonlethal sampling method to monitor effects of environmental

variables and contaminants was prompted. As previous research indicated potential for mRNA-based analysis of epidermal mucus,[6,7] the analysis of epidermal mucus through transcriptomics was assessed for its potential as a nonlethal, toxicogenomic assessment tool.

First, transcriptomic analysis of epidermal mucus from four lake trout populations was used to identify gene expression changes brought about by differences in environmental variables among lakes. The study was conducted at the Experimental Lakes Area in Canada as the lakes in the area have extensive long-term monitoring data on biotic and environmental variables. Results of RNA sequencing indicated that transcriptomic analysis of mucus was able to discern unique transcriptomic profiles among lake trout populations residing in different lakes. Moreover, a mixed linear model indicated that certain environmental variables accounted for portions of transcriptomic variability among lake trout populations, and included alkalinity, dissolved oxygen, and productivity. However, about 32% of transcriptomic variance was not accounted for by the mixed linear model, suggesting epigenetics, presence of pathogens, and other variables may have also prompted transcriptomic differences among populations. Interestingly, the two lake trout populations that had the most divergent transcriptomic profiles from all other populations resided in lakes that were used for whole-lake experiments with contaminants in the past. Thus, it is possible that the clear transcriptomic differences in these populations may be a result of genomic changes brought about by past stressor exposure. Overall, results of the study indicated that RNA sequencing of epidermal mucus is a viable tool to study transcriptomic differences among

geographically-distinct fish populations without the use of lethal sampling. For example, analysis of mucus could be useful for comparative transcriptomic studies interested in identifying mechanisms of adaptation among populations residing in different environments, especially in endangered species.

Further research is needed to better account for the effects of additional biotic and abiotic variables on transcriptomic responses observed among the four lake trout populations. First, given the dysregulation of immune-related genes, it would be beneficial to survey the lakes used in the study for presence of parasites or skin lesions. Moreover, characterizing the presence of bacteria or viruses would provide further insight on the molecular immune responses seen. Although viral transcripts were observed to be expressed in the present study, using a more adequate analysis targeted towards the microbiome would yield more robust results. In order to assess microbial communities, 16S rRNA sequencing could be performed on epidermal mucus collected from the four lake trout populations which would allow for identification, classification, and quantitation of microbial communities. Through 16S sequencing, the use of mucus could potentially be expanded to nonlethally monitor presence of harmful bacteria or viruses in fish. Development of such a tool would be beneficial for aquaculture applications as well as monitoring health of wild populations.

The potential for epigenetic modifications in lake trout populations that were subject to previous whole-lake stressor exposure also warrants additional research. Exposure to stress may potentially result in epigenomic imprinting, which has been shown to be regulated by DNA methylation (among other mechanisms).[8] Thus, future

studies could use high-throughput technologies to measure DNA methylation profiles (such as bisulfite-conversion-based sequencing) throughout the genome. Moreover, differential methylation analysis among lake trout from a stressor-exposed lake and lake trout from a reference lake could identify differentially methylated loci/regions (DML/DMR). Further downstream functional or enrichment analysis of genes overlapping with the DML/DMR would provide insight on the biological significance of epigenetic changes. Overall, the proposed epigenetic analysis could greatly further our understanding of the long-lasting effects contaminants may have on populations.

In addition to evaluating environmental variables on biota populations, the transcriptomic analysis of epidermal mucus for field-based ecotoxicology studies was also assessed. Spills of the petroleum derivative, dilbit were conducted within enclosures on a lake at the Experimental Lakes Area; although most of the dilbit was contained in the enclosures, low levels of dilbit entered the lake leading to potential exposure of lake trout. Concentrations reached a maximum of 4.4 μg/L ΣPAH, but generally remained below 1 μg/L ΣPAH. In order to assess potential effects of dilbit constituents in the lake, epidermal mucus was collected and sequenced from lake trout before and after dilbit treatments. First, transcriptomic analysis of mucus was able to discern unique transcriptional patterns among non-exposed and exposed individuals. Moreover, differential gene expression analysis identified dysregulation of genes involved in intermediary metabolism. More specifically, upregulation of gluconeogenic transcripts and downregulation of glycolytic transcripts was observed, indicative of stress-induced metabolic changes. Therefore, the gene expression changes identified in the present study

support previous studies which identified shifts in energy metabolism in fish exposed to dilbit.[9,10] Aside from genes involved in energy metabolism, there was trend of *cyp1a3* upregulation, a well-known biomarker of PAH exposure, which suggests direct molecular changes in response to dilbit.

Overall, transcriptomic analysis of mucus was shown to be a sensitive exposure monitoring tool, being able to identify molecular changes induced by dilbit even at relatively low environmental concentrations. However, further research will be needed before transcriptomic analysis of mucus can be used to monitor the magnitude and geographic extent of effects associated with oil spills. Most importantly, the time required to see transcriptomic changes within the mucus following contaminant exposure will need to be characterized. In order to address this gap in knowledge, future time-course experiments with oil should be considered. For example, mucus samples can be collected at multiple time points during as well as after oil exposure, which will generate a better understanding of when molecular responses began within mucus and how long lasting they are. By quantifying the temporal trends of gene expression in mucus, the window of molecular responses following oil exposure will be better understood, increasing the reliability of mucus as an oil exposure assessment tool.

Another limitation is that transcriptomic patterns within the mucus have yet to be compared to actively metabolizing tissues commonly used in gene expression studies. Thus, future studies will need to compare transcriptional responses in the mucus to that of tissues commonly analyzed for molecular impairment following oil exposure, including liver, muscle, and heart. These studies will need to compare differences in both the

profile of genes that are altered as well as the magnitude of dysregulation of select genes such as *cyp1a*. By understanding how expression in mucus compares relative to expression in well-characterized tissues, the potential physiological impacts of gene expression detected in mucus can be better understood. With further research, transcriptomic analysis will allow for catch-and-release, nonlethal sampling of fish populations for exposure monitoring following oil spills or other contaminant exposure.

Aside from development of mucus as a nonlethal exposure assessment tool, further research is needed to quantify potential higher order effects that may result from transcriptomic changes observed in lake trout following dilbit exposure. Currently, a majority of research on dilbit toxicity in fish has focused on early life stage fish, with little to no focus on potential impairments in adult fish. However, in the present study, transcriptomic responses suggested alteration in energetics in adult lake trout, which may have effects at higher levels of biological organization. Thus, it could be fruitful to consider additional molecular, individual, and population level endpoints during future dilbit experiments at the Experimental Lakes Area. For example, stress-induced energetic changes were suggested by transcriptomic responses in dilbit-exposed lake trout; in order to confirm these responses, blood samples could be nonlethally collected from individuals and analyzed for cortisol levels. Moreover, long-term assessment of condition index before and after dilbit additions could provide insight on potential changes in growth as a result of dilbit exposure. In order to assess the impacts of dilbit on reproductive and recruitment success, long term population sampling data before and after dilbit additions could be used to create age structure diagrams. Overall, the

consideration of higher level responses would provide a more complete understanding of how dilbit spills may impact adult freshwater fish and subsequent effects at the population level.

References

(1) Schlenk, D.; Sapozhnikova, Y.; Irwin, M. A.; Xie, L.; Hwang, W.; Reddy, S.; Brownawell, B. J.; Armstrong, J.; Kelly, M.; Montagne, D. E.; et al. In Vivo Bioassay-Guided Fractionation of Marine Sediment Extracts From the Southern California Bight, Usa, for Estrogenic Activity. *Environ. Toxicol. Chem.* **2005**, *24* (11), 2820. https://doi.org/10.1897/05-116R.1.

(2) Maruya, K. A.; Vidal-Dorsch, D. E.; Bay, S. M.; Kwon, J. W.; Xia, K.; Armbrust, K. L. Organic Contaminants of Emerging Concern in Sediments and Flatfish Collected near Outfalls Discharging Treated Wastewater Effluent to the Southern California Bight. *Environ. Toxicol. Chem.* **2012**, *31* (12), 2683–2688. https://doi.org/10.1002/etc.2003.

(3) Ann Rempel, M.; Reyes, J.; Steinert, S.; Hwang, W.; Armstrong, J.; Sakamoto, K.; Kelley, K.; Schlenk, D. Evaluation of Relationships between Reproductive Metrics, Gender and Vitellogenin Expression in Demersal Flatfish Collected near the Municipal Wastewater Outfall of Orange County, California, USA. *Aquat. Toxicol.* **2006**, *77* (3), 241–249. https://doi.org/10.1016/j.aquatox.2005.12.007.

(4) Forsgren, K. L.; Bay, S. M.; Vidal-Dorsch, D. E.; Deng, X.; Lu, G.; Armstrong, J.; Gully, J. R.; Schlenk, D. Annual and Seasonal Evaluation of Reproductive Status in Hornyhead Turbot at Municipal Wastewater Outfalls in the Southern California Bight. *Environ. Toxicol. Chem.* **2012**, *31* (12), 2701–2710. https://doi.org/10.1002/etc.2006.

(5) Burns, E. S.; Armstrong, J.; Tang, D.; Sakamoto, K.; Lowe, C. G. The Residency, Movement Patterns and Habitat Association of Several Demersal Fish Species to the Orange County Sanitation District Wastewater Outfall. *Mar. Pollut. Bull.* **2019**, *149*, 110638. https://doi.org/https://doi.org/10.1016/j.marpolbul.2019.110638.

(6) Greer, J. B.; Andrzejczyk, N. E.; Mager, E. M.; Stieglitz, J. D.; Benetti, D.; Grosell, M.; Schlenk, D. Whole-Transcriptome Sequencing of Epidermal Mucus as a Novel Method for Oil Exposure Assessment in Juvenile Mahi-Mahi (Coryphaena Hippurus). *Environ. Sci. Technol. Lett.* **2019**, *6*, 538–544. https://doi.org/10.1021/acs.estlett.9b00479.

(7) Ren, Y.; Zhao, H.; Su, B.; Peatman, E.; Li, C. Expression Profiling Analysis of Immune-Related Genes in Channel Catfish (Ictalurus Punctatus) Skin Mucus Following Flavobacterium Columnare Challenge. *Fish Shellfish Immunol.* **2015**, *46* (2), 537–542. https://doi.org/10.1016/j.fsi.2015.07.021.

(8) Zucchi, F. C. R.; Yao, Y.; Metz, G. A. The Secret Language of Destiny: Stress Imprinting and Transgenerational Origins of Disease. *Front. Genet.* **2012**, *3*, 96. https://doi.org/10.3389/fgene.2012.00096.

(9) Alderman, S. L.; Lin, F.; Gillis, T. E.; Farrell, A. P.; Kennedy, C. J. Developmental and Latent Effects of Diluted Bitumen Exposure on Early Life Stages of Sockeye Salmon (Oncorhynchus Nerka). *Aquat. Toxicol.* **2018**, *202*, 6–15. https://doi.org/10.1016/j.aquatox.2018.06.014.

(10) Avey, S. R.; Kennedy, C. J.; Farrell, A. P.; Gillis, T. E.; Alderman, S. L. Effects of Diluted Bitumen Exposure on Atlantic Salmon Smolts: Molecular and Metabolic Responses in Relation to Swimming Performance. *Aquat. Toxicol.* **2020**, *221* (September 2019), 105423. https://doi.org/10.1016/j.aquatox.2020.105423.

APPENDIX A:
Gene Expression Data from Chapter 2

Table A-1. List of all significant differentially expressed transcripts (FDR adjusted $p \leq 0.05$) ranked by p value in lake trout epidermal mucus among all lake-by-lake comparisons.

Rank	Gene Symbol	Full Name	log2 Fold Change	p-adj
		Lake 223 vs Lake 224		
224 is the base e.g. Positive FC = upregulated in Lake 223 relative to Lake 224				
1	COL14A1	Collagen alpha-1(XIV) chain	4.49	1.09E-24
2	URGCP	Up-regulator of cell proliferation	11.32	4.53E-22
3	Fam111a	Protein FAM111A	5.47	2.76E-21
4	GIMAP8	GTPase IMAP family member 8	10.14	3.93E-17
5	Urgcp	Up-regulator of cell proliferation	4.78	3.68E-16
6	Gvin1	Interferon-induced very large GTPase 1	2.71	1.34E-14
7	pol	Retrovirus-related Pol polyprotein from transposon gypsy	2.70	6.44E-14
8	#N/A	Transposable element Tcb1 transposase	1.94	1.06E-13
9	RNF213	E3 ubiquitin-protein ligase RNF213	8.93	1.54E-12
10	C2orf16	Uncharacterized protein C2orf16	4.54	5.46E-12
11	#N/A	Class I histocompatibility antigen, F10 alpha chain	9.11	1.00E-11
12	GIMAP5	GTPase IMAP family member 5	8.94	1.48E-11
13	GIMAP7	GTPase IMAP family member 7	9.80	2.75E-11
14	RNF213	E3 ubiquitin-protein ligase RNF213	8.74	5.62E-11
15	krt13	Keratin, type I cytoskeletal 13	1.77	9.93E-11
16	H2-K1	H-2 class I histocompatibility antigen, K-B alpha chain	5.06	1.33E-10
17	IFI44	Interferon-induced protein 44	8.53	8.26E-10
18	SPRR3	Small proline-rich protein 3	3.90	1.42E-09
19	Krt15	Keratin, type I cytoskeletal 15	4.49	3.41E-09
20	Nlrp1a	NACHT, LRR and PYD domains-containing protein 1a	2.31	3.79E-09
21	ORF1	RNA-directed RNA polymerase	8.45	3.81E-09
22	#N/A	Intermediate filament protein ON3	1.80	4.46E-09
23	Abi1	Abl interactor 1	4.76	5.52E-09
24	Hspa12a	Heat shock 70 kDa protein 12A	10.28	1.16E-08
25	Eppk1	Epiplakin	-3.32	1.17E-08
26	Art5	Ecto-ADP-ribosyltransferase 5	4.30	1.20E-08
27	tc1a	Transposable element Tc1 transposase	1.81	1.72E-08
28	ATP8A2	Phospholipid-transporting ATPase IB	-2.47	1.78E-08
29	Dusp5	Dual specificity protein phosphatase 5	-7.92	3.28E-08
30	HSP90AA1	Heat shock protein HSP 90-alpha	6.57	4.10E-08
31	YWHAH	14-3-3 protein eta	1.98	6.21E-08
32	ARPC1A	Actin-related protein 2/3 complex subunit 1A	1.90	6.46E-08
33	MDV087	Uncharacterized gene 87 protein	3.55	6.66E-08
34	Nt5c1a	Cytosolic 5'-nucleotidase 1A	1.98	8.21E-08
35	Plec	Plectin	-3.48	1.20E-07
36	IGFBP3	Insulin-like growth factor-binding protein 3	-4.55	1.23E-07
37	NUGGC	Nuclear GTPase SLIP-GC	-4.63	1.52E-07
38	#N/A	Nectin-1	-1.52	1.97E-07
39	tc1a	Transposable element Tc1 transposase	2.21	2.41E-07
40	CLDN4	Claudin-4	2.73	3.42E-07
41	#N/A	Transposable element Tcb1 transposase	2.33	3.79E-07
42	TY3B-I	Transposon Ty3-I Gag-Pol polyprotein	9.42	4.52E-07
43	hsp90a.1	Heat shock protein HSP 90-alpha 1	5.75	4.75E-07
44	#N/A	DLA class I histocompatibility antigen, A9/A9 alpha chain	2.86	5.00E-07
45	mapk14a	Mitogen-activated protein kinase 14A	-3.45	5.30E-07
46	EGR1	Early growth response protein 1	-2.15	6.80E-07

47	GVINP1	Interferon-induced very large GTPase 1	8.01	7.60E-07
48	krt18	Keratin, type I cytoskeletal 18	3.61	9.14E-07
49	SOCS3	Suppressor of cytokine signaling 3	-3.73	1.04E-06
50	ECU02_0740i	Ubiquitin	2.05	1.11E-06
51	MGST3	Microsomal glutathione S-transferase 3	3.50	1.14E-06
52	krt13	Keratin, type I cytoskeletal 13	1.98	1.14E-06
53	pol	Pol polyprotein	-3.58	1.38E-06
54	#N/A	ES1 protein homolog, mitochondrial	2.70	1.42E-06
55	jockey\pol	RNA-directed DNA polymerase from mobile element jockey	2.05	1.44E-06
56	RNF14	E3 ubiquitin-protein ligase RNF14	2.20	1.48E-06
57	TY3B-I	Transposon Ty3-I Gag-Pol polyprotein	8.46	1.60E-06
58	ORF1	Replicase polyprotein	7.76	1.61E-06
59	IGFBP3	Insulin-like growth factor-binding protein 3	-6.39	1.65E-06
60	Cps1	Carbamoyl-phosphate synthase [ammonia], mitochondrial	-3.91	1.85E-06
61	#N/A	Intermediate filament protein ON3	3.29	2.04E-06
62	NPTX1	Neuronal pentraxin-1	8.05	2.38E-06
63	Plec	Plectin	-2.91	2.38E-06
64	hsp90ab1	Heat shock protein HSP 90-beta	4.93	2.55E-06
65	B3GNT2	N-acetyllactosaminide beta-1,3-N-acetylglucosaminyltransferase 2	2.14	2.62E-06
66	gag-pol	Gag-Pol polyprotein	6.98	2.87E-06
67	URGCP	Up-regulator of cell proliferation	7.43	2.87E-06
68	#N/A	ERV-BabFcenv provirus ancestral Env polyprotein	7.55	3.16E-06
69	#N/A	Transposable element Tcb1 transposase	2.36	3.46E-06
70	Cldn4	Claudin-4	2.86	3.64E-06
71	Tmem238	Transmembrane protein 238	2.42	3.71E-06
72	Urgcp	Up-regulator of cell proliferation	3.52	4.10E-06
73	krt13	Keratin, type I cytoskeletal 13	1.43	4.39E-06
74	HEPACAM2	HEPACAM family member 2	7.55	4.40E-06
75	APOC1	Apolipoprotein C-I	7.94	4.49E-06
76	HSP90AB1	Heat shock protein HSP 90-beta	5.74	4.49E-06
77	PLEKHA5	Pleckstrin homology domain-containing family A member 5	-1.64	4.53E-06
78	vUbi	Ubiquitin-like protein	2.36	4.88E-06
79	#N/A	Transposable element Tcb2 transposase	2.37	5.28E-06
80	Mslnl	Mesothelin-like protein	2.28	5.69E-06
81	Arf2	ADP-ribosylation factor 2	2.27	6.45E-06
82	#N/A	Transposable element Tcb1 transposase	2.32	6.51E-06
83	GIMAP5	GTPase IMAP family member 5	5.00	6.59E-06
84	Gimap4	GTPase IMAP family member 4	-7.76	6.68E-06
85	Trp53inp1	Tumor protein p53-inducible nuclear protein 1	1.45	6.96E-06
86	Foxd1	Forkhead box protein D1	8.04	7.29E-06
87	fut11	Alpha-(1,3)-fucosyltransferase 11	2.32	7.35E-06
88	Endod1	Endonuclease domain-containing 1 protein	-6.60	7.47E-06
89	SH2D4A	SH2 domain-containing protein 4A	3.09	7.56E-06
90	#N/A	Peroxiredoxin	3.33	7.70E-06
91	Nme1	Nucleoside diphosphate kinase A	2.25	9.34E-06
92	Tmed9	Transmembrane emp24 domain-containing protein 9	2.22	9.49E-06
93	Nlrp1b	NACHT, LRR and PYD domains-containing protein 1b allele 1 {ECO:0000303|PubMed:16429160}	-4.29	1.04E-05
94	Enah	Protein enabled homolog	2.54	1.11E-05
95	TNIP1	TNFAIP3-interacting protein 1	1.55	1.16E-05
96	aste1	Protein asteroid homolog 1	2.63	1.27E-05
97	SYNE2	Nesprin-2	-1.84	1.29E-05
98	ATP5MC2	ATP synthase F(0) complex subunit C2, mitochondrial	2.16	1.31E-05
99	BTNL9	Butyrophilin-like protein 9	7.37	1.35E-05
100	#N/A	Neoverrucotoxin subunit beta	-5.56	1.62E-05
101	krt13	Keratin, type I cytoskeletal 13	2.61	1.63E-05
102	PRSS27	Serine protease 27	2.91	1.81E-05
103	selenow	Selenoprotein W	2.05	1.85E-05
104	HSPA12A	Heat shock 70 kDa protein 12A	7.10	1.92E-05
105	PEG10	Retrotransposon-derived protein PEG10	8.45	1.95E-05
106	DCTN3	Dynactin subunit 3	2.19	1.98E-05
107	URGCP	Up-regulator of cell proliferation	1.54	2.08E-05
108	FAT2	Protocadherin Fat 2	-2.48	2.08E-05
109	ABCB1	Multidrug resistance protein 1	4.49	2.10E-05
110	Krt8	Keratin, type II cytoskeletal 8	3.23	2.30E-05
111	Clta	Clathrin light chain A	2.15	2.34E-05

112	Amot	Angiomotin	-1.82	2.65E-05
113	Cps1	Carbamoyl-phosphate synthase [ammonia], mitochondrial	-3.58	2.67E-05
114	Gtpbp2	GTP-binding protein 2	3.18	2.73E-05
115	PDE4DIP	Myomegalin	-2.79	2.78E-05
116	UGT2A3	UDP-glucuronosyltransferase 2A3	7.73	2.87E-05
117	mtap	S-methyl-5'-thioadenosine phosphorylase {ECO:0000255|HAMAP-Rule:MF_03155}	-1.90	2.93E-05
118	#N/A	Transposable element Tcb2 transposase	1.74	2.99E-05
119	#N/A	Transposable element Tcb1 transposase	3.10	3.00E-05
120	KRT8	Keratin, type II cytoskeletal 8	1.72	3.03E-05
121	hba4	Hemoglobin subunit alpha-4	6.59	3.22E-05
122	egr1	Early growth response protein 1	-1.89	3.79E-05
123	ATP5F1B	ATP synthase subunit beta, mitochondrial	1.83	3.89E-05
124	#N/A	Histone H1	-1.69	4.88E-05
125	plk1	Serine/threonine-protein kinase PLK1	-3.61	5.05E-05
126	ARHGAP18	Rho GTPase-activating protein 18	1.64	5.25E-05
127	Eci1	Enoyl-CoA delta isomerase 1, mitochondrial	2.52	5.50E-05
128	#N/A	Stonustoxin subunit beta	-1.42	5.60E-05
129	brk1	Probable protein BRICK1	2.52	6.11E-05
130	hsp90a.1	Heat shock protein HSP 90-alpha 1	5.25	6.16E-05
131	CHN2	Beta-chimaerin	-2.29	6.33E-05
132	tcaf	TRPM8 channel-associated factor homolog	2.82	6.89E-05
133	SLC25A5	ADP/ATP translocase 2	2.80	6.89E-05
134	Krt20	Keratin, type I cytoskeletal 20	1.81	6.96E-05
135	Serp1	Stress-associated endoplasmic reticulum protein 1	2.40	7.02E-05
136	junb	Transcription factor jun-B	-1.45	7.74E-05
137	MYH9	Myosin-9	1.24	7.74E-05
138	RNF138	E3 ubiquitin-protein ligase RNF138 {ECO:0000305}	3.39	8.07E-05
139	gag	Nucleic-acid-binding protein from mobile element jockey	-1.95	8.17E-05
140	#N/A	DLA class I histocompatibility antigen, A9/A9 alpha chain	0.98	8.26E-05
141	hbb1	Hemoglobin subunit beta-1	6.75	8.62E-05
142	#N/A	Transposable element Tcb1 transposase	1.68	8.68E-05
143	selenof	15 kDa selenoprotein	1.78	8.80E-05
144	GFPT2	Glutamine--fructose-6-phosphate aminotransferase [isomerizing] 2	1.37	9.26E-05
145	Enc1	Ectoderm-neural cortex protein 1	5.19	9.53E-05
146	#N/A	LisH domain and HEAT repeat-containing protein KIAA1468 homolog	-2.18	0.0001
147	HEXB	Beta-hexosaminidase subunit beta	2.87	0.0001
148	SH2D3A	SH2 domain-containing protein 3A	-2.12	0.0001
149	JUN	Transcription factor AP-1	-1.86	0.0001
150	CD74	HLA class II histocompatibility antigen gamma chain	2.01	0.0001
151	#N/A	Transposable element Tcb1 transposase	-0.80	0.0001
152	rps15	40S ribosomal protein S15	2.45	0.0001
153	Clec4e	C-type lectin domain family 4 member E	3.03	0.0001
154	Higd1a	HIG1 domain family member 1A, mitochondrial	1.97	0.0001
155	GNPAT	Dihydroxyacetone phosphate acyltransferase	-1.83	0.0001
156	Nupr1	Nuclear protein 1 {ECO:0000305}	3.37	0.0001
157	Taldo1	Transaldolase	2.20	0.0001
158	GRB7	Growth factor receptor-bound protein 7	2.02	0.0001
159	araQ	L-arabinose transport system permease protein AraQ	6.65	0.0001
160	KRT7	Keratin, type II cytoskeletal 7	-2.09	0.0001
161	POF1B	Protein POF1B	-5.45	0.0001
162	#N/A	Calmodulin	1.46	0.0001
163	#N/A	ES1 protein homolog, mitochondrial	1.90	0.0001
164	GIMAP8	GTPase IMAP family member 8	8.07	0.0002
165	GRK5	G protein-coupled receptor kinase 5	-1.96	0.0002
166	egr1	Early growth response protein 1	-2.67	0.0002
167	Tmed9	Transmembrane emp24 domain-containing protein 9	1.80	0.0002
168	ARID1B	AT-rich interactive domain-containing protein 1B	-2.42	0.0002
169	HSD17B3	Testosterone 17-beta-dehydrogenase 3	-2.45	0.0002
170	SYNE2	Nesprin-2	-1.75	0.0002
171	Krt17	Keratin, type I cytoskeletal 17	1.58	0.0002
172	rnasekb	Ribonuclease kappa-B	2.12	0.0002
173	TNMD	Tenomodulin	-3.00	0.0002
174	ACTR2	Actin-related protein 2	2.04	0.0002
175	Tnik	Traf2 and NCK-interacting protein kinase	-2.51	0.0002
176	jag1b	Protein jagged-1b	-2.32	0.0002

177	pol	Retrovirus-related Pol polyprotein from transposon 297	7.50	0.0002
178	rhoaa	Rho-related GTP-binding protein RhoA-A {ECO:0000305}	1.15	0.0002
179	tcaf	TRPM8 channel-associated factor homolog	6.49	0.0002
180	STK17A	Serine/threonine-protein kinase 17A	1.83	0.0002
181	eif3h	Eukaryotic translation initiation factor 3 subunit H	2.24	0.0002
182	SYNE2	Nesprin-2	-1.62	0.0002
183	tc1a	Transposable element Tc1 transposase	2.02	0.0002
184	DAAM1	Disheveled-associated activator of morphogenesis 1	3.11	0.0002
185	acer1	Alkaline ceramidase 1	1.83	0.0002
186	amotl2a	Angiomotin-like 2a	1.83	0.0002
187	Flnc	Filamin-C	3.31	0.0003
188	ATP8B1	Phospholipid-transporting ATPase IC	1.44	0.0003
189	Fat2	Protocadherin Fat 2	-5.37	0.0003
190	UBA52	Ubiquitin-60S ribosomal protein L40	2.21	0.0003
191	DOCK1	Dedicator of cytokinesis protein 1	-1.32	0.0003
192	Ppfibp2	Liprin-beta-2	-1.87	0.0003
193	xkr9	XK-related protein 9	4.34	0.0003
194	Vamp8	Vesicle-associated membrane protein 8	2.12	0.0003
195	ERBB3	Receptor tyrosine-protein kinase erbB-3	-2.26	0.0003
196	CACNB1	Voltage-dependent L-type calcium channel subunit beta-1	3.91	0.0003
197	UBE2V1	Ubiquitin-conjugating enzyme E2 variant 1	1.93	0.0003
198	#N/A	Pancreatic alpha-amylase	-2.47	0.0003
199	NOD2	Nucleotide-binding oligomerization domain-containing protein 2	-2.00	0.0003
200	MYL9	Myosin regulatory light polypeptide 9	2.14	0.0003
201	Nlrc3	Protein NLRC3	-1.41	0.0003
202	Slco2b1	Solute carrier organic anion transporter family member 2B1	-2.96	0.0004
203	ARPC1A	Actin-related protein 2/3 complex subunit 1A	2.04	0.0004
204	krt13	Keratin, type I cytoskeletal 13	2.71	0.0004
205	hook1	Protein Hook homolog 1	-1.90	0.0004
206	Rab25	Ras-related protein Rab-25	2.43	0.0004
207	ssr1	Translocon-associated protein subunit alpha	2.41	0.0004
208	ARHGEF12	Rho guanine nucleotide exchange factor 12	-2.56	0.0004
209	hbb4	Hemoglobin subunit beta-4	6.12	0.0004
210	GIMAP7	GTPase IMAP family member 7	4.46	0.0004
211	FLNC	Filamin-C	2.80	0.0004
212	Litaf	Lipopolysaccharide-induced tumor necrosis factor-alpha factor homolog	2.96	0.0004
213	NF1	Neurofibromin	-1.33	0.0004
214	CHD6	Chromodomain-helicase-DNA-binding protein 6	-1.76	0.0004
215	Flnc	Filamin-C	2.70	0.0004
216	hddc3	Guanosine-3',5'-bis(diphosphate) 3'-pyrophosphohydrolase MESH1	2.29	0.0004
217	Chn2	Beta-chimaerin	-2.06	0.0004
218	PLXDC2	Plexin domain-containing protein 2	-2.46	0.0004
219	ier2	Immediate early response gene 2 protein	-2.63	0.0004
220	ARF4	ADP-ribosylation factor 4	1.32	0.0004
221	#N/A	Lipoma HMGIC fusion partner homolog	-1.70	0.0004
222	IFI30	Gamma-interferon-inducible lysosomal thiol reductase	1.42	0.0004
223	blcap	Bladder cancer-associated protein	2.12	0.0005
224	GSTP1	Glutathione S-transferase P	2.98	0.0005
225	ATP5PD	ATP synthase subunit d, mitochondrial	2.33	0.0005
226	ptprf	Receptor-type tyrosine-protein phosphatase F	-1.24	0.0005
227	ATOX1	Copper transport protein ATOX1	2.10	0.0005
228	#N/A	LisH domain and HEAT repeat-containing protein KIAA1468	-2.95	0.0005
229	pgap3	Post-GPI attachment to proteins factor 3	1.85	0.0005
230	SLC25A11	Mitochondrial 2-oxoglutarate/malate carrier protein	2.09	0.0005
231	Celsr1	Cadherin EGF LAG seven-pass G-type receptor 1	-1.37	0.0005
232	AGR3	Anterior gradient protein 3	1.57	0.0005
233	VPS52	Vacuolar protein sorting-associated protein 52 homolog	2.48	0.0005
234	Dgkb	Diacylglycerol kinase beta	-1.76	0.0005
235	sema3d	Semaphorin-3D	-3.20	0.0005
236	TPD52L2	Tumor protein D54	1.19	0.0006
237	RASSF8	Ras association domain-containing protein 8	2.17	0.0006
238	nr4a1	Nuclear receptor subfamily 4 group A member 1	-2.56	0.0006
239	TSTA3	GDP-L-fucose synthase	-5.65	0.0006
240	AIMP2	Aminoacyl tRNA synthase complex-interacting multifunctional protein 2	1.80	0.0006
241	CYTH3	Cytohesin-3	3.06	0.0006
242	SRCAP	Helicase SRCAP	-1.37	0.0006

243	Flnc	Filamin-C	3.01	0.0006
244	TMEM132C	Transmembrane protein 132C	6.71	0.0007
245	eef1b	Elongation factor 1-beta	1.90	0.0007
246	#N/A	Transposable element Tcb2 transposase	1.40	0.0007
247	smdt1	Essential MCU regulator, mitochondrial	1.94	0.0007
248	Sppl2a	Signal peptide peptidase-like 2A {ECO:0000250|UniProtKB:Q8TCT8}	0.89	0.0007
249	CLDN4	Claudin-4	2.46	0.0007
250	CCNI	Cyclin-I	2.05	0.0007
251	psbA2	Photosystem II protein D1 2 {ECO:0000255|HAMAP-Rule:MF_01379}	6.62	0.0007
252	Enc1	Ectoderm-neural cortex protein 1	4.29	0.0007
253	Atp5mc3	ATP synthase F(0) complex subunit C3, mitochondrial	2.28	0.0007
254	FAM43A	Protein FAM43A	1.64	0.0007
255	atf4	Cyclic AMP-dependent transcription factor ATF-4	1.37	0.0007
256	ANK3	Ankyrin-3	-2.09	0.0007
257	Syne2	Nesprin-2	-2.92	0.0007
258	oaz1b	Ornithine decarboxylase antizyme 2	1.80	0.0007
259	Myl6	Myosin light polypeptide 6	1.42	0.0007
260	PTBP1	Polypyrimidine tract-binding protein 1	1.44	0.0007
261	jade1	Protein Jade-1	-2.16	0.0008
262	NUMBL	Numb-like protein	-1.71	0.0008
263	RASSF3	Ras association domain-containing protein 3	1.37	0.0008
264	PIBF1	Progesterone-induced-blocking factor 1	-2.92	0.0008
265	cyp1a3	Cytochrome P450 1A3	3.71	0.0008
266	HIPK1	Homeodomain-interacting protein kinase 1	-1.84	0.0008
267	jag1b	Protein jagged-1b	-2.23	0.0008
268	pdcl3	Phosducin-like protein 3	2.13	0.0008
269	Dnmt3a	DNA (cytosine-5)-methyltransferase 3A	-5.32	0.0008
270	Ppia	Peptidyl-prolyl cis-trans isomerase A	1.71	0.0008
271	mvp	Major vault protein	1.68	0.0009
272	fam20b	Glycosaminoglycan xylosylkinase {ECO:0000250|UniProtKB:O75063}	1.24	0.0009
273	MFAP3L	Microfi brillar-associated protein 3-like	-1.70	0.0009
274	SYNE2	Nesprin-2	-1.61	0.0009
275	PPIP5K1	Inositol hexakisphosphate and diphosphoinositol-pentakisphosphate kinase 1	-2.46	0.0009
276	TPP1	Tripeptidyl-peptidase 1	3.38	0.0010
277	ARPC1A	Actin-related protein 2/3 complex subunit 1A	1.90	0.0010
278	pnrc2	Proline-rich nuclear receptor coactivator 2	1.95	0.0010
279	SLC25A5	ADP/ATP translocase 2	2.52	0.0010
280	RHOU	Rho-related GTP-binding protein RhoU	-1.81	0.0010
281	CLDN3	Claudin-3	2.09	0.0011
282	GMDS	GDP-mannose 4,6 dehydratase	1.37	0.0011
283	psmb9-a	Proteasome subunit beta type-9	1.34	0.0011
284	Snrk	SNF-related serine/threonine-protein kinase	4.81	0.0011
285	CCL13	C-C motif chemokine 13	3.22	0.0011
286	UBE2V1	Ubiquitin-conjugating enzyme E2 variant 1	1.93	0.0011
287	Ptgr1	Prostaglandin reductase 1	2.31	0.0011
288	CCL3	C-C motif chemokine 3	2.86	0.0011
289	HDLBP	Vigilin	1.66	0.0011
290	Fis1	Mitochondrial fission 1 protein	1.85	0.0011
291	Efhd2	EF-hand domain-containing protein D2	1.91	0.0011
292	Mien1	Migration and invasion enhancer 1	1.73	0.0011
293	ARL4A	ADP-ribosylation factor-like protein 4A	2.39	0.0011
294	YBX1	Nuclease-sensitive element-binding protein 1	1.99	0.0011
295	SULT2B1	Sulfotransferase family cytosolic 2B member 1	-2.07	0.0011
296	b2m	Beta-2-microglobulin	1.19	0.0011
297	bsdc1	BSD domain-containing protein 1	1.33	0.0011
298	TRAK2	Trafficking kinesin-binding protein 2	-1.50	0.0012
299	Slc9a5	Sodium/hydrogen exchanger 5	3.78	0.0012
300	Nos2	Nitric oxide synthase, inducible	4.84	0.0012
301	RPL10	60S ribosomal protein L10	2.24	0.0012
302	Tf2-9	Transposon Tf2-9 polyprotein	-2.00	0.0012
303	TRIM58	E3 ubiquitin-protein ligase TRIM58	2.70	0.0012
304	Tnrc18	Trinucleotide repeat-containing gene 18 protein	-1.32	0.0012
305	Eps8l2	Epidermal growth factor receptor kinase substrate 8-like protein 2	2.43	0.0012
306	alcama	CD166 antigen homolog A	1.61	0.0013
307	ptprf	Receptor-type tyrosine-protein phosphatase F	-2.64	0.0013

308	Nudt3	Diphosphoinositol polyphosphate phosphohydrolase 1	1.67	0.0013
309	dennd5b	DENN domain-containing protein 5B	-2.98	0.0013
310	NMES1	Normal mucosa of esophagus-specific gene 1 protein	2.30	0.0013
311	TMEM50A	Transmembrane protein 50A	1.31	0.0013
312	Cpeb2	Cytoplasmic polyadenylation element-binding protein 2	4.11	0.0013
313	#N/A	Transposon TX1 uncharacterized 149 kDa protein	-1.80	0.0013
314	KRT15	Keratin, type I cytoskeletal 15	3.94	0.0013
315	ELP1	Elongator complex protein 1	-1.45	0.0013
316	EIF4EBP2	Eukaryotic translation initiation factor 4E-binding protein 2	2.06	0.0013
317	PFF0380w	Protein PFF0380w	1.28	0.0013
318	cav1	Caveolin-1	1.71	0.0013
319	Tf2-9	Transposon Tf2-9 polyprotein	5.24	0.0013
320	Edrf1	Erythroid differentiation-related factor 1	-1.37	0.0013
321	Pold1	DNA polymerase delta catalytic subunit	-2.47	0.0013
322	ppdpfb	Pancreatic progenitor cell differentiation and proliferation factor B	2.28	0.0014
323	#N/A	RNA-directed RNA polymerase	-7.00	0.0014
324	TPRN	Taperin	2.45	0.0014
325	Pgm5	Phosphoglucomutase-like protein 5	-5.39	0.0014
326	Bcar3	Breast cancer anti-estrogen resistance protein 3	-2.02	0.0014
327	tpr	Nucleoprotein TPR	-1.65	0.0014
328	Trim39	E3 ubiquitin-protein ligase TRIM39	-2.14	0.0014
329	pol	Pol polyprotein	5.48	0.0014
330	Syne2	Nesprin-2	-1.82	0.0014
331	Ap1s3	AP-1 complex subunit sigma-3	1.55	0.0014
332	ARHGEF26	Rho guanine nucleotide exchange factor 26	1.81	0.0015
333	Atp5mf	ATP synthase subunit f, mitochondrial	2.29	0.0015
334	rps3-a	40S ribosomal protein S3-A	2.36	0.0015
335	SDCBP	Syntenin-1	1.61	0.0015
336	#N/A	LisH domain and HEAT repeat-containing protein KIAA1468 homolog	-1.84	0.0015
337	PGBD4	PiggyBac transposable element-derived protein 4	-1.31	0.0016
338	Cisd1	CDGSH iron-sulfur domain-containing protein 1	2.16	0.0016
339	Aak1	AP2-associated protein kinase 1	-4.41	0.0016
340	TRIM16	Tripartite motif-containing protein 16	0.94	0.0016
341	COX5B	Cytochrome c oxidase subunit 5B, mitochondrial	1.65	0.0017
342	tmbim6	Probable Bax inhibitor 1	1.66	0.0017
343	PEG10	Retrotransposon-derived protein PEG10	-1.70	0.0017
344	CASP6	Caspase-6	1.09	0.0017
345	fam162b	Protein FAM162B	1.71	0.0017
346	Tnik	Traf2 and NCK-interacting protein kinase	-2.08	0.0018
347	alpha	Capsid protein alpha	-6.92	0.0018
348	SYNPO	Synaptopodin	2.14	0.0018
349	ada	Adenosine deaminase	-1.29	0.0018
350	srrt	Serrate RNA effector molecule homolog	-1.27	0.0019
351	#N/A	Transposable element Tcb2 transposase	1.62	0.0019
352	Btn1a1	Butyrophilin subfamily 1 member A1	-1.60	0.0019
353	ifna3	Interferon a3 {ECO:0000303|PubMed:25080482}	-2.38	0.0019
354	Tf2-8	Transposon Tf2-8 polyprotein	4.77	0.0019
355	Rpl39	60S ribosomal protein L39	2.26	0.0019
356	CTSB	Cathepsin B	2.31	0.0019
357	slc40a1	Solute carrier family 40 member 1	1.90	0.0020
358	#N/A	Transposable element Tcb1 transposase	-2.41	0.0020
359	pxdn	Peroxidasin	5.61	0.0020
360	Cdc42ep4	Cdc42 effector protein 4	2.31	0.0020
361	#N/A	Salivary plasminogen activator beta	-4.06	0.0021
362	PSAP	Prosaposin	1.61	0.0021
363	tc1a	Transposable element Tc1 transposase	-0.83	0.0021
364	epd	Ependymin	3.34	0.0021
365	#N/A	Cystatin	4.96	0.0021
366	Pol	LINE-1 retrotransposable element ORF2 protein	-2.57	0.0021
367	Stard13	StAR-related lipid transfer protein 13	7.44	0.0021
368	NFE2L2	Nuclear factor erythroid 2-related factor 2	4.61	0.0021
369	Ubl3	Ubiquitin-like protein 3	1.30	0.0022
370	Rab5a	Ras-related protein Rab-5A	1.81	0.0022
371	Me3	NADP-dependent malic enzyme, mitochondrial	5.33	0.0022
372	AHNAK	Neuroblast differentiation-associated protein AHNAK	2.30	0.0023
373	rpl18a	60S ribosomal protein L18a	2.16	0.0023

374	rnf44	RING finger protein 44	-2.28	0.0023
375	Slc17a5	Sialin	1.95	0.0023
376	ARHGAP28	Rho GTPase-activating protein 28	2.09	0.0023
377	gag-pol	Gag-Pol polyprotein	-1.48	0.0024
378	ZDHHC6	Palmitoyltransferase ZDHHC6	1.47	0.0024
379	Ppp1ca	Serine/threonine-protein phosphatase PP1-alpha catalytic subunit	1.58	0.0024
380	psbA2	Photosystem II protein D1 2 {ECO:0000255|HAMAP-Rule:MF_01379}	7.38	0.0024
381	spt5	Transcription elongation factor spt5	-4.77	0.0024
382	TJP1	Tight junction protein ZO-1	1.83	0.0024
383	Kiaa1109	Uncharacterized protein KIAA1109	-1.10	0.0024
384	BCAR3	Breast cancer anti-estrogen resistance protein 3	-2.69	0.0024
385	med17	Mediator of RNA polymerase II transcription subunit 17	1.48	0.0025
386	#N/A	Thymosin beta-12	1.22	0.0025
387	ATP5MC3	ATP synthase F(0) complex subunit C3, mitochondrial	1.86	0.0025
388	EIF5A	Eukaryotic translation initiation factor 5A-1	1.86	0.0025
389	TCN1	Transcobalamin-1	3.19	0.0025
390	SUDS3	Sin3 histone deacetylase corepressor complex component SDS3	-5.00	0.0025
391	#N/A	Transposable element Tcb1 transposase	1.00	0.0025
392	ywhaba	14-3-3 protein beta/alpha-A	1.83	0.0025
393	RTN3	Reticulon-3	1.43	0.0026
394	PDZD2	PDZ domain-containing protein 2	-2.09	0.0026
395	gprc6a	G-protein coupled receptor family C group 6 member A	3.04	0.0026
396	rps10	40S ribosomal protein S10	1.91	0.0026
397	EFNB1	Ephrin-B1	-1.74	0.0026
398	RNF14	E3 ubiquitin-protein ligase RNF14	7.13	0.0027
399	ptprf	Receptor-type tyrosine-protein phosphatase F	-2.63	0.0027
400	RTP2	Receptor-transporting protein 2	2.31	0.0027
401	RAB19	Ras-related protein Rab-19	3.04	0.0027
402	tax1bp1b	Tax1-binding protein 1 homolog B	0.92	0.0027
403	GRAMD4	GRAM domain-containing protein 4	-1.39	0.0027
404	PARD6A	Partitioning defective 6 homolog alpha	2.45	0.0027
405	Cd74	H-2 class II histocompatibility antigen gamma chain	1.07	0.0028
406	MAML3	Mastermind-like protein 3	-2.02	0.0028
407	cka	Casein kinase II subunit alpha	-1.14	0.0028
408	EIF3F	Eukaryotic translation initiation factor 3 subunit F	2.16	0.0028
409	nccrp1	F-box only protein 50	2.14	0.0028
410	ACADSB	Short/branched chain specific acyl-CoA dehydrogenase, mitochondrial	2.78	0.0029
411	Hk1	Hexokinase-1	-1.60	0.0029
412	PPP2R1B	Serine/threonine-protein phosphatase 2A 65 kDa regulatory subunit A beta isoform	1.12	0.0029
413	hsp70	Heat shock 70 kDa protein	3.24	0.0029
414	#N/A	60S acidic ribosomal protein P2	2.29	0.0029
415	Slc25a5	ADP/ATP translocase 2	2.29	0.0029
416	Megf11	Multiple epidermal growth factor-like domains protein 11	6.94	0.0030
417	SLC39A11	Zinc transporter ZIP11	0.97	0.0030
418	SPRR3	Small proline-rich protein 3	1.43	0.0030
419	ZC3HAV1	Zinc finger CCCH-type antiviral protein 1	1.14	0.0030
420	eif4ebp3l	Eukaryotic translation initiation factor 4E-binding protein 3-like	3.32	0.0031
421	Zdbf2	DBF4-type zinc finger-containing protein 2 homolog	-1.92	0.0031
422	cct3	T-complex protein 1 subunit gamma	2.32	0.0031
423	Stx11	Syntaxin-11	2.03	0.0031
424	Pcbp2	Poly(rC)-binding protein 2	2.14	0.0031
425	#N/A	Polyubiquitin	2.87	0.0031
426	Fat2	Protocadherin Fat 2	-4.29	0.0032
427	RNF114	E3 ubiquitin-protein ligase RNF114	2.04	0.0032
428	SLC25A5	ADP/ATP translocase 2	2.18	0.0033
429	Pgd	6-phosphogluconate dehydrogenase, decarboxylating	1.71	0.0033
430	usp15	Ubiquitin carboxyl-terminal hydrolase 15	-5.02	0.0033
431	#N/A	GRAM domain-containing protein 1C	1.30	0.0034
432	STARD13	StAR-related lipid transfer protein 13	6.29	0.0034
433	Itpr2	Inositol 1,4,5-trisphosphate receptor type 2	-1.25	0.0034
434	Tnik	Traf2 and NCK-interacting protein kinase	-1.88	0.0034
435	Cgas	Cyclic GMP-AMP synthase	1.78	0.0034
436	TMEM131L	Transmembrane protein 131-like	-1.50	0.0034
437	banf1	Barrier-to-autointegration factor	2.83	0.0034
438	ZNF462	Zinc finger protein 462	1.52	0.0034

439	Ptbp3	Polypyrimidine tract-binding protein 3	0.87	0.0034
440	zcchc4	Zinc finger CCHC domain-containing protein 4	-1.87	0.0035
441	fgfr1a	Fibroblast growth factor receptor 1-A	-3.85	0.0035
442	CASK	Peripheral plasma membrane protein CASK	-1.73	0.0035
443	PCDHGC3	Protocadherin gamma-C3	-3.06	0.0035
444	Srsf5	Serine/arginine-rich splicing factor 5	-1.24	0.0036
445	#N/A	Tubulin beta chain	2.29	0.0036
446	#N/A	RNA-directed RNA polymerase	-6.82	0.0036
447	RAB9A	Ras-related protein Rab-9A	1.89	0.0036
448	PLEKHA5	Pleckstrin homology domain-containing family A member 5	-1.15	0.0036
449	grhl2	Grainyhead-like protein 2 homolog	-2.91	0.0036
450	STYK1	Tyrosine-protein kinase STYK1	1.04	0.0036
451	Cmpk2	UMP-CMP kinase 2, mitochondrial	4.95	0.0036
452	PARD3	Partitioning defective 3 homolog	-2.42	0.0036
453	GDI2	Rab GDP dissociation inhibitor beta	1.62	0.0037
454	Itpr2	Inositol 1,4,5-trisphosphate receptor type 2	-2.07	0.0037
455	ORF56	Uncharacterized protein ORF56	2.54	0.0037
456	Hpgd	15-hydroxyprostaglandin dehydrogenase [NAD(+)]	2.02	0.0037
457	Ccl28	C-C motif chemokine 28	-1.37	0.0037
458	npc2	Epididymal secretory protein E1	1.82	0.0037
459	TAX1BP3	Tax1-binding protein 3	2.05	0.0038
460	Lpar6	Lysophosphatidic acid receptor 6	-1.64	0.0038
461	Dennd3	DENN domain-containing protein 3	-1.40	0.0039
462	ppp1cb	Serine/threonine-protein phosphatase PP1-beta catalytic subunit	1.85	0.0039
463	PAWR	PRKC apoptosis WT1 regulator protein	-1.59	0.0039
464	sh2d4a	SH2 domain-containing protein 4A	2.77	0.0039
465	#N/A	Class I histocompatibility antigen, F10 alpha chain	11.27	0.0039
466	RPL14	60S ribosomal protein L14	1.72	0.0039
467	hsp70	Heat shock 70 kDa protein	3.24	0.0040
468	COPS7B	COP9 signalosome complex subunit 7b	1.58	0.0040
469	#N/A	Uncharacterized protein C1orf106 homolog	-1.68	0.0040
470	ABLIM2	Actin-binding LIM protein 2	1.40	0.0040
471	dennd5b	DENN domain-containing protein 5B	-2.79	0.0041
472	EZR	Ezrin	1.50	0.0041
473	TNFRSF1A	Tumor necrosis factor receptor superfamily member 1A	1.39	0.0041
474	VDAC2	Voltage-dependent anion-selective channel protein 2	1.07	0.0041
475	UQCR11	Cytochrome b-c1 complex subunit 10	1.72	0.0041
476	#N/A	Amino-terminal enhancer of split	1.36	0.0041
477	VGLL1	Transcription cofactor vestigial-like protein 1	2.24	0.0042
478	GAD1	Glutamate decarboxylase 1	2.60	0.0042
479	VAPB	Vesicle-associated membrane protein-associated protein B	1.19	0.0042
480	hsp70	Heat shock 70 kDa protein	3.18	0.0042
481	Capn2	Calpain-2 catalytic subunit	1.89	0.0042
482	PXN1	Jeltraxin	2.58	0.0042
483	Rpl28	60S ribosomal protein L28	1.98	0.0042
484	mx2	Interferon-induced GTP-binding protein Mx2	1.14	0.0042
485	ERVFC1	Endogenous retrovirus group FC1 Env polyprotein	-1.81	0.0043
486	Atf5	Cyclic AMP-dependent transcription factor ATF-5	2.37	0.0043
487	NYAP2	Neuronal tyrosine-phosphorylated phosphoinositide-3-kinase adapter 2	3.72	0.0043
488	#N/A	Membrane progestin receptor beta	5.33	0.0043
489	Cadps2	Calcium-dependent secretion activator 2	-1.10	0.0044
490	cyc	Cytochrome c	3.13	0.0044
491	Ndufs2	NADH dehydrogenase [ubiquinone] iron-sulfur protein 2, mitochondrial	-1.44	0.0044
492	cnpy3	Protein canopy homolog 3	2.55	0.0044
493	Kcnk2	Potassium channel subfamily K member 2	-2.35	0.0044
494	MROH1	Maestro heat-like repeat-containing protein family member 1	-0.98	0.0044
495	PPP2CB	Serine/threonine-protein phosphatase 2A catalytic subunit beta isoform	1.17	0.0044
496	tmem263-b	Transmembrane protein 263-B	-5.16	0.0046
497	FLNB	Filamin-B	3.67	0.0046
498	Rps26	40S ribosomal protein S26	2.03	0.0046
499	PPP2CB	Serine/threonine-protein phosphatase 2A catalytic subunit beta isoform	1.41	0.0047
500	tchp	Trichoplein keratin filament-binding protein	6.05	0.0047
501	CKAP4	Cytoskeleton-associated protein 4	1.96	0.0047
502	FAT1	Protocadherin Fat 1	-4.50	0.0047
503	ID1	DNA-binding protein inhibitor ID-1	2.21	0.0047
504	ANXA11	Annexin A11	0.80	0.0047

505	ERBB3	Receptor tyrosine-protein kinase erbB-3	-4.13	0.0047
506	CREG1	Protein CREG1	2.50	0.0047
507	alas1	5-aminolevulinate synthase, nonspecific, mitochondrial	2.46	0.0047
508	VWA7	von Willebrand factor A domain-containing protein 7	-5.29	0.0048
509	RBMS1	RNA-binding motif, single-stranded-interacting protein 1	1.64	0.0048
510	ZBED5	Zinc finger BED domain-containing protein 5	-0.71	0.0048
511	RPS5	40S ribosomal protein S5	2.08	0.0048
512	ID1	DNA-binding protein inhibitor ID-1	2.64	0.0048
513	kdelr3	ER lumen protein-retaining receptor 3	1.55	0.0049
514	Dennd3	DENN domain-containing protein 3	-1.84	0.0049
515	PNP	Purine nucleoside phosphorylase	1.31	0.0049
516	Mtss1	Metastasis suppressor protein 1	-2.19	0.0050
517	aldh1l1	Cytosolic 10-formyltetrahydrofolate dehydrogenase	6.02	0.0050
518	TRPM5	Transient receptor potential cation channel subfamily M member 5	4.35	0.0050
519	SULT3A1	Amine sulfotransferase	2.46	0.0050
520	USP54	Inactive ubiquitin carboxyl-terminal hydrolase 54	2.75	0.0050
521	arf1	ADP-ribosylation factor 1	2.08	0.0051
522	NDUFB9	NADH dehydrogenase [ubiquinone] 1 beta subcomplex subunit 9	1.77	0.0051
523	#N/A	Transposable element Tcb1 transposase	1.60	0.0051
524	DRAM2	DNA damage-regulated autophagy modulator protein 2	1.56	0.0051
525	ergic2	Endoplasmic reticulum-Golgi intermediate compartment protein 2	1.57	0.0051
526	mts	Serine/threonine-protein phosphatase PP2A	1.13	0.0052
527	rxrba	Retinoic acid receptor RXR-beta-A	1.39	0.0052
528	lmbr1l	Limb region 1 homolog-like protein	-2.26	0.0052
529	DDX17	Probable ATP-dependent RNA helicase DDX17	-2.60	0.0052
530	Snx3	Sorting nexin-3	1.84	0.0053
531	cops8	COP9 signalosome complex subunit 8	1.58	0.0053
532	Cep170b	Centrosomal protein of 170 kDa protein B	-1.88	0.0053
533	Gas7	Growth arrest-specific protein 7	6.62	0.0053
534	PPFIA3	Liprin-alpha-3	-3.18	0.0054
535	GPX2	Glutathione peroxidase 2	2.46	0.0054
536	rpl27	60S ribosomal protein L27	1.97	0.0054
537	mapk8a	Mitogen-activated protein kinase 8A	-4.58	0.0055
538	c1galt1a	Glycoprotein-N-acetylgalactosamine 3-beta-galactosyltransferase 1-A	-1.51	0.0055
539	CNDP2	Cytosolic non-specific dipeptidase	2.23	0.0055
540	PDE4DIP	Myomegalin	-2.70	0.0055
541	CLDN8	Claudin-8	1.90	0.0055
542	GNGT2	Guanine nucleotide-binding protein G(I)/G(S)/G(O) subunit gamma-T2	3.34	0.0055
543	GDPD1	Glycerophosphodiester phosphodiesterase domain-containing protein 1	-1.27	0.0056
544	NLRP3	NACHT, LRR and PYD domains-containing protein 3	-2.27	0.0057
545	copg2	Coatomer subunit gamma-2	1.25	0.0057
546	B4GALNT1	Beta-1,4 N-acetylgalactosaminyltransferase 1	3.65	0.0058
547	SSR3	Translocon-associated protein subunit gamma	1.41	0.0058
548	lsm12a	Protein LSM12 homolog A	1.75	0.0058
549	Oxa1l	Mitochondrial inner membrane protein OXA1L	-4.60	0.0058
550	Tf2-9	Transposon Tf2-9 polyprotein	3.05	0.0059
551	hsp90ab1	Heat shock protein HSP 90-beta	1.43	0.0060
552	TSTA3	GDP-L-fucose synthase	-4.69	0.0060
553	Atp5f1d	ATP synthase subunit delta, mitochondrial	1.49	0.0060
554	Pgap1	GPI inositol-deacylase	-1.55	0.0060
555	Tm9sf1	Transmembrane 9 superfamily member 1	1.37	0.0061
556	CRY2	Cryptochrome-2	-1.65	0.0061
557	Rpl23	60S ribosomal protein L23	1.95	0.0061
558	Adarb1	Double-stranded RNA-specific editase 1	-2.11	0.0061
559	Pard6b	Partitioning defective 6 homolog beta	2.52	0.0061
560	Map1lc3b	Microtubule-associated proteins 1A/1B light chain 3B	1.71	0.0061
561	Cpeb2	Cytoplasmic polyadenylation element-binding protein 2	3.95	0.0062
562	LTBP1	Latent-transforming growth factor beta-binding protein 1	4.66	0.0062
563	mid1ip1b	Mid1-interacting protein 1-B	1.48	0.0062
564	GALNT8	Probable polypeptide N-acetylgalactosaminyltransferase 8	1.05	0.0063
565	SVOP	Synaptic vesicle 2-related protein	-1.40	0.0063
566	FLNC	Filamin-C	3.30	0.0063
567	EPB41L2	Band 4.1-like protein 2	-1.10	0.0063
568	WDR77	Methylosome protein 50	1.57	0.0063
569	Lactb	Serine beta-lactamase-like protein LACTB, mitochondrial	-5.08	0.0064
570	MAP4K4	Mitogen-activated protein kinase kinase kinase kinase 4	-2.06	0.0064

571	METTL14	N6-adenosine-methyltransferase subunit METTL14	-2.05	0.0064
572	LMO7	LIM domain only protein 7	1.48	0.0064
573	rpl36a	60S ribosomal protein L36a	1.59	0.0065
574	#N/A	Intermediate filament protein ON3	2.10	0.0065
575	rps18	40S ribosomal protein S18	2.02	0.0065
576	PLCH2	1-phosphatidylinositol 4,5-bisphosphate phosphodiesterase eta-2	-1.28	0.0066
577	aste1	Protein asteroid homolog 1	4.36	0.0066
578	p1	RNA-directed RNA polymerase	6.69	0.0067
579	rpl13a	60S ribosomal protein L13a	1.86	0.0067
580	jag1b	Protein jagged-1b	-1.65	0.0068
581	amotl2a	Angiomotin-like 2a	2.49	0.0068
582	QSOX1	Sulfhydryl oxidase 1	2.84	0.0068
583	rps13	40S ribosomal protein S13	2.15	0.0068
584	SMCR8	Smith-Magenis syndrome chromosomal region candidate gene 8 protein	-1.72	0.0068
585	RAB2A	Ras-related protein Rab-2A	1.27	0.0068
586	Ubap2l	Ubiquitin-associated protein 2-like	-2.41	0.0068
587	Naf1	H/ACA ribonucleoprotein complex non-core subunit NAF1	-1.67	0.0068
588	COMMD1	COMM domain-containing protein 1	1.37	0.0068
589	AMBRA1	Activating molecule in BECN1-regulated autophagy protein 1	-1.82	0.0069
590	FLNC	Filamin-C	3.03	0.0069
591	SERF2	Small EDRK-rich factor 2	1.45	0.0069
592	RNF13	E3 ubiquitin-protein ligase RNF13	-4.87	0.0069
593	tspan31	Tetraspanin-31	-1.73	0.0069
594	zcchc4	Zinc finger CCHC domain-containing protein 4	-1.93	0.0070
595	NLRP12	NACHT, LRR and PYD domains-containing protein 12	-1.26	0.0070
596	SLC25A6	ADP/ATP translocase 3	2.16	0.0071
597	NRG4	Pro-neuregulin-4, membrane-bound isoform	2.03	0.0071
598	CNGA3	Cyclic nucleotide-gated cation channel alpha-3	6.80	0.0071
599	Ppfia3	Liprin-alpha-3	-1.93	0.0072
600	sema3d	Semaphorin-3D	-5.35	0.0072
601	Rpl26	60S ribosomal protein L26	2.10	0.0072
602	anxa2-a	Annexin A2-A	3.59	0.0072
603	SLC2A2	Solute carrier family 2, facilitated glucose transporter member 2	-2.15	0.0073
604	Morc2a	MORC family CW-type zinc finger protein 2A	-4.34	0.0073
605	MYH9	Myosin-9	1.70	0.0073
606	GIMAP2	GTPase IMAP family member 2	6.35	0.0074
607	CHL1	Neural cell adhesion molecule L1-like protein	-1.39	0.0074
608	CLDN4	Claudin-4	2.07	0.0074
609	ddit4l	DNA damage-inducible transcript 4-like protein	2.03	0.0074
610	SYNDIG1L	Synapse differentiation-inducing gene protein 1-like	2.14	0.0075
611	Atp5po	ATP synthase subunit O, mitochondrial	1.47	0.0076
612	RAB7A	Ras-related protein Rab-7a	1.18	0.0076
613	Dock8	Dedicator of cytokinesis protein 8	-2.07	0.0076
614	SEC22B	Vesicle-trafficking protein SEC22b	1.76	0.0076
615	GNAS	Guanine nucleotide-binding protein G(s) subunit alpha	-2.74	0.0076
616	slc40a1	Solute carrier family 40 member 1	1.98	0.0076
617	PFN2	Profilin-2	1.84	0.0077
618	Ice1	Little elongation complex subunit 1	-2.24	0.0077
619	RDX	Radixin	1.60	0.0077
620	tc1a	Transposable element Tc1 transposase	-1.04	0.0077
621	rps25	40S ribosomal protein S25	1.72	0.0077
622	serpinb1	Leukocyte elastase inhibitor	1.69	0.0077
623	eif3m	Eukaryotic translation initiation factor 3 subunit M	1.82	0.0078
624	def6	Differentially expressed in FDCP 6 homolog	-1.57	0.0078
625	Ngef	Ephexin-1	1.03	0.0078
626	GIT2	ARF GTPase-activating protein GIT2	-1.01	0.0079
627	DNASE1L3	Deoxyribonuclease gamma	2.86	0.0079
628	phka2	Phosphorylase b kinase regulatory subunit alpha, liver isoform	-1.61	0.0079
629	eef1a	Elongation factor 1-alpha	1.82	0.0079
630	EIF2S3	Eukaryotic translation initiation factor 2 subunit 3	1.97	0.0079
631	Dennd3	DENN domain-containing protein 3	1.61	0.0079
632	ZCCHC14	Zinc finger CCHC domain-containing protein 14	-4.79	0.0079
633	NLRC3	Protein NLRC3	-1.34	0.0079
634	ATP5MC1	ATP synthase F(0) complex subunit C1, mitochondrial	1.75	0.0079
635	Tomm7	Mitochondrial import receptor subunit TOM7 homolog	2.21	0.0080
636	Skil	Ski-like protein	2.47	0.0081

637	TSPAN3	Tetraspanin-3	1.65	0.0081
638	TUBGCP5	Gamma-tubulin complex component 5	-1.99	0.0082
639	hsc71	Heat shock cognate 70 kDa protein	2.04	0.0082
640	SCAPER	S phase cyclin A-associated protein in the endoplasmic reticulum	-1.43	0.0082
641	KRTCAP2	Keratinocyte-associated protein 2 {ECO:0000250|UniProtKB:Q8N6L1}	1.75	0.0082
642	yipf3	Protein YIPF3	1.65	0.0082
643	Eef1d	Elongation factor 1-delta	1.76	0.0083
644	CXCR3	C-X-C chemokine receptor type 3	2.92	0.0083
645	Rhog	Rho-related GTP-binding protein RhoG	1.91	0.0083
646	Spata13	Spermatogenesis-associated protein 13	3.36	0.0083
647	WWC1	Protein KIBRA	1.03	0.0083
648	PRKACA	cAMP-dependent protein kinase catalytic subunit alpha	1.53	0.0084
649	pol	Retrovirus-related Pol polyprotein from transposon opus	-3.53	0.0084
650	Mapk12	Mitogen-activated protein kinase 12	-2.90	0.0085
651	Vamp3	Vesicle-associated membrane protein 3	1.69	0.0085
652	Pogz	Pogo transposable element with ZNF domain	-1.66	0.0085
653	GLO1	Lactoylglutathione lyase	-4.65	0.0085
654	Kiaa1671	Uncharacterized protein KIAA1671	1.10	0.0085
655	rpl11	60S ribosomal protein L11	1.92	0.0086
656	Atp11a	Probable phospholipid-transporting ATPase IH	-1.68	0.0086
657	TP53INP2	Tumor protein p53-inducible nuclear protein 2	1.48	0.0086
658	ext1b	Exostosin-1b	-4.88	0.0086
659	Rps9	40S ribosomal protein S9	1.78	0.0086
660	mvp	Major vault protein	1.66	0.0086
661	rps13	40S ribosomal protein S13	1.96	0.0087
662	CCT5	T-complex protein 1 subunit epsilon	1.91	0.0087
663	selenot1a	Selenoprotein T1a	1.48	0.0087
664	PRDX5	Peroxiredoxin-5, mitochondrial	1.67	0.0087
665	cmas	N-acylneuraminate cytidylyltransferase	1.01	0.0087
666	Tf2-9	Transposon Tf2-9 polyprotein	1.30	0.0088
667	mynn	Myoneurin	-4.91	0.0088
668	PDLIM2	PDZ and LIM domain protein 2	1.62	0.0088
669	exsA	Spore coat assembly protein ExsA	2.14	0.0089
670	PARD6B	Partitioning defective 6 homolog beta	1.63	0.0090
671	abcG23	ABC transporter G family member 23	1.28	0.0090
672	AMOT	Angiomotin	-1.41	0.0091
673	KRT19	Keratin, type I cytoskeletal 19	-2.44	0.0091
674	FP1	Adhesive plaque matrix protein	-2.16	0.0091
675	NFIB	Nuclear factor 1 B-type	-0.77	0.0091
676	ABHD10	Mycophenolic acid acyl-glucuronide esterase, mitochondrial	2.14	0.0092
677	SNRNP70	U1 small nuclear ribonucleoprotein 70 kDa	-1.22	0.0092
678	mvp	Major vault protein	0.97	0.0092
679	NLRP12	NACHT, LRR and PYD domains-containing protein 12	-1.35	0.0092
680	ANKRD26	Ankyrin repeat domain-containing protein 26	-1.76	0.0092
681	JUN	Transcription factor AP-1	-1.04	0.0093
682	ldhb	L-lactate dehydrogenase B chain	2.17	0.0094
683	Trim35	Tripartite motif-containing protein 35	-2.06	0.0096
684	Rps16	40S ribosomal protein S16	1.82	0.0096
685	CEP85L	Centrosomal protein of 85 kDa-like	-1.84	0.0096
686	kdelr2	ER lumen protein-retaining receptor 2	1.38	0.0096
687	SCIN	Adseverin	2.54	0.0096
688	tmem127	Transmembrane protein 127	1.43	0.0097
689	Rps3	40S ribosomal protein S3	1.89	0.0097
690	GPX4	Phospholipid hydroperoxide glutathione peroxidase, mitochondrial	1.76	0.0098
691	HIP1R	Huntingtin-interacting protein 1-related protein	0.92	0.0098
692	APOLD1	Apolipoprotein L domain-containing protein 1	-1.78	0.0098
693	TMEM131L	Transmembrane protein 131-like	-1.44	0.0098
694	Itpr2	Inositol 1,4,5-trisphosphate receptor type 2	-1.24	0.0098
695	Etfa	Electron transfer flavoprotein subunit alpha, mitochondrial	-3.51	0.0099
696	Atp5f1a	ATP synthase subunit alpha, mitochondrial	1.36	0.0099
697	cfl2	Cofilin-2	2.05	0.0099
698	Txn2	Thioredoxin, mitochondrial	1.73	0.0100
699	Sqstm1	Sequestosome-1	1.93	0.0100
700	chtf18	Chromosome transmission fidelity protein 18 homolog	-3.41	0.0100
701	#N/A	S-antigen protein	-5.59	0.0100
702	mkrn1	Probable E3 ubiquitin-protein ligase makorin-1	1.41	0.0100

703	KIAA0232	Uncharacterized protein KIAA0232	1.12	0.0101
704	ERBB3	Receptor tyrosine-protein kinase erbB-3	-1.92	0.0102
705	actb	Actin, cytoplasmic 1	1.61	0.0102
706	pol	Retrovirus-related Pol polyprotein from transposon 17.6	-2.02	0.0102
707	rpl36	60S ribosomal protein L36	1.75	0.0103
708	EPB41L2	Band 4.1-like protein 2	-1.22	0.0104
709	SH2D5	SH2 domain-containing protein 5	-3.37	0.0104
710	SLA	Src-like-adapter	-4.28	0.0104
711	rasgrp1	RAS guanyl-releasing protein 1	-1.03	0.0104
712	CS	Circumsporozoite protein	1.36	0.0105
713	Dsp	Desmoplakin	-3.07	0.0105
714	#N/A	Transposable element Tcb1 transposase	1.22	0.0105
715	#N/A	Glycine--tRNA ligase	1.06	0.0105
716	ORMDL2	ORM1-like protein 2	1.25	0.0105
717	xkr9	XK-related protein 9	2.73	0.0106
718	ATP6V0C	V-type proton ATPase 16 kDa proteolipid subunit	2.24	0.0106
719	Aimp1	Aminoacyl tRNA synthase complex-interacting multifunctional protein 1	1.94	0.0107
720	RPL21	60S ribosomal protein L21	1.79	0.0107
721	ARHGEF10L	Rho guanine nucleotide exchange factor 10-like protein	-1.46	0.0107
722	Arl4d	ADP-ribosylation factor-like protein 4D	1.34	0.0107
723	GPR34	Probable G-protein coupled receptor 34	4.49	0.0108
724	ctsd	Cathepsin D	1.77	0.0109
725	ATP6V1E1	V-type proton ATPase subunit E 1	1.40	0.0109
726	gprc6a	G-protein coupled receptor family C group 6 member A	3.09	0.0110
727	Timp2	Metalloproteinase inhibitor 2	4.24	0.0110
728	ITPR2	Inositol 1,4,5-trisphosphate receptor type 2	-1.21	0.0110
729	MTHFD2	Bifunctional methylenetetrahydrofolate dehydrogenase/cyclohydrolase, mitochondrial	2.68	0.0111
730	ANKK1	Ankyrin repeat and protein kinase domain-containing protein 1	1.74	0.0111
731	Itpr2	Inositol 1,4,5-trisphosphate receptor type 2	-1.03	0.0112
732	trim71	E3 ubiquitin-protein ligase TRIM71	4.54	0.0112
733	#N/A	Transposable element Tcb1 transposase	-0.85	0.0112
734	#N/A	Transposable element Tcb2 transposase	2.79	0.0113
735	Cpeb2	Cytoplasmic polyadenylation element-binding protein 2	3.10	0.0113
736	tmem11	Transmembrane protein 11, mitochondrial	2.00	0.0113
737	med10	Mediator of RNA polymerase II transcription subunit 10	2.33	0.0113
738	PRKCD	Protein kinase C delta type	0.93	0.0113
739	Cyba	Cytochrome b-245 light chain	1.53	0.0114
740	#N/A	UPF0461 protein C5orf24 homolog	1.51	0.0114
741	ATP8A2	Phospholipid-transporting ATPase IB	-1.92	0.0114
742	uvssa	UV-stimulated scaffold protein A	-1.37	0.0115
743	ubac1	Ubiquitin-associated domain-containing protein 1	-4.87	0.0115
744	Eps8l2	Epidermal growth factor receptor kinase substrate 8-like protein 2	1.85	0.0115
745	mapk8b	Mitogen-activated protein kinase 8B	-2.22	0.0115
746	Lxn	Latexin	1.92	0.0116
747	Tf2-9	Transposon Tf2-9 polyprotein	-5.14	0.0116
748	ZBED9	SCAN domain-containing protein 3	-2.93	0.0116
749	Syne3	Nesprin-3	1.96	0.0117
750	Klf5	Krueppel-like factor 5	-1.48	0.0117
751	psma2	Proteasome subunit alpha type-2	1.70	0.0119
752	ccdc80	Coiled-coil domain-containing protein 80	4.43	0.0119
753	PCDHA5	Protocadherin alpha-5	-5.17	0.0119
754	PPFIBP2	Liprin-beta-2	-2.12	0.0120
755	thrb	Thyroid hormone receptor beta	-0.92	0.0120
756	CEACAM1	Carcinoembryonic antigen-related cell adhesion molecule 1	4.07	0.0120
757	arhgap21	Rho GTPase-activating protein 21	-1.00	0.0120
758	FOXK2	Forkhead box protein K2	2.01	0.0120
759	CAPZA1	F-actin-capping protein subunit alpha-1	1.22	0.0120
760	hba	Hemoglobin subunit alpha	8.74	0.0120
761	VIT	Vitrin	-3.90	0.0120
762	RNH1	Ribonuclease inhibitor	-0.96	0.0121
763	#N/A	Zinc-binding protein A33	2.47	0.0121
764	GRHL2	Grainyhead-like protein 2 homolog	-2.09	0.0123
765	tpx2-a	Targeting protein for Xklp2-A	-5.12	0.0123
766	ADAMTSL5	ADAMTS-like protein 5	2.76	0.0125
767	Mdh1	Malate dehydrogenase, cytoplasmic	1.69	0.0126

768	afap1l1	Actin filament-associated protein 1-like 1	-2.24	0.0126
769	cluh	Clustered mitochondria protein homolog	-1.25	0.0126
770	#N/A	Transposable element Tcb1 transposase	1.29	0.0127
771	EZR	Ezrin	1.54	0.0127
772	rpl19	60S ribosomal protein L19	1.56	0.0127
773	#N/A	Intestinal mucin-like protein	-2.15	0.0127
774	RBM47	RNA-binding protein 47	1.04	0.0127
775	DNAAF5	Dynein assembly factor 5, axonemal	-1.90	0.0127
776	#N/A	Costars family protein ABRACL	1.58	0.0128
777	BNIPL	Bcl-2/adenovirus E1B 19 kDa-interacting protein 2-like protein	0.88	0.0128
778	#N/A	Cystatin-B	2.12	0.0128
779	ATP6V1G1	V-type proton ATPase subunit G 1	1.68	0.0128
780	Nlrc3	Protein NLRC3	-1.79	0.0128
781	B9d1	B9 domain-containing protein 1	-3.18	0.0128
782	arid5b	AT-rich interactive domain-containing protein 5B	-4.77	0.0128
783	cpeb4	Cytoplasmic polyadenylation element-binding protein 4	3.73	0.0128
784	rps27	40S ribosomal protein S27	1.67	0.0129
785	rhoaa	Rho-related GTP-binding protein RhoA-A {ECO:0000305}	1.49	0.0129
786	CLDN4	Claudin-4	2.21	0.0130
787	#N/A	Spartin	1.57	0.0130
788	ANXA13	Annexin A13	2.89	0.0131
789	#N/A	Transposon TX1 uncharacterized 149 kDa protein	-1.67	0.0131
790	Arhgap27	Rho GTPase-activating protein 27	0.88	0.0131
791	Kiaa1671	Uncharacterized protein KIAA1671	1.25	0.0131
792	Nlrc3	Protein NLRC3	-1.17	0.0132
793	GADL1	Acidic amino acid decarboxylase GADL1	1.77	0.0132
794	Fcgr3	Low affinity immunoglobulin gamma Fc region receptor III	2.39	0.0132
795	Dst	Dystonin	-1.99	0.0133
796	shroom1	Protein Shroom1	1.76	0.0133
797	Grsf1	G-rich sequence factor 1	-1.02	0.0133
798	uspl1	SUMO-specific isopeptidase USPL1	-1.63	0.0133
799	DPM3	Dolichol-phosphate mannosyltransferase subunit 3	2.18	0.0135
800	#N/A	Lipocalin	-2.01	0.0135
801	pol	Retrovirus-related Pol polyprotein from transposon 297	-1.23	0.0135
802	Pde4dip	Myomegalin	-2.61	0.0136
803	NXF1	Nuclear RNA export factor 1	-1.98	0.0136
804	SEMA6D	Semaphorin-6D	1.68	0.0136
805	AHNAK	Neuroblast differentiation-associated protein AHNAK	1.82	0.0137
806	fgfr1a	Fibroblast growth factor receptor 1-A	-2.98	0.0137
807	fgfr1a	Fibroblast growth factor receptor 1-A	-2.59	0.0137
808	ATP6V0E2	V-type proton ATPase subunit e 2	2.06	0.0137
809	DEPTOR	DEP domain-containing mTOR-interacting protein	-2.40	0.0137
810	Cpa1	Carboxypeptidase A1	2.70	0.0138
811	Tmem9b	Transmembrane protein 9B	1.18	0.0138
812	Tf2-6	Transposon Tf2-6 polyprotein	1.48	0.0138
813	txn	Thioredoxin	3.33	0.0138
814	gerIA	Spore germination protein GerIA	-2.35	0.0138
815	ADGRL3	Adhesion G protein-coupled receptor L3	2.28	0.0138
816	Ceacam1	Carcinoembryonic antigen-related cell adhesion molecule 1	3.27	0.0139
817	Cd6	T-cell differentiation antigen CD6	-1.93	0.0139
818	eef1g	Elongation factor 1-gamma	1.65	0.0139
819	ATP7A	Copper-transporting ATPase 1	2.28	0.0140
820	GPX2	Glutathione peroxidase 2	3.14	0.0140
821	Arpc4	Actin-related protein 2/3 complex subunit 4	1.31	0.0140
822	KPNA2	Importin subunit alpha-1	-4.72	0.0141
823	Ifi35	Interferon-induced 35 kDa protein homolog	0.89	0.0141
824	eif3k	Eukaryotic translation initiation factor 3 subunit K	1.79	0.0141
825	Cldn23	Claudin-23	1.42	0.0141
826	ANK3	Ankyrin-3	-2.56	0.0143
827	Hmmr	Hyaluronan-mediated motility receptor	-4.05	0.0143
828	MYH9	Myosin-9	1.25	0.0143
829	Tmbim4	Protein lifeguard 4	1.42	0.0144
830	Fam83b	Protein FAM83B {ECO:0000305}	-1.27	0.0144
831	RPL7	60S ribosomal protein L7	1.63	0.0144
832	K12H4.7	Putative serine protease K12H4.7	2.60	0.0144
833	ENO1	Alpha-enolase	2.13	0.0144

834	UTRN	Utrophin	1.30	0.0145
835	ARHGDIA	Rho GDP-dissociation inhibitor 1	1.35	0.0145
836	p1	RNA-directed RNA polymerase	4.81	0.0145
837	MUC5AC	Mucin-5AC {ECO:0000305}	-2.64	0.0145
838	#N/A	Annexin A5	1.26	0.0146
839	dkf-2	Serine/threonine-protein kinase dkf-2 {ECO:0000303|PubMed:17728253}	-4.67	0.0147
840	KCNK2	Potassium channel subfamily K member 2	-2.02	0.0148
841	pol	Retrovirus-related Pol polyprotein from transposon 297	2.78	0.0148
842	ZNF41	Zinc finger protein 41	-3.72	0.0148
843	chmp5	Charged multivesicular body protein 5	1.07	0.0148
844	IFI44	Interferon-induced protein 44	-2.62	0.0149
845	IL34	Interleukin-34	-1.77	0.0150
846	ATP8A2	Phospholipid-transporting ATPase IB	-1.81	0.0150
847	PDE4DIP	Myomegalin	-1.89	0.0150
848	lamtor4	Ragulator complex protein LAMTOR4	1.74	0.0150
849	Pol	LINE-1 retrotransposable element ORF2 protein	-3.26	0.0150
850	Tf2-9	Transposon Tf2-9 polyprotein	-1.28	0.0150
851	AHNAK	Neuroblast differentiation-associated protein AHNAK	1.85	0.0150
852	EVPL	Envoplakin	0.75	0.0151
853	APBB2	Amyloid beta A4 precursor protein-binding family B member 2	3.19	0.0151
854	ATP5PB	ATP synthase F(0) complex subunit B1, mitochondrial	1.24	0.0152
855	#N/A	RNA-directed RNA polymerase beta chain	9.02	0.0152
856	EPRS	Bifunctional glutamate/proline--tRNA ligase	1.29	0.0152
857	TSC22D3	TSC22 domain family protein 3	1.58	0.0152
858	GIMAP4	GTPase IMAP family member 4	-2.10	0.0154
859	sspH2	E3 ubiquitin-protein ligase sspH2	0.96	0.0155
860	TAGLN	Transgelin	2.61	0.0155
861	tdrd7b	Tudor domain-containing protein 7B	1.69	0.0155
862	CACNB1	Voltage-dependent L-type calcium channel subunit beta-1	4.83	0.0156
863	#N/A	Ferritin, heavy subunit	2.21	0.0156
864	nap1l1	Nucleosome assembly protein 1-like 1	1.71	0.0156
865	RTL1	Retrotransposon-like protein 1	2.32	0.0156
866	GPS2	G protein pathway suppressor 2	2.06	0.0156
867	#N/A	Melanoma-associated antigen G1	-1.45	0.0157
868	rps23	40S ribosomal protein S23	1.99	0.0157
869	afap1l1	Actin filament-associated protein 1-like 1	-1.97	0.0157
870	PSTPIP2	Proline-serine-threonine phosphatase-interacting protein 2	-1.52	0.0157
871	TRIM21	E3 ubiquitin-protein ligase TRIM21	-2.00	0.0158
872	tpi1b	Triosephosphate isomerase B	1.79	0.0158
873	CALD1	Caldesmon, smooth muscle	-1.38	0.0158
874	rps18	40S ribosomal protein S18	1.74	0.0159
875	NDUFS8	NADH dehydrogenase [ubiquinone] iron-sulfur protein 8, mitochondrial	1.56	0.0159
876	rps3-b	40S ribosomal protein S3-B	1.88	0.0160
877	CAPN9	Calpain-9	1.07	0.0160
878	gnb2l1	Guanine nucleotide-binding protein subunit beta-2-like 1	1.67	0.0160
879	Ipo11	Importin-11	-1.84	0.0160
880	NGFR	Tumor necrosis factor receptor superfamily member 16	-3.27	0.0161
881	ZNF235	Zinc finger protein 235	-2.39	0.0162
882	ELMSAN1	ELM2 and SANT domain-containing protein 1	-2.04	0.0162
883	SAT1	Diamine acetyltransferase 1	1.20	0.0163
884	DNAJC7	DnaJ homolog subfamily C member 7	-1.49	0.0163
885	rpl34	60S ribosomal protein L34	2.00	0.0164
886	trio	Triple functional domain protein	-3.94	0.0164
887	PDZD2	PDZ domain-containing protein 2	-1.89	0.0164
888	rps15	40S ribosomal protein S15	1.69	0.0165
889	tdp2	Tyrosyl-DNA phosphodiesterase 2	1.58	0.0165
890	rpl37	60S ribosomal protein L37	1.72	0.0167
891	ELP1	Elongator complex protein 1	-1.40	0.0167
892	Rbl1	Retinoblastoma-like protein 1	-1.40	0.0168
893	Tanc2	Protein TANC2	2.12	0.0168
894	Zcchc2	Zinc finger CCHC domain-containing protein 2	-3.06	0.0168
895	#N/A	RNA-dependent RNA polymerase	3.89	0.0169
896	CAPZB	F-actin-capping protein subunit beta	1.25	0.0169
897	PRKCH	Protein kinase C eta type	1.43	0.0170
898	PTPRA	Receptor-type tyrosine-protein phosphatase alpha	-1.58	0.0170
899	BTF3	Transcription factor BTF3	1.82	0.0171

900	TMEM30A	Cell cycle control protein 50A	0.89	0.0171
901	PIAS1	E3 SUMO-protein ligase PIAS1	-1.37	0.0171
902	mpp1	55 kDa erythrocyte membrane protein	2.13	0.0171
903	#N/A	RNA-directed RNA polymerase	-5.08	0.0171
904	WARS	Tryptophan--tRNA ligase, cytoplasmic	1.44	0.0171
905	rps11	40S ribosomal protein S11	1.88	0.0173
906	#N/A	Stonustoxin subunit alpha	-2.26	0.0175
907	rpl13	60S ribosomal protein L13	1.70	0.0175
908	rpl31	60S ribosomal protein L31	1.64	0.0175
909	Dleu7	Leukemia-associated protein 7 homolog	4.17	0.0176
910	Eprs	Bifunctional glutamate/proline--tRNA ligase	0.92	0.0176
911	Pfn2	Profilin-2	1.61	0.0176
912	#N/A	Adiponectin receptor protein 2	1.14	0.0176
913	brox	BRO1 domain-containing protein BROX	1.69	0.0176
914	LTBP2	Latent-transforming growth factor beta-binding protein 2	3.66	0.0176
915	DACH1	Dachshund homolog 1	-3.87	0.0176
916	ERBB3	Receptor tyrosine-protein kinase erbB-3	-2.57	0.0176
917	PIN1	Peptidyl-prolyl cis-trans isomerase NIMA-interacting 1	1.75	0.0177
918	sdhb	Succinate dehydrogenase [ubiquinone] iron-sulfur subunit, mitochondrial	-4.50	0.0177
919	tc1a	Transposable element Tc1 transposase	0.87	0.0177
920	RAB8A	Ras-related protein Rab-8A	1.24	0.0178
921	ext1b	Exostosin-1b	-1.51	0.0178
922	RAB11A	Ras-related protein Rab-11A	1.19	0.0179
923	ARHGAP5	Rho GTPase-activating protein 5	-1.44	0.0179
924	yipf6	Protein YIPF6	1.79	0.0180
925	CRABP2	Cellular retinoic acid-binding protein 2	-1.23	0.0180
926	Rbm4	RNA-binding protein 4	-1.76	0.0180
927	ZNF185	Zinc finger protein 185	1.67	0.0182
928	PLCD1	1-phosphatidylinositol 4,5-bisphosphate phosphodiesterase delta-1	2.59	0.0183
929	Klf4	Krueppel-like factor 4	-2.31	0.0183
930	ppp1r3cb	Protein phosphatase 1 regulatory subunit 3C-B	2.87	0.0184
931	LINC00269	Putative uncharacterized protein encoded by LINC00269	2.28	0.0184
932	STX5	Syntaxin-5	1.06	0.0184
933	Trim29	Tripartite motif-containing protein 29	1.63	0.0184
934	sumo1	Small ubiquitin-related modifier 1	1.72	0.0184
935	MAP4K4	Mitogen-activated protein kinase kinase kinase kinase 4	-3.11	0.0184
936	SSR2	Translocon-associated protein subunit beta	1.28	0.0185
937	Dtx3l	E3 ubiquitin-protein ligase DTX3L	1.97	0.0185
938	PDLIM5	PDZ and LIM domain protein 5	-1.69	0.0186
939	V-SEA	Tyrosine-protein kinase transforming protein SEA	-4.76	0.0186
940	STX6	Syntaxin-6	-1.81	0.0186
941	DNAJB4	DnaJ homolog subfamily B member 4	1.65	0.0187
942	fgfr1a	Fibroblast growth factor receptor 1-A	-3.70	0.0188
943	CD59	CD59 glycoprotein	1.78	0.0188
944	BTN2A1	Butyrophilin subfamily 2 member A1	-1.41	0.0189
945	Kiaa1109	Uncharacterized protein KIAA1109	-1.23	0.0190
946	#N/A	Transposable element Tcb1 transposase	2.67	0.0190
947	Tbc1d15	TBC1 domain family member 15	1.21	0.0190
948	Gdpd2	Glycerophosphoinositol inositolphosphodiesterase GDPD2	-1.28	0.0191
949	Gss	Glutathione synthetase	-3.84	0.0191
950	sdha	Succinate dehydrogenase [ubiquinone] flavoprotein subunit, mitochondrial	-2.66	0.0191
951	BICD1	Protein bicaudal D homolog 1	-2.88	0.0191
952	#N/A	FYN-binding protein	1.63	0.0191
953	pef1	Peflin	2.20	0.0191
954	Ube2w	Ubiquitin-conjugating enzyme E2 W	1.06	0.0193
955	HACD2	Very-long-chain (3R)-3-hydroxyacyl-CoA dehydratase 2 {ECO:0000305}	2.44	0.0193
956	DDX17	Probable ATP-dependent RNA helicase DDX17	-1.29	0.0193
957	tbc1d31	TBC1 domain family member 31	-1.63	0.0194
958	#N/A	L-rhamnose-binding lectin CSL2 {ECO:0000303|Ref.1}	-3.21	0.0194
959	Rps20	40S ribosomal protein S20	1.88	0.0194
960	opa1	Dynamin-like 120 kDa protein, mitochondrial	-4.54	0.0195
961	farsa	Phenylalanine--tRNA ligase alpha subunit	2.22	0.0196
962	srebf2	Sterol regulatory element-binding protein 2	1.01	0.0196
963	LMO7	LIM domain only protein 7	1.36	0.0196
964	sept8a	Septin-8-A	1.25	0.0196
965	POF1B	Protein POF1B	-4.23	0.0197

966	aste1	Protein asteroid homolog 1	3.03	0.0197
967	Rab14	Ras-related protein Rab-14	1.44	0.0197
968	lap-2	Putative aminopeptidase W07G4.4	1.32	0.0197
969	ST3GAL1	CMP-N-acetylneuraminate-beta-galactosamide-alpha-2,3-sialyltransferase 1	2.37	0.0198
970	#N/A	Uncharacterized protein DKFZp434B061	1.96	0.0198
971	pol	Pol polyprotein	-3.24	0.0199
972	Ralb	Ras-related protein Ral-B	1.95	0.0200
973	Clta	Clathrin light chain A	1.70	0.0200
974	#N/A	Tubulin alpha chain	1.66	0.0200
975	ARPC1B	Actin-related protein 2/3 complex subunit 1B	1.84	0.0202
976	PEG10	Retrotransposon-derived protein PEG10	1.38	0.0202
977	IRF3	Interferon regulatory factor 3	2.14	0.0202
978	#N/A	PERQ amino acid-rich with GYF domain-containing protein 2	-1.64	0.0202
979	jag1b	Protein jagged-1b	-1.68	0.0203
980	DERA	Deoxyribose-phosphate aldolase	1.18	0.0203
981	TRIM69	E3 ubiquitin-protein ligase TRIM69	1.37	0.0203
982	#N/A	H-2 class II histocompatibility antigen, I-E alpha chain	1.06	0.0203
983	CENPV	Centromere protein V	1.96	0.0204
984	Chst11	Carbohydrate sulfotransferase 11	-4.39	0.0204
985	SFMBT2	Scm-like with four MBT domains protein 2	-4.64	0.0204
986	Mtss1	Metastasis suppressor protein 1	-1.44	0.0204
987	#N/A	Transposable element Tcb1 transposase	2.44	0.0204
988	Pcbp2	Poly(rC)-binding protein 2	1.13	0.0205
989	Pdpk1	3-phosphoinositide-dependent protein kinase 1	1.31	0.0207
990	VIL1	Villin-1	2.36	0.0208
991	CACNB2	Voltage-dependent L-type calcium channel subunit beta-2	3.45	0.0209
992	DNAJC7	DnaJ homolog subfamily C member 7	1.14	0.0209
993	BIRC6	Baculoviral IAP repeat-containing protein 6	-1.42	0.0209
994	ptprf	Receptor-type tyrosine-protein phosphatase F	-2.87	0.0209
995	Tuba1c	Tubulin alpha-1C chain	1.94	0.0209
996	Acox3	Peroxisomal acyl-coenzyme A oxidase 3	-4.60	0.0210
997	Rab1A	Ras-related protein Rab-1A	1.47	0.0210
998	COL6A2	Collagen alpha-2(VI) chain	-3.04	0.0211
999	GNE	Bifunctional UDP-N-acetylglucosamine 2-epimerase/N-acetylmannosamine kinase	1.30	0.0211
1000	rpl9	60S ribosomal protein L9	1.68	0.0212
1001	rps7	40S ribosomal protein S7	1.85	0.0212
1002	Eps15l1	Epidermal growth factor receptor substrate 15-like 1	1.39	0.0213
1003	snrpd3	Small nuclear ribonucleoprotein Sm D3	-4.38	0.0213
1004	NCOA7	Nuclear receptor coactivator 7	-1.27	0.0213
1005	banf1	Barrier-to-autointegration factor	1.17	0.0213
1006	cyp2m1	Cytochrome P450 2M1	3.73	0.0214
1007	Tmem131	Transmembrane protein 131	1.50	0.0214
1008	FAM83B	Protein FAM83B {ECO:0000305}	-0.95	0.0214
1009	PEBP1	Phosphatidylethanolamine-binding protein 1	2.73	0.0214
1010	GTF2IRD2	General transcription factor II-I repeat domain-containing protein 2	-4.74	0.0214
1011	CPAMD8	C3 and PZP-like alpha-2-macroglobulin domain-containing protein 8	-4.38	0.0214
1012	rpl18	60S ribosomal protein L18	1.70	0.0215
1013	Pol	LINE-1 retrotransposable element ORF2 protein	1.33	0.0215
1014	Nlrc3	Protein NLRC3	-1.43	0.0216
1015	TMEM64	Transmembrane protein 64	-4.42	0.0217
1016	agtrap	Type-1 angiotensin II receptor-associated protein-like	3.37	0.0217
1017	Ssh1	Protein phosphatase Slingshot homolog 1	-3.81	0.0218
1018	Ntf4	Neurotrophin-4	-4.51	0.0219
1019	chid1	Chitinase domain-containing protein 1	-1.48	0.0220
1020	PEG10	Retrotransposon-derived protein PEG10	-4.55	0.0220
1021	VDAC2	Voltage-dependent anion-selective channel protein 2	1.33	0.0221
1022	GHITM	Growth hormone-inducible transmembrane protein	1.35	0.0221
1023	Iscu	Iron-sulfur cluster assembly enzyme ISCU, mitochondrial	1.98	0.0221
1024	#N/A	Uncharacterized 51.9 kDa protein in rps4-rps11 intergenic region	1.40	0.0222
1025	Kiaa1109	Uncharacterized protein KIAA1109	-2.26	0.0222
1026	Tf2-9	Transposon Tf2-9 polyprotein	2.60	0.0223
1027	PTGER4	Prostaglandin E2 receptor EP4 subtype	-2.03	0.0223
1028	NBEAL1	Neurobeachin-like protein 1	1.30	0.0223
1029	Ranbp3	Ran-binding protein 3	-3.04	0.0223

1030	#N/A	Cytochrome c oxidase subunit 6A, mitochondrial	1.70	0.0224
1031	stard3	StAR-related lipid transfer protein 3	1.02	0.0225
1032	POLD1	DNA polymerase delta catalytic subunit	-1.36	0.0226
1033	FLNC	Filamin-C	3.15	0.0226
1034	ORF2	RNA-directed RNA polymerase	8.89	0.0226
1035	Slc35a2	UDP-galactose translocator	1.07	0.0227
1036	TJP1	Tight junction protein ZO-1	1.51	0.0227
1037	Arhgdia	Rho GDP-dissociation inhibitor 1 {ECO:0000250|UniProtKB:P19803}	1.41	0.0228
1038	Scin	Adseverin	2.16	0.0228
1039	#N/A	14-3-3 protein beta/alpha-2	1.48	0.0229
1040	Tmprss4	Transmembrane protease serine 4	1.51	0.0230
1041	S100A13	Protein S100-A13	1.75	0.0230
1042	kremen1	Kremen protein 1	-1.19	0.0231
1043	At2g29580	Zinc finger CCCH domain-containing protein 25	0.79	0.0231
1044	pno1	RNA-binding protein PNO1	2.25	0.0231
1045	CLCN3	H(+)/Cl(-) exchange transporter 3	1.23	0.0231
1046	rpl11	60S ribosomal protein L11	1.70	0.0232
1047	phka2	Phosphorylase b kinase regulatory subunit alpha, liver isoform	-2.51	0.0232
1048	#N/A	RNA-directed RNA polymerase beta chain	9.87	0.0232
1049	HTATIP2	Oxidoreductase HTATIP2	1.57	0.0233
1050	B3GNT2	N-acetyllactosaminide beta-1,3-N-acetylglucosaminyltransferase 2	2.18	0.0234
1051	ier2	Immediate early response gene 2 protein	-1.73	0.0234
1052	RB1CC1	RB1-inducible coiled-coil protein 1	1.71	0.0234
1053	Pcdh20	Protocadherin-20	-4.94	0.0234
1054	Cdc42	Cell division control protein 42 homolog	1.10	0.0234
1055	Rpl12	60S ribosomal protein L12	1.55	0.0234
1056	ZNF271	Zinc finger protein 271	-0.97	0.0235
1057	rpl30	60S ribosomal protein L30	1.82	0.0235
1058	MYH11	Myosin-11	-1.32	0.0235
1059	Cask	Peripheral plasma membrane protein CASK	-1.29	0.0236
1060	Ctss	Cathepsin S	1.15	0.0236
1061	rpl35	60S ribosomal protein L35	1.68	0.0237
1062	DMGDH	Dimethylglycine dehydrogenase, mitochondrial	-4.69	0.0237
1063	letm1	LETM1 and EF-hand domain-containing protein 1, mitochondrial	-1.32	0.0238
1064	Snx18	Sorting nexin-18	2.37	0.0238
1065	Znf771	Zinc finger protein 771	-4.45	0.0238
1066	AP1M1	AP-1 complex subunit mu-1	1.34	0.0239
1067	NBEAL1	Neurobeachin-like protein 1	1.08	0.0240
1068	Cep295	Centrosomal protein of 295 kDa {ECO:0000250|UniProtKB:Q9C0D2}	-1.11	0.0240
1069	amotl2a	Angiomotin-like 2a	2.57	0.0242
1070	Rpl17	60S ribosomal protein L17	1.49	0.0242
1071	MUC5B	Mucin-5B	-2.21	0.0242
1072	LRRK1	Leucine-rich repeat serine/threonine-protein kinase 1	-0.90	0.0242
1073	tp53	Cellular tumor antigen p53	1.65	0.0243
1074	PCF11	Pre-mRNA cleavage complex 2 protein Pcf11	-2.61	0.0243
1075	CEP170B	Centrosomal protein of 170 kDa protein B	-1.71	0.0246
1076	ADK	Adenosine kinase	-4.29	0.0247
1077	BRI3	Brain protein I3	1.69	0.0247
1078	Dnajb2	DnaJ homolog subfamily B member 2	2.17	0.0247
1079	rpl31	60S ribosomal protein L31	1.83	0.0248
1080	chd8	Chromodomain-helicase-DNA-binding protein 8	-1.38	0.0248
1081	atp6v0d1	V-type proton ATPase subunit d 1	1.54	0.0249
1082	gamt	Guanidinoacetate N-methyltransferase	3.63	0.0249
1083	ran	GTP-binding nuclear protein Ran	1.54	0.0251
1084	#N/A	Stonustoxin subunit beta	-2.24	0.0251
1085	MTR	Methionine synthase	-1.53	0.0251
1086	Sfpq	Splicing factor, proline- and glutamine-rich	-0.92	0.0251
1087	EMC9	ER membrane protein complex subunit 9	1.24	0.0252
1088	EIF4G2	Eukaryotic translation initiation factor 4 gamma 2	1.74	0.0253
1089	PCDHA2	Protocadherin alpha-2	-2.83	0.0253
1090	purb	Transcriptional activator protein Pur-beta	1.54	0.0254
1091	mdh1	Malate dehydrogenase, cytoplasmic	1.69	0.0254
1092	TNS3	Tensin-3	-4.63	0.0255
1093	fam50a	Protein FAM50A	1.36	0.0255
1094	AHNAK	Neuroblast differentiation-associated protein AHNAK	1.39	0.0256
1095	ATP6V1E1	V-type proton ATPase subunit E 1	1.51	0.0256

1096	TM9SF4	Transmembrane 9 superfamily member 4	1.21	0.0256
1097	Hmbs	Porphobilinogen deaminase	-1.69	0.0257
1098	CTSB	Cathepsin B	2.35	0.0257
1099	URGCP	Up-regulator of cell proliferation	1.25	0.0257
1100	ZMYM1	Zinc finger MYM-type protein 1	-1.52	0.0258
1101	NPDC1	Neural proliferation differentiation and control protein 1	2.17	0.0258
1102	KIF3B	Kinesin-like protein KIF3B	-1.07	0.0258
1103	IST1	IST1 homolog	1.42	0.0260
1104	RTase	Probable RNA-directed DNA polymerase from transposon BS	1.64	0.0260
1105	SLC25A20	Mitochondrial carnitine/acylcarnitine carrier protein	2.43	0.0260
1106	C11orf65	Uncharacterized protein C11orf65	-1.74	0.0260
1107	Gimap8	GTPase IMAP family member 8	1.65	0.0261
1108	MTHFD1	C-1-tetrahydrofolate synthase, cytoplasmic	7.12	0.0261
1109	moxd1	DBH-like monooxygenase protein 1 homolog	-4.29	0.0261
1110	IGFBP4	Insulin-like growth factor-binding protein 4	4.76	0.0261
1111	Myo9b	Unconventional myosin-IXb	-0.83	0.0262
1112	RPL5	60S ribosomal protein L5	1.52	0.0262
1113	igf1r	Insulin-like growth factor 1 receptor	-2.38	0.0262
1114	CARD8	Caspase recruitment domain-containing protein 8	-1.34	0.0263
1115	MYBL2	Myb-related protein B	-1.79	0.0263
1116	#N/A	Transposable element Tcb2 transposase	-1.04	0.0263
1117	RAP1B	Ras-related protein Rap-1b	1.66	0.0264
1118	Nlrp3	NACHT, LRR and PYD domains-containing protein 3	-1.33	0.0264
1119	ELOVL1	Elongation of very long chain fatty acids protein 1	1.63	0.0264
1120	#N/A	Transposable element Tcb2 transposase	-1.93	0.0264
1121	GDI2	Rab GDP dissociation inhibitor beta	1.46	0.0264
1122	ric8b	Synembryn-B	1.07	0.0265
1123	TEX2	Testis-expressed sequence 2 protein	-4.48	0.0265
1124	pdcd10b	Programmed cell death protein 10-B	1.20	0.0265
1125	Rab27a	Ras-related protein Rab-27A	1.87	0.0265
1126	Nlrp1b	NACHT, LRR and PYD domains-containing protein 1b allele 5	-1.76	0.0265
1127	ARHGEF12	Rho guanine nucleotide exchange factor 12	-1.73	0.0265
1128	hook1	Protein Hook homolog 1	-1.97	0.0265
1129	NASP	Nuclear autoantigenic sperm protein	-3.95	0.0266
1130	#N/A	Transposable element Tcb1 transposase	-0.87	0.0267
1131	Mfsd3	Major facilitator superfamily domain-containing protein 3	1.73	0.0267
1132	Ergic3	Endoplasmic reticulum-Golgi intermediate compartment protein 3	0.95	0.0268
1133	Fau	40S ribosomal protein S30	1.60	0.0268
1134	CD276	CD276 antigen	-2.36	0.0269
1135	IL1R1	Interleukin-1 receptor type 1	-1.15	0.0269
1136	Bloc1s2	Biogenesis of lysosome-related organelles complex 1 subunit 2	1.95	0.0270
1137	MED13L	Mediator of RNA polymerase II transcription subunit 13-like	-1.07	0.0271
1138	NCF4	Neutrophil cytosol factor 4	1.20	0.0271
1139	WBP2	WW domain-binding protein 2	1.44	0.0271
1140	SYNE1	Nesprin-1	-1.28	0.0271
1141	aste1	Protein asteroid homolog 1	2.02	0.0272
1142	rps21	40S ribosomal protein S21	1.35	0.0272
1143	MTHFD1	C-1-tetrahydrofolate synthase, cytoplasmic	5.14	0.0272
1144	dhx32	Putative pre-mRNA-splicing factor ATP-dependent RNA helicase DHX32	1.87	0.0273
1145	#N/A	UPF0729 protein C18orf32 homolog	1.44	0.0273
1146	#N/A	LINE-1 retrotransposable element ORF2 protein	-4.01	0.0273
1147	APLP2	Amyloid-like protein 2	2.60	0.0274
1148	#N/A	Polyubiquitin	1.64	0.0275
1149	Pik3cb	Phosphatidylinositol 4,5-bisphosphate 3-kinase catalytic subunit beta isoform	-1.94	0.0275
1150	FRZB	Secreted frizzled-related protein 3	3.26	0.0276
1151	#N/A	Transposable element Tcb1 transposase	0.88	0.0276
1152	FRK	Tyrosine-protein kinase FRK	1.54	0.0277
1153	#N/A	Transposable element Tcb1 transposase	1.55	0.0277
1154	Gimap4	GTPase IMAP family member 4	1.89	0.0278
1155	degs1	Sphingolipid delta(4)-desaturase DES1	1.91	0.0279
1156	Tf2-9	Transposon Tf2-9 polyprotein	1.88	0.0281
1157	PHTF2	Putative homeodomain transcription factor 2	1.19	0.0281
1158	INPP4B	Type II inositol 3,4-bisphosphate 4-phosphatase	-1.42	0.0282
1159	#N/A	Probable DNA polymerase	-2.59	0.0282
1160	CEP250	Centrosome-associated protein CEP250	-2.16	0.0283

1161	Pepd	Xaa-Pro dipeptidase	1.70	0.0284
1162	#N/A	Retinol dehydrogenase 3	1.85	0.0284
1163	R3hdm2	R3H domain-containing protein 2	-4.38	0.0284
1164	samm50a	Sorting and assembly machinery component 50 homolog A	-3.47	0.0284
1165	POU2F1	POU domain, class 2, transcription factor 1	1.40	0.0285
1166	ARHGEF26	Rho guanine nucleotide exchange factor 26	-2.02	0.0285
1167	Synpo	Synaptopodin	1.48	0.0286
1168	AADAT	Kynurenine/alpha-aminoadipate aminotransferase, mitochondrial	-1.95	0.0286
1169	MYH9	Myosin-9	-1.27	0.0287
1170	TGFBR2	TGF-beta receptor type-2	-2.03	0.0288
1171	PSAP	Prosaposin	1.91	0.0288
1172	BSG	Basigin	1.04	0.0288
1173	SYT16	Synaptotagmin-16	2.16	0.0289
1174	RAB5C	Ras-related protein Rab-5C	1.79	0.0289
1175	EPB41	Protein 4.1	-1.13	0.0290
1176	Kctd5	BTB/POZ domain-containing protein KCTD5	1.24	0.0290
1177	RBMS1	RNA-binding motif, single-stranded-interacting protein 1	1.58	0.0290
1178	B4galnt3	Beta-1,4-N-acetylgalactosaminyltransferase 3	-1.92	0.0291
1179	Sacs	Sacsin	-4.58	0.0291
1180	USP32	Ubiquitin carboxyl-terminal hydrolase 32	-1.32	0.0293
1181	gna14	Guanine nucleotide-binding protein subunit alpha-14	2.17	0.0293
1182	dlgap1	Disks large-associated protein 1	1.80	0.0293
1183	Tf2-9	Transposon Tf2-9 polyprotein	-2.59	0.0293
1184	#N/A	RNA-directed RNA polymerase beta chain	8.51	0.0293
1185	rhbdf1	Inactive rhomboid protein 1	1.14	0.0294
1186	SLC25A22	Mitochondrial glutamate carrier 1	-1.86	0.0294
1187	FHDC1	FH2 domain-containing protein 1	-1.55	0.0294
1188	MYCBP2	E3 ubiquitin-protein ligase MYCBP2	-1.24	0.0295
1189	krt18	Keratin, type I cytoskeletal 18	1.88	0.0295
1190	LTBP2	Latent-transforming growth factor beta-binding protein 2	4.76	0.0296
1191	St3gal3	CMP-N-acetylneuraminate-beta-1,4-galactoside alpha-2,3-sialyltransferase	-1.15	0.0296
1192	Srsf4	Serine/arginine-rich splicing factor 4	-1.44	0.0296
1193	SVIL	Supervillin	-1.70	0.0297
1194	STRN	Striatin	1.01	0.0298
1195	Capn1	Calpain-1 catalytic subunit	-0.97	0.0298
1196	gprc6a	G-protein coupled receptor family C group 6 member A	2.18	0.0299
1197	scoca	Short coiled-coil protein A	1.57	0.0300
1198	ITM2B	Integral membrane protein 2B	1.51	0.0300
1199	smarcb1a	SWI/SNF-related matrix-associated actin-dependent regulator of chromatin subfamily B member 1-A	-1.70	0.0300
1200	QSOX1	Sulfhydryl oxidase 1	2.46	0.0300
1201	rbm5	RNA-binding protein 5	-0.83	0.0300
1202	Rps14	40S ribosomal protein S14	1.60	0.0301
1203	uimc1	BRCA1-A complex subunit RAP80	-1.05	0.0301
1204	gnb1	Guanine nucleotide-binding protein G(I)/G(S)/G(T) subunit beta-1	0.79	0.0301
1205	#N/A	Transposable element Tcb1 transposase	-0.50	0.0301
1206	cpeb4	Cytoplasmic polyadenylation element-binding protein 4	3.75	0.0301
1207	TMED2	Transmembrane emp24 domain-containing protein 2	1.34	0.0303
1208	Trpm4	Transient receptor potential cation channel subfamily M member 4	-1.39	0.0303
1209	TNMD	Tenomodulin	-2.76	0.0303
1210	Kmt2c	Histone-lysine N-methyltransferase 2C	-1.04	0.0303
1211	trio	Triple functional domain protein	-1.16	0.0303
1212	Aldh18a1	Delta-1-pyrroline-5-carboxylate synthase	-2.64	0.0304
1213	TY3B-I	Transposon Ty3-I Gag-Pol polyprotein	-4.51	0.0304
1214	pim2	Serine/threonine-protein kinase pim-2	1.29	0.0304
1215	HMMR	Hyaluronan mediated motility receptor	-2.58	0.0305
1216	Nlrc3	Protein NLRC3	-2.04	0.0305
1217	Rps27	40S ribosomal protein S27	1.96	0.0305
1218	STYK1	Tyrosine-protein kinase STYK1	1.60	0.0306
1219	ANKK1	Ankyrin repeat and protein kinase domain-containing protein 1	1.61	0.0306
1220	Moe	Moesin/ezrin/radixin homolog 1 {ECO:0000250|UniProtKB:P46150}	1.63	0.0308
1221	AATK	Serine/threonine-protein kinase LMTK1	3.46	0.0308
1222	AHR	Aryl hydrocarbon receptor	-3.17	0.0308
1223	Cd63	CD63 antigen	1.35	0.0308
1224	AKAP11	A-kinase anchor protein 11	1.37	0.0309
1225	ZNF462	Zinc finger protein 462	-1.72	0.0310

1226	trio	Triple functional domain protein	-3.69	0.0310
1227	SLC17A5	Sialin	1.32	0.0310
1228	Sfrp1	Secreted frizzled-related protein 1	-4.64	0.0310
1229	CERK	Ceramide kinase	-2.06	0.0311
1230	#N/A	Ras-related protein ORAB-1	1.60	0.0311
1231	Pacsin3	Protein kinase C and casein kinase II substrate protein 3	-1.41	0.0311
1232	Gja10	Gap junction alpha-10 protein	-4.22	0.0312
1233	rps19	40S ribosomal protein S19	1.43	0.0313
1234	NDUFC1	NADH dehydrogenase [ubiquinone] 1 subunit C1, mitochondrial	1.88	0.0313
1235	Cenpe	Centromere-associated protein E {ECO:0000312|EMBL:AAR85498.1}	-2.38	0.0313
1236	RAB19	Ras-related protein Rab-19	1.26	0.0313
1237	ORF1-ORF2	RNA-directed RNA polymerase	8.62	0.0314
1238	NEFM	Neurofilament medium polypeptide	-1.48	0.0314
1239	GDPD5	Glycerophosphodiester phosphodiesterase domain-containing protein 5	4.76	0.0314
1240	#N/A	Stonustoxin subunit beta	-1.43	0.0315
1241	bccip	Protein BCCIP homolog	1.64	0.0315
1242	ABCC4	Multidrug resistance-associated protein 4	3.02	0.0315
1243	mettl14	N6-adenosine-methyltransferase subunit METTL14	-3.60	0.0315
1244	ETS2	Protein C-ets-2	-2.79	0.0316
1245	#N/A	Transposable element Tcb1 transposase	-0.66	0.0316
1246	fahd2	Fumarylacetoacetate hydrolase domain-containing protein 2	1.64	0.0317
1247	Taf12	Transcription initiation factor TFIID subunit 12	1.48	0.0317
1248	Tpd52l1	Tumor protein D53	1.13	0.0317
1249	AIFM3	Apoptosis-inducing factor 3	2.35	0.0317
1250	rft2	Riboflavin transporter 2	2.16	0.0319
1251	sema3d	Semaphorin-3D	-4.05	0.0320
1252	sh2d4a	SH2 domain-containing protein 4A	2.13	0.0321
1253	ZNF81	Zinc finger protein 81	-4.32	0.0321
1254	DIAPH3	Protein diaphanous homolog 3	-1.02	0.0323
1255	gatC	Aspartyl/glutamyl-tRNA(Asn/Gln) amidotransferase subunit C	4.47	0.0323
1256	CCT7	T-complex protein 1 subunit eta	1.72	0.0323
1257	Cdh26	Cadherin-like protein 26	-1.10	0.0323
1258	rps4	40S ribosomal protein S4	1.60	0.0324
1259	scrib	Protein scribble homolog	-2.44	0.0324
1260	SPECC1	Cytospin-B	1.52	0.0325
1261	COX7B	Cytochrome c oxidase subunit 7B, mitochondrial	1.52	0.0325
1262	MNCb-2990	Uncharacterized protein C14orf119 homolog	1.54	0.0325
1263	FRZB	Secreted frizzled-related protein 3	3.06	0.0326
1264	Rpl38	60S ribosomal protein L38	1.38	0.0326
1265	Fcrl5	Fc receptor-like protein 5	-2.88	0.0326
1266	Nudcd2	NudC domain-containing protein 2	1.89	0.0326
1267	Trim39	E3 ubiquitin-protein ligase TRIM39	0.82	0.0326
1268	ERG28	Probable ergosterol biosynthetic protein 28	1.50	0.0327
1269	PSAP	Prosaposin	1.14	0.0327
1270	ACTN4	Alpha-actinin-4 {ECO:0000305}	1.31	0.0328
1271	PPL	Periplakin	1.18	0.0328
1272	Pctp	Phosphatidylcholine transfer protein	1.31	0.0329
1273	egr1	Early growth response protein 1	-2.19	0.0330
1274	ccdc80	Coiled-coil domain-containing protein 80	3.61	0.0332
1275	KLF5	Krueppel-like factor 5	-1.45	0.0332
1276	rps27a	Ubiquitin-40S ribosomal protein S27a	1.39	0.0333
1277	rpl15	60S ribosomal protein L15	1.58	0.0334
1278	ndrg2	Protein NDRG2	-2.48	0.0335
1279	SPINK2	Serine protease inhibitor Kazal-type 2	1.49	0.0336
1280	Ndufa13	NADH dehydrogenase [ubiquinone] 1 alpha subcomplex subunit 13	1.28	0.0337
1281	STK26	Serine/threonine-protein kinase 26 {ECO:0000305}	1.08	0.0337
1282	krt8	Keratin, type II cytoskeletal 8	0.75	0.0337
1283	ELMSAN1	ELM2 and SANT domain-containing protein 1	-4.40	0.0338
1284	NAA25	N-alpha-acetyltransferase 25, NatB auxiliary subunit	-1.02	0.0338
1285	Palld	Palladin	2.74	0.0340
1286	CDKN1B	Cyclin-dependent kinase inhibitor 1B	1.08	0.0341
1287	LIG3	DNA ligase 3	-1.52	0.0342
1288	ARHGAP17	Rho GTPase-activating protein 17	0.95	0.0343
1289	PCDHGC5	Protocadherin gamma-C5	-3.17	0.0344
1290	TBC1D10A	TBC1 domain family member 10A	1.12	0.0344
1291	#N/A	Transposable element Tcb2 transposase	0.56	0.0344

1292	TMEM243	Transmembrane protein 243	2.09	0.0346
1293	Tmem8a	Transmembrane protein 8A	-1.11	0.0347
1294	Tmed7	Transmembrane emp24 domain-containing protein 7	1.39	0.0349
1295	Ppp2cb	Serine/threonine-protein phosphatase 2A catalytic subunit beta isoform	1.55	0.0350
1296	Hnrnpul1	Heterogeneous nuclear ribonucleoprotein U-like protein 1	-0.99	0.0350
1297	DSP	Desmoplakin	-1.64	0.0350
1298	cygb2	Cytoglobin-2	3.13	0.0350
1299	VAPA	Vesicle-associated membrane protein-associated protein A	1.23	0.0352
1300	eef1as	Elongation factor 1-alpha, somatic form	1.93	0.0352
1301	SZT2	Protein SZT2	-1.50	0.0353
1302	RPL6	60S ribosomal protein L6	1.35	0.0353
1303	K02A2.6	Uncharacterized protein K02A2.6	-1.72	0.0353
1304	#N/A	Transposable element Tcb2 transposase	-1.12	0.0353
1305	LRP1	Low-density lipoprotein receptor-related protein 1	-1.38	0.0355
1306	WDR74	WD repeat-containing protein 74	-1.67	0.0356
1307	ANXA4	Annexin A4	1.12	0.0356
1308	DLG5	Disks large homolog 5	-1.23	0.0356
1309	Gsr	Glutathione reductase, mitochondrial	1.56	0.0357
1310	rpl34	60S ribosomal protein L34	1.70	0.0357
1311	SPT6	Transcription elongation factor SPT6	-2.59	0.0358
1312	ATP5F1E	ATP synthase subunit epsilon, mitochondrial	1.83	0.0358
1313	PLXNB1	Plexin-B1	-2.10	0.0358
1314	Scarb2	Lysosome membrane protein 2	1.25	0.0358
1315	NCAPG	Condensin complex subunit 3	-3.36	0.0358
1316	SYNE3	Nesprin-3	1.59	0.0358
1317	ATP11A	Probable phospholipid-transporting ATPase IH	-1.41	0.0358
1318	DSC3	Desmocollin-3	2.23	0.0358
1319	cxadr	Coxsackievirus and adenovirus receptor homolog	1.27	0.0358
1320	TAGLN	Transgelin	2.01	0.0358
1321	Chst2	Carbohydrate sulfotransferase 2	1.73	0.0358
1322	Adpgk	ADP-dependent glucokinase	1.04	0.0358
1323	ELMO2	Engulfment and cell motility protein 2	-2.15	0.0359
1324	grhl2	Grainyhead-like protein 2 homolog	-1.30	0.0360
1325	FNBP4	Formin-binding protein 4	-0.82	0.0360
1326	SZT2	Protein SZT2	-1.22	0.0360
1327	fgfr1a	Fibroblast growth factor receptor 1-A	-2.72	0.0360
1328	tmem258	Transmembrane protein 258	1.48	0.0360
1329	EIF4G3	Eukaryotic translation initiation factor 4 gamma 3	-1.66	0.0362
1330	#N/A	Intestinal mucin-like protein	2.16	0.0362
1331	amotl2a	Angiomotin-like 2a	2.01	0.0362
1332	HDAC7	Histone deacetylase 7	1.77	0.0363
1333	cdk-4	Cyclin-dependent kinase 4 homolog {ECO:0000305}	3.14	0.0363
1334	LRRFIP1	Leucine-rich repeat flightless-interacting protein 1	1.49	0.0363
1335	PTPRO	Receptor-type tyrosine-protein phosphatase O	-4.62	0.0363
1336	Spats2	Spermatogenesis-associated serine-rich protein 2	1.09	0.0364
1337	CTDSP2	Carboxy-terminal domain RNA polymerase II polypeptide A small phosphatase 2	1.13	0.0365
1338	psbA1	Photosystem II protein D1 1 {ECO:0000255|HAMAP-Rule:MF_01379}	6.94	0.0366
1339	Cct5	T-complex protein 1 subunit epsilon	2.34	0.0366
1340	ankrd37	Ankyrin repeat domain-containing protein 37	2.30	0.0367
1341	#N/A	Transposable element Tcb1 transposase	-0.59	0.0367
1342	Pol	LINE-1 retrotransposable element ORF2 protein	-2.80	0.0367
1343	Usp9x	Probable ubiquitin carboxyl-terminal hydrolase FAF-X	1.21	0.0367
1344	TRPM7	Transient receptor potential cation channel subfamily M member 7	-1.27	0.0368
1345	Edem3	ER degradation-enhancing alpha-mannosidase-like protein 3	-4.20	0.0369
1346	57/58	DNA polymerase	2.00	0.0369
1347	VDAC1	Voltage-dependent anion-selective channel protein 1	1.46	0.0370
1348	HIP1R	Huntingtin-interacting protein 1-related protein	1.26	0.0370
1349	CLDN3	Claudin-3	2.17	0.0371
1350	IFI44	Interferon-induced protein 44	1.90	0.0371
1351	kit	Mast/stem cell growth factor receptor Kit	2.30	0.0371
1352	Cd68	Macrosialin	0.95	0.0372
1353	FXYD6	FXYD domain-containing ion transport regulator 6	-3.40	0.0372
1354	Bnipl	Bcl-2/adenovirus E1B 19 kDa-interacting protein 2-like protein	-4.09	0.0372
1355	Phf14	PHD finger protein 14	-2.07	0.0372
1356	ATP6V0B	V-type proton ATPase 21 kDa proteolipid subunit	1.22	0.0373

1357	CDK17	Cyclin-dependent kinase 17	-4.33	0.0373
1358	RPL22	60S ribosomal protein L22	1.42	0.0373
1359	TOB1	Protein Tob1	0.94	0.0375
1360	Neu1	Sialidase-1	2.64	0.0375
1361	Csde1	Cold shock domain-containing protein E1	-1.15	0.0376
1362	cep290	Centrosomal protein of 290 kDa	-1.70	0.0376
1363	MALT1	Mucosa-associated lymphoid tissue lymphoma translocation protein 1	0.83	0.0376
1364	Phf6	PHD finger protein 6	-3.62	0.0377
1365	nol10	Nucleolar protein 10	-1.83	0.0377
1366	SLC25A21	Mitochondrial 2-oxodicarboxylate carrier	-4.43	0.0377
1367	junb	Transcription factor jun-B	-1.30	0.0377
1368	FAM200A	Protein FAM200A	2.15	0.0377
1369	Jmjd7	JmjC domain-containing protein 7	1.91	0.0378
1370	FAM169A	Soluble lamin-associated protein of 75 kDa	-1.02	0.0378
1371	CACNA1B	Voltage-dependent N-type calcium channel subunit alpha-1B	-1.81	0.0378
1372	yipf4	Protein YIPF4	0.94	0.0379
1373	CTTNBP2NL	CTTNBP2 N-terminal-like protein	1.61	0.0380
1374	ARPC1B	Actin-related protein 2/3 complex subunit 1B	1.75	0.0380
1375	VGLL4	Transcription cofactor vestigial-like protein 4	-2.04	0.0381
1376	#N/A	Cytochrome c oxidase subunit 6C-1	1.57	0.0383
1377	rps3a	40S ribosomal protein S3a {ECO:0000255|HAMAP-Rule:MF_03122}	1.51	0.0384
1378	GIMAP2	GTPase IMAP family member 2	0.99	0.0384
1379	PLXNB2	Plexin-B2	-0.89	0.0384
1380	tmem167b	Protein kish-B	1.65	0.0384
1381	Rhobtb2	Rho-related BTB domain-containing protein 2	-1.72	0.0385
1382	TMEM121	Transmembrane protein 121	3.33	0.0385
1383	wwc2	Protein WWC2	1.02	0.0385
1384	FDFT1	Squalene synthase	1.54	0.0385
1385	Gtpbp1	GTP-binding protein 1	1.77	0.0385
1386	Snx18	Sorting nexin-18	1.61	0.0386
1387	ITM2B	Integral membrane protein 2B	0.76	0.0386
1388	Cdc25a	M-phase inducer phosphatase 1	-3.86	0.0386
1389	cfl1-a	Cofilin-1-A	1.08	0.0386
1390	GAD1	Glutamate decarboxylase 1	2.54	0.0387
1391	CHD4	Chromodomain-helicase-DNA-binding protein 4	-1.94	0.0387
1392	ICE1	Little elongation complex subunit 1	-2.23	0.0387
1393	SNTB1	Beta-1-syntrophin	2.98	0.0387
1394	TMEM131	Transmembrane protein 131	1.61	0.0387
1395	Prkce	Protein kinase C epsilon type	-1.44	0.0388
1396	GLUL	Glutamine synthetase	1.03	0.0388
1397	med15	Mediator of RNA polymerase II transcription subunit 15	-1.45	0.0388
1398	FASN	Fatty acid synthase	1.82	0.0391
1399	Gramd4	GRAM domain-containing protein 4	-1.14	0.0392
1400	Psmd7	26S proteasome non-ATPase regulatory subunit 7	1.80	0.0392
1401	NLRP1	NACHT, LRR and PYD domains-containing protein 1	-0.96	0.0392
1402	ncoa2	Nuclear receptor coactivator 2 {ECO:0000303|PubMed:17583703}	-1.24	0.0392
1403	TRIM25	E3 ubiquitin/ISG15 ligase TRIM25	-0.95	0.0393
1404	Tspo	Translocator protein	1.67	0.0393
1405	got2	Aspartate aminotransferase, mitochondrial	1.86	0.0393
1406	ddt	D-dopachrome decarboxylase	1.72	0.0394
1407	SLC35A4	Probable UDP-sugar transporter protein SLC35A4	1.81	0.0395
1408	ARCN1	Coatomer subunit delta	0.73	0.0395
1409	ANK3	Ankyrin-3	-2.67	0.0395
1410	Hdac1	Histone deacetylase 1	-1.31	0.0395
1411	DSP	Desmoplakin	-1.19	0.0395
1412	MYO1D	Unconventional myosin-Id	1.22	0.0395
1413	Jund	Transcription factor jun-D	-1.51	0.0396
1414	tc1a	Transposable element Tc1 transposase	1.46	0.0396
1415	Nt5dc2	5'-nucleotidase domain-containing protein 2	-1.44	0.0396
1416	ENDOD1	Endonuclease domain-containing 1 protein	-6.03	0.0397
1417	Arhgef12	Rho guanine nucleotide exchange factor 12	-1.38	0.0398
1418	Cit	Citron Rho-interacting kinase	-5.51	0.0398
1419	CCSER1	Serine-rich coiled-coil domain-containing protein 1	-1.61	0.0398
1420	Enc1	Ectoderm-neural cortex protein 1	4.99	0.0399
1421	rps6	40S ribosomal protein S6	1.38	0.0399
1422	cav2	Caveolin-2	1.38	0.0400

1423	Mybl1	Myb-related protein A	-2.26	0.0401
1424	ZFP36L1	Zinc finger protein 36, C3H1 type-like 1	1.16	0.0401
1425	#N/A	Natterin-like protein	-5.66	0.0401
1426	Myo9b	Unconventional myosin-IXb	-1.03	0.0403
1427	RHA2	Rhodotorucin-A peptides type 2	-2.05	0.0403
1428	CERS5	Ceramide synthase 5	1.46	0.0403
1429	cep131	Centrosomal protein of 131 kDa	6.89	0.0404
1430	CCR3	C-C chemokine receptor type 3	5.11	0.0406
1431	Vmp1	Vacuole membrane protein 1	-2.02	0.0408
1432	RBM5	RNA-binding protein 5	-1.68	0.0408
1433	#N/A	Glutathione S-transferase A	2.49	0.0408
1434	PALLD	Palladin	2.89	0.0409
1435	Myo1e	Unconventional myosin-Ie	0.83	0.0409
1436	tc1a	Transposable element Tc1 transposase	-0.68	0.0410
1437	Plekhg5	Pleckstrin homology domain-containing family G member 5	-2.25	0.0411
1438	Cntn1	Contactin-1	1.03	0.0412
1439	Ube2l3	Ubiquitin-conjugating enzyme E2 L3	1.51	0.0412
1440	AP3S2	AP-3 complex subunit sigma-2	2.20	0.0412
1441	pim2	Serine/threonine-protein kinase pim-2	1.32	0.0412
1442	MXD4	Max dimerization protein 4	1.44	0.0412
1443	pol	RNA-directed DNA polymerase from mobile element jockey	-1.25	0.0412
1444	MAP3K14	Mitogen-activated protein kinase kinase kinase 14	-0.88	0.0413
1445	PHF20	PHD finger protein 20	-1.25	0.0414
1446	MTHFS	5-formyltetrahydrofolate cyclo-ligase	3.35	0.0415
1447	ELOVL6	Elongation of very long chain fatty acids protein 6 {ECO:0000255|HAMAP-Rule:MF_03206, ECO:0000305}	1.03	0.0415
1448	#N/A	Intermediate filament protein ON3	2.99	0.0416
1449	CCNG1	Cyclin-G1	1.77	0.0416
1450	chtf18	Chromosome transmission fidelity protein 18 homolog	-3.83	0.0417
1451	POLR3A	DNA-directed RNA polymerase III subunit RPC1	-1.50	0.0419
1452	#N/A	Transposon TX1 uncharacterized 149 kDa protein	4.35	0.0419
1453	Nsd2	Histone-lysine N-methyltransferase NSD2	-2.63	0.0419
1454	ATP6V1B2	V-type proton ATPase subunit B, brain isoform	1.01	0.0419
1455	MLKL	Mixed lineage kinase domain-like protein	-0.88	0.0419
1456	ndel1a	Nuclear distribution protein nudE-like 1-A	1.52	0.0419
1457	SEPTIN7	Septin-7	1.46	0.0420
1458	PNISR	Arginine/serine-rich protein PNISR	-0.95	0.0421
1459	Rab25	Ras-related protein Rab-25	1.66	0.0421
1460	AIFM1	Apoptosis-inducing factor 1, mitochondrial	-1.46	0.0421
1461	DSP	Desmoplakin	-2.51	0.0422
1462	FRMD1	FERM domain-containing protein 1	-1.07	0.0422
1463	VASP	Vasodilator-stimulated phosphoprotein	1.29	0.0423
1464	SPAG9	C-Jun-amino-terminal kinase-interacting protein 4	-1.32	0.0423
1465	ITPR1	Inositol 1,4,5-trisphosphate receptor type 1	-3.49	0.0424
1466	Palld	Palladin	2.10	0.0424
1467	SKI	Ski oncogene	-1.26	0.0424
1468	Alg5	Dolichyl-phosphate beta-glucosyltransferase	1.00	0.0424
1469	Snx9	Sorting nexin-9	-1.25	0.0425
1470	#N/A	Natterin-like protein	-1.59	0.0425
1471	Mybl1	Myb-related protein A	-4.49	0.0425
1472	ADAM17	Disintegrin and metalloproteinase domain-containing protein 17	-3.70	0.0425
1473	EXOSC1	Exosome complex component CSL4	1.02	0.0426
1474	actr2a	Actin-related protein 2-A	1.04	0.0427
1475	WDR81	WD repeat-containing protein 81	1.91	0.0428
1476	Ccl20	C-C motif chemokine 20	4.34	0.0428
1477	FLNC	Filamin-C	2.36	0.0428
1478	sltm	SAFB-like transcription modulator	-0.99	0.0429
1479	max	Protein max	1.15	0.0430
1480	Tet3	Methylcytosine dioxygenase TET3	1.25	0.0430
1481	CHD3	Chromodomain-helicase-DNA-binding protein 3	-4.63	0.0430
1482	ARID1B	AT-rich interactive domain-containing protein 1B	-1.04	0.0431
1483	EPS8L1	Epidermal growth factor receptor kinase substrate 8-like protein 1	1.44	0.0431
1484	Ppp2cb	Serine/threonine-protein phosphatase 2A catalytic subunit beta isoform	1.43	0.0431
1485	Ncor1	Nuclear receptor corepressor 1	-1.04	0.0431
1486	Sugt1	Protein SGT1 homolog {ECO:0000250|UniProtKB:Q08446}	1.20	0.0431
1487	URGCP	Up-regulator of cell proliferation	-8.44	0.0432

1488	ddx42	ATP-dependent RNA helicase DDX42	-0.85	0.0432
1489	YPEL5	Protein yippee-like 5	1.71	0.0432
1490	yap1	Transcriptional coactivator YAP1	-1.46	0.0432
1491	ARID1B	AT-rich interactive domain-containing protein 1B	-1.92	0.0433
1492	svopl	Putative transporter SVOPL	1.50	0.0433
1493	CDC20	Cell division cycle protein 20 homolog	1.47	0.0434
1494	Gpank1	G patch domain and ankyrin repeat-containing protein 1	2.68	0.0434
1495	rps24	40S ribosomal protein S24	1.23	0.0435
1496	NCOA7	Nuclear receptor coactivator 7	-1.26	0.0436
1497	ST13	Hsc70-interacting protein	1.40	0.0436
1498	PLEKHA7	Pleckstrin homology domain-containing family A member 7	-4.27	0.0436
1499	Hip1r	Huntingtin-interacting protein 1-related protein	1.50	0.0437
1500	rpl10a	60S ribosomal protein L10a	1.51	0.0438
1501	ACTR2	Actin-related protein 2	-2.28	0.0438
1502	PTGDR2	Prostaglandin D2 receptor 2	-4.49	0.0438
1503	ARAP2	Arf-GAP with Rho-GAP domain, ANK repeat and PH domain-containing protein 2	-4.22	0.0438
1504	ANPEP	Aminopeptidase N	1.92	0.0438
1505	CGN	Cingulin	1.67	0.0438
1506	Ccni	Cyclin-I	1.04	0.0438
1507	p1	RNA-directed RNA polymerase	8.50	0.0439
1508	VMP1	Vacuole membrane protein 1	-1.77	0.0439
1509	Gtf2f2	General transcription factor IIF subunit 2	-1.75	0.0439
1510	SLC29A1	Equilibrative nucleoside transporter 1	-4.47	0.0441
1511	Rpl32	60S ribosomal protein L32	1.54	0.0441
1512	anks1b	Ankyrin repeat and sterile alpha motif domain-containing protein 1B	-1.58	0.0441
1513	TP63	Tumor protein 63	-1.15	0.0441
1514	#N/A	Tubulin alpha chain	1.21	0.0441
1515	Mga	MAX gene-associated protein	-1.10	0.0441
1516	MPEG1	Macrophage-expressed gene 1 protein	2.05	0.0442
1517	RNF7	RING-box protein 2	1.84	0.0443
1518	RPL3	60S ribosomal protein L3	-2.48	0.0443
1519	#N/A	UPF0764 protein C16orf89 homolog	2.11	0.0443
1520	GIMAP4	GTPase IMAP family member 4	-5.74	0.0443
1521	Dsp	Desmoplakin	-5.46	0.0443
1522	Lamp1	Lysosome-associated membrane glycoprotein 1	1.27	0.0446
1523	MFSD13A	Transmembrane protein 180 {ECO:0000250|UniProtKB:Q14CX5}	2.20	0.0446
1524	CIPC	CLOCK-interacting pacemaker	-2.20	0.0446
1525	FAXDC2	Fatty acid hydroxylase domain-containing protein 2	1.47	0.0447
1526	Msl1	Male-specific lethal 1 homolog	-4.09	0.0447
1527	SLCO5A1	Solute carrier organic anion transporter family member 5A1	-4.50	0.0449
1528	Anxa4	Annexin A4	1.25	0.0450
1529	SFMBT2	Scm-like with four MBT domains protein 2	-1.42	0.0451
1530	TASP1	Threonine aspartase 1	-2.21	0.0451
1531	HHLA2	HERV-H LTR-associating protein 2	1.40	0.0452
1532	RBM5	RNA-binding protein 5	-1.04	0.0452
1533	sumo3l	Small ubiquitin-related modifier 3-like	1.59	0.0452
1534	Syt1	Synaptotagmin 1	1.31	0.0452
1535	UTY	Histone demethylase UTY	-1.78	0.0453
1536	UBP1	Upstream-binding protein 1	-1.00	0.0456
1537	BACH2	Transcription regulator protein BACH2	1.37	0.0456
1538	CHD9	Chromodomain-helicase-DNA-binding protein 9	-0.80	0.0456
1539	KIF21A	Kinesin-like protein KIF21A	-0.98	0.0456
1540	KCTD20	BTB/POZ domain-containing protein KCTD20	1.73	0.0456
1541	CLCC1	Chloride channel CLIC-like protein 1	1.65	0.0457
1542	PARP3	Poly [ADP-ribose] polymerase 3	1.98	0.0457
1543	PRDX1	Peroxiredoxin-1	1.29	0.0457
1544	Tspan1	Tetraspanin-1	2.84	0.0457
1545	MATR3	Matrin-3	-1.05	0.0457
1546	rpl7a	60S ribosomal protein L7a	1.54	0.0458
1547	ubqJ	Polyubiquitin-J	0.81	0.0459
1548	Plpp4	Phospholipid phosphatase 4 {ECO:0000250|UniProtKB:Q5VZY2}	0.94	0.0459
1549	TSPAN3	Tetraspanin-3	4.29	0.0459
1550	NCAPG	Condensin complex subunit 3	-3.20	0.0459
1551	Mga	MAX gene-associated protein	-1.12	0.0459
1552	Lrp4	Low-density lipoprotein receptor-related protein 4	-2.29	0.0459

1553	COL20A1	Collagen alpha-1(XX) chain	-1.87	0.0460
1554	grhl2	Grainyhead-like protein 2 homolog	-1.24	0.0461
1555	LEPR	Leptin receptor	-3.40	0.0461
1556	yars	Tyrosine--tRNA ligase, cytoplasmic	2.56	0.0462
1557	VDAC1	Voltage-dependent anion-selective channel protein 1	1.51	0.0462
1558	Slc25a18	Mitochondrial glutamate carrier 2	-2.01	0.0462
1559	#N/A	Transposable element Tcb2 transposase	-0.83	0.0463
1560	POLR2I	DNA-directed RNA polymerase II subunit RPB9	1.77	0.0463
1561	AGL	Glycogen debranching enzyme {ECO:0000250|UniProtKB:P35573}	-4.51	0.0463
1562	ZNF32	Zinc finger protein 32	-4.29	0.0464
1563	PEG10	Retrotransposon-derived protein PEG10	-1.37	0.0465
1564	STXBP5	Syntaxin-binding protein 5	-1.08	0.0465
1565	TBCB	Tubulin-folding cofactor B	1.75	0.0465
1566	MFAP3L	Microfi brillar-associated protein 3-like	1.79	0.0468
1567	Epb41l1	Band 4.1-like protein 1	-0.92	0.0468
1568	ZNF236	Zinc finger protein 236	-2.09	0.0468
1569	RTL1	Retrotransposon-like protein 1	-2.42	0.0468
1570	#N/A	14-3-3 protein beta/alpha-1	1.46	0.0468
1571	SYT1	Synaptotagmin-1	2.38	0.0468
1572	Fam219b	Protein FAM219B	1.71	0.0469
1573	#N/A	Transposon TX1 uncharacterized 149 kDa protein	-1.38	0.0469
1574	trim71	E3 ubiquitin-protein ligase TRIM71	3.24	0.0470
1575	TRAP1	Heat shock protein 75 kDa, mitochondrial	1.74	0.0470
1576	SSBP2	Single-stranded DNA-binding protein 2	-1.50	0.0471
1577	GNS	N-acetylglucosamine-6-sulfatase	1.30	0.0472
1578	Kiaa1109	Uncharacterized protein KIAA1109	-1.41	0.0472
1579	UBXN4	UBX domain-containing protein 4	1.61	0.0473
1580	#N/A	Niban-like protein 1	-1.78	0.0473
1581	SLC6A11	Sodium- and chloride-dependent GABA transporter 3	-3.70	0.0474
1582	#N/A	Myosin heavy chain, skeletal muscle, adult	2.90	0.0475
1583	Pc	Pyruvate carboxylase, mitochondrial	-1.15	0.0477
1584	ldhb	L-lactate dehydrogenase B chain	1.59	0.0477
1585	cct3	T-complex protein 1 subunit gamma	0.98	0.0477
1586	shcbp1-b	SHC SH2 domain-binding protein 1 homolog B	-2.54	0.0477
1587	NINL	Ninein-like protein	1.88	0.0478
1588	TECPR1	Tectonin beta-propeller repeat-containing protein 1	-3.71	0.0478
1589	CLIC4	Chloride intracellular channel protein 4	4.78	0.0479
1590	tmem251	Transmembrane protein 251	1.78	0.0479
1591	ANK3	Ankyrin-3	-2.12	0.0480
1592	Cebpd	CCAAT/enhancer-binding protein delta	-1.85	0.0480
1593	ppp1cc	Serine/threonine-protein phosphatase PP1-gamma catalytic subunit	1.48	0.0481
1594	Hcfc1	Host cell factor 1	-1.57	0.0481
1595	rpl35a	60S ribosomal protein L35a	1.48	0.0481
1596	#N/A	Gastrula zinc finger protein XlCGF8.2DB	-4.50	0.0482
1597	Bfar	Bifunctional apoptosis regulator	0.76	0.0482
1598	#N/A	RNA-directed DNA polymerase homolog	3.48	0.0482
1599	CGREF1	Cell growth regulator with EF hand domain protein 1	-1.37	0.0482
1600	tc3a	Transposable element Tc3 transposase	0.94	0.0482
1601	MARVELD3	MARVEL domain-containing protein 3	1.25	0.0482
1602	LIN7C	Protein lin-7 homolog C	1.74	0.0483
1603	GLCCI1	Glucocorticoid-induced transcript 1 protein	1.92	0.0483
1604	Xdh	Xanthine dehydrogenase/oxidase	3.09	0.0486
1605	FOSL2	Fos-related antigen 2	-3.37	0.0487
1606	STAT1	Signal transducer and activator of transcription 1	-1.17	0.0487
1607	Dnase1l3	Deoxyribonuclease gamma	1.87	0.0487
1608	Ctnnd1	Catenin delta-1	-1.72	0.0487
1609	V-SEA	Tyrosine-protein kinase transforming protein SEA	-2.94	0.0487
1610	URH1	Probable uridine nucleosidase 1	-1.84	0.0487
1611	Bard1	BRCA1-associated RING domain protein 1	-4.12	0.0488
1612	#N/A	Transposon TX1 uncharacterized 149 kDa protein	-1.28	0.0488
1613	FUNDC1	FUN14 domain-containing protein 1	1.45	0.0488
1614	#N/A	Cornifin alpha	1.84	0.0489
1615	TACC1	Transforming acidic coiled-coil-containing protein 1	-0.59	0.0491
1616	gskip	GSK3-beta interaction protein	1.25	0.0491
1617	SRSF11	Serine/arginine-rich splicing factor 11	-1.10	0.0491
1618	SEPTIN4	Septin-4	1.88	0.0491

1619	ZNF568	Zinc finger protein 568	-3.03	0.0494
1620	pol	Retrovirus-related Pol polyprotein from transposon opus	3.22	0.0494
1621	STK36	Serine/threonine-protein kinase 36	-4.45	0.0495
1622	Myh9	Myosin-9	1.20	0.0495
1623	#N/A	Tubulin alpha-1 chain	1.74	0.0498
1624	krt13	Keratin, type I cytoskeletal 13	1.90	0.0499
1625	FBP1	Fructose-1,6-bisphosphatase 1	2.34	0.0499
1626	KLF9	Krueppel-like factor 9	-2.05	0.0499
1627	tc1a	Transposable element Tc1 transposase	-0.85	0.0499
1628	ube2d2	Ubiquitin-conjugating enzyme E2 D2	1.35	0.0499

Lake 223 vs Lake 373

373 is the base e.g. Positive FC = upregulated in Lake 223 relative to Lake 373

1	cyp3a27	Cytochrome P450 3A27	4.80	1.35E-26
2	Fam111a	Protein FAM111A	5.98	9.28E-26
3	Nt5c1a	Cytosolic 5'-nucleotidase 1A	4.10	9.43E-26
4	GIMAP4	GTPase IMAP family member 4	-5.96	6.47E-20
5	MDV087	Uncharacterized gene 87 protein	11.00	2.77E-19
6	H2-K1	H-2 class I histocompatibility antigen, K-B alpha chain	7.22	3.00E-19
7	gag-pol	Gag-Pol polyprotein	-3.85	5.33E-17
8	Vwa7	von Willebrand factor A domain-containing protein 7	6.37	2.03E-16
9	GIMAP4	GTPase IMAP family member 4	-10.02	8.98E-16
10	Psmb8	Proteasome subunit beta type-8	9.53	1.56E-14
11	Urgcp	Up-regulator of cell proliferation	5.82	1.95E-14
12	samhd1	Deoxynucleoside triphosphate triphosphohydrolase SAMHD1	4.12	3.64E-14
13	vtg1	Vitellogenin	9.30	4.66E-14
14	B4GALNT1	Beta-1,4 N-acetylgalactosaminyltransferase 1	4.12	8.54E-14
15	Nos2	Nitric oxide synthase, inducible	7.75	3.03E-13
16	ERVV-1	Endogenous retrovirus group V member 1 Env polyprotein	-3.45	3.10E-13
17	NLRP3	NACHT, LRR and PYD domains-containing protein 3	-4.33	1.05E-12
18	NUGGC	Nuclear GTPase SLIP-GC	-5.38	1.11E-12
19	vtg1	Vitellogenin	8.91	2.10E-12
20	cyp3a27	Cytochrome P450 3A27	4.59	6.71E-12
21	LECASAL	Mannose-specific lectin	-9.01	1.25E-11
22	RNF213	E3 ubiquitin-protein ligase RNF213	8.45	1.61E-10
23	IFI30	Gamma-interferon-inducible lysosomal thiol reductase	2.69	2.81E-10
24	pol	Retrovirus-related Pol polyprotein from transposon gypsy	3.48	3.10E-10
25	Eppk1	Epiplakin	-3.94	3.83E-10
26	GIMAP7	GTPase IMAP family member 7	9.33	4.87E-10
27	#N/A	Class I histocompatibility antigen, F10 alpha chain	8.62	5.23E-10
28	cyp1a3	Cytochrome P450 1A3	5.63	8.73E-10
29	GIMAP4	GTPase IMAP family member 4	8.14	1.80E-09
30	RNF213	E3 ubiquitin-protein ligase RNF213	8.26	3.13E-09
31	Iigp1	Interferon-inducible GTPase 1	6.58	3.29E-09
32	GPR50	Melatonin-related receptor	4.88	4.60E-09
33	GIMAP7	GTPase IMAP family member 7	9.11	7.87E-09
34	Vwa7	von Willebrand factor A domain-containing protein 7	5.45	1.19E-08
35	Plec	Plectin	-3.96	1.33E-08
36	ENDOD1	Endonuclease domain-containing 1 protein	-8.33	1.84E-08
37	#N/A	RNA-dependent RNA polymerase	8.19	2.44E-08
38	#N/A	Neoverrucotoxin subunit beta	-6.57	4.39E-08
39	Hspa12a	Heat shock 70 kDa protein 12A	9.81	4.56E-08
40	#N/A	Natterin-like protein	-5.27	6.71E-08
41	#N/A	Intestinal mucin-like protein	-3.19	8.52E-08
42	Plec	Plectin	-3.44	8.63E-08
43	DEPTOR	DEP domain-containing mTOR-interacting protein	-3.20	9.63E-08
44	ORF1	RNA-directed RNA polymerase	7.97	1.10E-07
45	NLRC3	Protein NLRC3	4.68	1.18E-07
46	#N/A	DLA class I histocompatibility antigen, A9/A9 alpha chain	2.66	1.47E-07
47	plk1	Serine/threonine-protein kinase PLK1	-4.68	1.49E-07
48	SOCS3	Suppressor of cytokine signaling 3	-3.80	2.14E-07
49	COL6A2	Collagen alpha-2(VI) chain	-4.68	2.26E-07

50	#N/A	Natterin-like protein	-6.04	2.90E-07
51	cnpy3	Protein canopy homolog 3	3.89	5.96E-07
52	hsp90a.1	Heat shock protein HSP 90-alpha 1	5.63	7.99E-07
53	Nlrp1b	NACHT, LRR and PYD domains-containing protein 1b allele 1 {ECO	-4.97	8.45E-07
54	ABCB1	Multidrug resistance protein 1	5.62	8.57E-07
55	GBP2	Guanylate-binding protein 2	7.71	1.01E-06
56	MUC5B	Mucin-5B	-3.47	1.21E-06
57	HSP90AB1	Heat shock protein HSP 90-beta	5.04	1.60E-06
58	GIMAP5	GTPase IMAP family member 5	5.47	1.68E-06
59	ERVFC1	Endogenous retrovirus group FC1 Env polyprotein	-6.19	3.50E-06
60	ANO9	Anoctamin-9	-2.38	4.47E-06
61	ALOXE3	Hydroperoxide isomerase ALOXE3	-5.72	4.65E-06
62	Ptgr1	Prostaglandin reductase 1	5.02	5.07E-06
63	mapk14a	Mitogen-activated protein kinase 14A	-4.00	6.15E-06
64	SAMD9L	Sterile alpha motif domain-containing protein 9-like	-1.98	6.93E-06
65	sspH2	E3 ubiquitin-protein ligase sspH2	2.18	7.58E-06
66	CCL3	C-C motif chemokine 3	4.19	7.98E-06
67	Plekhf1	Pleckstrin homology domain-containing family F member 1	2.35	1.05E-05
68	#N/A	Transposable element Tcb1 transposase	3.48	1.24E-05
69	#N/A	Natterin-like protein	-7.55	1.26E-05
70	ORF56	Uncharacterized protein ORF56	3.67	1.28E-05
71	PLAU	Urokinase-type plasminogen activator	-4.71	1.33E-05
72	vUbi	Ubiquitin-like protein	2.47	1.36E-05
73	hbb1	Hemoglobin subunit beta-1	7.70	1.41E-05
74	IFI44	Interferon-induced protein 44	5.73	1.55E-05
75	#N/A	ES1 protein homolog, mitochondrial	2.42	1.65E-05
76	AHCYL2	Putative adenosylhomocysteinase 3	-6.53	1.73E-05
77	DSP	Desmoplakin	-1.86	2.09E-05
78	ECU02_0740i	Ubiquitin	2.06	2.11E-05
79	p65	Proline-rich P65 protein	3.40	2.15E-05
80	HSPA12A	Heat shock 70 kDa protein 12A	8.38	2.20E-05
81	ORF1	Replicase polyprotein	7.28	2.28E-05
82	SYNE1	Nesprin-1	-2.09	2.29E-05
83	AHCYL2	Adenosylhomocysteinase 3	-6.54	2.29E-05
84	SH2D3A	SH2 domain-containing protein 3A	-2.80	2.32E-05
85	MUC5AC	Mucin-5AC {ECO	-3.62	2.81E-05
86	Tf2-9	Transposon Tf2-9 polyprotein	4.73	3.22E-05
87	NCAPG	Condensin complex subunit 3	-5.04	3.43E-05
88	hsp90ab1	Heat shock protein HSP 90-beta	3.95	3.51E-05
89	PSAP	Prosaposin	2.62	3.88E-05
90	tc1a	Transposable element Tc1 transposase	-2.22	4.00E-05
91	#N/A	Class I histocompatibility antigen, F10 alpha chain	-6.44	4.02E-05
92	PDZD2	PDZ domain-containing protein 2	-2.57	4.15E-05
93	DTX3L	E3 ubiquitin-protein ligase DTX3L	6.93	4.38E-05
94	Slco2b1	Solute carrier organic anion transporter family member 2B1	-3.13	4.67E-05
95	Foxd1	Forkhead box protein D1	7.56	5.30E-05
96	CD74	HLA class II histocompatibility antigen gamma chain	2.08	5.72E-05
97	PDZD2	PDZ domain-containing protein 2	-2.46	6.00E-05
98	fam50a	Protein FAM50A	2.28	7.86E-05
99	SLC25A20	Mitochondrial carnitine/acylcarnitine carrier protein	7.01	8.26E-05
100	PEG10	Retrotransposon-derived protein PEG10	7.95	8.73E-05
101	ERBB3	Receptor tyrosine-protein kinase erbB-3	-2.72	0.0001
102	TGL2	Protein-glutamine gamma-glutamyltransferase 2	-2.62	0.0001
103	#N/A	Salivary plasminogen activator beta	-4.30	0.0001
104	KLF5	Krueppel-like factor 5	-1.64	0.0001
105	Ddr1	Epithelial discoidin domain-containing receptor 1	-2.61	0.0001
106	Rsbn1	Round spermatid basic protein 1	4.59	0.0001
107	Tf2-9	Transposon Tf2-9 polyprotein	-1.97	0.0001
108	VMP1	Vacuole membrane protein 1	-3.18	0.0001
109	PDE4DIP	Myomegalin	-2.91	0.0001
110	#N/A	Uncharacterized protein C1orf106 homolog	-2.70	0.0001
111	#N/A	Natterin-like protein	-4.57	0.0001
112	IGFBP3	Insulin-like growth factor-binding protein 3	-4.23	0.0001
113	IGFBP3	Insulin-like growth factor-binding protein 3	-6.36	0.0002
114	GIMAP7	GTPase IMAP family member 7	5.23	0.0002
115	ANO9	Anoctamin-9	-1.92	0.0002

116	ANXA13	Annexin A13	6.67	0.0002
117	FAT2	Protocadherin Fat 2	-2.60	0.0002
118	#N/A	Zinc-binding protein A33	6.53	0.0002
119	hba4	Hemoglobin subunit alpha-4	5.37	0.0002
120	SAMD9	Sterile alpha motif domain-containing protein 9	-3.86	0.0002
121	ARHGDIA	Rho GDP-dissociation inhibitor 1	1.63	0.0002
122	UGT2A3	UDP-glucuronosyltransferase 2A3	7.24	0.0002
123	Me3	NADP-dependent malic enzyme, mitochondrial	6.90	0.0002
124	Cd200	OX-2 membrane glycoprotein	-3.65	0.0002
125	GMNC	Geminin coiled-coil domain-containing protein 1	6.55	0.0002
126	Tf2-9	Transposon Tf2-9 polyprotein	7.81	0.0002
127	GPX2	Glutathione peroxidase 2	2.91	0.0003
128	POF1B	Protein POF1B	-4.88	0.0003
129	NBEA	Neurobeachin	6.62	0.0003
130	pim2	Serine/threonine-protein kinase pim-2	1.64	0.0003
131	RTL1	Retrotransposon-like protein 1	6.55	0.0003
132	#N/A	Stonustoxin subunit alpha	1.43	0.0003
133	Cotl1	Coactosin-like protein {ECO	2.94	0.0003
134	#N/A	Intermediate filament protein ON3	1.38	0.0003
135	Dgkb	Diacylglycerol kinase beta	-1.95	0.0003
136	#N/A	Stonustoxin subunit alpha	5.53	0.0003
137	SLC25A15	Mitochondrial ornithine transporter 1	-3.43	0.0004
138	Plekhg5	Pleckstrin homology domain-containing family G member 5	-2.56	0.0004
139	Bcar3	Breast cancer anti-estrogen resistance protein 3	-2.68	0.0004
140	#N/A	NACHT, LRR and PYD domains-containing protein 9	6.63	0.0004
141	Samd9l	Sterile alpha motif domain-containing protein 9-like	-5.80	0.0004
142	BTN1A1	Butyrophilin subfamily 1 member A1	-3.00	0.0004
143	#N/A	Neoverrucotoxin subunit beta	6.48	0.0004
144	znf598	Zinc finger protein 598	-1.49	0.0005
145	GIMAP4	GTPase IMAP family member 4	2.53	0.0005
146	rhbdf2	Inactive rhomboid protein 2	-1.64	0.0005
147	Dsp	Desmoplakin	-1.79	0.0005
148	Tmem238	Transmembrane protein 238	2.12	0.0005
149	#N/A	Myomodulin neuropeptides	-3.41	0.0005
150	Peg10	Retrotransposon-derived protein PEG10	3.42	0.0006
151	IFFO1	Intermediate filament family orphan 1	3.38	0.0006
152	PDLIM5	PDZ and LIM domain protein 5	-2.39	0.0006
153	Mtss1	Metastasis suppressor protein 1	-2.54	0.0007
154	#N/A	Natterin-like protein	-2.39	0.0007
155	SAMHD1	Deoxynucleoside triphosphate triphosphohydrolase SAMHD1	6.39	0.0007
156	ccnf	Cyclin-F	-4.27	0.0007
157	CEACAM1	Carcinoembryonic antigen-related cell adhesion molecule 1	6.16	0.0008
158	pol	Retrovirus-related Pol polyprotein from transposon gypsy	-4.99	0.0008
159	Cpeb2	Cytoplasmic polyadenylation element-binding protein 2	3.84	0.0009
160	pxdn	Peroxidasin	6.50	0.0009
161	#N/A	Lipocalin	-3.11	0.0009
162	GVINP1	Interferon-induced very large GTPase 1	3.95	0.0010
163	Pol	LINE-1 retrotransposable element ORF2 protein	3.07	0.0010
164	DDR1	Epithelial discoidin domain-containing receptor 1	-2.68	0.0010
165	ORF39	Uncharacterized protein ORF39	4.88	0.0011
166	sdha	Succinate dehydrogenase [ubiquinone] flavoprotein subunit, mitochondrial	-4.58	0.0011
167	PEG10	Retrotransposon-derived protein PEG10	-5.76	0.0011
168	Peg10	Retrotransposon-derived protein PEG10	2.72	0.0011
169	Tf2-9	Transposon Tf2-9 polyprotein	3.49	0.0011
170	VWA7	von Willebrand factor A domain-containing protein 7	-6.01	0.0011
171	DSC1	Desmocollin-1	-6.64	0.0011
172	Gimap4	GTPase IMAP family member 4	2.48	0.0012
173	NCAPG	Condensin complex subunit 3	-4.83	0.0012
174	CACNA1B	Voltage-dependent N-type calcium channel subunit alpha-1B	6.53	0.0012
175	DCT	L-dopachrome tautomerase	-5.56	0.0012
176	RNF138	E3 ubiquitin-protein ligase RNF138 {ECO	3.73	0.0012
177	Ywhaz	14-3-3 protein zeta/delta	-1.95	0.0012
178	Baiap2	Brain-specific angiogenesis inhibitor 1-associated protein 2	-2.39	0.0012
179	Gtpbp2	GTP-binding protein 2	2.64	0.0012
180	#N/A	Nectin-1	-1.61	0.0012
181	SUN1	SUN domain-containing protein 1	7.29	0.0013

182	slc16a10	Monocarboxylate transporter 10	3.69	0.0013
183	krt18	Keratin, type I cytoskeletal 18	3.06	0.0014
184	melk	Maternal embryonic leucine zipper kinase	-5.74	0.0014
185	MPZL2	Myelin protein zero-like protein 2	1.73	0.0014
186	Tf2-9	Transposon Tf2-9 polyprotein	2.82	0.0014
187	GNE	Bifunctional UDP-N-acetylglucosamine 2-epimerase/N-acetylmannosamine kinase	1.88	0.0015
188	RT1-B	Rano class II histocompatibility antigen, A beta chain	1.49	0.0015
189	hsp70	Heat shock 70 kDa protein	3.48	0.0015
190	HI_0712	Probable hemoglobin and hemoglobin-haptoglobin-binding protein 3	-3.16	0.0015
191	ERBB3	Receptor tyrosine-protein kinase erbB-3	-3.30	0.0015
192	Tf2-8	Transposon Tf2-8 polyprotein	5.93	0.0015
193	SFMBT2	Scm-like with four MBT domains protein 2	-1.55	0.0016
194	Plekhg5	Pleckstrin homology domain-containing family G member 5	-2.99	0.0016
195	hsp70	Heat shock 70 kDa protein	3.51	0.0016
196	STARD13	StAR-related lipid transfer protein 13	7.16	0.0016
197	hsp70	Heat shock 70 kDa protein	3.53	0.0016
198	PEBP1	Phosphatidylethanolamine-binding protein 1	5.50	0.0016
199	Pde4dip	Myomegalin	-3.39	0.0017
200	ERBB3	Receptor tyrosine-protein kinase erbB-3	-2.59	0.0017
201	TRAPPC12	Trafficking protein particle complex subunit 12	2.91	0.0017
202	Rgs12	Regulator of G-protein signaling 12	-5.34	0.0018
203	#N/A	Natterin-like protein	-6.46	0.0018
204	Ogfr	Opioid growth factor receptor	-5.38	0.0019
205	NLRC3	Protein NLRC3	-5.98	0.0019
206	HCAR2	Hydroxycarboxylic acid receptor 2	-4.00	0.0019
207	araQ	L-arabinose transport system permease protein AraQ	6.17	0.0020
208	sibA	Integrin beta-like protein A	-4.56	0.0020
209	ERBB3	Receptor tyrosine-protein kinase erbB-3	-4.62	0.0021
210	Kcnj10	ATP-sensitive inward rectifier potassium channel 10	5.29	0.0021
211	krt18	Keratin, type I cytoskeletal 18	2.38	0.0022
212	Haspin	Serine/threonine-protein kinase haspin	-4.32	0.0022
213	HSP90AA1	Heat shock protein HSP 90-alpha	3.74	0.0023
214	PCDHGC3	Protocadherin gamma-C3	-3.22	0.0023
215	Syne2	Nesprin-2	-1.66	0.0024
216	SLC17A5	Sialin	2.30	0.0024
217	Vmp1	Vacuole membrane protein 1	-2.97	0.0024
218	Cenpe	Centromere-associated protein E {ECO	-3.17	0.0025
219	mapk8a	Mitogen-activated protein kinase 8A	-5.37	0.0025
220	FAT1	Protocadherin Fat 1	-5.10	0.0025
221	TMEM132C	Transmembrane protein 132C	6.16	0.0027
222	hbb4	Hemoglobin subunit beta-4	4.88	0.0027
223	eif4ebp3l	Eukaryotic translation initiation factor 4E-binding protein 3-like	3.74	0.0027
224	agap1	Arf-GAP with GTPase, ANK repeat and PH domain-containing protein 1	4.49	0.0028
225	Csrnp2	Cysteine/serine-rich nuclear protein 2	-4.11	0.0028
226	slc40a1	Solute carrier family 40 member 1	2.36	0.0028
227	NLRP1	NACHT, LRR and PYD domains-containing protein 1	1.69	0.0028
228	TPP1	Tripeptidyl-peptidase 1	3.03	0.0028
229	AHCYL2	Putative adenosylhomocysteinase 3	-3.88	0.0029
230	RTP2	Receptor-transporting protein 2	2.24	0.0029
231	tpr	Nucleoprotein TPR	-1.86	0.0029
232	Atf5	Cyclic AMP-dependent transcription factor ATF-5	3.22	0.0029
233	AQP3	Aquaporin-3	-4.08	0.0029
234	CDKN1B	Cyclin-dependent kinase inhibitor 1B	2.77	0.0029
235	Dsp	Desmoplakin	-5.58	0.0030
236	Fat2	Protocadherin Fat 2	-5.01	0.0031
237	AGAP3	Arf-GAP with GTPase, ANK repeat and PH domain-containing protein 3	4.13	0.0031
238	Ddx5	Probable ATP-dependent RNA helicase DDX5	-1.30	0.0031
239	Dsg2	Desmoglein-2	-6.21	0.0031
240	ndrg1-b	Protein NDRG1-B	4.64	0.0032
241	DIAPH3	Protein diaphanous homolog 3	-3.12	0.0032
242	#N/A	Lipocalin	-2.71	0.0034
243	Cit	Citron Rho-interacting kinase	-5.95	0.0034
244	tir-1	Sterile alpha and TIR motif-containing protein tir-1	-5.62	0.0034
245	Fcer1g	High affinity immunoglobulin epsilon receptor subunit gamma	2.96	0.0035
246	SLCO2A1	Solute carrier organic anion transporter family member 2A1	-2.46	0.0035

247	ANLN	Actin-binding protein anillin	-3.49	0.0036
248	jag1b	Protein jagged-1b	-1.93	0.0036
249	SLC25A22	Mitochondrial glutamate carrier 1	-2.04	0.0036
250	GNGT2	Guanine nucleotide-binding protein G(I)/G(S)/G(O) subunit gamma-T2	3.60	0.0036
251	dennd5b	DENN domain-containing protein 5B	-2.67	0.0036
252	CACNA1B	Voltage-dependent N-type calcium channel subunit alpha-1B	5.64	0.0036
253	GADD45A	Growth arrest and DNA damage-inducible protein GADD45 alpha	2.66	0.0037
254	#N/A	Transposable element Tcb1 transposase	3.64	0.0039
255	afap1l1	Actin filament-associated protein 1-like 1	-2.02	0.0040
256	Nupr1	Nuclear protein 1 {ECO	2.71	0.0040
257	Cps1	Carbamoyl-phosphate synthase [ammonia], mitochondrial	-3.37	0.0042
258	tpx2-a	Targeting protein for Xklp2-A	-5.85	0.0042
259	hsp90a.1	Heat shock protein HSP 90-alpha 1	3.90	0.0042
260	tacc3	Transforming acidic coiled-coil-containing protein 3	-3.80	0.0043
261	#N/A	ES1 protein homolog, mitochondrial	2.13	0.0044
262	Ghsr	Growth hormone secretagogue receptor type 1	-5.36	0.0045
263	aste1	Protein asteroid homolog 1	6.89	0.0045
264	ATP8A2	Phospholipid-transporting ATPase IB	-2.21	0.0045
265	#N/A	Stonustoxin subunit beta	1.63	0.0046
266	fmnl3	Formin-like protein 3	3.31	0.0047
267	C1orf127	Uncharacterized protein C1orf127	-5.86	0.0047
268	ACADSB	Short/branched chain specific acyl-CoA dehydrogenase, mitochondrial	2.86	0.0048
269	Lrat	Lecithin retinol acyltransferase	-6.36	0.0048
270	ZFP36L1	Zinc finger protein 36, C3H1 type-like 1	1.91	0.0048
271	Tf2-9	Transposon Tf2-9 polyprotein	3.36	0.0048
272	IRF1	Interferon regulatory factor 1	1.23	0.0048
273	ndel1a	Nuclear distribution protein nudE-like 1-A	2.53	0.0049
274	MPTX	Mucosal pentraxin	6.83	0.0049
275	Vtcn1	V-set domain containing T-cell activation inhibitor 1	-4.89	0.0051
276	ETS2	Protein C-ets-2	-2.87	0.0051
277	pnrc2	Proline-rich nuclear receptor coactivator 2	1.77	0.0051
278	NFE2L2	Nuclear factor erythroid 2-related factor 2	3.28	0.0051
279	TY3B-G	Transposon Ty3-G Gag-Pol polyprotein	3.47	0.0052
280	krt13	Keratin, type I cytoskeletal 13	2.01	0.0052
281	Igfbp6	Insulin-like growth factor-binding protein 6	-8.15	0.0052
282	ARPC1B	Actin-related protein 2/3 complex subunit 1B	1.80	0.0053
283	AHCYL2	Adenosylhomocysteinase 3	-5.33	0.0053
284	PCDHA5	Protocadherin alpha-5	-5.48	0.0053
285	ppp1r3cb	Protein phosphatase 1 regulatory subunit 3C-B	4.09	0.0055
286	Map2	Microtubule-associated protein 2	2.18	0.0055
287	CLSPN	Claspin	-5.55	0.0056
288	il1b	Interleukin-1 beta	5.75	0.0056
289	Tf2-6	Transposon Tf2-6 polyprotein	-5.52	0.0056
290	YRK	Proto-oncogene tyrosine-protein kinase Yrk	4.69	0.0058
291	LTBP2	Latent-transforming growth factor beta-binding protein 2	6.49	0.0059
292	cpeb4	Cytoplasmic polyadenylation element-binding protein 4	4.52	0.0059
293	Dsc2	Desmocollin-2	-2.26	0.0059
294	Slamf9	SLAM family member 9	2.24	0.0060
295	CTSB	Cathepsin B	2.85	0.0060
296	Rac2	Ras-related C3 botulinum toxin substrate 2	3.30	0.0061
297	NOTCH3	Neurogenic locus notch homolog protein 3	-2.50	0.0062
298	ARPC1B	Actin-related protein 2/3 complex subunit 1B	1.60	0.0062
299	PCDHA2	Protocadherin alpha-2	-3.25	0.0063
300	smc2	Structural maintenance of chromosomes protein 2	-3.05	0.0064
301	ADAP1	Arf-GAP with dual PH domain-containing protein 1	-1.80	0.0064
302	SLCO2B1	Solute carrier organic anion transporter family member 2B1	-3.05	0.0065
303	PLCG1	1-phosphatidylinositol 4,5-bisphosphate phosphodiesterase gamma-1	6.75	0.0065
304	tpx2-b	Targeting protein for Xklp2-B	-3.76	0.0066
305	Map2	Microtubule-associated protein 2	2.13	0.0066
306	Stard13	StAR-related lipid transfer protein 13	6.95	0.0067
307	Mybl1	Myb-related protein A	-3.23	0.0067
308	VPS52	Vacuolar protein sorting-associated protein 52 homolog	2.75	0.0068
309	rasgrp1	RAS guanyl-releasing protein 1	-1.18	0.0068
310	RPTN	Repetin	-2.64	0.0069
311	ARHGAP6	Rho GTPase-activating protein 6	-3.90	0.0070
312	Rab7a	Ras-related protein Rab-7a	1.73	0.0070

313	GBP1	Guanylate-binding protein 1	1.67	0.0070
314	Slc17a5	Sialin	2.07	0.0071
315	STYK1	Tyrosine-protein kinase STYK1	1.31	0.0072
316	57/58	DNA polymerase	2.54	0.0072
317	OSMR	Oncostatin-M-specific receptor subunit beta	-4.85	0.0072
318	ORF60	Uncharacterized protein ORF60	-1.93	0.0072
319	sema3d	Semaphorin-3D	-2.90	0.0073
320	PPE21	Uncharacterized PPE family protein PPE21	-3.22	0.0073
321	57/58	DNA polymerase	2.71	0.0074
322	GRK5	G protein-coupled receptor kinase 5	-1.98	0.0074
323	Tnik	Traf2 and NCK-interacting protein kinase	-2.15	0.0077
324	Zfp36l1	Zinc finger protein 36, C3H1 type-like 1	2.18	0.0077
325	cahz	Carbonic anhydrase	2.00	0.0078
326	DGKB	Diacylglycerol kinase beta	-1.45	0.0078
327	foxa1-a	Forkhead box protein A1-A	3.26	0.0079
328	Ccl20	C-C motif chemokine 20	5.35	0.0079
329	FHDC1	FH2 domain-containing protein 1	-2.07	0.0079
330	melk	Maternal embryonic leucine zipper kinase	-5.71	0.0080
331	ANK3	Ankyrin-3	-1.68	0.0080
332	ncapd2	Condensin complex subunit 1	-3.39	0.0080
333	Rgs12	Regulator of G-protein signaling 12	-4.05	0.0081
334	Iscu	Iron-sulfur cluster assembly enzyme ISCU, mitochondrial	2.10	0.0082
335	#N/A	Class I histocompatibility antigen, F10 alpha chain	10.78	0.0082
336	ZFAND5	AN1-type zinc finger protein 5	-2.96	0.0082
337	Ncaph	Condensin complex subunit 2	-5.16	0.0083
338	GLO1	Lactoylglutathione lyase	-5.20	0.0084
339	CTSB	Cathepsin B	2.03	0.0084
340	tacc3	Transforming acidic coiled-coil-containing protein 3	-5.01	0.0085
341	MUC5AC	Mucin-5AC {ECO	2.48	0.0085
342	Hpgd	15-hydroxyprostaglandin dehydrogenase [NAD(+)]	1.95	0.0085
343	Enah	Protein enabled homolog	2.22	0.0085
344	RTP3	Receptor-transporting protein 3	2.21	0.0086
345	Abca1	ATP-binding cassette sub-family A member 1	-5.42	0.0086
346	pol	Pol polyprotein	5.63	0.0087
347	KNTC1	Kinetochore-associated protein 1	-5.29	0.0087
348	Fblim1	Filamin-binding LIM protein 1	-2.50	0.0088
349	#N/A	Calmodulin	-2.43	0.0089
350	ptprf	Receptor-type tyrosine-protein phosphatase F	-1.27	0.0091
351	NUMA1	Nuclear mitotic apparatus protein 1 {ECO	-4.80	0.0091
352	GIMAP2	GTPase IMAP family member 2	6.49	0.0092
353	gag-pol	Gag-Pol polyprotein	2.69	0.0092
354	RNF225	RING finger protein 225 {ECO	1.48	0.0092
355	Kpna2	Importin subunit alpha-1	-1.93	0.0093
356	mapk8b	Mitogen-activated protein kinase 8B	-2.71	0.0094
357	Mefv	Pyrin	1.39	0.0095
358	Unc80	Protein unc-80 homolog	4.26	0.0096
359	Angptl3	Angiopoietin-related protein 3	-5.71	0.0096
360	OSTN	Osteocrin	6.48	0.0096
361	MKI67	Antigen KI-67	-3.27	0.0097
362	COL20A1	Collagen alpha-1(XX) chain	-2.66	0.0097
363	fabp3	Fatty acid-binding protein, heart	-2.42	0.0099
364	Rgs12	Regulator of G-protein signaling 12	-4.69	0.0102
365	Cpa1	Carboxypeptidase A1	2.69	0.0103
366	Tpd52l1	Tumor protein D53	1.35	0.0104
367	Cebpd	CCAAT/enhancer-binding protein delta	-1.68	0.0104
368	LEPR	Leptin receptor	-4.07	0.0104
369	Cldn4	Claudin-4	1.97	0.0104
370	kif11	Kinesin-like protein KIF11 {ECO	-3.02	0.0106
371	KRT7	Keratin, type II cytoskeletal 7	-2.15	0.0106
372	incenp-a	Inner centromere protein A	-4.47	0.0106
373	PDE4DIP	Myomegalin	-3.07	0.0106
374	FBP1	Fructose-1,6-bisphosphatase 1	3.37	0.0107
375	Angptl3	Angiopoietin-related protein 3	-5.23	0.0107
376	Endod1	Endonuclease domain-containing 1 protein	-2.31	0.0108
377	KRT15	Keratin, type I cytoskeletal 15	2.77	0.0108
378	Cpeb2	Cytoplasmic polyadenylation element-binding protein 2	4.03	0.0109

379	CYTH2	Cytohesin-2	4.63	0.0109
380	slc16a10	Monocarboxylate transporter 10	3.15	0.0110
381	epd	Ependymin	3.51	0.0110
382	Fhl1	Four and a half LIM domains protein 1	4.64	0.0110
383	Tnik	Traf2 and NCK-interacting protein kinase	-1.88	0.0111
384	#N/A	Membrane progestin receptor beta	4.34	0.0111
385	S100A13	Protein S100-A13	1.79	0.0111
386	SLC29A1	Equilibrative nucleoside transporter 1	-4.80	0.0111
387	mafb	Transcription factor MafB	2.78	0.0112
388	ARL4A	ADP-ribosylation factor-like protein 4A	2.10	0.0113
389	CD22	B-cell receptor CD22	4.03	0.0115
390	Eps8l2	Epidermal growth factor receptor kinase substrate 8-like protein 2	1.98	0.0116
391	TNC	Tenascin	1.46	0.0116
392	bhmt	Betaine--homocysteine S-methyltransferase 1	-3.30	0.0116
393	BICD1	Protein bicaudal D homolog 1	-3.27	0.0116
394	JUN	Transcription factor AP-1	1.94	0.0117
395	PLCG1	1-phosphatidylinositol 4,5-bisphosphate phosphodiesterase gamma-1	6.46	0.0118
396	NPTX1	Neuronal pentraxin-1	4.23	0.0119
397	tc1a	Transposable element Tc1 transposase	-0.76	0.0119
398	Fcgr3	Low affinity immunoglobulin gamma Fc region receptor III	3.11	0.0121
399	TAGAP	T-cell activation Rho GTPase-activating protein	2.09	0.0121
400	GNPAT	Dihydroxyacetone phosphate acyltransferase	-1.78	0.0125
401	tchp	Trichoplein keratin filament-binding protein	6.30	0.0126
402	Flnc	Filamin-C	2.59	0.0126
403	cyp2m1	Cytochrome P450 2M1	4.83	0.0127
404	nos2	Nitric oxide synthase, inducible	2.08	0.0128
405	Klf8	Krueppel-like factor 8	-1.41	0.0128
406	Sema3a	Semaphorin-3A	6.54	0.0129
407	Atp11a	Probable phospholipid-transporting ATPase IH	-1.62	0.0129
408	FAM83G	Protein FAM83G	-1.61	0.0130
409	CXCR3	C-X-C chemokine receptor type 3	3.35	0.0130
410	#N/A	Protein LAP2	2.52	0.0132
411	pol	Retrovirus-related Pol polyprotein from transposon opus	4.02	0.0134
412	IGFBP4	Insulin-like growth factor-binding protein 4	5.51	0.0134
413	Kpna2	Importin subunit alpha-1	-3.19	0.0137
414	b2m	Beta-2-microglobulin	1.02	0.0137
415	#N/A	Ferritin, heavy subunit	2.00	0.0139
416	#N/A	Intestinal mucin-like protein	2.46	0.0139
417	MAPKBP1	Mitogen-activated protein kinase-binding protein 1	-1.78	0.0140
418	cdk-4	Cyclin-dependent kinase 4 homolog {ECO	4.15	0.0141
419	Cps1	Carbamoyl-phosphate synthase [ammonia], mitochondrial	-3.05	0.0144
420	Stx11	Syntaxin-11	1.79	0.0144
421	BDH1	D-beta-hydroxybutyrate dehydrogenase, mitochondrial	-2.25	0.0144
422	YWHAH	14-3-3 protein eta	1.65	0.0144
423	CLCF1	Cardiotrophin-like cytokine factor 1	-3.71	0.0144
424	#N/A	Transposon TX1 uncharacterized 149 kDa protein	-1.96	0.0145
425	EEF2	Elongation factor 2	1.42	0.0146
426	Fosl2	Fos-related antigen 2	-2.44	0.0146
427	RPL3	60S ribosomal protein L3	-2.93	0.0149
428	MBNL1	Muscleblind-like protein 1	1.55	0.0149
429	FRZB	Secreted frizzled-related protein 3	4.90	0.0151
430	slc40a1	Solute carrier family 40 member 1	2.79	0.0151
431	shcbp1-b	SHC SH2 domain-binding protein 1 homolog B	-3.23	0.0151
432	Map7d1	MAP7 domain-containing protein 1	-5.35	0.0152
433	Mtss1	Metastasis suppressor protein 1	-1.45	0.0152
434	gamt	Guanidinoacetate N-methyltransferase	3.06	0.0153
435	inaK	Ice nucleation protein	-5.84	0.0154
436	V-TCR	Viral T-cell receptor beta chain-like T17T-22	2.36	0.0155
437	Ceacam1	Carcinoembryonic antigen-related cell adhesion molecule 1	3.90	0.0156
438	Rac2	Ras-related C3 botulinum toxin substrate 2	2.45	0.0156
439	Fat2	Protocadherin Fat 2	-4.41	0.0158
440	Gimap4	GTPase IMAP family member 4	-2.72	0.0158
441	Nfkb2	Nuclear factor NF-kappa-B p100 subunit	1.74	0.0158
442	#N/A	Negative regulator of reactive oxygen species	4.75	0.0159
443	grhl2	Grainyhead-like protein 2 homolog	-1.65	0.0161
444	Dst	Dystonin	1.83	0.0162

445	DUSP7	Dual specificity protein phosphatase 7	-2.10	0.0163
446	Prim2	DNA primase large subunit	-5.42	0.0163
447	PGM5	Phosphoglucomutase-like protein 5	-5.14	0.0163
448	Ndrg3	Protein NDRG3	-1.77	0.0163
449	Cnn3	Calponin-3	-5.03	0.0164
450	KIF4A	Chromosome-associated kinesin KIF4A	-4.88	0.0164
451	ptprf	Receptor-type tyrosine-protein phosphatase F	-2.55	0.0165
452	SLC4A2	Anion exchange protein 2	4.51	0.0166
453	PARD3	Partitioning defective 3 homolog	-2.77	0.0166
454	C1QA	Complement C1q subcomponent subunit A	2.40	0.0168
455	Kcnk2	Potassium channel subfamily K member 2 {ECO	-2.39	0.0168
456	Gimap4	GTPase IMAP family member 4	2.34	0.0169
457	HI_0258	Putative glycosyltransferase HI_0258	-4.08	0.0172
458	V-ERBB	Tyrosine-protein kinase transforming protein erbB	-1.95	0.0172
459	Plk1	Serine/threonine-protein kinase PLK1	-4.07	0.0173
460	SLC29A1	Equilibrative nucleoside transporter 1	-4.58	0.0173
461	GJB6	Gap junction beta-6 protein	3.16	0.0175
462	PXN1	Jeltraxin	2.42	0.0176
463	SERF2	Small EDRK-rich factor 2	1.62	0.0177
464	Pold1	DNA polymerase delta catalytic subunit	-2.66	0.0179
465	APLP2	Amyloid-like protein 2	2.25	0.0179
466	ARHGAP18	Rho GTPase-activating protein 18	1.68	0.0179
467	ncapd2	Condensin complex subunit 1	-3.29	0.0180
468	TSPAN3	Tetraspanin-3	6.42	0.0180
469	Tgm2	Protein-glutamine gamma-glutamyltransferase 2	-4.74	0.0181
470	SAMD9	Sterile alpha motif domain-containing protein 9	-4.31	0.0182
471	phka2	Phosphorylase b kinase regulatory subunit alpha, liver isoform	-1.55	0.0183
472	CX3CR1	CX3C chemokine receptor 1	6.34	0.0183
473	#N/A	Transposable element Tcb2 transposase	-1.70	0.0183
474	#N/A	Natterin-like protein	-3.99	0.0184
475	jag1b	Protein jagged-1b	-2.22	0.0185
476	ZBED9	SCAN domain-containing protein 3	-1.36	0.0185
477	zbtb16a	Zinc finger and BTB domain-containing protein 16-A {ECO	1.67	0.0185
478	Dtx3l	E3 ubiquitin-protein ligase DTX3L	6.31	0.0185
479	FGFBP1	Fibroblast growth factor-binding protein 1	-5.09	0.0187
480	PRELID1	PRELI domain-containing protein 1, mitochondrial	-1.72	0.0188
481	GRAMD4	GRAM domain-containing protein 4	-1.22	0.0188
482	mxi1	Max-interacting protein 1	1.73	0.0188
483	Cerk	Ceramide kinase	2.01	0.0190
484	cep44	Centrosomal protein of 44 kDa	-4.91	0.0191
485	DDIT3	DNA damage-inducible transcript 3 protein	1.96	0.0192
486	GIMAP2	GTPase IMAP family member 2	4.58	0.0192
487	SGSM1	Small G protein signaling modulator 1	-3.63	0.0196
488	ARPC1A	Actin-related protein 2/3 complex subunit 1A	1.11	0.0196
489	MDV087	Uncharacterized gene 87 protein	-1.07	0.0196
490	#N/A	Peroxiredoxin	2.07	0.0197
491	RSBN1	Round spermatid basic protein 1	3.59	0.0197
492	SYNE2	Nesprin-2	-1.60	0.0197
493	Ubl3	Ubiquitin-like protein 3	1.64	0.0198
494	SLC12A2	Solute carrier family 12 member 2	-2.50	0.0198
495	ARHGAP20	Rho GTPase-activating protein 20	6.20	0.0199
496	Clta	Clathrin light chain A	1.48	0.0201
497	Chsy1	Chondroitin sulfate synthase 1	-2.98	0.0201
498	KRT19	Keratin, type I cytoskeletal 19	-2.03	0.0201
499	Lifr	Leukemia inhibitory factor receptor	-4.77	0.0202
500	Cyba	Cytochrome b-245 light chain	1.68	0.0203
501	vmp1	Vacuole membrane protein 1	-2.35	0.0203
502	Rgs12	Regulator of G-protein signaling 12	-1.57	0.0203
503	ptprf	Receptor-type tyrosine-protein phosphatase F	-3.04	0.0205
504	agtrap	Type-1 angiotensin II receptor-associated protein-like	4.37	0.0205
505	SCIN	Adseverin	2.34	0.0206
506	CTDSP2	Carboxy-terminal domain RNA polymerase II polypeptide A small phosphatase 2	1.12	0.0206
507	gprc6a	G-protein coupled receptor family C group 6 member A	3.17	0.0207
508	Fh	Fumarate hydratase, mitochondrial	-3.24	0.0207
509	MUC5AC	Mucin-5AC {ECO	2.23	0.0209

510	IQGAP3	Ras GTPase-activating-like protein IQGAP3	-4.68	0.0209
511	#N/A	Lysozyme C II	2.53	0.0212
512	Syne2	Nesprin-2	-2.74	0.0212
513	znf395	Zinc finger protein 395	1.82	0.0212
514	PPP2R3A	Serine/threonine-protein phosphatase 2A regulatory subunit B" subunit alpha	2.65	0.0212
515	cpeb4	Cytoplasmic polyadenylation element-binding protein 4	4.67	0.0213
516	#N/A	Intermediate filament protein ON3	2.79	0.0213
517	Sgsm1	Small G protein signaling modulator 1	-4.69	0.0214
518	BTN1A1	Butyrophilin subfamily 1 member A1	1.50	0.0215
519	PLCH2	1-phosphatidylinositol 4,5-bisphosphate phosphodiesterase eta-2	-1.82	0.0216
520	KCNK2	Potassium channel subfamily K member 2	-2.12	0.0219
521	xkr9	XK-related protein 9	2.83	0.0219
522	RTN3	Reticulon-3	0.97	0.0219
523	FXYD6	FXYD domain-containing ion transport regulator 6	-3.73	0.0221
524	ext1b	Exostosin-1b	-2.10	0.0221
525	MYO9B	Unconventional myosin-IXb	-1.04	0.0223
526	KIF4B	Chromosome-associated kinesin KIF4B	-3.87	0.0223
527	p1	RNA-directed RNA polymerase	6.22	0.0224
528	dennd5b	DENN domain-containing protein 5B	-2.42	0.0226
529	PTPRJ	Receptor-type tyrosine-protein phosphatase eta	2.50	0.0227
530	Btnl2	Butyrophilin-like protein 2	-3.92	0.0227
531	Igsf8	Immunoglobulin superfamily member 8	-1.78	0.0229
532	Pepd	Xaa-Pro dipeptidase	2.01	0.0230
533	ARHGEF12	Rho guanine nucleotide exchange factor 12	-2.42	0.0230
534	CCL2	C-C motif chemokine 2	6.00	0.0231
535	LRP1	Prolow-density lipoprotein receptor-related protein 1	2.42	0.0232
536	POL	Retrovirus-related Pol polyprotein from transposon 412	-4.10	0.0235
537	#N/A	Intermediate filament protein ON3	1.99	0.0238
538	Alk	ALK tyrosine kinase receptor	-5.20	0.0239
539	Trp53inp1	Tumor protein p53-inducible nuclear protein 1	1.50	0.0239
540	midn	Midnolin	-2.45	0.0239
541	RGL1	Ral guanine nucleotide dissociation stimulator-like 1	-2.96	0.0241
542	Rdh13	Retinol dehydrogenase 13	-4.81	0.0244
543	Ttc39a	Tetratricopeptide repeat protein 39A	1.47	0.0244
544	MPEG1	Macrophage-expressed gene 1 protein	2.30	0.0247
545	GBGT1	Globoside alpha-1,3-N-acetylgalactosaminyltransferase 1	1.58	0.0248
546	cyfip2	Cytoplasmic FMR1-interacting protein 2	3.56	0.0248
547	hba	Hemoglobin subunit alpha	8.27	0.0248
548	CTSB	Cathepsin B	2.38	0.0248
549	Cytip	Cytohesin-interacting protein	3.05	0.0250
550	CRY1	Cryptochrome-1	-2.13	0.0252
551	CDKN1B	Cyclin-dependent kinase inhibitor 1B	1.26	0.0254
552	KIF20B	Kinesin-like protein KIF20B {ECO	-4.09	0.0257
553	Mapk12	Mitogen-activated protein kinase 12	-3.29	0.0260
554	smc2	Structural maintenance of chromosomes protein 2	-2.95	0.0260
555	Abca1	ATP-binding cassette sub-family A member 1	-5.76	0.0260
556	SLC16A9	Monocarboxylate transporter 9	2.03	0.0262
557	CENPV	Centromere protein V	1.94	0.0262
558	kit	Mast/stem cell growth factor receptor Kit	2.57	0.0262
559	Mpped2	Metallophosphoesterase MPPED2	4.17	0.0263
560	Deptor	DEP domain-containing mTOR-interacting protein	-2.08	0.0264
561	Itpr2	Inositol 1,4,5-trisphosphate receptor type 2	-1.57	0.0265
562	PTPRA	Receptor-type tyrosine-protein phosphatase alpha	-1.80	0.0266
563	sh3bp4	SH3 domain-binding protein 4	-3.14	0.0266
564	VCL	Vinculin	-1.60	0.0266
565	kdelr3	ER lumen protein-retaining receptor 3	1.46	0.0267
566	mtap	S-methyl-5'-thioadenosine phosphorylase {ECO	-2.17	0.0267
567	CKAP2	Cytoskeleton-associated protein 2	-5.03	0.0268
568	IQGAP3	Ras GTPase-activating-like protein IQGAP3	-4.89	0.0268
569	Il9r	Interleukin-9 receptor	4.47	0.0268
570	PCNX1	Pecanex-like protein 1	1.36	0.0270
571	nusap1	Nucleolar and spindle-associated protein 1	-5.15	0.0274
572	Lifr	Leukemia inhibitory factor receptor	-1.72	0.0277
573	Ap1b1	AP-1 complex subunit beta-1	-4.93	0.0277
574	PIAS2	E3 SUMO-protein ligase PIAS2	-1.46	0.0277

575	GIMAP7	GTPase IMAP family member 7	4.16	0.0279
576	PTGDR2	Prostaglandin D2 receptor 2	-4.94	0.0281
577	#N/A	Cathepsin L	2.65	0.0283
578	CA6	Carbonic anhydrase 6	-1.79	0.0284
579	UTRN	Utrophin	1.25	0.0285
580	PAQR6	Progestin and adipoQ receptor family member 6	1.25	0.0285
581	tmed1	Transmembrane emp24 domain-containing protein 1	2.09	0.0285
582	wwc2	Protein WWC2	1.62	0.0287
583	SH2D5	SH2 domain-containing protein 5	-3.25	0.0288
584	aste1	Protein asteroid homolog 1	-2.66	0.0289
585	ORF34	Uncharacterized protein ORF34	5.31	0.0289
586	ABL2	Abelson tyrosine-protein kinase 2	-2.13	0.0290
587	PRIM1	DNA primase small subunit	-2.66	0.0292
588	ZBTB11	Zinc finger and BTB domain-containing protein 11	-1.62	0.0292
589	Tf2-9	Transposon Tf2-9 polyprotein	1.76	0.0293
590	ARAP1	Arf-GAP with Rho-GAP domain, ANK repeat and PH domain-containing protein 1	4.49	0.0293
591	#N/A	Transposon TX1 uncharacterized 149 kDa protein	1.72	0.0293
592	SLC12A2	Solute carrier family 12 member 2	-2.72	0.0293
593	yipf4	Protein YIPF4	0.96	0.0295
594	DNM2	Dynamin-2	2.69	0.0296
595	#N/A	RNA-directed RNA polymerase beta chain	8.54	0.0296
596	Ank3	Ankyrin-3	-1.49	0.0297
597	grip2	Glutamate receptor-interacting protein 2	3.63	0.0298
598	AP3S2	AP-3 complex subunit sigma-2	2.02	0.0298
599	TRIM11	E3 ubiquitin-protein ligase TRIM11	1.90	0.0298
600	sult1st3	Cytosolic sulfotransferase 3	1.87	0.0300
601	Sqstm1	Sequestosome-1	2.29	0.0300
602	TACC3	Transforming acidic coiled-coil-containing protein 3	-4.61	0.0301
603	Cdh26	Cadherin-like protein 26	-4.56	0.0301
604	tax1bp1b	Tax1-binding protein 1 homolog B	-2.79	0.0301
605	Dtx1	E3 ubiquitin-protein ligase DTX1	3.47	0.0302
606	Limd2	LIM domain-containing protein 2	2.32	0.0302
607	xkr9	XK-related protein 9	3.19	0.0302
608	ATP11A	Probable phospholipid-transporting ATPase IH	-1.61	0.0302
609	Nsd1	Histone-lysine N-methyltransferase, H3 lysine-36 and H4 lysine-20 specific	-2.25	0.0304
610	ADAP1	Arf-GAP with dual PH domain-containing protein 1	-1.94	0.0304
611	CCL25	C-C motif chemokine 25	-2.86	0.0305
612	sod1	Superoxide dismutase [Cu-Zn]	-1.55	0.0306
613	ZCCHC14	Zinc finger CCHC domain-containing protein 14	-5.25	0.0306
614	SLC2A2	Solute carrier family 2, facilitated glucose transporter member 2	-2.44	0.0307
615	cct3	T-complex protein 1 subunit gamma	2.45	0.0308
616	Gvin1	Interferon-induced very large GTPase 1	2.31	0.0311
617	GABRG3	Gamma-aminobutyric acid receptor subunit gamma-3	2.78	0.0311
618	CLIC6	Chloride intracellular channel protein 6	-2.63	0.0312
619	Lepr	Leptin receptor	-3.78	0.0314
620	#N/A	Lipoma HMGIC fusion partner homolog	-1.40	0.0314
621	Taok1	Serine/threonine-protein kinase TAO1	1.96	0.0315
622	FSCN1	Fascin	-3.36	0.0317
623	Rnh1	Ribonuclease inhibitor	1.63	0.0317
624	Gpsm2	G-protein-signaling modulator 2	-4.97	0.0317
625	npc2	Epididymal secretory protein E1	1.57	0.0317
626	Diaph3	Protein diaphanous homolog 3	-3.17	0.0318
627	MOG	Myelin-oligodendrocyte glycoprotein	-1.12	0.0318
628	FAM180A	Protein FAM180A	-4.31	0.0318
629	Sik2	Serine/threonine-protein kinase SIK2	-1.94	0.0318
630	SLC43A2	Large neutral amino acids transporter small subunit 4	3.56	0.0318
631	FRY	Protein furry homolog	1.71	0.0318
632	pol	Pol polyprotein	2.71	0.0318
633	Nlrc3	Protein NLRC3	-4.46	0.0318
634	St5	Suppression of tumorigenicity 5 protein	-1.09	0.0318
635	gprc6a	G-protein coupled receptor family C group 6 member A	3.30	0.0318
636	Cndp2	Cytosolic non-specific dipeptidase	1.49	0.0320
637	Dusp7	Dual specificity protein phosphatase 7	-2.34	0.0321
638	FBXL6	F-box/LRR-repeat protein 6	1.88	0.0323

639	pol	Pol polyprotein	-3.04	0.0324
640	nrg1	Pro-neuregulin-1, membrane-bound isoform	-1.96	0.0324
641	MTA2	Metastasis-associated protein MTA2	-4.65	0.0324
642	SLC43A3	Solute carrier family 43 member 3	5.98	0.0325
643	ZNF180	Zinc finger protein 180	1.27	0.0326
644	KLHL6	Kelch-like protein 6	2.52	0.0329
645	cluh	Clustered mitochondria protein homolog {ECO	-1.56	0.0329
646	COL20A1	Collagen alpha-1(XX) chain	-3.68	0.0329
647	Sox9	Transcription factor SOX-9	1.82	0.0331
648	RT1-Ba	Rano class II histocompatibility antigen, B alpha chain	1.94	0.0331
649	PSAP	Prosaposin	1.66	0.0333
650	THAP4	THAP domain-containing protein 4	-2.71	0.0335
651	pxdn	Peroxidasin	6.23	0.0336
652	TOP2B	DNA topoisomerase 2-beta	-4.52	0.0337
653	STMN1	Stathmin	-2.47	0.0337
654	C1s	Complement C1s subcomponent	2.41	0.0338
655	Nlrp1a	NACHT, LRR and PYD domains-containing protein 1a	2.23	0.0339
656	DSP	Desmoplakin	-1.74	0.0342
657	hey1	Hairy/enhancer-of-split related with YRPW motif protein 1	1.31	0.0343
658	DDX5	Probable ATP-dependent RNA helicase DDX5	-1.33	0.0343
659	SAMD9L	Sterile alpha motif domain-containing protein 9-like	-2.99	0.0345
660	chac2	Putative glutathione-specific gamma-glutamylcyclotransferase 2 {ECO	2.49	0.0348
661	plk1	Serine/threonine-protein kinase PLK1	-4.65	0.0348
662	Ctnna2	Catenin alpha-2	-4.71	0.0348
663	ACTN4	Alpha-actinin-4 {ECO	-4.54	0.0349
664	KCNK13	Potassium channel subfamily K member 13	-4.55	0.0352
665	Tspan33	Tetraspanin-33	-4.73	0.0352
666	Gabrp	Gamma-aminobutyric acid receptor subunit pi	-2.35	0.0353
667	#N/A	Protein CASC5	-3.54	0.0354
668	G3BP1	Ras GTPase-activating protein-binding protein 1	-1.62	0.0354
669	apoeb	Apolipoprotein Eb	-1.62	0.0354
670	ccdc80	Coiled-coil domain-containing protein 80	4.54	0.0354
671	CIT	Citron Rho-interacting kinase	-4.63	0.0356
672	CTNND1	Catenin delta-1	-1.70	0.0356
673	slc16a10	Monocarboxylate transporter 10	2.75	0.0357
674	Eomes	Eomesodermin homolog	6.03	0.0358
675	Espl1	Separin	-4.77	0.0359
676	PRKCH	Protein kinase C eta type	1.63	0.0362
677	rxrba	Retinoic acid receptor RXR-beta-A	1.12	0.0362
678	rps13	40S ribosomal protein S13	1.52	0.0362
679	ATP6V1E1	V-type proton ATPase subunit E 1	1.64	0.0363
680	optn	Optineurin	1.24	0.0363
681	PHLPP1	PH domain leucine-rich repeat-containing protein phosphatase 1	2.12	0.0364
682	QSOX1	Sulfhydryl oxidase 1	2.29	0.0365
683	zranb1b	Ubiquitin thioesterase zranb1-B	1.87	0.0366
684	RASAL2	Ras GTPase-activating protein nGAP	1.46	0.0366
685	FAM200A	Protein FAM200A	1.88	0.0367
686	NLRC3	Protein NLRC3	1.21	0.0367
687	BUB1	Mitotic checkpoint serine/threonine-protein kinase BUB1	-2.89	0.0367
688	ATP6V1B2	V-type proton ATPase subunit B, brain isoform	1.17	0.0368
689	SLK	STE20-like serine/threonine-protein kinase	3.11	0.0368
690	gag-pol	Gag-Pol polyprotein	4.08	0.0369
691	Smoc2	SPARC-related modular calcium-binding protein 2	1.55	0.0370
692	#N/A	Transposon TX1 uncharacterized 149 kDa protein	2.89	0.0371
693	PHYPADRAFT_61094	Bryoporin {ECO	-1.73	0.0371
694	SLC6A13	Sodium- and chloride-dependent GABA transporter 2	-5.58	0.0372
695	Arf2	ADP-ribosylation factor 2	1.32	0.0374
696	Add3	Gamma-adducin	-1.78	0.0375
697	Samd9l	Sterile alpha motif domain-containing protein 9-like	-3.32	0.0376
698	selenow	Selenoprotein W	1.45	0.0376
699	SYNPO	Synaptopodin	1.89	0.0377
700	Mpped2	Metallophosphoesterase MPPED2	3.48	0.0377
701	NUMA1	Nuclear mitotic apparatus protein 1 {ECO	-4.50	0.0378
702	Cdc25a	M-phase inducer phosphatase 1	-4.25	0.0378
703	LMNB1	Lamin-B1	-1.78	0.0378

704	Tnpo2	Transportin-2	-1.13	0.0378
705	Prf1	Perforin-1	2.56	0.0379
706	PRDM1	PR domain zinc finger protein 1	-4.77	0.0379
707	Dnase1l3	Deoxyribonuclease gamma	2.80	0.0380
708	PGBD3	PiggyBac transposable element-derived protein 3	-1.11	0.0380
709	FRZB	Secreted frizzled-related protein 3	4.04	0.0382
710	bbip1	BBSome-interacting protein 1	1.61	0.0383
711	Sec14l1	SEC14-like protein 1 {ECO	1.90	0.0383
712	K12H4.7	Putative serine protease K12H4.7	2.50	0.0383
713	DNM1	Dynamin-1	2.66	0.0383
714	ERVPABLB-1	Endogenous retrovirus group PABLB member 1 Env polyprotein	3.32	0.0383
715	eef1as	Elongation factor 1-alpha, somatic form	1.75	0.0383
716	#N/A	Stonustoxin subunit beta	3.40	0.0383
717	Zc3h12a	Ribonuclease ZC3H12A	1.85	0.0384
718	Tjp1	Tight junction protein ZO-1	-2.29	0.0388
719	DSG1	Desmoglein-1	-5.52	0.0388
720	ADAM23	Disintegrin and metalloproteinase domain-containing protein 23	2.66	0.0388
721	ERN1	Serine/threonine-protein kinase/endoribonuclease IRE1	1.55	0.0390
722	NLRC3	Protein NLRC3	-4.42	0.0391
723	Fcer1g	High affinity immunoglobulin epsilon receptor subunit gamma	2.64	0.0392
724	CDC42EP2	Cdc42 effector protein 2	-1.89	0.0392
725	pssA	CDP-diacylglycerol--serine O-phosphatidyltransferase	1.77	0.0392
726	Coro1c	Coronin-1C	2.31	0.0393
727	OAZ	Ornithine decarboxylase antizyme 1	3.02	0.0395
728	HMGB3	High mobility group protein B3	2.99	0.0395
729	Gpr119	Glucose-dependent insulinotropic receptor	-2.14	0.0396
730	Map1lc3b	Microtubule-associated proteins 1A/1B light chain 3B	1.58	0.0397
731	NMRK2	Nicotinamide riboside kinase 2	-3.01	0.0397
732	Gabarapl2	Gamma-aminobutyric acid receptor-associated protein-like 2	1.66	0.0397
733	MR1	Major histocompatibility complex class I-related gene protein	1.58	0.0398
734	PRKCH	Protein kinase C eta type	1.71	0.0399
735	#N/A	WASH complex subunit strumpellin	-1.39	0.0401
736	FMNL1	Formin-like protein 1	1.85	0.0401
737	tc1a	Transposable element Tc1 transposase	-2.05	0.0401
738	Dsp	Desmoplakin	-2.32	0.0403
739	Endod1	Endonuclease domain-containing 1 protein	2.33	0.0403
740	B9d1	B9 domain-containing protein 1	-3.08	0.0403
741	afap1l1	Actin filament-associated protein 1-like 1	-2.25	0.0403
742	Sema3d	Semaphorin-3D	-3.38	0.0403
743	NEDD4	E3 ubiquitin-protein ligase NEDD4	-2.32	0.0404
744	Mthfd1	C-1-tetrahydrofolate synthase, cytoplasmic	4.16	0.0404
745	#N/A	Transposable element Tcb2 transposase	1.55	0.0405
746	CD53	Leukocyte surface antigen CD53	2.74	0.0407
747	RAB7A	Ras-related protein Rab-7a	0.94	0.0407
748	GIMAP7	GTPase IMAP family member 7	1.67	0.0408
749	Lpar3	Lysophosphatidic acid receptor 3	-2.83	0.0408
750	#N/A	RNA-directed RNA polymerase beta chain	9.40	0.0408
751	Sfrp1	Secreted frizzled-related protein 1	-4.50	0.0408
752	SOX9	Transcription factor SOX-9	1.39	0.0410
753	#N/A	Transposable element Tcb2 transposase	-0.99	0.0410
754	CARD11	Caspase recruitment domain-containing protein 11	-1.97	0.0410
755	PER2	Period circadian protein homolog 2	-3.58	0.0411
756	Add3	Gamma-adducin	-1.58	0.0411
757	GPX2	Glutathione peroxidase 2	1.91	0.0412
758	Sash3	SAM and SH3 domain-containing protein 3	2.10	0.0412
759	CSK	Tyrosine-protein kinase CSK	2.12	0.0413
760	ORF2	RNA-directed RNA polymerase	8.41	0.0414
761	alas1	5-aminolevulinate synthase, nonspecific, mitochondrial	2.03	0.0414
762	Sugt1	Protein SGT1 homolog {ECO	1.16	0.0415
763	NCAPD3	Condensin-2 complex subunit D3	-3.77	0.0415
764	CYTH1	Cytohesin-1	3.51	0.0416
765	pol	Pol polyprotein	-1.63	0.0418
766	RNF135	E3 ubiquitin-protein ligase RNF135	-1.45	0.0420
767	Scn2a	Sodium channel protein type 2 subunit alpha	4.15	0.0421
768	NPDC1	Neural proliferation differentiation and control protein 1	2.12	0.0421
769	CMA1	Chymase	2.75	0.0421

770	IL17REL	Putative interleukin-17 receptor E-like	-2.56	0.0422
771	Sik2	Serine/threonine-protein kinase SIK2	-2.41	0.0422
772	Ppp4r1	Serine/threonine-protein phosphatase 4 regulatory subunit 1	1.64	0.0422
773	C1ql4	Complement C1q-like protein 4	9.99	0.0423
774	DSP	Desmoplakin	-1.59	0.0423
775	Glod4	Glyoxalase domain-containing protein 4	1.96	0.0423
776	PCDHGA4	Protocadherin gamma-A4	-1.91	0.0425
777	tcaf	TRPM8 channel-associated factor homolog	3.52	0.0426
778	VGLL1	Transcription cofactor vestigial-like protein 1	1.66	0.0426
779	WDR81	WD repeat-containing protein 81	2.22	0.0427
780	wsb1	WD repeat and SOCS box-containing protein 1	1.19	0.0430
781	HEPACAM2	HEPACAM family member 2	4.20	0.0430
782	Map2	Microtubule-associated protein 2	2.01	0.0432
783	LMNA	Lamin-A	-1.03	0.0433
784	DOCK1	Dedicator of cytokinesis protein 1	-1.13	0.0433
785	Nupr1	Nuclear protein 1 {ECO	1.41	0.0434
786	GNAS	Guanine nucleotide-binding protein G(s) subunit alpha	-3.08	0.0434
787	Fosl2	Fos-related antigen 2	-4.22	0.0434
788	THEMIS	Protein THEMIS	2.97	0.0436
789	Abca1	ATP-binding cassette sub-family A member 1	-4.93	0.0437
790	GIMAP5	GTPase IMAP family member 5	2.37	0.0438
791	CACNB1	Voltage-dependent L-type calcium channel subunit beta-1	2.71	0.0438
792	eif3h	Eukaryotic translation initiation factor 3 subunit H {ECO	1.55	0.0440
793	PCDHGC5	Protocadherin gamma-C5	-3.05	0.0443
794	MFSD13A	Transmembrane protein 180 {ECO	1.99	0.0445
795	Scin	Adseverin	1.93	0.0445
796	tpi1b	Triosephosphate isomerase B	1.51	0.0446
797	NFE2L1	Nuclear factor erythroid 2-related factor 1	3.77	0.0446
798	Abca1	ATP-binding cassette sub-family A member 1	-4.88	0.0447
799	PNP	Purine nucleoside phosphorylase	1.39	0.0448
800	MTCL1	Microtubule cross-linking factor 1	3.18	0.0448
801	egr2b	Early growth response protein 2b	3.17	0.0448
802	Mycbpap	MYCBP-associated protein	-4.02	0.0448
803	BTN2A1	Butyrophilin subfamily 2 member A1	3.43	0.0448
804	pol	Pro-Pol polyprotein	-4.39	0.0450
805	TSC22D1	TSC22 domain family protein 1	2.19	0.0452
806	Slc17a5	Sialin	1.71	0.0452
807	Nlrc3	Protein NLRC3	1.03	0.0453
808	SSTR5	Somatostatin receptor type 5	2.22	0.0453
809	PPP1R16A	Protein phosphatase 1 regulatory subunit 16A	1.42	0.0455
810	ugt3	UDP-glucuronosyltransferase	3.57	0.0459
811	Enc1	Ectoderm-neural cortex protein 1	1.70	0.0460
812	SASH1	SAM and SH3 domain-containing protein 1	1.49	0.0460
813	Serp1	Stress-associated endoplasmic reticulum protein 1	1.48	0.0460
814	NASP	Nuclear autoantigenic sperm protein	-4.21	0.0460
815	#N/A	Transposon TX1 uncharacterized 149 kDa protein	2.22	0.0461
816	GNB3	Guanine nucleotide-binding protein G(I)/G(S)/G(T) subunit beta-3	4.27	0.0462
817	Atp5mf	ATP synthase subunit f, mitochondrial	1.64	0.0464
818	CLIC6	Chloride intracellular channel protein 6	3.28	0.0465
819	Btn1a1	Butyrophilin subfamily 1 member A1	-1.38	0.0465
820	MTHFD2	Bifunctional methylenetetrahydrofolate dehydrogenase/cyclohydrolase, mitochondrial	2.12	0.0466
821	SPI1	Transcription factor PU.1	2.05	0.0466
822	tamm41	Phosphatidate cytidylyltransferase, mitochondrial	1.89	0.0467
823	BTNL9	Butyrophilin-like protein 9	2.99	0.0467
824	IL7R	Interleukin-7 receptor subunit alpha	2.64	0.0468
825	sema3d	Semaphorin-3D	-4.06	0.0469
826	MTSS1	Metastasis suppressor protein 1	-1.22	0.0469
827	Tmem238	Transmembrane protein 238	1.95	0.0471
828	lcp1	Plastin-2	2.07	0.0472
829	#N/A	Histone H3.2	-1.39	0.0472
830	ARHGAP20	Rho GTPase-activating protein 20	4.90	0.0473
831	krt8	Keratin, type II cytoskeletal 8	2.10	0.0474
832	ncapg2	Condensin-2 complex subunit G2	-3.11	0.0476
833	SLC15A2	Solute carrier family 15 member 2	2.37	0.0476
834	SAT1	Diamine acetyltransferase 1	1.81	0.0477

835	ASPM	Abnormal spindle-like microcephaly-associated protein homolog	-3.77	0.0477
836	slc15a4	Solute carrier family 15 member 4	1.80	0.0477
837	CRY2	Cryptochrome-2	-4.79	0.0479
838	KNTC1	Kinetochore-associated protein 1	-4.82	0.0480
839	rps15	40S ribosomal protein S15	1.47	0.0480
840	nfil3	Nuclear factor interleukin-3-regulated protein	-1.48	0.0481
841	Gvin1	Interferon-induced very large GTPase 1	4.87	0.0481
842	EXOC3	Exocyst complex component 3	-3.06	0.0483
843	PCDHGC3	Protocadherin gamma-C3	-4.57	0.0483
844	Hnrnph2	Heterogeneous nuclear ribonucleoprotein H2	-1.41	0.0483
845	AHNAK	Neuroblast differentiation-associated protein AHNAK	2.00	0.0483
846	#N/A	Vespryn	-4.04	0.0483
847	PDLIM5	PDZ and LIM domain protein 5	-2.01	0.0484
848	#N/A	Stonustoxin subunit alpha	-1.71	0.0484
849	GJB6	Gap junction beta-6 protein	2.15	0.0484
850	#N/A	Transposable element Tcb1 transposase	-0.81	0.0485
851	ctsd	Cathepsin D	1.65	0.0485
852	pol	RNA-directed DNA polymerase from mobile element jockey	-2.38	0.0485
853	LRP1	Low-density lipoprotein receptor-related protein 1	2.96	0.0486
854	Ctnna2	Catenin alpha-2	-4.53	0.0487
855	Dleu7	Leukemia-associated protein 7 homolog	3.84	0.0487
856	MAML3	Mastermind-like protein 3	-1.77	0.0487
857	NRG4	Pro-neuregulin-4, membrane-bound isoform	1.64	0.0491
858	Chl1	Neural cell adhesion molecule L1-like protein	-2.18	0.0491
859	Hhatl	Protein-cysteine N-palmitoyltransferase HHAT-like protein	1.42	0.0491
860	Igf1r	Insulin-like growth factor 1 receptor	-3.87	0.0492
861	Psmc3ip	Homologous-pairing protein 2 homolog	-4.11	0.0492
862	pol	RNA-directed DNA polymerase from mobile element jockey	-1.08	0.0493
863	PKP3	Plakophilin-3	-1.20	0.0495
864	ADAP1	Arf-GAP with dual PH domain-containing protein 1	-4.43	0.0496
865	Tbc1d9	TBC1 domain family member 9	2.20	0.0496
866	ADCY8	Adenylate cyclase type 8	-5.63	0.0497
867	BCAR3	Breast cancer anti-estrogen resistance protein 3	-2.16	0.0498
868	SH3BGRL3	SH3 domain-binding glutamic acid-rich-like protein 3	1.87	0.0498
869	Cpxm2	Inactive carboxypeptidase-like protein X2	-5.52	0.0500
870	Msn	Moesin	2.27	0.0500
871	jag1b	Protein jagged-1b	-1.57	0.0500
872	DACH1	Dachshund homolog 1	-3.88	0.0500

Lake 223 vs Lake 260

260 is the base e.g. Positive FC = upregulated in Lake 223 relative to Lake 260

1	PLA2G4C	Cytosolic phospholipase A2 gamma	-7.58	3.61E-23
2	GIMAP4	GTPase IMAP family member 4	-6.95	2.67E-20
3	Mr1	Major histocompatibility complex class I-related gene protein	4.78	1.64E-19
4	Nt5c1a	Cytosolic 5'-nucleotidase 1A	5.03	2.46E-17
5	PLA2G4C	Cytosolic phospholipase A2 gamma	-3.08	6.93E-17
6	Gvin1	Interferon-induced very large GTPase 1	3.90	5.73E-16
7	cyp3a27	Cytochrome P450 3A27	5.66	1.52E-14
8	URGCP	Up-regulator of cell proliferation	6.52	8.98E-12
9	Urgcp	Up-regulator of cell proliferation	5.10	9.79E-12
10	URGCP	Up-regulator of cell proliferation	5.85	9.82E-12
11	MDV087	Uncharacterized gene 87 protein	7.89	1.14E-11
12	#N/A	DLA class I histocompatibility antigen, A9/A9 alpha chain	5.15	3.22E-11
13	DNAAF5	Dynein assembly factor 5, axonemal	-4.08	3.95E-11
14	H2-K1	H-2 class I histocompatibility antigen, K-B alpha chain	6.95	1.45E-10
15	vtg1	Vitellogenin	8.29	1.66E-10
16	URGCP	Up-regulator of cell proliferation	3.01	2.39E-10
17	GIMAP4	GTPase IMAP family member 4	-8.93	4.08E-10
18	PRB3	Basic salivary proline-rich protein 3	-9.28	7.24E-10
19	Urgcp	Up-regulator of cell proliferation	4.37	1.52E-09
20	Psmb8	Proteasome subunit beta type-8	7.80	2.28E-09
21	Dlec1	Deleted in lung and esophageal cancer protein 1 homolog	-4.05	2.39E-09

22	URGCP	Up-regulator of cell proliferation	3.19	2.43E-09
23	GPR50	Melatonin-related receptor	6.28	2.51E-09
24	Gvin1	Interferon-induced very large GTPase 1	5.28	3.67E-09
25	DLEC1	Deleted in lung and esophageal cancer protein 1	-5.03	1.14E-08
26	Mslnl	Mesothelin-like protein	6.16	1.86E-08
27	cyp3a27	Cytochrome P450 3A27	5.57	4.54E-08
28	rnasel3	Ribonuclease-like 3 {ECO:0000303|PubMed:16861230}	-8.13	9.24E-08
29	vtg1	Vitellogenin	7.17	9.61E-08
30	Gimap4	GTPase IMAP family member 4	7.70	1.08E-07
31	DLEC1	Deleted in lung and esophageal cancer protein 1	-4.14	1.39E-07
32	Fh	Fumarate hydratase, mitochondrial	-3.46	1.68E-07
33	GVINP1	Interferon-induced very large GTPase 1	6.01	1.69E-07
34	Mslnl	Mesothelin-like protein	4.83	2.26E-07
35	NLRC3	Protein NLRC3	6.91	8.35E-07
36	IFI44	Interferon-induced protein 44	3.99	9.66E-07
37	Nlrc3	Protein NLRC3	2.02	1.76E-06
38	GIMAP7	GTPase IMAP family member 7	7.54	2.40E-06
39	#N/A	Stonustoxin subunit beta	2.62	2.72E-06
40	P4HA2	Prolyl 4-hydroxylase subunit alpha-2	-4.18	3.26E-06
41	AHNAK	Neuroblast differentiation-associated protein AHNAK	1.91	3.56E-06
42	#N/A	Stonustoxin subunit beta	1.97	4.95E-06
43	plk1	Serine/threonine-protein kinase PLK1	-4.10	9.07E-06
44	krt13	Keratin, type I cytoskeletal 13	2.30	9.16E-06
45	Cldn4	Claudin-4	2.16	9.55E-06
46	Cpa1	Carboxypeptidase A1	5.04	9.76E-06
47	GIMAP4	GTPase IMAP family member 4	6.40	1.03E-05
48	#N/A	L-rhamnose-binding lectin CSL2 {ECO:0000303|Ref.1}	-5.31	1.10E-05
49	PDLIM2	PDZ and LIM domain protein 2	2.38	1.18E-05
50	#N/A	Natterin-like protein	-5.74	1.25E-05
51	ADAP1	Arf-GAP with dual PH domain-containing protein 1	-3.28	1.31E-05
52	CLDN4	Claudin-4	3.14	1.52E-05
53	HSP90AA1	Heat shock protein HSP 90-alpha	7.65	1.77E-05
54	CARD8	Caspase recruitment domain-containing protein 8	-2.32	2.05E-05
55	TNIP1	TNFAIP3-interacting protein 1	2.22	2.30E-05
56	Litaf	Lipopolysaccharide-induced tumor necrosis factor-alpha factor homolog	4.11	2.32E-05
57	hsp70	Heat shock 70 kDa protein	4.93	2.32E-05
58	RNH1	Ribonuclease inhibitor	3.12	2.88E-05
59	mapk14a	Mitogen-activated protein kinase 14A	-3.31	3.65E-05
60	hsp90a.1	Heat shock protein HSP 90-alpha 1	6.56	4.10E-05
61	GIMAP7	GTPase IMAP family member 7	6.69	4.20E-05
62	Hpgd	15-hydroxyprostaglandin dehydrogenase [NAD(+)]	2.69	4.32E-05
63	Sqstm1	Sequestosome-1	3.62	4.35E-05
64	TCN1	Transcobalamin-1	6.82	4.47E-05
65	Krt17	Keratin, type I cytoskeletal 17	1.71	4.56E-05
66	Urgcp	Up-regulator of cell proliferation	5.06	4.66E-05
67	Hspa12a	Heat shock 70 kDa protein 12A	8.00	4.69E-05
68	#N/A	Class I histocompatibility antigen, F10 alpha chain	6.24	4.88E-05
69	hsp70	Heat shock 70 kDa protein	4.53	4.99E-05
70	IFI44	Interferon-induced protein 44	6.31	6.11E-05
71	HSP90AB1	Heat shock protein HSP 90-beta	5.57	6.62E-05
72	#N/A	Intermediate filament protein ON3	1.85	6.99E-05
73	mid1ip1b	Mid1-interacting protein 1-B	1.90	7.34E-05
74	krt13	Keratin, type I cytoskeletal 13	2.69	7.70E-05
75	COL14A1	Collagen alpha-1(XIV) chain	4.81	8.71E-05
76	Ngef	Ephexin-1	1.98	9.52E-05
77	pol	Pol polyprotein	2.43	9.63E-05
78	MUC22	Mucin-22	-2.84	0.0001
79	Gtpbp2	GTP-binding protein 2	3.85	0.0001
80	ANXA11	Annexin A11	1.75	0.0001
81	IGFBP3	Insulin-like growth factor-binding protein 3	-4.43	0.0001
82	HI_0258	Putative glycosyltransferase HI_0258	-6.08	0.0001
83	AHNAK	Neuroblast differentiation-associated protein AHNAK	1.80	0.0001
84	ddit4l	DNA damage-inducible transcript 4-like protein	4.08	0.0001
85	#N/A	Natterin-like protein	-6.34	0.0001
86	hsp70	Heat shock 70 kDa protein	4.23	0.0001
87	#N/A	LINE-1 retrotransposable element ORF2 protein	-7.17	0.0001

88	ORF1	RNA-directed RNA polymerase	6.25	0.0001
89	ACADSB	Short/branched chain specific acyl-CoA dehydrogenase, mitochondrial	4.06	0.0001
90	hsp90ab1	Heat shock protein HSP 90-beta	5.35	0.0002
91	SH2D3A	SH2 domain-containing protein 3A	-1.99	0.0002
92	FBXO7	F-box only protein 7	-2.65	0.0002
93	#N/A	PCTP-like protein	1.99	0.0002
94	GIMAP4	GTPase IMAP family member 4	1.59	0.0002
95	IFI30	Gamma-interferon-inducible lysosomal thiol reductase	2.51	0.0002
96	Igf2r	Cation-independent mannose-6-phosphate receptor	6.30	0.0002
97	HARBI1	Putative nuclease HARBI1	2.10	0.0002
98	#N/A	Natterin-like protein	-5.29	0.0002
99	CLDN8	Claudin-8	2.04	0.0002
100	#N/A	Transposon TX1 uncharacterized 149 kDa protein	-5.13	0.0002
101	Smoc2	SPARC-related modular calcium-binding protein 2	2.89	0.0002
102	Evpl	Envoplakin	2.04	0.0002
103	SEC23A	Protein transport protein Sec23A	2.16	0.0002
104	GIMAP5	GTPase IMAP family member 5	6.05	0.0002
105	#N/A	Natterin-like protein	-7.47	0.0003
106	#N/A	GRAM domain-containing protein 1C	1.87	0.0003
107	GIMAP7	GTPase IMAP family member 7	3.55	0.0003
108	TRIM16	Tripartite motif-containing protein 16	1.00	0.0003
109	SH2D4A	SH2 domain-containing protein 4A	5.80	0.0003
110	Mefv	Pyrin	2.64	0.0003
111	Cit	Citron Rho-interacting kinase	-6.08	0.0004
112	Plekhf1	Pleckstrin homology domain-containing family F member 1	2.24	0.0004
113	Osbpl6	Oxysterol-binding protein-related protein 6	1.67	0.0004
114	nos2	Nitric oxide synthase, inducible	4.40	0.0004
115	Ggps1	Geranylgeranyl pyrophosphate synthase	-2.37	0.0004
116	AHNAK	Neuroblast differentiation-associated protein AHNAK	2.07	0.0004
117	GAD1	Glutamate decarboxylase 1	5.64	0.0004
118	NLRP12	NACHT, LRR and PYD domains-containing protein 12	2.45	0.0004
119	MAML3	Mastermind-like protein 3	-2.34	0.0004
120	NLRP1	NACHT, LRR and PYD domains-containing protein 1	1.48	0.0005
121	CLDN4	Claudin-4	4.07	0.0005
122	Ap1s3	AP-1 complex subunit sigma-3	2.52	0.0005
123	alas1	5-aminolevulinate synthase, nonspecific, mitochondrial	3.38	0.0005
124	OGDH	2-oxoglutarate dehydrogenase, mitochondrial	-2.55	0.0005
125	Pwp2	Periodic tryptophan protein 2 homolog	-3.55	0.0006
126	CD74	HLA class II histocompatibility antigen gamma chain	3.55	0.0006
127	ARPC1A	Actin-related protein 2/3 complex subunit 1A	1.52	0.0006
128	Gpr119	Glucose-dependent insulinotropic receptor	-2.88	0.0006
129	SAT1	Diamine acetyltransferase 1	2.47	0.0006
130	ERVPABLB-1	Endogenous retrovirus group PABLB member 1 Env polyprotein	5.71	0.0006
131	GIMAP7	GTPase IMAP family member 7	3.81	0.0006
132	znf395	Zinc finger protein 395	2.56	0.0006
133	wwox	WW domain-containing oxidoreductase	-2.31	0.0006
134	Snx18	Sorting nexin-18	3.44	0.0007
135	MXD4	Max dimerization protein 4	2.43	0.0007
136	HELZ2	Helicase with zinc finger domain 2	2.80	0.0007
137	krt13	Keratin, type I cytoskeletal 13	2.73	0.0007
138	SYT7	Synaptotagmin-7	-5.32	0.0007
139	cyp1a3	Cytochrome P450 1A3	4.20	0.0008
140	Pol	LINE-1 retrotransposable element ORF2 protein	-3.10	0.0008
141	#N/A	Neoverrucotoxin subunit beta	-4.49	0.0008
142	Dennd3	DENN domain-containing protein 3	2.10	0.0009
143	Tnik	Traf2 and NCK-interacting protein kinase	-2.72	0.0009
144	VGLL1	Transcription cofactor vestigial-like protein 1	2.34	0.0009
145	NLRC3	Protein NLRC3	5.77	0.0009
146	hbb4	Hemoglobin subunit beta-4	5.14	0.0009
147	tc3a	Transposable element Tc3 transposase	2.76	0.0010
148	Hip1r	Huntingtin-interacting protein 1-related protein	1.54	0.0010
149	PPL	Periplakin	1.48	0.0010
150	Nfkb2	Nuclear factor NF-kappa-B p100 subunit	1.74	0.0010
151	SAT1	Diamine acetyltransferase 1	2.28	0.0010
152	#N/A	LINE-1 retrotransposable element ORF2 protein	-7.71	0.0010
153	Stx11	Syntaxin-11	3.12	0.0010

154	cnpy3	Protein canopy homolog 3	3.14	0.0010
155	uck1	Uridine-cytidine kinase 1	-3.45	0.0010
156	MYL9	Myosin regulatory light polypeptide 9	2.63	0.0010
157	tdrd7b	Tudor domain-containing protein 7B	2.74	0.0011
158	LITAF	Lipopolysaccharide-induced tumor necrosis factor-alpha factor homolog	2.59	0.0011
159	#N/A	Lipoma HMGIC fusion partner homolog	-1.97	0.0011
160	CNBP	Cellular nucleic acid-binding protein	-3.34	0.0011
161	Eif4g3	Eukaryotic translation initiation factor 4 gamma 3	-6.07	0.0011
162	Trim39	E3 ubiquitin-protein ligase TRIM39	1.96	0.0011
163	ALOXE3	Hydroperoxide isomerase ALOXE3	-3.39	0.0011
164	Myo1e	Unconventional myosin-Ie	1.63	0.0012
165	Sec31b	Protein transport protein Sec31B	-2.70	0.0012
166	GPX2	Glutathione peroxidase 2	4.35	0.0012
167	TRIM25	E3 ubiquitin/ISG15 ligase TRIM25	1.54	0.0012
168	#N/A	Stonustoxin subunit alpha	2.30	0.0012
169	mkrn1	Probable E3 ubiquitin-protein ligase makorin-1	1.77	0.0012
170	URGCP	Up-regulator of cell proliferation	5.97	0.0013
171	PDZD2	PDZ domain-containing protein 2	-2.11	0.0013
172	Gpr108	Protein GPR108	-2.08	0.0013
173	Tf2-9	Transposon Tf2-9 polyprotein	-2.05	0.0013
174	chmp4c	Charged multivesicular body protein 4c	2.53	0.0013
175	FARP1	FERM, RhoGEF and pleckstrin domain-containing protein 1	-2.37	0.0013
176	PFN1	Profilin-1	2.59	0.0013
177	#N/A	Spartin	2.12	0.0013
178	Casp8	Caspase-8	2.87	0.0014
179	Nampt	Nicotinamide phosphoribosyltransferase	2.56	0.0014
180	HSPA12A	Heat shock 70 kDa protein 12A	7.30	0.0014
181	#N/A	Intermediate filament protein ON3	3.29	0.0015
182	pla2g4a	Cytosolic phospholipase A2	2.28	0.0015
183	AHNAK	Neuroblast differentiation-associated protein AHNAK	2.58	0.0015
184	MCL1	Induced myeloid leukemia cell differentiation protein Mcl-1 homolog	1.84	0.0015
185	C8orf44	Putative uncharacterized protein C8orf44	-5.62	0.0015
186	ENPP	Enterin neuropeptides	-3.72	0.0016
187	CLDN4	Claudin-4	4.15	0.0016
188	AHNAK	Neuroblast differentiation-associated protein AHNAK	2.81	0.0016
189	Arl4d	ADP-ribosylation factor-like protein 4D	2.27	0.0016
190	MCL1	Induced myeloid leukemia cell differentiation protein Mcl-1 homolog	2.68	0.0016
191	Clta	Clathrin light chain A	2.06	0.0016
192	pim2	Serine/threonine-protein kinase pim-2	1.96	0.0016
193	Tf2-9	Transposon Tf2-9 polyprotein	-2.16	0.0017
194	eif3h	Eukaryotic translation initiation factor 3 subunit H	2.74	0.0017
195	GIMAP4	GTPase IMAP family member 4	1.41	0.0017
196	LMO7	LIM domain only protein 7	3.01	0.0017
197	hsp90a.1	Heat shock protein HSP 90-alpha 1	4.39	0.0018
198	USP43	Ubiquitin carboxyl-terminal hydrolase 43	-5.41	0.0018
199	DUSP5	Dual specificity protein phosphatase 5	3.03	0.0018
200	banf1	Barrier-to-autointegration factor	3.98	0.0018
201	Cpeb2	Cytoplasmic polyadenylation element-binding protein 2	4.21	0.0018
202	HHLA2	HERV-H LTR-associating protein 2	2.31	0.0018
203	#N/A	Antho-RFamide neuropeptides type 2	-2.73	0.0019
204	ARPC1B	Actin-related protein 2/3 complex subunit 1B	2.80	0.0019
205	mx2	Interferon-induced GTP-binding protein Mx2	1.69	0.0019
206	AHNAK	Neuroblast differentiation-associated protein AHNAK	2.73	0.0019
207	MIMI_R795	Probable bifunctional E2/E3 enzyme R795	2.82	0.0019
208	STAT3	Signal transducer and activator of transcription 3	1.84	0.0019
209	#N/A	Transposable element Tcb2 transposase	-3.26	0.0020
210	Mknk2	MAP kinase-interacting serine/threonine-protein kinase 2	1.81	0.0020
211	REL	Proto-oncogene c-Rel	2.32	0.0020
212	#N/A	Peroxiredoxin	2.89	0.0020
213	CGN	Cingulin	3.51	0.0020
214	PTPRZ1	Receptor-type tyrosine-protein phosphatase zeta	-2.44	0.0020
215	NUGGC	Nuclear GTPase SLIP-GC	-2.95	0.0020
216	MTHFD2	Bifunctional methylenetetrahydrofolate dehydrogenase/cyclohydrolase, mitochondrial	3.77	0.0021
217	GVINP1	Interferon-induced very large GTPase 1	5.82	0.0021
218	Dop1b	Protein dopey-2	2.51	0.0021

219	nfkb2	Nuclear factor NF-kappa-B p100 subunit	1.89	0.0021
220	WDR59	WD repeat-containing protein 59	-2.59	0.0022
221	Rab32	Ras-related protein Rab-32	4.57	0.0022
222	#N/A	Transposon TX1 uncharacterized 149 kDa protein	-2.14	0.0023
223	Tnfrsf22	Tumor necrosis factor receptor superfamily member 22	3.69	0.0023
224	DUSP1	Dual specificity protein phosphatase 1	2.91	0.0023
225	hbb1	Hemoglobin subunit beta-1	6.01	0.0023
226	Nos2	Nitric oxide synthase, inducible	4.04	0.0023
227	Trim29	Tripartite motif-containing protein 29	2.61	0.0023
228	Dsp	Desmoplakin	-3.33	0.0024
229	ARL4A	ADP-ribosylation factor-like protein 4A	2.12	0.0024
230	SULF2	Extracellular sulfatase Sulf-2	-4.37	0.0024
231	DLEC1	Deleted in lung and esophageal cancer protein 1	-3.37	0.0024
232	CARD6	Caspase recruitment domain-containing protein 6	1.87	0.0025
233	ubqJ	Polyubiquitin-J	2.45	0.0025
234	jag1b	Protein jagged-1b	-2.05	0.0025
235	TRIM27	Zinc finger protein RFP	-2.37	0.0025
236	amotl2a	Angiomotin-like 2a	1.92	0.0026
237	Fam214b	Protein FAM214B	2.74	0.0026
238	Dsp	Desmoplakin	-6.61	0.0026
239	#N/A	Ferritin, heavy subunit	3.34	0.0028
240	krt18	Keratin, type I cytoskeletal 18	4.84	0.0028
241	cct3	T-complex protein 1 subunit gamma	4.41	0.0028
242	gna11	Guanine nucleotide-binding protein subunit alpha-11	5.14	1.0000
243	Rab7a	Ras-related protein Rab-7a	3.41	0.0028
244	SLC25A5	ADP/ATP translocase 2	3.00	0.0028
245	STYK1	Tyrosine-protein kinase STYK1	2.28	0.0028
246	naa60	N-alpha-acetyltransferase 60	-2.62	0.0029
247	rps13	40S ribosomal protein S13	2.73	0.0029
248	EVPL	Envoplakin	1.25	0.0029
249	#N/A	Zinc finger protein ENSP00000375192	-5.53	0.0030
250	RELB	Transcription factor RelB	1.65	0.0030
251	Rabgap1	Rab GTPase-activating protein 1	1.48	0.0031
252	Tmod3	Tropomodulin-3	1.59	0.0031
253	RAB7A	Ras-related protein Rab-7a	1.64	0.0031
254	BCAR3	Breast cancer anti-estrogen resistance protein 3	-2.62	0.0031
255	Atf3	Cyclic AMP-dependent transcription factor ATF-3	2.27	0.0031
256	Sacs	Sacsin	2.32	0.0031
257	PTBP1	Polypyrimidine tract-binding protein 1	1.86	0.0031
258	PARP14	Poly [ADP-ribose] polymerase 14	2.10	0.0032
259	SUPT20H	Transcription factor SPT20 homolog	-2.54	0.0032
260	PARP14	Poly [ADP-ribose] polymerase 14	1.74	0.0032
261	ANLN	Actin-binding protein anillin	-3.07	0.0032
262	cpeb4	Cytoplasmic polyadenylation element-binding protein 4	6.09	0.0032
263	Higd1a	HIG1 domain family member 1A, mitochondrial	2.07	0.0032
264	Tmprss4	Transmembrane protease serine 4	2.18	0.0033
265	alcama	CD166 antigen homolog A	1.75	0.0033
266	Efhd2	EF-hand domain-containing protein D2	2.48	0.0033
267	mfsd2ab	Sodium-dependent lysophosphatidylcholine symporter 1-B	-2.51	0.0033
268	ORF1	Replicase polyprotein	5.57	0.0034
269	YBX1	Nuclease-sensitive element-binding protein 1	2.56	0.0034
270	#N/A	Transposon TX1 uncharacterized 149 kDa protein	-2.82	0.0034
271	Tf2-6	Transposon Tf2-6 polyprotein	2.35	0.0034
272	KRT8	Keratin, type II cytoskeletal 8	1.83	0.0035
273	Stat1	Signal transducer and activator of transcription 1	1.74	0.0035
274	MUC22	Mucin-22	-2.88	0.0035
275	paqr5b	Membrane progestin receptor gamma-B	2.14	0.0035
276	YWHAH	14-3-3 protein eta	1.81	0.0036
277	Kcnj10	ATP-sensitive inward rectifier potassium channel 10	5.49	0.0037
278	pim2	Serine/threonine-protein kinase pim-2	2.43	0.0037
279	Enc1	Ectoderm-neural cortex protein 1	6.01	0.0037
280	FGD4	FYVE, RhoGEF and PH domain-containing protein 4	-2.02	0.0037
281	hddc3	Guanosine-3',5'-bis(diphosphate) 3'-pyrophosphohydrolase MESH1	2.56	0.0038
282	F5	Coagulation factor V	-3.19	0.0038
283	#N/A	Polyubiquitin	4.16	0.0038
284	Scin	Adseverin	2.98	0.0039

285	Krt20	Keratin, type I cytoskeletal 20	2.56	0.0039
286	PIBF1	Progesterone-induced-blocking factor 1	-2.97	0.0039
287	Nfkbia	NF-kappa-B inhibitor alpha	1.91	0.0040
288	CENPV	Centromere protein V	3.42	0.0040
289	Xrcc1	DNA repair protein XRCC1	-2.44	0.0040
290	#N/A	Stonustoxin subunit alpha	5.97	0.0041
291	TPD52	Tumor protein D52	2.87	0.0041
292	#N/A	LINE-1 retrotransposable element ORF2 protein	-4.98	0.0041
293	krt18	Keratin, type I cytoskeletal 18	2.52	0.0042
294	Arrdc3	Arrestin domain-containing protein 3	2.71	0.0042
295	IRF3	Interferon regulatory factor 3	4.26	0.0042
296	fam160a2	FTS and Hook-interacting protein homolog	-2.22	0.0042
297	QSOX1	Sulfhydryl oxidase 1	3.48	0.0043
298	DOP1B	Protein dopey-2	2.35	0.0043
299	Gpr141	Probable G-protein coupled receptor 141	-2.11	0.0044
300	Vamp8	Vesicle-associated membrane protein 8	2.02	0.0044
301	ctsd	Cathepsin D	3.54	0.0044
302	LMO7	LIM domain only protein 7	2.49	0.0044
303	HERC5	E3 ISG15--protein ligase HERC5	3.58	0.0044
304	mapk1	Mitogen-activated protein kinase 1	-4.17	0.0045
305	Moe	Moesin/ezrin/radixin homolog 1 {ECO:0000250|UniProtKB:P46150}	2.28	0.0045
306	VPS52	Vacuolar protein sorting-associated protein 52 homolog	4.27	0.0046
307	RASSF8	Ras association domain-containing protein 8	2.56	0.0046
308	EZR	Ezrin	2.32	0.0047
309	AHNAK	Neuroblast differentiation-associated protein AHNAK	2.62	0.0047
310	Dhx58	Probable ATP-dependent RNA helicase DHX58	2.30	0.0047
311	LIAT1	Protein LIAT1 {ECO:0000305}	-2.27	0.0047
312	#N/A	RNA-directed RNA polymerase beta chain	6.84	0.0047
313	Ldlrap1	Low density lipoprotein receptor adapter protein 1	-2.77	0.0047
314	RALGAPA1	Ral GTPase-activating protein subunit alpha-1	5.32	1.0000
315	Gimap4	GTPase IMAP family member 4	2.48	0.0048
316	ELOVL6	Elongation of very long chain fatty acids protein 6	1.47	0.0048
317	Ngef	Ephexin-1	1.91	0.0048
318	CCNG2	Cyclin-G2	2.23	0.0048
319	ELOVL1	Elongation of very long chain fatty acids protein 1	2.57	0.0048
320	GIMAP5	GTPase IMAP family member 5	2.36	0.0048
321	krt13	Keratin, type I cytoskeletal 13	1.74	0.0048
322	#N/A	Stonustoxin subunit beta	1.40	0.0048
323	MALT1	Mucosa-associated lymphoid tissue lymphoma translocation protein 1	1.63	0.0048
324	farsa	Phenylalanine--tRNA ligase alpha subunit	3.04	0.0048
325	TRAK2	Trafficking kinesin-binding protein 2	-2.58	0.0049
326	Tmem131	Transmembrane protein 131	2.87	0.0049
327	SEC24C	Protein transport protein Sec24C	1.66	0.0050
328	K12H4.7	Putative serine protease K12H4.7	3.92	0.0050
329	Cgas	Cyclic GMP-AMP synthase	2.46	0.0050
330	MCTP2	Multiple C2 and transmembrane domain-containing protein 2	2.03	0.0050
331	TY3B-G	Transposon Ty3-G Gag-Pol polyprotein	1.35	0.0050
332	Mep1b	Meprin A subunit beta	3.64	0.0050
333	FN1	Fibronectin	-6.90	0.0051
334	DTX3L	E3 ubiquitin-protein ligase DTX3L	5.17	1.0000
335	WWC1	Protein KIBRA	1.50	0.0051
336	ABCC10	Multidrug resistance-associated protein 7	4.10	0.0052
337	Prc1	Protein regulator of cytokinesis 1 {ECO:0000312|MGI:MGI:1858961}	-5.28	1.0000
338	#N/A	Transposon TX1 uncharacterized 149 kDa protein	-2.08	0.0053
339	Prss27	Serine protease 27	1.76	0.0054
340	Zfhx4	Zinc finger homeobox protein 4	-4.50	0.0054
341	Slc25a5	ADP/ATP translocase 2	2.11	0.0055
342	Stat3	Signal transducer and activator of transcription 3	1.86	0.0055
343	#N/A	Prothoracicostatic peptide	-3.47	0.0055
344	#N/A	Death ligand signal enhancer	3.27	0.0056
345	FMNL1	Formin-like protein 1	3.58	0.0056
346	#N/A	LINE-1 retrotransposable element ORF2 protein	-5.41	0.0056
347	Gabarapl2	Gamma-aminobutyric acid receptor-associated protein-like 2	2.28	0.0057
348	gna14	Guanine nucleotide-binding protein subunit alpha-14	3.43	0.0058
349	ptprf	Receptor-type tyrosine-protein phosphatase F	-1.28	0.0059
350	#N/A	RNA-dependent RNA polymerase	3.59	0.0059

351	Gvin1	Interferon-induced very large GTPase 1	2.18	0.0059
352	Kiaa1671	Uncharacterized protein KIAA1671	2.17	0.0059
353	NINL	Ninein-like protein	4.29	0.0059
354	krt18	Keratin, type I cytoskeletal 18	2.42	0.0059
355	ybx2-a	Y-box-binding protein 2-A	1.54	0.0060
356	sdha	Succinate dehydrogenase [ubiquinone] flavoprotein subunit, mitochondrial	-3.61	0.0060
357	GADD45A	Growth arrest and DNA damage-inducible protein GADD45 alpha	3.31	0.0061
358	BNIPL	Bcl-2/adenovirus E1B 19 kDa-interacting protein 2-like protein	1.32	0.0061
359	#N/A	Stonustoxin subunit beta	2.64	0.0061
360	PNP	Purine nucleoside phosphorylase	1.51	0.0063
361	ctsd	Cathepsin D	2.39	0.0063
362	TRAP1	Heat shock protein 75 kDa, mitochondrial	2.70	0.0063
363	lsm12a	Protein LSM12 homolog A	3.25	0.0064
364	TEX2	Testis-expressed sequence 2 protein	2.19	0.0064
365	At5g39570	Uncharacterized protein At5g39570	-3.13	0.0064
366	HLF	Hepatic leukemia factor	3.29	0.0064
367	YRK	Proto-oncogene tyrosine-protein kinase Yrk	5.06	1.0000
368	CAPN9	Calpain-9	1.50	0.0065
369	xiap	E3 ubiquitin-protein ligase XIAP {ECO:0000250|UniProtKB:P98170}	1.85	0.0065
370	#N/A	ES1 protein homolog, mitochondrial	2.02	0.0065
371	STAP2	Signal-transducing adaptor protein 2	1.91	0.0066
372	PSAP	Prosaposin	2.18	0.0066
373	aste1	Protein asteroid homolog 1	2.91	0.0066
374	RHA2	Rhodotorucin-A peptides type 2	-2.73	0.0067
375	SCIN	Adseverin	3.51	0.0067
376	ANKK1	Ankyrin repeat and protein kinase domain-containing protein 1	2.62	0.0067
377	rps10	40S ribosomal protein S10	2.31	0.0068
378	CXCL8	Interleukin-8	4.93	0.0069
379	Kctd5	BTB/POZ domain-containing protein KCTD5	2.19	0.0069
380	ZBTB11	Zinc finger and BTB domain-containing protein 11	-2.52	0.0069
381	#N/A	Saxiphilin	5.31	1.0000
382	Tmem238	Transmembrane protein 238	1.61	0.0069
383	cfl2	Cofilin-2	2.60	0.0069
384	RNF138	E3 ubiquitin-protein ligase RNF138 {ECO:0000305}	4.53	1.0000
385	fut11	Alpha-(1,3)-fucosyltransferase 11	1.84	0.0070
386	Snx18	Sorting nexin-18	4.14	0.0070
387	EZR	Ezrin	1.79	0.0071
388	ORF	Putative enzymatic polyprotein	-5.50	1.0000
389	FBP1	Fructose-1,6-bisphosphatase 1	5.03	0.0071
390	#N/A	Natterin-like protein	-2.33	0.0072
391	GNE	Bifunctional UDP-N-acetylglucosamine 2-epimerase/N-acetylmannosamine kinase	1.90	0.0072
392	TMPRSS13	Transmembrane protease serine 13	3.06	0.0073
393	#N/A	Transposon TX1 uncharacterized 82 kDa protein	-1.69	0.0073
394	gnb1	Guanine nucleotide-binding protein G(I)/G(S)/G(T) subunit beta-1	1.44	0.0073
395	F5	Coagulation factor V	-1.94	0.0073
396	Fhl1	Four and a half LIM domains protein 1	5.23	1.0000
397	HERC3	Probable E3 ubiquitin-protein ligase HERC3	3.80	0.0074
398	Serp1	Stress-associated endoplasmic reticulum protein 1	2.28	0.0074
399	npc2	Epididymal secretory protein E1	2.32	0.0075
400	Arhgap27	Rho GTPase-activating protein 27	1.58	0.0075
401	CTSB	Cathepsin B	3.92	0.0076
402	STAT1	Signal transducer and activator of transcription 1	1.28	0.0076
403	#N/A	Transposon TX1 uncharacterized 149 kDa protein	-2.49	0.0076
404	ARPC1B	Actin-related protein 2/3 complex subunit 1B	1.61	0.0077
405	TIGD1	Tigger transposable element-derived protein 1	-6.31	0.0077
406	ssr1	Translocon-associated protein subunit alpha	2.63	0.0077
407	STYK1	Tyrosine-protein kinase STYK1	1.72	0.0077
408	Herc4	Probable E3 ubiquitin-protein ligase HERC4	2.97	0.0078
409	ORF2	RNA-directed RNA polymerase	6.72	0.0078
410	ARHGEF26	Rho guanine nucleotide exchange factor 26	2.69	0.0078
411	exsA	Spore coat assembly protein ExsA	-2.53	0.0078
412	slc39a9-b	Zinc transporter ZIP9-B	-2.42	0.0078
413	ucp2	Mitochondrial uncoupling protein 2	1.68	0.0078
414	Ikbkg	NF-kappa-B essential modulator	-1.72	0.0079
415	GLRX3	Glutaredoxin-3	-2.11	0.0079

416	hsc71	Heat shock cognate 70 kDa protein	2.50	0.0079
417	ZNF185	Zinc finger protein 185	3.24	0.0080
418	Rab11fip1	Rab11 family-interacting protein 1	1.38	0.0080
419	NLRC3	Protein NLRC3	2.88	0.0080
420	Cfl2	Cofilin-2	1.89	0.0080
421	tcaf	TRPM8 channel-associated factor homolog	2.22	0.0080
422	mpp1	55 kDa erythrocyte membrane protein	4.29	0.0080
423	RASGEF1C	Ras-GEF domain-containing family member 1C	3.73	0.0080
424	Tesk2	Dual specificity testis-specific protein kinase 2	-2.68	0.0081
425	Cmpk2	UMP-CMP kinase 2, mitochondrial	5.22	1.0000
426	Arf2	ADP-ribosylation factor 2	1.79	0.0083
427	RNF225	RING finger protein 225 {ECO:0000312|HGNC:HGNC:51249}	1.93	0.0083
428	MPZL2	Myelin protein zero-like protein 2	-2.19	0.0083
429	DDB_G0268948	Putative methyltransferase DDB_G0268948	4.46	1.0000
430	eif4ebp3l	Eukaryotic translation initiation factor 4E-binding protein 3-like	3.95	0.0084
431	TY3B-G	Transposon Ty3-G Gag-Pol polyprotein	-5.29	0.0084
432	Arhgef38	Rho guanine nucleotide exchange factor 38	1.69	0.0085
433	YPEL5	Protein yippee-like 5	3.56	0.0085
434	SAT1	Diamine acetyltransferase 1	2.64	0.0085
435	POU2F1	POU domain, class 2, transcription factor 1	2.08	0.0085
436	ORF56	Uncharacterized protein ORF56	2.91	0.0086
437	XBP1	X-box-binding protein 1 {ECO:0000250|UniProtKB:P17861}	1.49	0.0086
438	WWC1	Protein KIBRA	1.61	0.0087
439	YWHAE	14-3-3 protein epsilon	2.17	0.0087
440	ARAP1	Arf-GAP with Rho-GAP domain, ANK repeat and PH domain-containing protein 1	2.38	0.0087
441	ptprf	Receptor-type tyrosine-protein phosphatase F	-2.63	0.0087
442	ATP2A2	Sarcoplasmic/endoplasmic reticulum calcium ATPase 2	3.80	0.0088
443	GPX2	Glutathione peroxidase 2	2.96	0.0089
444	BICD1	Protein bicaudal D homolog 1	-3.19	0.0090
445	MAP3K5	Mitogen-activated protein kinase 5	1.71	0.0090
446	SAT1	Diamine acetyltransferase 1	3.56	0.0090
447	HMMR	Hyaluronan mediated motility receptor	-3.16	0.0090
448	SLC16A9	Monocarboxylate transporter 9	3.30	0.0091
449	Gpr119	Glucose-dependent insulinotropic receptor	-3.64	0.0091
450	HERC3	Probable E3 ubiquitin-protein ligase HERC3	3.44	0.0091
451	pol	Retrovirus-related Pol polyprotein from transposon 17.6	-6.03	0.0093
452	Lnx2	Ligand of Numb protein X 2	1.94	0.0093
453	DAPK3	Death-associated protein kinase 3	2.81	0.0093
454	Zdbf2	DBF4-type zinc finger-containing protein 2 homolog	-2.71	0.0093
455	IGFBP3	Insulin-like growth factor-binding protein 3	-4.99	0.0093
456	MTCL1	Microtubule cross-linking factor 1	5.11	1.0000
457	ERVK-5	Endogenous retrovirus group K member 5 Np9 protein	-5.34	0.0095
458	Tf2-9	Transposon Tf2-9 polyprotein	2.44	0.0096
459	Tbc1d15	TBC1 domain family member 15	1.77	0.0096
460	B3galt2	Beta-1,3-galactosyltransferase 2	2.13	0.0097
461	LDLRAP1	Low density lipoprotein receptor adapter protein 1	-3.79	0.0098
462	PDE4DIP	Myomegalin	-2.67	0.0098
463	samhd1	Deoxynucleoside triphosphate triphosphohydrolase SAMHD1	1.62	0.0098
464	SPT6	Transcription elongation factor SPT6	-3.42	0.0098
465	vUbi	Ubiquitin-like protein	3.93	0.0098
466	UBE2V1	Ubiquitin-conjugating enzyme E2 variant 1	2.32	0.0098
467	Eef1d	Elongation factor 1-delta	2.05	0.0099
468	GBP1	Guanylate-binding protein 1	1.15	0.0100
469	gag	Nucleic-acid-binding protein from mobile element jockey	-1.63	0.0100
470	APOD	Apolipoprotein D	3.62	0.0100
471	MGST3	Microsomal glutathione S-transferase 3	2.13	0.0101
472	TPRN	Taperin	3.07	0.0101
473	Sox9	Transcription factor SOX-9	2.41	0.0102
474	BTNL9	Butyrophilin-like protein 9	5.15	1.0000
475	NFE2L2	Nuclear factor erythroid 2-related factor 2	3.69	0.0102
476	Gvin1	Interferon-induced very large GTPase 1	2.70	0.0103
477	SECISBP2L	Selenocysteine insertion sequence-binding protein 2-like	1.78	0.0103
478	Nfkbia	NF-kappa-B inhibitor alpha	1.85	0.0105
479	UGT2A3	UDP-glucuronosyltransferase 2A3	5.53	0.0105
480	#N/A	Stonustoxin subunit alpha	-1.50	0.0105

481	PRDX5	Peroxiredoxin-5, mitochondrial	1.99	0.0105
482	GRB7	Growth factor receptor-bound protein 7	2.04	0.0106
483	ADAMTSL5	ADAMTS-like protein 5	3.26	0.0107
484	Itsn1	Intersectin-1	2.39	0.0107
485	Nfkb2	Nuclear factor NF-kappa-B p100 subunit	2.35	0.0107
486	L1RE1	LINE-1 retrotransposable element ORF1 protein	-5.23	0.0108
487	mx2	Interferon-induced GTP-binding protein Mx2	1.55	0.0108
488	Pcbp2	Poly(rC)-binding protein 2	1.98	0.0110
489	max	Protein max	1.88	0.0110
490	DLEC1	Deleted in lung and esophageal cancer protein 1	-2.98	0.0111
491	DNAJC7	DnaJ homolog subfamily C member 7	1.79	0.0111
492	Sdcbp	Syntenin-1	2.12	0.0111
493	NFE2L1	Nuclear factor erythroid 2-related factor 1	4.82	1.0000
494	ACTN4	Alpha-actinin-4 {ECO:0000305}	1.54	0.0113
495	Fgd3	FYVE, RhoGEF and PH domain-containing protein 3	1.46	0.0113
496	FLII	Protein flightless-1 homolog	-1.96	0.0114
497	ANXA13	Annexin A13	4.95	1.0000
498	Tf2-9	Transposon Tf2-9 polyprotein	6.10	0.0116
499	Atp8b1	Phospholipid-transporting ATPase IC	2.23	0.0117
500	ENDOD1	Endonuclease domain-containing 1 protein	4.79	0.0118
501	p1	RNA-directed RNA polymerase	5.35	1.0000
502	CREB3L4	Cyclic AMP-responsive element-binding protein 3-like protein 4	1.96	0.0119
503	CYTH1	Cytohesin-1	5.27	1.0000
504	Ptbp3	Polypyrimidine tract-binding protein 3	1.57	0.0121
505	Irs2	Insulin receptor substrate 2	2.50	0.0121
506	Pard6b	Partitioning defective 6 homolog beta	2.14	0.0122
507	SEMA6D	Semaphorin-6D	2.04	0.0122
508	#N/A	Intestinal mucin-like protein	-2.21	0.0122
509	Rora	Nuclear receptor ROR-alpha	3.18	0.0123
510	rxrba	Retinoic acid receptor RXR-beta-A	1.71	0.0123
511	Ctss	Cathepsin S	2.37	0.0123
512	PARP14	Poly [ADP-ribose] polymerase 14	1.67	0.0123
513	ABCA1	ATP-binding cassette sub-family A member 1	2.31	0.0124
514	psmb9-a	Proteasome subunit beta type-9	1.71	0.0124
515	Map4k4	Mitogen-activated protein kinase kinase kinase kinase 4	4.97	1.0000
516	hmx3	Homeobox protein HMX3	6.55	0.0125
517	KLF2	Krueppel-like factor 2	2.31	0.0126
518	eef1d	Elongation factor 1-delta	2.54	0.0126
519	Spata13	Spermatogenesis-associated protein 13	3.39	0.0128
520	Stambpl1	AMSH-like protease	2.64	0.0128
521	FASLG	Tumor necrosis factor ligand superfamily member 6	2.93	0.0129
522	afap1l1	Actin filament-associated protein 1-like 1	-1.99	0.0129
523	MIMI_L138	Uncharacterized protein L138	-3.36	0.0129
524	pol	Retrovirus-related Pol polyprotein from transposon 297	-3.99	0.0129
525	PRKD3	Serine/threonine-protein kinase D3	3.75	0.0130
526	EIF4EBP2	Eukaryotic translation initiation factor 4E-binding protein 2	2.27	0.0131
527	MCTP2	Multiple C2 and transmembrane domain-containing protein 2	2.58	0.0132
528	GNE	Bifunctional UDP-N-acetylglucosamine 2-epimerase/N-acetylmannosamine kinase	2.06	0.0133
529	GMNC	Geminin coiled-coil domain-containing protein 1	4.78	1.0000
530	Dleu7	Leukemia-associated protein 7 homolog	5.25	1.0000
531	pol	Pol polyprotein	-1.74	0.0134
532	#N/A	Stonustoxin subunit alpha	1.32	0.0135
533	amotl2a	Angiomotin-like 2a	4.34	0.0135
534	EPRS	Bifunctional glutamate/proline--tRNA ligase	1.53	0.0136
535	URGCP	Up-regulator of cell proliferation	3.67	0.0136
536	slc30a8	Zinc transporter 8	3.92	0.0136
537	Iscu	Iron-sulfur cluster assembly enzyme ISCU, mitochondrial	2.21	0.0136
538	B3GNT2	N-acetyllactosaminide beta-1,3-N-acetylglucosaminyltransferase 2	1.84	0.0136
539	DAPK3	Death-associated protein kinase 3	2.96	0.0136
540	Slc15a1	Solute carrier family 15 member 1	3.18	0.0137
541	PSAP	Prosaposin	2.17	0.0137
542	Elovl7	Elongation of very long chain fatty acids protein 7	2.23	0.0137
543	SPOP	Speckle-type POZ protein	4.72	1.0000
544	kit	Mast/stem cell growth factor receptor Kit	4.17	0.0138
545	RTL1	Retrotransposon-like protein 1	4.79	1.0000

546	foxp1b	Forkhead box protein P1-B	2.28	0.0140
547	mvp	Major vault protein	1.45	0.0140
548	Hebp2	Heme-binding protein 2	1.37	0.0140
549	RAB11A	Ras-related protein Rab-11A	2.63	0.0141
550	K02A2.6	Uncharacterized protein K02A2.6	-1.79	0.0141
551	ORF1-ORF2	RNA-directed RNA polymerase	6.46	0.0143
552	Zcchc2	Zinc finger CCHC domain-containing protein 2	1.40	0.0143
553	FLII	Protein flightless-1 homolog	-1.46	0.0143
554	notch1	Neurogenic locus notch homolog protein 1	3.13	0.0145
555	YME1L1	ATP-dependent zinc metalloprotease YME1L1	5.77	0.0145
556	krt13	Keratin, type I cytoskeletal 13	2.58	0.0146
557	MYH9	Myosin-9	1.92	0.0147
558	ARG2	Arginase-2, mitochondrial	2.84	0.0148
559	ZNF283	Zinc finger protein 283	-4.30	0.0148
560	ACTN1	Alpha-actinin-1	1.90	0.0148
561	#N/A	Transposon TX1 uncharacterized 149 kDa protein	-2.44	0.0149
562	Rab25	Ras-related protein Rab-25	2.81	0.0150
563	CTSB	Cathepsin B	2.08	0.0150
564	nusap1	Nucleolar and spindle-associated protein 1	-5.07	1.0000
565	cct3	T-complex protein 1 subunit gamma	2.71	0.0151
566	TPP1	Tripeptidyl-peptidase 1	3.40	0.0151
567	aldh1l1	Cytosolic 10-formyltetrahydrofolate dehydrogenase	6.03	0.0151
568	#N/A	RNA-directed RNA polymerase beta chain	6.35	0.0152
569	PRP2	Repetitive proline-rich cell wall protein 2	1.27	0.0154
570	Krt8	Keratin, type II cytoskeletal 8	2.66	0.0154
571	Matk	Megakaryocyte-associated tyrosine-protein kinase	3.77	0.0154
572	SULT2B1	Sulfotransferase family cytosolic 2B member 1	-1.81	0.0155
573	MYH9	Myosin-9	1.86	0.0155
574	Slc17a5	Sialin	2.45	0.0155
575	cyfip1	Cytoplasmic FMR1-interacting protein 1 homolog	1.77	0.0155
576	Srms	Tyrosine-protein kinase Srms	1.63	0.0155
577	#N/A	UPF0729 protein C18orf32 homolog	2.93	0.0156
578	SCEL	Sciellin	1.41	0.0157
579	Zfp36l1	Zinc finger protein 36, C3H1 type-like 1	3.79	0.0157
580	ppp1cb	Serine/threonine-protein phosphatase PP1-beta catalytic subunit	2.20	0.0157
581	#N/A	Transposon TX1 uncharacterized 149 kDa protein	-1.23	0.0158
582	PRDM1	PR domain zinc finger protein 1	2.53	0.0158
583	eif3m	Eukaryotic translation initiation factor 3 subunit M {ECO:0000255|HAMAP-Rule:MF_03012}	2.30	0.0158
584	ARPC1A	Actin-related protein 2/3 complex subunit 1A	2.12	0.0159
585	GLO1	Lactoylglutathione lyase	-5.65	1.0000
586	NCAPG	Condensin complex subunit 3	-3.71	0.0160
587	chtf18	Chromosome transmission fidelity protein 18 homolog	-3.31	0.0160
588	Taldo1	Transaldolase	2.19	0.0160
589	RAPGEF1	Rap guanine nucleotide exchange factor 1	4.87	1.0000
590	ATP6V0E2	V-type proton ATPase subunit e 2	2.32	0.0160
591	TAGLN	Transgelin	3.23	0.0160
592	EPS8L1	Epidermal growth factor receptor kinase substrate 8-like protein 1	1.66	0.0160
593	TMPRSS13	Transmembrane protease serine 13	4.09	0.0162
594	tmem167b	Protein kish-B	2.18	0.0162
595	PRKAR1A	cAMP-dependent protein kinase type I-alpha regulatory subunit	1.63	0.0163
596	PARP14	Poly [ADP-ribose] polymerase 14	1.56	0.0164
597	ZFAND5	AN1-type zinc finger protein 5	2.40	0.0164
598	Spats2	Spermatogenesis-associated serine-rich protein 2	1.53	0.0165
599	Nt5c1a	Cytosolic 5'-nucleotidase 1A	2.80	0.0165
600	Parp14	Poly [ADP-ribose] polymerase 14	1.72	0.0166
601	gse1	Genetic suppressor element 1	-2.23	0.0166
602	Sphk1	Sphingosine kinase 1	1.53	0.0166
603	RT1-B	Rano class II histocompatibility antigen, A beta chain	2.11	0.0166
604	Mxra7	Matrix-remodeling-associated protein 7	-2.77	0.0166
605	LRRFIP1	Leucine-rich repeat flightless-interacting protein 1	2.83	0.0167
606	LMO7	LIM domain only protein 7	1.73	0.0167
607	Ppfibp2	Liprin-beta-2	-1.66	0.0167
608	Sqstm1	Sequestosome-1	2.52	0.0168
609	Peg10	Retrotransposon-derived protein PEG10	2.33	0.0168
610	Magi1	Membrane-associated guanylate kinase, WW and PDZ domain-containing	2.05	0.0168

		protein 1		
611	Dgkb	Diacylglycerol kinase beta	-1.37	0.0169
612	SOX9	Transcription factor SOX-9	2.24	0.0170
613	radil	Ras-associating and dilute domain-containing protein	2.17	0.0170
614	GFPT2	Glutamine--fructose-6-phosphate aminotransferase [isomerizing] 2	1.37	0.0171
615	Pim1	Serine/threonine-protein kinase pim-1	1.53	0.0171
616	GIMAP4	GTPase IMAP family member 4	2.14	0.0172
617	Tbc1d2b	TBC1 domain family member 2B	-2.10	0.0173
618	GSN	Gelsolin	2.13	0.0173
619	LTBP1	Latent-transforming growth factor beta-binding protein 1	4.84	1.0000
620	RASSF3	Ras association domain-containing protein 3	1.48	0.0173
621	IL1R1	Interleukin-1 receptor type 1	-1.37	0.0174
622	pol	RNA-directed DNA polymerase from mobile element jockey	-1.06	0.0175
623	krt18-a	Keratin, type I cytoskeletal 18-A	1.47	0.0175
624	plcd3a	1-phosphatidylinositol 4,5-bisphosphate phosphodiesterase delta-3-A	4.00	0.0176
625	Tf2-9	Transposon Tf2-9 polyprotein	-1.88	0.0176
626	STRN	Striatin	1.40	0.0176
627	DCTN3	Dynactin subunit 3	2.48	0.0176
628	Ssh1	Protein phosphatase Slingshot homolog 1	2.10	0.0178
629	bsdc1	BSD domain-containing protein 1	2.01	0.0178
630	slc40a1	Solute carrier family 40 member 1	2.25	0.0178
631	PRKCD	Protein kinase C delta type	1.19	0.0178
632	eif3i	Eukaryotic translation initiation factor 3 subunit I	-1.97	0.0178
633	chtf18	Chromosome transmission fidelity protein 18 homolog	-4.36	0.0178
634	RBMS1	RNA-binding motif, single-stranded-interacting protein 1	1.93	0.0179
635	LGMN	Legumain	2.04	0.0179
636	UBA52	Ubiquitin-60S ribosomal protein L40	2.31	0.0181
637	Znfx1	NFX1-type zinc finger-containing protein 1	1.46	0.0181
638	arih1	E3 ubiquitin-protein ligase arih1	2.26	0.0181
639	#N/A	Nectin-1	1.80	0.0181
640	ILDR1	Immunoglobulin-like domain-containing receptor 1	2.01	0.0182
641	Syap1	Synapse-associated protein 1	1.48	0.0182
642	Cant1	Soluble calcium-activated nucleotidase 1	2.00	0.0183
643	myd88	Myeloid differentiation primary response protein MyD88	-2.19	0.0183
644	PLS3	Plastin-3	1.75	0.0185
645	Eps8l2	Epidermal growth factor receptor kinase substrate 8-like protein 2	2.15	0.0185
646	RAB2A	Ras-related protein Rab-2A	1.62	0.0186
647	#N/A	Stonustoxin subunit alpha	2.53	0.0187
648	Azin1	Antizyme inhibitor 1	1.96	0.0188
649	actr2a	Actin-related protein 2-A	1.63	0.0188
650	COL6A2	Collagen alpha-2(VI) chain	-3.13	0.0189
651	Kpna2	Importin subunit alpha-1	-2.63	0.0189
652	Jag1	Protein jagged-1	-5.66	0.0189
653	ppp6r3-a	Serine/threonine-protein phosphatase 6 regulatory subunit 3-A	1.26	0.0189
654	Nampt	Nicotinamide phosphoribosyltransferase	2.04	0.0190
655	#N/A	Natterin-like protein	-5.92	0.0192
656	ELL2	RNA polymerase II elongation factor ELL2	2.18	0.0192
657	IGFBP4	Insulin-like growth factor-binding protein 4	5.38	0.0193
658	#N/A	Membrane progestin receptor beta	4.30	0.0193
659	Ank3	Ankyrin-3	-1.93	0.0195
660	ATP5PB	ATP synthase F(0) complex subunit B1, mitochondrial	1.64	0.0195
661	#N/A	Transposable element Tcb1 transposase	-2.03	0.0196
662	trim71	E3 ubiquitin-protein ligase TRIM71	4.82	1.0000
663	amotl2a	Angiomotin-like 2a	2.14	0.0198
664	Pdpk1	3-phosphoinositide-dependent protein kinase 1	1.54	0.0198
665	PRC1	Protein regulator of cytokinesis 1 {ECO:0000312|HGNC:HGNC:9341}	-3.72	0.0199
666	#N/A	Absent in melanoma 1-like protein	1.15	0.0199
667	HIP1R	Huntingtin-interacting protein 1-related protein	1.75	0.0200
668	Rsbn1	Round spermatid basic protein 1	4.18	0.0200
669	Cenpe	Centromere-associated protein E {ECO:0000312|EMBL:AAR85498.1}	-2.28	0.0200
670	CCNG1	Cyclin-G1	2.46	0.0201
671	RPLP1	60S acidic ribosomal protein P1	2.16	0.0201
672	TPD52L2	Tumor protein D54	1.55	0.0202
673	foxa1-a	Forkhead box protein A1-A	4.28	0.0202
674	TMEM131	Transmembrane protein 131	2.25	0.0202
675	NPTX1	Neuronal pentraxin-1	4.39	0.0203

676	GNB3	Guanine nucleotide-binding protein G(I)/G(S)/G(T) subunit beta-3	3.96	0.0203
677	acsbg2	Long-chain-fatty-acid--CoA ligase ACSBG2	1.17	0.0204
678	GVINP1	Interferon-induced very large GTPase 1	3.61	0.0204
679	GAD1	Glutamate decarboxylase 1	4.39	1.0000
680	ATP6V1D	V-type proton ATPase subunit D	2.63	0.0205
681	Fis1	Mitochondrial fission 1 protein	1.96	0.0206
682	AATK	Serine/threonine-protein kinase LMTK1	5.02	1.0000
683	EPS8L2	Epidermal growth factor receptor kinase substrate 8-like protein 2	4.58	1.0000
684	an3	Putative ATP-dependent RNA helicase an3	1.12	0.0213
685	NDUFS8	NADH dehydrogenase [ubiquinone] iron-sulfur protein 8, mitochondrial	2.04	0.0213
686	PPP2CB	Serine/threonine-protein phosphatase 2A catalytic subunit beta isoform	2.19	0.0213
687	RNF186	RING finger protein 186	1.26	0.0214
688	Irf6	Interferon regulatory factor 6	2.10	0.0215
689	Dennd3	DENN domain-containing protein 3	1.66	0.0216
690	fam50a	Protein FAM50A	2.00	0.0216
691	hsc71	Heat shock cognate 70 kDa protein	2.30	0.0216
692	STAT1	Signal transducer and activator of transcription 1	1.48	0.0216
693	OR4S2	Olfactory receptor 4S2	-5.54	1.0000
694	Anpep	Aminopeptidase N	4.75	1.0000
695	Slc17a5	Sialin	2.21	0.0216
696	p65	Proline-rich P65 protein	2.29	0.0217
697	p1	RNA-directed RNA polymerase	6.32	0.0218
698	hba4	Hemoglobin subunit alpha-4	4.19	0.0219
699	#N/A	Class I histocompatibility antigen, F10 alpha chain	9.09	0.0219
700	RHOU	Rho-related GTP-binding protein RhoU	-1.66	0.0219
701	Cdc42ep4	Cdc42 effector protein 4	2.29	0.0219
702	CEP170B	Centrosomal protein of 170 kDa protein B	-2.43	0.0219
703	tmem263-b	Transmembrane protein 263-B	-5.83	0.0220
704	Lgals3	Galectin-3	2.70	0.0220
705	#N/A	Tubulin alpha chain	2.25	0.0221
706	Nupr1	Nuclear protein 1 {ECO:0000305}	3.47	0.0221
707	Nars2	Probable asparagine--tRNA ligase, mitochondrial	-2.39	0.0221
708	cpras1	Circularly permutated Ras protein 1	1.94	0.0221
709	CLDN4	Claudin-4	-2.73	0.0221
710	PPP1R15B	Protein phosphatase 1 regulatory subunit 15B	2.24	0.0223
711	CYTH2	Cytohesin-2	1.76	0.0225
712	optn	Optineurin	1.61	0.0225
713	Tf2-9	Transposon Tf2-9 polyprotein	-1.79	0.0226
714	GSN	Gelsolin	3.54	0.0226
715	TBK1	Serine/threonine-protein kinase TBK1	1.42	0.0226
716	ndh-2	NADH-ubiquinone oxidoreductase chain 2	-6.14	0.0227
717	spire1	Protein spire homolog 1	1.20	0.0228
718	SAMHD1	Deoxynucleoside triphosphate triphosphohydrolase SAMHD1	4.66	1.0000
719	isca1	Iron-sulfur cluster assembly 1 homolog, mitochondrial	-2.19	0.0229
720	pol	Retrovirus-related Pol polyprotein from transposon 297	-4.11	0.0229
721	ITPR3	Inositol 1,4,5-trisphosphate receptor type 3	2.03	0.0230
722	STAT1	Signal transducer and activator of transcription 1	1.44	0.0230
723	Enc1	Ectoderm-neural cortex protein 1	3.66	0.0230
724	ARF4	ADP-ribosylation factor 4	1.42	0.0231
725	#N/A	LINE-1 retrotransposable element ORF2 protein	-5.32	0.0232
726	Znf185	Zinc finger protein 185	1.63	0.0232
727	SH2D4B	SH2 domain-containing protein 4B	1.34	0.0232
728	#N/A	Transposable element Tcb1 transposase	-2.46	0.0233
729	rft2	Riboflavin transporter 2	3.47	0.0235
730	SULT3A1	Amine sulfotransferase	2.62	0.0236
731	Ppp1ca	Serine/threonine-protein phosphatase PP1-alpha catalytic subunit	1.81	0.0237
732	Sash1	SAM and SH3 domain-containing protein 1	1.17	0.0238
733	#N/A	Negative regulator of reactive oxygen species	4.76	1.0000
734	Setd2	Histone-lysine N-methyltransferase SETD2	-3.40	0.0239
735	COX17	Cytochrome c oxidase copper chaperone	-2.76	0.0241
736	Pcbp2	Poly(rC)-binding protein 2	2.57	0.0241
737	EIF2S3	Eukaryotic translation initiation factor 2 subunit 3	1.92	0.0241
738	Farp1	FERM, RhoGEF and pleckstrin domain-containing protein 1	-1.77	0.0242
739	smurf2	E3 ubiquitin-protein ligase SMURF2	1.85	0.0242
740	OAZ2	Ornithine decarboxylase antizyme 2	1.95	0.0242
741	Deptor	DEP domain-containing mTOR-interacting protein	-2.33	0.0243

742	CCT5	T-complex protein 1 subunit epsilon	2.35	0.0243
743	RALGAPA1	Ral GTPase-activating protein subunit alpha-1	3.82	1.0000
744	POU2F3	POU domain, class 2, transcription factor 3	1.89	0.0243
745	wwc1	Protein KIBRA	1.33	0.0245
746	Ube2w	Ubiquitin-conjugating enzyme E2 W	1.62	0.0245
747	BCL2L1	Bcl-2-like protein 1	2.84	0.0245
748	rps23	40S ribosomal protein S23	1.91	0.0246
749	IRF1	Interferon regulatory factor 1	1.43	0.0247
750	TSPAN8	Tetraspanin-8	3.73	0.0247
751	NCF2	Neutrophil cytosol factor 2	4.08	0.0247
752	jak1	Tyrosine-protein kinase JAK1	1.21	0.0247
753	Tnik	Traf2 and NCK-interacting protein kinase	-1.70	0.0247
754	SEMA7A	Semaphorin-7A	2.74	0.0250
755	#N/A	H-2 class II histocompatibility antigen, I-E alpha chain	1.69	0.0250
756	B4GALNT1	Beta-1,4 N-acetylgalactosaminyltransferase 1	2.56	0.0251
757	UBE2V1	Ubiquitin-conjugating enzyme E2 variant 1	2.44	0.0251
758	arl6	ADP-ribosylation factor-like protein 6	-2.62	0.0251
759	CRHR1	Corticotropin-releasing factor receptor 1	4.64	1.0000
760	TY3B-I	Transposon Ty3-I Gag-Pol polyprotein	-1.24	0.0255
761	Mgat3	Beta-1,4-mannosyl-glycoprotein 4-beta-N-acetylglucosaminyltransferase	-1.06	0.0255
762	kit	Mast/stem cell growth factor receptor Kit	2.29	0.0256
763	GIMAP5	GTPase IMAP family member 5	1.29	0.0256
764	Fam83e	Protein FAM83E {ECO:0000305}	3.24	1.0000
765	RNASET2	Ribonuclease T2	2.78	0.0256
766	Tf2-8	Transposon Tf2-8 polyprotein	4.20	0.0257
767	eef1b	Elongation factor 1-beta	2.13	0.0258
768	Ctsz	Cathepsin Z	2.23	0.0258
769	rpl34	60S ribosomal protein L34	2.44	0.0259
770	Vamp3	Vesicle-associated membrane protein 3	2.10	0.0259
771	atp6v0d1	V-type proton ATPase subunit d 1	2.21	0.0260
772	#N/A	Stonustoxin subunit beta	1.32	0.0261
773	mxi1	Max-interacting protein 1	-2.00	0.0261
774	#N/A	Transposable element Tcb1 transposase	2.55	0.0264
775	AHNAK	Neuroblast differentiation-associated protein AHNAK	2.52	0.0266
776	CTSB	Cathepsin B	2.99	0.0266
777	ZC3HAV1	Zinc finger CCCH-type antiviral protein 1	1.28	0.0266
778	dcun1d3	DCN1-like protein 3	1.64	0.0266
779	Ankrd55	Ankyrin repeat domain-containing protein 55	-5.86	0.0268
780	chac1	Glutathione-specific gamma-glutamylcyclotransferase 1 {ECO:0000250|UniProtKB:Q9BUX1}	1.92	0.0268
781	DPEP2	Dipeptidase 2	2.17	0.0270
782	zgc:73324	Coenzyme Q-binding protein COQ10 homolog, mitochondrial	5.43	0.0271
783	Csmd3	CUB and sushi domain-containing protein 3	-1.41	0.0271
784	GBP1	Guanylate-binding protein 1	1.00	0.0272
785	smdt1	Essential MCU regulator, mitochondrial	1.72	0.0275
786	LMO7	LIM domain only protein 7	3.10	0.0275
787	rhoaa	Rho-related GTP-binding protein RhoA-A {ECO:0000305}	1.29	0.0275
788	QSOX1	Sulfhydryl oxidase 1	2.85	0.0275
789	SUN1	SUN domain-containing protein 1	5.58	0.0277
790	Osbpl6	Oxysterol-binding protein-related protein 6	1.44	0.0279
791	SYNPO	Synaptopodin	2.61	0.0280
792	Ptgr1	Prostaglandin reductase 1	2.47	0.0280
793	ldhb	L-lactate dehydrogenase B chain	2.28	0.0280
794	mvp	Major vault protein	1.60	0.0280
795	Atf5	Cyclic AMP-dependent transcription factor ATF-5	3.67	0.0280
796	CACNA1B	Voltage-dependent N-type calcium channel subunit alpha-1B	4.61	1.0000
797	FOSL2	Fos-related antigen 2	1.98	0.0282
798	Eif1	Eukaryotic translation initiation factor 1	1.87	0.0282
799	srsf1	Serine/arginine-rich splicing factor 1	-1.64	0.0283
800	Trafd1	TRAF-type zinc finger domain-containing protein 1	2.61	0.0283
801	TRIM25	E3 ubiquitin/ISG15 ligase TRIM25	-1.77	0.0285
802	Sec14l1	SEC14-like protein 1 {ECO:0000305}	2.20	0.0286
803	Art5	Ecto-ADP-ribosyltransferase 5	2.37	0.0287
804	INPP5D	Phosphatidylinositol 3,4,5-trisphosphate 5-phosphatase 1	3.76	1.0000
805	blcap	Bladder cancer-associated protein	2.62	0.0287
806	MYO1D	Unconventional myosin-Id	2.04	0.0288

807	ZFAND5	AN1-type zinc finger protein 5	4.33	1.0000
808	rpl31	60S ribosomal protein L31	2.30	0.0289
809	MFSD13A	Transmembrane protein 180 {ECO:0000250|UniProtKB:Q14CX5}	2.95	0.0289
810	epd	Ependymin	3.33	0.0289
811	IL17RC	Interleukin-17 receptor C	1.26	0.0289
812	Dolpp1	Dolichyldiphosphatase 1	2.22	0.0290
813	#N/A	Tubulin beta chain	2.71	0.0290
814	SUSD6	Sushi domain-containing protein 6 {ECO:0000312|HGNC:HGNC:19956}	4.16	0.0290
815	URGCP	Up-regulator of cell proliferation	2.59	0.0290
816	NBEAL1	Neurobeachin-like protein 1	1.37	0.0291
817	PYGO2	Pygopus homolog 2	2.92	0.0292
818	krt18	Keratin, type I cytoskeletal 18	2.58	0.0292
819	isyna1-a	Inositol-3-phosphate synthase 1-A	3.66	0.0292
820	STIP1	Stress-induced-phosphoprotein 1	1.91	0.0292
821	EPRS	Bifunctional glutamate/proline--tRNA ligase	1.85	0.0293
822	grtp1a	Growth hormone-regulated TBC protein 1-A	2.32	0.0293
823	mts	Serine/threonine-protein phosphatase PP2A	1.39	0.0293
824	SYNE1	Nesprin-1	-1.65	0.0294
825	BRI3	Brain protein I3	2.41	0.0294
826	chtf18	Chromosome transmission fidelity protein 18 homolog	-5.80	0.0294
827	FNIP1	Folliculin-interacting protein 1	2.04	0.0295
828	EHD1	EH domain-containing protein 1 {ECO:0000305}	1.58	0.0295
829	TGas113e22.1	Histone H3.3	2.12	0.0296
830	#N/A	Transposable element Tcb2 transposase	2.63	0.0297
831	nav3	Neuron navigator 3	1.37	0.0297
832	CTSC	Dipeptidyl peptidase 1	1.68	0.0298
833	#N/A	Histone H3.3	2.17	0.0298
834	DUSP16	Dual specificity protein phosphatase 16	3.56	0.0298
835	ADAR	Double-stranded RNA-specific adenosine deaminase	1.28	0.0299
836	STX19	Syntaxin-19	3.04	0.0300
837	Idh1	Isocitrate dehydrogenase [NADP] cytoplasmic	1.40	0.0300
838	Cltc	Clathrin heavy chain 1	1.32	0.0300
839	xkr9	XK-related protein 9	3.34	0.0300
840	rps15	40S ribosomal protein S15	2.64	0.0300
841	Rab1b	Ras-related protein Rab-1B	1.51	0.0301
842	mvp	Major vault protein	2.01	0.0301
843	CENPF	Centromere protein F	-2.70	0.0303
844	CUX1	Protein CASP	1.33	0.0304
845	Atg4d	Cysteine protease ATG4D	1.80	0.0304
846	ATP5PD	ATP synthase subunit d, mitochondrial	2.67	0.0304
847	tc1a	Transposable element Tc1 transposase	1.43	0.0304
848	HEXB	Beta-hexosaminidase subunit beta	-2.20	0.0305
849	#N/A	Polyubiquitin	3.32	0.0305
850	MSRB3	Methionine-R-sulfoxide reductase B3	-1.92	0.0305
851	SDCBP	Syntenin-1	2.57	0.0305
852	FLNC	Filamin-C	3.03	1.0000
853	#N/A	Lectin BRA-3	-5.67	1.0000
854	DLEC1	Deleted in lung and esophageal cancer protein 1	-3.31	0.0307
855	Lamp1	Lysosome-associated membrane glycoprotein 1	1.94	0.0307
856	CLDN4	Claudin-4	2.15	0.0307
857	GTF2H4	General transcription factor IIH subunit 4	2.50	0.0307
858	FER	Tyrosine-protein kinase Fer	-2.11	0.0308
859	tdp2	Tyrosyl-DNA phosphodiesterase 2	2.57	0.0308
860	HI_0712	Probable hemoglobin and hemoglobin-haptoglobin-binding protein 3	-2.00	0.0309
861	midn	Midnolin	1.83	0.0309
862	ARHGAP18	Rho GTPase-activating protein 18	1.84	0.0309
863	HI_0712	Probable hemoglobin and hemoglobin-haptoglobin-binding protein 3	-2.59	0.0310
864	pol	Retrovirus-related Pol polyprotein from transposon gypsy	1.74	0.0310
865	RAB9A	Ras-related protein Rab-9A	3.31	0.0311
866	Klf6	Krueppel-like factor 6	2.03	0.0312
867	GOLGA4	Golgin subfamily A member 4	0.98	0.0312
868	#N/A	Transposable element Tcb1 transposase	-1.85	0.0312
869	MKNK2	MAP kinase-interacting serine/threonine-protein kinase 2	1.41	0.0314
870	Rnf213	E3 ubiquitin-protein ligase RNF213	2.21	0.0315
871	afap1l1	Actin filament-associated protein 1-like 1	-2.35	0.0315
872	ITPR3	Inositol 1,4,5-trisphosphate receptor type 3	2.87	0.0316

873	Homer2	Homer protein homolog 2	1.74	0.0317
874	Elob	Transcription elongation factor B polypeptide 2	2.09	0.0317
875	ANO7	Anoctamin-7	5.48	0.0318
876	#N/A	Cathepsin L	3.52	1.0000
877	MSN	Moesin	2.73	0.0318
878	Unc13a	Protein unc-13 homolog A	3.53	1.0000
879	PPP2CB	Serine/threonine-protein phosphatase 2A catalytic subunit beta isoform	2.03	0.0320
880	RAB44	Ras-related protein Rab-44	2.37	0.0321
881	TMEM132C	Transmembrane protein 132C	4.87	0.0321
882	jak1	Tyrosine-protein kinase JAK1	1.04	0.0322
883	Eif4enif1	Eukaryotic translation initiation factor 4E transporter	2.70	0.0322
884	Rpl23	60S ribosomal protein L23	2.38	0.0323
885	DGKD	Diacylglycerol kinase delta	4.65	1.0000
886	tc1a	Transposable element Tc1 transposase	1.26	0.0324
887	Atp5mf	ATP synthase subunit f, mitochondrial	2.70	0.0324
888	HID1	Protein HID1	3.12	0.0324
889	HSD17B14	17-beta-hydroxysteroid dehydrogenase 14	1.30	0.0325
890	boka	Bcl-2-related ovarian killer protein homolog A	-2.13	0.0325
891	DNAJB1	DnaJ homolog subfamily B member 1	2.42	0.0325
892	Tmem238	Transmembrane protein 238	2.92	0.0325
893	ERP44	Endoplasmic reticulum resident protein 44	1.49	0.0326
894	Cndp2	Cytosolic non-specific dipeptidase	1.80	0.0326
895	ARL1	ADP-ribosylation factor-like protein 1	1.62	0.0326
896	eef1g	Elongation factor 1-gamma	2.09	0.0327
897	Spag1	Sperm-associated antigen 1	2.26	0.0327
898	pssA	CDP-diacylglycerol--serine O-phosphatidyltransferase	2.64	0.0328
899	PMM2	Phosphomannomutase 2	1.53	0.0328
900	TFG	Protein TFG	1.84	0.0333
901	DDX3Y	ATP-dependent RNA helicase DDX3Y	1.49	0.0334
902	EVPL	Envoplakin	1.04	0.0334
903	Ier5	Immediate early response gene 5 protein	1.92	0.0334
904	ASNS	Asparagine synthetase [glutamine-hydrolyzing]	1.98	0.0335
905	URGCP	Up-regulator of cell proliferation	3.42	0.0335
906	Cpeb2	Cytoplasmic polyadenylation element-binding protein 2	3.87	0.0336
907	CYBB	Cytochrome b-245 heavy chain	3.40	1.0000
908	KIAA1324	UPF0577 protein KIAA1324	2.80	0.0339
909	cxadr	Coxsackievirus and adenovirus receptor homolog	1.57	0.0339
910	GLUL	Glutamine synthetase	1.44	0.0339
911	CYB5R3	NADH-cytochrome b5 reductase 3	3.90	0.0339
912	ppdpfb	Pancreatic progenitor cell differentiation and proliferation factor B	1.79	0.0339
913	mylipa	E3 ubiquitin-protein ligase MYLIP-A	1.77	0.0341
914	#N/A	Sugar phosphate exchanger 2	1.48	0.0341
915	HSPA4	Heat shock 70 kDa protein 4	2.00	0.0341
916	APOD	Apolipoprotein D	4.23	0.0341
917	GNGT2	Guanine nucleotide-binding protein G(I)/G(S)/G(O) subunit gamma-T2	4.08	0.0342
918	rpl11	60S ribosomal protein L11	1.88	0.0343
919	IST1	IST1 homolog	1.73	0.0343
920	DAAM2	Disheveled-associated activator of morphogenesis 2	2.93	0.0344
921	PLSCR2	Phospholipid scramblase 2	1.89	0.0344
922	TJP1	Tight junction protein ZO-1	1.62	0.0345
923	KIF4A	Chromosome-associated kinesin KIF4A	-4.23	1.0000
924	rps18	40S ribosomal protein S18	2.17	0.0345
925	pnrc2	Proline-rich nuclear receptor coactivator 2	1.29	0.0345
926	got2	Aspartate aminotransferase, mitochondrial	3.22	1.0000
927	#N/A	Adiponectin receptor protein 2	1.60	0.0346
928	DUSP6	Dual specificity protein phosphatase 6	2.56	0.0346
929	rasef	Ras and EF-hand domain-containing protein	2.02	0.0347
930	PNN	Pinin	-1.61	0.0347
931	Map2	Microtubule-associated protein 2	2.00	0.0347
932	gC	Envelope glycoprotein C	2.95	0.0349
933	Mboat1	Lysophospholipid acyltransferase 1	4.37	0.0350
934	Pol	LINE-1 retrotransposable element ORF2 protein	1.67	0.0354
935	Nudt3	Diphosphoinositol polyphosphate phosphohydrolase 1	1.53	0.0354
936	SGPL1	Sphingosine-1-phosphate lyase 1	1.76	0.0355
937	B3GALT2	Beta-1,3-galactosyltransferase 2	1.40	0.0355
938	F2rl1	Proteinase-activated receptor 2	1.89	0.0355

939	PDZD2	PDZ domain-containing protein 2	-1.71	0.0356
940	CAMK1	Calcium/calmodulin-dependent protein kinase type 1	2.39	0.0357
941	melk	Maternal embryonic leucine zipper kinase	-3.94	1.0000
942	KANSL1	KAT8 regulatory NSL complex subunit 1	0.99	0.0357
943	Rdx	Radixin	1.50	0.0358
944	Nrdc	Nardilysin	-2.02	0.0358
945	Plcd1	1-phosphatidylinositol 4,5-bisphosphate phosphodiesterase delta-1	2.70	0.0359
946	Etnk1	Ethanolamine kinase 1	1.12	0.0359
947	cahz	Carbonic anhydrase	2.39	0.0359
948	GDI2	Rab GDP dissociation inhibitor beta	1.89	0.0359
949	Tnfaip3	Tumor necrosis factor alpha-induced protein 3	2.05	0.0359
950	Fcgr3	Low affinity immunoglobulin gamma Fc region receptor III	3.66	1.0000
951	Traf5	TNF receptor-associated factor 5	2.42	0.0361
952	GNB3	Guanine nucleotide-binding protein G(I)/G(S)/G(T) subunit beta-3	5.59	0.0362
953	GIMAP5	GTPase IMAP family member 5	3.21	0.0363
954	tram1l1	Translocating chain-associated membrane protein 1-like 1	1.44	0.0363
955	GVINP1	Interferon-induced very large GTPase 1	1.79	0.0363
956	FNIP1	Folliculin-interacting protein 1	2.20	0.0363
957	Dtx3l	E3 ubiquitin-protein ligase DTX3L	1.93	0.0364
958	eif3g	Eukaryotic translation initiation factor 3 subunit G	1.97	0.0365
959	#N/A	LINE-1 retrotransposable element ORF2 protein	-5.91	0.0365
960	rpl36a	60S ribosomal protein L36a	2.19	0.0366
961	actb	Actin, cytoplasmic 1	1.85	0.0367
962	ROCK2	Rho-associated protein kinase 2	1.46	0.0367
963	#N/A	Transposable element Tcb1 transposase	-2.51	0.0367
964	DSC3	Desmocollin-3	3.11	0.0367
965	eef1as	Elongation factor 1-alpha, somatic form	3.06	0.0368
966	fam83h	Protein FAM83H {ECO:0000305}	1.99	0.0368
967	farsa	Phenylalanine--tRNA ligase alpha subunit	2.83	0.0368
968	FP1	Adhesive plaque matrix protein	-3.38	0.0368
969	ARF6	ADP-ribosylation factor 6	1.73	0.0369
970	AGR3	Anterior gradient protein 3	1.77	0.0369
971	ITSN2	Intersectin-2	1.17	0.0371
972	mef2d	Myocyte-specific enhancer factor 2D homolog	1.52	0.0371
973	SLC17A5	Sialin	2.05	0.0371
974	CDKN1B	Cyclin-dependent kinase inhibitor 1B	2.36	0.0372
975	CBS	Cystathionine beta-synthase {ECO:0000305}	2.44	0.0372
976	Dst	Dystonin	1.50	0.0373
977	COX8B	Cytochrome c oxidase subunit 8B, mitochondrial	2.85	0.0373
978	PCOLCE	Procollagen C-endopeptidase enhancer 1	-3.94	0.0373
979	PARD6A	Partitioning defective 6 homolog alpha	2.65	0.0373
980	GVINP1	Interferon-induced very large GTPase 1	2.75	0.0373
981	midn	Midnolin	2.46	0.0373
982	HDLBP	Vigilin	1.70	0.0374
983	Tm9sf1	Transmembrane 9 superfamily member 1	1.85	0.0374
984	Flrt1	Leucine-rich repeat transmembrane protein FLRT1	-3.31	0.0374
985	ARHGDIA	Rho GDP-dissociation inhibitor 1	2.04	0.0375
986	grip2	Glutamate receptor-interacting protein 2	3.68	1.0000
987	Dnase1l3	Deoxyribonuclease gamma	2.74	1.0000
988	KEAP1	Kelch-like ECH-associated protein 1	3.37	1.0000
989	ME2	NAD-dependent malic enzyme, mitochondrial	4.22	1.0000
990	TSC22D3	TSC22 domain family protein 3	-1.65	0.0378
991	SIK2	Serine/threonine-protein kinase SIK2	1.49	0.0378
992	#N/A	Transposable element Tcb1 transposase	-2.21	0.0379
993	Prdm11	PR domain-containing protein 11	-1.89	0.0379
994	#N/A	LINE-1 retrotransposable element ORF2 protein	-7.00	0.0380
995	arf1	ADP-ribosylation factor 1	2.23	0.0380
996	ATP5MC3	ATP synthase F(0) complex subunit C3, mitochondrial	1.88	0.0380
997	CLEC16A	Protein CLEC16A {ECO:0000305}	-1.76	0.0381
998	NBEAL1	Neurobeachin-like protein 1	1.08	0.0382
999	DARS	Aspartate--tRNA ligase, cytoplasmic	1.70	0.0383
1000	SRP72	Signal recognition particle subunit SRP72	1.17	0.0383
1001	ADAM23	Disintegrin and metalloproteinase domain-containing protein 23	3.72	1.0000
1002	vcp	Transitional endoplasmic reticulum ATPase	1.14	0.0384
1003	camsap1b	Calmodulin-regulated spectrin-associated protein 1-B	-1.73	0.0386
1004	OR1D5	Olfactory receptor 1D5	-5.07	1.0000

1005	STAT1	Signal transducer and activator of transcription 1	1.66	0.0389
1006	SSR2	Translocon-associated protein subunit beta	1.31	0.0391
1007	#N/A	LINE-1 retrotransposable element ORF2 protein	-5.00	0.0391
1008	USP54	Inactive ubiquitin carboxyl-terminal hydrolase 54	3.00	0.0392
1009	selenof	15 kDa selenoprotein	1.72	0.0393
1010	Galnt6	Polypeptide N-acetylgalactosaminyltransferase 6	1.17	0.0393
1011	Dock8	Dedicator of cytokinesis protein 8	4.51	1.0000
1012	HERC6	Probable E3 ubiquitin-protein ligase HERC6	2.08	0.0394
1013	SCIN	Adseverin	2.17	0.0395
1014	Ica1	Islet cell autoantigen 1	1.53	0.0396
1015	RAP1B	Ras-related protein Rap-1b	2.16	0.0396
1016	#N/A	LisH domain and HEAT repeat-containing protein KIAA1468	-2.43	0.0396
1017	TAOK1	Serine/threonine-protein kinase TAO1	1.90	0.0397
1018	CEACAM1	Carcinoembryonic antigen-related cell adhesion molecule 1	4.02	0.0397
1019	Ak4	Adenylate kinase 4, mitochondrial	3.74	1.0000
1020	GSPT2	Eukaryotic peptide chain release factor GTP-binding subunit ERF3B	1.86	0.0398
1021	CTNNBL1	Beta-catenin-like protein 1	1.30	0.0399
1022	MUC5B	Mucin-5B	-2.04	0.0401
1023	Sox9	Transcription factor SOX-9	2.82	0.0401
1024	UBN1	Ubinuclein-1	-2.18	0.0401
1025	PRKCH	Protein kinase C eta type	1.47	0.0401
1026	Cep170b	Centrosomal protein of 170 kDa protein B	-2.00	0.0402
1027	CNIH1	Protein cornichon homolog 1	2.82	0.0402
1028	PRKCD	Protein kinase C delta type	2.16	0.0403
1029	KIAA0232	Uncharacterized protein KIAA0232	1.27	0.0404
1030	nme6	Nucleoside diphosphate kinase 6	4.35	1.0000
1031	mxi1	Max-interacting protein 1	1.67	0.0405
1032	STK17B	Serine/threonine-protein kinase 17B	1.81	0.0405
1033	STK17A	Serine/threonine-protein kinase 17A	1.48	0.0405
1034	STX5	Syntaxin-5	1.35	0.0405
1035	Nsd1	Histone-lysine N-methyltransferase, H3 lysine-36 and H4 lysine-20 specific	-1.69	0.0406
1036	Hook3	Protein Hook homolog 3	-1.69	0.0406
1037	ESYT2	Extended synaptotagmin-2	1.60	0.0406
1038	Rnf213	E3 ubiquitin-protein ligase RNF213	1.14	0.0408
1039	L1RE1	LINE-1 retrotransposable element ORF1 protein	-6.33	0.0408
1040	CEP250	Centrosome-associated protein CEP250	-2.25	0.0408
1041	Rpl39	60S ribosomal protein L39	2.40	0.0411
1042	DOP1B	Protein dopey-2	1.80	0.0411
1043	Arhgap45	Minor histocompatibility protein HA-1	2.28	0.0412
1044	ENPP	Enterin neuropeptides	-2.12	0.0413
1045	Mknk1	MAP kinase-interacting serine/threonine-protein kinase 1	2.37	0.0413
1046	HIP1R	Huntingtin-interacting protein 1-related protein	1.50	0.0413
1047	ZFAND3	AN1-type zinc finger protein 3	1.57	0.0413
1048	#N/A	Sperm-specific antigen 2	2.07	0.0414
1049	ldlr-a	Low-density lipoprotein receptor 1	1.32	0.0414
1050	CYTH2	Cytohesin-2	3.74	1.0000
1051	ZFAND5	AN1-type zinc finger protein 5	1.89	0.0415
1052	pksL	Polyketide synthase PksL	2.94	0.0415
1053	ABCA12	ATP-binding cassette sub-family A member 12	1.19	0.0416
1054	etf1	Eukaryotic peptide chain release factor subunit 1	2.19	0.0416
1055	purb	Transcriptional activator protein Pur-beta	2.06	0.0416
1056	STK26	Serine/threonine-protein kinase 26 {ECO:0000305}	1.63	0.0418
1057	TESC	Calcineurin B homologous protein 3	1.49	0.0419
1058	UPK1A	Uroplakin-1a	1.34	0.0419
1059	Znf32	Zinc finger protein 32	4.44	1.0000
1060	VASP	Vasodilator-stimulated phosphoprotein	2.65	0.0421
1061	ATP5F1B	ATP synthase subunit beta, mitochondrial	1.34	0.0421
1062	rps13	40S ribosomal protein S13	2.04	0.0422
1063	PDPK1	3-phosphoinositide-dependent protein kinase 1	2.69	0.0424
1064	DAAM2	Disheveled-associated activator of morphogenesis 2	2.63	0.0424
1065	glyr1	Putative oxidoreductase GLYR1	1.47	0.0425
1066	RPL10	60S ribosomal protein L10	2.24	0.0425
1067	AMBRA1	Activating molecule in BECN1-regulated autophagy protein 1	-1.88	0.0426
1068	RAB5C	Ras-related protein Rab-5C	2.21	0.0427
1069	VPS4B	Vacuolar protein sorting-associated protein 4B	1.28	0.0427

1070	rpl13a	60S ribosomal protein L13a	2.03	0.0428
1071	Eprs	Bifunctional glutamate/proline--tRNA ligase	1.09	0.0428
1072	CSK	Tyrosine-protein kinase CSK	3.38	1.0000
1073	CLDN3	Claudin-3	3.71	0.0428
1074	C16orf89	UPF0764 protein C16orf89	-4.01	0.0429
1075	TRIM47	Tripartite motif-containing protein 47	1.25	0.0431
1076	CRY2	Cryptochrome-2	2.06	0.0431
1077	Tf2-9	Transposon Tf2-9 polyprotein	3.29	0.0432
1078	eef1a	Elongation factor 1-alpha	3.71	1.0000
1079	Fntb	Protein farnesyltransferase subunit beta	-1.91	0.0433
1080	#N/A	UPF0764 protein C16orf89 homolog	3.41	0.0434
1081	CLCN7	H(+)/Cl(-) exchange transporter 7	-2.12	0.0434
1082	AHNAK	Neuroblast differentiation-associated protein AHNAK	1.70	0.0434
1083	amotl2a	Angiomotin-like 2a	2.62	0.0434
1084	ABLIM2	Actin-binding LIM protein 2	1.59	0.0434
1085	lcp1	Plastin-2	2.42	0.0435
1086	kdelr3	ER lumen protein-retaining receptor 3	1.61	0.0435
1087	ARHGAP17	Rho GTPase-activating protein 17	-1.42	0.0436
1088	GPCPD1	Glycerophosphocholine phosphodiesterase GPCPD1	-3.16	0.0437
1089	PLLP	Plasmolipin	2.66	0.0438
1090	#N/A	Glycerol-3-phosphate transporter	1.34	0.0438
1091	UTRN	Utrophin	1.49	0.0438
1092	Rnh1	Ribonuclease inhibitor	1.78	0.0438
1093	oaz1b	Ornithine decarboxylase antizyme 2	1.26	0.0439
1094	tpi1a	Triosephosphate isomerase A	2.59	0.0440
1095	Pfn2	Profilin-2	2.12	0.0440
1096	nr4a1	Nuclear receptor subfamily 4 group A member 1	1.92	0.0441
1097	SLC16A3	Monocarboxylate transporter 4	2.12	0.0441
1098	ABCF2	ATP-binding cassette sub-family F member 2	1.50	0.0441
1099	fyna	Tyrosine-protein kinase fyna	2.38	0.0442
1100	REXO2	Oligoribonuclease, mitochondrial	4.52	1.0000
1101	ITPR3	Inositol 1,4,5-trisphosphate receptor type 3	1.90	0.0443
1102	rpl11	60S ribosomal protein L11	1.98	0.0444
1103	cops8	COP9 signalosome complex subunit 8	2.02	0.0444
1104	#N/A	Calmodulin	1.60	0.0446
1105	GMPR2	GMP reductase 2 {ECO:0000255|HAMAP-Rule:MF_03195}	5.36	1.0000
1106	IVL	Involucrin	-2.14	0.0449
1107	cyc	Cytochrome c	3.61	0.0449
1108	rps6	40S ribosomal protein S6	2.06	0.0449
1109	UQCR10	Cytochrome b-c1 complex subunit 9	2.97	0.0450
1110	hsp90ab1	Heat shock protein HSP 90-beta	1.76	0.0450
1111	ADAM28	Disintegrin and metalloproteinase domain-containing protein 28	1.17	0.0452
1112	Tfap2c	Transcription factor AP-2 gamma	2.46	0.0452
1113	Taf12	Transcription initiation factor TFIID subunit 12	2.03	0.0452
1114	ube2d2	Ubiquitin-conjugating enzyme E2 D2	1.35	0.0452
1115	MYH9	Myosin-9	1.41	0.0453
1116	EPRS	Bifunctional glutamate/proline--tRNA ligase	1.63	0.0453
1117	RAF1	RAF proto-oncogene serine/threonine-protein kinase	-1.86	0.0453
1118	SLF2	SMC5-SMC6 complex localization factor protein 2	-2.20	0.0454
1119	CARD14	Caspase recruitment domain-containing protein 14	1.46	0.0455
1120	RASEF	Ras and EF-hand domain-containing protein	2.16	0.0455
1121	eef1a	Elongation factor 1-alpha	2.07	0.0455
1122	SYT7	Synaptotagmin-7	-4.93	1.0000
1123	rps25	40S ribosomal protein S25	2.26	0.0455
1124	Sugt1	Protein SGT1 homolog {ECO:0000250|UniProtKB:Q08446}	1.63	0.0456
1125	smc2	Structural maintenance of chromosomes protein 2	-2.08	0.0456
1126	FAM200A	Protein FAM200A	2.46	0.0459
1127	Rps26	40S ribosomal protein S26	2.30	0.0459
1128	smc2	Structural maintenance of chromosomes protein 2	-2.45	0.0460
1129	CACNB1	Voltage-dependent L-type calcium channel subunit beta-1	3.31	0.0460
1130	tc1a	Transposable element Tc1 transposase	-3.15	0.0460
1131	Cldn23	Claudin-23	1.83	0.0460
1132	cct3	T-complex protein 1 subunit gamma	1.57	0.0460
1133	an3	Putative ATP-dependent RNA helicase an3	1.31	0.0463
1134	Chmp4b	Charged multivesicular body protein 4b	2.15	0.0464
1135	arhgap45	Minor histocompatibility protein HA-1	2.11	0.0465

1136	agtrap	Type-1 angiotensin II receptor-associated protein-like	4.33	1.0000
1137	GRK5	G protein-coupled receptor kinase 5	1.52	0.0465
1138	Gda	Guanine deaminase	3.01	0.0466
1139	Cd82	CD82 antigen	1.71	0.0466
1140	RPL21	60S ribosomal protein L21	2.69	0.0468
1141	cyp2m1	Cytochrome P450 2M1	3.91	1.0000
1142	NUMA1	Nuclear mitotic apparatus protein 1 {ECO:0000312|HGNC:HGNC:8059}	-3.78	1.0000
1143	#N/A	Putative uncharacterized protein ENSP00000383309	-2.12	0.0469
1144	Espl1	Separin	-4.59	1.0000
1145	RAB19	Ras-related protein Rab-19	3.93	1.0000
1146	#N/A	Natterin-like protein	-3.55	0.0470
1147	#N/A	Spartin	1.76	0.0471
1148	Cdc42	Cell division control protein 42 homolog	1.47	0.0473
1149	TRIM58	E3 ubiquitin-protein ligase TRIM58	2.56	0.0473
1150	ECU02_0740i	Ubiquitin	2.50	0.0475
1151	HCLS1	Hematopoietic lineage cell-specific protein	2.31	0.0475
1152	axin2	Axin-2	-1.00	0.0475
1153	UTY	Histone demethylase UTY	-1.10	0.0475
1154	Magi1	Membrane-associated guanylate kinase, WW and PDZ domain-containing protein 1	1.50	0.0476
1155	Ano7	Anoctamin-7	3.85	0.0477
1156	pol	Pol polyprotein	1.22	0.0478
1157	#N/A	Adiponectin receptor protein 1	1.07	0.0478
1158	FLVCR2	Feline leukemia virus subgroup C receptor-related protein 2	3.39	1.0000
1159	mfsd2b	Major facilitator superfamily domain-containing protein 2B	1.77	0.0480
1160	rasef	Ras and EF-hand domain-containing protein	1.81	0.0481
1161	CTDSP2	Carboxy-terminal domain RNA polymerase II polypeptide A small phosphatase 2	1.38	0.0481
1162	tcaf	TRPM8 channel-associated factor homolog	3.58	0.0481
1163	CHKA	Choline kinase alpha	2.40	0.0482
1164	rpl19	60S ribosomal protein L19	1.72	0.0482
1165	Tmed9	Transmembrane emp24 domain-containing protein 9	2.52	0.0483
1166	FRK	Tyrosine-protein kinase FRK	1.86	0.0485
1167	Grasp	General receptor for phosphoinositides 1-associated scaffold protein	2.14	0.0485
1168	ATP2A3	Sarcoplasmic/endoplasmic reticulum calcium ATPase 3	5.25	1.0000
1169	def6	Differentially expressed in FDCP 6 homolog	2.64	0.0486
1170	gse1	Genetic suppressor element 1	-1.84	0.0486
1171	TRIM11	E3 ubiquitin-protein ligase TRIM11	2.66	0.0486
1172	tbc1d31	TBC1 domain family member 31	-1.74	0.0487
1173	Map4k1	Mitogen-activated protein kinase kinase kinase kinase 1	1.55	0.0487
1174	TBCB	Tubulin-folding cofactor B	2.50	0.0487
1175	STAT1	Signal transducer and activator of transcription 1	1.86	0.0487
1176	Pepd	Xaa-Pro dipeptidase	2.44	0.0487
1177	SUCO	SUN domain-containing ossification factor	2.09	0.0487
1178	Rab1A	Ras-related protein Rab-1A	1.67	0.0487
1179	#N/A	Bicaudal D-related protein 1	3.01	0.0488
1180	ORF34	Uncharacterized protein ORF34	5.27	1.0000
1181	cct3	T-complex protein 1 subunit gamma	1.73	0.0488
1182	Atg16l1	Autophagy-related protein 16-1	-2.00	0.0489
1183	znf521	Zinc finger protein 521	4.39	1.0000
1184	Ppfibp2	Liprin-beta-2	-2.44	0.0490
1185	Mien1	Migration and invasion enhancer 1	1.43	0.0491
1186	Eprs	Bifunctional glutamate/proline--tRNA ligase	2.49	0.0491
1187	pol	Pol polyprotein	4.59	1.0000
1188	JUN	Transcription factor AP-1	1.11	0.0491
1189	TY3B-I	Transposon Ty3-I Gag-Pol polyprotein	-3.51	0.0492
1190	ANXA4	Annexin A4	2.23	0.0492
1191	brox	BRO1 domain-containing protein BROX	1.86	0.0492
1192	Rps23	40S ribosomal protein S23	3.50	0.0493
1193	PAX9	Paired box protein Pax-9	3.94	1.0000
1194	tdrd7b	Tudor domain-containing protein 7B	3.58	0.0494
1195	ARPC1A	Actin-related protein 2/3 complex subunit 1A	2.17	0.0494
1196	GOLGA4	Golgin subfamily A member 4	2.12	0.0495
1197	slc40a1	Solute carrier family 40 member 1	2.12	0.0496
1198	ATP8A2	Phospholipid-transporting ATPase IB	-1.41	0.0497
1199	kita	Mast/stem cell growth factor receptor kita	2.28	0.0497

1200	ATOX1	Copper transport protein ATOX1	2.36	0.0497
1201	USP54	Inactive ubiquitin carboxyl-terminal hydrolase 54	2.74	0.0497
1202	TMCO3	Transmembrane and coiled-coil domain-containing protein 3	-1.68	0.0498
1203	Rnf213	E3 ubiquitin-protein ligase RNF213	1.99	0.0498
1204	BTF3L4	Transcription factor BTF3 homolog 4	3.90	0.0498
1205	GSTP1	Glutathione S-transferase P	2.21	0.0499
1206	med10	Mediator of RNA polymerase II transcription subunit 10	2.42	0.0499
1207	Pol	LINE-1 retrotransposable element ORF2 protein	-6.20	0.0500
1208	ACTR2	Actin-related protein 2	2.59	0.0500

Lake 224 vs Lake 373

373 is the base e.g. Positive FC = upregulated in Lake 224 relative to Lake 373

1	GIMAP4	GTPase IMAP family member 4	-11.74	2.40E-22
2	MDV087	Uncharacterized gene 87 protein	11.03	3.37E-21
3	cyp3a27	Cytochrome P450 3A27	5.63	6.82E-20
4	cyp3a27	Cytochrome P450 3A27	5.52	6.88E-19
5	samhd1	Deoxynucleoside triphosphate triphosphohydrolase SAMHD1	5.42	1.20E-18
6	MDV087	Uncharacterized gene 87 protein	-4.16	1.30E-18
7	ERVV-1	Endogenous retrovirus group V member 1 Env polyprotein	-4.67	1.47E-17
8	vtg1	Vitellogenin	9.99	8.54E-16
9	ERVFC1	Endogenous retrovirus group FC1 Env polyprotein	-3.96	8.75E-16
10	vtg1	Vitellogenin	9.71	3.47E-15
11	Urgcp	Up-regulator of cell proliferation	7.24	4.45E-15
12	GIMAP8	GTPase IMAP family member 8	-9.69	1.64E-14
13	Pol	LINE-1 retrotransposable element ORF2 protein	4.08	1.50E-13
14	URGCP	Up-regulator of cell proliferation	-10.47	5.35E-13
15	slc22a6	Solute carrier family 22 member 6	-9.10	5.69E-13
16	#N/A	Ladderlectin	5.63	6.62E-13
17	#N/A	Transposon TX1 uncharacterized 149 kDa protein	3.15	4.14E-12
18	#N/A	Transposon TX1 uncharacterized 149 kDa protein	2.71	2.95E-11
19	GIMAP5	GTPase IMAP family member 5	-8.54	3.18E-11
20	C1ql4	Complement C1q-like protein 4	8.99	5.01E-11
21	#N/A	Transposon TX1 uncharacterized 149 kDa protein	3.60	7.71E-11
22	GIMAP4	GTPase IMAP family member 4	-3.82	8.48E-11
23	SLC22A6	Solute carrier family 22 member 6	-8.61	9.08E-11
24	ENPP	Enterin neuropeptides	2.68	9.12E-11
25	Art5	Ecto-ADP-ribosyltransferase 5	-5.30	9.71E-11
26	SAMD9	Sterile alpha motif domain-containing protein 9	-8.81	1.19E-10
27	CACNA1B	Voltage-dependent N-type calcium channel subunit alpha-1B	8.40	1.74E-10
28	IFFO1	Intermediate filament family orphan 1	4.46	1.74E-10
29	COL14A1	Collagen alpha-1(XIV) chain	-4.20	3.88E-10
30	gag-pol	Gag-Pol polyprotein	5.70	6.44E-10
31	AHCYL2	Putative adenosylhomocysteinase 3	-8.48	1.07E-09
32	#N/A	Stonustoxin subunit beta	2.62	1.39E-09
33	AHCYL2	Putative adenosylhomocysteinase 3	-8.27	2.27E-09
34	Fam111a	Protein FAM111A	-8.69	2.86E-09
35	AHCYL2	Adenosylhomocysteinase 3	-8.28	3.32E-09
36	#N/A	Stonustoxin subunit beta	8.02	4.18E-09
37	Ogfr	Opioid growth factor receptor	-9.01	7.39E-09
38	#N/A	Class I histocompatibility antigen, F10 alpha chain	-8.19	7.91E-09
39	Samd9l	Sterile alpha motif domain-containing protein 9-like	-8.24	8.59E-09
40	GIMAP4	GTPase IMAP family member 4	8.06	2.04E-08
41	pol	Retrovirus-related Pol polyprotein from transposon gypsy	-7.44	2.20E-08
42	gag-pol	Gag-Pol polyprotein	-2.29	2.72E-08
43	Traf7	E3 ubiquitin-protein ligase TRAF7	-3.87	3.74E-08
44	GVINP1	Interferon-induced very large GTPase 1	5.68	4.40E-08
45	#N/A	Transposon TX1 uncharacterized 149 kDa protein	2.61	5.30E-08
46	#N/A	Transposon TX1 uncharacterized 149 kDa protein	4.42	7.90E-08
47	#N/A	Ladderlectin	-9.15	8.75E-08
48	CACNA1B	Voltage-dependent N-type calcium channel subunit alpha-1B	7.15	1.09E-07
49	gag-pol	Gag-Pol polyprotein	7.02	1.14E-07
50	Pik3cb	Phosphatidylinositol 4,5-bisphosphate 3-kinase catalytic subunit beta isoform	3.07	1.56E-07

51	Nlrc3	Protein NLRC3	7.32	1.96E-07
52	ENDOD1	Endonuclease domain-containing 1 protein	6.09	2.44E-07
53	#N/A	NACHT, LRR and PYD domains-containing protein 9	7.71	2.89E-07
54	BTN2A1	Butyrophilin subfamily 2 member A1	5.35	3.09E-07
55	#N/A	Actin, muscle	2.13	4.45E-07
56	gag-pol	Gag-Pol polyprotein	-7.77	5.74E-07
57	URGCP	Up-regulator of cell proliferation	-8.01	6.25E-07
58	Iigp1	Interferon-inducible GTPase 1	5.80	6.76E-07
59	LECASAL	Mannose-specific lectin	-5.88	7.62E-07
60	NLRC3	Protein NLRC3	4.35	9.57E-07
61	GIMAP7	GTPase IMAP family member 7	5.20	1.01E-06
62	Gimap4	GTPase IMAP family member 4	6.31	1.08E-06
63	GVINP1	Interferon-induced very large GTPase 1	-8.38	1.17E-06
64	Nt5c1a	Cytosolic 5'-nucleotidase 1A	2.18	1.19E-06
65	Gvin1	Interferon-induced very large GTPase 1	6.31	1.39E-06
66	Pgm5	Phosphoglucomutase-like protein 5	7.42	1.44E-06
67	#N/A	Neoverrucotoxin subunit beta	7.26	1.60E-06
68	GBP2	Guanylate-binding protein 2	7.23	1.60E-06
69	Peg10	Retrotransposon-derived protein PEG10	2.52	2.02E-06
70	PPIP5K1	Inositol hexakisphosphate and diphosphoinositol-pentakisphosphate kinase 1	2.18	3.16E-06
71	Endod1	Endonuclease domain-containing 1 protein	4.27	3.19E-06
72	TY3B-I	Transposon Ty3-I Gag-Pol polyprotein	-10.08	3.26E-06
73	Mycbpap	MYCBP-associated protein	-6.39	3.52E-06
74	Lpin2	Phosphatidate phosphatase LPIN2	3.48	4.17E-06
75	sibA	Integrin beta-like protein A	-5.74	4.40E-06
76	TSTA3	GDP-L-fucose synthase	7.03	4.76E-06
77	tir-1	Sterile alpha and TIR motif-containing protein tir-1	-7.34	4.77E-06
78	Iffo1	Intermediate filament family orphan 1	6.82	5.02E-06
79	ENDOD1	Endonuclease domain-containing 1 protein	4.94	6.55E-06
80	#N/A	ERV-BabFcenv provirus ancestral Env polyprotein	-7.18	7.38E-06
81	RTL1	Retrotransposon-like protein 1	6.61	8.77E-06
82	AHCYL2	Adenosylhomocysteinase 3	-7.05	8.88E-06
83	NLRC3	Protein NLRC3	6.71	1.02E-05
84	TRPM5	Transient receptor potential cation channel subfamily M member 5	-4.98	1.05E-05
85	TSTA3	GDP-L-fucose synthase	6.78	1.29E-05
86	#N/A	RNA-directed RNA polymerase	8.34	1.63E-05
87	#N/A	Stonustoxin subunit alpha	7.81	2.31E-05
88	Lrat	Lecithin retinol acyltransferase	-8.10	2.37E-05
89	alpha	Capsid protein alpha	8.26	2.41E-05
90	IFI44	Interferon-induced protein 44	4.32	2.44E-05
91	ZNF235	Zinc finger protein 235	3.83	2.55E-05
92	Ikbip	Inhibitor of nuclear factor kappa-B kinase-interacting protein	5.78	2.58E-05
93	ERVFC1	Endogenous retrovirus group FC1 Env polyprotein	5.68	2.70E-05
94	Tspan33	Tetraspanin-33	2.16	3.14E-05
95	pol	Retrovirus-related Pol polyprotein from transposon 297	-4.63	3.27E-05
96	CA4	Carbonic anhydrase 4	3.80	3.39E-05
97	Trpm5	Transient receptor potential cation channel subfamily M member 5	-6.86	3.96E-05
98	#N/A	Transposon TX1 uncharacterized 149 kDa protein	2.12	4.48E-05
99	Vwa7	von Willebrand factor A domain-containing protein 7	5.52	4.83E-05
100	Urgcp	Up-regulator of cell proliferation	-4.03	4.96E-05
101	TY3B-G	Transposon Ty3-G Gag-Pol polyprotein	4.39	5.75E-05
102	SAMD9	Sterile alpha motif domain-containing protein 9	-5.16	6.12E-05
103	Mog	Myelin-oligodendrocyte glycoprotein	-6.62	7.46E-05
104	#N/A	RNA-directed RNA polymerase	8.17	7.46E-05
105	TY3B-I	Transposon Ty3-I Gag-Pol polyprotein	-10.61	0.0001
106	TRPM5	Transient receptor potential cation channel subfamily M member 5	-4.56	0.0001
107	ARHGAP8	Rho GTPase-activating protein 8	2.45	0.0001
108	ATP5PD	ATP synthase subunit d, mitochondrial	-1.72	0.0001
109	SAMHD1	Deoxynucleoside triphosphate triphosphohydrolase SAMHD1	6.51	0.0002
110	TRAPPC12	Trafficking protein particle complex subunit 12	3.07	0.0002
111	p65	Proline-rich P65 protein	3.40	0.0002
112	EPN2	Epsin-2	-7.56	0.0002
113	ZNF613	Zinc finger protein 613	-6.58	0.0002
114	Ndufs2	NADH dehydrogenase [ubiquinone] iron-sulfur protein 2, mitochondrial	1.94	0.0002
115	Matr3	Matrin-3	6.54	0.0002

116	CACNA1E	Voltage-dependent R-type calcium channel subunit alpha-1E	6.76	0.0002
117	ORF39	Uncharacterized protein ORF39	3.99	0.0002
118	aste1	Protein asteroid homolog 1	-3.45	0.0002
119	RNF14	E3 ubiquitin-protein ligase RNF14	-6.55	0.0002
120	Alk	ALK tyrosine kinase receptor	-6.96	0.0003
121	SAMD9L	Sterile alpha motif domain-containing protein 9-like	-4.62	0.0003
122	Mr1	Major histocompatibility complex class I-related gene protein	1.39	0.0003
123	AHNAK	Neuroblast differentiation-associated protein AHNAK	6.19	0.0003
124	MYCBPAP	MYCBP-associated protein	-5.14	0.0003
125	MPZL2	Myelin protein zero-like protein 2	2.23	0.0003
126	pol	Pol polyprotein	6.04	0.0003
127	Smoc2	SPARC-related modular calcium-binding protein 2	1.97	0.0003
128	GMNC	Geminin coiled-coil domain-containing protein 1	6.07	0.0004
129	Tomm5	Mitochondrial import receptor subunit TOM5 homolog {ECO:0000250|UniProtKB:Q8N4H5}	2.48	0.0004
130	BTN1A1	Butyrophilin subfamily 1 member A1	-2.31	0.0004
131	Samd9l	Sterile alpha motif domain-containing protein 9-like	-4.59	0.0004
132	Cd6	T-cell differentiation antigen CD6	2.37	0.0004
133	Ctnna2	Catenin alpha-2	-6.45	0.0004
134	TRIML1	Probable E3 ubiquitin-protein ligase TRIML1	5.79	0.0004
135	CARD8	Caspase recruitment domain-containing protein 8	2.30	0.0004
136	marveld2	MARVEL domain-containing protein 2	6.41	0.0004
137	#N/A	Stonustoxin subunit beta	1.87	0.0004
138	pol	Retrovirus-related Pol polyprotein from transposon 297	-9.31	0.0004
139	Tf2-9	Transposon Tf2-9 polyprotein	6.50	0.0004
140	egr1	Early growth response protein 1	2.92	0.0005
141	IFFO1	Intermediate filament family orphan 1	5.70	0.0005
142	Abi1	Abl interactor 1	-3.58	0.0005
143	tlcd2	TLC domain-containing protein 2	-2.63	0.0005
144	CFB	Complement factor B	5.59	0.0005
145	Bace2	Beta-secretase 2	-2.17	0.0006
146	ADAP1	Arf-GAP with dual PH domain-containing protein 1	-6.26	0.0006
147	fbxl15	F-box/LRR-repeat protein 15	2.97	0.0006
148	Peg10	Retrotransposon-derived protein PEG10	3.15	0.0007
149	NLRP3	NACHT, LRR and PYD domains-containing protein 3	-2.00	0.0007
150	Dsg2	Desmoglein-2	-5.50	0.0007
151	PRKD3	Serine/threonine-protein kinase D3	6.16	0.0007
152	Gvin1	Interferon-induced very large GTPase 1	3.44	0.0007
153	TRIM68	E3 ubiquitin-protein ligase TRIM68	1.34	0.0008
154	#N/A	Poly(A) polymerase type 3	2.08	0.0008
155	DCT	L-dopachrome tautomerase	-4.81	0.0008
156	ZER1	Protein zer-1 homolog	3.41	0.0008
157	DSG1	Desmoglein-1	-7.23	0.0008
158	ADAP1	Arf-GAP with dual PH domain-containing protein 1	-5.03	0.0008
159	SAMD9L	Sterile alpha motif domain-containing protein 9-like	-1.42	0.0009
160	FBXO3	F-box only protein 3	-2.92	0.0009
161	NLRC3	Protein NLRC3	2.22	0.0009
162	MAL2	Protein MAL2	2.19	0.0011
163	Ghsr	Growth hormone secretagogue receptor type 1	-4.39	0.0012
164	GIMAP8	GTPase IMAP family member 8	-6.26	0.0013
165	Scn2a	Sodium channel protein type 2 subunit alpha	4.47	0.0013
166	Dcxr	L-xylulose reductase	5.46	0.0013
167	pol	Pol polyprotein	-5.11	0.0013
168	egr1	Early growth response protein 1	3.09	0.0013
169	tert	Telomerase reverse transcriptase {ECO:0000303|PubMed:18312429}	2.45	0.0014
170	krt18	Keratin, type I cytoskeletal 18	-1.91	0.0014
171	PF14_0175	Protein PF14_0175	3.42	0.0014
172	IL13RA2	Interleukin-13 receptor subunit alpha-2	-6.14	0.0015
173	Cacna1a	Voltage-dependent P/Q-type calcium channel subunit alpha-1A	5.97	0.0015
174	GIMAP4	GTPase IMAP family member 4	-5.98	0.0016
175	Dsg1a	Desmoglein-1-alpha	-3.69	0.0016
176	Mycbpap	MYCBP-associated protein	-4.70	0.0016
177	SPTBN4	Spectrin beta chain, non-erythrocytic 4	-6.86	0.0017
178	Gimap4	GTPase IMAP family member 4	3.35	0.0017
179	gmnc	Geminin coiled-coil domain-containing protein 1	5.73	0.0018
180	IFI30	Gamma-interferon-inducible lysosomal thiol reductase	1.33	0.0019

181	ANKRD44	Serine/threonine-protein phosphatase 6 regulatory ankyrin repeat subunit B	5.78	0.0020
182	VWA7	von Willebrand factor A domain-containing protein 7	6.51	0.0020
183	NLRP1	NACHT, LRR and PYD domains-containing protein 1	1.74	0.0020
184	Urgcp	Up-regulator of cell proliferation	-1.57	0.0020
185	Tnfaip3	Tumor necrosis factor alpha-induced protein 3	1.21	0.0021
186	Mefv	Pyrin	1.75	0.0021
187	Map2	Microtubule-associated protein 2	2.76	0.0023
188	Pabpc1	Polyadenylate-binding protein 1	5.67	0.0023
189	Tf2-6	Transposon Tf2-6 polyprotein	-5.21	0.0024
190	rnf2-a	E3 ubiquitin-protein ligase RING2-A	-2.74	0.0026
191	SLC25A5	ADP/ATP translocase 2	-1.79	0.0027
192	Dock8	Dedicator of cytokinesis protein 8	2.48	0.0027
193	sspH2	E3 ubiquitin-protein ligase sspH2	1.30	0.0029
194	ZNF214	Zinc finger protein 214	1.32	0.0029
195	AQP3	Aquaporin-3	-3.79	0.0030
196	B4galt5	Beta-1,4-galactosyltransferase 5	-1.62	0.0030
197	ATP5MC1	ATP synthase F(0) complex subunit C1, mitochondrial	-1.58	0.0030
198	Tf2-9	Transposon Tf2-9 polyprotein	2.30	0.0030
199	cka	Casein kinase II subunit alpha	1.11	0.0031
200	ENTPD2	Ectonucleoside triphosphate diphosphohydrolase 2	-4.70	0.0032
201	IFI44	Interferon-induced protein 44	2.48	0.0032
202	GADL1	Acidic amino acid decarboxylase GADL1	-1.62	0.0033
203	#N/A	FMRFamide-related neuropeptides	2.97	0.0034
204	TY3B-I	Transposon Ty3-I Gag-Pol polyprotein	-6.65	0.0035
205	Vtcn1	V-set domain containing T-cell activation inhibitor 1	-2.91	0.0035
206	h2afv	Histone H2A.V	-1.89	0.0036
207	Capn2	Calpain-2 catalytic subunit	-2.44	0.0037
208	inaK	Ice nucleation protein	-6.12	0.0037
209	h2afx	Histone H2AX	-1.87	0.0038
210	CYP51A1	Lanosterol 14-alpha demethylase	-2.15	0.0038
211	sod1	Superoxide dismutase [Cu-Zn]	-1.52	0.0039
212	tc1a	Transposable element Tc1 transposase	-1.42	0.0039
213	ZBED5	Zinc finger BED domain-containing protein 5	-3.11	0.0041
214	Tf2-9	Transposon Tf2-9 polyprotein	3.96	0.0041
215	pol	Retrovirus-related Pol polyprotein from transposon opus	2.60	0.0042
216	ATP5MC2	ATP synthase F(0) complex subunit C2, mitochondrial	-1.44	0.0043
217	#N/A	Myomodulin neuropeptides	-2.30	0.0043
218	Mybl1	Myb-related protein A	5.86	0.0044
219	Eci1	Enoyl-CoA delta isomerase 1, mitochondrial	-2.28	0.0046
220	sqv-7	UDP-sugar transporter sqv-7	3.02	0.0047
221	Tmem8a	Transmembrane protein 8A	2.01	0.0047
222	SLA	Src-like-adapter	3.24	0.0047
223	SLC25A5	ADP/ATP translocase 2	-1.48	0.0048
224	URGCP	Up-regulator of cell proliferation	2.37	0.0049
225	ATP5F1B	ATP synthase subunit beta, mitochondrial	-1.42	0.0049
226	krt8	Keratin, type II cytoskeletal 8	-1.17	0.0049
227	ier2	Immediate early response gene 2 protein	2.71	0.0050
228	chac2	Putative glutathione-specific gamma-glutamylcyclotransferase 2	2.99	0.0051
229	JUN	Transcription factor AP-1	2.56	0.0053
230	#N/A	Transposable element Tcb1 transposase	-2.75	0.0055
231	Ankrd27	Ankyrin repeat domain-containing protein 27	3.07	0.0057
232	krt13	Keratin, type I cytoskeletal 13	-1.60	0.0057
233	DNAAF5	Dynein assembly factor 5, axonemal	2.17	0.0058
234	Nme1	Nucleoside diphosphate kinase A	-1.98	0.0059
235	#N/A	Retinol dehydrogenase 3	-2.30	0.0063
236	Sds	L-serine dehydratase/L-threonine deaminase	5.78	0.0063
237	IKBIP	Inhibitor of nuclear factor kappa-B kinase-interacting protein	3.40	0.0064
238	Itgb4	Integrin beta-4	-4.90	0.0065
239	Cd5l	CD5 antigen-like	2.09	0.0065
240	PC	Pyruvate carboxylase, mitochondrial	-6.45	0.0066
241	HEXB	Beta-hexosaminidase subunit beta	-2.95	0.0066
242	ANO9	Anoctamin-9	-1.55	0.0068
243	HEPACAM2	HEPACAM family member 2	-5.00	0.0073
244	jarid2b	Protein Jumonji	1.89	0.0076
245	eef1b	Elongation factor 1-beta	-1.34	0.0078

246	#N/A	Transposable element Tcb1 transposase	1.89	0.0080
247	ZBTB46	Zinc finger and BTB domain-containing protein 46	1.67	0.0081
248	TRPM5	Transient receptor potential cation channel subfamily M member 5	-6.49	0.0082
249	Vwa7	von Willebrand factor A domain-containing protein 7	5.90	0.0084
250	frrs1	Putative ferric-chelate reductase 1	-2.73	0.0084
251	CTBP2	C-terminal-binding protein 2	-4.57	0.0089
252	pol	Pol polyprotein	2.56	0.0090
253	Syt14	Synaptotagmin-14	4.11	0.0090
254	tc1a	Transposable element Tc1 transposase	-3.21	0.0091
255	tc1a	Transposable element Tc1 transposase	-2.85	0.0091
256	ranbp10	Ran-binding protein 10	3.62	0.0093
257	nccrp1	F-box only protein 50	-1.77	0.0093
258	DCXR	L-xylulose reductase	3.62	0.0094
259	lamc1	Laminin subunit gamma-1	-7.02	0.0094
260	ALOXE3	Hydroperoxide isomerase ALOXE3	-3.69	0.0094
261	Tcf7l2	Transcription factor 7-like 2	2.04	0.0099
262	Gvin1	Interferon-induced very large GTPase 1	4.14	0.0100
263	Ap1s2	AP-1 complex subunit sigma-2	-1.03	0.0102
264	FRY	Protein furry homolog	2.08	0.0102
265	TSPAN3	Tetraspanin-3	-1.37	0.0102
266	ZSWIM5	Zinc finger SWIM domain-containing protein 5	-4.17	0.0105
267	ORF1	Replicase polyprotein	-6.61	0.0107
268	mt-co2	Cytochrome c oxidase subunit 2	6.81	0.0107
269	RHA2	Rhodotorucin-A peptides type 2	2.18	0.0112
270	Rsbn1	Round spermatid basic protein 1	3.70	0.0116
271	#N/A	Probable voltage-dependent N-type calcium channel subunit alpha-1B	5.58	0.0120
272	ADSL	Adenylosuccinate lyase	1.74	0.0121
273	Gvin1	Interferon-induced very large GTPase 1	5.03	0.0125
274	#N/A	Transmembrane protein 97	-2.45	0.0126
275	ahcy-b	Adenosylhomocysteinase B	-1.95	0.0127
276	CD40	Tumor necrosis factor receptor superfamily member 5	1.68	0.0129
277	ENTPD2	Ectonucleoside triphosphate diphosphohydrolase 2	-5.23	0.0130
278	pol	Retrovirus-related Pol polyprotein from transposon 297	1.66	0.0132
279	serpinb1	Leukocyte elastase inhibitor	-1.42	0.0134
280	ANO9	Anoctamin-9	-1.50	0.0134
281	RCBTB1	RCC1 and BTB domain-containing protein 1	4.43	0.0135
282	VDAC2	Voltage-dependent anion-selective channel protein 2	-1.52	0.0135
283	rplP	50S ribosomal protein L16 {ECO:0000255|HAMAP-Rule:MF_01342}	-6.91	0.0138
284	Gvin1	Interferon-induced very large GTPase 1	-1.86	0.0141
285	TNIK	TRAF2 and NCK-interacting protein kinase	2.05	0.0141
286	Cspg4	Chondroitin sulfate proteoglycan 4	-6.26	0.0147
287	P2RX5	P2X purinoceptor 5	3.17	0.0148
288	ADAP1	Arf-GAP with dual PH domain-containing protein 1	-4.79	0.0148
289	Rgs2	Regulator of G-protein signaling 2	1.98	0.0149
290	SEC24B	Protein transport protein Sec24B	-2.60	0.0151
291	sort1	Sortilin	-0.80	0.0154
292	NOS	Nitric oxide synthase	1.44	0.0155
293	fmnl3	Formin-like protein 3	3.16	0.0159
294	gag-pol	Gag-Pol polyprotein	2.34	0.0159
295	Epn3	Epsin-3	-5.20	0.0161
296	hook1	Protein Hook homolog 1	1.88	0.0161
297	#N/A	Transposable element Tcb1 transposase	1.45	0.0163
298	SLC35A1	CMP-sialic acid transporter	-1.87	0.0164
299	krt13	Keratin, type I cytoskeletal 13	-1.17	0.0167
300	#N/A	Stonustoxin subunit alpha	1.02	0.0169
301	#N/A	Arrestin red cell isoform 2	3.54	0.0169
302	B3GALT5	Beta-1,3-galactosyltransferase 5	1.72	0.0170
303	ENDOD1	Endonuclease domain-containing 1 protein	-6.81	0.0171
304	Ppia	Peptidyl-prolyl cis-trans isomerase A	-1.12	0.0172
305	#N/A	Zinc-binding protein A33	3.43	0.0173
306	Son	Protein SON	2.20	0.0178
307	TAGAP	T-cell activation Rho GTPase-activating protein	2.12	0.0179
308	TRIM29	Tripartite motif-containing protein 29	-6.19	0.0179
309	Mpped2	Metallophosphoesterase MPPED2	4.11	0.0180
310	DIP2A	Disco-interacting protein 2 homolog A	1.30	0.0180
311	GIMAP4	GTPase IMAP family member 4	1.92	0.0180

312	tcf21	Transcription factor 21 {ECO:0000312|EMBL:AAI07969.1}	3.66	0.0183
313	trim71	E3 ubiquitin-protein ligase TRIM71	-3.65	0.0186
314	URGCP	Up-regulator of cell proliferation	7.11	0.0187
315	#N/A	Stonustoxin subunit beta	2.68	0.0191
316	SULT2B1	Sulfotransferase family cytosolic 2B member 1	1.46	0.0193
317	#N/A	Transposon TX1 uncharacterized 149 kDa protein	-3.20	0.0193
318	CLCN1	Chloride channel protein 1	-3.78	0.0193
319	CPXM1	Probable carboxypeptidase X1	-6.06	0.0195
320	Dip2a	Disco-interacting protein 2 homolog A	1.49	0.0198
321	GRB7	Growth factor receptor-bound protein 7	-1.61	0.0201
322	LMNA	Lamin-A	-1.20	0.0201
323	PSMD13	26S proteasome non-ATPase regulatory subunit 13	-1.57	0.0202
324	CACNA1E	Voltage-dependent R-type calcium channel subunit alpha-1E	4.44	0.0211
325	SLC35A1	CMP-sialic acid transporter	-1.76	0.0212
326	SORCS1	VPS10 domain-containing receptor SorCS1	3.03	0.0216
327	Btn1a1	Butyrophilin subfamily 1 member A1	1.31	0.0216
328	Peg10	Retrotransposon-derived protein PEG10	2.13	0.0219
329	B4GALT5	Beta-1,4-galactosyltransferase 5	-1.82	0.0223
330	RTL1	Retrotransposon-like protein 1	-2.88	0.0230
331	MEGF11	Multiple epidermal growth factor-like domains protein 11	-6.19	0.0232
332	#N/A	Transposable element Tcb1 transposase	-1.84	0.0233
333	Nlrc3	Protein NLRC3	1.50	0.0233
334	Kcnj10	ATP-sensitive inward rectifier potassium channel 10	4.30	0.0235
335	mxb	Interferon-induced GTP-binding protein MxB	2.89	0.0235
336	PHYPADRAFT_61094	Bryoporin	-1.67	0.0235
337	SQLE	Squalene monooxygenase	-1.48	0.0238
338	MYBL1	Myb-related protein A	5.16	0.0240
339	Nop56	Nucleolar protein 56	1.68	0.0242
340	ZNF177	Zinc finger protein 177	3.05	0.0242
341	Ndrg3	Protein NDRG3	-1.51	0.0245
342	Raver2	Ribonucleoprotein PTB-binding 2	4.53	0.0246
343	krt13	Keratin, type I cytoskeletal 13	-1.50	0.0252
344	Phf14	PHD finger protein 14	2.19	0.0253
345	HGFAC	Hepatocyte growth factor activator	-6.26	0.0257
346	Cpxm2	Inactive carboxypeptidase-like protein X2	-5.48	0.0258
347	krt13	Keratin, type I cytoskeletal 13	-1.41	0.0259
348	CASP13	Caspase-13	3.18	0.0261
349	ADGRL3	Adhesion G protein-coupled receptor L3 {ECO:0000312|HGNC:HGNC:20974}	3.52	0.0261
350	Gdpd2	Glycerophosphoinositol inositolphosphodiesterase GDPD2	2.72	0.0261
351	RSBN1	Round spermatid basic protein 1	3.56	0.0266
352	KIF13B	Kinesin-like protein KIF13B	2.63	0.0267
353	Cacna1e	Voltage-dependent R-type calcium channel subunit alpha-1E	5.52	0.0267
354	NLRC3	Protein NLRC3	6.09	0.0270
355	Entpd2	Ectonucleoside triphosphate diphosphohydrolase 2	-2.95	0.0271
356	HI_0258	Putative glycosyltransferase HI_0258	-2.64	0.0272
357	ch25h	Cholesterol 25-hydroxylase-like protein	1.98	0.0273
358	pro-pol	Pro-Pol polyprotein	4.22	0.0284
359	ANKRD27	Ankyrin repeat domain-containing protein 27	2.23	0.0287
360	Cacna1e	Voltage-dependent R-type calcium channel subunit alpha-1E	6.10	0.0289
361	ST3GAL1	CMP-N-acetylneuraminate-beta-galactosamide-alpha-2,3-sialyltransferase 1	-2.58	0.0290
362	Megf11	Multiple epidermal growth factor-like domains protein 11	-6.30	0.0293
363	#N/A	Stonustoxin subunit beta	1.30	0.0293
364	Ctnna2	Catenin alpha-2	-4.42	0.0296
365	RNF14	E3 ubiquitin-protein ligase RNF14	-1.42	0.0302
366	VPS13A	Vacuolar protein sorting-associated protein 13A	1.74	0.0307
367	Cpxm1	Probable carboxypeptidase X1	-5.92	0.0318
368	CHN2	Beta-chimaerin	1.68	0.0320
369	#N/A	DLA class I histocompatibility antigen, A9/A9 alpha chain	-0.97	0.0324
370	RGS4	Regulator of G-protein signaling 4	-3.98	0.0325
371	DENND4A	C-myc promoter-binding protein	4.33	0.0331
372	iws1	Protein IWS1 homolog	-1.89	0.0332
373	gpat3	Glycerol-3-phosphate acyltransferase 3	-3.00	0.0332
374	Ost4	Dolichyl-diphosphooligosaccharide--protein glycosyltransferase subunit	-1.71	0.0333

		4		
375	NEFM	Neurofilament medium polypeptide	1.48	0.0343
376	SAC3	Actin-3	1.60	0.0344
377	Dhx34	Probable ATP-dependent RNA helicase DHX34	2.36	0.0346
378	Nme1	Nucleoside diphosphate kinase A	-1.40	0.0346
379	Psmd2	26S proteasome non-ATPase regulatory subunit 2	-1.34	0.0351
380	IL17REL	Putative interleukin-17 receptor E-like	-1.79	0.0355
381	MEFV	Pyrin	4.13	0.0361
382	efna5b	Ephrin-A5b	-2.64	0.0365
383	EIF5A	Eukaryotic translation initiation factor 5A-1	-1.14	0.0368
384	HDLBP	Vigilin	-1.08	0.0369
385	Pcdh20	Protocadherin-20	3.95	0.0370
386	TY3B-G	Transposon Ty3-G Gag-Pol polyprotein	1.17	0.0370
387	USP48	Ubiquitin carboxyl-terminal hydrolase 48	2.04	0.0372
388	blw	ATP synthase subunit alpha, mitochondrial	2.13	0.0375
389	PARD6B	Partitioning defective 6 homolog beta	-1.78	0.0377
390	cdh4	Cadherin-4	-4.63	0.0379
391	DSG2	Desmoglein-2	-3.18	0.0380
392	hook1	Protein Hook homolog 1	1.80	0.0385
393	JMJD1C	Probable JmjC domain-containing histone demethylation protein 2C	1.17	0.0386
394	klhl26	Kelch-like protein 26	3.92	0.0389
395	NLRC3	Protein NLRC3	1.27	0.0404
396	K02A2.6	Uncharacterized protein K02A2.6	1.78	0.0409
397	krt8	Keratin, type II cytoskeletal 8	-1.25	0.0410
398	GIMAP2	GTPase IMAP family member 2	6.08	0.0411
399	pef1	Peflin	-1.90	0.0416
400	BTN2A1	Butyrophilin subfamily 2 member A1	1.31	0.0417
401	#N/A	Antho-RFamide neuropeptides type 2	1.83	0.0418
402	Sdc2	Syndecan-2	-1.99	0.0421
403	Pgap1	GPI inositol-deacylase	1.25	0.0422
404	F5	Coagulation factor V	2.14	0.0424
405	Rab1A	Ras-related protein Rab-1A	-1.22	0.0431
406	Znf768	Zinc finger protein 768	-2.84	0.0431
407	FBXO10	F-box only protein 10	6.16	0.0433
408	Tf2-9	Transposon Tf2-9 polyprotein	3.44	0.0435
409	fabp3	Fatty acid-binding protein, heart	-1.53	0.0439
410	Cpxm1	Probable carboxypeptidase X1	-4.16	0.0444
411	Mpped2	Metallophosphoesterase MPPED2	3.49	0.0448
412	RCBTB1	RCC1 and BTB domain-containing protein 1	1.05	0.0448
413	Moe	Moesin/ezrin/radixin homolog 1 {ECO:0000250|UniProtKB:P46150}	-1.27	0.0458
414	agap1	Arf-GAP with GTPase, ANK repeat and PH domain-containing protein 1	3.82	0.0458
415	Lrp1	Prolow-density lipoprotein receptor-related protein 1	4.60	0.0463
416	Tinagl1	Tubulointerstitial nephritis antigen-like	-2.94	0.0463
417	#N/A	Transposable element Tcb1 transposase	6.06	0.0469
418	TRIM21	E3 ubiquitin-protein ligase TRIM21	1.06	0.0472
419	krt13	Keratin, type I cytoskeletal 13	-1.84	0.0483
420	GBGT1	Globoside alpha-1,3-N-acetylgalactosaminyltransferase 1	1.47	0.0486
421	ZMYM5	Zinc finger MYM-type protein 5	5.81	0.0489
422	Urgcp	Up-regulator of cell proliferation	-2.55	0.0491
423	#N/A	Calmodulin	-1.07	0.0491
424	RPL7	60S ribosomal protein L7	-1.34	0.0496
425	Tmprss4	Transmembrane protease serine 4	-1.24	0.0497
426	Samd5	Sterile alpha motif domain-containing protein 5	1.13	0.0499

Lake 260 vs Lake 224

224 is the base e.g. Positive FC = upregulated in Lake 260 relative to Lake 224

1	PLA2G4C	Cytosolic phospholipase A2 gamma	8.10	5.68E-28
2	Mr1	Major histocompatibility complex class I-related gene protein	-5.25	3.89E-26
3	#N/A	Stonustoxin subunit beta	-4.08	4.09E-23
4	PLA2G4C	Cytosolic phospholipase A2 gamma	2.63	7.88E-22
5	Gvin1	Interferon-induced very large GTPase 1	-4.15	2.49E-17
6	GIMAP4	GTPase IMAP family member 4	10.69	5.59E-15
7	GIMAP8	GTPase IMAP family member 8	9.56	8.96E-15

8	GIMAP8	GTPase IMAP family member 8	9.66	1.65E-14
9	MDV087	Uncharacterized gene 87 protein	-7.96	1.88E-14
10	GIMAP4	GTPase IMAP family member 4	4.80	2.54E-13
11	cyp3a27	Cytochrome P450 3A27	-6.52	1.00E-12
12	TY3B-I	Transposon Ty3-I Gag-Pol polyprotein	12.51	3.81E-12
13	rnasel3	Ribonuclease-like 3 {ECO:0000303|PubMed:16861230}	9.90	4.78E-12
14	URGCP	Up-regulator of cell proliferation	-3.15	1.13E-11
15	PRB3	Basic salivary proline-rich protein 3	7.60	1.56E-11
16	GVINP1	Interferon-induced very large GTPase 1	-7.77	1.62E-11
17	vtg1	Vitellogenin	-8.68	1.62E-11
18	MDV087	Uncharacterized gene 87 protein	3.58	1.62E-11
19	cyp3a27	Cytochrome P450 3A27	-6.51	2.36E-11
20	#N/A	Ladderlectin	-6.74	3.45E-11
21	URGCP	Up-regulator of cell proliferation	-8.03	5.55E-11
22	TY3B-I	Transposon Ty3-I Gag-Pol polyprotein	11.94	7.65E-11
23	#N/A	Class I histocompatibility antigen, F10 alpha chain	10.09	1.56E-10
24	vtg1	Vitellogenin	-8.23	1.60E-10
25	DLEC1	Deleted in lung and esophageal cancer protein 1	4.07	1.66E-10
26	RNF213	E3 ubiquitin-protein ligase RNF213	8.72	2.40E-10
27	#N/A	Actin	-3.75	3.11E-10
28	Urgcp	Up-regulator of cell proliferation	-5.83	4.22E-10
29	Abi1	Abl interactor 1	6.35	5.18E-10
30	SYT7	Synaptotagmin-7	8.41	1.30E-09
31	EGR1	Early growth response protein 1	-3.92	2.05E-09
32	pol	Pol polyprotein	-3.06	2.75E-09
33	pol	Retrovirus-related Pol polyprotein from transposon 297	6.74	5.80E-09
34	Pik3cb	Phosphatidylinositol 4,5-bisphosphate 3-kinase catalytic subunit beta isoform	-3.42	7.48E-09
35	ier2	Immediate early response gene 2 protein	-2.94	1.53E-08
36	STAT1	Signal transducer and activator of transcription 1	-2.16	2.67E-08
37	USP43	Ubiquitin carboxyl-terminal hydrolase 43	8.52	2.69E-08
38	Tf2-9	Transposon Tf2-9 polyprotein	3.67	2.86E-08
39	CRY2	Cryptochrome-2	-3.73	3.72E-08
40	#N/A	Stonustoxin subunit beta	-4.01	4.55E-08
41	HEXB	Beta-hexosaminidase subunit beta	4.97	5.85E-08
42	nr4a1	Nuclear receptor subfamily 4 group A member 1	-4.53	9.15E-08
43	#N/A	Transposable element Tcb2 transposase	4.49	1.07E-07
44	pol	Retrovirus-related Pol polyprotein from transposon opus	8.36	1.13E-07
45	Smoc2	SPARC-related modular calcium-binding protein 2	-3.24	1.35E-07
46	Dlec1	Deleted in lung and esophageal cancer protein 1 homolog	2.95	1.49E-07
47	exsA	Spore coat assembly protein ExsA	4.61	2.96E-07
48	GIMAP2	GTPase IMAP family member 2	7.22	3.01E-07
49	DUSP1	Dual specificity protein phosphatase 1	-4.49	3.34E-07
50	KIFAP3	Kinesin-associated protein 3	2.32	3.45E-07
51	gag-pol	Gag-Pol polyprotein	-6.60	4.41E-07
52	DLEC1	Deleted in lung and esophageal cancer protein 1	3.10	5.04E-07
53	ier2	Immediate early response gene 2 protein	-3.82	5.30E-07
54	NLRP1	NACHT, LRR and PYD domains-containing protein 1	-1.69	6.16E-07
55	JUN	Transcription factor AP-1	-2.17	7.33E-07
56	ABCB1	Multidrug resistance protein 1	3.70	7.59E-07
57	tc1a	Transposable element Tc1 transposase	-1.66	8.01E-07
58	Nt5c1a	Cytosolic 5'-nucleotidase 1A	-3.07	8.01E-07
59	Atf3	Cyclic AMP-dependent transcription factor ATF-3	-3.33	8.21E-07
60	RNF213	E3 ubiquitin-protein ligase RNF213	8.05	8.35E-07
61	NLRC3	Protein NLRC3	-6.53	1.24E-06
62	RALGAPA1	Ral GTPase-activating protein subunit alpha-1	-6.44	1.40E-06
63	#N/A	Stonustoxin subunit alpha	-1.64	1.69E-06
64	Nrdc	Nardilysin	3.09	1.70E-06
65	Dusp5	Dual specificity protein phosphatase 5	-6.80	1.84E-06
66	fos	Proto-oncogene c-Fos	-4.10	2.08E-06
67	SPRR3	Small proline-rich protein 3	4.18	2.33E-06
68	tchp	Trichoplein keratin filament-binding protein	7.07	2.97E-06
69	Nlrc3	Protein NLRC3	-1.83	3.49E-06
70	pol	Retrovirus-related Pol polyprotein from transposon opus	-6.12	5.93E-06
71	#N/A	Transposable element Tcb1 transposase	3.17	6.24E-06
72	cep131	Centrosomal protein of 131 kDa	7.51	6.62E-06

73	DUSP5	Dual specificity protein phosphatase 5	-4.35	7.27E-06
74	HI_0258	Putative glycosyltransferase HI_0258	4.49	7.55E-06
75	GVQW1	Protein GVQW1	8.51	8.70E-06
76	Klf4	Krueppel-like factor 4	-3.30	9.62E-06
77	HARBI1	Putative nuclease HARBI1	-2.18	1.06E-05
78	samhd1	Deoxynucleoside triphosphate triphosphohydrolase SAMHD1	-2.92	1.09E-05
79	RALGAPA1	Ral GTPase-activating protein subunit alpha-1	-3.89	1.11E-05
80	CACNA1B	Voltage-dependent N-type calcium channel subunit alpha-1B	-5.94	1.13E-05
81	Tnrc18	Trinucleotide repeat-containing gene 18 protein	-2.15	1.19E-05
82	P4HA2	Prolyl 4-hydroxylase subunit alpha-2	2.52	1.26E-05
83	Mycbpap	MYCBP-associated protein	5.45	1.32E-05
84	#N/A	LINE-1 retrotransposable element ORF2 protein	6.69	1.40E-05
85	egr1	Early growth response protein 1	-3.82	1.43E-05
86	CACNA1B	Voltage-dependent N-type calcium channel subunit alpha-1B	-6.13	1.45E-05
87	#N/A	Stonustoxin subunit alpha	-8.10	1.52E-05
88	STAT1	Signal transducer and activator of transcription 1	-2.88	1.57E-05
89	Fam111a	Protein FAM111A	4.16	1.59E-05
90	#N/A	Transposable element Tcb1 transposase	3.89	1.64E-05
91	Pim1	Serine/threonine-protein kinase pim-1	-2.64	1.69E-05
92	Tf2-9	Transposon Tf2-9 polyprotein	-2.83	1.81E-05
93	FBXO7	F-box only protein 7	2.92	1.81E-05
94	junb	Transcription factor jun-B	-2.75	1.91E-05
95	FARP1	FERM, RhoGEF and pleckstrin domain-containing protein 1	2.80	1.93E-05
96	Chd6	Chromodomain-helicase-DNA-binding protein 6	-3.91	2.16E-05
97	Ggps1	Geranylgeranyl pyrophosphate synthase	3.40	2.19E-05
98	#N/A	Transposable element Tcb1 transposase	3.96	2.21E-05
99	Dennd3	DENN domain-containing protein 3	-2.16	2.34E-05
100	#N/A	Transposable element Tcb1 transposase	3.80	2.58E-05
101	pol	Retrovirus-related Pol polyprotein from transposon 297	11.58	2.72E-05
102	hsd17b12b	Very-long-chain 3-oxoacyl-CoA reductase-B {ECO:0000305}	5.57	2.83E-05
103	Mefv	Pyrin	-2.97	3.06E-05
104	PPP1R15B	Protein phosphatase 1 regulatory subunit 15B	-3.74	3.08E-05
105	ifna3	Interferon a3 {ECO:0000303|PubMed:25080482}	-4.59	3.33E-05
106	MIMI_R795	Probable bifunctional E2/E3 enzyme R795	-2.79	3.47E-05
107	GIMAP4	GTPase IMAP family member 4	-6.31	3.64E-05
108	ENDOD1	Endonuclease domain-containing 1 protein	-6.24	3.65E-05
109	Gpr119	Glucose-dependent insulinotropic receptor	3.88	3.76E-05
110	KRT19	Keratin, type I cytoskeletal 19	-3.42	4.28E-05
111	MUC22	Mucin-22	1.86	4.29E-05
112	TNMD	Tenomodulin	-4.41	4.33E-05
113	pol	Retrovirus-related Pol polyprotein from transposon 17.6	7.81	4.46E-05
114	rpsC	30S ribosomal protein S3	7.66	4.48E-05
115	#N/A	Stonustoxin subunit beta	-1.70	4.87E-05
116	gag-pol	Gag-Pol polyprotein	-5.31	5.11E-05
117	TPD52	Tumor protein D52	-2.69	5.20E-05
118	GIMAP5	GTPase IMAP family member 5	6.50	1
119	TIGD1	Tigger transposable element-derived protein 1	8.09	5.32E-05
120	Fh	Fumarate hydratase, mitochondrial	2.43	5.37E-05
121	#N/A	Transposable element Tcb1 transposase	4.15	5.37E-05
122	fos	Proto-oncogene c-Fos	-3.72	5.43E-05
123	eif3i	Eukaryotic translation initiation factor 3 subunit I	2.78	6.09E-05
124	#N/A	Transposable element Tcb1 transposase	5.29	6.16E-05
125	TRIM17	E3 ubiquitin-protein ligase TRIM17	-5.58	6.24E-05
126	HEBP2	Heme-binding protein 2	2.69	6.59E-05
127	#N/A	Class I histocompatibility antigen, F10 alpha chain	-5.08	6.61E-05
128	RALGAPA1	Ral GTPase-activating protein subunit alpha-1	-4.82	6.67E-05
129	Samd9l	Sterile alpha motif domain-containing protein 9-like	5.34	6.98E-05
130	tc1a	Transposable element Tc1 transposase	3.91	7.76E-05
131	Jund	Transcription factor jun-D	-3.21	8.18E-05
132	ITA	Inhibitor of apoptosis protein	-1.34	8.25E-05
133	egr1	Early growth response protein 1	-2.84	9.14E-05
134	tc1a	Transposable element Tc1 transposase	-1.23	9.50E-05
135	Fam111a	Protein FAM111A	4.97	9.52E-05
136	#N/A	ERV-BabFcenv provirus ancestral Env polyprotein	6.91	0.0001
137	hook1	Protein Hook homolog 1	-1.92	0.0001
138	tc1a	Transposable element Tc1 transposase	3.78	0.0001

139	Endod1	Endonuclease domain-containing 1 protein	-5.31	0.0001
140	#N/A	Melanoma-associated antigen G1	-2.56	0.0001
141	Pgm5	Phosphoglucomutase-like protein 5	-6.41	0.0001
142	ENDOD1	Endonuclease domain-containing 1 protein	-5.68	0.0001
143	DUSP5	Dual specificity protein phosphatase 5	-2.59	0.0001
144	#N/A	Transposon TX1 uncharacterized 149 kDa protein	3.60	0.0001
145	hook1	Protein Hook homolog 1	-2.44	0.0001
146	Gvin1	Interferon-induced very large GTPase 1	7.52	0.0001
147	Gimap4	GTPase IMAP family member 4	-5.88	0.0002
148	jockey\pol	RNA-directed DNA polymerase from mobile element jockey	4.09	0.0002
149	#N/A	LINE-1 retrotransposable element ORF2 protein	7.69	0.0002
150	GLRX3	Glutaredoxin-3	2.60	0.0002
151	#N/A	Transposable element Tcb1 transposase	2.76	0.0002
152	NLRP12	NACHT, LRR and PYD domains-containing protein 12	-2.39	0.0002
153	DDB_G0268948	Putative methyltransferase DDB_G0268948	-4.99	0.0002
154	NLRP3	NACHT, LRR and PYD domains-containing protein 3	-5.74	0.0002
155	rplN	50S ribosomal protein L14	7.06	1.0000
156	Igf2r	Cation-independent mannose-6-phosphate receptor	-5.83	0.0002
157	#N/A	Transposable element Tcb1 transposase	3.86	0.0002
158	#N/A	Transposable element Tcb1 transposase	3.43	0.0002
159	#N/A	Stonustoxin subunit beta	-1.61	0.0002
160	F5	Coagulation factor V	3.23	0.0002
161	SOCS3	Suppressor of cytokine signaling 3	-3.35	0.0002
162	PEG10	Retrotransposon-derived protein PEG10	-5.36	0.0002
163	Ldlrap1	Low density lipoprotein receptor adapter protein 1	3.11	0.0002
164	tc1a	Transposable element Tc1 transposase	-1.16	0.0002
165	egr1	Early growth response protein 1	-5.78	0.0003
166	SYT7	Synaptotagmin-7	6.72	1.0000
167	ZNF568	Zinc finger protein 568	-6.05	0.0003
168	GBGT1	Globoside alpha-1,3-N-acetylgalactosaminyltransferase 1	-1.32	0.0003
169	GSN	Gelsolin	-3.37	0.0004
170	#N/A	Transposable element Tcb1 transposase	-3.62	0.0004
171	#N/A	Transposable element Tcb2 transposase	3.73	0.0004
172	Tf2-9	Transposon Tf2-9 polyprotein	5.06	0.0004
173	IMMP1L	Mitochondrial inner membrane protease subunit 1	3.32	0.0004
174	slc39a9-b	Zinc transporter ZIP9-B	2.80	0.0004
175	#N/A	Transposable element Tcb1 transposase	3.19	0.0004
176	MYH11	Myosin-11	-1.72	0.0004
177	uck1	Uridine-cytidine kinase 1	3.74	0.0004
178	brk1	Probable protein BRICK1	2.13	0.0005
179	FOSL2	Fos-related antigen 2	-5.57	0.0005
180	Ankrd55	Ankyrin repeat domain-containing protein 55	7.57	0.0005
181	CLDN4	Claudin-4	4.28	0.0005
182	ERVV-1	Endogenous retrovirus group V member 1 Env polyprotein	3.17	0.0005
183	gag-pol	Gag-Pol polyprotein	6.34	1.0000
184	AKAP13	A-kinase anchor protein 13	-1.22	0.0005
185	TSPAN3	Tetraspanin-3	-5.13	1.0000
186	moaE2	Molybdopterin synthase catalytic subunit 2	7.97	0.0006
187	SUPT20H	Transcription factor SPT20 homolog	2.42	0.0006
188	Lpin2	Phosphatidate phosphatase LPIN2	-2.76	0.0006
189	tc1a	Transposable element Tc1 transposase	3.40	0.0006
190	GIMAP7	GTPase IMAP family member 7	-3.03	0.0006
191	Nlrc3	Protein NLRC3	-5.31	0.0006
192	#N/A	Stonustoxin subunit beta	-5.34	0.0006
193	Gvin1	Interferon-induced very large GTPase 1	-3.04	0.0007
194	Znf32	Zinc finger protein 32	-5.21	0.0007
195	Nfkb2	Nuclear factor NF-kappa-B p100 subunit	-1.52	0.0007
196	DDX17	Probable ATP-dependent RNA helicase DDX17	-3.21	0.0007
197	Tspan33	Tetraspanin-33	-2.11	0.0007
198	RNH1	Ribonuclease inhibitor	-2.55	0.0007
199	SULF2	Extracellular sulfatase Sulf-2	4.11	0.0007
200	#N/A	Transposable element Tcb2 transposase	-1.81	0.0007
201	mfsd2ab	Sodium-dependent lysophosphatidylcholine symporter 1-B	3.04	0.0007
202	Fbxo11	F-box only protein 11	-2.07	0.0007
203	MUC22	Mucin-22	3.83	0.0008
204	MIMI_L138	Uncharacterized protein L138	3.47	0.0008

205	GPATCH8	G patch domain-containing protein 8	-1.38	0.0008
206	Fah	Fumarylacetoacetase	5.05	0.0008
207	ARAP1	Arf-GAP with Rho-GAP domain, ANK repeat and PH domain-containing protein 1	-2.51	0.0009
208	Znfx1	NFX1-type zinc finger-containing protein 1	-1.74	0.0009
209	rnasekb	Ribonuclease kappa-B	2.03	0.0009
210	OGDH	2-oxoglutarate dehydrogenase, mitochondrial	2.02	0.0009
211	egr1	Early growth response protein 1	-2.48	0.0009
212	DLEC1	Deleted in lung and esophageal cancer protein 1	2.80	0.0009
213	CD276	CD276 antigen	-3.52	0.0010
214	#N/A	LINE-1 retrotransposable element ORF2 protein	6.79	0.0010
215	ROCK2	Rho-associated protein kinase 2	-1.96	0.0010
216	#N/A	Transposable element Tcb1 transposase	3.07	0.0010
217	TSTA3	GDP-L-fucose synthase	-5.27	0.0010
218	Hook3	Protein Hook homolog 3	2.01	0.0010
219	Klf4	Krueppel-like factor 4	-3.91	0.0010
220	RELB	Transcription factor RelB	-1.83	0.0010
221	#N/A	Transposable element Tcb1 transposase	2.84	0.0010
222	znf395	Zinc finger protein 395	-1.93	0.0010
223	trim33	E3 ubiquitin-protein ligase TRIM33	-5.27	0.0011
224	HI_0712	Probable hemoglobin and hemoglobin-haptoglobin-binding protein 3	3.95	0.0011
225	#N/A	Histone H1	-2.15	0.0011
226	SHMT2	Serine hydroxymethyltransferase, mitochondrial	-1.68	0.0011
227	#N/A	Probable DNA polymerase	-3.12	0.0012
228	jockey\pol	RNA-directed DNA polymerase from mobile element jockey	-5.04	1.0000
229	dcaf15	DDB1- and CUL4-associated factor 15	1.85	0.0012
230	TRIML1	Probable E3 ubiquitin-protein ligase TRIML1	-5.53	0.0012
231	C16orf89	UPF0764 protein C16orf89	5.85	0.0013
232	LAMA3	Laminin subunit alpha-3	-4.89	1.0000
233	Fntb	Protein farnesyltransferase subunit beta	2.12	0.0013
234	LINC00269	Putative uncharacterized protein encoded by LINC00269	4.20	0.0013
235	Ralgapa1	Ral GTPase-activating protein subunit alpha-1	-4.03	0.0014
236	RTL1	Retrotransposon-like protein 1	-4.86	1.0000
237	IFI44	Interferon-induced protein 44	-2.67	0.0015
238	HERC5	E3 ISG15--protein ligase HERC5	-5.29	0.0015
239	Trim58	E3 ubiquitin-protein ligase TRIM58	-4.86	1.0000
240	GIMAP8	GTPase IMAP family member 8	2.82	0.0016
241	FN1	Fibronectin	5.24	0.0016
242	PEG10	Retrotransposon-derived protein PEG10	7.24	1.0000
243	Kiaa1109	Uncharacterized protein KIAA1109	-3.09	0.0016
244	RNF186	RING finger protein 186	-1.60	0.0016
245	#N/A	Transposable element Tcb1 transposase	3.91	0.0016
246	Glod4	Glyoxalase domain-containing protein 4	2.90	0.0016
247	IRS2	Insulin receptor substrate 2	-1.65	0.0017
248	#N/A	RNA-directed RNA polymerase	-6.61	0.0017
249	#N/A	Stonustoxin subunit beta	-2.49	0.0017
250	naa60	N-alpha-acetyltransferase 60	2.85	0.0017
251	PRODH	Proline dehydrogenase 1, mitochondrial {ECO:0000250|UniProtKB:O43272}	-1.61	0.0017
252	#N/A	Amino-terminal enhancer of split	1.83	0.0018
253	Arl5b	ADP-ribosylation factor-like protein 5B	-3.23	0.0018
254	IFFO1	Intermediate filament family orphan 1	-2.87	0.0018
255	AHNAK	Neuroblast differentiation-associated protein AHNAK	-5.73	0.0018
256	PGBD4	PiggyBac transposable element-derived protein 4	-3.30	0.0018
257	YME1L1	ATP-dependent zinc metalloprotease YME1L1	-4.89	1.0000
258	TSTA3	GDP-L-fucose synthase	-5.03	1.0000
259	Pik3c2a	Phosphatidylinositol 4-phosphate 3-kinase C2 domain-containing subunit alpha	-3.87	0.0018
260	PIAS1	E3 SUMO-protein ligase PIAS1	-1.99	0.0018
261	mau2	MAU2 chromatid cohesion factor homolog	-4.80	1.0000
262	Dsp	Desmoplakin	-2.61	0.0018
263	tc1a	Transposable element Tc1 transposase	-1.37	0.0019
264	Capn2	Calpain-2 catalytic subunit	2.06	0.0019
265	Gpr141	Probable G-protein coupled receptor 141	2.55	0.0019
266	HERC3	Probable E3 ubiquitin-protein ligase HERC3	-5.27	0.0019
267	ALYREF	THO complex subunit 4	-2.33	0.0019

268	ACSL3	Long-chain-fatty-acid--CoA ligase 3	-1.48	0.0020
269	COX17	Cytochrome c oxidase copper chaperone	3.33	0.0020
270	midn	Midnolin	-3.03	0.0021
271	Mslnl	Mesothelin-like protein	-4.44	0.0021
272	fbxl15	F-box/LRR-repeat protein 15	-2.47	0.0021
273	alpha	Capsid protein alpha	-6.53	0.0022
274	KRT7	Keratin, type II cytoskeletal 7	-3.00	0.0022
275	Nfkbia	NF-kappa-B inhibitor alpha	-2.35	0.0022
276	FOSL2	Fos-related antigen 2	-3.09	0.0024
277	#N/A	Transposable element Tcb1 transposase	2.50	0.0024
278	Itih4	Inter alpha-trypsin inhibitor, heavy chain 4	4.56	0.0024
279	#N/A	Transposon TX1 uncharacterized 149 kDa protein	2.86	0.0025
280	#N/A	Uncharacterized protein DKFZp434B061	3.16	0.0025
281	NAT16	Probable N-acetyltransferase 16	-4.68	1.0000
282	Rnh1	Ribonuclease inhibitor	-4.93	1.0000
283	PTPRZ1	Receptor-type tyrosine-protein phosphatase zeta	2.11	0.0027
284	sox2	Transcription factor Sox-2	-4.96	1.0000
285	GIMAP7	GTPase IMAP family member 7	-3.68	0.0029
286	ARRDC1	Arrestin domain-containing protein 1	-1.44	0.0029
287	Btnl2	Butyrophilin-like protein 2	-5.03	1.0000
288	Ppfia3	Liprin-alpha-3	-2.51	0.0029
289	RAB11A	Ras-related protein Rab-11A	1.71	0.0029
290	miefl	Mitochondrial dynamics protein MID51	-4.74	1.0000
291	MCTP2	Multiple C2 and transmembrane domain-containing protein 2	-1.63	0.0030
292	EEF2	Elongation factor 2	2.22	0.0032
293	DCXR	L-xylulose reductase	-4.62	1.0000
294	#N/A	Transposable element Tcb2 transposase	-2.66	0.0032
295	ATP13A3	Probable cation-transporting ATPase 13A3	-4.36	0.0033
296	TASOR	Protein TASOR {ECO:0000305}	-1.44	0.0033
297	PTPDC1	Protein tyrosine phosphatase domain-containing protein 1	3.30	0.0034
298	Saci_1252	Uncharacterized protein Saci_1252	-1.52	0.0034
299	ADAM28	Disintegrin and metalloproteinase domain-containing protein 28	-1.68	0.0034
300	TACC1	Transforming acidic coiled-coil-containing protein 1	-1.07	0.0035
301	PLEKHA5	Pleckstrin homology domain-containing family A member 5	-1.35	0.0035
302	NBPF12	Neuroblastoma breakpoint family member 12	2.23	0.0036
303	Asl	Argininosuccinate lyase	3.30	0.0036
304	#N/A	Nuclear factor 7, ovary	-3.94	0.0036
305	Nlrp3	NACHT, LRR and PYD domains-containing protein 3	-4.78	1.0000
306	aste1	Protein asteroid homolog 1	-2.46	0.0037
307	iws1	Protein IWS1 homolog	2.72	0.0038
308	PTK2B	Protein-tyrosine kinase 2-beta	-1.55	0.0038
309	#N/A	Death ligand signal enhancer	-2.92	0.0038
310	Dock8	Dedicator of cytokinesis protein 8	-2.50	0.0039
311	Gpr108	Protein GPR108	1.75	0.0039
312	#N/A	Transposable element Tcb2 transposase	2.88	0.0040
313	tc1a	Transposable element Tc1 transposase	-1.25	0.0040
314	#N/A	RNA-directed RNA polymerase	-6.44	0.0041
315	#N/A	Transposable element Tcb1 transposase	3.10	0.0041
316	pol	Pol polyprotein	-5.03	1.0000
317	B3GALT1	Beta-1,3-galactosyltransferase 1	-1.87	0.0042
318	Tnfaip3	Tumor necrosis factor alpha-induced protein 3	-1.80	0.0042
319	DNAAF5	Dynein assembly factor 5, axonemal	2.10	0.0042
320	X-element\ORF2	Probable RNA-directed DNA polymerase from transposon X-element	-4.78	1.0000
321	PGBD3	PiggyBac transposable element-derived protein 3	-1.83	0.0044
322	GIMAP4	GTPase IMAP family member 4	-3.90	0.0045
323	Eci1	Enoyl-CoA delta isomerase 1, mitochondrial	2.79	0.0045
324	ADAM17	Disintegrin and metalloproteinase domain-containing protein 17	-4.70	1.0000
325	#N/A	Putative uncharacterized protein ENSP00000383309	2.78	0.0046
326	Arfgap1	ADP-ribosylation factor GTPase-activating protein 1	-1.45	0.0046
327	BTN2A1	Butyrophilin subfamily 2 member A1	-3.11	0.0046
328	gpr183	G-protein coupled receptor 183	2.34	0.0049
329	PDE4DIP	Myomegalin	2.35	0.0049
330	STAT1	Signal transducer and activator of transcription 1	-3.00	0.0050
331	ENPP	Enterin neuropeptides	3.43	0.0051
332	HI_0712	Probable hemoglobin and hemoglobin-haptoglobin-binding protein 3	3.11	0.0052
333	BAIAP2L1	Brain-specific angiogenesis inhibitor 1-associated protein 2-like protein 1	2.61	0.0052

334	secY	Protein translocase subunit SecY	5.43	1.0000
335	EPB41	Protein 4.1	-1.70	0.0053
336	oaz1a	Ornithine decarboxylase antizyme 1	1.45	0.0053
337	Epb41l1	Band 4.1-like protein 1	-1.28	0.0053
338	Tf2-9	Transposon Tf2-9 polyprotein	1.63	0.0053
339	sacm1la	Phosphatidylinositide phosphatase SAC1-A	-4.72	1.0000
340	MED12	Mediator of RNA polymerase II transcription subunit 12	-4.47	1.0000
341	Mau2	MAU2 chromatid cohesion factor homolog	-2.19	0.0055
342	PTK2B	Protein-tyrosine kinase 2-beta	-1.55	0.0055
343	#N/A	Transposable element Tcb2 transposase	3.10	0.0055
344	Itch	E3 ubiquitin-protein ligase Itchy	-1.34	0.0055
345	ARID1A	AT-rich interactive domain-containing protein 1A	-3.96	0.0055
346	JUN	Transcription factor AP-1	-2.58	0.0055
347	PHF12	PHD finger protein 12	-4.50	1.0000
348	FKBP5	Peptidyl-prolyl cis-trans isomerase FKBP5	-1.82	0.0055
349	GIMAP4	GTPase IMAP family member 4	-1.62	0.0056
350	WIPI2	WD repeat domain phosphoinositide-interacting protein 2	-1.76	0.0056
351	Tf2-9	Transposon Tf2-9 polyprotein	1.30	0.0056
352	Trp53inp1	Tumor protein p53-inducible nuclear protein 1	1.61	0.0056
353	pol	Retrovirus-related Pol polyprotein from transposon 17.6	5.53	0.0056
354	PTBP3	Polypyrimidine tract-binding protein 3	-1.95	0.0056
355	STAT1	Signal transducer and activator of transcription 1-alpha/beta	-1.64	0.0058
356	Ptprz1	Receptor-type tyrosine-protein phosphatase zeta	-3.87	0.0058
357	Phf21a	PHD finger protein 21A	-4.47	1.0000
358	Tf2-9	Transposon Tf2-9 polyprotein	2.73	0.0061
359	Tf2-9	Transposon Tf2-9 polyprotein	1.45	0.0063
360	GRHL1	Grainyhead-like protein 1 homolog	-1.59	0.0063
361	MYO9B	Unconventional myosin-IXb	-1.41	0.0063
362	GBE1	1,4-alpha-glucan-branching enzyme	-4.42	1.0000
363	Myo9b	Unconventional myosin-IXb	-1.45	0.0066
364	MYH9	Myosin-9	-1.52	0.0067
365	CEBPB	CCAAT/enhancer-binding protein beta	-3.37	0.0067
366	aste1	Protein asteroid homolog 1	-2.26	0.0068
367	PIAS1	E3 SUMO-protein ligase PIAS1	-3.31	0.0068
368	#N/A	Protein C9orf72 homolog	-4.26	1.0000
369	SMCR8	Smith-Magenis syndrome chromosomal region candidate gene 8 protein	-4.04	0.0069
370	Plxnb2	Plexin-B2	-1.58	0.0069
371	TAOK3	Serine/threonine-protein kinase TAO3	-2.49	0.0069
372	STOML2	Stomatin-like protein 2, mitochondrial	2.39	0.0070
373	Mtmr1	Myotubularin-related protein 1	-1.51	0.0070
374	#N/A	Pancreatic alpha-amylase	-2.54	0.0070
375	cka	Casein kinase II subunit alpha	-2.09	0.0071
376	NLRC3	Protein NLRC3	-2.88	0.0072
377	#N/A	Transposable element Tcb2 transposase	2.46	0.0073
378	SAMHD1	Deoxynucleoside triphosphate triphosphohydrolase SAMHD1	-4.73	1.0000
379	#N/A	Zinc-binding protein A33	-2.92	0.0074
380	#N/A	Stonustoxin subunit alpha	-2.14	0.0074
381	Flrt1	Leucine-rich repeat transmembrane protein FLRT1	2.58	0.0074
382	Ddx5	Probable ATP-dependent RNA helicase DDX5	-2.27	0.0075
383	RAF1	RAF proto-oncogene serine/threonine-protein kinase	2.30	0.0076
384	Gimap4	GTPase IMAP family member 4	-3.72	0.0076
385	phlda2	Pleckstrin homology-like domain family A member 2	-1.87	0.0076
386	TNFSF14	Tumor necrosis factor ligand superfamily member 14	-3.92	0.0076
387	UBP1	Upstream-binding protein 1	-1.79	0.0077
388	Samd9l	Sterile alpha motif domain-containing protein 9-like	4.73	0.0077
389	Pwp2	Periodic tryptophan protein 2 homolog	2.64	0.0078
390	Parp14	Poly [ADP-ribose] polymerase 14	-1.64	0.0078
391	rbm5	RNA-binding protein 5	-1.65	0.0079
392	B4GALNT1	Beta-1,4 N-acetylgalactosaminyltransferase 1	-1.35	0.0080
393	Dhx58	Probable ATP-dependent RNA helicase DHX58	-2.23	0.0081
394	Osbpl6	Oxysterol-binding protein-related protein 6	-1.59	0.0082
395	#N/A	Salivary plasminogen activator beta	-3.68	0.0082
396	L1RE1	LINE-1 retrotransposable element ORF1 protein	10.59	0.0083
397	tc1a	Transposable element Tc1 transposase	2.69	0.0083
398	#N/A	Transposable element Tcb2 transposase	-1.12	0.0085
399	SLMAP	Sarcolemmal membrane-associated protein	-2.01	0.0086

400	#N/A	Transposon TX1 uncharacterized 149 kDa protein	2.33	0.0087
401	RNF19A	E3 ubiquitin-protein ligase RNF19A	-1.44	0.0087
402	TMEM8A	Transmembrane protein 8A	-1.72	0.0087
403	Farp1	FERM, RhoGEF and pleckstrin domain-containing protein 1	1.78	0.0088
404	#N/A	LINE-1 retrotransposable element ORF2 protein	7.47	0.0088
405	Parp14	Poly [ADP-ribose] polymerase 14	-2.80	0.0088
406	CRTAC1	Cartilage acidic protein 1	2.69	0.0089
407	F2rl1	Proteinase-activated receptor 2	-2.71	0.0089
408	Cltc	Clathrin heavy chain 1	3.13	0.0089
409	nr4a1	Nuclear receptor subfamily 4 group A member 1	-4.34	0.0091
410	SLA	Src-like-adapter	-3.95	1.0000
411	BTG2	Protein BTG2	-2.06	0.0092
412	SYNE2	Nesprin-2	-1.20	0.0092
413	Znf32	Zinc finger protein 32	-1.93	0.0093
414	pol	Retrovirus-related Pol polyprotein from transposon opus	9.49	0.0093
415	Atg16l1	Autophagy-related protein 16-1	2.30	0.0094
416	Dgcr8	Microprocessor complex subunit DGCR8	-1.55	0.0094
417	APOLD1	Apolipoprotein L domain-containing protein 1	-1.83	0.0096
418	Casp8	Caspase-8	-2.37	0.0096
419	#N/A	Transposable element Tcb1 transposase	2.90	0.0096
420	ANXA1	Annexin A1	-2.48	0.0097
421	MYO9B	Unconventional myosin-IXb	-1.37	0.0097
422	ZNF283	Zinc finger protein 283	4.39	0.0098
423	SAMD9L	Sterile alpha motif domain-containing protein 9-like	-1.39	0.0098
424	MYB	Transcriptional activator Myb	-1.47	0.0098
425	Tf2-9	Transposon Tf2-9 polyprotein	1.34	0.0099
426	#N/A	LisH domain and HEAT repeat-containing protein KIAA1468 homolog	1.87	0.0099
427	nav3	Neuron navigator 3	-1.55	0.0099
428	SEC23A	Protein transport protein Sec23A	-1.84	0.0100
429	RNH1	Ribonuclease inhibitor	-1.59	0.0101
430	Kif5b	Kinesin-1 heavy chain	-4.75	1.0000
431	#N/A	Stonustoxin subunit beta	-1.55	0.0101
432	GIP	Copia protein	-1.35	0.0102
433	RC3H1	Roquin-1	-4.32	1.0000
434	EIF4G1	Eukaryotic translation initiation factor 4 gamma 1	-1.25	0.0103
435	Dcxr	L-xylulose reductase	-4.42	1.0000
436	Tnfaip3	Tumor necrosis factor alpha-induced protein 3	-2.16	0.0103
437	Zfhx4	Zinc finger homeobox protein 4	2.86	0.0104
438	TRIM27	Zinc finger protein RFP	2.24	0.0105
439	DDX5	Probable ATP-dependent RNA helicase DDX5	-2.39	0.0106
440	klhl26	Kelch-like protein 26	-4.49	1.0000
441	Arrdc3	Arrestin domain-containing protein 3	-2.23	0.0107
442	Jmjd1c	Probable JmjC domain-containing histone demethylation protein 2C	-1.17	0.0108
443	PTGS2	Prostaglandin G/H synthase 2	-2.46	0.0109
444	DLEC1	Deleted in lung and esophageal cancer protein 1	2.81	0.0109
445	jag1b	Protein jagged-1b	-1.46	0.0109
446	Pcdh20	Protocadherin-20	-5.26	0.0109
447	vimp	Selenoprotein S	1.41	0.0111
448	Dennd3	DENN domain-containing protein 3	-1.68	0.0112
449	#N/A	Stonustoxin subunit alpha	-1.83	0.0112
450	Gss	Glutathione synthetase	-3.54	1.0000
451	URGCP	Up-regulator of cell proliferation	-1.68	0.0113
452	WIPI1	WD repeat domain phosphoinositide-interacting protein 1	-1.37	0.0114
453	#N/A	Transposable element Tcb1 transposase	2.54	0.0118
454	USP2	Ubiquitin carboxyl-terminal hydrolase 2	-3.27	0.0118
455	TY3B-G	Transposon Ty3-G Gag-Pol polyprotein	3.67	0.0118
456	Pol	LINE-1 retrotransposable element ORF2 protein	-1.57	0.0119
457	MCL1	Induced myeloid leukemia cell differentiation protein Mcl-1 homolog	-1.68	0.0119
458	GVINP1	Interferon-induced very large GTPase 1	-3.57	0.0119
459	Nlrp1b	NACHT, LRR and PYD domains-containing protein 1b allele 3	-1.90	0.0120
460	GMNC	Geminin coiled-coil domain-containing protein 1	-4.31	1.0000
461	Tesk2	Dual specificity testis-specific protein kinase 2	1.92	0.0123
462	ROCK2	Rho-associated protein kinase 2	-3.25	0.0123
463	Ankrd27	Ankyrin repeat domain-containing protein 27	-3.14	0.0123
464	#N/A	Antho-RFamide neuropeptides type 2	1.73	0.0124
465	Gvin1	Interferon-induced very large GTPase 1	-2.59	0.0124

466	pol	RNA-directed DNA polymerase from mobile element jockey	1.30	0.0125
467	Card14	Caspase recruitment domain-containing protein 14	-1.75	0.0125
468	IFFO1	Intermediate filament family orphan 1	-4.02	1.0000
469	pol	RNA-directed DNA polymerase from mobile element jockey	-1.88	0.0127
470	Cd40	Tumor necrosis factor receptor superfamily member 5	-2.63	0.0128
471	ZNF79	Zinc finger protein 79	-4.23	1.0000
472	GOLGA4	Golgin subfamily A member 4	-2.16	0.0130
473	Map4k4	Mitogen-activated protein kinase kinase kinase kinase 4	-4.84	1.0000
474	ddx42	ATP-dependent RNA helicase DDX42	-1.05	0.0131
475	KIF5B	Kinesin-1 heavy chain	-4.40	1.0000
476	TPD52	Tumor protein D52	-2.23	0.0132
477	marveld2	MARVEL domain-containing protein 2	-4.65	1.0000
478	gag-pol	Gag-Pol polyprotein	-4.23	1.0000
479	tc1a	Transposable element Tc1 transposase	3.23	0.0133
480	EXOC2	Exocyst complex component 2	-1.35	0.0135
481	Kcnj10	ATP-sensitive inward rectifier potassium channel 10	-4.47	1.0000
482	Mctp2	Multiple C2 and transmembrane domain-containing protein 2	1.74	0.0136
483	MYH10	Myosin-10	-2.92	0.0137
484	tc1a	Transposable element Tc1 transposase	2.61	0.0137
485	SIK2	Serine/threonine-protein kinase SIK2	-4.85	1.0000
486	Rnf213	E3 ubiquitin-protein ligase RNF213	-1.96	0.0139
487	DERA	Deoxyribose-phosphate aldolase	1.11	0.0139
488	#N/A	Transposable element Tcb2 transposase	-1.20	0.0139
489	pkn2	Serine/threonine-protein kinase N2	1.73	0.0139
490	C16orf89	UPF0764 protein C16orf89	8.00	0.0141
491	Kdm4a	Lysine-specific demethylase 4A	-4.50	1.0000
492	NUMBL	Numb-like protein	-1.65	0.0144
493	elavl1-a	ELAV-like protein 1-A	-2.25	0.0145
494	Khnyn	Protein KHNYN	-1.74	0.0145
495	Ptpn21	Tyrosine-protein phosphatase non-receptor type 21	1.58	0.0145
496	Nlrp12	NACHT, LRR and PYD domains-containing protein 12	-1.78	0.0145
497	Adgrg2	Adhesion G-protein coupled receptor G2	-1.73	0.0145
498	B3galt2	Beta-1,3-galactosyltransferase 2	-1.81	0.0148
499	ADSL	Adenylosuccinate lyase	-2.14	0.0148
500	RBM5	RNA-binding protein 5	-1.46	0.0148
501	Vps13a	Vacuolar protein sorting-associated protein 13A	-1.01	0.0149
502	MYH9	Myosin-9	-1.93	0.0149
503	atl2	Atlastin-2	-3.85	1.0000
504	Wipi1	WD repeat domain phosphoinositide-interacting protein 1	-1.61	0.0153
505	RNF216	E3 ubiquitin-protein ligase RNF216	-2.14	0.0156
506	mtbp	Mdm2-binding protein	-2.39	0.0156
507	NR1D2	Nuclear receptor subfamily 1 group D member 2	-1.34	0.0156
508	ANKRD27	Ankyrin repeat domain-containing protein 27	-2.30	0.0156
509	PARP12	Poly [ADP-ribose] polymerase 12	-2.24	0.0156
510	DLEC1	Deleted in lung and esophageal cancer protein 1	2.43	0.0158
511	NLRC3	Protein NLRC3	-1.58	0.0159
512	#N/A	Myosin heavy chain, embryonic smooth muscle isoform	-1.59	0.0159
513	Ngef	Ephexin-1	-1.46	0.0159
514	BIRC2	Baculoviral IAP repeat-containing protein 2	-1.41	0.0160
515	AMOT	Angiomotin	-1.33	0.0161
516	xpot	Exportin-T	-1.85	0.0161
517	KIF3B	Kinesin-like protein KIF3B	-1.51	0.0161
518	#N/A	Transposable element Tcb1 transposase	1.14	0.0162
519	#N/A	Transposable element Tcb1 transposase	-1.29	0.0162
520	#N/A	Stonustoxin subunit alpha	-2.77	0.0162
521	arid5b	AT-rich interactive domain-containing protein 5B	-4.38	1.0000
522	Tf2-6	Transposon Tf2-6 polyprotein	-1.68	0.0163
523	Parp14	Poly [ADP-ribose] polymerase 14	-1.33	0.0163
524	SLK	STE20-like serine/threonine-protein kinase	-1.68	0.0164
525	L1RE1	LINE-1 retrotransposable element ORF1 protein	4.51	0.0166
526	ERVK-5	Endogenous retrovirus group K member 5 Np9 protein	6.58	0.0170
527	Tf2-9	Transposon Tf2-9 polyprotein	1.93	0.0170
528	PKP3	Plakophilin-3	-1.65	0.0170
529	MYO9B	Unconventional myosin-IXb	-1.13	0.0170
530	CREB3L4	Cyclic AMP-responsive element-binding protein 3-like protein 4	-1.55	0.0170
531	gna11	Guanine nucleotide-binding protein subunit alpha-11	-1.50	0.0170

532	Hbs1l	HBS1-like protein	-3.76	1.0000
533	ITGA11	Integrin alpha-11	6.54	1.0000
534	cep170b	Centrosomal protein of 170 kDa protein B	-2.24	0.0171
535	arg2-a	Arginase, non-hepatic 1	-3.52	0.0172
536	DAAM1	Disheveled-associated activator of morphogenesis 1	-0.99	0.0173
537	RNF19A	E3 ubiquitin-protein ligase RNF19A	1.06	0.0175
538	SVIL	Supervillin	-2.43	0.0176
539	TPP2	Tripeptidyl-peptidase 2	-3.74	1.0000
540	Zdhhc18	Palmitoyltransferase ZDHHC18	-4.36	1.0000
541	Rbm4	RNA-binding protein 4	-2.39	0.0179
542	#N/A	Nuclear factor 7, ovary	-1.46	0.0180
543	ETS2	Protein C-ets-2	-1.40	0.0180
544	FAM200A	Protein FAM200A	-4.62	1.0000
545	Endov	Endonuclease V	2.54	0.0181
546	#N/A	Saxiphilin	-5.89	0.0181
547	plekha8	Pleckstrin homology domain-containing family A member 8	-1.19	0.0181
548	fen1	Flap endonuclease 1 {ECO:0000255|HAMAP-Rule:MF_03140}	-4.12	1.0000
549	Ptpn12	Tyrosine-protein phosphatase non-receptor type 12	-1.01	0.0183
550	VPS13A	Vacuolar protein sorting-associated protein 13A	-3.34	1.0000
551	PPA1	Inorganic pyrophosphatase	-1.12	0.0183
552	#N/A	Stonustoxin subunit beta	-1.21	0.0184
553	Rnf213	E3 ubiquitin-protein ligase RNF213	-1.81	0.0185
554	Rnf213	E3 ubiquitin-protein ligase RNF213	-1.58	0.0186
555	MINK1	Misshapen-like kinase 1	-1.64	0.0187
556	TSC22D3	TSC22 domain family protein 3	1.73	0.0187
557	ncoa2	Nuclear receptor coactivator 2	-1.92	0.0188
558	uhrf1bp1l	UHRF1-binding protein 1-like	-1.51	0.0189
559	TASOR	Protein TASOR {ECO:0000305}	-1.68	0.0189
560	Mybl1	Myb-related protein A	-2.78	0.0190
561	Ptgis	Prostacyclin synthase	-3.00	0.0191
562	tc1a	Transposable element Tc1 transposase	2.57	0.0191
563	TNKS	Tankyrase-1	-2.24	0.0191
564	Rnf213	E3 ubiquitin-protein ligase RNF213	-2.51	0.0191
565	PLEKHA5	Pleckstrin homology domain-containing family A member 5	-2.25	0.0193
566	MANF	Mesencephalic astrocyte-derived neurotrophic factor	-2.18	0.0193
567	#N/A	Transposable element Tcb1 transposase	-1.08	0.0193
568	#N/A	Sodium/potassium/calcium exchanger 6, mitochondrial	-1.14	0.0193
569	POU2F3	POU domain, class 2, transcription factor 3	-1.27	0.0194
570	sdha	Succinate dehydrogenase [ubiquinone] flavoprotein subunit, mitochondrial	3.85	0.0194
571	Cldn4	Claudin-4	2.44	0.0199
572	#N/A	RNA-directed RNA polymerase	-4.69	1.0000
573	Tnfrsf22	Tumor necrosis factor receptor superfamily member 22	-3.05	0.0200
574	Fbxo11	F-box only protein 11	-1.61	0.0200
575	tc1a	Transposable element Tc1 transposase	-1.55	0.0201
576	Ube2l3	Ubiquitin-conjugating enzyme E2 L3	-2.89	0.0201
577	n4bp1	NEDD4-binding protein 1	-2.66	0.0204
578	SLC25A22	Mitochondrial glutamate carrier 1	-2.36	0.0205
579	PARP14	Poly [ADP-ribose] polymerase 14	-1.26	0.0205
580	nos2	Nitric oxide synthase, inducible	-3.45	0.0205
581	Gvin1	Interferon-induced very large GTPase 1	-2.74	0.0206
582	#N/A	Uncharacterized 51.9 kDa protein in rps4-rps11 intergenic region	2.08	0.0206
583	Rabgap1	Rab GTPase-activating protein 1	-1.12	0.0207
584	ERVFC1	Endogenous retrovirus group FC1 Env polyprotein	-2.76	0.0207
585	Tsc22d3	TSC22 domain family protein 3	-2.08	0.0207
586	MYL6	Myosin light polypeptide 6	-4.09	1.0000
587	Phf6	PHD finger protein 6	-2.06	0.0207
588	ATP2A3	Sarcoplasmic/endoplasmic reticulum calcium ATPase 3	-4.60	1.0000
589	IFI44	Interferon-induced protein 44	-2.91	0.0208
590	SH2D7	SH2 domain-containing protein 7	-1.26	0.0209
591	Parp12	Poly [ADP-ribose] polymerase 12	-2.27	0.0209
592	Itih3	Inter-alpha-trypsin inhibitor heavy chain H3	4.77	1.0000
593	Cux1	Homeobox protein cut-like 1	-0.96	0.0210
594	tc1a	Transposable element Tc1 transposase	3.32	0.0211
595	tc1a	Transposable element Tc1 transposase	-1.28	0.0211
596	RTL1	Retrotransposon-like protein 1	1.74	0.0212
597	arih1	E3 ubiquitin-protein ligase arih1	-1.96	0.0212

598	tc1a	Transposable element Tc1 transposase	2.87	0.0214
599	ndh-2	NADH-ubiquinone oxidoreductase chain 2	4.62	0.0214
600	nfkb2	Nuclear factor NF-kappa-B p100 subunit	-1.43	0.0214
601	CACNA1E	Voltage-dependent R-type calcium channel subunit alpha-1E	-4.22	1.0000
602	FER	Tyrosine-protein kinase Fer	2.09	0.0215
603	Ikbkg	NF-kappa-B essential modulator	1.50	0.0216
604	Nop56	Nucleolar protein 56	-2.57	0.0217
605	Gvin1	Interferon-induced very large GTPase 1	-2.77	0.0217
606	Dsg4	Desmoglein-4	-1.87	0.0219
607	uck2a	Uridine-cytidine kinase 2-A	-2.11	0.0219
608	sbf2	Myotubularin-related protein 13	-1.40	0.0219
609	HIP1R	Huntingtin-interacting protein 1-related protein	-2.16	0.0221
610	strip1	Striatin-interacting protein 1 homolog	-1.74	0.0223
611	vps33b	Vacuolar protein sorting-associated protein 33B	1.10	0.0224
612	#N/A	UPF0271 protein PPA0282	6.83	1.0000
613	C4	Complement C4	4.72	0.0225
614	MCTP2	Multiple C2 and transmembrane domain-containing protein 2	-2.31	0.0225
615	PRKAR1A	cAMP-dependent protein kinase type I-alpha regulatory subunit	-1.56	0.0225
616	NEFH	Neurofilament heavy polypeptide	-3.66	0.0225
617	Ddx5	Probable ATP-dependent RNA helicase DDX5	-1.24	0.0225
618	vipr1	Vasoactive intestinal polypeptide receptor	-4.58	1.0000
619	DEPDC5	DEP domain-containing protein 5	-1.33	0.0226
620	BTN2A1	Butyrophilin subfamily 2 member A1	-1.13	0.0226
621	Tnik	Traf2 and NCK-interacting protein kinase	-2.74	0.0226
622	ugcg-a	Ceramide glucosyltransferase-A	-1.92	0.0226
623	gerIA	Spore germination protein GerIA	-2.50	0.0227
624	CLCN7	H(+)/Cl(-) exchange transporter 7	2.17	0.0228
625	Itsn1	Intersectin-1	-2.17	0.0229
626	Myo9b	Unconventional myosin-IXb	-1.04	0.0229
627	NLRP3	NACHT, LRR and PYD domains-containing protein 3	-1.97	0.0230
628	PIK3C2B	Phosphatidylinositol 4-phosphate 3-kinase C2 domain-containing subunit beta	-1.78	0.0230
629	PBRM1	Protein polybromo-1	-3.63	1.0000
630	BAD	Bcl2-associated agonist of cell death	-3.08	0.0231
631	ZNF174	Zinc finger protein 174	-4.29	1.0000
632	Zmym5	Zinc finger MYM-type protein 5	-2.48	0.0232
633	ncor1	Nuclear receptor corepressor 1	-1.34	0.0233
634	Sds	L-serine dehydratase/L-threonine deaminase	-4.49	1.0000
635	Nfkbia	NF-kappa-B inhibitor alpha	-1.69	0.0234
636	TLE3	Transducin-like enhancer protein 3	-4.27	1.0000
637	Mslnl	Mesothelin-like protein	-2.56	0.0235
638	Crebbp	CREB-binding protein	-2.22	0.0235
639	Kmt2c	Histone-lysine N-methyltransferase 2C	-1.18	0.0236
640	PSTPIP2	Proline-serine-threonine phosphatase-interacting protein 2	-2.00	0.0238
641	ELMSAN1	ELM2 and SANT domain-containing protein 1	-2.38	0.0240
642	#N/A	LINE-1 retrotransposable element ORF2 protein	6.31	1.0000
643	GTF3C1	General transcription factor 3C polypeptide 1	-1.79	0.0242
644	Fbxo44	F-box only protein 44	-3.51	0.0243
645	b9d1	B9 domain-containing protein 1	-3.92	1.0000
646	ALKBH1	DNA oxidative demethylase ALKBH1	-4.20	1.0000
647	#N/A	Protein FAM208B	-1.39	0.0244
648	SIK2	Serine/threonine-protein kinase SIK2	-2.08	0.0244
649	TBC1D22B	TBC1 domain family member 22B	-1.20	0.0245
650	ATP8A2	Phospholipid-transporting ATPase IB	-1.10	0.0245
651	CLEC16A	Protein CLEC16A {ECO:0000305}	1.62	0.0246
652	ppp1r3cb	Protein phosphatase 1 regulatory subunit 3C-B	-2.65	0.0248
653	VPS13A	Vacuolar protein sorting-associated protein 13A	-4.18	1.0000
654	NUP98	Nuclear pore complex protein Nup98-Nup96	-4.27	1.0000
655	OR1D5	Olfactory receptor 1D5	3.69	1.0000
656	rbm18	Probable RNA-binding protein 18	-2.22	0.0249
657	Sppl2a	Signal peptide peptidase-like 2A {ECO:0000250|UniProtKB:Q8TCT8}	1.97	0.0251
658	ZBED5	Zinc finger BED domain-containing protein 5	-3.05	0.0251
659	NMES1	Normal mucosa of esophagus-specific gene 1 protein	1.73	0.0251
660	#N/A	Actin, muscle	-2.24	0.0252
661	ZFC3H1	Zinc finger C3H1 domain-containing protein	-1.81	0.0252
662	Ap1g2	AP-1 complex subunit gamma-like 2	-4.12	1.0000

663	CYTH2	Cytohesin-2	-3.38	1.0000
664	Tf2-9	Transposon Tf2-9 polyprotein	-1.23	0.0254
665	#N/A	Protein LAP2	-1.15	0.0255
666	slc43a2	Large neutral amino acids transporter small subunit 4	-3.60	0.0255
667	#N/A	WASH complex subunit CCDC53	-4.27	1.0000
668	THA2	Probable low-specificity L-threonine aldolase 2	-4.02	1.0000
669	GTF2IRD2B	General transcription factor II-I repeat domain-containing protein 2B	-1.15	0.0258
670	PARP15	Poly [ADP-ribose] polymerase 15	-1.87	0.0258
671	GNAI3	Guanine nucleotide-binding protein G(k) subunit alpha	-3.29	0.0258
672	TMEM183A	Transmembrane protein 183A	-3.99	1.0000
673	CLIC3	Chloride intracellular channel protein 3	-1.12	0.0260
674	FRY	Protein furry homolog	-1.55	0.0263
675	RBM5	RNA-binding protein 5	-1.42	0.0264
676	RNF213	E3 ubiquitin-protein ligase RNF213	-1.93	0.0264
677	DAPK3	Death-associated protein kinase 3	-2.63	0.0264
678	#N/A	Vespryn	-4.19	1.0000
679	#N/A	Blastomere cadherin	-3.47	1.0000
680	Eif4enif1	Eukaryotic translation initiation factor 4E transporter	-2.55	0.0266
681	CYTH1	Cytohesin-1	-4.65	1.0000
682	KRT16	Keratin, type I cytoskeletal 16	-2.45	0.0267
683	BRPF1	Peregrin	-2.68	0.0267
684	Ptgis	Prostacyclin synthase	-1.86	0.0267
685	TNRC18	Trinucleotide repeat-containing gene 18 protein	-1.18	0.0269
686	PRELID3B	PRELI domain containing protein 3B	-2.82	0.0269
687	CCNG2	Cyclin-G2	-2.10	0.0269
688	PPIP5K1	Inositol hexakisphosphate and diphosphoinositol-pentakisphosphate kinase 1	-1.19	0.0271
689	ORF	Putative enzymatic polyprotein	3.45	0.0271
690	Wasf1	Wiskott-Aldrich syndrome protein family member 1	-3.54	1.0000
691	WNK1	Serine/threonine-protein kinase WNK1	-1.33	0.0271
692	Drg2	Developmentally-regulated GTP-binding protein 2	-2.78	0.0272
693	GMPR2	GMP reductase 2 {ECO:0000255|HAMAP-Rule:MF_03195}	-4.15	1.0000
694	RPS6KA5	Ribosomal protein S6 kinase alpha-5	-4.15	1.0000
695	Matk	Megakaryocyte-associated tyrosine-protein kinase	-3.64	0.0273
696	F5	Coagulation factor V	1.82	0.0276
697	ERCC8	DNA excision repair protein ERCC-8	1.82	0.0276
698	PLXNA1	Plexin-A1	-1.09	0.0278
699	FANCA	Fanconi anemia group A protein	-1.26	0.0278
700	hook2	Protein Hook homolog 2	-1.19	0.0281
701	invs	Inversin	-2.73	0.0281
702	ITPR3	Inositol 1,4,5-trisphosphate receptor type 3	-2.61	0.0283
703	aco-2	Probable aconitate hydratase, mitochondrial	-4.00	1.0000
704	Zswim6	Zinc finger SWIM domain-containing protein 6	-1.26	0.0285
705	UBA1	Ubiquitin-like modifier-activating enzyme 1	-2.80	0.0286
706	tyrp1	5,6-dihydroxyindole-2-carboxylic acid oxidase	-5.41	0.0286
707	Gss	Glutathione synthetase	-1.59	0.0287
708	Cacna1a	Voltage-dependent P/Q-type calcium channel subunit alpha-1A	-4.24	1.0000
709	IVL	Involucrin	1.85	0.0287
710	rilpl1	RILP-like protein 1	-3.66	1.0000
711	R3HDM2	R3H domain-containing protein 2	-4.27	1.0000
712	CTBP2	C-terminal-binding protein 2	-4.14	1.0000
713	PRDM1	PR domain zinc finger protein 1	-1.88	0.0291
714	Iigp1	Interferon-inducible GTPase 1	2.65	0.0291
715	Cd82	CD82 antigen	-2.10	0.0292
716	PLCD1	1-phosphatidylinositol 4,5-bisphosphate phosphodiesterase delta-1	2.25	0.0292
717	KLHL35	Kelch-like protein 35	-3.67	1.0000
718	#N/A	Transposable element Tcb1 transposase	-1.18	0.0294
719	THOC2	THO complex subunit 2	-1.20	0.0295
720	Setd5	SET domain-containing protein 5	-1.71	0.0295
721	CEPT1	Choline/ethanolaminephosphotransferase 1	-1.78	0.0296
722	Arid4b	AT-rich interactive domain-containing protein 4B	-1.91	0.0297
723	TY3B-G	Transposon Ty3-G Gag-Pol polyprotein	-1.56	0.0298
724	#N/A	Transmembrane protein 5	-3.90	1.0000
725	tmem186	Transmembrane protein 186	2.70	0.0300
726	GATAD2A	Transcriptional repressor p66-alpha	-3.99	1.0000
727	pol	Retrovirus-related Pol polyprotein from transposon 17.6	1.15	0.0300

728	#N/A	Transposable element Tcb1 transposase	-0.96	0.0302
729	esrp2	Epithelial splicing regulatory protein 2	-1.08	0.0302
730	Rora	Nuclear receptor ROR-alpha	-2.70	0.0302
731	MYB	Transcriptional activator Myb	-1.26	0.0302
732	ANAPC1	Anaphase-promoting complex subunit 1	-3.92	1.0000
733	CHD2	Chromodomain-helicase-DNA-binding protein 2	-1.45	0.0304
734	rab4b	Ras-related protein Rab-4B	-3.91	1.0000
735	ROCK1	Rho-associated protein kinase 1	-2.28	0.0305
736	tc1a	Transposable element Tc1 transposase	2.52	0.0306
737	PCOLCE	Procollagen C-endopeptidase enhancer 1	2.88	0.0306
738	Mbd2	Methyl-CpG-binding domain protein 2	-3.12	0.0306
739	Tle3	Transducin-like enhancer protein 3	-3.84	0.0309
740	VWA7	von Willebrand factor A domain-containing protein 7	-4.72	1.0000
741	gmnc	Geminin coiled-coil domain-containing protein 1	-3.98	1.0000
742	Cadps2	Calcium-dependent secretion activator 2	-0.97	0.0313
743	POLR3A	DNA-directed RNA polymerase III subunit RPC1	-1.99	0.0313
744	TYK2	Non-receptor tyrosine-protein kinase TYK2	-1.22	0.0314
745	Zfp27	Zinc finger protein 27	-1.75	0.0315
746	#N/A	Transposon TX1 uncharacterized 149 kDa protein	1.84	0.0316
747	CLIP1	CAP-Gly domain-containing linker protein 1	-2.17	0.0318
748	Osbpl6	Oxysterol-binding protein-related protein 6	-1.28	0.0318
749	KIF13B	Kinesin-like protein KIF13B	-0.93	0.0318
750	Tor1a	Torsin-1A	-3.27	1.0000
751	HLF	Hepatic leukemia factor	-2.76	0.0319
752	usp37	Ubiquitin carboxyl-terminal hydrolase 37	-3.91	1.0000
753	ERN1	Serine/threonine-protein kinase/endoribonuclease IRE1	-2.43	0.0319
754	JUN	Transcription factor AP-1	-1.74	0.0319
755	#N/A	Zinc finger protein ENSP00000375192	6.56	0.0320
756	Rapgefl1	Rap guanine nucleotide exchange factor-like 1	-1.20	0.0321
757	ARNT2	Aryl hydrocarbon receptor nuclear translocator 2	-1.38	0.0321
758	tc1a	Transposable element Tc1 transposase	-1.37	0.0322
759	Phf6	PHD finger protein 6	-2.64	1.0000
760	ERN1	Serine/threonine-protein kinase/endoribonuclease IRE1	-2.95	0.0322
761	RICTOR	Rapamycin-insensitive companion of mTOR	-3.14	1.0000
762	ANKRD44	Serine/threonine-protein phosphatase 6 regulatory ankyrin repeat subunit B	-4.02	1.0000
763	NAMPT	Nicotinamide phosphoribosyltransferase	-2.69	0.0324
764	TRIM8	Probable E3 ubiquitin-protein ligase TRIM8	1.04	0.0325
765	vcp	Transitional endoplasmic reticulum ATPase	-3.35	1.0000
766	EIF4G1	Eukaryotic translation initiation factor 4 gamma 1	-3.88	1.0000
767	Usp15	Ubiquitin carboxyl-terminal hydrolase 15	-1.63	0.0328
768	gorab	RAB6-interacting golgin	1.94	0.0329
769	#N/A	LINE-1 retrotransposable element ORF2 protein	7.32	0.0329
770	#N/A	Transposable element Tcb1 transposase	-0.97	0.0329
771	INPP5D	Phosphatidylinositol 3,4,5-trisphosphate 5-phosphatase 1	-3.66	0.0332
772	pol	Pol polyprotein	-4.43	1.0000
773	CTIF	CBP80/20-dependent translation initiation factor	-3.93	1.0000
774	PHLPP1	PH domain leucine-rich repeat-containing protein phosphatase 1	2.39	0.0336
775	CACNA1E	Voltage-dependent R-type calcium channel subunit alpha-1E	-4.12	1.0000
776	#N/A	LINE-1 retrotransposable element ORF2 protein	8.19	0.0337
777	Upf1	Regulator of nonsense transcripts 1	-2.00	0.0338
778	CHD6	Chromodomain-helicase-DNA-binding protein 6	-1.23	0.0338
779	CCP110	Centriolar coiled-coil protein of 110 kDa	-3.69	1.0000
780	FMNL1	Formin-like protein 1	-3.06	0.0341
781	Rnf213	E3 ubiquitin-protein ligase RNF213	-1.64	0.0341
782	#N/A	Arginase, hepatic	-2.72	0.0341
783	Adgre4	Adhesion G protein-coupled receptor E4	-4.34	1.0000
784	Chd7	Chromodomain-helicase-DNA-binding protein 7	-1.27	0.0342
785	SUDS3	Sin3 histone deacetylase corepressor complex component SDS3	-3.79	0.0343
786	FLII	Protein flightless-1 homolog	1.67	0.0344
787	STK17A	Serine/threonine-protein kinase 17A	-1.84	0.0344
788	#N/A	Transposable element Tcb1 transposase	-1.31	0.0345
789	NT5C2	Cytosolic purine 5'-nucleotidase	-2.16	0.0345
790	CCL3	C-C motif chemokine 3	2.01	0.0346
791	SLC1A4	Neutral amino acid transporter A	-1.95	0.0346
792	#N/A	PCTP-like protein	-1.53	0.0346
793	#N/A	Snake venom metalloprotease inhibitor 02D01	2.41	0.0347

794	myb	Transcriptional activator Myb	-3.36	0.0348
795	Slc25a3	Phosphate carrier protein, mitochondrial	1.62	0.0348
796	Ints4	Integrator complex subunit 4	-2.35	0.0350
797	nlrc5	Protein NLRC5	-1.90	0.0350
798	#N/A	LINE-1 retrotransposable element ORF2 protein	7.10	0.0351
799	Ankrd27	Ankyrin repeat domain-containing protein 27	-1.82	0.0351
800	Pabpc1	Polyadenylate-binding protein 1	-3.90	1.0000
801	Kmt2c	Histone-lysine N-methyltransferase 2C	-1.40	0.0352
802	Sacs	Sacsin	-4.20	1.0000
803	STAT4	Signal transducer and activator of transcription 4	-2.26	0.0352
804	supt6h	Transcription elongation factor SPT6	-2.18	0.0353
805	IP6K1	Inositol hexakisphosphate kinase 1	1.00	0.0356
806	tc1a	Transposable element Tc1 transposase	-1.17	0.0356
807	mef2d	Myocyte-specific enhancer factor 2D homolog	-1.34	0.0357
808	MXD4	Max dimerization protein 4	-1.01	0.0357
809	Golga4	Golgin subfamily A member 4	-1.56	0.0357
810	R3HDM1	R3H domain-containing protein 1	1.45	0.0358
811	foxc1a	Forkhead box C1-A	-1.97	0.0358
812	Eif4g3	Eukaryotic translation initiation factor 4 gamma 3	-3.09	1.0000
813	ASAP2	Arf-GAP with SH3 domain, ANK repeat and PH domain-containing protein 2	-2.37	0.0360
814	inpp5f	Phosphatidylinositide phosphatase SAC2	-1.40	0.0360
815	jhdm1db	Lysine-specific demethylase 7B	-1.27	0.0360
816	RCBTB1	RCC1 and BTB domain-containing protein 1	-1.63	0.0360
817	ZNF518A	Zinc finger protein 518A	-4.17	1.0000
818	UGGT1	UDP-glucose:glycoprotein glucosyltransferase 1	-1.05	0.0361
819	pol	Retrovirus-related Pol polyprotein from transposon 297	-1.70	0.0363
820	krt18	Keratin, type I cytoskeletal 18	-2.19	0.0363
821	NLRC3	Protein NLRC3	-8.51	0.0364
822	Dnmt3a	DNA (cytosine-5)-methyltransferase 3A	-3.05	1.0000
823	Rnf213	E3 ubiquitin-protein ligase RNF213	-1.28	0.0365
824	SUCO	SUN domain-containing ossification factor	-1.94	0.0365
825	MCTP2	Multiple C2 and transmembrane domain-containing protein 2	-3.41	1.0000
826	Afdn	Afadin	-0.95	0.0368
827	METTL22	Methyltransferase-like protein 22	-2.03	0.0369
828	Dock8	Dedicator of cytokinesis protein 8	-4.03	1.0000
829	ext1b	Exostosin-1b	-1.54	0.0369
830	Endod1	Endonuclease domain-containing 1 protein	-3.12	0.0370
831	TY3B-I	Transposon Ty3-I Gag-Pol polyprotein	-4.13	1.0000
832	AGO4	Protein argonaute-4 {ECO:0000255|HAMAP-Rule:MF_03033}	-1.15	0.0372
833	GRK5	G protein-coupled receptor kinase 5	-1.33	0.0373
834	FUBP3	Far upstream element-binding protein 3	-1.20	0.0375
835	TNRC18	Trinucleotide repeat-containing gene 18 protein	-1.34	0.0375
836	RB1CC1	RB1-inducible coiled-coil protein 1	-3.23	1.0000
837	ucp2	Mitochondrial uncoupling protein 2	-1.43	0.0375
838	TRIM14	Tripartite motif-containing protein 14	-3.07	0.0375
839	Nlrc3	Protein NLRC3	-1.58	0.0376
840	Ythdc1	YTH domain-containing protein 1	1.79	0.0376
841	MYO9B	Unconventional myosin-IXb	-1.45	0.0377
842	Rad54l2	Helicase ARIP4	-4.01	1.0000
843	HDAC7	Histone deacetylase 7	-3.94	1.0000
844	EIF4G3	Eukaryotic translation initiation factor 4 gamma 3	-1.28	0.0382
845	cep131	Centrosomal protein of 131 kDa	3.29	0.0382
846	ucp2	Mitochondrial uncoupling protein 2	-4.47	1.0000
847	MORC2	MORC family CW-type zinc finger protein 2	-1.36	0.0384
848	ASAP3	Arf-GAP with SH3 domain, ANK repeat and PH domain-containing protein 3	-0.84	0.0384
849	BIN2	Bridging integrator 2	-2.02	0.0387
850	MCTP2	Multiple C2 and transmembrane domain-containing protein 2	-1.14	0.0388
851	Plekha6	Pleckstrin homology domain-containing family A member 6	-1.77	0.0389
852	ZNF726	Zinc finger protein 726	-1.53	0.0389
853	GRHL1	Grainyhead-like protein 1 homolog	-1.30	0.0390
854	Mep1b	Meprin A subunit beta	-2.86	0.0390
855	Dab2ip	Disabled homolog 2-interacting protein	-1.24	0.0391
856	Rufy2	RUN and FYVE domain-containing protein 2	-3.06	1.0000
857	PARP14	Poly [ADP-ribose] polymerase 14	-2.00	0.0392

858	CAMK2D	Calcium/calmodulin-dependent protein kinase type II delta chain	1.78	0.0393
859	pol	Retrovirus-related Pol polyprotein from transposon opus	-4.36	1.0000
860	Syt14	Synaptotagmin-14	-3.44	1.0000
861	Gjb3	Gap junction beta-3 protein	-3.04	0.0393
862	Plec	Plectin	-2.17	0.0393
863	CERK	Ceramide kinase	-2.28	0.0394
864	Chd6	Chromodomain-helicase-DNA-binding protein 6	-1.30	0.0394
865	C2orf16	Uncharacterized protein C2orf16	2.81	0.0394
866	FOS	Proto-oncogene c-Fos	-4.30	1.0000
867	Brd2	Bromodomain-containing protein 2	-1.20	0.0395
868	KIAA0355	Uncharacterized protein KIAA0355	-2.13	0.0396
869	#N/A	Transposable element Tcb1 transposase	-3.18	1.0000
870	#N/A	Glycerol-3-phosphate transporter	-1.62	0.0396
871	CHD2	Chromodomain-helicase-DNA-binding protein 2	-0.99	0.0397
872	RFX7	DNA-binding protein RFX7	-2.30	0.0397
873	DGKD	Diacylglycerol kinase delta	2.57	0.0398
874	F5	Coagulation factor V	2.25	0.0398
875	Nrdc	Nardilysin	3.62	1.0000
876	PRRC2C	Protein PRRC2C	-3.12	1.0000
877	Osbpl6	Oxysterol-binding protein-related protein 6	-1.14	0.0399
878	Usp9x	Probable ubiquitin carboxyl-terminal hydrolase FAF-X	-2.09	0.0399
879	Fosl1	Fos-related antigen 1	-3.84	0.0399
880	mvp	Major vault protein	-2.16	0.0400
881	cpped1	Serine/threonine-protein phosphatase CPPED1	-3.83	1.0000
882	NLRC3	Protein NLRC3	-2.06	0.0400
883	CHD9	Chromodomain-helicase-DNA-binding protein 9	-1.01	0.0400
884	KANK1	KN motif and ankyrin repeat domain-containing protein 1	-3.60	0.0401
885	ELL2	RNA polymerase II elongation factor ELL2	-1.63	0.0401
886	CHN2	Beta-chimaerin	-1.29	0.0401
887	ENDOD1	Endonuclease domain-containing 1 protein	-5.65	0.0402
888	ARG2	Arginase-2, mitochondrial	-3.57	0.0402
889	Col28a1	Collagen alpha-1(XXVIII) chain	-3.90	1.0000
890	#N/A	78 kDa glucose-regulated protein	-1.68	0.0404
891	mxi1	Max-interacting protein 1	2.12	0.0405
892	KRTAP4-3	Keratin-associated protein 4-3	2.14	0.0406
893	Sec31b	Protein transport protein Sec31B	1.72	0.0406
894	#N/A	Transposable element Tcb1 transposase	-1.39	0.0406
895	smarcb1a	SWI/SNF-related matrix-associated actin-dependent regulator of chromatin subfamily B member 1-A	-2.08	0.0408
896	TFRC	Transferrin receptor protein 1	-2.45	0.0409
897	Gramd4	GRAM domain-containing protein 4	-2.42	0.0410
898	vmp1	Vacuole membrane protein 1	-4.98	1.0000
899	Evpl	Envoplakin	-2.16	0.0410
900	PROKR2	Prokineticin receptor 2	-3.89	1.0000
901	#N/A	Transposable element Tcb1 transposase	-1.00	0.0414
902	CPT1A	Carnitine O-palmitoyltransferase 1, liver isoform	-3.80	1.0000
903	Eif4g3	Eukaryotic translation initiation factor 4 gamma 3	-1.62	0.0415
904	Fbxo11	F-box only protein 11	-1.13	0.0416
905	pol	RNA-directed DNA polymerase from mobile element jockey	-3.98	1.0000
906	ZNF235	Zinc finger protein 235	-2.42	0.0417
907	BAZ2B	Bromodomain adjacent to zinc finger domain protein 2B	-1.41	0.0417
908	AUTS2	Autism susceptibility gene 2 protein	-1.79	0.0418
909	Tf2-8	Transposon Tf2-8 polyprotein	-1.17	0.0419
910	#N/A	LINE-1 retrotransposable element ORF2 protein	9.72	0.0419
911	ATP8B4	Probable phospholipid-transporting ATPase IM	-3.71	1.0000
912	tc3a	Transposable element Tc3 transposase	-1.84	0.0420
913	PNP	Purine nucleoside phosphorylase	-2.84	0.0420
914	foxp1b	Forkhead box protein P1-B	-1.66	0.0420
915	ARHGEF12	Rho guanine nucleotide exchange factor 12	-1.54	0.0420
916	mfsd5	Molybdate-anion transporter	2.59	0.0421
917	TRAPPC12	Trafficking protein particle complex subunit 12	-0.97	0.0422
918	Rab7a	Ras-related protein Rab-7a	-2.26	0.0422
919	paqr5b	Membrane progestin receptor gamma-B	-1.52	0.0422
920	CDA	Cytidine deaminase	2.52	0.0422
921	TJP2	Tight junction protein ZO-2	-1.01	0.0422
922	Lpar6	Lysophosphatidic acid receptor 6	-1.42	0.0422

923	eef1d	Elongation factor 1-delta	-1.93	0.0422
924	At5g39570	Uncharacterized protein At5g39570	2.21	0.0422
925	smc5	Structural maintenance of chromosomes protein 5	-1.30	0.0422
926	Bcor	BCL-6 corepressor	1.57	0.0423
927	chmp4c	Charged multivesicular body protein 4c	-1.49	0.0424
928	STAT4	Signal transducer and activator of transcription 4	-1.53	0.0424
929	#N/A	Transposable element Tcb1 transposase	-0.74	0.0425
930	PTPRO	Receptor-type tyrosine-protein phosphatase O	-4.25	1.0000
931	Lpcat4	Lysophospholipid acyltransferase LPCAT4	-1.89	0.0427
932	RTase	Probable RNA-directed DNA polymerase from transposon BS	1.45	0.0427
933	gse1	Genetic suppressor element 1	1.76	0.0428
934	GXYLT1	Glucoside xylosyltransferase 1	-1.87	0.0434
935	RNF213	E3 ubiquitin-protein ligase RNF213	-1.49	0.0436
936	PITPNM2	Membrane-associated phosphatidylinositol transfer protein 2	-1.13	0.0436
937	ATP11A	Probable phospholipid-transporting ATPase IH	-0.97	0.0436
938	Cd2ap	CD2-associated protein	-1.76	0.0437
939	Acsl4	Long-chain-fatty-acid--CoA ligase 4	-3.78	1.0000
940	PTK2B	Protein-tyrosine kinase 2-beta	-1.30	0.0439
941	Acaca	Acetyl-CoA carboxylase 1	-1.14	0.0439
942	U2SURP	U2 snRNP-associated SURP motif-containing protein	-1.03	0.0440
943	Pgap1	GPI inositol-deacylase	-1.02	0.0441
944	PARP12	Poly [ADP-ribose] polymerase 12	-2.51	0.0441
945	TJP3	Tight junction protein ZO-3	-1.55	0.0442
946	prpf39	Pre-mRNA-processing factor 39	-1.61	0.0446
947	tc1a	Transposable element Tc1 transposase	-0.90	0.0446
948	grhl3	Grainyhead-like protein 3 homolog	-1.11	0.0447
949	HELZ2	Helicase with zinc finger domain 2	-2.22	0.0448
950	STAT1	Signal transducer and activator of transcription 1	-1.30	0.0448
951	PARP14	Poly [ADP-ribose] polymerase 14	-0.96	0.0448
952	#N/A	cTAGE family member 5	-1.21	0.0448
953	ZNF79	Zinc finger protein 79	-3.05	1.0000
954	Gtf2f2	General transcription factor IIF subunit 2	-1.73	0.0449
955	plekha7	Pleckstrin homology domain-containing family A member 7	-2.33	0.0450
956	TMCC3	Transmembrane and coiled-coil domains protein 3	-1.84	0.0451
957	#N/A	cTAGE family member 5	-1.96	0.0452
958	Amot	Angiomotin	-1.15	0.0453
959	GIMAP4	GTPase IMAP family member 4	-5.36	0.0453
960	VPS13A	Vacuolar protein sorting-associated protein 13A	-3.05	1.0000
961	ANXA11	Annexin A11	-0.98	0.0455
962	Dnase1l3	Deoxyribonuclease gamma	-2.76	0.0458
963	WDR41	WD repeat-containing protein 41	-2.12	0.0462
964	FRYL	Protein furry homolog-like	-3.00	0.0462
965	NLRP12	NACHT, LRR and PYD domains-containing protein 12	-1.36	0.0462
966	GFPT1	Glutamine--fructose-6-phosphate aminotransferase [isomerizing] 1	-1.07	0.0462
967	Pde9a	High affinity cGMP-specific 3',5'-cyclic phosphodiesterase 9A	-2.27	0.0463
968	Morc2a	MORC family CW-type zinc finger protein 2A	-1.19	0.0463
969	v1g172254	L-2-hydroxyglutarate dehydrogenase, mitochondrial	-3.76	1.0000
970	Liat1	Protein LIAT1 {ECO:0000305|PubMed:25369936}	-3.77	1.0000
971	SMCR8	Smith-Magenis syndrome chromosomal region candidate gene 8 protein	-1.89	0.0466
972	Prkaa2	5'-AMP-activated protein kinase catalytic subunit alpha-2	-2.84	0.0467
973	ACSL3	Long-chain-fatty-acid--CoA ligase 3	-2.12	0.0468
974	INPP4B	Type II inositol 3,4-bisphosphate 4-phosphatase	-1.31	0.0468
975	Hid1	Protein HID1	-4.36	1.0000
976	Abcc3	Canalicular multispecific organic anion transporter 2	-1.93	0.0469
977	ADAM28	Disintegrin and metalloproteinase domain-containing protein 28	-2.46	0.0469
978	ITM2B	Integral membrane protein 2B	1.10	0.0469
979	FKBP5	Peptidyl-prolyl cis-trans isomerase FKBP5	-3.16	0.0471
980	Ugt8	2-hydroxyacylsphingosine 1-beta-galactosyltransferase	-4.23	1.0000
981	KDM5C	Lysine-specific demethylase 5C	-2.94	0.0474
982	Fbxw7	F-box/WD repeat-containing protein 7	-1.98	0.0475
983	PARP14	Poly [ADP-ribose] polymerase 14	-1.52	0.0475
984	NLRC3	Protein NLRC3	-2.28	0.0475
985	AP3S2	AP-3 complex subunit sigma-2	1.97	0.0476
986	jak1	Tyrosine-protein kinase JAK1	-0.84	0.0477
987	GBP1	Guanylate-binding protein 1	-0.71	0.0479
988	RAB44	Ras-related protein Rab-44	-2.32	0.0480

989	#N/A	Transposable element Tcb2 transposase	2.52	0.0480
990	Smarcad1	SWI/SNF-related matrix-associated actin-dependent regulator of chromatin subfamily A containing DEAD/H box 1	-3.89	1.0000
991	WDR43	WD repeat-containing protein 43	-3.14	0.0480
992	crtac1	Cartilage acidic protein 1	1.97	0.0480
993	#N/A	Transmembrane protein 56	-2.82	1.0000
994	HI_0712	Probable hemoglobin and hemoglobin-haptoglobin-binding protein 3	3.11	0.0481
995	25	Probable ATP-dependent helicase 25	-2.37	0.0482
996	Sqstm1	Sequestosome-1	-1.64	0.0482
997	gna11	Guanine nucleotide-binding protein subunit alpha-11	-3.81	1.0000
998	HIF1A	Hypoxia-inducible factor 1-alpha	-1.97	0.0482
999	Dnm2	Dynamin-2	-0.91	0.0484
1000	RNF14	E3 ubiquitin-protein ligase RNF14	1.24	0.0484
1001	OGFR	Opioid growth factor receptor	-2.40	1.0000
1002	Polr1e	DNA-directed RNA polymerase I subunit RPA49	-3.51	1.0000
1003	#N/A	von Willebrand factor A domain-containing protein 9	-3.11	1.0000
1004	EPRS	Bifunctional glutamate/proline--tRNA ligase	-1.75	0.0492
1005	Tnik	Traf2 and NCK-interacting protein kinase	-1.21	0.0492
1006	#N/A	LINE-1 retrotransposable element ORF2 protein	7.65	0.0492
1007	noc4l	Nucleolar complex protein 4 homolog	-4.02	1.0000
1008	Ier5	Immediate early response gene 5 protein	-1.70	0.0494
1009	pssA	CDP-diacylglycerol--serine O-phosphatidyltransferase	-2.40	0.0495
1010	FAM83B	Protein FAM83B	-1.44	0.0495
1011	SSH1	Protein phosphatase Slingshot homolog 1	-1.92	0.0497
1012	DUSP6	Dual specificity protein phosphatase 6	-2.26	0.0500

Lake 260 vs Lake 373

373 is the base e.g. Positive FC = upregulated in Lake 260 relative to Lake 373

1	PLA2G4C	Cytosolic phospholipase A2 gamma	7.81	3.70E-23
2	Vwa7	von Willebrand factor A domain-containing protein 7	5.93	2.71E-19
3	PLA2G4C	Cytosolic phospholipase A2 gamma	2.53	3.34E-16
4	PRB3	Basic salivary proline-rich protein 3	10.55	8.79E-13
5	DNAAF5	Dynein assembly factor 5, axonemal	4.20	1.81E-12
6	#N/A	Transposon TX1 uncharacterized 149 kDa protein	3.76	4.50E-12
7	Mr1	Major histocompatibility complex class I-related gene protein	-3.96	6.92E-11
8	Pol	LINE-1 retrotransposable element ORF2 protein	4.68	1.01E-10
9	#N/A	Transposon TX1 uncharacterized 149 kDa protein	4.51	1.49E-10
10	Gvin1	Interferon-induced very large GTPase 1	-3.40	1.65E-10
11	Vwa7	von Willebrand factor A domain-containing protein 7	5.11	2.10E-10
12	DLEC1	Deleted in lung and esophageal cancer protein 1	4.08	2.45E-10
13	#N/A	LINE-1 retrotransposable element ORF2 protein	24.59	2.61E-10
14	C1ql4	Complement C1q-like protein 4	9.31	3.79E-10
15	Iigp1	Interferon-inducible GTPase 1	8.34	4.19E-10
16	#N/A	Class I histocompatibility antigen, F10 alpha chain	9.58	2.16E-09
17	CARD8	Caspase recruitment domain-containing protein 8	3.37	3.04E-09
18	#N/A	Transposon TX1 uncharacterized 149 kDa protein	5.59	1.06E-08
19	rnasel3	Ribonuclease-like 3 {ECO:0000303|PubMed:16861230}	8.05	1.41E-08
20	RNF213	E3 ubiquitin-protein ligase RNF213	8.21	1.42E-08
21	SAMD9L	Sterile alpha motif domain-containing protein 9-like	-2.92	9.19E-08
22	#N/A	Transposable element Tcb1 transposase	5.60	9.61E-08
23	ENDOD1	Endonuclease domain-containing 1 protein	-7.95	1.38E-07
24	ABCB1	Multidrug resistance protein 1	4.83	1.71E-07
25	slc22a6	Solute carrier family 22 member 6	-7.01	2.72E-07
26	FARP1	FERM, RhoGEF and pleckstrin domain-containing protein 1	2.74	2.82E-07
27	#N/A	Transposon TX1 uncharacterized 149 kDa protein	5.68	3.12E-07
28	ORF39	Uncharacterized protein ORF39	5.89	3.38E-07
29	MPZL2	Myelin protein zero-like protein 2	3.85	3.67E-07
30	USP43	Ubiquitin carboxyl-terminal hydrolase 43	8.01	5.24E-07
31	#N/A	Class I histocompatibility antigen, F10 alpha chain	-7.46	7.57E-07
32	URGCP	Up-regulator of cell proliferation	-5.68	8.79E-07
33	ERVFC1	Endogenous retrovirus group FC1 Env polyprotein	-5.68	1.02E-06
34	GIMAP8	GTPase IMAP family member 8	3.40	1.06E-06
35	GIMAP2	GTPase IMAP family member 2	5.39	1.28E-06

36	IFI44	Interferon-induced protein 44	-4.18	1.34E-06
37	TGL2	Protein-glutamine gamma-glutamyltransferase 2	-2.95	1.67E-06
38	ENPP	Enterin neuropeptides	3.24	1.93E-06
39	Fam111a	Protein FAM111A	4.71	1.98E-06
40	aste1	Protein asteroid homolog 1	-3.38	2.49E-06
41	#N/A	Transposon TX1 uncharacterized 149 kDa protein	3.00	2.85E-06
42	#N/A	Transposon TX1 uncharacterized 149 kDa protein	2.99	2.96E-06
43	Mr1	Major histocompatibility complex class I-related gene protein	-6.34	4.86E-06
44	pol	Pol polyprotein	-2.80	5.85E-06
45	SLC22A6	Solute carrier family 22 member 6	-6.49	5.92E-06
46	#N/A	Poly(A) polymerase type 3	2.66	7.46E-06
47	TY3B-G	Transposon Ty3-G Gag-Pol polyprotein	8.26	7.86E-06
48	tchp	Trichoplein keratin filament-binding protein	7.29	7.90E-06
49	SAMD9	Sterile alpha motif domain-containing protein 9	-6.73	8.99E-06
50	ZFAND5	AN1-type zinc finger protein 5	-4.91	1.03E-05
51	RNF213	E3 ubiquitin-protein ligase RNF213	7.53	1.17E-05
52	Dlec1	Deleted in lung and esophageal cancer protein 1 homolog	3.02	1.46E-05
53	plekha8	Pleckstrin homology domain-containing family A member 8	-2.30	1.66E-05
54	#N/A	LINE-1 retrotransposable element ORF2 protein	7.05	1.88E-05
55	LINC00269	Putative uncharacterized protein encoded by LINC00269	6.50	2.05E-05
56	NLRC3	Protein NLRC3	-6.14	2.35E-05
57	AHCYL2	Putative adenosylhomocysteinase 3	-6.34	2.62E-05
58	Gvin1	Interferon-induced very large GTPase 1	-4.56	2.76E-05
59	#N/A	Antho-RFamide neuropeptides type 2	3.52	3.59E-05
60	mxi1	Max-interacting protein 1	3.50	4.34E-05
61	AHCYL2	Putative adenosylhomocysteinase 3	-6.15	4.75E-05
62	GVQW1	Protein GVQW1	7.99	4.98E-05
63	PCOLCE	Procollagen C-endopeptidase enhancer 1	6.97	5.34E-05
64	PRDM1	PR domain zinc finger protein 1	-3.42	6.37E-05
65	RALGAPA1	Ral GTPase-activating protein subunit alpha-1	-6.02	6.41E-05
66	AHCYL2	Adenosylhomocysteinase 3	-6.17	6.42E-05
67	#N/A	Transposon TX1 uncharacterized 149 kDa protein	3.73	6.42E-05
68	samhd1	Deoxynucleoside triphosphate triphosphohydrolase SAMHD1	2.42	6.48E-05
69	URGCP	Up-regulator of cell proliferation	-5.11	6.90E-05
70	KRT19	Keratin, type I cytoskeletal 19	-3.05	6.95E-05
71	exsA	Spore coat assembly protein ExsA	3.74	7.39E-05
72	SLA1	Actin cytoskeleton-regulatory complex protein SLA1	2.31	7.72E-05
73	cep131	Centrosomal protein of 131 kDa	7.02	8.00E-05
74	#N/A	Transposon TX1 uncharacterized 149 kDa protein	5.26	8.00E-05
75	Pwp2	Periodic tryptophan protein 2 homolog	3.42	8.71E-05
76	midn	Midnolin	-3.94	8.78E-05
77	pol	Retrovirus-related Pol polyprotein from transposon gypsy	-5.40	8.78E-05
78	Tf2-9	Transposon Tf2-9 polyprotein	2.67	8.85E-05
79	Ptgis	Prostacyclin synthase	-4.30	9.04E-05
80	#N/A	Class I histocompatibility antigen, F10 alpha chain	-6.06	9.46E-05
81	GBP2	Guanylate-binding protein 2	7.14	0.0001
82	Mslnl	Mesothelin-like protein	-5.24	0.0001
83	Samd9l	Sterile alpha motif domain-containing protein 9-like	-6.17	0.0001
84	SOCS3	Suppressor of cytokine signaling 3	-3.47	0.0001
85	Nlrc3	Protein NLRC3	-5.71	0.0001
86	Urgcp	Up-regulator of cell proliferation	-4.22	0.0002
87	uck1	Uridine-cytidine kinase 1	3.98	0.0002
88	Gpr108	Protein GPR108	2.35	0.0002
89	V-ERBB	Tyrosine-protein kinase transforming protein erbB	-2.37	0.0002
90	sibA	Integrin beta-like protein A	-6.26	0.0002
91	FN1	Fibronectin	8.18	0.0002
92	MCTP2	Multiple C2 and transmembrane domain-containing protein 2	-2.43	0.0002
93	eif3i	Eukaryotic translation initiation factor 3 subunit I	2.55	0.0002
94	Plekhg5	Pleckstrin homology domain-containing family G member 5	-3.00	0.0002
95	#N/A	LINE-1 retrotransposable element ORF2 protein	6.69	0.0002
96	Ptgis	Prostacyclin synthase	-3.76	0.0002
97	NBPF12	Neuroblastoma breakpoint family member 12	3.72	0.0002
98	URGCP	Up-regulator of cell proliferation	-6.66	0.0002
99	Ythdc1	YTH domain-containing protein 1	3.01	0.0002
100	pol	Retrovirus-related Pol polyprotein from transposon opus	-5.23	0.0002
101	#N/A	Ladderlectin	-7.12	0.0002

102	V-ERBB	Tyrosine-protein kinase transforming protein erbB	-2.21	0.0002
103	BTN1A1	Butyrophilin subfamily 1 member A1	-4.34	0.0003
104	#N/A	Transposable element Tcb1 transposase	2.84	0.0003
105	TIGD1	Tigger transposable element-derived protein 1	7.57	0.0003
106	S100a1	Protein S100-A1	-2.90	0.0003
107	Glod4	Glyoxalase domain-containing protein 4	3.84	0.0003
108	L1RE1	LINE-1 retrotransposable element ORF1 protein	6.33	0.0003
109	Chrna2	Neuronal acetylcholine receptor subunit alpha-2	3.62	0.0003
110	midn	Midnolin	-3.73	0.0003
111	Ikbip	Inhibitor of nuclear factor kappa-B kinase-interacting protein	5.69	0.0003
112	pol	Retrovirus-related Pol polyprotein from transposon 17.6	7.31	0.0003
113	PFA0170c	Putative zinc carboxypeptidase PFA0170c	2.52	0.0003
114	F5	Coagulation factor V	3.95	0.0003
115	#N/A	Transposable element Tcb2 transposase	3.57	0.0003
116	DLEC1	Deleted in lung and esophageal cancer protein 1	2.54	0.0003
117	EEF2	Elongation factor 2	2.33	0.0003
118	rpsC	30S ribosomal protein S3 {ECO:0000255|HAMAP-Rule:MF_01309}	7.16	0.0004
119	MUC22	Mucin-22	1.98	0.0004
120	krt13	Keratin, type I cytoskeletal 13	-2.41	0.0004
121	HLF	Hepatic leukemia factor	-4.36	0.0004
122	PFE0100w	RING finger protein PFE0100w	3.65	0.0004
123	URGCP	Up-regulator of cell proliferation	-2.15	0.0004
124	DEPTOR	DEP domain-containing mTOR-interacting protein	-2.92	0.0004
125	Pol	LINE-1 retrotransposable element ORF2 protein	2.23	0.0005
126	At5g39570	Uncharacterized protein At5g39570	3.68	0.0005
127	Tsc22d3	TSC22 domain family protein 3	-2.69	0.0005
128	ADAP1	Arf-GAP with dual PH domain-containing protein 1	2.38	0.0005
129	NLRP3	NACHT, LRR and PYD domains-containing protein 3	-3.01	0.0005
130	SUPT20H	Transcription factor SPT20 homolog	2.89	0.0005
131	#N/A	Transposon TX1 uncharacterized 149 kDa protein	2.89	0.0005
132	Traf7	E3 ubiquitin-protein ligase TRAF7	-4.56	0.0005
133	Ddx5	Probable ATP-dependent RNA helicase DDX5	-2.27	0.0006
134	PLAU	Urokinase-type plasminogen activator	-4.27	0.0006
135	COL14A1	Collagen alpha-1(XIV) chain	-4.60	0.0006
136	FGD4	FYVE, RhoGEF and PH domain-containing protein 4	2.73	0.0007
137	Itih4	Inter alpha-trypsin inhibitor, heavy chain 4	5.45	0.0007
138	PARP12	Poly [ADP-ribose] polymerase 12	-2.78	0.0007
139	#N/A	Transposable element Tcb2 transposase	-2.42	0.0007
140	myd88	Myeloid differentiation primary response protein MyD88	2.77	0.0007
141	Ndrg3	Protein NDRG3	-2.40	0.0007
142	DUSP5	Dual specificity protein phosphatase 5	-4.82	0.0007
143	Btnl2	Butyrophilin-like protein 2	-5.56	0.0007
144	grhl3	Grainyhead-like protein 3 homolog	-2.17	0.0007
145	Csrnp2	Cysteine/serine-rich nuclear protein 2	-4.56	0.0008
146	#N/A	Saxiphilin	-5.76	0.0008
147	CCL3	C-C motif chemokine 3	3.37	0.0008
148	ANXA11	Annexin A11	-2.03	0.0008
149	AQP3	Aquaporin-3	-5.04	0.0008
150	Moe	Moesin/ezrin/radixin homolog 1 {ECO:0000250|UniProtKB:P46150}	-1.99	0.0009
151	naa60	N-alpha-acetyltransferase 60	3.00	0.0009
152	Evpl	Envoplakin	-2.84	0.0009
153	Tmprss4	Transmembrane protease serine 4	-1.99	0.0009
154	Ikbkg	NF-kappa-B essential modulator	2.31	0.0009
155	Gvin1	Interferon-induced very large GTPase 1	7.00	0.0010
156	Setd2	Histone-lysine N-methyltransferase SETD2	3.81	0.0010
157	#N/A	Stonustoxin subunit beta	-5.38	0.0010
158	Ywhaz	14-3-3 protein zeta/delta	-2.33	0.0010
159	FOSL2	Fos-related antigen 2	-5.48	0.0010
160	PNP	Purine nucleoside phosphorylase	-4.35	0.0010
161	Cfh	Complement factor H	-5.32	0.0010
162	#N/A	Melanoma-associated antigen G1	-2.52	0.0011
163	PGBD3	PiggyBac transposable element-derived protein 3	-2.00	0.0011
164	GVINP1	Interferon-induced very large GTPase 1	-6.33	0.0011
165	RGL1	Ral guanine nucleotide dissociation stimulator-like 1	-5.02	0.0012
166	IP6K1	Inositol hexakisphosphate kinase 1	1.61	0.0012
167	STAT1	Signal transducer and activator of transcription 1	-2.49	0.0013

168	YME1L1	ATP-dependent zinc metalloprotease YME1L1	-5.28	0.0013
169	ABCF2	ATP-binding cassette sub-family F member 2	-2.11	0.0013
170	#N/A	Salivary plasminogen activator beta	-3.98	0.0013
171	tc3a	Transposable element Tc3 transposase	-3.07	0.0013
172	TRIB2	Tribbles homolog 2	-5.66	0.0013
173	DDB_G0268948	Putative methyltransferase DDB_G0268948	-4.85	0.0014
174	NLRP12	NACHT, LRR and PYD domains-containing protein 12	-2.09	0.0014
175	Trim58	E3 ubiquitin-protein ligase TRIM58	-5.34	0.0014
176	SYT7	Synaptotagmin-7	4.31	0.0014
177	#N/A	LINE-1 retrotransposable element ORF2 protein	4.78	0.0014
178	Klf4	Krueppel-like factor 4	-4.14	0.0014
179	AP3S2	AP-3 complex subunit sigma-2	2.99	0.0014
180	Art5	Ecto-ADP-ribosyltransferase 5	-3.61	0.0015
181	Igf2r	Cation-independent mannose-6-phosphate receptor	-5.61	0.0015
182	midn	Midnolin	-4.12	0.0015
183	SAMD9L	Sterile alpha motif domain-containing protein 9-like	-5.64	0.0015
184	GSN	Gelsolin	-3.86	0.0016
185	WDR59	WD repeat-containing protein 59	2.37	0.0016
186	AHNAK	Neuroblast differentiation-associated protein AHNAK	-2.59	0.0016
187	gna11	Guanine nucleotide-binding protein subunit alpha-11	-5.85	0.0016
188	Gimap4	GTPase IMAP family member 4	-5.32	0.0016
189	URGCP	Up-regulator of cell proliferation	-2.29	0.0016
190	PHLPP1	PH domain leucine-rich repeat-containing protein phosphatase 1	3.51	0.0017
191	DSP	Desmoplakin	-1.98	0.0017
192	HELZ2	Helicase with zinc finger domain 2	-2.87	0.0017
193	DOK3	Docking protein 3	-3.01	0.0017
194	moaE2	Molybdopterin synthase catalytic subunit 2	7.47	0.0017
195	Tf2-9	Transposon Tf2-9 polyprotein	3.12	0.0017
196	TJP3	Tight junction protein ZO-3	-2.13	0.0018
197	#N/A	NACHT, LRR and PYD domains-containing protein 9	6.45	1.0000
198	SAMD9	Sterile alpha motif domain-containing protein 9	-5.42	0.0018
199	Igfbp6	Insulin-like growth factor-binding protein 6	-5.76	0.0018
200	TCNA	Sialidase	2.79	0.0018
201	Fosl2	Fos-related antigen 2	-3.75	0.0018
202	OSBPL3	Oxysterol-binding protein-related protein 3	-2.37	0.0019
203	ENPP	Enterin neuropeptides	4.26	0.0019
204	ABCG2	ATP-binding cassette sub-family G member 2	2.74	0.0019
205	Sdc2	Syndecan-2	-3.60	0.0019
206	Btn1a1	Butyrophilin subfamily 1 member A1	1.48	0.0019
207	HERC5	E3 ISG15--protein ligase HERC5	-4.65	0.0019
208	CNBP	Cellular nucleic acid-binding protein	3.41	0.0020
209	Fosl1	Fos-related antigen 1	-5.93	0.0020
210	Ankrd55	Ankyrin repeat domain-containing protein 55	7.07	0.0021
211	GLRX3	Glutaredoxin-3	2.22	0.0021
212	Son	Protein SON	2.98	0.0021
213	EPS8L2	Epidermal growth factor receptor kinase substrate 8-like protein 2	-5.73	0.0022
214	Samd9l	Sterile alpha motif domain-containing protein 9-like	-5.44	0.0022
215	Nfkbia	NF-kappa-B inhibitor alpha	-2.86	0.0023
216	SULF2	Extracellular sulfatase Sulf-2	4.00	0.0023
217	Casp8	Caspase-8	-2.77	0.0024
218	STK17A	Serine/threonine-protein kinase 17A	-2.37	0.0024
219	Rdx	Radixin	-1.82	0.0024
220	Sec31b	Protein transport protein Sec31B	2.58	0.0024
221	MR1	Major histocompatibility complex class I-related gene protein	2.09	0.0025
222	PTGIS	Prostacyclin synthase	-3.96	0.0026
223	AHNAK	Neuroblast differentiation-associated protein AHNAK	-2.80	0.0027
224	DLEC1	Deleted in lung and esophageal cancer protein 1	2.86	0.0028
225	RHA2	Rhodotorucin-A peptides type 2	2.69	0.0028
226	fam160a2	FTS and Hook-interacting protein homolog	2.24	0.0029
227	EZR	Ezrin	-1.67	0.0029
228	pdlim7	PDZ and LIM domain protein 7	-1.78	0.0030
229	Kpna3	Importin subunit alpha-4	-2.15	0.0031
230	nr4a2	Nuclear receptor subfamily 4 group A member 2	-5.34	0.0032
231	Hook3	Protein Hook homolog 3	2.08	0.0032
232	Xrcc1	DNA repair protein XRCC1	2.53	0.0032
233	Card14	Caspase recruitment domain-containing protein 14	-2.07	0.0032

234	Mybl1	Myb-related protein A	-3.82	0.0033
235	#N/A	Transposon TX1 uncharacterized 149 kDa protein	2.41	0.0033
236	PGBD4	PiggyBac transposable element-derived protein 4	-3.41	0.0033
237	NR1D2	Nuclear receptor subfamily 1 group D member 2	-1.80	0.0034
238	SYT7	Synaptotagmin-7	6.20	1.0000
239	slc39a9-b	Zinc transporter ZIP9-B	2.70	0.0034
240	PKP3	Plakophilin-3	-2.22	0.0034
241	krt13	Keratin, type I cytoskeletal 13	-2.67	0.0035
242	PPL	Periplakin	-1.83	0.0035
243	F5	Coagulation factor V	2.47	0.0035
244	Tnrc18	Trinucleotide repeat-containing gene 18 protein	-2.19	0.0035
245	tc3a	Transposable element Tc3 transposase	-2.43	0.0035
246	CIITA	MHC class II transactivator	2.40	0.0036
247	#N/A	Stonustoxin subunit beta	-2.56	0.0037
248	Mbd2	Methyl-CpG-binding domain protein 2	-3.84	0.0037
249	FBXO7	F-box only protein 7	2.37	0.0037
250	TMEM63B	CSC1-like protein 2	-1.86	0.0037
251	Ap1g2	AP-1 complex subunit gamma-like 2	-5.23	0.0038
252	wwox	WW domain-containing oxidoreductase	2.01	0.0038
253	Ggps1	Geranylgeranyl pyrophosphate synthase	1.70	0.0038
254	#N/A	Glycerol-3-phosphate transporter	-2.14	0.0038
255	Dsg4	Desmoglein-4	-2.51	0.0038
256	ILDR1	Immunoglobulin-like domain-containing receptor 1	-2.23	0.0039
257	Nars2	Probable asparagine--tRNA ligase, mitochondrial	2.32	0.0039
258	krt13	Keratin, type I cytoskeletal 13	-2.35	0.0039
259	Anxa11	Annexin A11	-2.11	0.0039
260	GIMAP5	GTPase IMAP family member 5	-2.52	0.0040
261	DOK1	Docking protein 1	-2.96	0.0040
262	ZNF283	Zinc finger protein 283	5.31	0.0040
263	Dsc2	Desmocollin-2	-2.66	0.0041
264	Hsd3b7	3 beta-hydroxysteroid dehydrogenase type 7	-3.30	0.0041
265	Osbpl6	Oxysterol-binding protein-related protein 6	-1.97	0.0041
266	pol	RNA-directed DNA polymerase from mobile element jockey	-3.11	0.0042
267	tir-1	Sterile alpha and TIR motif-containing protein tir-1	-5.28	0.0042
268	HERC3	Probable E3 ubiquitin-protein ligase HERC3	-4.54	0.0043
269	Itih3	Inter-alpha-trypsin inhibitor heavy chain H3	6.33	1.0000
270	Lrtm2	Leucine-rich repeat and transmembrane domain-containing protein 2	1.77	0.0044
271	Lnx2	Ligand of Numb protein X 2	-2.55	0.0044
272	#N/A	Vespryn	-5.15	1.0000
273	TCN1	Transcobalamin-1	-5.29	0.0046
274	RGS4	Regulator of G-protein signaling 4	-5.84	0.0046
275	VMP1	Vacuole membrane protein 1	-2.59	0.0046
276	#N/A	Translation initiation factor IF-2	7.08	0.0046
277	secY	Protein translocase subunit SecY	6.25	1.0000
278	DDR1	Epithelial discoidin domain-containing receptor 1	-1.85	0.0046
279	#N/A	Peptide chain release factor 2 {ECO:0000255|HAMAP-Rule:MF_00094}	6.89	0.0046
280	PRELID3B	PRELI domain containing protein 3B	-4.17	0.0047
281	RNH1	Ribonuclease inhibitor	-2.32	0.0049
282	MXD4	Max dimerization protein 4	-1.95	0.0049
283	plcd3a	1-phosphatidylinositol 4,5-bisphosphate phosphodiesterase delta-3-A	-4.12	0.0049
284	Epha2	Ephrin type-A receptor 2	-5.04	1.0000
285	CEBPB	CCAAT/enhancer-binding protein beta	-3.63	0.0051
286	FBXO3	F-box only protein 3	-3.27	0.0052
287	SLC25A22	Mitochondrial glutamate carrier 1	-2.58	0.0053
288	B3galt2	Beta-1,3-galactosyltransferase 2	-1.88	0.0053
289	LNX2	Ligand of Numb protein X 2	-2.83	0.0055
290	#N/A	Nuclear factor 7, ovary	-1.86	0.0055
291	STAT1	Signal transducer and activator of transcription 1	-1.75	0.0055
292	PEG10	Retrotransposon-derived protein PEG10	6.76	1.0000
293	CD276	CD276 antigen	-4.33	0.0056
294	gag-pol	Gag-Pol polyprotein	-2.25	0.0056
295	Urgcp	Up-regulator of cell proliferation	-4.49	0.0056
296	Anxa1	Annexin A1	-1.90	0.0056
297	Azin1	Antizyme inhibitor 1	-1.88	0.0057
298	ALYREF	THO complex subunit 4	-2.14	0.0057
299	#N/A	41 kDa spicule matrix protein	2.38	0.0057

300	Rora	Nuclear receptor ROR-alpha	-3.38	0.0059
301	F2rl1	Proteinase-activated receptor 2	-3.26	0.0062
302	SAMD9L	Sterile alpha motif domain-containing protein 9-like	-2.93	0.0063
303	Tnfrsf22	Tumor necrosis factor receptor superfamily member 22	-3.26	0.0064
304	ORF60	Uncharacterized protein ORF60	-2.02	0.0064
305	AHCYL2	Adenosylhomocysteinase 3	-4.98	1.0000
306	aste1	Protein asteroid homolog 1	-4.30	0.0065
307	Klf4	Krueppel-like factor 4	-3.13	0.0065
308	Clec4f	C-type lectin domain family 4 member F	4.72	0.0065
309	Sptb	Spectrin beta chain, erythrocytic	6.49	1.0000
310	Kr	Protein krueppel	-4.99	1.0000
311	Ogfr	Opioid growth factor receptor	-4.50	0.0067
312	phactr4a	Phosphatase and actin regulator 4A	-1.80	0.0067
313	PAK4	Serine/threonine-protein kinase PAK 4	-2.50	0.0067
314	ACTN1	Alpha-actinin-1	-2.02	0.0068
315	SEC23A	Protein transport protein Sec23A	-2.13	0.0068
316	GIMAP5	GTPase IMAP family member 5	-2.08	0.0068
317	Dsg2	Desmoglein-2	-5.23	0.0069
318	NUP98	Nuclear pore complex protein Nup98-Nup96	-4.81	1.0000
319	Igsf8	Immunoglobulin superfamily member 8	-1.94	0.0070
320	Adgrg2	Adhesion G-protein coupled receptor G2	-2.34	0.0070
321	PLA2G7	Platelet-activating factor acetylhydrolase	-1.77	0.0071
322	Galnt6	Polypeptide N-acetylgalactosaminyltransferase 6	-1.39	0.0071
323	mx2	Interferon-induced GTP-binding protein Mx2	-1.61	0.0073
324	tc1a	Transposable element Tc1 transposase	-1.23	0.0073
325	EGFR	Epidermal growth factor receptor	-1.51	0.0073
326	Asl	Argininosuccinate lyase	3.30	0.0074
327	USP2	Ubiquitin carboxyl-terminal hydrolase 2	-4.15	0.0075
328	ESYT3	Extended synaptotagmin-3	-1.24	0.0075
329	#N/A	Nectin-1	-2.19	0.0076
330	DDX5	Probable ATP-dependent RNA helicase DDX5	-2.47	0.0076
331	DUSP1	Dual specificity protein phosphatase 1	-4.07	0.0077
332	Mctp2	Multiple C2 and transmembrane domain-containing protein 2	1.91	0.0079
333	pla2g4a	Cytosolic phospholipase A2	-2.41	0.0080
334	TPD52	Tumor protein D52	-2.73	0.0080
335	F5	Coagulation factor V	4.65	0.0082
336	KLF5	Krueppel-like factor 5	-1.48	0.0082
337	SAT1	Diamine acetyltransferase 1	-2.05	0.0083
338	KRT7	Keratin, type II cytoskeletal 7	-3.16	0.0085
339	ldlr-a	Low-density lipoprotein receptor 1	-1.98	0.0085
340	TJP3	Tight junction protein ZO-3	-1.86	0.0086
341	G3BP1	Ras GTPase-activating protein-binding protein 1	-2.30	0.0087
342	Eif4g3	Eukaryotic translation initiation factor 4 gamma 3	-2.02	0.0088
343	Pim1	Serine/threonine-protein kinase pim-1	-2.85	0.0088
344	pat	Protein Pat	-1.48	0.0089
345	DAPK3	Death-associated protein kinase 3	-2.35	0.0090
346	NUGGC	Nuclear GTPase SLIP-GC	-2.52	0.0090
347	WIPI2	WD repeat domain phosphoinositide-interacting protein 2	-1.82	0.0091
348	LIAT1	Protein LIAT1 {ECO:0000305}	1.92	0.0093
349	Dsp	Desmoplakin	-2.34	0.0093
350	Map2	Microtubule-associated protein 2	2.53	0.0094
351	BAIAP2L1	Brain-specific angiogenesis inhibitor 1-associated protein 2-like protein 1	-3.21	0.0095
352	SCEL	Sciellin	-2.29	0.0095
353	GRHL3	Grainyhead-like protein 3 homolog {ECO:0000312|HGNC:HGNC:25839}	-2.07	0.0096
354	Eppk1	Epiplakin	-2.89	0.0096
355	Tf2-9	Transposon Tf2-9 polyprotein	-2.18	0.0097
356	Urgcp	Up-regulator of cell proliferation	-3.24	0.0097
357	arih1	E3 ubiquitin-protein ligase arih1	-2.31	0.0098
358	FOSL2	Fos-related antigen 2	-2.53	0.0099
359	Nos2	Nitric oxide synthase, inducible	3.67	0.0102
360	RALGAPA1	Ral GTPase-activating protein subunit alpha-1	-4.29	0.0103
361	slc43a2	Large neutral amino acids transporter small subunit 4	-4.35	0.0103
362	Baiap2l1	Brain-specific angiogenesis inhibitor 1-associated protein 2-like protein 1	-3.95	0.0104
363	Plekhg5	Pleckstrin homology domain-containing family G member 5	-2.53	0.0104
364	ACTN4	Alpha-actinin-4 {ECO:0000305}	-1.45	0.0104
365	Sik2	Serine/threonine-protein kinase SIK2	-2.06	0.0104

366	KLF5	Krueppel-like factor 5	-2.17	0.0104
367	HEBP2	Heme-binding protein 2	2.88	0.0104
368	frrs1	Putative ferric-chelate reductase 1	-3.88	0.0105
369	CCNG2	Cyclin-G2	-2.65	0.0105
370	Parp12	Poly [ADP-ribose] polymerase 12	-2.69	0.0105
371	Ipo7	Importin-7	-1.77	0.0105
372	PHTF2	Putative homeodomain transcription factor 2	-2.88	0.0105
373	PDCD6IP	Programmed cell death 6-interacting protein	-1.08	0.0105
374	GIMAP8	GTPase IMAP family member 8	2.29	0.0106
375	RELB	Transcription factor RelB	-2.22	0.0107
376	#N/A	Uncharacterized protein in mobD 3'region	2.88	0.0107
377	Mycbpap	MYCBP-associated protein	-4.55	0.0108
378	#N/A	Death ligand signal enhancer	-2.86	0.0108
379	Plec	Plectin	-2.70	0.0108
380	PIAS1	E3 SUMO-protein ligase PIAS1	-1.89	0.0108
381	ASNS	Asparagine synthetase [glutamine-hydrolyzing]	-1.81	0.0109
382	MANF	Mesencephalic astrocyte-derived neurotrophic factor	-1.87	0.0109
383	ANO9	Anoctamin-9	-2.02	0.0109
384	tyrp1	5,6-dihydroxyindole-2-carboxylic acid oxidase	-4.81	1.0000
385	Ngef	Ephexin-1	-1.73	0.0110
386	#N/A	Calmodulin	-1.93	0.0110
387	Tinagl1	Tubulointerstitial nephritis antigen-like	-4.84	1.0000
388	KIFAP3	Kinesin-associated protein 3	2.07	0.0111
389	#N/A	Niban-like protein 1	-1.50	0.0111
390	#N/A	Uncharacterized protein DKFZp434B061	2.48	0.0112
391	#N/A	Nuclear factor 7, ovary	-3.68	0.0113
392	Nampt	Nicotinamide phosphoribosyltransferase	-3.36	0.0114
393	ANXA1	Annexin A1	-1.76	0.0114
394	hsd17b12b	Very-long-chain 3-oxoacyl-CoA reductase-B {ECO:0000305}	4.10	0.0115
395	#N/A	Stonustoxin subunit alpha	-2.51	0.0116
396	GADL1	Acidic amino acid decarboxylase GADL1	-2.56	0.0117
397	Ndufs2	NADH dehydrogenase [ubiquinone] iron-sulfur protein 2, mitochondrial	1.65	0.0117
398	Hspa4	Heat shock 70 kDa protein 4	-3.23	0.0119
399	ARG2	Arginase-2, mitochondrial	-3.38	0.0120
400	jup	Junction plakoglobin	-2.05	0.0120
401	NLRC3	Protein NLRC3	-4.53	0.0121
402	OGDH	2-oxoglutarate dehydrogenase, mitochondrial	2.15	0.0121
403	DSC1	Desmocollin-1	-4.82	0.0122
404	GVINP1	Interferon-induced very large GTPase 1	-3.63	0.0123
405	#N/A	Transposable element Tcb1 transposase	3.46	0.0123
406	Brd2	Bromodomain-containing protein 2	-1.62	0.0124
407	Bace2	Beta-secretase 2	-2.03	0.0125
408	IVL	Involucrin	2.17	0.0125
409	25	Probable ATP-dependent helicase 25	-1.95	0.0125
410	pol	Retrovirus-related Pol polyprotein from transposon 17.6	4.45	0.0127
411	gpat3	Glycerol-3-phosphate acyltransferase 3	-4.92	1.0000
412	#N/A	Uncharacterized protein C1orf106 homolog	-2.19	0.0128
413	ZFAND5	AN1-type zinc finger protein 5	-2.75	0.0129
414	Tf2-9	Transposon Tf2-9 polyprotein	1.87	0.0129
415	C8orf44	Putative uncharacterized protein C8orf44	6.57	0.0130
416	Kiaa1671	Uncharacterized protein KIAA1671	-1.85	0.0131
417	Abi1	Abl interactor 1	2.78	0.0132
418	Cbx4	E3 SUMO-protein ligase CBX4	-2.98	0.0132
419	DDX17	Probable ATP-dependent RNA helicase DDX17	-2.62	0.0133
420	NLRP3	NACHT, LRR and PYD domains-containing protein 3	-4.72	1.0000
421	EGFR	Epidermal growth factor receptor	-2.41	0.0135
422	LAMP1	Lysosome-associated membrane glycoprotein 1	2.13	0.0137
423	OSBPL3	Oxysterol-binding protein-related protein 3	-1.62	0.0137
424	CLEC16A	Protein CLEC16A {ECO:0000305}	1.96	0.0138
425	#N/A	LINE-1 retrotransposable element ORF2 protein	9.21	0.0138
426	PTGS2	Prostaglandin G/H synthase 2	-2.87	0.0139
427	LITAF	Lipopolysaccharide-induced tumor necrosis factor-alpha factor homolog	-2.32	0.0139
428	URGCP	Up-regulator of cell proliferation	-3.54	0.0140
429	#N/A	Transposable element Tcb1 transposase	-1.77	0.0140
430	ucp2	Mitochondrial uncoupling protein 2	-1.52	0.0140
431	Rgs12	Regulator of G-protein signaling 12	-3.99	0.0140

432	Fblim1	Filamin-binding LIM protein 1	-2.61	0.0141
433	Parp14	Poly [ADP-ribose] polymerase 14	-1.77	0.0141
434	YWHAE	14-3-3 protein epsilon	-1.90	0.0141
435	SAT1	Diamine acetyltransferase 1	-2.46	0.0142
436	C16orf89	UPF0764 protein C16orf89	5.53	0.0142
437	Irf6	Interferon regulatory factor 6	-2.29	0.0142
438	TGM1	Protein-glutamine gamma-glutamyltransferase K	-2.59	0.0145
439	Wasl	Neural Wiskott-Aldrich syndrome protein	-1.39	0.0145
440	Khnyn	Protein KHNYN	-1.90	0.0146
441	Zswim6	Zinc finger SWIM domain-containing protein 6	-1.64	0.0147
442	Ptprz1	Receptor-type tyrosine-protein phosphatase zeta	-3.61	0.0148
443	FKBP5	Peptidyl-prolyl cis-trans isomerase FKBP5	-3.77	0.0149
444	GIMAP4	GTPase IMAP family member 4	-3.43	1.0000
445	ANO9	Anoctamin-9	-1.61	0.0151
446	Lrp2	Low-density lipoprotein receptor-related protein 2	-5.04	1.0000
447	Ap1s2	AP-1 complex subunit sigma-2	-1.53	0.0151
448	Osbpl6	Oxysterol-binding protein-related protein 6	-1.55	0.0151
449	Nlrc3	Protein NLRC3	5.93	1.0000
450	ABCC8	ATP-binding cassette sub-family C member 8	-4.06	0.0152
451	myb	Transcriptional activator Myb	-3.87	0.0152
452	NFKBIZ	NF-kappa-B inhibitor zeta	-1.24	0.0153
453	MCTP2	Multiple C2 and transmembrane domain-containing protein 2	-2.68	0.0156
454	gna14	Guanine nucleotide-binding protein subunit alpha-14	-3.49	0.0156
455	Tnfrsf22	Tumor necrosis factor receptor superfamily member 22	-2.44	0.0157
456	CASP3	Caspase-3	-3.13	0.0158
457	COX17	Cytochrome c oxidase copper chaperone	3.02	0.0158
458	#N/A	Arginase, hepatic	-2.63	0.0159
459	#N/A	Stonustoxin subunit alpha	-1.10	0.0161
460	inaK	Ice nucleation protein	-5.42	0.0165
461	EVPL	Envoplakin	-1.48	0.0167
462	PFB0145c	Uncharacterized protein PFB0145c	3.17	0.0167
463	TGas113e22.1	Histone H3.3	-2.06	0.0168
464	Sqstm1	Sequestosome-1	-2.43	0.0168
465	Klf8	Krueppel-like factor 8	-1.51	0.0170
466	NUP98A	Nuclear pore complex protein NUP98A {ECO:0000303|PubMed:21189294}	-3.23	0.0172
467	FAM8A1	Protein FAM8A1	1.71	0.0173
468	Fam111a	Protein FAM111A	-3.84	0.0174
469	SPT6	Transcription elongation factor SPT6	2.48	0.0174
470	#N/A	Transposable element Tcb2 transposase	-1.65	0.0175
471	CTRL	Chymotrypsin-like protease CTRL-1	-4.29	0.0175
472	dip2ba	Disco-interacting protein 2 homolog B-A	-2.11	0.0177
473	wee1-a	Wee1-like protein kinase 1-A	-2.29	0.0177
474	zgc:73324	Coenzyme Q-binding protein COQ10 homolog, mitochondrial	-4.80	1.0000
475	Fosl2	Fos-related antigen 2	-4.99	0.0177
476	Mslnl	Mesothelin-like protein	-3.48	0.0177
477	Dtx4	E3 ubiquitin-protein ligase DTX4	-1.95	0.0179
478	SH3GLB2	Endophilin-B2	-1.48	0.0179
479	Sik2	Serine/threonine-protein kinase SIK2	-2.81	0.0179
480	Sdcbp	Syntenin-1	-1.93	0.0183
481	grhl3	Grainyhead-like protein 3 homolog	-1.53	0.0184
482	TEAD1	Transcriptional enhancer factor TEF-1	-2.29	0.0185
483	#N/A	Collagen type IV alpha-3-binding protein	-1.66	0.0187
484	sacm1la	Phosphatidylinositide phosphatase SAC1-A	-4.64	1.0000
485	CTNND1	Catenin delta-1	-2.18	0.0189
486	PLA2G7	Platelet-activating factor acetylhydrolase	-2.32	0.0189
487	Atf3	Cyclic AMP-dependent transcription factor ATF-3	-3.28	0.0190
488	arhgap45	Minor histocompatibility protein HA-1	-2.76	0.0192
489	Mog	Myelin-oligodendrocyte glycoprotein	-4.56	1.0000
490	DYRK3	Dual specificity tyrosine-phosphorylation-regulated kinase 3	-2.94	0.0192
491	Upf1	Regulator of nonsense transcripts 1	-2.07	0.0193
492	Myo5b	Unconventional myosin-Vb	-3.38	0.0194
493	CDC40	Pre-mRNA-processing factor 17	-4.87	1.0000
494	Lrat	Lecithin retinol acyltransferase	-4.90	0.0195
495	DSC1	Desmocollin-1	-5.32	0.0196
496	NEDD4	E3 ubiquitin-protein ligase NEDD4	-1.93	0.0196

497	#N/A	LisH domain and HEAT repeat-containing protein KIAA1468 homolog	1.72	0.0197
498	efna1	Ephrin-A1	-2.84	0.0198
499	Srpk2	SRSF protein kinase 2	3.63	1.0000
500	Abcf2	ATP-binding cassette sub-family F member 2	-2.28	0.0202
501	ERVK-5	Endogenous retrovirus group K member 5 Np9 protein	7.29	0.0203
502	HEXB	Beta-hexosaminidase subunit beta	2.25	0.0204
503	CLIC3	Chloride intracellular channel protein 3	-1.36	0.0204
504	SFXN1	Sideroflexin-1	-3.77	0.0207
505	#N/A	LINE-1 retrotransposable element ORF2 protein	6.83	0.0207
506	Rnf213	E3 ubiquitin-protein ligase RNF213	-2.58	0.0208
507	TRIM16L	Tripartite motif-containing protein 16-like protein	-2.16	0.0208
508	STK40	Serine/threonine-protein kinase 40	-1.94	0.0208
509	STK40	Serine/threonine-protein kinase 40	-2.16	0.0211
510	ERBB3	Receptor tyrosine-protein kinase erbB-3	-1.69	0.0213
511	#N/A	Myosin light chain 3, skeletal muscle isoform	-2.87	0.0213
512	Rps6ka3	Ribosomal protein S6 kinase alpha-3	-4.39	1.0000
513	arg2-a	Arginase, non-hepatic 1	-3.51	0.0214
514	Krt17	Keratin, type I cytoskeletal 17	-1.62	0.0214
515	PTGS2	Prostaglandin G/H synthase 2	-2.79	0.0214
516	#N/A	Uncharacterized protein KIAA0930 homolog	1.88	0.0214
517	Rnh1	Ribonuclease inhibitor	-4.72	1.0000
518	SH2D7	SH2 domain-containing protein 7	-1.65	0.0217
519	#N/A	LINE-1 retrotransposable element ORF2 protein	7.16	0.0219
520	ITPR3	Inositol 1,4,5-trisphosphate receptor type 3	-3.04	0.0220
521	Eif4g2	Eukaryotic translation initiation factor 4 gamma 2	-2.00	0.0221
522	jak1	Tyrosine-protein kinase JAK1	-1.36	0.0221
523	AHNAK	Neuroblast differentiation-associated protein AHNAK	-2.48	0.0221
524	mri1	Methylthioribose-1-phosphate isomerase	1.40	0.0222
525	DSP	Desmoplakin	-1.95	0.0222
526	Tmod3	Tropomodulin-3	-1.58	0.0223
527	plxna4	Plexin-A4	-3.37	0.0223
528	PCYT2	Ethanolamine-phosphate cytidylyltransferase	-3.22	0.0225
529	Adgre1	Adhesion G protein-coupled receptor E2	-4.55	1.0000
530	Baiap2	Brain-specific angiogenesis inhibitor 1-associated protein 2	-1.78	0.0226
531	tc1a	Transposable element Tc1 transposase	-1.25	0.0227
532	PRELID3B	PRELI domain containing protein 3B	-3.26	0.0227
533	Tpsg1	Tryptase gamma	-4.89	0.0229
534	Snx18	Sorting nexin-18	-2.45	0.0231
535	MCL1	Induced myeloid leukemia cell differentiation protein Mcl-1 homolog	-1.96	0.0232
536	RPTN	Repetin	-2.38	0.0232
537	SEC24B	Protein transport protein Sec24B	-3.30	0.0234
538	Peg10	Retrotransposon-derived protein PEG10	1.58	0.0235
539	Acaca	Acetyl-CoA carboxylase 1	-1.59	0.0236
540	ppp1r3cb	Protein phosphatase 1 regulatory subunit 3C-B	-3.14	0.0236
541	#N/A	Calmodulin	-2.20	0.0236
542	efna5b	Ephrin-A5b	-3.06	0.0239
543	ADAM8	Disintegrin and metalloproteinase domain-containing protein 8	-2.80	0.0240
544	#N/A	Lectin BRA-3	5.30	0.0241
545	#N/A	Stonustoxin subunit beta	-1.26	0.0242
546	HARBI1	Putative nuclease HARBI1	-1.45	0.0245
547	SRP72	Signal recognition particle subunit SRP72	-1.42	0.0246
548	#N/A	Myomodulin neuropeptides	-2.08	0.0246
549	FBXW7	F-box/WD repeat-containing protein 7	-1.87	0.0246
550	GJB3	Gap junction beta-3 protein	-4.46	1.0000
551	ZDHHC4	Probable palmitoyltransferase ZDHHC4	-3.92	1.0000
552	CGN	Cingulin	-3.12	0.0248
553	RAB3IL1	Guanine nucleotide exchange factor for Rab-3A	1.62	0.0248
554	Kdm4a	Lysine-specific demethylase 4A	-4.56	1.0000
555	DDX3X	ATP-dependent RNA helicase DDX3X	-1.48	0.0250
556	grhl3	Grainyhead-like protein 3 homolog	-1.64	0.0250
557	Alk	ALK tyrosine kinase receptor	-4.84	1.0000
558	mfsd2ab	Sodium-dependent lysophosphatidylcholine symporter 1-B	2.20	0.0250
559	ugcg-a	Ceramide glucosyltransferase-A	-2.16	0.0252
560	Nrdc	Nardilysin	4.08	1.0000
561	ZNF613	Zinc finger protein 613	-4.48	1.0000
562	tc1a	Transposable element Tc1 transposase	2.90	0.0253

563	tc3a	Transposable element Tc3 transposase	-1.46	0.0253
564	ADAM17	Disintegrin and metalloproteinase domain-containing protein 17	-4.59	1.0000
565	PRP2	Repetitive proline-rich cell wall protein 2	-2.14	0.0255
566	Tf2-9	Transposon Tf2-9 polyprotein	3.92	0.0255
567	farsa	Phenylalanine--tRNA ligase alpha subunit	-2.14	0.0255
568	PDCD6	Programmed cell death protein 6	-2.70	0.0256
569	SLC20A1	Sodium-dependent phosphate transporter 1	2.66	0.0256
570	ABL2	Abelson tyrosine-protein kinase 2	-2.36	0.0256
571	Plec	Plectin	-2.52	0.0257
572	Tf2-9	Transposon Tf2-9 polyprotein	2.25	0.0259
573	PPE21	Uncharacterized PPE family protein PPE21	-3.19	0.0260
574	spag1a	Sperm-associated antigen 1A	-1.73	0.0260
575	K02A2.6	Uncharacterized protein K02A2.6	1.49	0.0261
576	DSC2	Desmocollin-2	-5.12	1.0000
577	hsc71	Heat shock cognate 70 kDa protein	-1.58	0.0264
578	Nlrc3	Protein NLRC3	-4.07	0.0264
579	PPP4R1	Serine/threonine-protein phosphatase 4 regulatory subunit 1	-1.77	0.0266
580	IKBIP	Inhibitor of nuclear factor kappa-B kinase-interacting protein	3.19	1.0000
581	PF14_0175	Protein PF14_0175	2.86	1.0000
582	Fgd3	FYVE, RhoGEF and PH domain-containing protein 3	-1.62	0.0267
583	NFKBIZ	NF-kappa-B inhibitor zeta	-1.62	0.0267
584	#N/A	Actin	-2.48	0.0268
585	ABCC4	Multidrug resistance-associated protein 4	-1.64	0.0269
586	Arl5b	ADP-ribosylation factor-like protein 5B	-3.33	0.0270
587	MYO9B	Unconventional myosin-IXb	-1.22	0.0271
588	TRAK2	Trafficking kinesin-binding protein 2	2.31	0.0272
589	Tmco3	Transmembrane and coiled-coil domain-containing protein 3	1.70	0.0272
590	Chd6	Chromodomain-helicase-DNA-binding protein 6	-3.07	0.0272
591	TRIM27	Zinc finger protein RFP	1.92	0.0273
592	COG1	Conserved oligomeric Golgi complex subunit 1	-1.44	0.0274
593	krt8	Keratin, type II cytoskeletal 8	-1.83	0.0275
594	Anxa3	Annexin A3	-1.66	0.0276
595	Mep1b	Meprin A subunit beta	-2.98	0.0276
596	CD40	Tumor necrosis factor receptor superfamily member 5	-2.12	0.0276
597	NUP98	Nuclear pore complex protein Nup98-Nup96	-2.00	0.0279
598	PPP1R15B	Protein phosphatase 1 regulatory subunit 15B	-3.42	0.0279
599	tc1a	Transposable element Tc1 transposase	-1.17	0.0280
600	#N/A	Transposon TX1 uncharacterized 149 kDa protein	-1.95	0.0280
601	PTGS2	Prostaglandin G/H synthase 2	-3.98	0.0283
602	#N/A	Transposable element Tcb1 transposase	2.76	0.0284
603	EZR	Ezrin	-1.62	0.0284
604	ADAP1	Arf-GAP with dual PH domain-containing protein 1	-3.64	1.0000
605	ELOVL1	Elongation of very long chain fatty acids protein 1	-1.79	0.0285
606	Zswim6	Zinc finger SWIM domain-containing protein 6	-2.14	0.0285
607	ucp2	Mitochondrial uncoupling protein 2	-4.40	1.0000
608	DSG2	Desmoglein-2	-3.85	0.0289
609	GALNT6	Polypeptide N-acetylgalactosaminyltransferase 6	-1.26	0.0289
610	Fntb	Protein farnesyltransferase subunit beta	2.20	0.0290
611	DSP	Desmoplakin	-1.72	0.0291
612	Anxa3	Annexin A3	-1.81	0.0291
613	atp8b1	Phospholipid-transporting ATPase IC	-1.49	0.0292
614	EVPL	Envoplakin	-1.23	0.0293
615	psmb4	Proteasome subunit beta type-4	-1.75	0.0293
616	Gstm5	Glutathione S-transferase Mu 5	-0.87	0.0293
617	vcp	Transitional endoplasmic reticulum ATPase	-3.80	1.0000
618	Rin2	Ras and Rab interactor 2	-4.43	1.0000
619	Frmd4b	FERM domain-containing protein 4B	-3.54	1.0000
620	Tbc1d2b	TBC1 domain family member 2B	1.78	0.0300
621	Lifr	Leukemia inhibitory factor receptor	-1.86	0.0301
622	#N/A	Probable DNA polymerase	-2.88	0.0302
623	nr4a1	Nuclear receptor subfamily 4 group A member 1	-3.28	0.0302
624	NEK3	Serine/threonine-protein kinase Nek3	2.43	0.0302
625	RNF14	E3 ubiquitin-protein ligase RNF14	-4.44	1.0000
626	ddit4l	DNA damage-inducible transcript 4-like protein	-3.26	0.0304
627	myo1c-a	Unconventional myosin-Ic-A	-1.55	0.0305
628	RTP3	Receptor-transporting protein 3	2.30	0.0305

629	SLC46A2	Thymic stromal cotransporter homolog	-2.76	0.0307
630	phlda2	Pleckstrin homology-like domain family A member 2	-2.41	0.0310
631	Flrt1	Leucine-rich repeat transmembrane protein FLRT1	2.73	0.0311
632	#N/A	Transposable element Tcb1 transposase	-1.41	0.0313
633	#N/A	L-rhamnose-binding lectin CSL2 {ECO:0000303|Ref.1}	2.94	0.0315
634	BAIAP3	BAI1-associated protein 3	3.88	1.0000
635	rhcg	Ammonium transporter Rh type C	1.88	0.0317
636	Socs1	Suppressor of cytokine signaling 1	2.43	0.0319
637	PTPN1	Tyrosine-protein phosphatase non-receptor type 1	-2.13	0.0319
638	Gjb3	Gap junction beta-3 protein	-2.89	0.0319
639	CLCN1	Chloride channel protein 1	-4.23	1.0000
640	wee1-b	Wee1-like protein kinase 1-B	-2.48	0.0322
641	SLC1A4	Neutral amino acid transporter A	-2.03	0.0322
642	ARHGEF15	Rho guanine nucleotide exchange factor 15	-1.13	0.0324
643	mtus1a	Microtubule-associated tumor suppressor 1 homolog A	-2.02	0.0324
644	ZBED5	Zinc finger BED domain-containing protein 5	-1.98	0.0324
645	KPNA3	Importin subunit alpha-4	-1.77	0.0325
646	STK17B	Serine/threonine-protein kinase 17B	-2.10	0.0325
647	Arap1	Arf-GAP with Rho-GAP domain, ANK repeat and PH domain-containing protein 1	-1.28	0.0325
648	BIN2	Bridging integrator 2	-1.75	0.0325
649	CLDN4	Claudin-4	-2.21	0.0326
650	gse1	Genetic suppressor element 1	1.98	0.0328
651	sort1	Sortilin	-1.82	0.0329
652	rhbdf2	Inactive rhomboid protein 2	-1.20	0.0330
653	NIPA2	Magnesium transporter NIPA2	-2.58	0.0331
654	Gpsm2	G-protein-signaling modulator 2	-4.61	1.0000
655	Trp53inp1	Tumor protein p53-inducible nuclear protein 1	1.68	0.0332
656	#N/A	S-antigen protein	-2.68	0.0332
657	HIP1R	Huntingtin-interacting protein 1-related protein	-2.37	0.0332
658	HMGCR	3-hydroxy-3-methylglutaryl-coenzyme A reductase	-1.87	0.0334
659	#N/A	78 kDa glucose-regulated protein	-1.64	0.0334
660	Il10rb	Interleukin-10 receptor subunit beta	-3.22	0.0335
661	GTF2IRD2	General transcription factor II-I repeat domain-containing protein 2A	-1.89	0.0337
662	Dsp	Desmoplakin	-1.58	0.0337
663	TSPAN14	Tetraspanin-14	-1.66	0.0338
664	Gpr141	Probable G-protein coupled receptor 141	1.71	0.0340
665	HARBI1	Putative nuclease HARBI1	1.08	0.0340
666	Acsl4	Long-chain-fatty-acid--CoA ligase 4	-4.28	1.0000
667	LRP2	Low-density lipoprotein receptor-related protein 2	-4.48	1.0000
668	#N/A	DLA class I histocompatibility antigen, A9/A9 alpha chain	-2.66	0.0342
669	mvp	Major vault protein	-1.69	0.0342
670	ttll3	Tubulin monoglycylase TTLL3	3.33	0.0342
671	Tp53bp2	Apoptosis-stimulating of p53 protein 2	-2.52	0.0342
672	Tacstd2	Tumor-associated calcium signal transducer 2	-1.99	0.0342
673	#N/A	WASH complex subunit strumpellin	-1.56	0.0342
674	MAPKAPK2	MAP kinase-activated protein kinase 2	-2.00	0.0342
675	PIAS1	E3 SUMO-protein ligase PIAS1	-3.30	0.0343
676	RELB	Transcription factor RelB homolog	-3.77	1.0000
677	Eif1	Eukaryotic translation initiation factor 1	-1.93	0.0345
678	#N/A	Transposon TX1 uncharacterized 149 kDa protein	2.39	0.0345
679	sspH2	E3 ubiquitin-protein ligase sspH2	1.72	0.0345
680	TRIM11	E3 ubiquitin-protein ligase TRIM11	1.83	0.0346
681	Ngef	Ephexin-1	-1.41	0.0347
682	krt8	Keratin, type II cytoskeletal 8	-1.79	0.0347
683	PTGS2	Prostaglandin G/H synthase 2	-2.91	0.0348
684	B4galt5	Beta-1,4-galactosyltransferase 5	-1.94	0.0348
685	RBM25	RNA-binding protein 25	1.79	0.0349
686	MTA2	Metastasis-associated protein MTA2	-4.29	1.0000
687	ext1b	Exostosin-1b	-2.11	0.0350
688	NIPAL4	Magnesium transporter NIPA4	-2.60	0.0350
689	GK	Glycerol kinase	-4.19	1.0000
690	Myo9b	Unconventional myosin-IXb	-1.46	0.0351
691	DUSP7	Dual specificity protein phosphatase 7	-1.63	0.0351
692	PLCH2	1-phosphatidylinositol 4,5-bisphosphate phosphodiesterase eta-2	-2.14	0.0351
693	Tecpr1	Tectonin beta-propeller repeat-containing protein 1	5.19	0.0352

694	Herc4	Probable E3 ubiquitin-protein ligase HERC4	-2.95	0.0352
695	PYDC1	Pyrin domain-containing protein 1 {ECO:0000305}	-2.45	0.0352
696	TPP2	Tripeptidyl-peptidase 2	-3.85	1.0000
697	ARAP1	Arf-GAP with Rho-GAP domain, ANK repeat and PH domain-containing protein 1	-2.08	0.0354
698	ACSL3	Long-chain-fatty-acid--CoA ligase 3	-1.24	0.0355
699	IGFBP1	Insulin-like growth factor-binding protein 1	2.01	0.0358
700	Dusp7	Dual specificity protein phosphatase 7	-2.54	0.0358
701	Rnf213	E3 ubiquitin-protein ligase RNF213	-2.05	0.0359
702	gtf2f2	General transcription factor IIF subunit 2	-2.22	0.0359
703	STXBP2	Syntaxin-binding protein 2	-1.39	0.0361
704	#N/A	FMRFamide-related neuropeptides	2.09	0.0361
705	SEC24C	Protein transport protein Sec24C	-1.22	0.0362
706	Prss27	Serine protease 27	-1.83	0.0364
707	KPNA3	Importin subunit alpha-4	-1.64	0.0366
708	MSRB3	Methionine-R-sulfoxide reductase B3	1.87	0.0367
709	rpl19	60S ribosomal protein L19	-3.40	1.0000
710	SAT1	Diamine acetyltransferase 1	-1.67	0.0369
711	FLNB	Filamin-B	-2.12	0.0369
712	TSPAN3	Tetraspanin-3	-4.33	1.0000
713	PARP12	Poly [ADP-ribose] polymerase 12	-3.03	0.0373
714	NISCH	Nischarin	1.73	0.0374
715	C1orf127	Uncharacterized protein C1orf127	-4.03	0.0374
716	ZFC3H1	Zinc finger C3H1 domain-containing protein	-2.11	0.0375
717	MAP7D1	MAP7 domain-containing protein 1	-3.87	0.0376
718	CD200	OX-2 membrane glycoprotein	-3.34	0.0377
719	hsd17b12a	Very-long-chain 3-oxoacyl-CoA reductase-A {ECO:0000305}	-1.59	0.0380
720	Pias2	E3 SUMO-protein ligase PIAS2	-1.53	0.0383
721	Cfl2	Cofilin-2	-1.35	0.0383
722	Lamc2	Laminin subunit gamma-2	-4.61	0.0383
723	ATP5MC1	ATP synthase F(0) complex subunit C1, mitochondrial	-3.11	0.0384
724	Zc3h12a	Ribonuclease ZC3H12A	-1.52	0.0387
725	Lpcat4	Lysophospholipid acyltransferase LPCAT4	-1.89	0.0391
726	Gak	Cyclin-G-associated kinase	-1.42	0.0391
727	MDV087	Uncharacterized gene 87 protein	-1.33	0.0394
728	ARHGAP4	Rho GTPase-activating protein 4	-2.38	0.0394
729	Map7d1	MAP7 domain-containing protein 1	-4.26	0.0395
730	arf4	ADP-ribosylation factor 4	-2.23	0.0395
731	nme6	Nucleoside diphosphate kinase 6	2.79	0.0396
732	Abce1	ATP-binding cassette sub-family E member 1	-1.37	0.0397
733	ANXA1	Annexin A1	-2.21	0.0397
734	Srms	Tyrosine-protein kinase Srms	-1.27	0.0398
735	tc1a	Transposable element Tc1 transposase	-1.28	0.0398
736	ddit4	DNA damage-inducible transcript 4 protein	-2.63	0.0399
737	FASN	Fatty acid synthase	-2.70	0.0399
738	STAT1	Signal transducer and activator of transcription 1	-2.64	0.0399
739	Mtss1	Metastasis suppressor protein 1	-2.72	0.0399
740	STAT1	Signal transducer and activator of transcription 1	-1.51	0.0401
741	Casp3	Caspase-3	-3.87	1.0000
742	Sergef	Secretion-regulating guanine nucleotide exchange factor	2.43	0.0402
743	chmp4c	Charged multivesicular body protein 4c	-1.69	0.0403
744	MIMI_R795	Probable bifunctional E2/E3 enzyme R795	-2.01	0.0403
745	EIF4A1	Eukaryotic initiation factor 4A-I	-1.86	0.0404
746	Lrp2	Low-density lipoprotein receptor-related protein 2	-3.95	1.0000
747	Gcc2	GRIP and coiled-coil domain-containing protein 2	-2.94	0.0404
748	Jund	Transcription factor jun-D	-3.03	0.0405
749	fam76b	Protein FAM76B	-1.82	0.0405
750	#N/A	Transposable element Tcb1 transposase	2.14	0.0406
751	PER2	Period circadian protein homolog 2	-3.41	0.0407
752	RDH12	Retinol dehydrogenase 12	-3.58	0.0407
753	hsd17b12a	Very-long-chain 3-oxoacyl-CoA reductase-A {ECO:0000305}	-3.34	0.0407
754	SDC4	Syndecan-4	-2.49	0.0407
755	SSR1	Translocon-associated protein subunit alpha	-3.69	1.0000
756	tc1a	Transposable element Tc1 transposase	-1.38	0.0409
757	Krt20	Keratin, type I cytoskeletal 20	-2.11	0.0409
758	PLN	Cardiac phospholamban	-4.41	1.0000

759	nfil3	Nuclear factor interleukin-3-regulated protein	-1.82	0.0411
760	ZMYM6	Zinc finger MYM-type protein 6	-2.89	0.0411
761	Kiaa1109	Uncharacterized protein KIAA1109	-2.86	0.0411
762	Zfhx4	Zinc finger homeobox protein 4	3.33	0.0411
763	HI_0712	Probable hemoglobin and hemoglobin-haptoglobin-binding protein 3	2.46	0.0413
764	Sdcbp	Syntenin-1	-2.89	0.0415
765	#N/A	Transposable element Tcb1 transposase	-1.67	0.0416
766	Dsp	Desmoplakin	-2.06	0.0416
767	Rasa2	Ras GTPase-activating protein 2	-1.43	0.0418
768	#N/A	Transposable element Tcb1 transposase	2.08	0.0419
769	Snrpg	Small nuclear ribonucleoprotein G	-2.05	0.0420
770	B3GALT1	Beta-1,3-galactosyltransferase 1	-1.62	0.0421
771	OVOL1	Putative transcription factor Ovo-like 1	-1.61	0.0423
772	Vmp1	Vacuole membrane protein 1	-2.42	0.0423
773	Fbxo44	F-box only protein 44	-3.57	0.0424
774	ZNF568	Zinc finger protein 568	-5.16	1.0000
775	IMMP1L	Mitochondrial inner membrane protease subunit 1	2.65	0.0424
776	Plekha6	Pleckstrin homology domain-containing family A member 6	-2.25	0.0426
777	EPS8L1	Epidermal growth factor receptor kinase substrate 8-like protein 1	-1.35	0.0427
778	Ralgapa1	Ral GTPase-activating protein subunit alpha-1	-3.55	1.0000
779	PLEKHA5	Pleckstrin homology domain-containing family A member 5	-2.35	0.0428
780	tc1a	Transposable element Tc1 transposase	-1.58	0.0428
781	Frmd4a	FERM domain-containing protein 4A	-1.30	0.0429
782	#N/A	Stonustoxin subunit beta	-1.55	0.0429
783	ELF4	ETS-related transcription factor Elf-4	-1.47	0.0430
784	NR1D2	Nuclear receptor subfamily 1 group D member 2	-2.40	0.0430
785	APOD	Apolipoprotein D	-2.90	0.0432
786	Plxnb2	Plexin-B2	-1.54	0.0432
787	Serinc3	Serine incorporator 3	-2.74	0.0434
788	GALNT6	Polypeptide N-acetylgalactosaminyltransferase 6	-1.48	0.0437
789	NOS	Nitric oxide synthase	1.62	0.0437
790	DAPK3	Death-associated protein kinase 3	-2.81	0.0437
791	HSPA4	Heat shock 70 kDa protein 4	-1.46	0.0440
792	dnajc2	DnaJ homolog subfamily C member 2	-3.30	1.0000
793	SH2D4A	SH2 domain-containing protein 4A	-5.47	0.0442
794	GRHL3	Grainyhead-like protein 3 homolog {ECO:0000312|HGNC:HGNC:25839}	-1.70	0.0442
795	Mafk	Transcription factor MafK	-1.74	0.0442
796	MTSS1	Metastasis suppressor protein 1	-1.66	0.0442
797	ROCK2	Rho-associated protein kinase 2	-3.45	0.0443
798	gadl1	Acidic amino acid decarboxylase GADL1	-2.06	0.0443
799	LIMA1	LIM domain and actin-binding protein 1	-3.58	0.0444
800	TMCO3	Transmembrane and coiled-coil domain-containing protein 3	1.80	0.0445
801	ADAP1	Arf-GAP with dual PH domain-containing protein 1	-2.20	0.0445
802	HIF1A	Hypoxia-inducible factor 1-alpha	-2.35	0.0445
803	#N/A	Protein groucho-1	-4.22	1.0000
804	slc20a1b	Sodium-dependent phosphate transporter 1-B	-1.98	0.0447
805	EIF5	Eukaryotic translation initiation factor 5	-1.46	0.0448
806	NR4A3	Nuclear receptor subfamily 4 group A member 3	-3.70	0.0448
807	Rps23	40S ribosomal protein S23	-3.21	0.0448
808	Entpd4	Ectonucleoside triphosphate diphosphohydrolase 4	-1.19	0.0449
809	P4HA2	Prolyl 4-hydroxylase subunit alpha-2	1.80	0.0449
810	Rnf213	E3 ubiquitin-protein ligase RNF213	-1.59	0.0451
811	KLF5	Krueppel-like factor 5	-1.93	0.0451
812	SGSM1	Small G protein signaling modulator 1	-2.85	0.0452
813	Arhgap45	Minor histocompatibility protein HA-1	-2.70	0.0452
814	rpusd1	RNA pseudouridylate synthase domain-containing protein 1	-2.25	0.0452
815	#N/A	Transposable element Tcb1 transposase	-1.08	0.0452
816	MAN1C1	Mannosyl-oligosaccharide 1,2-alpha-mannosidase IC	-4.33	1.0000
817	Ubl3	Ubiquitin-like protein 3	1.71	0.0454
818	INPP5A	Type I inositol 1,4,5-trisphosphate 5-phosphatase	-2.58	0.0454
819	Dsg2	Desmoglein-2	-3.57	0.0456
820	ERP44	Endoplasmic reticulum resident protein 44	-1.35	0.0458
821	Pol	LINE-1 retrotransposable element ORF2 protein	-1.87	0.0458
822	Fbxw7	F-box/WD repeat-containing protein 7 {ECO:0000305}	-2.25	0.0458
823	Fgl1	Fibrinogen-like protein 1	-4.18	1.0000
824	ITGA11	Integrin alpha-11	6.02	1.0000

825	UAP1	UDP-N-acetylhexosamine pyrophosphorylase	-1.95	0.0462
826	NLRP1	NACHT, LRR and PYD domains-containing protein 1	-0.99	0.0463
827	Tf2-9	Transposon Tf2-9 polyprotein	1.60	0.0463
828	CLOCK	Circadian locomoter output cycles protein kaput	-1.91	0.0463
829	HNRNPD	Heterogeneous nuclear ribonucleoprotein D0	-1.28	0.0464
830	DSP	Desmoplakin	-2.05	0.0464
831	#N/A	Transposable element Tcb1 transposase	1.81	0.0465
832	AGO4	Protein argonaute-4 {ECO:0000255|HAMAP-Rule:MF_03033}	-1.30	0.0467
833	Erf	ETS domain-containing transcription factor ERF	-1.81	0.0468
834	G3BP2	Ras GTPase-activating protein-binding protein 2	-2.21	0.0468
835	alcama	CD166 antigen homolog A	-1.64	0.0472
836	c1galt1b	Glycoprotein-N-acetylgalactosamine 3-beta-galactosyltransferase 1-B	-1.91	0.0472
837	ERBB3	Receptor tyrosine-protein kinase erbB-3	-2.23	0.0473
838	COL13A1	Collagen alpha-1(XIII) chain	3.19	0.0473
839	valA	2-epi-5-epi-valiolone synthase {ECO:0000303|PubMed:16151088}	-2.59	0.0474
840	Itch	E3 ubiquitin-protein ligase Itchy	-1.37	0.0475
841	Spag1	Sperm-associated antigen 1	-2.07	0.0475
842	GIP	Copia protein	-1.19	0.0475
843	Myo5a	Unconventional myosin-Va	2.99	0.0475
844	PTGS2	Prostaglandin G/H synthase 2	-2.57	0.0476
845	LMO7	LIM domain only protein 7	-1.25	0.0478
846	vmp1	Vacuole membrane protein 1	-4.10	1.0000
847	Tle3	Transducin-like enhancer protein 3	-3.71	0.0479
848	CRY2	Cryptochrome-2	-2.21	0.0480
849	MYL6B	Myosin light chain 6B	-1.82	0.0481
850	EIF4G2	Eukaryotic translation initiation factor 4 gamma 2	-1.54	0.0481
851	GRB7	Growth factor receptor-bound protein 7	-1.74	0.0484
852	Rab5a	Ras-related protein Rab-5A	-1.68	0.0485
853	PRDM1	PR domain zinc finger protein 1	-3.89	1.0000
854	PHF12	PHD finger protein 12	-4.43	1.0000
855	Ak4	Adenylate kinase 4, mitochondrial	-3.48	1.0000
856	Rab1A	Ras-related protein Rab-1A	-1.51	0.0487
857	ZBED5	Zinc finger BED domain-containing protein 5	-3.32	0.0488
858	cyfip1	Cytoplasmic FMR1-interacting protein 1 homolog	-1.39	0.0488
859	Osbpl6	Oxysterol-binding protein-related protein 6	-1.44	0.0488
860	FOXN3	Forkhead box protein N3	-2.58	0.0488
861	tpr	Nucleoprotein TPR	-1.41	0.0488
862	#N/A	Histone H3.3	-2.07	0.0493
863	KRT20	Keratin, type I cytoskeletal 20	-1.94	0.0495
864	ORF46	Probable major glycoprotein	-1.80	0.0496
865	ZFAND5	AN1-type zinc finger protein 5	-3.66	1.0000
866	Tf2-9	Transposon Tf2-9 polyprotein	2.56	0.0496
867	ZBED9	SCAN domain-containing protein 3	-2.60	0.0496
868	MAPKBP1	Mitogen-activated protein kinase-binding protein 1	-1.56	0.0496
869	Map4k4	Mitogen-activated protein kinase kinase kinase kinase 4	-1.78	0.0496
870	setd6	N-lysine methyltransferase setd6	-2.84	0.0496
871	N4BP2	NEDD4-binding protein 2	-2.23	0.0496
872	CRY2	Cryptochrome-2	-4.40	1.0000
873	Spint1	Kunitz-type protease inhibitor 1	-1.46	0.0497
874	xpot	Exportin-T	-1.61	0.0497
875	ocln	Occludin	-1.31	0.0498
876	HCFC1	Host cell factor 1	-2.44	0.0498
877	FKBP5	Peptidyl-prolyl cis-trans isomerase FKBP5	-1.86	0.0499
878	hsd17b12	Very-long-chain 3-oxoacyl-CoA reductase {ECO:0000305}	2.31	0.0499
879	Znf768	Zinc finger protein 768	-2.45	0.0499

APPENDIX B:
Gene Expression Data from Chapter 3

Table B-1. List of all differentially expressed transcripts (FDR adjusted $p \leq 0.05$) in epidermal mucus ranked by p value among 2018 and 2019 baseline samples.

Gene Symbol	UniProt ID and Full Gene Name	log2 Fold Change	*p*-adj
RRT15	RRT15_YEAST Regulator of rDNA transcription protein 15	13.72	2.39E-46
Tes	TES_MOUSE Testin	9.56	6.91E-27
#N/A	YCX91_PHAAO Uncharacterized protein ORF91	16.14	1.46E-26
stac3	STAC3_DANRE SH3 and cysteine-rich domain-containing protein 3	10.34	2.63E-23
ART2	ART2_YEAST Putative uncharacterized protein ART2	11.10	7.06E-21
ciao1b	CIO1B_SALSA Probable cytosolic iron-sulfur protein assembly protein ciao1-B	-11.47	3.16E-20
secE	SECE_METMP Protein translocase subunit SecE	7.10	1.84E-18
pnp	PNP_DESRM Polyribonucleotide nucleotidyltransferase	13.78	1.30E-17
TAR1	TAR1_YEAST Protein TAR1	-4.38	2.02E-17
#N/A	S10I_ICTPU Ictacalcin	-9.14	2.46E-17
Nlrc3	NLRC3_MOUSE Protein NLRC3	14.16	5.16E-17
bioB	BIOB_MAGMM Biotin synthase {ECO:0000255|HAMAP-Rule:MF_01694}	13.76	5.24E-17
#N/A	YCX91_PHAAO Uncharacterized protein ORF91	12.44	4.05E-16
TAR1	TAR1_YEAST Protein TAR1	13.40	4.05E-16
L	L_RABVB Large structural protein	-14.16	2.62E-15
pksG	PKSG_BACSU Polyketide biosynthesis 3-hydroxy-3-methylglutaryl-ACP synthase PksG	11.76	2.81E-14
MT-ND2	NU2M_LAMFL NADH-ubiquinone oxidoreductase chain 2	12.75	1.63E-13
TAR1-A	TAR1_KLULA Protein TAR1	11.48	2.53E-13
Tnik	TNIK_MOUSE Traf2 and NCK-interacting protein kinase	-2.74	2.53E-13
#N/A	YCX91_PHAAO Uncharacterized protein ORF91	12.72	2.53E-13
rplp0	RLA0_DANRE 60S acidic ribosomal protein P0	-5.69	1.42E-11
Rpl12	RL12_MOUSE 60S ribosomal protein L12	-4.45	2.50E-11
#N/A	#N/A	-4.03	4.28E-09
Rps20	RS20_RAT 40S ribosomal protein S20	-6.58	9.31E-09
#N/A	#N/A	5.33	1.02E-08
rnasel3	RNSL3_DANRE Ribonuclease-like 3 {ECO:0000303|PubMed:16861230}	-3.27	1.61E-08
dbnl-a	DBNLA_XENLA Drebrin-like protein A	-8.04	1.73E-08
Tnik	TNIK_MOUSE Traf2 and NCK-interacting protein kinase	-3.22	3.32E-08
At1g05670	PPR12_ARATH Pentatricopeptide repeat-containing protein At1g05670, mitochondrial	4.52	3.32E-08
#N/A	FA63A_BOVIN Protein FAM63A	-3.35	3.32E-08
#N/A	RLA0_RANSY 60S acidic ribosomal protein P0	-4.32	3.67E-08
rep	R1AB_BCHK4 Replicase polyprotein 1ab	-5.02	4.67E-08
#N/A	NDB4G_UROYA Antimicrobial peptide UyCT1 {ECO:0000303|PubMed:23182832}	-3.71	5.74E-08
RPL5	RL5_CHICK 60S ribosomal protein L5	-4.27	8.14E-08
rps24	RS24_TAKRU 40S ribosomal protein S24	-5.12	8.21E-08
Nlrc3	NLRC3_MOUSE Protein NLRC3	-6.32	8.87E-08
#N/A	#N/A	6.18	1.76E-07
#N/A	#N/A	7.68	2.12E-07
MT-ND2	NU2M_SALSA NADH-ubiquinone oxidoreductase chain 2	8.50	2.34E-07
Mmaa	MMAA_MOUSE Methylmalonic aciduria type A homolog, mitochondrial	-7.62	2.80E-07
rrm2	RIR2_DANRE Ribonucleoside-diphosphate reductase subunit M2	-3.16	2.91E-07
#N/A	#N/A	5.73	3.27E-07
Nop14	NOP14_MOUSE Nucleolar protein 14	8.06	5.09E-07
SODB	SODF_ENTHI Superoxide dismutase [Fe]	5.10	6.14E-07
SH3BGRL3	SH3L3_HUMAN SH3 domain-binding glutamic acid-rich-like protein 3	3.86	6.91E-07
murC	MURC_BACCZ UDP-N-acetylmuramate--L-alanine ligase {	7.98	1.30E-06
Cebpd	CEBPD_RAT CCAAT/enhancer-binding protein delta	-7.55	2.74E-06
#N/A	MIA3_HUMAN Melanoma inhibitory activity protein 3	-5.96	2.74E-06
#N/A	#N/A	5.61	3.19E-06
#N/A	#N/A	3.97	3.95E-06
ttn-1	TTN1_CAEEL Titin homolog {ECO:0000303|PubMed:12381307}	7.55	4.42E-06
#N/A	#N/A	8.42	4.50E-06

SEC16	SEC16_PICST COPII coat assembly protein SEC16	2.32	5.56E-06
#N/A	#N/A	5.36	5.74E-06
cirbp	CIRBP_XENTR Cold-inducible RNA-binding protein	-6.45	5.75E-06
TNFRSF1A	TNR1A_BOVIN Tumor necrosis factor receptor superfamily member 1A	5.11	6.34E-06
psd	PSD_CLOBJ Phosphatidylserine decarboxylase proenzyme	7.47	7.75E-06
SLC25A1	TXTP_BOVIN Tricarboxylate transport protein, mitochondrial	4.38	8.17E-06
#N/A	YCX91_PHAAO Uncharacterized protein ORF91	8.74	9.72E-06
rps27	RS27_XENLA 40S ribosomal protein S27	-6.56	1.11E-05
#N/A	YMO3_PANSE Uncharacterized protein in mobD 3'region	4.45	1.16E-05
EIF4A2	IF4A2_CHICK Eukaryotic initiation factor 4A-II	-5.45	1.17E-05
#N/A	#N/A	5.15	1.20E-05
#N/A	#N/A	7.96	1.25E-05
HDHD2	HDHD2_HUMAN Haloacid dehalogenase-like hydrolase domain-containing protein 2	-2.92	1.38E-05
#N/A	#N/A	6.64	1.45E-05
LMO7	LMO7_HUMAN LIM domain only protein 7	-7.47	1.56E-05
nadA	NADA_GEOTN Quinolinate synthase A {ECO:0000255|HAMAP-Rule:MF_00569}	3.05	1.67E-05
jockey\pol	RTJK_DROFU RNA-directed DNA polymerase from mobile element jockey	3.19	2.23E-05
#N/A	#N/A	2.54	2.37E-05
COPE	COPE_BOVIN Coatomer subunit epsilon	-3.55	2.76E-05
#N/A	IF2_CLOPH Translation initiation factor IF-2 {ECO:0000255|HAMAP-Rule:MF_00100}	7.01	3.00E-05
glmM	GLMM_VIBVU Phosphoglucosamine mutase {ECO:0000255|HAMAP-Rule:MF_01554}	-3.23	3.00E-05
ADNP2	ADNP2_HUMAN ADNP homeobox protein 2	4.53	3.18E-05
#N/A	ION3_CARAU Intermediate filament protein ON3	-6.81	3.30E-05
rpl31	RL31_PAROL 60S ribosomal protein L31	-7.32	3.43E-05
#N/A	YB3_XENLA B box-binding protein	-7.69	3.43E-05
rps4	RS4_ICTPU 40S ribosomal protein S4	-4.23	3.43E-05
nqrA	NQRA_VIBAN Na(+)-translocating NADH-quinone reductase subunit A {ECO:0000255|HAMAP-Rule:MF_00425}	3.00	3.77E-05
Prdm1	PRDM1_MOUSE PR domain zinc finger protein 1	-3.69	3.93E-05
Txnl4a	TXN4A_MOUSE Thioredoxin-like protein 4A	-5.23	4.13E-05
STB2	STB2_YEAST Protein STB2	-8.32	4.36E-05
#N/A	#N/A	3.58	5.62E-05
#N/A	#N/A	3.95	6.14E-05
RTase	RTBS_DROME Probable RNA-directed DNA polymerase from transposon BS	2.25	6.14E-05
rlmC	RLMC_HAEIE 23S rRNA (uracil(747)-C(5))-methyltransferase RlmC {ECO:0000255|HAMAP-Rule:MF_01012}	-5.00	6.60E-05
RPL3L	RL3L_BOVIN 60S ribosomal protein L3-like	-5.07	6.72E-05
pnrc2	PNRC2_SALSA Proline-rich nuclear receptor coactivator 2	2.64	6.87E-05
Plec	PLEC_MOUSE Plectin	-5.46	7.10E-05
#N/A	LORF2_HUMAN LINE-1 retrotransposable element ORF2 protein	6.12	7.11E-05
slc35c1	FUCT1_NEMVE GDP-fucose transporter 1	2.78	7.14E-05
Slmap	SLMAP_RAT Sarcolemmal membrane-associated protein	6.07	7.20E-05
HMGB2	HMGB2_CHICK High mobility group protein B2	-3.05	7.44E-05
TYMP	TYPH_HUMAN Thymidine phosphorylase	6.73	8.05E-05
#N/A	#N/A	5.91	8.55E-05
RNH1	RINI_PIG Ribonuclease inhibitor	3.58	8.55E-05
RPLP1	RLA1_CHICK 60S acidic ribosomal protein P1	-7.27	8.69E-05
fdhD	FDHD_WOLSU Sulfurtransferase FdhD {ECO:0000255|HAMAP-Rule:MF_00187}	4.24	1.08E-04
pol	RTJK_DROME RNA-directed DNA polymerase from mobile element jockey	2.76	1.18E-04
TAR1	TAR1_YEAST Protein TAR1	4.22	1.22E-04
TPO2	TPO2_YEAST Polyamine transporter 2	5.98	1.26E-04
Grm3	GRM3_MOUSE Metabotropic glutamate receptor 3	3.95	1.29E-04
RPTN	RPTN_HUMAN Repetin	2.86	1.36E-04
#N/A	#N/A	6.06	1.54E-04
#N/A	#N/A	4.35	1.60E-04
ddl	DDL_RHOE4 D-alanine--D-alanine ligase {ECO:0000255|HAMAP-Rule:MF_00047}	6.11	1.60E-04
Tm6sf2	TM6S2_RAT Transmembrane 6 superfamily member 2	3.87	1.71E-04
ciao1b	CIO1B_SALSA Probable cytosolic iron-sulfur protein assembly protein ciao1-B	-2.51	1.71E-04
#N/A	#N/A	4.47	1.83E-04
X-element\ORF2	RTXE_DROME Probable RNA-directed DNA polymerase from transposon X-element	2.57	1.83E-04
#N/A	TCB1_CAEBR Transposable element Tcb1 transposase	3.97	1.85E-04
pgcA	PGCA_STAS1 Phosphoglucomutase	3.75	1.89E-04
YSL7	YSL7_ARATH Probable metal-nicotianamine transporter YSL7	1.92	1.91E-04
TMP	TMP_BPDP1 Tape measure protein	2.79	1.96E-04

#N/A	VP6_ROTGA Intermediate capsid protein VP6	2.54	1.96E-04
#N/A	#N/A	1.46	1.98E-04
#N/A	YMO3_PANSE Uncharacterized protein in mobD 3'region	4.23	1.98E-04
surE	SURE_DINSH 5'-nucleotidase SurE {ECO:0000255|HAMAP-Rule:MF_00060}	3.65	1.98E-04
#N/A	#N/A	2.80	1.98E-04
#N/A	TCB1_CAEBR Transposable element Tcb1 transposase	3.77	1.98E-04
#N/A	CISY_TETTH Citrate synthase, mitochondrial	-3.37	1.98E-04
#N/A	#N/A	3.68	1.98E-04
klhl3	KLHL3_DANRE Kelch-like protein 3	7.64	2.19E-04
#N/A	#N/A	3.61	2.20E-04
rps24	RS24_TAKRU 40S ribosomal protein S24	-6.86	2.40E-04
MT-ND5	NU5M_SALSA NADH-ubiquinone oxidoreductase chain 5	-3.39	2.40E-04
rpl27a	RL27A_XENLA 60S ribosomal protein L27a	-5.66	2.61E-04
PLCG2	PLCG2_HUMAN 1-phosphatidylinositol 4,5-bisphosphate phosphodiesterase gamma-2	-7.05	2.61E-04
#N/A	#N/A	5.82	2.71E-04
Iars1	SYIC_MOUSE Isoleucine--tRNA ligase, cytoplasmic	-7.12	2.72E-04
#N/A	#N/A	-6.69	1.00E+0 0
#N/A	#N/A	7.42	2.80E-04
#N/A	#N/A	7.75	2.80E-04
Setd2	SETD2_MOUSE Histone-lysine N-methyltransferase SETD2	5.62	2.80E-04
NLRP12	NAL12_HUMAN NACHT, LRR and PYD domains-containing protein 12	4.24	2.80E-04
#N/A	#N/A	2.58	2.80E-04
glmU	GLMU_HYDS0 Bifunctional protein GlmU {ECO:0000255|HAMAP-Rule:MF_01631}	3.85	2.81E-04
ligA	DNLJ_ANADF DNA ligase {ECO:0000255|HAMAP-Rule:MF_01588}	4.02	2.81E-04
#N/A	#N/A	3.97	2.82E-04
Habp2	HABP2_MOUSE Hyaluronan-binding protein 2	-2.66	3.06E-04
#N/A	#N/A	2.65	3.15E-04
#N/A	#N/A	6.05	3.26E-04
MT-ND2	NU2M_SALSA NADH-ubiquinone oxidoreductase chain 2	5.82	3.26E-04
dapA	DAPA_NEIMF 4-hydroxy-tetrahydrodipicolinate synthase	3.07	3.32E-04
TAN1	TAN1_YEAST tRNA acetyltransferase TAN1	3.06	3.36E-04
#N/A	TCB1_CAEBR Transposable element Tcb1 transposase	2.17	3.37E-04
g6pd	G6PD_TAKRU Glucose-6-phosphate 1-dehydrogenase	3.88	3.46E-04
#N/A	TCB2_CAEBR Transposable element Tcb2 transposase	6.10	4.02E-04
creD	CRED_ECOLI Inner membrane protein CreD	2.83	4.02E-04
tc1a	TC1A_CAEEL Transposable element Tc1 transposase	3.23	4.02E-04
ABI1	ABI1_HUMAN Abl interactor 1	3.82	4.03E-04
miaB	MIAB_ARTS2 tRNA-2-methylthio-N(6)-dimethylallyladenosine synthase {ECO:0000255|HAMAP-Rule:MF_01864}	7.11	4.08E-04
cpy1	CBPY_SCHPO Carboxypeptidase Y	4.78	4.14E-04
TRIM14	TRI14_HUMAN Tripartite motif-containing protein 14	4.80	4.19E-04
#N/A	#N/A	3.72	4.29E-04
BQ2027_M B2259	Y2259_MYCBO Uncharacterized SURF1-like protein Mb2259	5.62	4.45E-04
IML1	IML1_USTMA Vacuolar membrane-associated protein IML1	2.31	4.45E-04
tc1a	TC1A_CAEEL Transposable element Tc1 transposase	3.01	4.75E-04
K02A2.6	YRD6_CAEEL Uncharacterized protein K02A2.6	2.49	4.92E-04
#N/A	#N/A	-6.48	1.00E+0 0
Rps14	RS14_MOUSE 40S ribosomal protein S14	-7.02	4.99E-04
#N/A	YTX2_XENLA Transposon TX1 uncharacterized 149 kDa protein	2.29	5.01E-04
phactr4-b	PHR4B_XENLA Phosphatase and actin regulator 4-B	6.24	5.14E-04
wdr26	WDR26_DANRE WD repeat-containing protein 26	5.07	5.14E-04
RRT15	RRT15_YEAST Regulator of rDNA transcription protein 15	3.96	5.53E-04
#N/A	#N/A	3.63	5.68E-04
rpsa	RSSA_SALSA 40S ribosomal protein SA {ECO:0000255|HAMAP-Rule:MF_03016}	-5.63	5.79E-04
yheD	YHED_BACSU Endospore coat-associated protein YheD	6.45	5.85E-04
SOCS3	SOCS3_CHICK Suppressor of cytokine signaling 3	-2.46	5.88E-04
rps2	RS2_ICTPU 40S ribosomal protein S2	-3.26	5.99E-04
#N/A	#N/A	4.88	6.45E-04
#N/A	#N/A	3.26	6.45E-04
#N/A	#N/A	5.96	6.60E-04
Rpl12	RL12_MOUSE 60S ribosomal protein L12	-4.32	6.61E-04
#N/A	LIN1_NYCCO LINE-1 reverse transcriptase homolog	2.99	6.64E-04
IARS1	SYIC_HUMAN Isoleucine--tRNA ligase, cytoplasmic	5.22	6.83E-04

#N/A	#N/A	2.34	6.83E-04
ERVPABLB-1	ERB1_HUMAN Endogenous retrovirus group PABLB member 1 Env polyprotein	2.64	6.84E-04
TRV_01442	ACUK_TRIVH Transcription activator of gluconeogenesis TRV_01442	5.74	7.06E-04
#N/A	#N/A	3.29	7.08E-04
ZB8	PAL2_ORYSJ Phenylalanine ammonia-lyase	-3.43	7.17E-04
csf1r1	CSF11_TAKRU Macrophage colony-stimulating factor 1 receptor 1	6.27	7.59E-04
tc1a	TC1A_CAEEL Transposable element Tc1 transposase	3.24	7.70E-04
#N/A	#N/A	2.61	7.70E-04
SGA1	AMYG_YEAST Glucoamylase, intracellular sporulation-specific	2.31	7.75E-04
#N/A	ALDOA_SALSA Fructose-bisphosphate aldolase A {ECO:0000303|PubMed:23786287}	4.96	7.82E-04
cysS	SYC_BAUCH Cysteine--tRNA ligase {ECO:0000255|HAMAP-Rule:MF_00041}	-2.97	7.82E-04
#N/A	#N/A	4.68	7.82E-04
#N/A	YL004_HUMAN Putative uncharacterized protein FLJ45999	3.86	8.16E-04
#N/A	GLNA_RHOSH Glutamine synthetase	5.22	8.29E-04
jockey\pol	RTJK_DROFU RNA-directed DNA polymerase from mobile element jockey	1.94	8.58E-04
MELTF	TRFM_RABIT Melanotransferrin	5.73	8.62E-04
EFR3	EFR3_COCIM Protein EFR3	4.78	8.85E-04
HERC1	HERC1_HUMAN Probable E3 ubiquitin-protein ligase HERC1	5.18	8.89E-04
#N/A	YMO3_PANSE Uncharacterized protein in mobD 3'region	3.73	9.34E-04
TPK3	TPK3_ORYSJ Thiamine pyrophosphokinase 3	6.06	9.41E-04
pol	RTJK_DROME RNA-directed DNA polymerase from mobile element jockey	4.09	9.47E-04
RTase	RTBS_DROME Probable RNA-directed DNA polymerase from transposon BS	2.95	9.48E-04
A	VGA_BPS13 A' protein	-3.54	9.48E-04
#N/A	#N/A	3.39	0.0010
#N/A	#N/A	5.03	0.0010
Stx3	STX3_MOUSE Syntaxin-3	-7.12	0.0011
Rpl38	RL38_RAT 60S ribosomal protein L38	-5.68	1.0000
#N/A	#N/A	3.12	0.0011
#N/A	PVDB_PLAKN Duffy receptor beta form	2.64	0.0011
CHT2	CHI2_CANAL Chitinase 2	3.92	0.0011
ART2	ART2_YEAST Putative uncharacterized protein ART2	4.18	0.0012
#N/A	#N/A	4.05	0.0012
#N/A	TCB1_CAEBR Transposable element Tcb1 transposase	1.92	0.0012
ZBED5	ZBED5_CANLF Zinc finger BED domain-containing protein 5	2.74	0.0012
Mag	MAG_RAT Myelin-associated glycoprotein	4.62	0.0012
#N/A	SDPR_RAT Serum deprivation-response protein	2.00	0.0013
Ttn	TITIN_MOUSE Titin	3.27	0.0013
#N/A	#N/A	2.41	0.0013
#N/A	#N/A	2.55	0.0013
bigA	BIGA_SALTY Putative surface-exposed virulence protein BigA	5.82	0.0013
Pls1	PLSI_MOUSE Plastin-1	5.03	0.0013
eef1ao	EF1A2_XENLA Elongation factor 1-alpha, oocyte form	-2.61	0.0013
GATAD2A	P66A_HUMAN Transcriptional repressor p66-alpha	-6.40	1.0000
#N/A	#N/A	-2.78	0.0014
#N/A	#N/A	4.15	0.0014
Paxbp1	PAXB1_MOUSE PAX3- and PAX7-binding protein 1	5.53	0.0014
focA	FOCA_ECOLI Probable formate transporter 1	4.02	0.0014
Tril	TRIL_MOUSE TLR4 interactor with leucine rich repeats	3.76	0.0014
#N/A	#N/A	3.21	0.0014
Sun1	SUN1_MOUSE SUN domain-containing protein 1	3.09	0.0014
#N/A	#N/A	5.71	0.0014
#N/A	#N/A	5.60	0.0014
#N/A	#N/A	3.52	0.0014
MJ0138	Y138_METJA Putative glutamine amidotransferase-like protein MJ0138	4.21	0.0014
#N/A	#N/A	5.80	0.0014
tc1a	TC1A_CAEEL Transposable element Tc1 transposase	5.58	0.0014
TRIM11	TRI11_BOVIN E3 ubiquitin-protein ligase TRIM11	3.56	0.0014
#N/A	#N/A	3.45	0.0015
lap-2	YH24_CAEEL Putative aminopeptidase W07G4.4	-6.10	0.0015
#N/A	#N/A	5.87	0.0015
#N/A	#N/A	-6.32	1.0000
#N/A	#N/A	3.86	0.0015
Cobll1	COBL1_MOUSE Cordon-bleu protein-like 1	2.49	0.0015
#N/A	LORF2_HUMAN LINE-1 retrotransposable element ORF2 protein	3.07	0.0015

#N/A	#N/A	4.27	0.0015
ANO5	ANO5_HUMAN Anoctamin-5	5.59	0.0015
tc1a	TC1A_CAEEL Transposable element Tc1 transposase	2.79	0.0015
infB	IF2_BORBU Translation initiation factor IF-2	4.33	0.0015
ureF	UREF_RUEST Urease accessory protein UreF {ECO:0000255|HAMAP-Rule:MF_01385}	4.49	0.0016
#N/A	#N/A	2.76	0.0016
ANXA11	ANX11_HUMAN Annexin A11	4.92	0.0016
hisH	HIS5_BACFN Imidazole glycerol phosphate synthase subunit HisH {ECO:0000255|HAMAP-Rule:MF_00278}	1.96	0.0016
SNX9	SNX9_HUMAN Sorting nexin-9	2.02	0.0016
FAM133	F133_CHICK Protein FAM133	-3.32	0.0016
dpp3	DPP3_NEMVE Dipeptidyl peptidase 3	2.76	0.0016
#N/A	#N/A	3.77	0.0017
#N/A	FMRA_CALPA Antho-RFamide neuropeptides	3.71	0.0017
per	PER_DROPS Period circadian protein	5.64	0.0017
RPS5	RS5_HUMAN 40S ribosomal protein S5	-3.42	0.0017
#N/A	#N/A	3.80	0.0017
TAR1	TAR1_YEAST Protein TAR1	3.84	0.0017
#N/A	TCB1_CAEBR Transposable element Tcb1 transposase	4.01	0.0017
#N/A	VDAC1_SOLTU Mitochondrial outer membrane protein porin of 34 kDa	4.96	0.0017
rpl13a	RL13A_SALTR 60S ribosomal protein L13a	-2.62	0.0017
VAPA	VAPA_PONAB Vesicle-associated membrane protein-associated protein A	3.82	0.0018
Ldb3	LDB3_MOUSE LIM domain-binding protein 3	3.50	0.0018
STIM1	STIM1_HUMAN Stromal interaction molecule 1	-3.67	0.0018
#N/A	#N/A	5.22	0.0018
#N/A	#N/A	2.05	0.0019
#N/A	CUG1A_TENMO Pupal cuticle protein G1A	5.21	0.0019
#N/A	#N/A	4.72	0.0019
Nlrc3	NLRC3_MOUSE Protein NLRC3	3.56	0.0019
GTF2E1	T2EA_BOVIN General transcription factor IIE subunit 1	3.32	0.0019
dlg1	DLG1_DROME Disks large 1 tumor suppressor protein	3.89	0.0020
#N/A	#N/A	3.12	0.0020
#N/A	#N/A	4.02	0.0020
SV2C	SV2C_HUMAN Synaptic vesicle glycoprotein 2C	4.10	0.0020
NFYB	NFYB_BOVIN Nuclear transcription factor Y subunit beta	-4.46	0.0020
ybx1	YBOX1_XENLA Nuclease-sensitive element-binding protein 1	4.94	0.0020
PSAP	SAP_BOVIN Prosaposin	-3.12	0.0020
#N/A	PERQ1_MOUSE PERQ amino acid-rich with GYF domain-containing protein 1	-5.10	0.0020
ECU11_1100	SYIC_ENCCU Probable isoleucine--tRNA ligase, cytoplasmic	-2.40	0.0020
#N/A	TCB2_CAEBR Transposable element Tcb2 transposase	3.65	0.0020
GM2	CRGM2_CHIID Gamma-crystallin M2	4.40	0.0020
med19a	MD19A_DANRE Mediator of RNA polymerase II transcription subunit 19-A	4.89	0.0020
frr	RRF_ZYMMO Ribosome-recycling factor {ECO:0000255|HAMAP-Rule:MF_00040}	3.19	0.0021
TGas006m08.1	H4_XENTR Histone H4	-1.73	0.0022
#N/A	#N/A	3.84	0.0022
serS	SYS_CHLPN Serine--tRNA ligase {ECO:0000255|HAMAP-Rule:MF_00176}	4.16	0.0023
RPL5	RL5_CHICK 60S ribosomal protein L5	-2.28	0.0023
Saci_1674	Y1674_SULAC Uncharacterized protein Saci_1674	4.61	0.0023
HMGN3	HMGN3_CHICK High mobility group nucleosome-binding domain-containing protein 3	5.22	0.0023
#N/A	#N/A	2.19	0.0023
FBXO2	FBX2_BOVIN F-box only protein 2	4.91	0.0023
PME2	PME2_ARATH Pectinesterase 2	3.29	0.0023
TENM2	TEN2_CHICK Teneurin-2	3.94	0.0023
CCDC15	CCD15_HUMAN Coiled-coil domain-containing protein 15	3.14	0.0023
#N/A	LEC_GALNI Mannose-specific lectin	-2.40	0.0023
A2M	A2MG_PONAB Alpha-2-macroglobulin	2.89	0.0023
unc-31	CAPS_CAEBR Calcium-dependent secretion activator	4.17	0.0023
MSRB1	MSRB1_BOVIN Methionine-R-sulfoxide reductase B1	4.60	0.0024
#N/A	#N/A	5.69	0.0024
#N/A	#N/A	4.09	0.0024
dbnl-a	DBNLA_XENLA Drebrin-like protein A	4.72	0.0024
#N/A	#N/A	4.64	0.0025
nppa	ANF_OREMO Natriuretic peptides A	-3.96	0.0025
pol	RTJK_DROME RNA-directed DNA polymerase from mobile element jockey	3.09	0.0025

b2m	B2MG_ICTPU Beta-2-microglobulin	-4.21	0.0025
ERVV-2	ERVV2_HUMAN Endogenous retrovirus group V member 2 Env polyprotein	5.22	0.0025
ATG12	ATG12_PICGU Ubiquitin-like protein ATG12	5.10	0.0025
DHRS13	DHR13_BOVIN Dehydrogenase/reductase SDR family member 13	5.54	0.0025
ORF2	CAPSD_PASV1 Capsid polyprotein VP90	5.43	0.0025
GPR179	GP179_HUMAN Probable G-protein coupled receptor 179	3.95	0.0025
plsB	PLSB_PHOLL Glycerol-3-phosphate acyltransferase	5.02	0.0025
#N/A	#N/A	2.90	0.0025
hisC	HIS8_CAMJD Histidinol-phosphate aminotransferase	4.59	0.0025
#N/A	SMAKA_XENLA Small membrane A-kinase anchor protein	5.02	0.0025
#N/A	#N/A	4.20	0.0025
#N/A	#N/A	5.19	0.0025
#N/A	#N/A	5.16	0.0025
rny	RNY_LEUCK Ribonuclease Y {ECO:0000255|HAMAP-Rule:MF_00335}	4.57	0.0025
#N/A	#N/A	3.21	0.0025
ALOXE3	LOXE3_HUMAN Hydroperoxide isomerase ALOXE3	-2.92	0.0025
#N/A	TCB1_CAEBR Transposable element Tcb1 transposase	2.74	0.0026
CCL21	CCL21_MACMU C-C motif chemokine 21	3.32	0.0026
#N/A	TCB1_CAEBR Transposable element Tcb1 transposase	2.87	0.0026
PLCXD1	PLCX1_HUMAN PI-PLC X domain-containing protein 1	3.16	0.0026
ATG12	ATG12_PICGU Ubiquitin-like protein ATG12	4.81	0.0026
#N/A	#N/A	2.45	0.0026
ycf80	YCF80_GUITH Uncharacterized protein ycf80	5.61	0.0026
#N/A	#N/A	3.74	0.0027
ligA	DNLJ_PSEU5 DNA ligase {ECO:0000255|HAMAP-Rule:MF_01588}	2.29	0.0027
#N/A	#N/A	3.38	0.0027
#N/A	#N/A	5.75	0.0027
MJ0463	SUI1_METJA Protein translation factor SUI1 homolog	-2.59	0.0027
FKBP3	FKBP3_BOVIN Peptidyl-prolyl cis-trans isomerase FKBP3	2.06	0.0027
tc3a	TC3A_CAEEL Transposable element Tc3 transposase	4.88	0.0027
MYO18B	MY18B_HUMAN Unconventional myosin-XVIIIb	-6.03	1.0000
#N/A	#N/A	5.22	0.0028
cep170b	C170B_XENTR Centrosomal protein of 170 kDa protein B	-2.27	0.0028
Cmklr1	CML1_RAT Chemokine-like receptor 1	4.08	0.0028
#N/A	#N/A	3.82	0.0028
SPBPJ4664.02	YHU2_SCHPO Uncharacterized threonine-rich GPI-anchored glycoprotein PJ4664.02	5.47	0.0029
#N/A	TCB1_CAEBR Transposable element Tcb1 transposase	2.83	0.0029
dpp3	DPP3_NEMVE Dipeptidyl peptidase 3	2.92	0.0029
WDTC1	WDTC1_HUMAN WD and tetratricopeptide repeats protein 1	-2.25	0.0029
#N/A	#N/A	-2.52	0.0030
#N/A	TCB2_CAEBR Transposable element Tcb2 transposase	4.55	0.0031
#N/A	#N/A	2.99	0.0031
rpl36a	RL36A_TAKRU 60S ribosomal protein L36a	-4.54	0.0031
Trdn	TRDN_RAT Triadin	-5.28	0.0031
priS	PRIS_THEVO DNA primase small subunit PriS {ECO:0000255|HAMAP-Rule:MF_00700}	2.95	0.0031
Pdss1	DPS1_MOUSE Decaprenyl-diphosphate synthase subunit 1	-1.82	0.0031
uvrC	UVRC_LACGA UvrABC system protein C {ECO:0000255|HAMAP-Rule:MF_00203}	-2.99	0.0032
#N/A	Y481_PSYCK Maf-like protein Pcryo_0481 {ECO:0000255|HAMAP-Rule:MF_00528}	2.94	0.0032
#N/A	#N/A	3.19	0.0032
tc1a	TC1A_CAEEL Transposable element Tc1 transposase	4.17	0.0033
jockey\pol	RTJK_DROFU RNA-directed DNA polymerase from mobile element jockey	2.75	0.0033
#N/A	#N/A	2.32	0.0033
#N/A	#N/A	3.12	0.0033
#N/A	#N/A	3.50	0.0033
Acaca	ACACA_MOUSE Acetyl-CoA carboxylase 1	-7.16	0.0033
Srsf4	SRSF4_MOUSE Serine/arginine-rich splicing factor 4	-3.33	0.0034
#N/A	TCB1_CAEBR Transposable element Tcb1 transposase	2.62	0.0034
PRICKLE1	PRIC1_HUMAN Prickle-like protein 1	4.57	0.0034
MARCKSL1	MRP_HUMAN MARCKS-related protein	-2.80	0.0034
#N/A	#N/A	2.17	0.0034
#N/A	TCB2_CAEBR Transposable element Tcb2 transposase	2.37	0.0034
#N/A	#N/A	2.68	0.0034
#N/A	TCB2_CAEBR Transposable element Tcb2 transposase	2.46	0.0034

b2m	B2MG_ICTPU Beta-2-microglobulin	3.19	0.0034
ART2	ART2_YEAST Putative uncharacterized protein ART2	2.90	0.0034
#N/A	#N/A	4.22	0.0034
#N/A	#N/A	3.21	0.0034
#N/A	#N/A	2.68	0.0034
HOXD12	HXD12_CHICK Homeobox protein Hox-D12	2.44	0.0034
ERVFC1	EFC1_HUMAN Endogenous retrovirus group FC1 Env polyprotein	3.38	0.0034
pol	RTJK_DROME RNA-directed DNA polymerase from mobile element jockey	2.02	0.0034
#N/A	#N/A	5.84	0.0035
RNH1	RINI_PIG Ribonuclease inhibitor	4.87	0.0035
CCDC15	CCD15_HUMAN Coiled-coil domain-containing protein 15	3.67	0.0035
PLEKHA5	PKHA5_HUMAN Pleckstrin homology domain-containing family A member 5	-1.23	0.0035
#N/A	TCB1_CAEBR Transposable element Tcb1 transposase	4.87	0.0035
#N/A	H3_URECA Histone H3	-1.88	0.0035
NLRP3	NLRP3_BOVIN NACHT, LRR and PYD domains-containing protein 3	3.45	0.0035
cirbp-b	CIRBB_XENLA Cold-inducible RNA-binding protein B	-3.03	0.0036
murC	MURC_JANMA UDP-N-acetylmuramate--L-alanine ligase	5.22	0.0036
#N/A	#N/A	5.73	0.0037
SOV	DI3L2_ARATH DIS3-like exonuclease 2 {ECO:0000255|HAMAP-Rule:MF_03045}	2.94	0.0038
jockey\pol	RTJK_DROFU RNA-directed DNA polymerase from mobile element jockey	2.58	0.0038
#N/A	#N/A	2.07	0.0038
vps36	VPS36_DANRE Vacuolar protein-sorting-associated protein 36	1.63	0.0039
argC	ARGC_PELTS N-acetyl-gamma-glutamyl-phosphate reductase	3.58	0.0039
EIF4A1	IF4A1_PONAB Eukaryotic initiation factor 4A-I	-3.03	0.0039
RPL32	RL32_BOVIN 60S ribosomal protein L32	-5.75	0.0039
tc1a	TC1A_CAEEL Transposable element Tc1 transposase	3.46	0.0039
ZNF468	ZN468_HUMAN Zinc finger protein 468	-6.17	1.0000
yap1	YAP1_DANRE Transcriptional coactivator YAP1	2.97	0.0039
#N/A	GLNA_BACFR Glutamine synthetase	2.95	0.0039
Cntrl	CNTRL_MOUSE Centriolin	4.53	0.0039
#N/A	#N/A	3.67	0.0040
#N/A	TCB1_CAEBR Transposable element Tcb1 transposase	5.41	0.0041
ybcI	YBCI_BACSU Uncharacterized protein YbcI	4.05	0.0041
#N/A	#N/A	2.53	0.0041
#N/A	#N/A	2.84	0.0042
TBL1XR1	TBL1R_HUMAN F-box-like/WD repeat-containing protein TBL1XR1	6.17	0.0042
#N/A	NDB4G_UROYA Antimicrobial peptide UyCT1 {ECO:0000303|PubMed:23182832}	-2.37	0.0042
TBCA	TBCA_CHICK Tubulin-specific chaperone A	3.07	0.0043
#N/A	TCB1_CAEBR Transposable element Tcb1 transposase	2.40	0.0043
jockey\pol	RTJK_DROFU RNA-directed DNA polymerase from mobile element jockey	1.64	0.0043
#N/A	#N/A	3.30	0.0043
#N/A	#N/A	4.98	0.0043
ANK2	ANK2_HUMAN Ankyrin-2	3.94	0.0043
#N/A	HM14A_CHICK Non-histone chromosomal protein HMG-14A	-4.35	1.0000
#N/A	TCB2_CAEBR Transposable element Tcb2 transposase	3.12	0.0044
SO_1816	Y1816_SHEON UPF0319 protein SO_1816 {ECO:0000255|HAMAP-Rule:MF_00789}	4.92	0.0045
tc1a	TC1A_CAEEL Transposable element Tc1 transposase	3.54	0.0046
OR4D10	OR4DA_HUMAN Olfactory receptor 4D10	3.61	0.0046
#N/A	#N/A	3.54	0.0047
tc1a	TC1A_CAEEL Transposable element Tc1 transposase	4.54	0.0047
psiJ	PSIJ_DICDI Protein psiJ	4.10	0.0047
RORB	RORB_HUMAN Nuclear receptor ROR-beta	2.19	0.0047
#N/A	#N/A	2.05	0.0048
RNF186	RN186_HUMAN RING finger protein 186	-1.50	0.0048
mdh	MDH_DESAP Malate dehydrogenase {ECO:0000255|HAMAP-Rule:MF_00487}	3.33	0.0049
tc1a	TC1A_CAEEL Transposable element Tc1 transposase	2.96	0.0049
Tmed2	TMED2_MOUSE Transmembrane emp24 domain-containing protein 2	4.52	0.0049
wdhd1	WDHD1_XENLA WD repeat and HMG-box DNA-binding protein 1	4.63	0.0050
#N/A	TCB1_CAEBR Transposable element Tcb1 transposase	5.30	0.0051
ND5	NU5M_BRAFL NADH-ubiquinone oxidoreductase chain 5	3.17	0.0051
rpl13a	RL13A_SALTR 60S ribosomal protein L13a	5.25	0.0051
Minpp1	MINP1_MOUSE Multiple inositol polyphosphate phosphatase 1	3.35	0.0051
#N/A	#N/A	4.54	0.0051
#N/A	#N/A	2.97	0.0051
Rps8	RS8_RAT 40S ribosomal protein S8	-2.02	0.0051
S	SPIKE_CVMA5 Spike glycoprotein	5.48	0.0051

GLS	GLSK_HUMAN Glutaminase kidney isoform, mitochondrial	5.01	0.0052
cdk-8	CDK8_CAEEL Cyclin-dependent kinase 8	4.25	0.0052
RPII	RPB1_PLAFD DNA-directed RNA polymerase II subunit RPB1	3.14	0.0052
#N/A	#N/A	2.29	0.0052
BUD3	BUD3_ASHGO Bud site selection protein 3 homolog	2.37	0.0052
SPAC26H5.02c	WRIP1_SCHPO ATPase WRNIP1 homolog C26H5.02c	2.58	0.0053
rps6	RS6_ONCMY 40S ribosomal protein S6	-3.96	0.0053
#N/A	TCB1_CAEBR Transposable element Tcb1 transposase	2.84	0.0053
#N/A	#N/A	3.28	0.0053
#N/A	#N/A	5.54	0.0054
tc1a	TC1A_CAEEL Transposable element Tc1 transposase	3.49	0.0054
LRP8	LRP8_CHICK Low-density lipoprotein receptor-related protein 8	-5.52	1.0000
rps3-a	RS31_XENLA 40S ribosomal protein S3-A	-3.29	0.0055
GIMAP4	GIMA4_HUMAN GTPase IMAP family member 4	2.16	0.0055
gatB	GATB_LACAC Aspartyl/glutamyl-tRNA(Asn/Gln) amidotransferase subunit B	4.71	0.0055
Nmul_A1548	GCS2_NITMU Putative glutamate--cysteine ligase 2	2.60	0.0055
#N/A	#N/A	5.24	0.0055
VOZ2	VOZ2_ARATH Transcription factor VOZ2	3.45	0.0055
GPR89B	GPHRB_HUMAN Golgi pH regulator B	3.30	0.0055
fp-1	FP1V1_PERVI Foot protein 1 variant 1	3.10	0.0055
#N/A	#N/A	4.90	0.0056
SAP13	SAP13_ARATH Zinc finger AN1 and C2H2 domain-containing stress-associated protein 13	4.13	0.0056
SEMA6D	SEM6D_PONAB Semaphorin-6D	4.52	0.0056
#N/A	#N/A	3.51	0.0057
CAD2	CADH2_ORYSJ Cinnamyl alcohol dehydrogenase 2	3.24	0.0057
#N/A	#N/A	2.62	0.0057
#N/A	#N/A	4.44	0.0057
mutS	MUTS_PROMT DNA mismatch repair protein MutS	-3.47	0.0058
tapt1	TAPT1_XENLA Transmembrane anterior posterior transformation protein 1 homolog	6.18	0.0058
tc1a	TC1A_CAEEL Transposable element Tc1 transposase	2.71	0.0058
#N/A	#N/A	2.21	0.0058
tc1a	TC1A_CAEEL Transposable element Tc1 transposase	3.06	0.0058
tc3a	TC3A_CAEEL Transposable element Tc3 transposase	3.57	0.0058
#N/A	#N/A	3.34	0.0058
#N/A	#N/A	3.39	0.0060
FAM186A	F186A_MOUSE Protein FAM186A	3.20	0.0060
#N/A	#N/A	-2.12	0.0060
TOP3A	TOP3A_ORYSJ DNA topoisomerase 3-alpha	3.40	0.0060
ncl	NUCL_XENLA Nucleolin	-2.13	0.0061
PEG3	PEG3_BOVIN Paternally-expressed gene 3 protein	5.35	0.0061
tsf	EFTS_DESPS Elongation factor Ts {ECO:0000255|HAMAP-Rule:MF_00050}	2.58	0.0063
Rplp1	RLA1_MOUSE 60S acidic ribosomal protein P1	-5.98	1.0000
#N/A	#N/A	2.41	0.0064
#N/A	TCB2_CAEBR Transposable element Tcb2 transposase	4.69	0.0064
MED8	MED8_YARLI Mediator of RNA polymerase II transcription subunit 8	3.65	0.0064
#N/A	#N/A	5.08	0.0064
YSL7	YSL7_ARATH Probable metal-nicotianamine transporter YSL7	1.10	0.0064
#N/A	TCB1_CAEBR Transposable element Tcb1 transposase	1.72	0.0064
#N/A	#N/A	3.17	0.0064
tc1a	TC1A_CAEEL Transposable element Tc1 transposase	5.66	0.0066
Ascc3	ASCC3_RAT Activating signal cointegrator 1 complex subunit 3	3.20	0.0066
Marcksl1	MRP_RAT MARCKS-related protein	-3.63	1.0000
uvrC	UVRC_KORVE UvrABC system protein C {ECO:0000255|HAMAP-Rule:MF_00203}	3.34	0.0066
glnE	GLNE_IDILO Glutamate-ammonia-ligase adenylyltransferase	3.62	0.0066
SSI2	STAD2_ORYSJ Stearoyl-[acyl-carrier-protein] 9-desaturase 2, chloroplastic	5.00	0.0066
Rpl17	RL17_RAT 60S ribosomal protein L17	-5.37	0.0066
flp-3	FLP03_CAEEL FMRFamide-like neuropeptides 3	3.67	0.0067
S	SPIKE_CVPR8 Spike glycoprotein	2.15	0.0067
Sprr1b	SPR1B_MOUSE Cornifin-B	4.75	0.0067
rps6	RS6_ONCMY 40S ribosomal protein S6	-3.56	0.0067
#N/A	#N/A	4.09	0.0068
#N/A	TCB1_CAEBR Transposable element Tcb1 transposase	2.59	0.0069
#N/A	TCB1_CAEBR Transposable element Tcb1 transposase	2.76	0.0069

#N/A	#N/A	-3.25	0.0069
c1galt1b	C1GTB_DANRE Glycoprotein-N-acetylgalactosamine 3-beta-galactosyltransferase 1-B	-2.95	0.0070
#N/A	YHS4_SCHPO Putative cell agglutination protein C947.04	1.83	0.0071
#N/A	#N/A	4.33	0.0072
#N/A	#N/A	3.45	0.0072
SPAC26H5.02c	WRIP1_SCHPO ATPase WRNIP1 homolog C26H5.02c	2.16	0.0072
jockey\pol	RTJK_DROFU RNA-directed DNA polymerase from mobile element jockey	5.03	0.0072
tc1a	TC1A_CAEEL Transposable element Tc1 transposase	2.55	0.0072
#N/A	#N/A	3.38	0.0072
HOXD12	HXD12_CHICK Homeobox protein Hox-D12	2.69	0.0072
TL1	TP1A_MALDO Thaumatin-like protein 1a	4.33	0.0073
GLI2	GLI2_CHICK Zinc finger protein GLI2 {ECO:0000305}	2.72	0.0073
MHR1	MHR1_CANAL Mitochondrial homologous recombination protein 1	2.45	0.0073
#N/A	TCB1_CAEBR Transposable element Tcb1 transposase	1.89	0.0073
PAQR3	PAQR3_HUMAN Progestin and adipoQ receptor family member 3	2.63	0.0073
#N/A	MYP_STRPU Major yolk protein	2.85	0.0073
#N/A	#N/A	4.35	0.0074
APOB	APOB_HUMAN Apolipoprotein B-100	5.06	0.0074
alkS	ALKS_PSEOL HTH-type transcriptional regulator AlkS	3.15	0.0074
gmppb	GMPPB_DANRE Mannose-1-phosphate guanyltransferase beta	2.53	0.0074
Syngr1	SNG1_RAT Synaptogyrin-1	3.09	0.0074
SESN1	SESN1_MACFA Sestrin-1	4.62	0.0074
RRT12	RRT12_YEAST Subtilase-type proteinase RRT12	-3.01	0.0075
#N/A	YTX2_XENLA Transposon TX1 uncharacterized 149 kDa protein	3.71	0.0075
cos	COS_DROPS Kinesin-like protein costa	3.54	0.0075
AS2	ASNS2_PEA Asparagine synthetase, root [glutamine-hydrolyzing]	4.38	0.0075
frr	RRF_ZYMMO Ribosome-recycling factor {ECO:0000255|HAMAP-Rule:MF_00040}	3.53	0.0076
#N/A	TCB1_CAEBR Transposable element Tcb1 transposase	4.19	0.0076
#N/A	TCB1_CAEBR Transposable element Tcb1 transposase	2.27	0.0076
jockey\pol	RTJK_DROFU RNA-directed DNA polymerase from mobile element jockey	1.85	0.0076
Map7d1	MA7D1_MOUSE MAP7 domain-containing protein 1	4.11	0.0077
Hcar2	HCAR2_RAT Hydroxycarboxylic acid receptor 2	2.55	0.0077
Fam120b	F120B_MOUSE Constitutive coactivator of peroxisome proliferator-activated receptor gamma	4.44	0.0077
glgC	GLGC_BACHD Glucose-1-phosphate adenylyltransferase	2.50	0.0078
CDC45	CDC45_HUMAN Cell division control protein 45 homolog	-3.87	0.0078
#N/A	TCB1_CAEBR Transposable element Tcb1 transposase	3.64	0.0079
RAD5	RAD5_DEBHA DNA repair protein RAD5	5.53	0.0079
MPH1	MPH1_KLULA ATP-dependent DNA helicase MPH1	2.21	0.0079
#N/A	#N/A	1.96	0.0080
RXFP1	RXFP1_PONAB Relaxin receptor 1	4.29	0.0080
flaA	FLAA_BORBU Flagellar filament outer layer protein	4.33	0.0080
#N/A	#N/A	3.14	0.0080
#N/A	TCB1_CAEBR Transposable element Tcb1 transposase	2.30	0.0081
TRIM16	TRI16_HUMAN Tripartite motif-containing protein 16	1.90	0.0081
tc1a	TC1A_CAEEL Transposable element Tc1 transposase	4.53	0.0082
ureC	URE1_PSEF5 Urease subunit alpha {ECO:0000255|HAMAP-Rule:MF_01953}	4.61	0.0082
tc1a	TC1A_CAEEL Transposable element Tc1 transposase	2.83	0.0083
NEK8	NEK8_HUMAN Serine/threonine-protein kinase Nek8	4.24	0.0084
#N/A	TCB1_CAEBR Transposable element Tcb1 transposase	2.81	0.0084
Os11g0109000	P2C73_ORYSJ Probable protein phosphatase 2C 73	2.36	0.0084
RORB	RORB_HUMAN Nuclear receptor ROR-beta	1.29	0.0084
#N/A	#N/A	3.58	0.0084
tc1a	TC1A_CAEEL Transposable element Tc1 transposase	3.50	0.0085
vlpE	VLPE_MYCHR Variant surface antigen E	5.10	0.0087
proA	PROA_PROMA Gamma-glutamyl phosphate reductase	5.42	0.0087
#N/A	#N/A	2.49	0.0088
fmt	FMT_AQUAE Methionyl-tRNA formyltransferase	4.04	0.0089
#N/A	#N/A	4.42	0.0089
galK	GAL1_CALS4 Galactokinase {ECO:0000255|HAMAP-Rule:MF_00246}	4.90	0.0089
ATG12	ATG12_PICGU Ubiquitin-like protein ATG12	2.93	0.0089
#N/A	TCB1_CAEBR Transposable element Tcb1 transposase	3.77	0.0090
trpE	TRPE_BUCPS Anthranilate synthase component 1	3.95	0.0090
tc1a	TC1A_CAEEL Transposable element Tc1 transposase	3.10	0.0090

Mob4	PHOCN_RAT MOB-like protein phocein	2.32	0.0090
QRICH2	QRIC2_HUMAN Glutamine-rich protein 2	3.83	0.0090
gpsA	GPDA_LACSS Glycerol-3-phosphate dehydrogenase [NAD(P)+] {ECO:0000255|HAMAP-Rule:MF_00394}	3.47	0.0090
#N/A	#N/A	4.08	0.0090
#N/A	#N/A	2.41	0.0090
VEF	VEF_GVTN Viral-enhancing factor	4.58	0.0092
KLHL33	KLH33_HUMAN Kelch-like protein 33	2.98	0.0092
GPA33	GPA33_HUMAN Cell surface A33 antigen	3.13	0.0092
Bard1	BARD1_MOUSE BRCA1-associated RING domain protein 1	3.90	0.0092
Msmp	MSMP_MOUSE Prostate-associated microseminoprotein	-4.56	0.0092
#N/A	TCB2_CAEBR Transposable element Tcb2 transposase	4.24	0.0092
#N/A	#N/A	4.59	0.0092
#N/A	#N/A	1.98	0.0092
rpl9	RL9_ICTPU 60S ribosomal protein L9	4.88	0.0092
tc1a	TC1A_CAEEL Transposable element Tc1 transposase	3.09	0.0093
pol	POL5_DROME Retrovirus-related Pol polyprotein from transposon opus	3.42	0.0093
#N/A	TCB2_CAEBR Transposable element Tcb2 transposase	3.76	0.0093
#N/A	TCB1_CAEBR Transposable element Tcb1 transposase	1.77	0.0094
Cd74	HG2A_RAT H-2 class II histocompatibility antigen gamma chain	-1.53	0.0094
FZD3	FZD3_HUMAN Frizzled-3	4.21	0.0094
#N/A	#N/A	3.07	0.0094
#N/A	#N/A	1.83	0.0094
#N/A	#N/A	2.85	0.0095
ITPRIPL2	IPIL2_HUMAN Inositol 1,4,5-trisphosphate receptor-interacting protein-like 2	3.58	0.0095
h2az2	H2AV_XENTR Histone H2A.V	-4.95	1.0000
#N/A	#N/A	3.48	0.0096
#N/A	#N/A	2.72	0.0096
PF10_0343	SANT_PLAF7 S-antigen protein	-3.44	0.0096
tc1a	TC1A_CAEEL Transposable element Tc1 transposase	2.38	0.0096
#N/A	#N/A	3.50	0.0097
tc1a	TC1A_CAEEL Transposable element Tc1 transposase	4.20	0.0097
BUD13	BUD13_CHICK BUD13 homolog	2.84	0.0097
#N/A	#N/A	4.10	0.0098
sstT	SSTT_CAMJD Serine/threonine transporter SstT {ECO:0000255|HAMAP-Rule:MF_01582}	2.72	0.0098
ZBED4	ZBED4_HUMAN Zinc finger BED domain-containing protein 4	3.86	0.0098
hsp90ab1	HS90B_DANRE Heat shock protein HSP 90-beta	-1.76	0.0099
#N/A	#N/A	4.90	0.0099
#N/A	TCB1_CAEBR Transposable element Tcb1 transposase	3.61	0.0099
#N/A	#N/A	4.47	0.0099
#N/A	#N/A	4.73	0.0099
#N/A	#N/A	3.92	0.0099
sur-2	MED23_CAEEL Mediator of RNA polymerase II transcription subunit 23	3.09	0.0100
NUGGC	SLIP_HUMAN Nuclear GTPase SLIP-GC	4.24	0.0100
unc119b	U119B_DANRE Protein unc-119 homolog B	3.91	0.0101
pckA	PCKA_CALS4 Phosphoenolpyruvate carboxykinase [ATP] {ECO:0000255|HAMAP-Rule:MF_00453}	4.81	0.0101
Vegfc	VEGFC_MOUSE Vascular endothelial growth factor C	4.42	0.0102
#N/A	TCB2_CAEBR Transposable element Tcb2 transposase	3.09	0.0102
#N/A	#N/A	2.52	0.0103
DENND1B	DEN1B_HUMAN DENN domain-containing protein 1B	4.67	0.0103
#N/A	TCB1_CAEBR Transposable element Tcb1 transposase	3.73	0.0103
At5g25860	FBL83_ARATH Putative F-box/LRR-repeat protein At5g25860	3.32	0.0103
TAR1	TAR1_YEAST Protein TAR1	4.73	0.0103
#N/A	TCB1_CAEBR Transposable element Tcb1 transposase	2.42	0.0103
tc1a	TC1A_CAEEL Transposable element Tc1 transposase	4.12	0.0103
#N/A	#N/A	3.88	0.0104
#N/A	MIA3_HUMAN Melanoma inhibitory activity protein 3	2.14	0.0104
U18	U18_HHV6U Putative immediate early glycoprotein	4.05	0.0104
tc1a	TC1A_CAEEL Transposable element Tc1 transposase	2.17	0.0104
#N/A	TCB2_CAEBR Transposable element Tcb2 transposase	4.87	0.0105
#N/A	#N/A	2.77	0.0105
Paf-AHalpha	PA1B2_DROME Platelet-activating factor acetylhydrolase IB subunit beta homolog	2.15	0.0105
atp-2	ATPB_NEUCR ATP synthase subunit beta, mitochondrial	2.49	0.0105

#N/A	#N/A	5.09	0.0105
ASPH	ASPH_HUMAN Aspartyl/asparaginyl beta-hydroxylase	-5.57	0.0106
#N/A	TCB2_CAEBR Transposable element Tcb2 transposase	4.19	0.0106
gag-pol	POL_BIV29 Gag-Pol polyprotein	2.77	0.0106
BTN1A1	BT1A1_HUMAN Butyrophilin subfamily 1 member A1	2.81	0.0106
#N/A	#N/A	4.89	0.0106
MJ0138	Y138_METJA Putative glutamine amidotransferase-like protein MJ0138	3.25	0.0107
Nlrc3	NLRC3_MOUSE Protein NLRC3	-4.22	0.0107
murC	MURC_BORA1 UDP-N-acetylmuramate--L-alanine ligase	4.57	0.0107
PIK3AP1	BCAP_HUMAN Phosphoinositide 3-kinase adapter protein 1	2.50	0.0107
GPR108	GP108_HUMAN Protein GPR108	4.45	0.0108
pol	RTJK_DROME RNA-directed DNA polymerase from mobile element jockey	1.68	0.0110
#N/A	#N/A	4.22	0.0111
Epb41l3	E41L3_MOUSE Band 4.1-like protein 3	-4.83	0.0113
#N/A	TCB1_CAEBR Transposable element Tcb1 transposase	2.29	0.0114
yqfO	GCH1L_BACSU GTP cyclohydrolase 1 type 2 homolog	3.40	0.0115
tc1a	TC1A_CAEEL Transposable element Tc1 transposase	3.41	0.0115
dlg1l	DLG1L_DANRE Discs large homolog 1-like protein	-4.16	1.0000
#N/A	STXB_SYNHO Stonustoxin subunit beta	2.78	0.0115
RPL14	RL14_PIG 60S ribosomal protein L14	-5.10	1.0000
Tcerg1	TCRG1_MOUSE Transcription elongation regulator 1	-1.71	0.0115
#N/A	STXB_SYNHO Stonustoxin subunit beta	-4.41	0.0115
#N/A	#N/A	4.05	0.0115
Sry	SRY_RAT Sex-determining region Y protein	2.41	0.0115
#N/A	#N/A	4.67	0.0116
Myo9a	MYO9A_RAT Unconventional myosin-IXa	-5.31	0.0116
RNF40	BRE1B_PONAB E3 ubiquitin-protein ligase BRE1B	2.79	0.0117
tc1a	TC1A_CAEEL Transposable element Tc1 transposase	4.13	0.0117
lat	LAT_MYCTU Probable L-lysine-epsilon aminotransferase	4.67	0.0117
#N/A	#N/A	2.45	0.0117
#N/A	#N/A	1.97	0.0117
#N/A	TCB1_CAEBR Transposable element Tcb1 transposase	3.75	0.0117
tc1a	TC1A_CAEEL Transposable element Tc1 transposase	2.27	0.0118
MmarC7_1414	KAE1B_METM7 Probable bifunctional tRNA threonylcarbamoyladenosine biosynthesis protein {ECO:0000255|HAMAP-Rule:MF_01447}	4.24	0.0119
#N/A	#N/A	3.60	0.0121
#N/A	TCB1_CAEBR Transposable element Tcb1 transposase	3.61	0.0121
#N/A	#N/A	4.42	0.0121
ETNK2	EKI2_HUMAN Ethanolamine kinase 2	1.47	0.0121
#N/A	#N/A	4.33	0.0122
GAPDH	G3P_COTJA Glyceraldehyde-3-phosphate dehydrogenase	3.82	0.0122
#N/A	#N/A	2.18	0.0122
Palb2	PALB2_MOUSE Partner and localizer of BRCA2	4.08	0.0122
SSRP1	SSRP1_CHICK FACT complex subunit SSRP1	-2.11	0.0123
pol	RTJK_DROME RNA-directed DNA polymerase from mobile element jockey	4.31	0.0124
#N/A	TCB2_CAEBR Transposable element Tcb2 transposase	3.69	0.0124
#N/A	#N/A	2.32	0.0124
Itpr3	ITPR3_MOUSE Inositol 1,4,5-trisphosphate receptor type 3	-1.57	0.0125
rps6	RS6_ONCMY 40S ribosomal protein S6	-3.91	0.0125
#N/A	TCB1_CAEBR Transposable element Tcb1 transposase	2.68	0.0126
#N/A	TCB2_CAEBR Transposable element Tcb2 transposase	3.28	0.0126
TCEAL3	TCAL3_HUMAN Transcription elongation factor A protein-like 3	3.33	0.0126
#N/A	#N/A	4.08	0.0126
tc3a	TC3A_CAEEL Transposable element Tc3 transposase	3.51	0.0126
#N/A	#N/A	2.85	0.0126
#N/A	#N/A	4.04	0.0126
#N/A	TCB1_CAEBR Transposable element Tcb1 transposase	4.13	0.0126
Palb2	PALB2_MOUSE Partner and localizer of BRCA2	-4.33	0.0127
#N/A	#N/A	2.74	0.0127
#N/A	TCB1_CAEBR Transposable element Tcb1 transposase	2.52	0.0127
ccnb2	CCNB2_XENLA G2/mitotic-specific cyclin-B2	3.32	0.0128
#N/A	#N/A	3.45	0.0128
tc1a	TC1A_CAEEL Transposable element Tc1 transposase	2.27	0.0128
ycf2-A	YCF2_VITVI Protein Ycf2 {ECO:0000255|HAMAP-Rule:MF_01330}	4.52	0.0128
tc3a	TC3A_CAEEL Transposable element Tc3 transposase	4.13	0.0128
#N/A	#N/A	1.44	0.0128

#N/A	VDAC1_SOLTU Mitochondrial outer membrane protein porin of 34 kDa	2.21	0.0128
ribK	RIFK_SULTO Riboflavin kinase {ECO:0000255|HAMAP-Rule:MF_01285}	3.18	0.0129
#N/A	KIPK_ARATH Serine/threonine-protein kinase KIPK	2.73	0.0129
tum1	THTM_SCHPO Probable 3-mercaptopyruvate sulfurtransferase	4.23	0.0129
Rpl38	RL38_RAT 60S ribosomal protein L38	-4.31	0.0129
Prrc2a	PRC2A_MOUSE Protein PRRC2A	-1.97	0.0131
#N/A	#N/A	3.88	0.0131
Itpr3	ITPR3_MOUSE Inositol 1,4,5-trisphosphate receptor type 3	-2.41	0.0131
#N/A	#N/A	3.33	0.0132
TGM5	TGM5_HUMAN Protein-glutamine gamma-glutamyltransferase 5	-1.50	0.0132
pol	RTJK_DROME RNA-directed DNA polymerase from mobile element jockey	2.41	0.0135
asah2	ASAH2_DANRE Neutral ceramidase	2.75	0.0135
SFK1	SFK1_YEAST Protein SFK1	2.77	0.0136
tc1a	TC1A_CAEEL Transposable element Tc1 transposase	5.05	0.0136
BAZ2B	BAZ2B_HUMAN Bromodomain adjacent to zinc finger domain protein 2B	2.37	0.0136
PF14_0175	YPF17_PLAF7 Protein PF14_0175	4.25	0.0137
#N/A	#N/A	1.86	0.0138
#N/A	#N/A	4.46	0.0138
#N/A	STXA_SYNVE Neoverrucotoxin subunit alpha	3.86	0.0139
ITGA3	ITA3_BOVIN Integrin alpha-3	2.05	0.0139
Nrdc	NRDC_MOUSE Nardilysin	2.75	0.0140
Trim29	TRI29_MOUSE Tripartite motif-containing protein 29	4.64	0.0140
#N/A	#N/A	3.75	0.0141
#N/A	#N/A	3.54	0.0141
daf-31	DAF31_CAEEL N-alpha-acetyltransferase daf-31 {ECO:0000305}	4.58	0.0141
tc1a	TC1A_CAEEL Transposable element Tc1 transposase	3.06	0.0141
#N/A	TCB1_CAEBR Transposable element Tcb1 transposase	4.11	0.0141
#N/A	LAC1_HUMAN Ig lambda-1 chain C regions	3.37	0.0141
#N/A	#N/A	3.75	0.0141
#N/A	#N/A	4.60	0.0142
#N/A	#N/A	4.76	0.0142
#N/A	TCB2_CAEBR Transposable element Tcb2 transposase	2.46	0.0142
LRRFIP2	LRRF2_HUMAN Leucine-rich repeat flightless-interacting protein 2	-6.14	1.0000
#N/A	#N/A	3.31	0.0143
CD4	CD4_DELLE T-cell surface glycoprotein CD4	4.05	0.0143
#N/A	HV303_HUMAN Ig heavy chain V-III region 23 {ECO:0000305}	2.21	0.0145
pol	RTJK_DROME RNA-directed DNA polymerase from mobile element jockey	2.77	0.0147
At2g42990	GDL48_ARATH GDSL esterase/lipase At2g42990	4.63	0.0149
PFI0570w	GUF1_PLAF7 Translation factor GUF1 homolog, mitochondrial	4.29	0.0151
PSAP	SAP_BOVIN Prosaposin	4.07	0.0151
#N/A	TCB2_CAEBR Transposable element Tcb2 transposase	3.39	0.0151
PYGM	PYGM_HUMAN Glycogen phosphorylase, muscle form	-3.69	0.0151
SAR0496	ISPE_STAAR 4-diphosphocytidyl-2-C-methyl-D-erythritol kinase	3.49	0.0151
ESRP1	ESRP1_HUMAN Epithelial splicing regulatory protein 1	1.01	0.0152
tc1a	TC1A_CAEEL Transposable element Tc1 transposase	3.82	0.0152
RTase	RTBS_DROME Probable RNA-directed DNA polymerase from transposon BS	2.18	0.0152
#N/A	DCD_ARTCA Deoxycytidine triphosphate deaminase	4.15	0.0152
#N/A	#N/A	3.24	0.0152
ADNP2	ADNP2_HUMAN ADNP homeobox protein 2	4.62	0.0152
#N/A	TCB1_CAEBR Transposable element Tcb1 transposase	3.86	0.0152
#N/A	UBIQP_XENLA Polyubiquitin	-1.82	0.0152
#N/A	#N/A	3.76	0.0153
#N/A	#N/A	4.40	0.0153
#N/A	#N/A	3.26	0.0155
tc1a	TC1A_CAEEL Transposable element Tc1 transposase	3.44	0.0155
Plce1	PLCE1_MOUSE 1-phosphatidylinositol 4,5-bisphosphate phosphodiesterase epsilon-1	3.28	0.0155
KIF21A	KI21A_HUMAN Kinesin-like protein KIF21A	2.21	0.0155
#N/A	#N/A	4.34	0.0155
#N/A	#N/A	2.98	0.0156
atpG	ATPG_NOCSJ ATP synthase gamma chain {ECO:0000255|HAMAP-Rule:MF_00815}	3.78	0.0156
#N/A	#N/A	4.41	0.0157
#N/A	#N/A	1.60	0.0157
#N/A	#N/A	2.65	0.0158
tc1a	TC1A_CAEEL Transposable element Tc1 transposase	2.69	0.0158
tc1a	TC1A_CAEEL Transposable element Tc1 transposase	4.23	0.0158
Canx	CALX_RAT Calnexin	-1.53	0.0158

#N/A	TCB1_CAEBR Transposable element Tcb1 transposase	3.04	0.0158
vps10	VPS10_ASPTN Vacuolar protein sorting/targeting protein 10	-3.50	0.0159
rps6	RS6_ONCMY 40S ribosomal protein S6	-2.06	0.0159
ilvD	ILVD_STRT2 Dihydroxy-acid dehydratase {ECO:0000255|HAMAP-Rule:MF_00012}	4.65	0.0159
tc1a	TC1A_CAEEL Transposable element Tc1 transposase	3.96	0.0159
#N/A	#N/A	2.45	0.0160
#N/A	#N/A	2.38	0.0160
rpl4-b	RL4B_XENLA 60S ribosomal protein L4-B	-2.57	0.0161
#N/A	#N/A	4.01	0.0161
#N/A	#N/A	2.01	0.0162
tc1a	TC1A_CAEEL Transposable element Tc1 transposase	3.12	0.0162
abcC5	ABCC5_DICDI ABC transporter C family member 5	-1.36	0.0162
DUSP7	DUS7_HUMAN Dual specificity protein phosphatase 7	2.40	0.0162
Ppp1r15b	PR15B_MOUSE Protein phosphatase 1 regulatory subunit 15B	-2.59	0.0163
#N/A	TCB2_CAEBR Transposable element Tcb2 transposase	3.03	0.0164
atpA	ATPA_NITSB ATP synthase subunit alpha {ECO:0000255|HAMAP-Rule:MF_01346}	3.74	0.0165
DNASE1	DNAS1_BOVIN Deoxyribonuclease-1	3.25	0.0165
LONRF2	LONF2_HUMAN LON peptidase N-terminal domain and RING finger protein 2	3.31	0.0165
mt-co3	COX3_SALSA Cytochrome c oxidase subunit 3	3.53	0.0165
#N/A	#N/A	1.95	0.0165
Cast	ICAL_MOUSE Calpastatin	-6.36	1.0000
citF	CILA_HAEIN Citrate lyase alpha chain	4.50	0.0166
tc1a	TC1A_CAEEL Transposable element Tc1 transposase	2.86	0.0167
#N/A	#N/A	4.00	0.0168
dtpB	DTPB_PHOAA Dipeptide and tripeptide permease B {ECO:0000255|HAMAP-Rule:MF_01879}	4.41	0.0168
dop-4	DOPR4_CAEEL Dopamine receptor 4	4.58	0.0168
jockey\pol	RTJK_DROFU RNA-directed DNA polymerase from mobile element jockey	2.02	0.0168
RTase	RTBS_DROME Probable RNA-directed DNA polymerase from transposon BS	3.96	0.0168
menD	MEND_SYNS9 2-succinyl-5-enolpyruvyl-6-hydroxy-3-cyclohexene-1-carboxylate synthase {ECO:0000255|HAMAP-Rule:MF_01659}	3.87	0.0169
Fam187a	F187A_RAT Ig-like V-type domain-containing protein FAM187A	3.48	0.0169
#N/A	#N/A	3.22	0.0171
#N/A	#N/A	3.75	0.0171
PDAT2	PDAT2_ARATH Putative phospholipid:diacylglycerol acyltransferase 2	4.50	0.0171
#N/A	TCB1_CAEBR Transposable element Tcb1 transposase	4.49	0.0171
#N/A	#N/A	4.13	0.0171
CD2	CD2_MACFA T-cell surface antigen CD2	4.41	0.0172
#N/A	#N/A	3.41	0.0172
tc1a	TC1A_CAEEL Transposable element Tc1 transposase	3.35	0.0172
MAP7D2	MA7D2_HUMAN MAP7 domain-containing protein 2	-3.40	0.0172
#N/A	#N/A	2.52	0.0172
Rap1gap2	RPGP2_MOUSE Rap1 GTPase-activating protein 2	-5.17	1.0000
RTase	RTBS_DROME Probable RNA-directed DNA polymerase from transposon BS	2.27	0.0174
Pstpip1	PPIP1_MOUSE Proline-serine-threonine phosphatase-interacting protein 1	3.18	0.0175
Plac8l1	PL8L1_MOUSE PLAC8-like protein 1	4.82	0.0175
#N/A	#N/A	4.92	0.0175
hisA	HIS4_AERHH 1-(5-phosphoribosyl)-5-[(5-phosphoribosylamino)methylideneamino] imidazole-4-carboxamide isomerase {ECO:0000255|HAMAP-Rule:MF_01014}	4.45	0.0175
#N/A	TCB1_CAEBR Transposable element Tcb1 transposase	3.28	0.0175
#N/A	#N/A	4.72	0.0175
Cacna2d4	CA2D4_MOUSE Voltage-dependent calcium channel subunit alpha-2/delta-4	2.85	0.0177
#N/A	#N/A	2.09	0.0177
#N/A	TCB1_CAEBR Transposable element Tcb1 transposase	1.98	0.0179
#N/A	#N/A	1.70	0.0179
gmhA	GMHA_WOLSU Phosphoheptose isomerase {ECO:0000255|HAMAP-Rule:MF_00067}	3.58	0.0179
ier2	IER2_DANRE Immediate early response gene 2 protein	-2.36	0.0180
Ldb3	LDB3_MOUSE LIM domain-binding protein 3	3.46	0.0181
#N/A	#N/A	4.32	0.0181
#N/A	#N/A	2.79	0.0183
sspH2	SSPH2_SALTY E3 ubiquitin-protein ligase sspH2	3.51	0.0183
topA	TOP1_RICTY DNA topoisomerase 1 {ECO:0000255|HAMAP-Rule:MF_00952}	4.04	0.0183
foxred2	FXRD2_DANRE FAD-dependent oxidoreductase domain-containing protein 2	3.04	0.0183
#N/A	#N/A	3.63	0.0183
STG	CF015_PANTR Uncharacterized protein C6orf15 homolog	4.04	0.0183
ZBED9	SCND3_HUMAN SCAN domain-containing protein 3	2.34	0.0183

rpl9	RL9_ICTPU 60S ribosomal protein L9	-2.50	0.0184
tc1a	TC1A_CAEEL Transposable element Tc1 transposase	2.57	0.0186
Ctha_0558	Y558_CHLT3 UPF0234 protein Ctha_0558 {ECO:0000255|HAMAP-Rule:MF_00632}	2.76	0.0186
#N/A	#N/A	4.14	0.0186
lin1255	Y1255_LISIN Uncharacterized protein Lin1255/Lin1742	3.65	0.0186
#N/A	TCB2_CAEBR Transposable element Tcb2 transposase	3.98	0.0187
Proser2	PRSR2_MOUSE Proline and serine-rich protein 2	-6.68	0.0187
Ppp3r1	CANB1_RAT Calcineurin subunit B type 1	3.12	0.0187
tc1a	TC1A_CAEEL Transposable element Tc1 transposase	3.64	0.0188
tc1a	TC1A_CAEEL Transposable element Tc1 transposase	3.91	0.0188
#N/A	TCB1_CAEBR Transposable element Tcb1 transposase	3.49	0.0189
licA	LICA2_HAEIF Protein LicA	3.77	0.0191
#N/A	TCB2_CAEBR Transposable element Tcb2 transposase	3.79	0.0191
#N/A	#N/A	3.16	0.0191
miaA	MIAA_MYCGA tRNA dimethylallyltransferase {ECO:0000255|HAMAP-Rule:MF_00185}	2.76	0.0191
tc1a	TC1A_CAEEL Transposable element Tc1 transposase	3.88	0.0192
groL2	CH602_SALRD 60 kDa chaperonin 2 {ECO:0000255|HAMAP-Rule:MF_00600}	3.51	0.0192
#N/A	#N/A	2.24	0.0192
RTase	RTBS_DROME Probable RNA-directed DNA polymerase from transposon BS	1.48	0.0195
CYB5A	CYB5_PIG Cytochrome b5	4.29	0.0196
C1qc	C1QC_RAT Complement C1q subcomponent subunit C	3.21	0.0196
F5	FA5_HUMAN Coagulation factor V	3.03	0.0197
#N/A	#N/A	-8.75	0.0197
SLC27A6	S27A6_HUMAN Long-chain fatty acid transport protein 6	3.44	0.0197
#N/A	#N/A	2.80	0.0197
pol	RTJK_DROME RNA-directed DNA polymerase from mobile element jockey	1.61	0.0197
MIMI_R554	YR554_MIMIV Uncharacterized protein R554	2.71	0.0198
Trim25	TRI25_MOUSE E3 ubiquitin/ISG15 ligase TRIM25	3.64	0.0198
X-element\OR F2	RTXE_DROME Probable RNA-directed DNA polymerase from transposon X-element	1.81	0.0198
Ogfr	OGFR_MOUSE Opioid growth factor receptor	-2.37	0.0200
truD	TRUD_METTH Probable tRNA pseudouridine synthase D {ECO:0000255|HAMAP-Rule:MF_01082}	2.50	0.0200
AHNAK	AHNK_HUMAN Neuroblast differentiation-associated protein AHNAK	3.55	0.0201
Tnik	TNIK_MOUSE Traf2 and NCK-interacting protein kinase	-1.29	0.0201
#N/A	TCB1_CAEBR Transposable element Tcb1 transposase	2.29	0.0201
ART2	ART2_YEAST Putative uncharacterized protein ART2	3.14	0.0201
F	CAPSD_BPPHS Capsid protein F	-3.93	0.0201
GNAS	GNAS_CRIGR Guanine nucleotide-binding protein G(s) subunit alpha	1.91	0.0201
camkmt	CMKMT_XENLA Calmodulin-lysine N-methyltransferase	3.90	0.0201
#N/A	TCB1_CAEBR Transposable element Tcb1 transposase	3.27	0.0202
PRRC2B	PRC2B_HUMAN Protein PRRC2B	-1.20	0.0202
#N/A	#N/A	2.08	0.0204
cyp3a27	CP3AR_ONCMY Cytochrome P450 3A27	3.74	0.0204
#N/A	TCB1_CAEBR Transposable element Tcb1 transposase	4.31	0.0205
RTase	RTBS_DROME Probable RNA-directed DNA polymerase from transposon BS	1.47	0.0206
TCOF1	TCOF_HUMAN Treacle protein	-5.26	1.0000
panC/cmk	PANCY_PROM0 Bifunctional pantoate ligase/cytidylate kinase {ECO:0000255|HAMAP-Rule:MF_01349}	2.85	0.0206
#N/A	#N/A	-2.61	0.0207
RNF128	RN128_HUMAN E3 ubiquitin-protein ligase RNF128	4.55	0.0207
EIF5	IF5_HUMAN Eukaryotic translation initiation factor 5	-1.54	0.0208
#N/A	TCB2_CAEBR Transposable element Tcb2 transposase	4.45	0.0209
b2m	B2MG_ICTPU Beta-2-microglobulin	4.23	0.0209
Rbp2	RET2_RAT Retinol-binding protein 2	3.11	0.0209
Znf106	ZN106_MOUSE Zinc finger protein 106	3.13	0.0209
#N/A	#N/A	2.35	0.0210
#N/A	#N/A	1.69	0.0210
#N/A	#N/A	3.13	0.0210
#N/A	TCB1_CAEBR Transposable element Tcb1 transposase	4.44	0.0210
#N/A	#N/A	-2.52	0.0211
tc3a	TC3A_CAEEL Transposable element Tc3 transposase	4.40	0.0212
jockey\pol	RTJK_DROFU RNA-directed DNA polymerase from mobile element jockey	1.58	0.0212

#N/A	TCB1_CAEBR Transposable element Tcb1 transposase	4.39	0.0212
atpG	ATPG_LACDB ATP synthase gamma chain {ECO:0000255|HAMAP-Rule:MF_00815}	3.87	0.0212
Pbxip1	PBIP1_MOUSE Pre-B-cell leukemia transcription factor-interacting protein 1	3.48	0.0212
#N/A	H2B_SALTR Histone H2B	-1.84	0.0212
#N/A	#N/A	2.03	0.0212
RTase	RTBS_DROME Probable RNA-directed DNA polymerase from transposon BS	2.51	0.0212
#N/A	#N/A	2.84	0.0214
#N/A	#N/A	0.84	0.0215
slc30a9	ZNT9_XENLA Zinc transporter 9	2.80	0.0218
cxadr	CXAR_DANRE Coxsackievirus and adenovirus receptor homolog	2.22	0.0219
tc1a	TC1A_CAEEL Transposable element Tc1 transposase	2.27	0.0220
#N/A	#N/A	3.01	0.0222
agr2	AGR2_DANRE Anterior gradient protein 2 homolog	-5.74	0.0223
#N/A	#N/A	1.90	0.0223
#N/A	TCB1_CAEBR Transposable element Tcb1 transposase	1.76	0.0223
#N/A	GAD_SULSO D-gluconate/D-galactonate dehydratase {ECO:0000303|PubMed:15474024}	2.25	0.0223
#N/A	#N/A	3.06	0.0224
tc1a	TC1A_CAEEL Transposable element Tc1 transposase	2.39	0.0225
TP53INP1	T53I1_HUMAN Tumor protein p53-inducible nuclear protein 1	3.08	0.0225
RTase	RTBS_DROME Probable RNA-directed DNA polymerase from transposon BS	4.26	0.0227
gatD	GATD_METMA Glutamyl-tRNA(Gln) amidotransferase subunit D {ECO:0000255|HAMAP-Rule:MF_00586}	1.22	0.0229
#N/A	MIA3_MOUSE Melanoma inhibitory activity protein 3	3.29	0.0230
nr3c1	GCR_ONCMY Glucocorticoid receptor	1.82	0.0230
#N/A	TCB1_CAEBR Transposable element Tcb1 transposase	3.52	0.0231
LTB4R2	LT4R2_HUMAN Leukotriene B4 receptor 2	4.14	0.0231
ttn-1	TTN1_CAEEL Titin homolog {ECO:0000303|PubMed:12381307}	4.16	0.0232
RNF186	RN186_HUMAN RING finger protein 186	-1.50	0.0232
tc1a	TC1A_CAEEL Transposable element Tc1 transposase	3.82	0.0232
tc1a	TC1A_CAEEL Transposable element Tc1 transposase	2.85	0.0233
#N/A	#N/A	2.07	0.0233
#N/A	#N/A	3.31	0.0234
#N/A	STXB_SYNHO Stonustoxin subunit beta	3.70	0.0235
GIMAP4	GIMA4_HUMAN GTPase IMAP family member 4	1.85	0.0235
PARVG	PARVG_HUMAN Gamma-parvin	3.66	0.0236
IFFO1	IFFO1_HUMAN Intermediate filament family orphan 1	-4.35	0.0237
#N/A	#N/A	2.60	0.0238
Got2	AATM_MOUSE Aspartate aminotransferase, mitochondrial	3.12	0.0238
cahz	CAHZ_DANRE Carbonic anhydrase	3.20	0.0239
metG	SYM_PSEMY Methionine--tRNA ligase {ECO:0000255|HAMAP-Rule:MF_00098}	4.12	0.0240
SYNE1	SYNE1_HUMAN Nesprin-1	2.45	0.0240
TRIM16L	TR16L_HUMAN Tripartite motif-containing protein 16-like protein	-2.10	0.0240
#N/A	TCB1_CAEBR Transposable element Tcb1 transposase	3.39	0.0240
Cys	CRUST_PANBO Crustapain	4.36	0.0240
pdxA	PDXA_AROAE 4-hydroxythreonine-4-phosphate dehydrogenase {ECO:0000255|HAMAP-Rule:MF_00536}	4.15	0.0243
jockey\pol	RTJK_DROFU RNA-directed DNA polymerase from mobile element jockey	1.43	0.0243
psf-1	PSF1_CAEEL Probable DNA replication complex GINS protein PSF1	4.01	0.0243
#N/A	#N/A	4.06	0.0243
#N/A	TCB1_CAEBR Transposable element Tcb1 transposase	2.82	0.0243
Pla2g2e	PA2GE_MOUSE Group IIE secretory phospholipase A2	1.89	0.0243
#N/A	#N/A	4.43	0.0243
#N/A	#N/A	2.21	0.0243
#N/A	#N/A	2.59	0.0243
#N/A	#N/A	3.61	0.0243
trm1	TRM1_METM7 tRNA (guanine(26)-N(2))-dimethyltransferase	3.00	0.0243
pdxT	PDXT_TROWT Pyridoxal 5'-phosphate synthase subunit PdxT	2.17	0.0243
rplE	RL5_MAGSA 50S ribosomal protein L5 {ECO:0000255|HAMAP-Rule:MF_01333}	3.42	0.0243
Pou2f3	PO2F3_RAT POU domain, class 2, transcription factor 3	-2.31	0.0243
Bcell_0380	Y380_BACCJ Putative Gly-rich membrane protein Bcell_0380	2.55	0.0243
#N/A	TCB2_CAEBR Transposable element Tcb2 transposase	2.37	0.0243
#N/A	#N/A	2.32	0.0243
#N/A	TCB1_CAEBR Transposable element Tcb1 transposase	1.98	0.0245
Ptprr	PTPRR_MOUSE Receptor-type tyrosine-protein phosphatase R	3.93	0.0245
#N/A	LECM4_PSEPL C-type lectin lectoxin-Enh4	3.96	0.0245
cry3Ca	CR3CA_BACTK Pesticidal crystal protein Cry3Ca	2.01	0.0245

#N/A	#N/A	2.00	0.0246
#N/A	#N/A	2.90	0.0246
#N/A	CALM_STIJA Calmodulin	-3.67	1.0000
#N/A	#N/A	-3.73	1.0000
Hebp2	HEBP2_MOUSE Heme-binding protein 2	1.47	0.0246
#N/A	TCB1_CAEBR Transposable element Tcb1 transposase	3.05	0.0246
#N/A	#N/A	3.56	0.0246
#N/A	#N/A	3.65	0.0247
MAP4K4	M4K4_HUMAN Mitogen-activated protein kinase kinase kinase kinase 4	-2.33	0.0247
Cdc27	CDC27_MOUSE Cell division cycle protein 27 homolog	2.77	0.0247
rpl5-a	RL5A_XENLA 60S ribosomal protein L5-A	-4.73	0.0248
uvrB	UVRB_RICCK UvrABC system protein B {ECO:0000255|HAMAP-Rule:MF_00204}	2.05	0.0249
tc1a	TC1A_CAEEL Transposable element Tc1 transposase	3.50	0.0249
#N/A	#N/A	3.88	0.0249
Papolb	PAPOB_MOUSE Poly(A) polymerase beta	3.50	0.0249
ATG12	ATG12_PICGU Ubiquitin-like protein ATG12	3.97	0.0249
spp-11	SPP11_CAEEL Saposin-like protein 11	2.75	0.0249
Myo9a	MYO9A_RAT Unconventional myosin-IXa	-6.82	0.0249
FRS1	FRS1_ARATH Protein FAR1-RELATED SEQUENCE 1	2.42	0.0249
ileS	SYI_PHOLL Isoleucine--tRNA ligase {ECO:0000255|HAMAP-Rule:MF_02002}	-5.05	0.0250
#N/A	#N/A	1.72	0.0250
Lypla2	LYPA2_RAT Acyl-protein thioesterase 2	-3.07	0.0250
#N/A	LORF2_HUMAN LINE-1 retrotransposable element ORF2 protein	3.97	0.0250
SRRM1	SRRM1_CHICK Serine/arginine repetitive matrix protein 1	1.81	0.0250
ndel1b	NDL1B_DANRE Nuclear distribution protein nudE-like 1-B	3.13	0.0253
#N/A	#N/A	3.66	0.0254
jockey\pol	RTJK_DROFU RNA-directed DNA polymerase from mobile element jockey	1.51	0.0254
gdt1	GDT1_DICDI Probable inactive serine/threonine-protein kinase gdt1	4.21	0.0254
SAB1876c	LUKL2_STAAB Uncharacterized leukocidin-like protein 2	2.41	0.0254
#N/A	#N/A	3.62	0.0254
tc1a	TC1A_CAEEL Transposable element Tc1 transposase	3.74	0.0255
NRPC2	NRPC2_ARATH DNA-directed RNA polymerase III subunit 2 {ECO:0000305}	3.57	0.0255
Gpr158	GP158_RAT Probable G-protein coupled receptor 158	3.76	0.0256
#N/A	#N/A	2.26	0.0256
MINK1	MINK1_HUMAN Misshapen-like kinase 1	5.08	0.0256
#N/A	TCB2_CAEBR Transposable element Tcb2 transposase	3.23	0.0256
Arhgap17	RHG17_RAT Rho GTPase-activating protein 17	-2.05	0.0256
mnmG	MNMG_LACGA tRNA uridine 5-carboxymethylaminomethyl modification enzyme MnmG {ECO:0000255|HAMAP-Rule:MF_00129}	2.20	0.0256
#N/A	PERQ2_DANRE PERQ amino acid-rich with GYF domain-containing protein 2	-6.42	1.0000
#N/A	TCB2_CAEBR Transposable element Tcb2 transposase	2.83	0.0257
eef1g	EF1G_DANRE Elongation factor 1-gamma	-2.26	0.0257
tc1a	TC1A_CAEEL Transposable element Tc1 transposase	3.05	0.0257
mdfic	MDFIC_XENLA MyoD family inhibitor domain-containing protein	4.01	0.0258
aroB'	DHQS_ARCFU 3-dehydroquinate synthase {ECO:0000255|HAMAP-Rule:MF_01244}	3.78	0.0259
RTase	RTBS_DROME Probable RNA-directed DNA polymerase from transposon BS	1.43	0.0259
Lrrc10	LRC10_MOUSE Leucine-rich repeat-containing protein 10	3.77	0.0259
GATAD2A	P66A_HUMAN Transcriptional repressor p66-alpha	4.03	0.0260
#N/A	PO22_POPJA Retrovirus-related Pol polyprotein from type-1 retrotransposable element R2	2.69	0.0261
agr2	AGR2_DANRE Anterior gradient protein 2 homolog	2.43	0.0261
tc1a	TC1A_CAEEL Transposable element Tc1 transposase	2.93	0.0261
Rps20	RS20_RAT 40S ribosomal protein S20	-4.90	0.0261
#N/A	#N/A	4.42	0.0262
Cct2	TCPB_MOUSE T-complex protein 1 subunit beta	-6.52	1.0000
trpD	TRPD_PSESM Anthranilate phosphoribosyltransferase {ECO:0000255|HAMAP-Rule:MF_00211}	4.73	0.0262
Pogk	POGK_MOUSE Pogo transposable element with KRAB domain	2.12	0.0262
TAO1	TAO1_ARATH Disease resistance protein TAO1 {ECO:0000305}	2.91	0.0262
tc1a	TC1A_CAEEL Transposable element Tc1 transposase	3.31	0.0263
#N/A	#N/A	2.91	0.0263
tc1a	TC1A_CAEEL Transposable element Tc1 transposase	1.82	0.0264
#N/A	#N/A	2.52	0.0264
tc1a	TC1A_CAEEL Transposable element Tc1 transposase	3.86	0.0265
TMEM106A	T106A_HUMAN Transmembrane protein 106A	3.60	0.0266
#N/A	TCB1_CAEBR Transposable element Tcb1 transposase	1.92	0.0266

Camk2g	KCC2G_MOUSE Calcium/calmodulin-dependent protein kinase type II subunit gamma	3.62	0.0266
#N/A	#N/A	3.45	0.0266
Tnrc18	TNC18_MOUSE Trinucleotide repeat-containing gene 18 protein	-2.10	0.0266
#N/A	#N/A	2.34	0.0266
#N/A	TCB1_CAEBR Transposable element Tcb1 transposase	2.01	0.0266
RGR	RGR_HUMAN RPE-retinal G protein-coupled receptor	2.99	0.0266
ERVFC1	EFC1_HUMAN Endogenous retrovirus group FC1 Env polyprotein	1.84	0.0266
SUCLG1	SUCA_HUMAN Succinyl-CoA ligase [ADP/GDP-forming] subunit alpha, mitochondrial	-3.75	1.0000
MIMI_R871	YR871_MIMIV Uncharacterized protein R871	2.56	0.0266
YHR213W-B	YH21B_YEAST Uncharacterized protein YHR213W-B	3.02	0.0266
RHEB	RHEB_HUMAN GTP-binding protein Rheb	2.75	0.0266
#N/A	UL77_ELHVK Virion-packaging protein UL25 homolog	2.25	0.0267
skap2	SKAP2_DANRE Src kinase-associated phosphoprotein 2	2.79	0.0267
Ceacam5	CEAM5_MOUSE Carcinoembryonic antigen-related cell adhesion molecule 5	3.35	0.0267
jockey\pol	RTJK_DROFU RNA-directed DNA polymerase from mobile element jockey	2.82	0.0268
PIGK	GPI8_HUMAN GPI-anchor transamidase	4.47	0.0268
RTase	RTBS_DROME Probable RNA-directed DNA polymerase from transposon BS	1.96	0.0268
IMPDH	IMDH_TRIFO Inosine-5'-monophosphate dehydrogenase	2.49	0.0268
fos	FOS_TAKRU Proto-oncogene c-Fos	-2.96	0.0269
#N/A	#N/A	2.20	0.0271
#N/A	TCB2_CAEBR Transposable element Tcb2 transposase	2.14	0.0271
#N/A	TCB2_CAEBR Transposable element Tcb2 transposase	3.70	0.0271
ALOX5	LOX5_HUMAN Arachidonate 5-lipoxygenase	1.96	0.0271
#N/A	TCB1_CAEBR Transposable element Tcb1 transposase	2.94	0.0271
#N/A	TCB2_CAEBR Transposable element Tcb2 transposase	3.67	0.0271
Arhgap39	RHG39_MOUSE Rho GTPase-activating protein 39	-4.07	0.0272
#N/A	#N/A	-0.93	0.0272
#N/A	TCB2_CAEBR Transposable element Tcb2 transposase	2.86	0.0272
Pik3ap1	BCAP_MOUSE Phosphoinositide 3-kinase adapter protein 1	1.91	0.0272
HRC	SRCH_RABIT Sarcoplasmic reticulum histidine-rich calcium-binding protein	3.69	0.0273
#N/A	#N/A	2.61	0.0274
klp8	KLP8_SCHPO Kinesin-like protein 8	3.03	0.0274
CHD7	CHD7_HUMAN Chromodomain-helicase-DNA-binding protein 7	3.58	0.0274
#N/A	#N/A	3.00	0.0274
#N/A	#N/A	3.05	0.0274
THBD	TRBM_SAISC Thrombomodulin	4.15	0.0275
#N/A	#N/A	2.89	0.0275
PLAC8L1	PL8L1_HUMAN PLAC8-like protein 1	3.51	0.0276
tc1a	TC1A_CAEEL Transposable element Tc1 transposase	3.74	0.0276
#N/A	#N/A	3.16	0.0276
#N/A	TCB2_CAEBR Transposable element Tcb2 transposase	3.44	0.0276
#N/A	#N/A	2.75	0.0276
Igni_0686	ARGDC_IGNH4 Arginine decarboxylase proenzyme	4.19	0.0276
Nucb2	NUCB2_RAT Nucleobindin-2	-2.66	0.0276
ligA	DNLJ_GEODF DNA ligase {ECO:0000255|HAMAP-Rule:MF_01588}	3.65	0.0276
#N/A	#N/A	2.75	0.0276
tc1a	TC1A_CAEEL Transposable element Tc1 transposase	2.59	0.0276
#N/A	TCB2_CAEBR Transposable element Tcb2 transposase	3.64	0.0276
#N/A	#N/A	3.58	0.0276
#N/A	TCB2_CAEBR Transposable element Tcb2 transposase	2.10	0.0276
#N/A	#N/A	3.55	0.0276
COLGALT1	GT251_HUMAN Procollagen galactosyltransferase 1	3.12	0.0278
NT5C2	5NTC_CHICK Cytosolic purine 5'-nucleotidase	1.34	0.0279
#N/A	TCB1_CAEBR Transposable element Tcb1 transposase	2.02	0.0279
B3GALT2	B3GT2_HUMAN Beta-1,3-galactosyltransferase 2	1.63	0.0280
PAT1	PAT1_ARATH Scarecrow-like transcription factor PAT1	1.94	0.0281
#N/A	FUK_HUMAN L-fucose kinase	5.27	0.0281
#N/A	#N/A	2.04	0.0281
Pik3c2g	P3C2G_MOUSE Phosphatidylinositol 4-phosphate 3-kinase C2 domain-containing subunit gamma	1.98	0.0281
gag	GAGJ_DROFU Nucleic-acid-binding protein from mobile element jockey	2.38	0.0281
Abcb9	ABCB9_MOUSE ATP-binding cassette sub-family B member 9	4.86	0.0282
tc1a	TC1A_CAEEL Transposable element Tc1 transposase	3.05	0.0282

#N/A	YD023_HUMAN Putative uncharacterized protein FLJ45035	4.30	0.0282
#N/A	#N/A	3.90	0.0282
rpsP	RS16_BUCAP 30S ribosomal protein S16 {ECO:0000255|HAMAP-Rule:MF_00385}	4.29	0.0282
oaz1b	OAZ2_DANRE Ornithine decarboxylase antizyme 2	2.92	0.0282
#N/A	LORF2_HUMAN LINE-1 retrotransposable element ORF2 protein	1.64	0.0282
aurkb-a	AUKBA_XENLA Aurora kinase B-A	1.99	0.0282
#N/A	#N/A	3.04	0.0282
infB	IF2_BORBU Translation initiation factor IF-2	4.11	0.0283
Eif4a2	IF4A2_RAT Eukaryotic initiation factor 4A-II	-3.43	0.0285
#N/A	#N/A	3.38	0.0286
mpa	ARC_MYCVP Proteasome-associated ATPase {ECO:0000255|HAMAP-Rule:MF_02112}	4.13	0.0286
#N/A	#N/A	3.67	0.0286
GOS1	GOSR1_YEAST Golgi SNAP receptor complex member 1	3.86	0.0286
gnb2l1	GBLP_ORENI Guanine nucleotide-binding protein subunit beta-2-like 1	-6.31	1.0000
#N/A	#N/A	-3.46	0.0287
Paxbp1	PAXB1_MOUSE PAX3- and PAX7-binding protein 1	4.27	0.0288
#N/A	TCB1_CAEBR Transposable element Tcb1 transposase	3.19	0.0289
#N/A	#N/A	4.28	0.0289
jockey\pol	RTJK_DROFU RNA-directed DNA polymerase from mobile element jockey	2.06	0.0289
SCAI	SCAI_HUMAN Protein SCAI	-5.77	1.0000
Rnf186	RN186_MOUSE RING finger protein 186	-1.21	0.0290
#N/A	#N/A	2.92	0.0290
#N/A	PSGP_ONCMY Polysialoglycoprotein	3.43	0.0291
#N/A	#N/A	1.91	0.0291
CIRBP	CIRBP_PONAB Cold-inducible RNA-binding protein	-6.65	0.0291
EXOC3L4	EX3L4_HUMAN Exocyst complex component 3-like protein 4	3.52	0.0293
calm	CALM_EPIAK Calmodulin	-2.99	0.0293
fut11	FUT11_ORYLA Alpha-(1,3)-fucosyltransferase 11	1.91	0.0294
#N/A	#N/A	3.40	0.0294
tc1a	TC1A_CAEEL Transposable element Tc1 transposase	-2.34	0.0295
Trim39	TRI39_RAT E3 ubiquitin-protein ligase TRIM39	3.77	0.0296
#N/A	#N/A	2.71	0.0297
HMGB2	HMGB2_HUMAN High mobility group protein B2	-4.64	1.0000
Cox7a2	CX7A2_MOUSE Cytochrome c oxidase subunit 7A2, mitochondrial	2.31	0.0300
#N/A	#N/A	2.00	0.0301
TANC2	TANC2_HUMAN Protein TANC2	3.56	0.0301
#N/A	#N/A	2.04	0.0301
#N/A	TCB1_CAEBR Transposable element Tcb1 transposase	3.24	0.0301
#N/A	TCB1_CAEBR Transposable element Tcb1 transposase	3.75	0.0301
rpl7a	RL7A_TAKRU 60S ribosomal protein L7a	-4.88	0.0301
cbsB	CBSB_SULAC Cytochrome b558/566 subunit B	3.89	0.0301
tc1a	TC1A_CAEEL Transposable element Tc1 transposase	3.40	0.0301
tc1a	TC1A_CAEEL Transposable element Tc1 transposase	2.63	0.0301
lamtor4	LTOR4_DANRE Ragulator complex protein LAMTOR4	4.37	0.0301
pol	RTJK_DROME RNA-directed DNA polymerase from mobile element jockey	3.65	0.0302
proS	SYP_COLP3 Proline--tRNA ligase	2.12	0.0303
SAMD4B	SMAG2_HUMAN Protein Smaug homolog 2	2.27	0.0303
#N/A	TCB1_CAEBR Transposable element Tcb1 transposase	3.39	0.0304
#N/A	TCB1_CAEBR Transposable element Tcb1 transposase	3.52	0.0304
#N/A	ORF73_HHV8P Protein ORF73	2.69	0.0305
#N/A	HMGT_ONCMY High mobility group-T protein	2.93	0.0305
ERVPABL B-1	ERB1_HUMAN Endogenous retrovirus group PABLB member 1 Env polyprotein	3.28	0.0305
#N/A	#N/A	3.69	0.0305
#N/A	#N/A	2.73	0.0306
Setd2	SETD2_MOUSE Histone-lysine N-methyltransferase SETD2	-1.82	0.0306
#N/A	#N/A	3.41	0.0306
#N/A	#N/A	3.45	0.0307
MYH9	MYH9_CHICK Myosin-9	-0.94	0.0307
SYNPO2L	SYP2L_HUMAN Synaptopodin 2-like protein	3.21	0.0307
Efcab5	EFCB5_MOUSE EF-hand calcium-binding domain-containing protein 5	4.07	0.0308
rpmE2	RL31B_LACF3 50S ribosomal protein L31 type B	3.02	0.0310
Faah	FAAH1_MOUSE Fatty-acid amide hydrolase 1	3.84	0.0310
#N/A	TCB1_CAEBR Transposable element Tcb1 transposase	2.80	0.0310
truB	TRUB_OPITP tRNA pseudouridine synthase B	4.18	0.0310
RNF14	RNF14_HUMAN E3 ubiquitin-protein ligase RNF14	2.33	0.0311

tc1a	TC1A_CAEEL Transposable element Tc1 transposase	2.15	0.0311
#N/A	#N/A	1.93	0.0312
#N/A	TCB1_CAEBR Transposable element Tcb1 transposase	-1.33	0.0312
tc1a	TC1A_CAEEL Transposable element Tc1 transposase	3.33	0.0312
rtel1	RTEL1_DANRE Regulator of telomere elongation helicase 1	-4.26	0.0312
#N/A	#N/A	2.54	0.0312
rpiA	RPIA_LACDB Ribose-5-phosphate isomerase A	2.69	0.0312
TPS-mISO1	MISO1_PINCO Monofunctional isopimaradiene synthase, chloroplastic {ECO:0000303|PubMed:23370714}	4.58	0.0312
mtmr10	MTMRA_DANRE Myotubularin-related protein 10	1.51	0.0312
sodA	SODC1_DICDI Superoxide dismutase [Cu-Zn] 1	2.03	0.0312
#N/A	TCB1_CAEBR Transposable element Tcb1 transposase	4.37	0.0312
ACTR8	ARP8_BOVIN Actin-related protein 8	3.69	0.0312
tsf	EFTS_CHLCV Elongation factor Ts	3.87	0.0313
tif1	IF4A_NEOFI ATP-dependent RNA helicase eIF4A	-4.49	1.0000
topA	TOP1_RICTY DNA topoisomerase 1	3.77	0.0313
#N/A	#N/A	1.64	0.0313
PFD1115c	YD115_PLAF7 Uncharacterized protein PFD1115c	2.04	0.0313
JMJD1C	JHD2C_HUMAN Probable JmjC domain-containing histone demethylation protein 2C	-4.43	0.0313
#N/A	#N/A	2.91	0.0314
sigJ	SIGJ_DICDI SrfA-induced gene J protein	2.84	0.0314
Papola	PAPOA_MOUSE Poly(A) polymerase alpha	3.11	0.0314
pol	RTJK_DROME RNA-directed DNA polymerase from mobile element jockey	2.20	0.0315
tnpR	TNR1_ECOLI Transposon gamma-delta resolvase	1.38	0.0315
UKL1	UKL1_ARATH Uridine kinase-like protein 1, chloroplastic	3.60	0.0316
EXPA24	EXP24_ARATH Expansin-A24	3.57	0.0316
#N/A	#N/A	4.43	0.0318
#N/A	#N/A	3.32	0.0318
RTase	RTBS_DROME Probable RNA-directed DNA polymerase from transposon BS	2.62	0.0319
#N/A	TCB1_CAEBR Transposable element Tcb1 transposase	3.73	0.0320
#N/A	TCB1_CAEBR Transposable element Tcb1 transposase	3.29	0.0321
#N/A	#N/A	2.59	0.0321
rexB	ADDB_LACPL ATP-dependent helicase/deoxyribonuclease subunit B	4.38	0.0321
#N/A	TCB2_CAEBR Transposable element Tcb2 transposase	3.68	0.0322
Tead3	TEAD3_MOUSE Transcriptional enhancer factor TEF-5	2.47	0.0322
tc1a	TC1A_CAEEL Transposable element Tc1 transposase	1.79	0.0322
ASPH	ASPH_BOVIN Aspartyl/asparaginyl beta-hydroxylase	2.28	0.0322
PDE4DIP	MYOME_HUMAN Myomegalin	3.49	0.0322
tc1a	TC1A_CAEEL Transposable element Tc1 transposase	3.72	0.0323
trmD	TRMD_NITEU tRNA (guanine-N(1)-)-methyltransferase	2.75	0.0323
ssp5	SSP5_STRGN Agglutinin receptor	2.19	0.0323
tc1a	TC1A_CAEEL Transposable element Tc1 transposase	1.70	0.0323
#N/A	TCB1_CAEBR Transposable element Tcb1 transposase	1.70	0.0323
#N/A	TCB1_CAEBR Transposable element Tcb1 transposase	2.36	0.0323
#N/A	#N/A	-2.06	0.0323
#N/A	ACTC_TAKRU Actin, alpha cardiac	-1.26	0.0324
#N/A	F208B_MOUSE Protein FAM208B	-6.72	0.0325
#N/A	TCB1_CAEBR Transposable element Tcb1 transposase	-1.40	0.0325
Mme	NEP_MOUSE Neprilysin	3.31	0.0325
#N/A	CX023_HUMAN Uncharacterized protein CXorf23	3.83	0.0325
dnapkcs	PRKDC_DICDI DNA-dependent protein kinase catalytic subunit	2.74	0.0325
#N/A	#N/A	3.29	0.0330
Khdc3	KHDC3_RAT KH domain-containing protein 3	3.29	0.0330
pnrc2	PNRC2_SALSA Proline-rich nuclear receptor coactivator 2	1.61	0.0330
#N/A	#N/A	4.51	0.0330
Serp1	SERP1_RAT Stress-associated endoplasmic reticulum protein 1	3.15	0.0330
jockey\pol	RTJK_DROFU RNA-directed DNA polymerase from mobile element jockey	2.32	0.0330
tc1a	TC1A_CAEEL Transposable element Tc1 transposase	2.93	0.0330
GPR89B	GPHRB_HUMAN Golgi pH regulator B	3.37	0.0330
BAZ2B	BAZ2B_HUMAN Bromodomain adjacent to zinc finger domain protein 2B	-1.53	0.0331
#N/A	TCB1_CAEBR Transposable element Tcb1 transposase	2.85	0.0331
#N/A	#N/A	3.27	0.0332
pol	RTJK_DROME RNA-directed DNA polymerase from mobile element jockey	1.79	0.0333
tc1a	TC1A_CAEEL Transposable element Tc1 transposase	0.93	0.0334
#N/A	#N/A	2.09	0.0335
#N/A	#N/A	3.19	0.0335

Rnh1	RINI_RAT Ribonuclease inhibitor	1.45	0.0335
#N/A	#N/A	4.32	0.0335
Hat1	HAT1_MOUSE Histone acetyltransferase type B catalytic subunit	-2.39	0.0335
SEC16	SEC16_DEBHA COPII coat assembly protein SEC16	3.50	0.0335
RBM25	RBM25_HUMAN RNA-binding protein 25	3.63	1.0000
rpoC2	RPOC2_MAIZE DNA-directed RNA polymerase subunit beta"	3.10	0.0336
Lrrc4	LRRC4_RAT Leucine-rich repeat-containing protein 4	2.28	0.0337
#N/A	#N/A	4.84	0.0337
ZC3H13	ZC3HD_HUMAN Zinc finger CCCH domain-containing protein 13	-2.04	0.0338
#N/A	H33_HORVU Histone H3.3	3.76	0.0338
Slc35b1	S35B1_MOUSE Solute carrier family 35 member B1	2.73	0.0338
SLAMF8	SLAF8_HUMAN SLAM family member 8	2.60	0.0339
#N/A	TCB1_CAEBR Transposable element Tcb1 transposase	2.56	0.0339
#N/A	TCB2_CAEBR Transposable element Tcb2 transposase	1.21	0.0339
jockey\pol	RTJK_DROFU RNA-directed DNA polymerase from mobile element jockey	2.34	0.0339
Khdc3	KHDC3_RAT KH domain-containing protein 3	4.40	0.0340
gatC	GATC_DESMR Aspartyl/glutamyl-tRNA(Asn/Gln) amidotransferase subunit C	3.27	0.0340
#N/A	#N/A	3.68	0.0340
tc1a	TC1A_CAEEL Transposable element Tc1 transposase	3.56	0.0340
#N/A	FA84A_MOUSE Protein FAM84A	2.15	0.0340
#N/A	STXB_SYNHO Stonustoxin subunit beta	3.37	0.0340
Adgrf5	AGRF5_MOUSE Adhesion G protein-coupled receptor F5	2.90	0.0341
#N/A	#N/A	2.60	0.0341
tc1a	TC1A_CAEEL Transposable element Tc1 transposase	3.06	0.0343
#N/A	#N/A	4.19	0.0343
DDB_G0275411	Y5411_DICDI putative uncharacterized GPI-anchored protein DDB_G0275411	4.79	0.0343
BSG	BASI_CHICK Basigin	-3.31	1.0000
pepA	AMPA_GEOSM Probable cytosol aminopeptidase	-1.80	0.0345
HSPG2	PGBM_HUMAN Basement membrane-specific heparan sulfate proteoglycan core protein	-5.37	1.0000
Clec4e	CLC4E_RAT C-type lectin domain family 4 member E	-3.05	0.0345
sup-1	SUP1_CAEEL Protein SUP-1	3.69	0.0347
#N/A	#N/A	3.37	0.0347
HSD6	HSD6_ARATH 11-beta-hydroxysteroid dehydrogenase-like 6	3.64	1.0000
ATG12	ATG12_PICGU Ubiquitin-like protein ATG12	3.18	0.0348
pol	RTJK_DROME RNA-directed DNA polymerase from mobile element jockey	2.95	0.0348
#N/A	#N/A	2.25	0.0348
ileS	SYI_CHRVO Isoleucine--tRNA ligase	4.09	0.0348
#N/A	#N/A	3.39	0.0349
#N/A	#N/A	4.33	0.0349
#N/A	HB2C_PIG SLA class II histocompatibility antigen, DQ haplotype C beta chain	2.49	0.0349
RSBN1L	RSBNL_HUMAN Round spermatid basic protein 1-like protein	-4.34	1.0000
SPCC1494.01	YQK1_SCHPO UPF0676 protein C1494.01	3.96	0.0350
#N/A	#N/A	3.35	0.0350
#N/A	RLA0_RANSY 60S acidic ribosomal protein P0	2.00	0.0350
#N/A	TCB1_CAEBR Transposable element Tcb1 transposase	3.21	0.0351
JKAMP	JKAMP_HUMAN JNK1/MAPK8-associated membrane protein	4.06	0.0355
Rtn1	RTN1_RAT Reticulon-1	4.37	0.0355
#N/A	#N/A	4.16	0.0355
truD	TRUD_PSEPF tRNA pseudouridine synthase D	2.17	0.0355
#N/A	#N/A	1.74	0.0356
#N/A	#N/A	4.03	0.0362
#N/A	#N/A	3.02	0.0364
MMT1	MMT1_HORVU Methionine S-methyltransferase	3.35	0.0365
Sfri_2298	PSRP_SHEFN Putative phosphoenolpyruvate synthase regulatory protein	1.72	0.0365
Slc7a5	LAT1_RAT Large neutral amino acids transporter small subunit 1	4.00	0.0368
#N/A	TCB2_CAEBR Transposable element Tcb2 transposase	2.47	0.0369
phlda2	PHLA2_SALSA Pleckstrin homology-like domain family A member 2	-2.01	0.0369
ATL44	ATL44_ARATH RING-H2 finger protein ATL44	2.25	0.0369
panB	PANB_BACSK 3-methyl-2-oxobutanoate hydroxymethyltransferase	4.04	0.0369
Rpl13a	RL13A_RAT 60S ribosomal protein L13a	-5.11	1.0000
Laptm4b	LAP4B_RAT Lysosomal-associated transmembrane protein 4B	2.21	0.0369
hisS	SYH_NEOSM Histidine--tRNA ligase	3.17	0.0372
ZDHHC24	ZDH24_HUMAN Probable palmitoyltransferase ZDHHC24	-3.28	1.0000
#N/A	#N/A	2.73	0.0373

tc1a	TC1A_CAEEL Transposable element Tc1 transposase	3.16	0.0373
Patr-G	HLAG_PANTR Patr class I histocompatibility antigen, alpha chain G	1.73	0.0373
#N/A	TCB1_CAEBR Transposable element Tcb1 transposase	3.15	0.0373
#N/A	TCB2_CAEBR Transposable element Tcb2 transposase	1.79	0.0373
DNF3	ATC8_YEAST Probable phospholipid-transporting ATPase DNF3	2.20	0.0374
Slc29a1	S29A1_RAT Equilibrative nucleoside transporter 1	3.94	0.0374
#N/A	TCB1_CAEBR Transposable element Tcb1 transposase	3.51	0.0376
#N/A	TCB1_CAEBR Transposable element Tcb1 transposase	3.72	0.0376
ctp	DYL1_DROME Dynein light chain 1, cytoplasmic	-4.41	1.0000
pol	RTJK_DROME RNA-directed DNA polymerase from mobile element jockey	2.83	0.0376
QSOX1	QSOX1_CAVPO Sulfhydryl oxidase 1	-2.41	0.0376
Cnst	CNST_MOUSE Consortin	4.78	0.0376
Rpl37a-ps1	RL37P_RAT Putative 60S ribosomal protein L37a	3.69	0.0376
#N/A	#N/A	2.62	0.0376
Ephb6	EPHB6_RAT Ephrin type-B receptor 6	4.21	0.0376
#N/A	#N/A	3.57	0.0376
SRCAP	SRCAP_HUMAN Helicase SRCAP	-2.94	0.0377
tc1a	TC1A_CAEEL Transposable element Tc1 transposase	1.85	0.0378
tc1a	TC1A_CAEEL Transposable element Tc1 transposase	2.89	0.0378
#N/A	TCB2_CAEBR Transposable element Tcb2 transposase	4.00	0.0379
Akr7a3	ARK73_RAT Aflatoxin B1 aldehyde reductase member 3	3.02	0.0379
UL141	UL141_HCMVM Protein UL141	-4.19	1.0000
#N/A	#N/A	2.88	0.0379
TUBGCP3	GCP3_HUMAN Gamma-tubulin complex component 3	3.04	0.0379
F11r	JAM1_MOUSE Junctional adhesion molecule A	1.32	0.0379
GIP	COPIA_DROME Copia protein	2.41	0.0379
BNA5-2	KYNU2_PHANO Kynureninase 2	1.91	0.0379
RTase	RTBS_DROME Probable RNA-directed DNA polymerase from transposon BS	2.99	0.0379
#N/A	UBIQP_XENLA Polyubiquitin	3.66	1.0000
Fh	FUMH_MOUSE Fumarate hydratase, mitochondrial	2.25	0.0380
tc1a	TC1A_CAEEL Transposable element Tc1 transposase	3.36	0.0380
rps21	RS21_ICTPU 40S ribosomal protein S21	-4.36	1.0000
#N/A	#N/A	3.79	0.0382
#N/A	TCB1_CAEBR Transposable element Tcb1 transposase	3.84	0.0382
#N/A	#N/A	2.66	0.0382
scube2	SCUB2_DANRE Signal peptide, CUB and EGF-like domain-containing protein 2	2.12	0.0382
cyp3a40	C340_ORYLA Cytochrome P450 3A40	1.74	0.0382
#N/A	TCB2_CAEBR Transposable element Tcb2 transposase	2.97	0.0382
Arhgap21	RHG21_MOUSE Rho GTPase-activating protein 21	2.94	0.0382
rpl27a	RL27A_XENLA 60S ribosomal protein L27a	-5.97	1.0000
jockey\pol	RTJK_DROFU RNA-directed DNA polymerase from mobile element jockey	2.49	0.0382
cpsf6	CPSF6_DANRE Cleavage and polyadenylation specificity factor subunit 6	-2.64	0.0383
ITGA6	ITA6_CHICK Integrin alpha-6	3.34	0.0383
#N/A	#N/A	2.25	0.0383
RTT101	CUL8_YEAST Cullin-8	3.54	1.0000
tc1a	TC1A_CAEEL Transposable element Tc1 transposase	1.55	0.0384
gvpD	GVPD_HALMT Protein GvpD	3.52	0.0384
Dbnl	DBNL_MOUSE Drebrin-like protein	3.76	0.0385
ABC2731	Y2731_BACSK UPF0173 metal-dependent hydrolase ABC2731	3.49	0.0386
ptmaa	PTMAA_DANRE Prothymosin alpha-A	-2.54	0.0386
#N/A	#N/A	3.64	0.0386
BYE1	BYE1_YARLI Transcription factor BYE1	4.29	0.0386
chlN	CHLN_SYNJA Light-independent protochlorophyllide reductase subunit N	3.23	0.0387
brms1la	BM1LA_DANRE Breast cancer metastasis-suppressor 1-like protein-A	-2.84	0.0387
#N/A	TCB1_CAEBR Transposable element Tcb1 transposase	3.46	0.0387
Sh2d4b	SH24B_MOUSE SH2 domain-containing protein 4B	-1.60	0.0387
MYSM1	MYSM1_BRAFL Histone H2A deubiquitinase MYSM1	3.34	0.0387
RTase	RTBS_DROME Probable RNA-directed DNA polymerase from transposon BS	2.82	0.0387
wtap	FL2D_DANRE Pre-mRNA-splicing regulator WTAP	-3.37	0.0387
#N/A	TCB1_CAEBR Transposable element Tcb1 transposase	1.92	0.0387
RNF19A	RN19A_PIG E3 ubiquitin-protein ligase RNF19A	3.73	0.0387
#N/A	#N/A	-2.74	0.0387
ctaB	COXX_ROSCS Protoheme IX farnesyltransferase	1.69	0.0387
CSF1R	CSF1R_HUMAN Macrophage colony-stimulating factor 1 receptor	-5.37	1.0000
ACOX1	ACOX1_PHACI Peroxisomal acyl-coenzyme A oxidase 1	2.58	0.0388
Ank3	ANK3_MOUSE Ankyrin-3	1.82	0.0388

#N/A	#N/A	3.69	0.0389
Th	TY3H_MOUSE Tyrosine 3-monooxygenase	4.69	0.0390
TPRG1L	TPRGL_HUMAN Tumor protein p63-regulated gene 1-like protein	3.74	0.0390
#N/A	#N/A	3.48	0.0391
ADAM29	ADA29_HUMAN Disintegrin and metalloproteinase domain-containing protein 29	3.93	0.0391
#N/A	#N/A	3.05	0.0391
EIF4A3	RH2_ARATH DEAD-box ATP-dependent RNA helicase 2	1.72	0.0392
PRT1	EIF3B_CANGA Eukaryotic translation initiation factor 3 subunit B	3.94	0.0392
TBC1D2	TBD2A_BOVIN TBC1 domain family member 2A	3.70	0.0392
Hnrnpab	ROAA_MOUSE Heterogeneous nuclear ribonucleoprotein A/B	-5.37	1.0000
EIF5A	IF5A1_RABIT Eukaryotic translation initiation factor 5A-1	-5.37	1.0000
YEL1	YEL1_ASHGO Guanine-nucleotide exchange factor YEL1	3.44	0.0393
Ptpn12	PTN12_MOUSE Tyrosine-protein phosphatase non-receptor type 12	-1.22	0.0394
Kcnh1	KCNH1_RAT Potassium voltage-gated channel subfamily H member 1	3.39	0.0394
depdc7	DEPD7_DANRE DEP domain-containing protein 7	2.08	0.0396
tnpR	TNR1_ECOLI Transposon gamma-delta resolvase	3.32	0.0396
#N/A	TCB1_CAEBR Transposable element Tcb1 transposase	3.31	0.0396
#N/A	#N/A	1.77	0.0396
#N/A	TCB2_CAEBR Transposable element Tcb2 transposase	1.71	0.0397
CD47	CD47_BOVIN Leukocyte surface antigen CD47	1.54	0.0397
rnpA	RNPA_HELPY Ribonuclease P protein component	1.25	0.0398
Rab11fip1	RFIP1_MOUSE Rab11 family-interacting protein 1	3.74	0.0398
rpl24	RL24_GILMI 60S ribosomal protein L24	-6.59	0.0399
#N/A	#N/A	3.53	0.0400
#N/A	#N/A	3.71	0.0400
#N/A	LIN1_NYCCO LINE-1 reverse transcriptase homolog	3.34	0.0400
Tox	TOX_MOUSE Thymocyte selection-associated high mobility group box protein TOX	4.29	0.0400
MGST1	MGST1_PIG Microsomal glutathione S-transferase 1	3.10	0.0402
#N/A	#N/A	4.06	0.0403
jockey\pol	RTJK_DROFU RNA-directed DNA polymerase from mobile element jockey	3.31	0.0403
tc1a	TC1A_CAEEL Transposable element Tc1 transposase	3.60	1.0000
JUN	JUN_CHICK Transcription factor AP-1	-1.44	0.0403
#N/A	TCB1_CAEBR Transposable element Tcb1 transposase	1.59	0.0403
mdm1	MDM1_DANRE Nuclear protein MDM1	3.80	0.0403
CYTH1	CYH1_HUMAN Cytohesin-1	2.14	0.0403
szrd1	SZRD1_DANRE SUZ domain-containing protein 1	3.00	0.0403
RTase	RTBS_DROME Probable RNA-directed DNA polymerase from transposon BS	1.75	0.0403
GPR50	MTR1L_HUMAN Melatonin-related receptor	3.15	0.0403
mx2	MX2_ONCMY Interferon-induced GTP-binding protein Mx2	2.92	0.0403
#N/A	#N/A	3.54	1.0000
#N/A	#N/A	2.61	0.0404
LGALS1	LEG1_HUMAN Galectin-1	4.19	0.0404
Hipk3	HIPK3_MOUSE Homeodomain-interacting protein kinase 3	3.66	0.0404
QRICH2	QRIC2_HUMAN Glutamine-rich protein 2	2.79	0.0404
#N/A	#N/A	-2.46	0.0404
addA	ADDA_STRU0 ATP-dependent helicase/nuclease subunit A	1.88	0.0404
prtC	PRTC_DICCH Serralysin C	2.64	0.0404
plsB	PLSB_PHOLL Glycerol-3-phosphate acyltransferase	2.59	0.0405
Rpl12	RL12_MOUSE 60S ribosomal protein L12	5.24	0.0405
TUT4	TUT4_HUMAN Terminal uridylyltransferase 4	2.23	0.0405
#N/A	LIN1_NYCCO LINE-1 reverse transcriptase homolog	3.43	0.0405
hdac1-b	HDA1B_XENLA Probable histone deacetylase 1-B	-2.27	0.0406
#N/A	#N/A	2.06	0.0406
Snrnp70	RU17_MOUSE U1 small nuclear ribonucleoprotein 70 kDa	-2.29	0.0406
#N/A	#N/A	2.05	0.0409
GPT2	ALAT2_HUMAN Alanine aminotransferase 2	2.20	0.0409
#N/A	#N/A	-4.64	1.0000
CASP1	CASP1_FELCA Caspase-1	3.15	0.0409
GTF2H2	TF2H2_BOVIN General transcription factor IIH subunit 2	-3.60	1.0000
#N/A	#N/A	2.38	0.0410
hemC	HEM3_DESVM Porphobilinogen deaminase	2.85	0.0411
CORO1C	COR1C_HUMAN Coronin-1C	1.42	0.0411
arf3	ARF3_TAKRU ADP-ribosylation factor 3	1.80	0.0411
Fam222a	F222A_MOUSE Protein FAM222A	2.72	0.0411
#N/A	AFLL_ASPPA Versicolorin B desaturase	2.41	0.0412
#N/A	TCB1_CAEBR Transposable element Tcb1 transposase	3.02	0.0413

PputGB1_5045	Y5045_PSEPG UPF0301 protein PputGB1_5045	4.17	0.0413
tc1a	TC1A_CAEEL Transposable element Tc1 transposase	2.35	0.0413
ACE	ACE_CHICK Angiotensin-converting enzyme	-3.91	1.0000
#N/A	TCB1_CAEBR Transposable element Tcb1 transposase	1.97	0.0414
#N/A	#N/A	3.52	0.0415
wdr-20	WDR20_CAEEL WD repeat-containing protein 20 homolog {ECO:0000250|UniProtKB:Q8TBZ3}	2.28	0.0416
#N/A	TCB1_CAEBR Transposable element Tcb1 transposase	2.09	0.0416
rpl36a	RL36A_TAKRU 60S ribosomal protein L36a	-5.78	1.0000
#N/A	CC014_BOVIN Uncharacterized protein C3orf14 homolog	3.21	0.0417
#N/A	TCB2_CAEBR Transposable element Tcb2 transposase	2.25	0.0417
PLEKHA5	PKHA5_HUMAN Pleckstrin homology domain-containing family A member 5	3.07	0.0418
#N/A	#N/A	3.89	0.0419
ileS	SYI_SULDN Isoleucine--tRNA ligase	-5.89	1.0000
tc1a	TC1A_CAEEL Transposable element Tc1 transposase	3.26	0.0421
DOCK7	DOCK7_HUMAN Dedicator of cytokinesis protein 7	3.88	0.0422
tc1a	TC1A_CAEEL Transposable element Tc1 transposase	2.83	0.0422
Zbed4	ZBED4_MOUSE Zinc finger BED domain-containing protein 4	2.68	0.0422
#N/A	TCB1_CAEBR Transposable element Tcb1 transposase	3.58	0.0422
tc1a	TC1A_CAEEL Transposable element Tc1 transposase	2.16	0.0422
#N/A	#N/A	3.12	0.0422
#N/A	#N/A	2.00	0.0423
CMTM7	CKLF7_HUMAN CKLF-like MARVEL transmembrane domain-containing protein 7	2.46	0.0424
#N/A	DFNA5_HUMAN Non-syndromic hearing impairment protein 5	-2.40	0.0424
#N/A	#N/A	3.42	0.0424
#N/A	TCB1_CAEBR Transposable element Tcb1 transposase	3.78	0.0424
#N/A	CYT_ONCKE Cystatin	-5.43	1.0000
#N/A	TCB1_CAEBR Transposable element Tcb1 transposase	2.22	0.0424
Arrdc5	ARRD5_MOUSE Arrestin domain-containing protein 5	3.74	0.0425
#N/A	#N/A	3.63	0.0425
RTase	RTBS_DROME Probable RNA-directed DNA polymerase from transposon BS	1.41	0.0425
#N/A	TCB1_CAEBR Transposable element Tcb1 transposase	3.72	0.0425
katG	KATG_ACICJ Catalase-peroxidase	2.67	0.0426
krt13	K1C13_ONCMY Keratin, type I cytoskeletal 13	-3.02	0.0426
jockey\pol	RTJK_DROFU RNA-directed DNA polymerase from mobile element jockey	1.63	0.0428
jockey\pol	RTJK_DROFU RNA-directed DNA polymerase from mobile element jockey	3.40	0.0428
tc1a	TC1A_CAEEL Transposable element Tc1 transposase	3.59	1.0000
tmk	KTHY_METS5 Probable thymidylate kinase	1.49	0.0431
#N/A	#N/A	3.31	0.0431
#N/A	TCB1_CAEBR Transposable element Tcb1 transposase	1.65	0.0432
aspS	SYD_LACRJ Aspartate--tRNA ligase	3.80	0.0432
Nme3	NDK3_MOUSE Nucleoside diphosphate kinase 3	2.08	0.0433
pol	RTJK_DROME RNA-directed DNA polymerase from mobile element jockey	3.35	0.0433
skp1	SKP1_XENLA S-phase kinase-associated protein 1	2.86	0.0433
#N/A	Y1932_PASMU Uncharacterized protein PM1932	3.75	0.0433
#N/A	#N/A	-2.20	0.0433
HI_0258	Y258_HAEIN Putative glycosyltransferase HI_0258	3.09	0.0433
DUSP1	DUS1_HUMAN Dual specificity protein phosphatase 1	-2.03	0.0435
#N/A	TCB2_CAEBR Transposable element Tcb2 transposase	2.41	0.0437
mnmG	MNMG_SULMW tRNA uridine 5-carboxymethylaminomethyl modification enzyme MnmG	3.75	0.0438
#N/A	TCB1_CAEBR Transposable element Tcb1 transposase	3.70	0.0438
#N/A	TM56B_XENLA Transmembrane protein 56-B	1.96	0.0438
ade	ADEC_ECOL6 Adenine deaminase	3.75	0.0440
BBX	BBX_HUMAN HMG box transcription factor BBX	3.67	0.0440
nipblb	NIPLB_DANRE Nipped-B-like protein B	1.89	0.0441
mios-b	MIOB_XENLA WD repeat-containing protein mio-B	2.69	0.0441
#N/A	TCB1_CAEBR Transposable element Tcb1 transposase	2.13	0.0442
mceB	IM92_KLEPN Microcin E492 immunity protein	3.52	0.0443
44051	AUG8_ARATH AUGMIN subunit 8	2.67	0.0444
tc1a	TC1A_CAEEL Transposable element Tc1 transposase	1.90	0.0444
Uggt1	UGGG1_RAT UDP-glucose:glycoprotein glucosyltransferase 1	3.16	0.0445
qutR	QUTR_TALSN Quinate repressor protein	3.30	0.0446
#N/A	#N/A	1.74	0.0446
#N/A	TCB2_CAEBR Transposable element Tcb2 transposase	3.05	0.0446

#N/A	#N/A	2.23	0.0446
NLRC3	NLRC3_HUMAN Protein NLRC3	1.42	0.0446
CCDC12	CCD12_HUMAN Coiled-coil domain-containing protein 12	-4.51	1.0000
GAL3ST4	G3ST4_BOVIN Galactose-3-O-sulfotransferase 4	1.29	0.0448
#N/A	#N/A	4.05	0.0449
supt6h	SPT6H_DANRE Transcription elongation factor SPT6	-0.93	0.0452
#N/A	TCB1_CAEBR Transposable element Tcb1 transposase	3.77	0.0452
#N/A	#N/A	4.36	0.0452
pfp	PFP_PORGN Pyrophosphate--fructose 6-phosphate 1-phosphotransferase	3.55	0.0452
Smarca4	SMCA4_RAT Transcription activator BRG1	-2.75	0.0452
#N/A	H6_ONCMY Non-histone chromosomal protein H6	-5.80	1.0000
Nme1	NDKA_RAT Nucleoside diphosphate kinase A	-5.80	1.0000
#N/A	CG043_MOUSE Uncharacterized protein C7orf43 homolog	3.54	1.0000
#N/A	#N/A	3.56	0.0454
kefG	KEFG_YERPY Glutathione-regulated potassium-efflux system ancillary protein KefG	3.81	0.0454
WAR1	WAR1_CANAL Transcriptional regulator WAR1	2.49	0.0456
ywhaba	143BA_DANRE 14-3-3 protein beta/alpha-A	-1.13	0.0456
Ts	TYSY_DROME Thymidylate synthase	2.30	0.0456
YPR108W-A	YPR08_YEAST Uncharacterized protein YPR108W-A	4.29	0.0456
#N/A	SANT_PLAFF S-antigen protein	2.25	0.0456
#N/A	#N/A	3.87	0.0459
SLC39A11	S39AB_BOVIN Zinc transporter ZIP11	1.77	0.0459
STAT1	STAT1_HUMAN Signal transducer and activator of transcription 1-alpha/beta	3.85	0.0460
#N/A	TCB1_CAEBR Transposable element Tcb1 transposase	2.13	0.0460
tc1a	TC1A_CAEEL Transposable element Tc1 transposase	3.03	0.0461
PDLIM2	PDLI2_MACFA PDZ and LIM domain protein 2	3.93	0.0461
Msantd4	MSD4_MOUSE Myb/SANT-like DNA-binding domain-containing protein 4	-3.82	1.0000
#N/A	TCB2_CAEBR Transposable element Tcb2 transposase	1.90	0.0461
K12H4.7	YM67_CAEEL Putative serine protease K12H4.7	-2.71	0.0462
#N/A	TCB1_CAEBR Transposable element Tcb1 transposase	1.92	0.0463
#N/A	#N/A	2.94	0.0463
KMT2D	KMT2D_HUMAN Histone-lysine N-methyltransferase 2D	2.90	0.0464
EPAS1	EPAS1_HUMAN Endothelial PAS domain-containing protein 1	2.44	0.0464
matK	MATK_HORSA Maturase K	3.24	0.0464
#N/A	TCB1_CAEBR Transposable element Tcb1 transposase	3.34	0.0468
IL16	IL16_PANTR Pro-interleukin-16	-3.82	0.0469
PRKCH	KPCL_HUMAN Protein kinase C eta type	2.77	0.0469
tc1a	TC1A_CAEEL Transposable element Tc1 transposase	2.73	0.0471
#N/A	TCB1_CAEBR Transposable element Tcb1 transposase	1.77	0.0471
lpxK	LPXK_VEREI Tetraacyldisaccharide 4'-kinase	3.81	0.0471
tc1a	TC1A_CAEEL Transposable element Tc1 transposase	1.70	0.0471
#N/A	TCB1_CAEBR Transposable element Tcb1 transposase	3.15	0.0472
#N/A	#N/A	2.31	0.0472
tc1a	TC1A_CAEEL Transposable element Tc1 transposase	3.43	0.0472
#N/A	#N/A	2.58	0.0472
#N/A	#N/A	3.80	0.0472
gag-pol	POL_WDSV Gag-Pol polyprotein	3.19	0.0472
tc1a	TC1A_CAEEL Transposable element Tc1 transposase	3.70	0.0472
#N/A	#N/A	3.64	1.0000
#N/A	#N/A	3.93	0.0472
ycf78	YCF78_STIHE Uncharacterized membrane protein ycf78	3.06	0.0472
GIMAP7	GIMA7_HUMAN GTPase IMAP family member 7	1.47	0.0472
#N/A	#N/A	3.36	0.0473
#N/A	#N/A	3.17	0.0473
focA	FOCA_ECOLI Probable formate transporter 1	1.86	0.0473
ptmaa	PTMAA_DANRE Prothymosin alpha-A	-2.60	0.0473
Ehbp1l1	EH1L1_MOUSE EH domain-binding protein 1-like protein 1	-5.50	0.0473
#N/A	#N/A	2.71	0.0474
NIFU3	NIFU3_ARATH NifU-like protein 3, chloroplastic	-5.88	1.0000
#N/A	#N/A	2.72	0.0477
MIMI_R554	YR554_MIMIV Uncharacterized protein R554	2.54	0.0477
St3gal2	SIA4B_MOUSE CMP-N-acetylneuraminate-beta-galactosamide-alpha-2,3-sialyltransferase 2	3.42	0.0477
#N/A	#N/A	4.01	0.0478

#N/A	TCB1_CAEBR Transposable element Tcb1 transposase	1.66	0.0478
#N/A	TCB1_CAEBR Transposable element Tcb1 transposase	2.78	0.0478
rps10	RS10_NANEQ 30S ribosomal protein S10	1.89	0.0478
GIMAP4	GIMA4_HUMAN GTPase IMAP family member 4	2.55	0.0478
jockey\pol	RTJK_DROFU RNA-directed DNA polymerase from mobile element jockey	1.78	0.0479
RBBP6	RBBP6_HUMAN E3 ubiquitin-protein ligase RBBP6	4.18	0.0479
tmem45b	TM45B_DANRE Transmembrane protein 45B	2.40	0.0479
tc1a	TC1A_CAEEL Transposable element Tc1 transposase	2.34	0.0479
TNFAIP3	TNAP3_MACFA Tumor necrosis factor alpha-induced protein 3	2.87	0.0479
menD	MEND_PORGI 2-succinyl-5-enolpyruvyl-6-hydroxy-3-cyclohexene-1-carboxylate synthase	3.64	0.0480
#N/A	LIN1_NYCCO LINE-1 reverse transcriptase homolog	2.51	0.0481
RBM25	RBM25_HUMAN RNA-binding protein 25	-1.60	0.0481
TENM2	TEN2_HUMAN Teneurin-2	2.52	0.0481
X-element\ORF2	RTXE_DROME Probable RNA-directed DNA polymerase from transposon X-element	1.83	0.0481
SERINC3	SERC3_PONAB Serine incorporator 3	2.41	0.0482
#N/A	#N/A	3.11	0.0482
#N/A	#N/A	3.24	0.0482
Rbm12b1	R12BA_MOUSE RNA-binding protein 12B-A	4.55	0.0482
NEFH	NFH_HUMAN Neurofilament heavy polypeptide	2.03	0.0482
CASK	CSKP_HUMAN Peripheral plasma membrane protein CASK	3.55	0.0482
ube2d2	UB2D2_XENLA Ubiquitin-conjugating enzyme E2 D2	-2.64	0.0482
UMOD	UROM_PONAB Uromodulin	-3.70	1.0000
YTHDC1	YTDC1_HUMAN YTH domain-containing protein 1	2.72	0.0483
RTase	RTBS_DROME Probable RNA-directed DNA polymerase from transposon BS	1.96	0.0483
#N/A	TCB1_CAEBR Transposable element Tcb1 transposase	1.93	0.0484
RNF19A	RN19A_HUMAN E3 ubiquitin-protein ligase RNF19A	-4.38	1.0000
trip10	CIP4_DANRE Cdc42-interacting protein 4 homolog	1.71	0.0485
Amigo1	AMGO1_RAT Amphoterin-induced protein 1	4.26	0.0485
trpD	TRPD_PSESM Anthranilate phosphoribosyltransferase	3.38	0.0486
#N/A	#N/A	2.86	0.0486
#N/A	#N/A	3.08	0.0486
SYAP1	SYAP1_HUMAN Synapse-associated protein 1	-1.74	0.0487
#N/A	#N/A	3.43	1.0000
#N/A	#N/A	1.56	0.0487
FUT9	FUT9_CRIGR Alpha-(1,3)-fucosyltransferase 9	2.43	0.0487
#N/A	#N/A	2.87	0.0488
rppH	RPPH_ORITI RNA pyrophosphohydrolase	3.24	0.0488
tc1a	TC1A_CAEEL Transposable element Tc1 transposase	1.83	0.0490
#N/A	#N/A	2.24	0.0491
tc1a	TC1A_CAEEL Transposable element Tc1 transposase	2.85	0.0491
#N/A	#N/A	2.69	0.0491
Lpar6	LPAR6_RAT Lysophosphatidic acid receptor 6	1.93	0.0492
#N/A	#N/A	2.75	0.0492
h2az2	H2AV_XENTR Histone H2A.V	3.23	0.0493
#N/A	TCB1_CAEBR Transposable element Tcb1 transposase	2.12	0.0494
DMXL1	DMXL1_HUMAN DmX-like protein 1	2.68	0.0494
engB	ENGB_PELPB Probable GTP-binding protein EngB	4.21	0.0494
hsp70	HSP70_ONCTS Heat shock 70 kDa protein	-2.25	0.0494
ZBED5	ZBED5_HUMAN Zinc finger BED domain-containing protein 5	2.78	0.0494
#N/A	TCB2_CAEBR Transposable element Tcb2 transposase	3.43	0.0494
#N/A	#N/A	3.08	0.0494
Dapk2	DAPK2_MOUSE Death-associated protein kinase 2	-1.49	0.0494
#N/A	#N/A	2.56	0.0494
At3g16880	FBK57_ARATH Putative F-box/kelch-repeat protein At3g16880	3.70	0.0496
pho88	PHO88_SCHPO Inorganic phosphate transport protein pho88	2.46	0.0496
tc1a	TC1A_CAEEL Transposable element Tc1 transposase	2.94	0.0497
ube2d2	UB2D2_XENLA Ubiquitin-conjugating enzyme E2 D2	3.45	0.0497
SLC36A1	S36A1_HUMAN Proton-coupled amino acid transporter 1	2.90	0.0498
Elys	ELYS_DROME Protein ELYS homolog	3.44	1.0000
hisE	HIS2_VESOH Phosphoribosyl-ATP pyrophosphatase	2.72	0.0499

Table B-2. List of all differentially expressed transcripts (FDR adjusted $p \leq 0.1$) in epidermal mucus ranked by *p* value in dilbit-exposed lake trout compared 2018 baseline samples.

Gene Symbol	UniProtID and Full Gene Name	log2 Fold Change	*p*-adj
FRRS1	FRRS1_HUMAN Ferric-chelate reductase 1	3.00	2.72E-21
LMO7	LMO7_HUMAN LIM domain only protein 7	2.61	6.31E-17
HLF	HLF_HUMAN Hepatic leukemia factor	4.92	2.29E-16
CR1	CR1_HUMAN Complement receptor type 1	4.88	1.55E-14
HIP1R	HIP1R_HUMAN Huntingtin-interacting protein 1-related protein	2.66	1.05E-11
ST3GAL1	SIA4A_CHICK CMP-N-acetylneuraminate-beta-galactosamide-alpha-2,3-sialyltransferase 1	4.27	5.05E-11
Plec	PLEC_MOUSE Plectin	-3.96	5.05E-11
Kiaa1671	K1671_MOUSE Uncharacterized protein KIAA1671	2.27	9.32E-11
TGas006m08.1	H4_XENTR Histone H4	-3.33	1.86E-10
Hpgd	PGDH_MOUSE 15-hydroxyprostaglandin dehydrogenase [NAD(+)]	5.18	6.86E-10
GIMAP7	GIMA7_HUMAN GTPase IMAP family member 7	2.82	1.12E-09
Myo1e	MYO1E_MOUSE Unconventional myosin-Ie	2.84	1.12E-09
#N/A	#N/A	3.91	1.55E-09
EZR	EZRI_RABIT Ezrin	2.05	4.06E-09
PPL	PEPL_HUMAN Periplakin	2.17	4.71E-09
TAR1	TAR1_YEAST Protein TAR1	-3.02	9.51E-09
SEC23A	SC23A_CHICK Protein transport protein Sec23A	2.74	1.01E-08
AHNAK	AHNK_HUMAN Neuroblast differentiation-associated protein AHNAK	3.44	1.07E-08
Plec	PLEC_MOUSE Plectin	-4.41	1.08E-08
CAPN9	CAN9_HUMAN Calpain-9	2.20	1.28E-08
EVPL	EVPL_HUMAN Envoplakin	3.08	1.95E-08
WDTC1	WDTC1_HUMAN WD and tetratricopeptide repeats protein 1	-2.75	3.12E-08
Ly6g6d	LY66D_RAT Lymphocyte antigen 6 complex locus protein G6d	4.30	4.68E-08
MYH9	MYH9_CHICK Myosin-9	1.96	4.86E-08
#N/A	LEC_GALNI Mannose-specific lectin	-3.79	5.73E-08
RDX	RADI_HUMAN Radixin	3.16	5.73E-08
rrm2	RIR2_DANRE Ribonucleoside-diphosphate reductase subunit M2	-4.85	5.99E-08
Rrbp1	RRBP1_MOUSE Ribosome-binding protein 1	5.18	5.99E-08
Eps8l2	ES8L2_MOUSE Epidermal growth factor receptor kinase substrate 8-like protein 2	3.98	7.88E-08
MXD4	MAD4_HUMAN Max dimerization protein 4	3.28	1.73E-07
LITAF	LITAF_CHICK Lipopolysaccharide-induced tumor necrosis factor-alpha factor homolog	3.00	2.42E-07
mt-co1	COX1_ONCMY Cytochrome c oxidase subunit 1	3.77	2.53E-07
AHNAK	AHNK_HUMAN Neuroblast differentiation-associated protein AHNAK	2.83	2.63E-07
TUFT1	TUFT1_BOVIN Tuftelin {ECO:0000303|PubMed:1874744}	2.32	3.71E-07
Proser2	PRSR2_MOUSE Proline and serine-rich protein 2	5.38	5.08E-07
UPK1A	UPK1A_BOVIN Uroplakin-1a	2.53	5.70E-07
rps7	RS7_TAKRU 40S ribosomal protein S7	-2.30	5.97E-07
MYH9	MYH9_HUMAN Myosin-9	3.69	6.58E-07
RHOBTB1	RHBT1_HUMAN Rho-related BTB domain-containing protein 1	3.21	1.00E-06
SYNE1	SYNE1_HUMAN Nesprin-1	-3.68	1.15E-06
jag1b	JAG1B_DANRE Protein jagged-1b	-2.86	1.20E-06
AHNAK	AHNK_HUMAN Neuroblast differentiation-associated protein AHNAK	3.92	1.34E-06
#N/A	#N/A	5.34	1.34E-06
#N/A	H3_URECA Histone H3	-4.54	1.34E-06
AHNAK	AHNK_HUMAN Neuroblast differentiation-associated protein AHNAK	5.03	1.56E-06
APLP1	APLP1_HUMAN Amyloid-like protein 1	3.39	1.62E-06
LRP1	LRP1_CHICK Low-density lipoprotein receptor-related protein 1	-3.37	1.64E-06
#N/A	DFNA5_HUMAN Non-syndromic hearing impairment protein 5	-6.86	1.99E-06
Ly6g6d	LY66D_RAT Lymphocyte antigen 6 complex locus protein G6d	2.83	2.00E-06
OSBPL6	OSBL6_HUMAN Oxysterol-binding protein-related protein 6	2.18	2.00E-06
gmppb	GMPPB_DANRE Mannose-1-phosphate guanyltransferase beta	2.40	2.12E-06
Tf2-9	TF29_SCHPO Transposon Tf2-9 polyprotein	-2.65	2.19E-06
CAPZB	CAPZB_CHICK F-actin-capping protein subunit beta isoforms 1 and 2	2.23	2.19E-06
#N/A	TCB1_CAEBR Transposable element Tcb1 transposase	-3.00	2.32E-06

Map7d1	MA7D1_MOUSE MAP7 domain-containing protein 1	6.15	2.52E-06
rsmG	RSMG_METC4 Ribosomal RNA small subunit methyltransferase G {ECO:0000255|HAMAP-Rule:MF_00074}	-3.07	2.52E-06
Eppk1	EPIPL_MOUSE Epiplakin	-2.81	2.57E-06
Tf2-6	TF26_SCHPO Transposon Tf2-6 polyprotein	-2.02	4.60E-06
TSPAN8	TSN8_PONAB Tetraspanin-8	2.86	4.89E-06
cxadr	CXAR_DANRE Coxsackievirus and adenovirus receptor homolog	2.65	5.98E-06
TNIP1	TNIP1_HUMAN TNFAIP3-interacting protein 1	1.99	6.09E-06
#N/A	#N/A	2.51	6.23E-06
Tnik	TNIK_MOUSE Traf2 and NCK-interacting protein kinase	-3.60	6.83E-06
EPS8L1	ES8L1_HUMAN Epidermal growth factor receptor kinase substrate 8-like protein 1	3.01	7.69E-06
#N/A	H2B_SALTR Histone H2B	-2.70	8.50E-06
Rpl12	RL12_MOUSE 60S ribosomal protein L12	-2.82	8.50E-06
URGCP	URGCP_BOVIN Up-regulator of cell proliferation	2.79	1.16E-05
LMO7	LMO7_HUMAN LIM domain only protein 7	6.89	1.16E-05
PITPNA	PIPNA_RABIT Phosphatidylinositol transfer protein alpha isoform	2.40	1.19E-05
EVPL	EVPL_HUMAN Envoplakin	1.95	1.31E-05
#N/A	#N/A	4.02	1.34E-05
#N/A	SLP1_PINMG Shematrin-like protein 1	2.38	1.34E-05
Homer2	HOME2_RAT Homer protein homolog 2	2.40	1.56E-05
SYNE2	SYNE2_HUMAN Nesprin-2	-1.74	1.77E-05
#N/A	#N/A	2.83	2.17E-05
#N/A	#N/A	4.02	2.67E-05
Dsg2	DSG2_MOUSE Desmoglein-2	2.00	3.03E-05
GADL1	GADL1_BOVIN Acidic amino acid decarboxylase GADL1	2.89	3.38E-05
Myo5b	MYO5B_MOUSE Unconventional myosin-Vb	1.80	3.38E-05
SYNE2	SYNE2_HUMAN Nesprin-2	-3.47	3.95E-05
PLA2G4C	PA24C_HUMAN Cytosolic phospholipase A2 gamma	-2.33	3.95E-05
Klf2	KLF2_MOUSE Krueppel-like factor 2	2.78	3.97E-05
paqr5b	MPRGB_DANRE Membrane progestin receptor gamma-B	3.37	3.97E-05
Svmpi-Cce12	SVMI1_CERCE Snake venom metalloprotease inhibitor 02A10	4.19	4.10E-05
tcaf	TCAF_DANRE TRPM8 channel-associated factor homolog	1.96	4.27E-05
#N/A	H3_URECA Histone H3	-3.72	4.27E-05
PNP	PNPH_BOVIN Purine nucleoside phosphorylase	4.16	4.54E-05
Proser2	PRSR2_MOUSE Proline and serine-rich protein 2	3.72	4.95E-05
PLCD1	PLCD1_BOVIN 1-phosphatidylinositol 4,5-bisphosphate phosphodiesterase delta-1	4.01	4.95E-05
TMEM131	TM131_HUMAN Transmembrane protein 131	2.96	4.95E-05
Gnaq	GNAQ_MOUSE Guanine nucleotide-binding protein G(q) subunit alpha	3.36	4.96E-05
stk10	STK10_DANRE Serine/threonine-protein kinase 10	1.90	5.11E-05
Sqstm1	SQSTM_MOUSE Sequestosome-1	2.69	5.27E-05
Rnf186	RN186_MOUSE RING finger protein 186	-2.88	5.30E-05
FGD3	FGD3_HUMAN FYVE, RhoGEF and PH domain-containing protein 3	3.10	5.35E-05
PDLIM2	PDLI2_MACFA PDZ and LIM domain protein 2	6.20	5.59E-05
UU149	Y149_UREPA Uncharacterized protein UU149	3.23	6.48E-05
#N/A	#N/A	-3.26	6.57E-05
CGNL1	CGNL1_HUMAN Cingulin-like protein 1	2.88	6.73E-05
BTN1A1	BT1A1_HUMAN Butyrophilin subfamily 1 member A1	2.35	6.80E-05
RRT12	RRT12_YEAST Subtilase-type proteinase RRT12	-2.80	6.80E-05
Lrrk1	LRRK1_MOUSE Leucine-rich repeat serine/threonine-protein kinase 1	-2.79	7.25E-05
Dock8	DOCK8_MOUSE Dedicator of cytokinesis protein 8	-3.34	7.53E-05
Krt42	K1C42_RAT Keratin, type I cytoskeletal 42	-4.85	7.79E-05
COL6A2	CO6A2_CHICK Collagen alpha-2(VI) chain	-5.60	7.99E-05
HERC2	HERC2_HUMAN E3 ubiquitin-protein ligase HERC2	-1.47	8.00E-05
AHNAK	AHNK_HUMAN Neuroblast differentiation-associated protein AHNAK	2.83	8.98E-05
EIF4A1	IF4A1_PONAB Eukaryotic initiation factor 4A-I	-2.74	8.98E-05
rps2	RS2_ICTPU 40S ribosomal protein S2	-2.46	8.98E-05
Proser2	PRSR2_MOUSE Proline and serine-rich protein 2	5.67	1.15E-04
ANXA11	ANX11_HUMAN Annexin A11	6.10	1.17E-04
BRD7	BRD7_CHICK Bromodomain-containing protein 7	3.48	1.21E-04
cep170b	C170B_XENTR Centrosomal protein of 170 kDa protein B	-6.28	1.21E-04
SYNE1	SYNE1_HUMAN Nesprin-1	-4.92	1.22E-04
B4GALNT1	B4GN1_HUMAN Beta-1,4 N-acetylgalactosaminyltransferase 1	4.00	1.26E-04
TOP2A	TOP2A_CHICK DNA topoisomerase 2-alpha	-6.09	1.32E-04
#N/A	PVRL2_MOUSE Nectin-2	3.41	1.34E-04

ITPR2	ITPR2_HUMAN Inositol 1,4,5-trisphosphate receptor type 2	-2.54	1.36E-04
pssA	PSS_ECOLI CDP-diacylglycerol--serine O-phosphatidyltransferase	3.12	1.42E-04
Hsd3b7	3BHS7_MOUSE 3 beta-hydroxysteroid dehydrogenase type 7	4.04	1.44E-04
cxadr	CXAR_DANRE Coxsackievirus and adenovirus receptor homolog	3.75	1.46E-04
STK17A	ST17A_RABIT Serine/threonine-protein kinase 17A	2.38	1.50E-04
Cuzd1	CUZD1_MOUSE CUB and zona pellucida-like domain-containing protein 1	5.01	1.51E-04
Gtpbp2	GTPB2_MOUSE GTP-binding protein 2	4.71	1.52E-04
rpl9	RL9_ICTPU 60S ribosomal protein L9	-2.44	1.73E-04
NIAD	NIA_LEPMC Nitrate reductase [NADPH]	-5.37	1.86E-04
ALOXE3	LOXE3_HUMAN Hydroperoxide isomerase ALOXE3	-4.72	1.91E-04
#N/A	#N/A	2.14	1.94E-04
Sdr16c5	RDHE2_MOUSE Epidermal retinol dehydrogenase 2	4.47	2.02E-04
#N/A	#N/A	4.35	2.24E-04
myzap	MYZAP_XENTR Myocardial zonula adherens protein	1.97	2.24E-04
ZNF185	ZN185_HUMAN Zinc finger protein 185	2.81	2.42E-04
AHNAK	AHNK_HUMAN Neuroblast differentiation-associated protein AHNAK	4.24	2.53E-04
ncapd2	CND1_XENLA Condensin complex subunit 1	-5.92	2.78E-04
NCAPG	CND3_HUMAN Condensin complex subunit 3	-5.59	2.84E-04
Slc43a1	LAT3_MOUSE Large neutral amino acids transporter small subunit 3	2.66	2.86E-04
MT-ND5	NU5M_SALSA NADH-ubiquinone oxidoreductase chain 5	1.71	2.86E-04
AHNAK	AHNK_HUMAN Neuroblast differentiation-associated protein AHNAK	4.46	2.86E-04
alas1	HEM1_OPSTA 5-aminolevulinate synthase, nonspecific, mitochondrial	3.29	3.00E-04
EIF4A2	IF4A2_CHICK Eukaryotic initiation factor 4A-II	-4.50	3.20E-04
SPPL2A	SPP2A_HUMAN Signal peptide peptidase-like 2A {ECO:0000303|PubMed:15385547, ECO:0000312|HGNC:HGNC:30227}	5.27	3.28E-04
LMO7	LMO7_HUMAN LIM domain only protein 7	4.16	3.71E-04
BAHD1	BAHD1_ARATH BAHD acyltransferase At5g47980	4.17	4.27E-04
MCTP2	MCTP2_HUMAN Multiple C2 and transmembrane domain-containing protein 2	1.26	4.80E-04
#N/A	NATTL_DANRE Natterin-like protein	-2.67	5.22E-04
C6orf132	CF132_HUMAN Uncharacterized protein C6orf132	2.59	5.27E-04
PDLIM2	PDLI2_BOVIN PDZ and LIM domain protein 2	2.89	5.55E-04
MTH_1421	Y1421_METTH Uncharacterized protein MTH_1421	-1.86	5.95E-04
#N/A	GRM1C_HUMAN GRAM domain-containing protein 1C	2.78	6.10E-04
SPACA4	SACA4_BOVIN Sperm acrosome membrane-associated protein 4	2.94	6.45E-04
TMEM131	TM131_HUMAN Transmembrane protein 131	5.47	6.86E-04
Foxq1	FOXQ1_RAT Forkhead box protein Q1	3.39	6.90E-04
RUNX3	RUNX3_HUMAN Runt-related transcription factor 3	-2.28	6.90E-04
MT-CO2	COX2_TINMA Cytochrome c oxidase subunit 2	2.45	6.90E-04
AHNAK	AHNK_HUMAN Neuroblast differentiation-associated protein AHNAK	4.39	7.18E-04
Adgrg2	AGRG2_MOUSE Adhesion G-protein coupled receptor G2	1.66	7.26E-04
ESYT2	ESYT2_HUMAN Extended synaptotagmin-2	1.86	7.45E-04
ybx1	YBOX1_XENLA Nuclease-sensitive element-binding protein 1	5.59	7.45E-04
CENPF	CENPF_HUMAN Centromere protein F	-6.64	7.54E-04
NOS2	NOS2_CHICK Nitric oxide synthase, inducible	3.98	8.33E-04
SGPL1	SGPL1_HUMAN Sphingosine-1-phosphate lyase 1	2.49	8.63E-04
Trim16	TRI16_MOUSE Tripartite motif-containing protein 16	1.65	8.74E-04
#N/A	#N/A	1.33	8.90E-04
rt	POMT1_DROME Protein O-mannosyltransferase 1	-5.49	8.94E-04
mrh4	MRH4_ASPTN ATP-dependent RNA helicase mrh4, mitochondrial	-1.47	8.96E-04
AHNAK	AHNK_HUMAN Neuroblast differentiation-associated protein AHNAK	4.80	8.96E-04
TP_0404	Y404_TREPA Uncharacterized protein TP_0404	2.51	9.03E-04
Nlrc3	NLRC3_MOUSE Protein NLRC3	-2.49	9.03E-04
TAN1	TAN1_YEAST tRNA acetyltransferase TAN1	-2.81	9.03E-04
EEF2	EF2_CHICK Elongation factor 2	-1.87	9.68E-04
#N/A	#N/A	3.35	1.01E-03
WASF2	WASF2_HUMAN Wiskott-Aldrich syndrome protein family member 2	2.20	1.07E-03
Myh9	MYH9_MOUSE Myosin-9	1.57	1.08E-03
Serp1	SERP1_RAT Stress-associated endoplasmic reticulum protein 1	4.21	1.14E-03
Tnik	TNIK_MOUSE Traf2 and NCK-interacting protein kinase	-1.47	1.14E-03
HERC1	HERC1_HUMAN Probable E3 ubiquitin-protein ligase HERC1	-1.58	1.16E-03
cgn	CING_DANRE Cingulin	1.74	1.18E-03
MDN1	MDN1_HUMAN Midasin	-5.44	1.18E-03
MPN_639	Y639_MYCPN Uncharacterized lipoprotein MG439 homolog 6	-3.18	1.30E-03
Rps20	RS20_RAT 40S ribosomal protein S20	-4.66	1.34E-03
#N/A	#N/A	-5.32	1.36E-03
RPL29	RL29_MACFA 60S ribosomal protein L29	-2.58	1.37E-03

Ldlr	LDLR_RAT Low-density lipoprotein receptor	2.76	1.38E-03
dlx3b	DLX3B_DANRE Homeobox protein Dlx3b	3.24	1.38E-03
Tprn	TPRN_MOUSE Taperin	3.53	1.40E-03
Cdc42ep4	BORG4_MOUSE Cdc42 effector protein 4	3.39	1.44E-03
SPACA4	SACA4_HUMAN Sperm acrosome membrane-associated protein 4	2.69	1.45E-03
ABLIM1	ABLM1_HUMAN Actin-binding LIM protein 1	2.63	1.52E-03
Cds1	CDS1_RAT Phosphatidate cytidylyltransferase 1	2.29	1.54E-03
#N/A	#N/A	-3.79	1.56E-03
AHNAK	AHNK_HUMAN Neuroblast differentiation-associated protein AHNAK	2.48	1.57E-03
#N/A	#N/A	5.89	1.61E-03
junb	JUNB_CYPCA Transcription factor jun-B	-5.19	1.63E-03
ELOVL6	ELOV6_HUMAN Elongation of very long chain fatty acids protein 6 {ECO:0000255|HAMAP-Rule:MF_03206, ECO:0000305}	2.59	1.63E-03
Sarg	SARG_MOUSE Specifically androgen-regulated gene protein	2.87	1.63E-03
PARP14	PAR14_HUMAN Poly [ADP-ribose] polymerase 14	2.00	1.63E-03
ARG2	ARGI2_HUMAN Arginase-2, mitochondrial	3.84	1.64E-03
TBC1D5	TBCD5_HUMAN TBC1 domain family member 5	2.20	1.66E-03
Ppp1r14b	PP14B_RAT Protein phosphatase 1 regulatory subunit 14B	3.11	1.66E-03
#N/A	#N/A	2.39	1.85E-03
ubiG	UBIG_RHORT Ubiquinone biosynthesis O-methyltransferase {ECO:0000255|HAMAP-Rule:MF_00472}	3.20	1.88E-03
CLDN8	CLD8_HUMAN Claudin-8	2.07	1.93E-03
frrs1	FRRS1_DANRE Putative ferric-chelate reductase 1	2.26	1.93E-03
TGM1	TGM1_HUMAN Protein-glutamine gamma-glutamyltransferase K	2.73	2.03E-03
Tnik	TNIK_MOUSE Traf2 and NCK-interacting protein kinase	-1.40	2.04E-03
uspl1	USPL1_DANRE SUMO-specific isopeptidase USPL1	-3.26	2.04E-03
#N/A	#N/A	3.15	2.13E-03
Proser2	PRSR2_MOUSE Proline and serine-rich protein 2	6.14	2.14E-03
#N/A	BICR2_DANRE Bicaudal D-related protein 2	2.37	2.16E-03
#N/A	#N/A	2.19	2.22E-03
#N/A	#N/A	2.98	2.23E-03
HIP1R	HIP1R_HUMAN Huntingtin-interacting protein 1-related protein	1.93	2.24E-03
#N/A	PERQ1_MOUSE PERQ amino acid-rich with GYF domain-containing protein 1	2.21	2.27E-03
rlmC	RLMC_HAEIE 23S rRNA (uracil(747)-C(5))-methyltransferase RlmC {ECO:0000255|HAMAP-Rule:MF_01012}	-5.70	2.31E-03
gpt2	ALAT2_XENTR Alanine aminotransferase 2	2.37	2.33E-03
Sec14l1	S14L1_MOUSE SEC14-like protein 1 {ECO:0000305}	2.37	2.42E-03
pol	POL3_DROME Retrovirus-related Pol polyprotein from transposon 17.6	-2.24	2.42E-03
Higd1a	HIG1A_MOUSE HIG1 domain family member 1A, mitochondrial	2.69	2.43E-03
EML3	EMAL3_HUMAN Echinoderm microtubule-associated protein-like 3	-4.18	2.43E-03
#N/A	#N/A	4.00	2.48E-03
RPL5	RL5_CHICK 60S ribosomal protein L5	-2.29	2.48E-03
ybx1	YBOX1_XENLA Nuclease-sensitive element-binding protein 1	1.49	2.48E-03
Cdk6	CDK6_MOUSE Cyclin-dependent kinase 6	-5.69	2.48E-03
fam214a	F214A_DANRE Protein FAM214A	2.53	2.58E-03
#N/A	UBIQP_XENLA Polyubiquitin	5.28	2.61E-03
tax1bp1b	TXB1B_DANRE Tax1-binding protein 1 homolog B	1.57	2.61E-03
#N/A	#N/A	5.43	2.61E-03
#N/A	TBA_LEPDS Tubulin alpha chain	-4.61	2.61E-03
CERS5	CERS5_HUMAN Ceramide synthase 5	4.65	2.61E-03
At4g23580	FBK88_ARATH F-box/kelch-repeat protein At4g23580	3.44	2.61E-03
yap1	YAP1_DANRE Transcriptional coactivator YAP1	2.17	2.75E-03
CCL3	CCL3_HUMAN C-C motif chemokine 3	-4.66	2.82E-03
FSIP2	FSIP2_HUMAN Fibrous sheath-interacting protein 2	-5.50	2.82E-03
#N/A	#N/A	5.53	2.90E-03
#N/A	YTX2_XENLA Transposon TX1 uncharacterized 149 kDa protein	-3.57	2.92E-03
#N/A	AIM1_HUMAN Absent in melanoma 1 protein	1.19	2.92E-03
OSBPL3	OSBL3_HUMAN Oxysterol-binding protein-related protein 3	2.58	2.92E-03
HBEGF	HBEGF_CHICK Proheparin-binding EGF-like growth factor	5.05	2.92E-03
Upk3b	UPK3B_MOUSE Uroplakin-3b	2.28	2.94E-03
B3GALT2	B3GT2_PONAB Beta-1,3-galactosyltransferase 2	2.34	2.97E-03
#N/A	#N/A	3.25	2.97E-03
#N/A	#N/A	2.72	3.01E-03
Il22ra2	I22R2_MOUSE Interleukin-22 receptor subunit alpha-2	2.17	3.15E-03
gefW	GEFW_DICDI Ras guanine nucleotide exchange factor W	-6.66	3.15E-03
GPR50	MTR1L_HUMAN Melatonin-related receptor	4.44	3.15E-03

pepA	AMPA_GEOSM Probable cytosol aminopeptidase {ECO:0000255|HAMAP-Rule:MF_00181}	-2.46	3.15E-03
DSG2	DSG2_HUMAN Desmoglein-2	1.40	3.21E-03
Trim16	TRI16_MOUSE Tripartite motif-containing protein 16	2.47	3.26E-03
ncl	NUCL_XENLA Nucleolin	-2.24	3.30E-03
CLDN4	CLD4_BOVIN Claudin-4	2.77	3.30E-03
jag1b	JAG1B_DANRE Protein jagged-1b	-2.15	3.37E-03
ICE1	ICE1_HUMAN Little elongation complex subunit 1	-3.89	3.44E-03
SFMBT2	SMBT2_HUMAN Scm-like with four MBT domains protein 2	-5.59	3.44E-03
#N/A	#N/A	1.68	3.51E-03
#N/A	#N/A	4.69	3.54E-03
PPM2	TYW4_YEAST tRNA wybutosine-synthesizing protein 4	-6.27	3.54E-03
ybcI	YBCI_BACSU Uncharacterized protein YbcI	3.32	3.58E-03
b2m	B2MG_ICTPU Beta-2-microglobulin	2.95	3.58E-03
Cps1	CPSM_RAT Carbamoyl-phosphate synthase [ammonia], mitochondrial	-3.21	3.58E-03
chaf1a	CAF1A_DANRE Chromatin assembly factor 1 subunit A	-4.53	3.70E-03
At1g19060	Y1196_ARATH UPF0725 protein At1g19060	2.01	3.75E-03
TAR1	TAR1_YEAST Protein TAR1	-3.76	3.77E-03
#N/A	#N/A	4.27	3.80E-03
Klf4	KLF4_MOUSE Krueppel-like factor 4	2.89	3.80E-03
ARHGAP27	RHG27_HUMAN Rho GTPase-activating protein 27	1.34	3.80E-03
abhd17b	AB17B_XENLA Protein ABHD17B {ECO:0000305}	3.91	3.91E-03
Pol	LORF2_MOUSE LINE-1 retrotransposable element ORF2 protein	3.18	3.96E-03
#N/A	#N/A	2.89	3.96E-03
BCAR3	BCAR3_BOVIN Breast cancer anti-estrogen resistance protein 3	-3.26	4.00E-03
pol	RTJK_DROME RNA-directed DNA polymerase from mobile element jockey	4.68	4.19E-03
pilA	PILA_MYXXD Fimbrial protein	4.46	4.35E-03
CLDN4	CLD4_BOVIN Claudin-4	1.96	4.36E-03
Ocln	OCLN_RAT Occludin	2.11	4.41E-03
DUSP1	DUS1_HUMAN Dual specificity protein phosphatase 1	2.16	4.66E-03
ART2	ART2_YEAST Putative uncharacterized protein ART2	-2.34	4.71E-03
#N/A	YS003_HUMAN Uncharacterized protein LOC113230	4.37	4.71E-03
lap-2	YH24_CAEEL Putative aminopeptidase W07G4.4	-1.81	4.71E-03
ULK2	ULK2_HUMAN Serine/threonine-protein kinase ULK2	2.00	4.71E-03
Capn5	CAN5_MOUSE Calpain-5	1.97	4.74E-03
Ddx17	DDX17_MOUSE Probable ATP-dependent RNA helicase DDX17	-3.71	4.74E-03
SLC2A3	GTR3_CHICK Solute carrier family 2, facilitated glucose transporter member 3	-2.88	4.74E-03
ube2d2	UB2D2_XENLA Ubiquitin-conjugating enzyme E2 D2	4.62	4.96E-03
TJP3	ZO3_HUMAN Tight junction protein ZO-3	1.44	5.00E-03
septin7	SEPT7_XENLA Septin-7	3.39	5.00E-03
Hmmr	HMMR_RAT Hyaluronan-mediated motility receptor	-5.74	5.12E-03
TBC1D31	TBC31_HUMAN TBC1 domain family member 31	-2.85	5.12E-03
#N/A	#N/A	5.55	5.25E-03
Syne2	SYNE2_MOUSE Nesprin-2	-1.62	5.25E-03
#N/A	#N/A	2.77	5.31E-03
Trim16	TRI16_MOUSE Tripartite motif-containing protein 16	2.12	5.87E-03
#N/A	TCB2_CAEBR Transposable element Tcb2 transposase	-1.71	5.95E-03
#N/A	#N/A	4.20	5.95E-03
MUC15	MUC15_BOVIN Mucin-15	2.06	5.96E-03
midn	MIDN_DANRE Midnolin	3.13	5.98E-03
#N/A	#N/A	2.67	6.05E-03
rps3a	RS3A_SALSA 40S ribosomal protein S3a {ECO:0000255|HAMAP-Rule:MF_03122}	1.23	6.08E-03
#N/A	DFNA5_HUMAN Non-syndromic hearing impairment protein 5	-4.85	6.08E-03
CNKSR3	CNKR3_HUMAN Connector enhancer of kinase suppressor of ras 3	2.44	6.08E-03
YSL7	YSL7_ARATH Probable metal-nicotianamine transporter YSL7	1.77	6.08E-03
uspl1	USPL1_DANRE SUMO-specific isopeptidase USPL1	-4.76	6.22E-03
PTPRZ1	PTPRZ_HUMAN Receptor-type tyrosine-protein phosphatase zeta	-1.33	6.38E-03
#N/A	TCB2_CAEBR Transposable element Tcb2 transposase	4.42	6.43E-03
ANP32B	AN32B_BOVIN Acidic leucine-rich nuclear phosphoprotein 32 family member B	-4.98	6.55E-03
STRN	STRN_HUMAN Striatin	1.43	6.84E-03
glud1	DHE3_CHAAC Glutamate dehydrogenase, mitochondrial	4.02	6.88E-03
anln	ANLN_XENLA Actin-binding protein anillin	-5.22	7.39E-03
#N/A	NATTL_DANRE Natterin-like protein	-4.76	7.40E-03
sibE	SIBE_DICDI Integrin beta-like protein E	-5.84	7.41E-03
sh2d4a	SH24A_XENTR SH2 domain-containing protein 4A	2.55	7.96E-03

VSIG10L	VS10L_HUMAN V-set and immunoglobulin domain-containing protein 10-like	2.58	8.06E-03
Litaf	LITAF_RAT Lipopolysaccharide-induced tumor necrosis factor-alpha factor homolog	-3.70	8.09E-03
MDN1	MDN1_HUMAN Midasin	-2.20	8.09E-03
#N/A	#N/A	2.80	8.12E-03
lepA1	LEPA_METFK Elongation factor 4 {ECO:0000255|HAMAP-Rule:MF_00071}	4.33	8.44E-03
AHNAK	AHNK_HUMAN Neuroblast differentiation-associated protein AHNAK	5.18	8.65E-03
LARS2	SYLM_HUMAN Probable leucine--tRNA ligase, mitochondrial	-5.21	8.68E-03
Galnt6	GALT6_MOUSE Polypeptide N-acetylgalactosaminyltransferase 6	1.61	8.83E-03
grhl3	GRHL3_XENTR Grainyhead-like protein 3 homolog	2.07	8.89E-03
rps4	RS4_ICTPU 40S ribosomal protein S4	-3.33	9.22E-03
Tnik	TNIK_MOUSE Traf2 and NCK-interacting protein kinase	4.71	9.22E-03
efnb2a	EFNB2_DANRE Ephrin-B2a	2.66	9.22E-03
Ank3	ANK3_MOUSE Ankyrin-3	-6.05	9.22E-03
alr	ALR_NOSS1 Alanine racemase {ECO:0000255|HAMAP-Rule:MF_01201}	4.11	9.26E-03
Tacc1	TACC1_MOUSE Transforming acidic coiled-coil-containing protein 1	2.01	9.37E-03
TY3B-G	YG31B_YEAST Transposon Ty3-G Gag-Pol polyprotein	-1.88	9.59E-03
IKBKB	IKKB_HUMAN Inhibitor of nuclear factor kappa-B kinase subunit beta	-6.12	9.76E-03
SCEL	SCEL_HUMAN Sciellin	3.60	9.77E-03
#N/A	RLA0_RANSY 60S acidic ribosomal protein P0	-2.10	9.77E-03
thrb	THB_DANRE Thyroid hormone receptor beta	-1.70	9.79E-03
LRP4	LRP4_HUMAN Low-density lipoprotein receptor-related protein 4	-2.87	9.83E-03
LY75	LY75_MESAU Lymphocyte antigen 75	-1.65	1.00E-02
CASZ1	CASZ1_HUMAN Zinc finger protein castor homolog 1	5.44	1.00E-02
RBM25	RBM25_HUMAN RNA-binding protein 25	4.96	1.00E-02
DOCK10	DOC10_HUMAN Dedicator of cytokinesis protein 10	-4.76	1.01E-02
rep	R1AB_BCHK4 Replicase polyprotein 1ab	-4.50	1.03E-02
OAT	OAT_HUMAN Ornithine aminotransferase, mitochondrial	3.79	1.04E-02
alcama	C166A_DANRE CD166 antigen homolog A	2.16	1.04E-02
tpt1	TCTP_DANRE Translationally-controlled tumor protein homolog	1.47	1.04E-02
SVIL	SVIL_BOVIN Supervillin	-4.19	1.04E-02
#N/A	PPAF_PHAVU Fe(3+)-Zn(2+) purple acid phosphatase {ECO:0000303|PubMed:8001554}	-5.67	1.07E-02
Ddx17	DDX17_MOUSE Probable ATP-dependent RNA helicase DDX17	-2.35	1.07E-02
#N/A	#N/A	5.12	1.10E-02
Rgl1	RGL1_MOUSE Ral guanine nucleotide dissociation stimulator-like 1	2.17	1.10E-02
CUL9	CUL9_HUMAN Cullin-9	-1.03	1.10E-02
Wnk1	WNK1_RAT Serine/threonine-protein kinase WNK1	2.71	1.10E-02
#N/A	SYG_PROAC Glycine--tRNA ligase {ECO:0000255|HAMAP-Rule:MF_00253}	4.41	1.11E-02
smc2	SMC2_XENLA Structural maintenance of chromosomes protein 2	-4.80	1.11E-02
BNIPL	BNIPL_HUMAN Bcl-2/adenovirus E1B 19 kDa-interacting protein 2-like protein	1.91	1.14E-02
tmem150a	T150A_XENTR Transmembrane protein 150A	3.08	1.14E-02
Cit	CTRO_MOUSE Citron Rho-interacting kinase	-5.61	1.14E-02
Zdbf2	ZDBF2_MOUSE DBF4-type zinc finger-containing protein 2 homolog	2.59	1.14E-02
ERBB3	ERBB3_PONAB Receptor tyrosine-protein kinase erbB-3	1.98	1.15E-02
Tnik	TNIK_MOUSE Traf2 and NCK-interacting protein kinase	-2.54	1.15E-02
RTN3	RTN3_HUMAN Reticulon-3	3.36	1.15E-02
#N/A	#N/A	2.28	1.15E-02
HHLA2	HHLA2_HUMAN HERV-H LTR-associating protein 2	4.36	1.17E-02
Trim16	TRI16_MOUSE Tripartite motif-containing protein 16	1.99	1.17E-02
araB	ARAB_PECAS Ribulokinase {ECO:0000255|HAMAP-Rule:MF_00520}	3.35	1.19E-02
#N/A	#N/A	2.07	1.20E-02
Cluh	CLU_MOUSE Clustered mitochondria protein homolog {ECO:0000255|HAMAP-Rule:MF_03013}	-2.63	1.21E-02
HERC1	HERC1_HUMAN Probable E3 ubiquitin-protein ligase HERC1	-1.59	1.21E-02
IST1	IST1_BOVIN IST1 homolog	2.48	1.21E-02
ankhb	ANKHB_DANRE Progressive ankylosis protein homolog B	2.79	1.22E-02
ier2	IER2_DANRE Immediate early response gene 2 protein	-3.10	1.28E-02
Txnl4a	TXN4A_MOUSE Thioredoxin-like protein 4A	-4.00	1.29E-02
ENO1	ENOA_CHICK Alpha-enolase	-2.27	1.29E-02
Prdm1	PRDM1_MOUSE PR domain zinc finger protein 1	1.64	1.30E-02
DIP2A	DIP2A_HUMAN Disco-interacting protein 2 homolog A	-1.91	1.30E-02
mt-co2	COX2_ONCMY Cytochrome c oxidase subunit 2	1.43	1.32E-02
#N/A	TCB2_CAEBR Transposable element Tcb2 transposase	-1.10	1.33E-02
rps3-a	RS31_XENLA 40S ribosomal protein S3-A	-2.22	1.33E-02
#N/A	NATTL_DANRE Natterin-like protein	-5.93	1.33E-02

NRPC2	NRPC2_ARATH DNA-directed RNA polymerase III subunit 2 {ECO:0000305}	4.20	1.33E-02
#N/A	LECG_THANI Galactose-specific lectin nattectin	1.98	1.34E-02
#N/A	#N/A	4.75	1.34E-02
Rps14	RS14_MOUSE 40S ribosomal protein S14	-3.91	1.34E-02
IST1	IST1_BOVIN IST1 homolog	3.58	1.34E-02
#N/A	#N/A	3.77	1.36E-02
DOCK1	DOCK1_HUMAN Dedicator of cytokinesis protein 1	-2.29	1.36E-02
slc35c1	FUCT1_NEMVE GDP-fucose transporter 1	1.69	1.37E-02
Nqo1	NQO1_RAT NAD(P)H dehydrogenase [quinone] 1	2.76	1.38E-02
MT-ND5	NU5M_SALSA NADH-ubiquinone oxidoreductase chain 5	1.37	1.39E-02
Map2	MTAP2_RAT Microtubule-associated protein 2	2.42	1.39E-02
MCTP2	MCTP2_HUMAN Multiple C2 and transmembrane domain-containing protein 2	2.24	1.40E-02
TBC1D17	TBC17_HUMAN TBC1 domain family member 17	3.10	1.41E-02
#N/A	NATTL_DANRE Natterin-like protein	-3.69	1.45E-02
ARAP1	ARAP1_HUMAN Arf-GAP with Rho-GAP domain, ANK repeat and PH domain-containing protein 1	-1.41	1.46E-02
#N/A	#N/A	1.99	1.46E-02
wdhd1	WDHD1_XENLA WD repeat and HMG-box DNA-binding protein 1	-4.56	1.46E-02
dip2ba	DI2BA_DANRE Disco-interacting protein 2 homolog B-A	-2.71	1.46E-02
VPS13A	VP13A_HUMAN Vacuolar protein sorting-associated protein 13A	-1.51	1.47E-02
EPS8L1	ES8L1_HUMAN Epidermal growth factor receptor kinase substrate 8-like protein 1	1.59	1.49E-02
incenp-a	INCEA_XENLA Inner centromere protein A	-4.22	1.50E-02
#N/A	#N/A	4.09	1.50E-02
ARHGEF15	ARHGF_HUMAN Rho guanine nucleotide exchange factor 15	1.92	1.50E-02
DDR2	DDR2_HUMAN Discoidin domain-containing receptor 2	-3.03	1.50E-02
CDKN1C	CDN1C_HUMAN Cyclin-dependent kinase inhibitor 1C	2.67	1.50E-02
NLRC3	NLRC3_HUMAN Protein NLRC3	1.25	1.50E-02
#N/A	#N/A	2.35	1.52E-02
MYH11	MYH11_CHICK Myosin-11	-5.08	1.53E-02
#N/A	#N/A	1.95	1.55E-02
ASPM	ASPM_MACFA Abnormal spindle-like microcephaly-associated protein homolog	-5.16	1.56E-02
CLDN4	CLD4_BOVIN Claudin-4	2.23	1.57E-02
melk	MELK_DANRE Maternal embryonic leucine zipper kinase	-4.97	1.58E-02
TEAD3	TEAD3_CHICK Transcriptional enhancer factor TEF-5	1.94	1.58E-02
SYNE2	SYNE2_HUMAN Nesprin-2	-1.19	1.59E-02
MSH6	MSH6_HUMAN DNA mismatch repair protein Msh6	-5.03	1.60E-02
CHD9	CHD9_HUMAN Chromodomain-helicase-DNA-binding protein 9	-1.52	1.60E-02
RAB11A	RB11A_CHICK Ras-related protein Rab-11A	1.86	1.60E-02
TEF	TEF_CHICK Transcription factor VBP	1.88	1.62E-02
HELZ2	HELZ2_HUMAN Helicase with zinc finger domain 2	1.59	1.62E-02
SAFB	SAFB1_HUMAN Scaffold attachment factor B1	-2.09	1.63E-02
RTase	RTBS_DROME Probable RNA-directed DNA polymerase from transposon BS	-4.28	1.64E-02
#N/A	#N/A	4.56	1.67E-02
KRTCAP2	KTAP2_CANLF Keratinocyte-associated protein 2 {ECO:0000250|UniProtKB:Q8N6L1}	4.24	1.68E-02
#N/A	#N/A	-1.71	1.69E-02
GATAD2A	P66A_HUMAN Transcriptional repressor p66-alpha	4.56	1.69E-02
#N/A	#N/A	4.06	1.72E-02
DOCK2	DOCK2_HUMAN Dedicator of cytokinesis protein 2	-4.81	1.73E-02
KMT2A	KMT2A_HUMAN Histone-lysine N-methyltransferase 2A	-1.85	1.74E-02
TSPYL1	TSYL1_BOVIN Testis-specific Y-encoded-like protein 1	-4.05	1.76E-02
#N/A	#N/A	4.18	1.76E-02
Cdc34	UB2R1_MOUSE Ubiquitin-conjugating enzyme E2 R1	2.31	1.78E-02
M2	TARS_RHISY Taraxerol synthase	3.13	1.81E-02
TCN1	TCO1_HUMAN Transcobalamin-1	3.98	1.84E-02
#N/A	#N/A	4.99	1.84E-02
ANXA11	ANX11_HUMAN Annexin A11	1.97	1.84E-02
#N/A	#N/A	1.91	1.84E-02
GDPD5	GDPD5_HUMAN Glycerophosphodiester phosphodiesterase domain-containing protein 5	4.54	1.86E-02
#N/A	AIM1L_HUMAN Absent in melanoma 1-like protein	1.24	1.86E-02
#N/A	#N/A	-3.11	1.89E-02
lepA	LEPA_BUCBP Elongation factor 4 {ECO:0000255|HAMAP-Rule:MF_00071}	1.96	1.89E-02
Rab11fip1	RFIP1_MOUSE Rab11 family-interacting protein 1	4.88	1.89E-02

SPAG1	SPAG1_HUMAN Sperm-associated antigen 1	2.12	1.91E-02
#N/A	#N/A	-5.19	1.91E-02
ZC3H7B	Z3H7B_HUMAN Zinc finger CCCH domain-containing protein 7B	-3.14	1.91E-02
ADAM9	ADAM9_HUMAN Disintegrin and metalloproteinase domain-containing protein 9	1.66	1.91E-02
#N/A	#N/A	1.55	1.92E-02
Capn8	CAN8_RAT Calpain-8	-1.62	1.94E-02
NLRC3	NLRC3_HUMAN Protein NLRC3	2.52	1.94E-02
NEDD4L	NED4L_HUMAN E3 ubiquitin-protein ligase NEDD4-like	3.53	1.94E-02
ZFAND5	ZFAN5_HUMAN AN1-type zinc finger protein 5	3.50	1.96E-02
atp8b1	AT8B1_XENTR Phospholipid-transporting ATPase IC	1.49	1.96E-02
Adcy5	ADCY5_RAT Adenylate cyclase type 5	3.21	1.96E-02
ildr1	ILDR1_XENLA Immunoglobulin-like domain-containing receptor 1	1.96	1.97E-02
Cab39l	CB39L_MOUSE Calcium-binding protein 39-like	3.41	1.97E-02
KIF20B	KI20B_HUMAN Kinesin-like protein KIF20B {ECO:0000305}	-5.01	1.98E-02
Syne2	SYNE2_MOUSE Nesprin-2	-2.54	1.98E-02
SPATS2	SPAS2_HUMAN Spermatogenesis-associated serine-rich protein 2	1.98	1.98E-02
Cebpd	CEBPD_RAT CCAAT/enhancer-binding protein delta	-5.24	1.98E-02
rps6	RS6_ONCMY 40S ribosomal protein S6	-1.79	1.98E-02
ADAR	DSRAD_HUMAN Double-stranded RNA-specific adenosine deaminase	-1.95	1.98E-02
vps36	VPS36_DANRE Vacuolar protein-sorting-associated protein 36	1.24	1.99E-02
NLRC3	NLRC3_HUMAN Protein NLRC3	1.34	2.00E-02
Nsun5	NSUN5_MOUSE Probable 28S rRNA (cytosine-C(5))-methyltransferase	2.56	2.02E-02
ACTN4	ACTN4_HUMAN Alpha-actinin-4 {ECO:0000305}	1.05	2.03E-02
trio	TRIO_DANRE Triple functional domain protein	-2.69	2.04E-02
#N/A	#N/A	3.78	2.05E-02
KMT2D	KMT2D_HUMAN Histone-lysine N-methyltransferase 2D	-1.55	2.05E-02
GIMAP4	GIMA4_HUMAN GTPase IMAP family member 4	1.87	2.05E-02
dennd5b	DEN5B_DANRE DENN domain-containing protein 5B	-2.86	2.07E-02
abhd2a	ABH2A_DANRE Abhydrolase domain-containing protein 2-A	1.26	2.09E-02
ATM	ATM_HUMAN Serine-protein kinase ATM	-2.44	2.09E-02
Frk	FRK_MOUSE Tyrosine-protein kinase FRK	3.77	2.10E-02
Haspin	HASP_MOUSE Serine/threonine-protein kinase haspin	-5.02	2.12E-02
TNIP1	TNIP1_HUMAN TNFAIP3-interacting protein 1	2.20	2.12E-02
NBEAL1	NBEL1_HUMAN Neurobeachin-like protein 1	1.33	2.12E-02
chtf18	CTF18_XENLA Chromosome transmission fidelity protein 18 homolog	-4.43	2.12E-02
tpt1	TCTP_DANRE Translationally-controlled tumor protein homolog	2.33	2.12E-02
SPAG5	SPAG5_HUMAN Sperm-associated antigen 5	-4.99	2.14E-02
FAM83F	FA83F_HUMAN Protein FAM83F	1.56	2.14E-02
Slc25a5	ADT2_RAT ADP/ATP translocase 2	2.25	2.15E-02
Tnrc6a	TNR6A_MOUSE Trinucleotide repeat-containing gene 6A protein	-2.99	2.15E-02
Esyt1	ESYT1_MOUSE Extended synaptotagmin-1	-4.55	2.17E-02
#N/A	#N/A	5.03	2.20E-02
rrm2	RIR2_DANRE Ribonucleoside-diphosphate reductase subunit M2	-4.62	2.21E-02
CROCC	CROCC_HUMAN Rootletin	-2.46	2.23E-02
pim2	PIM2_DANRE Serine/threonine-protein kinase pim-2	3.50	2.23E-02
#N/A	#N/A	2.23	2.24E-02
GRK5	GRK5_HUMAN G protein-coupled receptor kinase 5	-2.08	2.25E-02
RAB11A	RB11A_CHICK Ras-related protein Rab-11A	1.77	2.27E-02
#N/A	DPOM_CLAPU Probable DNA polymerase	2.93	2.28E-02
jockey\pol	RTJK_DROFU RNA-directed DNA polymerase from mobile element jockey	1.80	2.29E-02
ccnd1	CCND1_DANRE G1/S-specific cyclin-D1	-4.20	2.29E-02
LARP1	LARP1_HUMAN La-related protein 1	-3.14	2.31E-02
RPL5	RL5_CHICK 60S ribosomal protein L5	-2.55	2.31E-02
frrs1	FRRS1_DANRE Putative ferric-chelate reductase 1	2.67	2.32E-02
#N/A	#N/A	-5.10	2.33E-02
dlx3b	DLX3B_DANRE Homeobox protein Dlx3b	2.56	2.33E-02
ZFP36L1	TISB_HUMAN Zinc finger protein 36, C3H1 type-like 1	-3.04	2.33E-02
#N/A	#N/A	3.03	2.33E-02
MCF2L	MCF2L_HUMAN Guanine nucleotide exchange factor DBS	-5.28	2.34E-02
DNAH6	DYH6_HUMAN Dynein heavy chain 6, axonemal	-3.61	2.36E-02
#N/A	#N/A	2.65	2.37E-02
ERVFC1	EFC1_HUMAN Endogenous retrovirus group FC1 Env polyprotein	2.76	2.38E-02
lrmp	LRMP_DANRE Lymphoid-restricted membrane protein	-5.17	2.38E-02
#N/A	#N/A	2.34	2.38E-02
rps3-a	RS31_XENLA 40S ribosomal protein S3-A	-5.23	2.38E-02

focA	FOCA_ECOLI Probable formate transporter 1	3.41	2.38E-02
APLP1	APLP1_HUMAN Amyloid-like protein 1	3.98	2.38E-02
ADCY9	ADCY9_CHICK Adenylate cyclase type 9	-1.91	2.38E-02
ivns1abpa	NS1BA_DANRE Influenza virus NS1A-binding protein homolog A	-2.08	2.38E-02
TGL2	TGM2_CHICK Protein-glutamine gamma-glutamyltransferase 2	-2.35	2.38E-02
MKI67	KI67_HUMAN Antigen KI-67	-4.89	2.38E-02
PC	PYC_BOVIN Pyruvate carboxylase, mitochondrial	-1.72	2.39E-02
Tprn	TPRN_MOUSE Taperin	3.96	2.39E-02
Klf6	KLF6_MOUSE Krueppel-like factor 6	-3.38	2.39E-02
Clta	CLCA_MOUSE Clathrin light chain A	1.63	2.41E-02
MT-ND5	NU5M_SALSA NADH-ubiquinone oxidoreductase chain 5	1.25	2.41E-02
FPV226	V226_FOWPN Probable serine/threonine-protein kinase FPV226	1.93	2.42E-02
PLEKHG4B	PKH4B_HUMAN Pleckstrin homology domain-containing family G member 4B	2.50	2.45E-02
#N/A	#N/A	-2.74	2.45E-02
TPD52L1	TPD53_HUMAN Tumor protein D53	4.41	2.47E-02
krt13	K1C13_ONCMY Keratin, type I cytoskeletal 13	-1.67	2.50E-02
Plec	PLEC_MOUSE Plectin	-2.42	2.51E-02
PCM1	PCM1_HUMAN Pericentriolar material 1 protein	3.54	2.54E-02
FAM83C	FA83C_HUMAN Protein FAM83C {ECO:0000305}	2.10	2.58E-02
RAB44	RAB44_HUMAN Ras-related protein Rab-44	-3.80	2.58E-02
MCM3	MCM3_CHICK DNA replication licensing factor MCM3	-4.42	2.58E-02
LRRC31	LRC31_HUMAN Leucine-rich repeat-containing protein 31	-2.94	2.60E-02
mknk2	MKNK2_XENTR MAP kinase-interacting serine/threonine-protein kinase 2	1.62	2.60E-02
trm1	TRM1_METM7 tRNA (guanine(26)-N(2))-dimethyltransferase {ECO:0000255|HAMAP-Rule:MF_00290}	-1.73	2.63E-02
RPS2	RS2_CRIGR 40S ribosomal protein S2	-2.88	2.63E-02
HMGCR	HMDH_BOVIN 3-hydroxy-3-methylglutaryl-coenzyme A reductase	2.19	2.65E-02
Wnk3	WNK3_MOUSE Serine/threonine-protein kinase WNK3	1.85	2.68E-02
Rin2	RIN2_MOUSE Ras and Rab interactor 2	-2.17	2.70E-02
prkcbb	KPCB_DANRE Protein kinase C beta type	-1.96	2.70E-02
pheS	SYFA_ALISL Phenylalanine--tRNA ligase alpha subunit {ECO:0000255|HAMAP-Rule:MF_00281}	-1.35	2.73E-02
Spag9	JIP4_MOUSE C-Jun-amino-terminal kinase-interacting protein 4	-1.82	2.73E-02
GRB7	GRB7_HUMAN Growth factor receptor-bound protein 7	3.15	2.73E-02
TJP1	ZO1_CANLF Tight junction protein ZO-1	2.18	2.75E-02
#N/A	CISY_TETTH Citrate synthase, mitochondrial	-3.68	2.75E-02
SLC22A6	S22A6_BOVIN Solute carrier family 22 member 6	-3.82	2.75E-02
Pard6b	PAR6B_MOUSE Partitioning defective 6 homolog beta	2.43	2.75E-02
#N/A	#N/A	4.58	2.78E-02
cnpy3	CNPY3_DANRE Protein canopy homolog 3	-4.79	1.00E+00
Vamp8	VAMP8_RAT Vesicle-associated membrane protein 8 {ECO:0000303|PubMed:10336434}	2.95	2.79E-02
spire1	SPIR1_DANRE Protein spire homolog 1	1.17	2.79E-02
ZNF679	ZN679_HUMAN Zinc finger protein 679	-4.87	2.81E-02
CELA1	CELA1_PIG Chymotrypsin-like elastase family member 1	2.95	2.85E-02
#N/A	#N/A	3.34	2.87E-02
PPIP5K1	VIP1_HUMAN Inositol hexakisphosphate and diphosphoinositol-pentakisphosphate kinase 1	-1.82	2.88E-02
Brwd3	BRWD3_MOUSE Bromodomain and WD repeat-containing protein 3	-1.76	2.89E-02
NLRP1	NLRP1_HUMAN NACHT, LRR and PYD domains-containing protein 1	4.07	2.90E-02
Slc25a5	ADT2_MOUSE ADP/ATP translocase 2	3.86	2.97E-02
Trim16	TRI16_MOUSE Tripartite motif-containing protein 16	1.64	2.98E-02
NCOR2	NCOR2_HUMAN Nuclear receptor corepressor 2	-4.33	2.98E-02
Mob4	PHOCN_RAT MOB-like protein phocein	1.46	2.99E-02
MPP6	MPP6_HUMAN MAGUK p55 subfamily member 6	1.71	3.00E-02
#N/A	#N/A	-4.00	3.00E-02
LEPR	LEPR_HUMAN Leptin receptor	-3.59	3.01E-02
GHRH	SLIB_HUMAN Somatoliberin	2.50	3.01E-02
SDC4	SDC4_CHICK Syndecan-4	1.89	3.01E-02
pat	PAT_ALCFA Phosphinothricin N-acetyltransferase {ECO:0000250|UniProtKB:Q57146}	-3.16	3.01E-02
krt13	K1C13_ONCMY Keratin, type I cytoskeletal 13	2.24	3.02E-02
LMO7	LMO7_HUMAN LIM domain only protein 7	2.18	3.04E-02
mdtC	MDTC_PECAS Multidrug resistance protein MdtC {ECO:0000255|HAMAP-Rule:MF_01424}	2.35	3.06E-02
b2m	B2MG_ICTPU Beta-2-microglobulin	2.38	3.08E-02

rplp0	RLA0_DANRE 60S acidic ribosomal protein P0	-2.20	3.08E-02
PTMS	PTMS_HUMAN Parathymosin	-4.39	3.09E-02
rps3a	RS3A_SALSA 40S ribosomal protein S3a {ECO:0000255|HAMAP-Rule:MF_03122}	-1.56	3.11E-02
#N/A	TCB1_CAEBR Transposable element Tcb1 transposase	1.74	3.12E-02
PCNT	PCNT_HUMAN Pericentrin	-1.63	3.14E-02
Bcor	BCOR_MOUSE BCL-6 corepressor	-3.63	3.14E-02
jarid2b	JARD2_DANRE Protein Jumonji	1.78	3.14E-02
LECASAL	ASAL_ALLSA Mannose-specific lectin	-4.54	3.14E-02
F2rl1	PAR2_MOUSE Proteinase-activated receptor 2	3.82	3.14E-02
Aloxe3	LOXE3_RAT Hydroperoxide isomerase ALOXE3	-2.45	3.14E-02
#N/A	#N/A	4.47	3.14E-02
#N/A	STXA_SYNVE Neoverrucotoxin subunit alpha	3.95	3.14E-02
PGBD4	PGBD4_HUMAN PiggyBac transposable element-derived protein 4	-2.14	3.16E-02
jak1	JAK1_DANRE Tyrosine-protein kinase JAK1	1.45	3.16E-02
ITA	BIR_CHICK Inhibitor of apoptosis protein	-1.19	3.20E-02
Cast	ICAL_RAT Calpastatin	4.44	3.21E-02
#N/A	FYB_HUMAN FYN-binding protein	1.57	3.26E-02
Tmem87a	TM87A_MOUSE Transmembrane protein 87A	-1.12	3.28E-02
SEMA6D	SEM6D_HUMAN Semaphorin-6D	-2.85	3.28E-02
Foxq1	FOXQ1_MOUSE Forkhead box protein Q1	2.78	3.28E-02
Med13	MED13_MOUSE Mediator of RNA polymerase II transcription subunit 13	-2.48	3.28E-02
rpl36a	RL36A_TAKRU 60S ribosomal protein L36a	-5.22	3.28E-02
YSL7	YSL7_ARATH Probable metal-nicotianamine transporter YSL7	1.48	3.29E-02
chac1	CHAC1_DANRE Glutathione-specific gamma-glutamylcyclotransferase 1 {ECO:0000250|UniProtKB:Q9BUX1}	1.90	3.32E-02
Tiam1	TIAM1_MOUSE T-lymphoma invasion and metastasis-inducing protein 1	1.97	3.32E-02
ELOVL7	ELOV7_BOVIN Elongation of very long chain fatty acids protein 7 {ECO:0000255|HAMAP-Rule:MF_03207, ECO:0000305}	3.41	3.34E-02
Sorl1	SORL_MOUSE Sortilin-related receptor	-1.32	3.38E-02
rpsG	RS7_SULNB 30S ribosomal protein S7 {ECO:0000255|HAMAP-Rule:MF_00480}	2.57	3.39E-02
#N/A	STXB_SYNHO Stonustoxin subunit beta	2.58	3.39E-02
SPAC26H5.02c	WRIP1_SCHPO ATPase WRNIP1 homolog C26H5.02c	1.66	3.40E-02
csnk1a1	KC1A_XENLA Casein kinase I isoform alpha	1.20	3.42E-02
RPL14	RL14_PIG 60S ribosomal protein L14	-4.19	3.46E-02
cadm4	CADM4_XENLA Cell adhesion molecule 4	1.98	3.46E-02
nuoC	NUOC_ROSS1 NADH-quinone oxidoreductase subunit C {ECO:0000255|HAMAP-Rule:MF_01357}	2.57	3.46E-02
TNFRSF12A	TNR12_HUMAN Tumor necrosis factor receptor superfamily member 12A	3.26	3.46E-02
MAP4K5	M4K5_HUMAN Mitogen-activated protein kinase kinase kinase kinase 5	-2.84	3.46E-02
DNMBP	DNMBP_HUMAN Dynamin-binding protein	1.38	3.46E-02
PPFIBP2	LIPB2_HUMAN Liprin-beta-2	-3.39	3.46E-02
IFI30	GILT_BOVIN Gamma-interferon-inducible lysosomal thiol reductase	-4.64	3.46E-02
Ralgds	GNDS_MOUSE Ral guanine nucleotide dissociation stimulator	4.07	3.47E-02
Ldlr	LDLR_RAT Low-density lipoprotein receptor	2.04	3.47E-02
SNRK	SNRK_HUMAN SNF-related serine/threonine-protein kinase	2.24	3.47E-02
axin2	AXIN2_DANRE Axin-2	-3.43	3.47E-02
Ccl28	CCL28_MOUSE C-C motif chemokine 28	-2.10	3.49E-02
mnmA	MNMA_NATTJ tRNA-specific 2-thiouridylase MnmA {ECO:0000255|HAMAP-Rule:MF_00144}	-2.79	3.49E-02
ERN1	ERN1_HUMAN Serine/threonine-protein kinase/endoribonuclease IRE1	2.76	3.53E-02
ght1	GHT1_SCHPO High-affinity glucose transporter ght1	2.54	3.61E-02
#N/A	ETUD1_MOUSE Elongation factor Tu GTP-binding domain-containing protein 1	-3.57	3.64E-02
#N/A	#N/A	3.04	3.64E-02
Sema4g	SEM4G_MOUSE Semaphorin-4G	3.21	3.66E-02
Spaca4	SACA4_MOUSE Sperm acrosome membrane-associated protein 4	1.79	3.66E-02
ncoa3	NCOA3_XENLA Nuclear receptor coactivator 3	-2.00	3.66E-02
BTK	BTK_HUMAN Tyrosine-protein kinase BTK	-3.53	3.66E-02
Akap5	AKAP5_MOUSE A-kinase anchor protein 5	-2.08	3.66E-02
Klf3	KLF3_MOUSE Krueppel-like factor 3	1.45	3.67E-02
pol	RTJK_DROME RNA-directed DNA polymerase from mobile element jockey	1.69	3.67E-02
SIPA1L1	SI1L1_HUMAN Signal-induced proliferation-associated 1-like protein 1	-4.42	3.67E-02
Syne3	SYNE3_MOUSE Nesprin-3	2.17	3.67E-02
TNKS1BP1	TB182_HUMAN 182 kDa tankyrase-1-binding protein	2.33	3.72E-02
ECU11_1100	SYIC_ENCCU Probable isoleucine--tRNA ligase, cytoplasmic	-3.49	3.74E-02

GMDS	GMDS_CRIGR GDP-mannose 4,6 dehydratase	1.25	3.76E-02
Taok1	TAOK1_MOUSE Serine/threonine-protein kinase TAO1	1.84	3.76E-02
VPS13B	VP13B_HUMAN Vacuolar protein sorting-associated protein 13B	-1.15	3.78E-02
FAM111A	F111A_HUMAN Protein FAM111A	3.32	3.78E-02
htt	HD_TAKRU Huntingtin	-1.00	3.82E-02
LMO7	LMO7_HUMAN LIM domain only protein 7	3.23	3.82E-02
Lifr	LIFR_RAT Leukemia inhibitory factor receptor	-4.76	1.00E+00
SH2D7	SH2D7_HUMAN SH2 domain-containing protein 7	-3.73	3.85E-02
Pde4dip	MYOME_MOUSE Myomegalin	-2.62	3.85E-02
tc1a	TC1A_CAEEL Transposable element Tc1 transposase	1.25	3.85E-02
THADA	THADA_HUMAN Thyroid adenoma-associated protein	-3.88	3.85E-02
Nampt	NAMPT_RAT Nicotinamide phosphoribosyltransferase	2.54	3.90E-02
KIF5C	KIF5C_HUMAN Kinesin heavy chain isoform 5C	-4.94	3.91E-02
BQ2027_MB2317	Y2317_MYCBO UPF0167 protein Mb2317	-3.79	3.91E-02
SPTBN1	SPTB2_HUMAN Spectrin beta chain, non-erythrocytic 1	-1.47	3.91E-02
#N/A	#N/A	2.02	3.93E-02
KDM5B	KDM5B_CHICK Lysine-specific demethylase 5B	-1.63	3.94E-02
HK1	HXK1_HUMAN Hexokinase-1	-3.11	3.95E-02
PF10_0343	SANT_PLAF7 S-antigen protein	-4.46	3.95E-02
#N/A	LORF2_HUMAN LINE-1 retrotransposable element ORF2 protein	1.45	3.96E-02
#N/A	NIBL1_RAT Niban-like protein 1	1.76	3.97E-02
FKBP5	FKBP5_HUMAN Peptidyl-prolyl cis-trans isomerase FKBP5	2.85	4.02E-02
RPTN	RPTN_HUMAN Repetin	4.23	4.02E-02
Tnik	TNIK_MOUSE Traf2 and NCK-interacting protein kinase	-1.49	4.05E-02
sstT	SSTT_CAMJD Serine/threonine transporter SstT {ECO:0000255|HAMAP-Rule:MF_01582}	2.92	4.05E-02
XPC	XPC_HUMAN DNA repair protein complementing XP-C cells	-3.76	4.05E-02
NLRP12	NAL12_HUMAN NACHT, LRR and PYD domains-containing protein 12	2.41	4.05E-02
fabZ	FABZ_XANC5 3-hydroxyacyl-[acyl-carrier-protein] dehydratase FabZ {ECO:0000255|HAMAP-Rule:MF_00406}	-2.30	4.05E-02
Proser2	PRSR2_MOUSE Proline and serine-rich protein 2	3.74	4.05E-02
GFPT1	GFPT1_HUMAN Glutamine--fructose-6-phosphate aminotransferase [isomerizing] 1	1.11	4.06E-02
hsp90ab1	HS90B_DANRE Heat shock protein HSP 90-beta	-1.32	4.08E-02
#N/A	LIN1_NYCCO LINE-1 reverse transcriptase homolog	3.16	4.09E-02
CCNG2	CCNG2_HUMAN Cyclin-G2	3.45	4.09E-02
RRT15	RRT15_YEAST Regulator of rDNA transcription protein 15	-2.03	4.10E-02
GLO1	LGUL_HUMAN Lactoylglutathione lyase	-5.11	4.13E-02
Edil3	EDIL3_MOUSE EGF-like repeat and discoidin I-like domain-containing protein 3	2.54	4.13E-02
ARAP1	ARAP1_HUMAN Arf-GAP with Rho-GAP domain, ANK repeat and PH domain-containing protein 1	-1.06	4.13E-02
Rab11fip1	RFIP1_MOUSE Rab11 family-interacting protein 1	4.90	4.15E-02
PDIA3	PDIA3_CHICK Protein disulfide-isomerase A3	-4.65	1.00E+00
LYST	LYST_BOVIN Lysosomal-trafficking regulator	2.57	4.15E-02
#N/A	TCB2_CAEBR Transposable element Tcb2 transposase	5.14	4.17E-02
ARRDC1	ARRD1_HUMAN Arrestin domain-containing protein 1	2.75	4.18E-02
Tnfrsf26	TNR26_MOUSE Tumor necrosis factor receptor superfamily member 26	3.02	4.19E-02
SLA1	SLA1_VANPO Actin cytoskeleton-regulatory complex protein SLA1	-1.36	4.19E-02
tsr1	TSR1_XENLA Pre-rRNA-processing protein TSR1 homolog	-4.24	4.27E-02
ST14	ST14_HUMAN Suppressor of tumorigenicity 14 protein	1.38	4.27E-02
metN	METN_RHILO Methionine import ATP-binding protein MetN {ECO:0000255|HAMAP-Rule:MF_01719}	2.58	4.29E-02
PRKCD	KPCD_HUMAN Protein kinase C delta type	1.85	4.29E-02
ART2	ART2_YEAST Putative uncharacterized protein ART2	-2.21	4.30E-02
Fam111a	F111A_MOUSE Protein FAM111A	2.76	4.31E-02
#N/A	#N/A	4.45	4.32E-02
ART2	ART2_YEAST Putative uncharacterized protein ART2	-2.60	4.32E-02
g6pd	G6PD_TAKRU Glucose-6-phosphate 1-dehydrogenase	-2.11	4.34E-02
hspa8	HSP7C_DANRE Heat shock cognate 71 kDa protein	2.15	4.34E-02
#N/A	#N/A	2.98	4.34E-02
Tnik	TNIK_MOUSE Traf2 and NCK-interacting protein kinase	-1.69	4.34E-02
ZNF180	ZN180_HUMAN Zinc finger protein 180	-4.64	1.00E+00
RBMS1	RBMS1_HUMAN RNA-binding motif, single-stranded-interacting protein 1	2.19	4.39E-02
CAD	PYR1_SQUAC CAD protein	-3.72	4.40E-02

Rpl3	RL3_RAT 60S ribosomal protein L3	-5.41	4.40E-02
WDFY4	WDFY4_HUMAN WD repeat- and FYVE domain-containing protein 4	-3.74	4.40E-02
Hip1r	HIP1R_MOUSE Huntingtin-interacting protein 1-related protein	1.25	4.44E-02
NF1	NF1_HUMAN Neurofibromin	-1.95	4.44E-02
trpS	SYW_THEMA Tryptophan--tRNA ligase	-2.15	4.45E-02
#N/A	LIN1_NYCCO LINE-1 reverse transcriptase homolog	2.12	4.45E-02
Pold1	DPOD1_MOUSE DNA polymerase delta catalytic subunit	-4.70	1.00E+00
Rnf213	RN213_MOUSE E3 ubiquitin-protein ligase RNF213	-0.92	4.49E-02
Rpl17	RL17_RAT 60S ribosomal protein L17	-5.17	4.49E-02
ADAM29	ADA29_HUMAN Disintegrin and metalloproteinase domain-containing protein 29	-1.34	4.50E-02
#N/A	MUC2L_RAT Intestinal mucin-like protein	2.30	4.50E-02
#N/A	#N/A	1.72	4.50E-02
ABCA12	ABCAC_HUMAN ATP-binding cassette sub-family A member 12	1.40	4.50E-02
PSD4	PSD4_HUMAN PH and SEC7 domain-containing protein 4	-4.76	1.00E+00
Map3k14	M3K14_MOUSE Mitogen-activated protein kinase kinase kinase 14	-1.35	4.58E-02
SAMD9	SAMD9_HUMAN Sterile alpha motif domain-containing protein 9	2.02	4.58E-02
CENPE	CENPE_HUMAN Centromere-associated protein E	-5.01	4.58E-02
FNBP4	FNBP4_HUMAN Formin-binding protein 4	-2.68	4.58E-02
#N/A	#N/A	2.12	4.58E-02
#N/A	#N/A	1.93	4.58E-02
sox8	SOX8_TETNG Transcription factor Sox-8	-2.78	4.66E-02
myo19	MYO19_XENLA Unconventional myosin-XIX	1.57	4.66E-02
SPEN	MINT_HUMAN Msx2-interacting protein	4.29	4.71E-02
Arhgap17	RHG17_RAT Rho GTPase-activating protein 17	-3.26	4.74E-02
U2surp	SR140_MOUSE U2 snRNP-associated SURP motif-containing protein	-3.18	4.76E-02
AMBRA1	AMRA1_HUMAN Activating molecule in BECN1-regulated autophagy protein 1	-4.35	4.77E-02
A2M	A2MG_PONAB Alpha-2-macroglobulin	2.75	4.82E-02
PLXNB1	PLXB1_HUMAN Plexin-B1	-4.13	1.00E+00
MYL6	MYL6_CHICK Myosin light polypeptide 6	1.77	4.89E-02
#N/A	#N/A	4.48	4.89E-02
Rabgap1	RBGP1_MOUSE Rab GTPase-activating protein 1	1.23	4.89E-02
PREX1	PREX1_HUMAN Phosphatidylinositol 3,4,5-trisphosphate-dependent Rac exchanger 1 protein	-3.88	4.91E-02
ccnd1	CCND1_DANRE G1/S-specific cyclin-D1	-3.22	4.92E-02
Coro1a	COR1A_RAT Coronin-1A	-4.11	1.00E+00
Zfp26	ZFP26_MOUSE Zinc finger protein 26	-3.13	4.95E-02
#N/A	#N/A	4.30	4.95E-02
PKN1	PKN1_HUMAN Serine/threonine-protein kinase N1	-5.25	4.98E-02
Top3a	TOP3A_MOUSE DNA topoisomerase 3-alpha	-2.53	5.01E-02
cyoA	CYOA_BUCAI Cytochrome bo(3) ubiquinol oxidase subunit 2	4.59	5.07E-02
max	MAX_DANRE Protein max	2.14	5.09E-02
PCP4L1	PC4L1_BOVIN Purkinje cell protein 4-like protein 1	-2.24	5.09E-02
#N/A	#N/A	2.87	5.09E-02
Tecta	TECTA_MOUSE Alpha-tectorin	-5.62	5.09E-02
#N/A	PCTL_HUMAN PCTP-like protein	2.68	5.09E-02
#N/A	#N/A	4.23	5.09E-02
IGFBP3	IBP3_HUMAN Insulin-like growth factor-binding protein 3	-2.59	5.09E-02
CAPNS1	CPNS1_PIG Calpain small subunit 1	3.73	5.11E-02
SCAMP2	SCAM2_HUMAN Secretory carrier-associated membrane protein 2	1.69	5.11E-02
#N/A	#N/A	3.80	5.11E-02
ACIN1	ACINU_HUMAN Apoptotic chromatin condensation inducer in the nucleus	-3.82	5.15E-02
grhl3	GRHL3_XENLA Grainyhead-like protein 3 homolog	1.24	5.16E-02
#N/A	TYB12_ONCMY Thymosin beta-12	-2.75	5.16E-02
Rab11fip1	RFIP1_MOUSE Rab11 family-interacting protein 1	3.26	5.16E-02
Sfpq	SFPQ_MOUSE Splicing factor, proline- and glutamine-rich	-5.10	5.20E-02
FKBP5	FKBP5_HUMAN Peptidyl-prolyl cis-trans isomerase FKBP5	2.87	5.22E-02
mutS	MUTS_PROMT DNA mismatch repair protein MutS {ECO:0000255|HAMAP-Rule:MF_00096}	-2.44	5.22E-02
JAK2	JAK2_PIG Tyrosine-protein kinase JAK2	-4.59	1.00E+00
Akap12	AKA12_MOUSE A-kinase anchor protein 12	-3.61	5.22E-02
hsc71	HSP70_ONCMY Heat shock cognate 70 kDa protein	1.91	5.22E-02
atg2a	ATG2A_XENTR Autophagy-related protein 2 homolog A	1.65	5.22E-02
RRT15	RRT15_YEAST Regulator of rDNA transcription protein 15	-2.28	5.33E-02
Arhgap35	RHG35_MOUSE Rho GTPase-activating protein 35	1.48	5.33E-02
#N/A	BICR1_MOUSE Bicaudal D-related protein 1	1.78	5.33E-02

EPS15L1	EP15R_HUMAN Epidermal growth factor receptor substrate 15-like 1	1.89	5.33E-02
LYST	LYST_HUMAN Lysosomal-trafficking regulator	-1.62	5.33E-02
KIAA0232	K0232_HUMAN Uncharacterized protein KIAA0232	1.23	5.35E-02
#N/A	BICR1_MOUSE Bicaudal D-related protein 1	1.60	5.36E-02
CPAMD8	CPMD8_HUMAN C3 and PZP-like alpha-2-macroglobulin domain-containing protein 8	-2.20	5.39E-02
Dennd2d	DEN2D_MOUSE DENN domain-containing protein 2D	-4.34	5.40E-02
F2rl1	PAR2_MOUSE Proteinase-activated receptor 2	3.02	5.42E-02
Os08g0242700	UP12_ORYSJ ACT domain-containing protein DS12, chloroplastic {ECO:0000305}	-1.69	5.46E-02
rlmH	RLMH_CAMLR Ribosomal RNA large subunit methyltransferase H {ECO:0000255|HAMAP-Rule:MF_00658}	2.87	5.46E-02
ZNF609	ZN609_HUMAN Zinc finger protein 609	-2.52	5.46E-02
ZP2	ZP2_BOVIN Zona pellucida sperm-binding protein 2	-2.81	5.46E-02
SCN2A	SCN2A_HUMAN Sodium channel protein type 2 subunit alpha	1.87	5.46E-02
rpoC	RPOC_CHLL2 DNA-directed RNA polymerase subunit beta' {ECO:0000255|HAMAP-Rule:MF_01322}	2.43	5.49E-02
ncapg2	CNDG2_XENLA Condensin-2 complex subunit G2	-4.10	1.00E+00
Patr-G	HLAG_PANTR Patr class I histocompatibility antigen, alpha chain G	1.67	5.52E-02
SPHK2	SPHK2_HUMAN Sphingosine kinase 2	2.46	5.53E-02
krt13	K1C13_ONCMY Keratin, type I cytoskeletal 13	-1.98	5.53E-02
Arid1a	ARI1A_MOUSE AT-rich interactive domain-containing protein 1A	-1.99	5.53E-02
#N/A	HRSL4_HUMAN Retinoic acid receptor responder protein 3	2.46	5.53E-02
Kiaa1109	K1109_MOUSE Uncharacterized protein KIAA1109	-1.38	5.55E-02
#N/A	#N/A	3.01	5.55E-02
Atrn	ATRN_MOUSE Attractin	-1.63	5.59E-02
FRY	FRY_HUMAN Protein furry homolog	-2.00	5.62E-02
STK26	STK26_HUMAN Serine/threonine-protein kinase 26 {ECO:0000305}	1.86	5.65E-02
PRKCH	KPCL_HUMAN Protein kinase C eta type	3.21	5.67E-02
VPS4B	VPS4B_BOVIN Vacuolar protein sorting-associated protein 4B	1.85	5.67E-02
STK35	STK35_HUMAN Serine/threonine-protein kinase 35	1.87	5.68E-02
Tf2-6	TF26_SCHPO Transposon Tf2-6 polyprotein	-1.35	5.69E-02
igf2bp1	IF2B1_DANRE Insulin-like growth factor 2 mRNA-binding protein 1	1.68	5.74E-02
TINF2	TINF2_HUMAN TERF1-interacting nuclear factor 2	-4.05	5.75E-02
Phldb1	PHLB1_RAT Pleckstrin homology-like domain family B member 1	1.40	5.76E-02
NLRC3	NLRC3_HUMAN Protein NLRC3	1.89	5.77E-02
stac3	STAC3_DANRE SH3 and cysteine-rich domain-containing protein 3	-2.41	5.77E-02
cnfn-b	CNFNB_XENLA Cornifelin homolog B	1.73	5.79E-02
scrib	SCRIB_DANRE Protein scribble homolog	-4.87	1.00E+00
NFKB1	NFKB1_CANLF Nuclear factor NF-kappa-B p105 subunit	-3.11	5.84E-02
PLA2R1	PLA2R_PONAB Secretory phospholipase A2 receptor	-2.27	5.85E-02
Nlrc3	NLRC3_MOUSE Protein NLRC3	-2.14	5.86E-02
GIMAP4	GIMA4_HUMAN GTPase IMAP family member 4	2.76	5.87E-02
nipblb	NIPLB_DANRE Nipped-B-like protein B	1.74	5.89E-02
DGKQ	DGKQ_HUMAN Diacylglycerol kinase theta	2.46	5.91E-02
A2m	A2MG_RAT Alpha-2-macroglobulin	-3.57	5.91E-02
#N/A	PRVB_OPSTA Parvalbumin beta	1.93	5.91E-02
SPBPJ4664.02	YHU2_SCHPO Uncharacterized threonine-rich GPI-anchored glycoprotein PJ4664.02	1.18	5.92E-02
Cpt1a	CPT1A_MOUSE Carnitine O-palmitoyltransferase 1, liver isoform	-4.62	6.01E-02
SLC2A2	GTR2_CHICK Solute carrier family 2, facilitated glucose transporter member 2	-2.62	6.03E-02
#N/A	#N/A	1.48	6.03E-02
Tmprss4	TMPS4_MOUSE Transmembrane protease serine 4	1.52	6.03E-02
SI	SUIS_HUMAN Sucrase-isomaltase, intestinal	5.15	6.03E-02
DNMT1	DNMT1_CHICK DNA (cytosine-5)-methyltransferase 1	-2.38	6.03E-02
BQ2027_MB2259	Y2259_MYCBO Uncharacterized SURF1-like protein Mb2259	-5.33	6.05E-02
Hmbs	HEM3_RAT Porphobilinogen deaminase	-2.61	6.05E-02
PDE4DIP	MYOME_HUMAN Myomegalin	-2.79	6.07E-02
DDB1	DDB1_CHICK DNA damage-binding protein 1	-2.13	6.08E-02
#N/A	#N/A	2.44	6.13E-02
#N/A	#N/A	2.87	6.13E-02
pth	PTH_DICNV Peptidyl-tRNA hydrolase {ECO:0000255|HAMAP-Rule:MF_00083}	4.27	6.15E-02
#N/A	#N/A	4.07	1.00E+00
samm50a	SAM5A_DANRE Sorting and assembly machinery component 50 homolog A	-3.78	6.20E-02

Grm3	GRM3_MOUSE Metabotropic glutamate receptor 3	-2.03	6.27E-02
ELF3	ELF3_HUMAN ETS-related transcription factor Elf-3	-1.91	6.27E-02
scrib	SCRIB_DANRE Protein scribble homolog	-3.55	6.27E-02
SAT1	SAT1_CHICK Diamine acetyltransferase 1	1.71	6.28E-02
Tf2-6	TF26_SCHPO Transposon Tf2-6 polyprotein	-1.88	6.30E-02
SCAPER	SCAPE_HUMAN S phase cyclin A-associated protein in the endoplasmic reticulum	-2.37	6.31E-02
#N/A	#N/A	3.16	6.33E-02
LARP4	LARP4_HUMAN La-related protein 4	-3.84	6.34E-02
Rbm47	RBM47_RAT RNA-binding protein 47	1.00	6.36E-02
ADGRF3	AGRF3_HUMAN Adhesion G-protein coupled receptor F3	-2.39	6.41E-02
actb	ACTB_SALSA Actin, cytoplasmic 1	3.78	6.43E-02
Eml1	EMAL1_MOUSE Echinoderm microtubule-associated protein-like 1	-1.62	6.43E-02
#N/A	EFCB_PAPAN ERV-BabFcenv provirus ancestral Env polyprotein	-4.49	6.46E-02
wee1-b	WEE1B_XENLA Wee1-like protein kinase 1-B	2.52	6.46E-02
ext1b	EXT1B_DANRE Exostosin-1b	-1.61	6.46E-02
PVR	PVR_HUMAN Poliovirus receptor	2.28	6.46E-02
Ppp1r9b	NEB2_RAT Neurabin-2	-4.07	6.46E-02
Myo9b	MYO9B_RAT Unconventional myosin-IXb	1.44	6.46E-02
Znf185	ZN185_MOUSE Zinc finger protein 185	1.30	6.46E-02
SNRNP70	RU17_HUMAN U1 small nuclear ribonucleoprotein 70 kDa	-1.98	6.46E-02
ANKRD50	ANR50_HUMAN Ankyrin repeat domain-containing protein 50	-3.60	6.49E-02
FLNA	FLNA_HUMAN Filamin-A	-2.49	6.49E-02
ERBB3	ERBB3_HUMAN Receptor tyrosine-protein kinase erbB-3	2.79	6.51E-02
Map7d1	MA7D1_MOUSE MAP7 domain-containing protein 1	2.57	6.56E-02
PTPN6	PTN6_HUMAN Tyrosine-protein phosphatase non-receptor type 6	-3.69	6.56E-02
Prpf8	PRP8_MOUSE Pre-mRNA-processing-splicing factor 8	-1.31	6.64E-02
MCL1	MCL1_CANLF Induced myeloid leukemia cell differentiation protein Mcl-1 homolog	2.09	6.64E-02
ybx1	YBOX1_XENLA Nuclease-sensitive element-binding protein 1	4.14	6.65E-02
#N/A	SLP1_PINMG Shematrin-like protein 1	2.97	6.66E-02
#N/A	#N/A	2.89	6.70E-02
PARP1	PARP1_CHICK Poly [ADP-ribose] polymerase 1	-4.01	1.00E+00
asna1	ASNA_DANRE ATPase asna1 {ECO:0000255|HAMAP-Rule:MF_03112}	4.08	1.00E+00
Slco2b1	SO2B1_RAT Solute carrier organic anion transporter family member 2B1	-2.95	6.75E-02
SEC61B	SC61B_PONAB Protein transport protein Sec61 subunit beta	3.32	6.75E-02
TAR1	TAR1_YEAST Protein TAR1	-2.06	6.80E-02
#N/A	#N/A	-4.31	6.83E-02
PLXNA1	PLXA1_HUMAN Plexin-A1	1.57	6.83E-02
NUP188	NU188_HUMAN Nucleoporin NUP188 homolog	-5.60	6.83E-02
CAPN2	CAN2_HUMAN Calpain-2 catalytic subunit	-2.26	6.86E-02
fam83h	FA83H_DANRE Protein FAM83H {ECO:0000305}	4.91	6.86E-02
#N/A	#N/A	3.75	6.86E-02
SLC27A4	S27A4_HUMAN Long-chain fatty acid transport protein 4	1.36	6.87E-02
Gab2	GAB2_MOUSE GRB2-associated-binding protein 2	1.89	6.87E-02
PLEKHA5	PKHA5_HUMAN Pleckstrin homology domain-containing family A member 5	2.71	6.88E-02
nodQ	NODQ_RHIME Bifunctional enzyme NodQ	2.30	6.92E-02
rpl13a	RL13A_SALTR 60S ribosomal protein L13a	-2.06	6.92E-02
PCDH1	PCDH1_HUMAN Protocadherin-1	1.58	6.92E-02
SZT2	SZT2_HUMAN Protein SZT2	-1.54	6.92E-02
mug79	MUG79_SCHPO Meiotically up-regulated gene 79 protein	2.27	6.93E-02
rpsa	RSSA_SALSA 40S ribosomal protein SA {ECO:0000255|HAMAP-Rule:MF_03016}	-2.61	6.96E-02
STAG1	STAG1_HUMAN Cohesin subunit SA-1	-2.90	6.99E-02
FLNC	FLNC_HUMAN Filamin-C	1.92	6.99E-02
#N/A	LAP2_HUMAN Protein LAP2	-1.76	6.99E-02
U2AF1	U2AF1_BOVIN Splicing factor U2AF 35 kDa subunit	-2.21	7.01E-02
ZDHHC14	ZDH14_HUMAN Probable palmitoyltransferase ZDHHC14	-2.74	7.02E-02
#N/A	#N/A	0.84	7.04E-02
nfil3	NFIL3_XENLA Nuclear factor interleukin-3-regulated protein	2.61	7.04E-02
chd8	CHD8_DANRE Chromodomain-helicase-DNA-binding protein 8	-1.79	7.05E-02
Srsf5	SRSF5_RAT Serine/arginine-rich splicing factor 5	-2.72	7.06E-02
SASH1	SASH1_HUMAN SAM and SH3 domain-containing protein 1	2.66	7.08E-02
thiE	THIE_THEVO Thiamine-phosphate synthase {ECO:0000255|HAMAP-Rule:MF_00097}	1.30	7.08E-02
rps27	RS27_XENLA 40S ribosomal protein S27	-3.80	7.08E-02

FZD10	FZD10_CHICK Frizzled-10	-3.26	7.11E-02
Kmt2d	KMT2D_MOUSE Histone-lysine N-methyltransferase 2D	2.36	7.13E-02
ART2	ART2_YEAST Putative uncharacterized protein ART2	-2.53	7.13E-02
prkci	KPCI_DANRE Protein kinase C iota type	1.79	7.13E-02
DYNC2H1	DYHC2_HUMAN Cytoplasmic dynein 2 heavy chain 1	-2.45	7.14E-02
ZNF195	ZN195_HUMAN Zinc finger protein 195	-1.87	7.15E-02
WNK3	WNK3_HUMAN Serine/threonine-protein kinase WNK3	1.71	7.16E-02
Serbp1	PAIRB_MOUSE Plasminogen activator inhibitor 1 RNA-binding protein	-1.93	7.23E-02
krt8	K2C8_DANRE Keratin, type II cytoskeletal 8	4.59	7.27E-02
Acbd3	GCP60_RAT Golgi resident protein GCP60	1.63	7.33E-02
#N/A	#N/A	1.76	7.33E-02
Cbx4	CBX4_MOUSE E3 SUMO-protein ligase CBX4	4.64	7.33E-02
rpl15	RL15_PARDA 60S ribosomal protein L15	-4.06	7.33E-02
Cfh	CFAH_MOUSE Complement factor H	3.82	7.33E-02
#N/A	#N/A	3.00	7.33E-02
Eif4b	IF4B_MOUSE Eukaryotic translation initiation factor 4B	-3.66	7.33E-02
Spea_2046	DGTL1_SHEPA Deoxyguanosinetriphosphate triphosphohydrolase-like protein {ECO:0000255|HAMAP-Rule:MF_01212}	1.97	7.36E-02
DUSP7	DUS7_HUMAN Dual specificity protein phosphatase 7	1.62	7.37E-02
ndhG	NU6C_IPOPU NAD(P)H-quinone oxidoreductase subunit 6, chloroplastic	1.39	7.38E-02
Prr15	PRR15_MOUSE Proline-rich protein 15	2.01	7.40E-02
Cdc5l	CDC5L_RAT Cell division cycle 5-like protein	-1.34	7.40E-02
NT5C2	5NTC_CHICK Cytosolic purine 5'-nucleotidase	1.40	7.47E-02
Ltc4s	LTC4S_RAT Leukotriene C4 synthase	-2.02	7.47E-02
RASA2	RASA2_HUMAN Ras GTPase-activating protein 2	-1.87	7.51E-02
ITPKB	IP3KB_HUMAN Inositol-trisphosphate 3-kinase B	2.51	7.52E-02
ptdss1	PTSS1_DANRE Phosphatidylserine synthase 1	1.60	7.52E-02
#N/A	#N/A	3.31	7.52E-02
Rru_A3059	Y3059_RHORT UPF0301 protein Rru_A3059 {ECO:0000255|HAMAP-Rule:MF_00758}	3.10	7.53E-02
#N/A	#N/A	4.50	7.55E-02
#N/A	VPRBP_MOUSE Protein VPRBP	-3.46	7.55E-02
sema4e	SEM4E_DANRE Semaphorin-4E	-2.26	7.56E-02
speE	SPEE_ALKEH Polyamine aminopropyltransferase {ECO:0000255|HAMAP-Rule:MF_00198}	2.38	7.56E-02
phactr4a	PHR4A_DANRE Phosphatase and actin regulator 4A	4.54	7.57E-02
#N/A	#N/A	1.86	7.57E-02
PPP2R3A	P2R3A_HUMAN Serine/threonine-protein phosphatase 2A regulatory subunit B" subunit alpha	2.63	7.57E-02
NOP9	NOP9_PODAN Nucleolar protein 9	3.30	7.57E-02
USP43	UBP43_HUMAN Ubiquitin carboxyl-terminal hydrolase 43	1.31	7.63E-02
esyt3	ESYT3_XENTR Extended synaptotagmin-3	0.84	7.67E-02
kdm2b	KDM2B_XENLA Lysine-specific demethylase 2B	-3.27	7.67E-02
#N/A	#N/A	4.85	7.68E-02
nbn	NBN_DANRE Nibrin	-4.78	1.00E+00
Myh9	MYH9_MOUSE Myosin-9	1.88	7.71E-02
#N/A	#N/A	2.18	7.73E-02
Cpeb3	CPEB3_MOUSE Cytoplasmic polyadenylation element-binding protein 3	-4.51	1.00E+00
Stap2	STAP2_MOUSE Signal-transducing adaptor protein 2	2.80	7.77E-02
KLHL24	KLH24_HUMAN Kelch-like protein 24	1.16	7.77E-02
Ddx58	DDX58_MOUSE Probable ATP-dependent RNA helicase DDX58	1.50	7.77E-02
KRAS	RASK_HUMAN GTPase KRas	2.33	7.77E-02
Picalm	PICAL_RAT Phosphatidylinositol-binding clathrin assembly protein	3.01	7.77E-02
#N/A	#N/A	2.83	7.80E-02
MAZ	MAZ_HUMAN Myc-associated zinc finger protein	-4.75	1.00E+00
#N/A	TCB1_CAEBR Transposable element Tcb1 transposase	-4.39	1.00E+00
glnE	GLNE_IDILO Glutamate-ammonia-ligase adenylyltransferase {ECO:0000255|HAMAP-Rule:MF_00802}	2.13	7.90E-02
GNE	GLCNE_HUMAN Bifunctional UDP-N-acetylglucosamine 2-epimerase/N-acetylmannosamine kinase	1.42	7.91E-02
MGA	MGAP_HUMAN MAX gene-associated protein	-3.68	7.91E-02
#N/A	#N/A	2.90	7.91E-02
hisS	SYH_NEOSM Histidine--tRNA ligase {ECO:0000255|HAMAP-Rule:MF_00127}	3.26	7.92E-02
DMXL1	DMXL1_HUMAN DmX-like protein 1	3.50	7.92E-02
PNPLA6	PLPL6_HUMAN Neuropathy target esterase	-2.10	7.92E-02

mtus1a	MTS1A_DANRE Microtubule-associated tumor suppressor 1 homolog A	3.04	7.92E-02
BAZ2A	BAZ2A_HUMAN Bromodomain adjacent to zinc finger domain protein 2A	3.69	7.92E-02
#N/A	EFCB_PAPAN ERV-BabFcenv provirus ancestral Env polyprotein	3.60	7.92E-02
creD	CRED_ECOLI Inner membrane protein CreD	2.24	7.92E-02
Smarca5	SMCA5_MOUSE SWI/SNF-related matrix-associated actin-dependent regulator of chromatin subfamily A member 5	-4.50	1.00E+00
FMRFa	FMRF_DROME FMRFamide-related peptides	1.89	7.92E-02
PIK3CG	PK3CG_PIG Phosphatidylinositol 4,5-bisphosphate 3-kinase catalytic subunit gamma isoform	-3.46	7.92E-02
Trim29	TRI29_MOUSE Tripartite motif-containing protein 29	2.15	7.92E-02
cldnd	CLDY_DANRE Claudin-like protein ZF-A89	4.02	1.00E+00
#N/A	TCB1_CAEBR Transposable element Tcb1 transposase	3.59	7.92E-02
ADGRG3	AGRG3_HUMAN Adhesion G protein-coupled receptor G3 {ECO:0000303|PubMed:25713288}	-3.83	7.92E-02
Mapk12	MK12_MOUSE Mitogen-activated protein kinase 12	-2.17	7.92E-02
TRO	TROP_HUMAN Trophinin	-1.24	7.94E-02
Rpl38	RL38_RAT 60S ribosomal protein L38	-3.29	7.99E-02
znf703	ZN703_DANRE Zinc finger protein 703	-3.57	8.00E-02
KIF14	KIF14_HUMAN Kinesin-like protein KIF14 {ECO:0000305}	-4.84	1.00E+00
Gpbp1l1	GPBL1_RAT Vasculin-like protein 1	-4.21	8.00E-02
TJP1	ZO1_HUMAN Tight junction protein ZO-1	4.26	8.00E-02
#N/A	#N/A	4.39	8.01E-02
RPS27L	RS27L_BOVIN 40S ribosomal protein S27-like	3.92	1.00E+00
NCKAP5	NCKP5_HUMAN Nck-associated protein 5	1.29	8.01E-02
cyp1a3	CP1A3_ONCMY Cytochrome P450 1A3	3.10	8.07E-02
URB1	NPA1P_HUMAN Nucleolar pre-ribosomal-associated protein 1	-4.38	1.00E+00
Fnbp4	FNBP4_MOUSE Formin-binding protein 4	-2.12	8.13E-02
P2RX1	P2RX1_HUMAN P2X purinoceptor 1	4.19	8.13E-02
B4GALT3	B4GT3_BOVIN Beta-1,4-galactosyltransferase 3	2.13	8.13E-02
SECISBP2L	SBP2L_HUMAN Selenocysteine insertion sequence-binding protein 2-like	1.55	8.13E-02
gcnt4	GCNT4_DANRE Beta-1,3-galactosyl-O-glycosyl-glycoprotein beta-1,6-N-acetylglucosaminyltransferase 4	3.14	8.14E-02
Kmt2d	KMT2D_MOUSE Histone-lysine N-methyltransferase 2D	-1.13	8.14E-02
Nlrc3	NLRC3_MOUSE Protein NLRC3	-1.80	8.16E-02
#N/A	#N/A	-1.43	8.16E-02
Tacstd2	TACD2_MOUSE Tumor-associated calcium signal transducer 2	1.23	8.18E-02
Cpsf1	CPSF1_MOUSE Cleavage and polyadenylation specificity factor subunit 1	-1.87	8.18E-02
Klc4	KLC4_RAT Kinesin light chain 4	2.81	8.18E-02
PPM1G	PPM1G_MACFA Protein phosphatase 1G	-3.47	8.24E-02
Specc1	CYTSB_MOUSE Cytospin-B	1.25	8.27E-02
fut11	FUT11_ORYLA Alpha-(1,3)-fucosyltransferase 11	1.21	8.28E-02
sibA	SIBA_DICDI Integrin beta-like protein A	3.90	1.00E+00
#N/A	#N/A	2.63	8.28E-02
MYOF	MYOF_HUMAN Myoferlin	-2.90	8.31E-02
TMEM131L	T131L_HUMAN Transmembrane protein 131-like	-2.10	8.34E-02
depdc7	DEPD7_DANRE DEP domain-containing protein 7	-3.11	8.34E-02
SLC9A5	SL9A5_HUMAN Sodium/hydrogen exchanger 5	3.73	8.34E-02
Itsn2	ITSN2_MOUSE Intersectin-2	2.13	8.34E-02
#N/A	#N/A	2.14	8.36E-02
#N/A	#N/A	1.99	8.36E-02
NAA15	NAA15_HUMAN N-alpha-acetyltransferase 15, NatA auxiliary subunit	-2.66	8.40E-02
#N/A	CE042_HUMAN Uncharacterized protein C5orf42	3.38	8.40E-02
ZBED5	ZBED5_CANLF Zinc finger BED domain-containing protein 5	2.16	8.40E-02
TFG	TFG_HUMAN Protein TFG	2.16	8.47E-02
NLRC3	NLRC3_HUMAN Protein NLRC3	3.10	8.47E-02
ELOVL1	ELOV1_HUMAN Elongation of very long chain fatty acids protein 1 {ECO:0000255|HAMAP-Rule:MF_03201, ECO:0000305}	1.94	8.48E-02
PNN	PININ_PONAB Pinin	-2.43	8.50E-02
rpsE	RS5_SALAI 30S ribosomal protein S5 {ECO:0000255|HAMAP-Rule:MF_01307}	2.53	8.51E-02
RTP2	RTP2_HUMAN Receptor-transporting protein 2	3.96	1.00E+00
#N/A	#N/A	1.80	8.54E-02
Nlrc3	NLRC3_MOUSE Protein NLRC3	-2.59	8.59E-02
CCNG2	CCNG2_HUMAN Cyclin-G2	3.31	8.59E-02
Dpp3	DPP3_RAT Dipeptidyl peptidase 3	-3.09	8.60E-02
Cldn3	CLD3_RAT Claudin-3	3.29	8.61E-02

Soga1	SOGA1_MOUSE Protein SOGA1	-2.81	8.65E-02
RGL1	RGL1_HUMAN Ral guanine nucleotide dissociation stimulator-like 1	4.00	1.00E+00
#N/A	#N/A	1.67	8.67E-02
ITSN2	ITSN2_HUMAN Intersectin-2	0.97	8.67E-02
PRUNE2	PRUN2_PONAB Protein prune homolog 2	3.18	8.67E-02
NEIL3	NEIL3_HUMAN Endonuclease 8-like 3	-3.22	8.70E-02
PIK3R3	P55G_BOVIN Phosphatidylinositol 3-kinase regulatory subunit gamma	-4.30	1.00E+00
TIAM1	TIAM1_HUMAN T-lymphoma invasion and metastasis-inducing protein 1	2.68	8.75E-02
Espl1	ESPL1_MOUSE Separin	-4.66	1.00E+00
tc1a	TC1A_CAEEL Transposable element Tc1 transposase	3.96	1.00E+00
npc2	NPC2_DANRE Epididymal secretory protein E1	2.93	8.78E-02
brms1la	BM1LA_DANRE Breast cancer metastasis-suppressor 1-like protein-A	-4.05	1.00E+00
PF14_0175	YPF17_PLAF7 Protein PF14_0175	-1.61	8.83E-02
KCNK1	KCNK1_HUMAN Potassium channel subfamily K member 1	2.02	8.85E-02
xynB	XYNB_NEOPA Endo-1,4-beta-xylanase B	3.76	8.87E-02
Ylpm1	YLPM1_MOUSE YLP motif-containing protein 1	-2.89	8.88E-02
SAT1	SAT1_CHICK Diamine acetyltransferase 1	3.34	8.89E-02
WDR7	WDR7_HUMAN WD repeat-containing protein 7	-5.38	8.89E-02
EHMT1	EHMT1_HUMAN Histone-lysine N-methyltransferase EHMT1	-2.56	8.92E-02
CUL9	CUL9_HUMAN Cullin-9	-1.85	8.93E-02
RPL6	RL6_HUMAN 60S ribosomal protein L6	-3.61	8.93E-02
#N/A	YD023_HUMAN Putative uncharacterized protein FLJ45035	3.63	8.94E-02
FAM49A	FA49A_CHICK Protein FAM49A	-4.38	1.00E+00
Ngef	NGEF_MOUSE Ephexin-1	1.47	9.00E-02
PSD3	PSD3_HUMAN PH and SEC7 domain-containing protein 3	-1.90	9.00E-02
Inpp4b	INP4B_MOUSE Type II inositol 3,4-bisphosphate 4-phosphatase	-2.74	9.01E-02
hpcR	HPCR_SHIFL Homoprotocatechuate degradative operon repressor	4.13	9.06E-02
#N/A	STXB_SYNHO Stonustoxin subunit beta	1.66	9.07E-02
SSRP1	SSRP1_CHICK FACT complex subunit SSRP1	-2.55	9.07E-02
FBF1	FBF1_CHICK Fas-binding factor 1 homolog	-4.11	9.07E-02
#N/A	#N/A	3.00	9.07E-02
#N/A	#N/A	4.24	9.08E-02
SAR1A	SAR1A_PIG GTP-binding protein SAR1a	2.06	9.08E-02
#N/A	FUK_HUMAN L-fucose kinase	-3.13	9.12E-02
apaf1	APAF_DANRE Apoptotic protease-activating factor 1	-1.22	9.18E-02
PAPOLA	PAPOA_HUMAN Poly(A) polymerase alpha	-2.63	9.19E-02
Adcy2	ADCY2_MOUSE Adenylate cyclase type 2	-3.41	9.19E-02
gefW	GEFW_DICDI Ras guanine nucleotide exchange factor W	-1.97	9.19E-02
#N/A	AIM1_HUMAN Absent in melanoma 1 protein	-1.35	9.19E-02
MYO3A	MYO3A_HUMAN Myosin-IIIa	3.34	9.20E-02
#N/A	#N/A	2.86	9.20E-02
ZNF799	ZN799_HUMAN Zinc finger protein 799	-3.88	1.00E+00
Tbc1d12	TBC12_MOUSE TBC1 domain family member 12	-2.26	9.20E-02
Arf2	ARF2_RAT ADP-ribosylation factor 2	1.45	9.20E-02
daf-1	DAF1_CAEEL Cell surface receptor daf-1	3.46	9.22E-02
Lonrf3	LONF3_MOUSE LON peptidase N-terminal domain and RING finger protein 3	1.97	9.26E-02
#N/A	FRIH_SALSA Ferritin, heavy subunit	4.02	1.00E+00
SLC25A17	PM34_HUMAN Peroxisomal membrane protein PMP34	-2.91	9.31E-02
CLIP1	CLIP1_HUMAN CAP-Gly domain-containing linker protein 1	-5.35	9.34E-02
REV1	REV1_CHICK DNA repair protein REV1	-2.17	9.37E-02
mcm7	MCM7_XENTR DNA replication licensing factor mcm7	-3.89	1.00E+00
#N/A	#N/A	2.40	9.40E-02
srrt	SRRT_DANRE Serrate RNA effector molecule homolog	-1.71	9.41E-02
NCOR2	NCOR2_HUMAN Nuclear receptor corepressor 2	2.79	9.50E-02
#N/A	#N/A	1.93	9.52E-02
TAR1	TAR1_YEAST Protein TAR1	-1.64	9.53E-02
naca	NACA_DANRE Nascent polypeptide-associated complex subunit alpha	-2.46	9.61E-02
LRP8	LRP8_CHICK Low-density lipoprotein receptor-related protein 8	3.02	9.61E-02
hdgfl2	HDGR2_DANRE Hepatoma-derived growth factor-related protein 2	-3.39	9.63E-02
Tf2-6	TF26_SCHPO Transposon Tf2-6 polyprotein	-1.02	9.70E-02
GIMAP2	GIMA2_HUMAN GTPase IMAP family member 2	-3.67	9.70E-02
rpmI	RL35_BLOPB 50S ribosomal protein L35 {ECO:0000255|HAMAP-Rule:MF_00514}	4.20	9.73E-02
Tom1l2	TM1L2_MOUSE TOM1-like protein 2	4.17	9.73E-02
PF14_0175	YPF17_PLAF7 Protein PF14_0175	1.39	9.73E-02
ERMAP	ERMAP_HUMAN Erythroid membrane-associated protein	1.78	9.78E-02

OVA1	SYMM_ARATH Methionine--tRNA ligase, chloroplastic/mitochondrial {ECO:0000305}	3.69	9.79E-02
rtel1	RTEL1_DANRE Regulator of telomere elongation helicase 1 {ECO:0000255|HAMAP-Rule:MF_03065}	-3.87	1.00E+00
PERP	PERP_HUMAN p53 apoptosis effector related to PMP-22	1.22	9.85E-02
#N/A	TCB2_CAEBR Transposable element Tcb2 transposase	4.14	9.85E-02
#N/A	#N/A	2.29	9.85E-02
#N/A	#N/A	3.61	9.85E-02
ELP1	ELP1_RABIT Elongator complex protein 1	-1.47	9.85E-02
IFFO1	IFFO1_HUMAN Intermediate filament family orphan 1	-5.03	9.91E-02
Smarca4	SMCA4_RAT Transcription activator BRG1	-4.06	9.92E-02
FER	FER_CANLF Tyrosine-protein kinase Fer	2.23	9.97E-02
Pik3c2g	P3C2G_MOUSE Phosphatidylinositol 4-phosphate 3-kinase C2 domain-containing subunit gamma	1.77	9.98E-02